School of Civil Engineering

Transfer Of Prestress By Pretensioned Wire Tendons

Paul Kong Yeow Liong

This thesis is presented as part of the requirements for the award of Degree of Master of Engineering of Curtin University of Technology

November 1993

Dedicated to my family

"I give thanks to Christ Jesus Our Lord, who has given me strength for my work."
(1 Timothy 1:12 GNB)

Education is what survives when what has been learnt has been forgotten.
(B. F. Skinner, 1964)

Acknowledgments

The work described in this dissertation was carried out in the Department of Civil Engineering at Curtin University of Technology between February 1992 and October 1993.

In acknowledgment of precious contributions and assistance extended to me during the course of this project, I wish to record my sincere and special thanks to the following:

First and foremost: Dr. I. J. Chandler, Senior Lecturer in the Department of Civil Engineering, for his continual supervision, guidance, advice, encouragement, empathy and friendship over the past two years. I am particularly grateful for his contributions to this thesis through the many fruitful discussions on the present study and also for intentionally setting up a special fund allocated for my project.

Mr. S. Douglas, Manager of Austrak Pty. Ltd., for his remarkable generosity in donating indented and plain prestressing wires which were used in the tests, and for his unceasing interest.

The Readymix Pty. Ltd., for providing the two commercial concrete mixes used in Tests 2 and 6.

Mr. R. Lewis, Mr. R. Cutter, Mr. M. Elliss, Mr. W. Dunn and Mr. D. Edwards, laboratory technicians in the Department of Civil Engineering, for their skilful technical assistance and dedication to this project. Their willingness to help has made my experience at Curtin University a memorable one.

Mr. S. Atkinson, the Technical Officer of the Computer Laboratories in the School of Engineering, for his excellent advice on the use of computers. It

is indeed a privilege to have befriended such an amiable acquaintance who had unfailingly been a source of enlightenment.

Mr. Y. M. Chin, Mr. E. S. V. Lo, Mr. K. P. Tanudjaja, Mr. F. K. Lim, Mr. S. Kramadibrata, Mr. M. B. M. Ilyas, Ms. N. Lloyd and Mr. A. Gupta, all colleagues from the Department of Civil Engineering who have livened up my stay. Special thanks is due to Mr. Y. M. Chin who had commendably helped me in almost all of the concrete castings, forever toiling to achieve perfect surface finishes on the beam specimens. His extraordinary commitment is well appreciated and the fruits of his work preciously savoured. I am also very thankful to Ms. N. Lloyd for her assistance in arranging for the deliveries of the high strength concrete mixes in Tests 2 and 6.

Dr. H. Nikraz, for his influential organising power in recruiting and mustering 'slave' labour for the concreting works of the test beams. I also wish to thank him for his intelligent arguments put forward to me in the friendliest possible manner during our few but inestimable meetings.

Mr. B. Dean and Mr. G. Longhurst, laboratory technicians in the Department of Mechanical Engineering, for assisting in the tensile testing of prestressing wires and also for examining the indentation profile of a 5 mm diameter Chevron wire tendon.

Mr. F. Steenson, Manager of Boiler Technics, for his assistance in my attempt to make a local laboratory steam curing system.

Mr. S. Malkani of RMAX Pty. Ltd., for donating polystyrene foam sheets required for making a steam curing chamber (although the chamber was not used due to the lack of readily available steam).

Ms. J. Yapp and Mr. A. Koh, who had certainly helped me in many ways which have eased this sojourn. The profound fellowship shared will be cherished for a long time to come.

Finally, I wish to express appreciation to the Australian International Development Assistance Bureau (AIDAB) for providing me with a two-year scholarship under the Equity and Merit Scholarship Scheme, without which this project would not have materialised.

Abstract

Key words: End zone, prestress transfer, wire tendon, transmission length, pull-in, plain wire, indented wire, concrete strength, size of wire, gradual release, sudden release, shock release, time dependent effects.

An empirical investigation into the transfer of prestress force from wire tendons to concrete in the end zones of pretensioned prestressed concrete beams was accomplished in this project. The experimental tests featured 56 small scale prestressed concrete beams.

Some of the factors influencing prestress transfer which were considered in the current tests are as follows:

(a) type of release - gradual, sudden or shock
(b) surface condition of the wire - plain or indented
(c) size of the wire
(d) concrete compressive strength at the time of transfer
(e) time dependent effects

Most of the tests involved gradual release of steel tendons with the prestressing force transferred in approximately ten equal increments. Sudden release in a single step was achieved by allowing the supporting abutments to retract rapidly. Shock release was implemented in some beams by angle grinding the wires. The type of release which gave the best quality of prestress transfer was gradual release. This was followed by sudden and shock releases respectively.

There were four types of wires used in the laboratory tests: namely the 5 mm dia. Plain, 5 mm dia. Chevron indented, 7 mm dia. Plain and 7 mm dia. Belgian indented wires. Transmission lengths were determined from strain distributions for these wires. Pull-ins of the wire tendons at the ends of the beams were also measured.

There was significant scatter in the experimental data. Different ranges of transmission lengths and pull-ins were obtained for the various types of wires used.

Three equations were derived for the 5 mm dia. Plain, 5 mm dia. Chevron and 7 mm dia. Plain wires, which linearly correlated pull-ins to the transmission lengths. These relationships provide a qualitative and quantitative method of indirectly monitoring for the transmission lengths through the measurements of pull-in.

Statistical inference tests proved that indented wires were superior in performance compared to plain wires, but the differences were more apparent for the pull-ins than for the transmission lengths.

Comparisons on the influence of tendon size substantiated that greater pull-ins occurred for larger wires but the differences were not significant for the transmission lengths.

For concrete strength at the time of transfer of less than 32 MPa, the transmission lengths and pull-ins were significantly larger than those for higher strengths. It is recommended that concrete strength at transfer be at least 32 MPa for pretensioned prestressed concrete.

Apart from the maturity and strength of concrete, the quality of a mix also influenced the transmission length and there was limited data to suggest that a better grade mix despite having lower strength at a more tender age could outperform a lower grade mix with greater strength released after a longer curing period.

Formulae for plain and indented wires were found by dimensional analysis which correlated the transmission length to the diameter of wire tendon and the stress/strength ratio of the prestressed beams.

Pull-ins increased significantly over 6 months but the changes in the transmission lengths were small. Normalised longitudinal strain distributions did not indicate that transmission lengths would remain unchanged over time.

Contents

Notation

The following notation is used throughout this dissertation. The first time any symbol is used, its meaning is provided in the text.

A_c	cross-sectional area of concrete specimen
A_p	cross-sectional area of prestressing steel
A_w	cross-sectional area of a prestressing wire
C'	factor to convert concrete cylinder strength to the equivalent cube strength after Murdock and Brook (1979)
D	diameter of concrete test cylinder
d	depth of the test beam
d_b	nominal diameter of a tendon
$d\Delta$	infinitesimal change in slip over the distance from x to x+dx
E_b	modulus of elasticity of concrete at the bottom of a test beam
E_c	modulus of elasticity of concrete (general notation)
E_{cj}	modulus of elasticity of concrete according to AS 3600 (1988)
$E_{c.transfer}$	modulus of elasticity of concrete at transfer
$E_{c.6month}$	modulus of elasticity of concrete at 6 months
E_p	modulus of elasticity of prestressing steel
E_t	modulus of elasticity of concrete at the top of a test beam
f'_c	characteristic compressive strength of concrete at 28 days
f'_{ci}	compressive strength of concrete at transfer after Cousins, Johnston and Zia (1990)
f_{cp}	compressive strength of concrete at transfer
f_p	tensile strength of prestressing tendon
f_s	tensile stress in the wire at a distance x along a beam
f_{se}	effective tendon stress
f_{si}	initial tendon stress
H	height of concrete test cylinder
H_a	alternative hypothesis in a statistical inference test
H_o	null hypothesis in a statistical inference test
K_t	constant in Equation 2.38 according to BS 8110:Part 1:1985

K_o	constant in Equation 2.46 after Chandler (1984)
L_p	transmission length of a tendon
$\hat{L}_p$	upper limit for transmission length in wire pretensioned prestressed beams
L_{pi}	initial transmission length of a tendon upon full prestress transfer
M_s	maturity of the concrete
m	modular ratio of steel over concrete
n_1, n_2	sizes of two samples in a statistical inference test
P	total force in the prestressing steel
r	correlation coefficient in regression analysis
r_w	radius of the prestressing wire after Janney (1954)
s_1, s_2	standard deviations of two samples in a statistical inference test
s_σ	ratio of the area under the effective tendon stress versus transmission length curve over a rectangular enclosed area of ($f_{se}\, L_p$)
s_τ	ratio of the area under the bond stress versus transmission length curve over a rectangular enclosed area of ($\tau_{cp}\, L_p$)
t	bonding force per unit length developed at the steel-concrete interface after Marshall and Krishnamurthy (1969)
t_{test}	t-distribution test statistic in a statistical inference test
U_t	uniform plastic bond stress after Cousins, Johnston and Zia (1990)
U_t'	equals to the ratio of $\frac{U_t}{\sqrt{f_{ci}'}}$ after Cousins, Johnston and Zia (1990)
u_t	concrete cube strength at transfer
V	coefficient of variation in statistical analysis
x	distance from the dead end of a pretensioned prestressed beam
$\bar{x}_1$, $\bar{x}_2$	means of two samples in a statistical inference test
y	'out of straightness' deflection function for the test beams
y''	curvature function for the test beams
z_{test}	normal distribution test statistic in a statistical inference test

α	level of significance in a statistical inference test (Figure 2.16)
ΔP_i	decrease in force from an initial prestress force
Δt	time interval of the hardening process for concrete
Δ_o	slip of the tendon relative to the concrete at the end face of a pretensioned prestressed concrete beam (ie. pull-in or end slip)
$\hat{\Delta}_o$	upper limit for pull-in in wire pretensioned prestressed beams
Δ_{oi}	initial pull-in of a tendon upon full prestress transfer
Δ_x	slip at a distance x from the end of a beam after Bruggeling (1986)
δL_p	change in transmission length over time
δx	an infinitesimal length of a pretensioned prestressed concrete beam

$\delta\Delta_o$	change in pull-in over time
$\delta\varepsilon$	differential longitudinal strain between steel and concrete
$\delta\theta$	angular change in the beam over the length of δx
ε	strain in the concrete after Lydon (1979)
ε_b	strain at the bottom of a test beam
ε_{co}	maximum longitudinal concrete compressive strain past the end zone due to full prestress transfer
ε_{curv}	strain in test beam due to curvature effect
ε_{cx}	concrete strain at a distance x from the end face after transfer
ε_o	concrete strain corresponding to σ_{max} after Lydon (1979)
ε_{se}	effective maximum tendon strain past the end zone after prestress transfer
ε_{si}	initial tendon strain before release of prestress
ε_{sx}	strain in tendon at a distance x from the end face of the beam after transfer
ε_t	strain at the top of a test beam
κ	curvature of the test beam (equals y")
λ	characteristic length after Guyon (1953)
μ	coefficient of friction between concrete and steel
μ_1, μ_2	means of two populations in a statistical inference test
ν	degrees of freedom in a t-distribution statistical inference test
ν_c	Poisson's ratio for concrete
ν_s	Poisson's ratio for steel
Φ	circumference of the tendon
$\emptyset$	indicates reference is made to the diameter of a tendon
$\emptyset_{cc.transfer}$	design creep factor at transfer
$\emptyset_{cc.6month}$	design creep factor at 6 months
σ	stress in the concrete after Lydon (1979)
σ_{co}	longitudinal axial stress in a prestressed concrete specimen, $\left(\frac{P}{A_c}\right)$
σ_{max}	maximum stress in the concrete after Lydon (1979)
σ_1, σ_2	standard deviations of two populations in a statistical inference test
τ	bond stress at the steel-concrete interface after Guyon (1953)
τ_{cp}	maximum bond stress in a tendon after Bruggeling (1986)
τ_{max}	maximum bond stress at the end of the beam after Guyon (1953)
τ_x	bond stress at a distance x from the beam end after Bruggeling (1986)
ψ	ratio of E_t over E_b

List of Figures

List of Tables

CHAPTER 1

Introduction

Structural concrete has the characteristic of being capable of sustaining greater loads in compression than in tension and as a consequence of its unreliable tensile strength, it is prone to cracking. Cracking can occur at micro- or macro-levels, with microcracks propagating in the material to form macrocracks which are visible to the naked eye.

Cracking can be initiated through volumetric change in concrete, from applied loads creating axial or flexural stresses, from shrinkage and plastic movements during and after casting, from creep effects over time or from thermal gradients. It needs to be controlled as it can be aesthetically unacceptable, causes loss of member stiffness resulting in large deflections and encourages moisture ingress which corrodes the steel. In order to control cracking, steel can be made an integral part of a concrete member as steel performs well in tension.

Steel reinforcement can be used in concrete in one of three forms; reinforced, prestressed or partially prestressed concrete. In conventional reinforced concrete, steel is "untensioned" and has the function of carrying tensile forces when the concrete cracks in the tensile zone thus shedding its load to the steel. Steel may not be required in the compression zone as concrete has the capacity to carry large compressive forces before showing any sign of distress.

Fully prestressed concrete involves the precompression of concrete prior to any service load being applied to the member. Since the member remains in an uncracked state within the range of the applied service loads, the overall performance will be enhanced. With no cracks, the full cross-sectional area of the member can contribute to its stiffness and thus provide a better control on deflection.

Partial prestressing bridges the gap between reinforced and fully prestressed concrete. While reinforced concrete is expected to crack with the application of service load and fully prestressed concrete is designed to be uncracked, partially prestressed concrete would crack within the service load range when its "decompression moment" has been surpassed and stresses in the extreme fibres of a concrete member has exceeded the tensile capacity.

Prestressing can be achieved by using steel wires, bars, strands or cables and they are referred to in general as steel "tendons". The basic principle is to stretch a tendon in tension and transfer this load into the concrete as compression. A concrete member can have its tendon(s) 'post-tensioned' or 'pretensioned'. In post-tensioning, the steel tendon located in a duct is stressed up ***after*** a cast concrete member has hardened and gained sufficient strength. In contrast, the steel tendon in a pretensioned prestressed concrete member is tensioned ***before*** casting the concrete around this steel tendon. Precompression of concrete is then effected through releasing the tendons from the restraining abutments.

The methods of force transfer are different in pretensioned and post-tensioned prestressed concrete. In post-tensioning, as the tendon is stressed, the reaction force is directly applied to the end of the member. The tendon is secured to positive anchorage plates at both ends of the member before being released. For pretensioned prestressed concrete, the steel tendon has to be tensioned and temporarily anchored to abutments. After the concrete is cast and has hardened, the prestressing force is transferred to the concrete by bond at the steel-concrete interface as detensioning occurs.

Therefore, post-tensioning and pretensioning are associated with end anchorage and bond transfer respectively as the mechanisms of prestress transfer. This may not be entirely true for pretensioning because

anchorage plates or other positive anchorages have been used to assist in the transfer of force. However, for this project the interest has been focused on pretensioned prestressed concrete beams without any other form of additional anchorage restraint.

An investigation was carried out to examine the effects of factors which influence prestress force transfer. In the laboratory tests performed, the effects due to different concrete strengths, sizes and types of wire tendons and types of releases were considered. In order to be able to determine the influence of these factors, measurements were taken to quantify the quality of prestress transfer in test beams.

As pretensioned steel is released, it sinks into the concrete and the total amount of slip at the end face of a member is called the "***pull-in***" or "end-slip". Since there is slippage, the full effective prestress cannot be developed at the end face of the member; in fact, it will take a certain distance from the end to develop the full effective prestress. This distance is called the "***transmission length***" or "transfer length". For each steel tendon in a pretensioned prestressed beam, there is one corresponding transmission length and pull-in at each end of the beam. The effect of the transfer of prestress is reflected in these two parameters and thus, the quality of the transfer can be determined from magnitudes of the observed transmission length and pull-in.

Chapter 2 describes previous research work accomplished in the area of pretensioned prestressed concrete. The author concentrated on work related to prestressing wires and not so much on strand (being the other type of more commonly used tendon), since Chandler (1984) had covered extensively the study of strand tendons.

The author's undertakings during the laboratory testing phase of this project is revealed in Chapter 3. Materials and formwork used in the testing programme, the different variables considered and also the testing procedure are elaborated.

The results and outcomes of analyses performed on the data obtained are presented in Chapter 4 of this dissertation. Apart from comparing results from the laboratory tests alone, the author also made cross-comparisons with results from previous investigations. Another highly pertinent

aspect covered in Chapter 4 is the relationship between transmission length and the corresponding pull-in. Establishing acceptable relationships between these two parameters for various types of wires would allow the transmission lengths to be estimated by only monitoring for the pull-ins, thus simplifying the method for controlling the quality of transfer since much more effort is required to evaluate the transmission lengths than the pull-ins. Apart from this, formulae were also established using dimensional analysis which related transmission length to the diameter of the wire tendon and stress/strength ratio (this is a function of the precompression concrete stress and concrete strength at transfer). Changes in the transmission length and pull-in due to long term effects such as creep and shrinkage were also examined.

Finally, Chapter 5 concludes on the findings of this project taking into account the existing but limited knowledge on the topic of end zones in prestressed concrete beams with pretensioned wire tendons.

CHAPTER 2

Fundamental Principles

2.1 Introduction

The rudiments associated with prestressed concrete with pretensioned tendons will be established in this chapter, allowing further developments discovered during the course of this project to be detailed in subsequent chapters.

A brief description of the materials used in making prestressed concrete will be presented. Various types of steel tendons available for pretensioning are considered.

The mechanics of prestress transfer from the steel to the surrounding concrete will be explained according to the many ways of transfer as proposed by previous investigators. Factors that affect the transfer of prestress are pointed out and their effects on tendons elaborated.

Some of the theoretical, semi-empirical and empirical formulae for determining the transmission length and pull-in are also summarised. Derivation of a relationship between the transmission length and pull-in of wire tendons is provided.

Since the results of this project were compared to those from previous investigations, the concrete strength at transfer had to be compatible

before any comparisons could be made. Much work done in Great Britain used the concrete 'cube' strength, therefore it was apt to provide conversion from cube strength to the equivalent cylinder strength.

The chapter concludes by discussing statistical approaches such as regression analysis and hypothesis testing which were used for analysing the results.

2.2 Materials

Special high strength steel and concrete are imperative to the manufacturing of pretensioned prestressed concrete. High strength concrete can attain high compressive capacity in a short period of time whilst the high strength steel can be strained sufficiently to cater for losses due to shrinkage, creep and relaxation effects without significantly losing the pretension.

2.2.1 Prestressing Tendons

The production of prestressing wires involves cold drawing of high carbon hot-rolled steel rods through a set of dies (Fogarasi, 1986). The dies can be used to impress indentations or grooves on the surface of the steel wires. The drawing process decreases the diameter of the wire and simultaneously causes longitudinal crystals to form on the surface. The wires are then stress-relieved to yield uniform elastic properties.

Prestressing wires are manufactured with diameters in the range of 2 mm to 16 mm and they are mainly circular in cross-section.

Cold drawn wires can be grouped together to make untwisted cables. Alternatively, they can be wound together helically to form prestressing strands. Seven-wire, uncoated stress-relieved strands are available with nominal diameters of 6.3, 7.9, 9.5, 11.1, 12.7, 15.2 and 17.8 mm.

A less common alternative for pretensioning is the use of prestressing bars, which are hot-rolled and usually stress-relieved. Prestressing bars have smaller tensile capacity than wires or strands.

Until recently, the reinforcing material has been kept strictly to high strength, uncoated steel wires or strands. However, the susceptibility of steel to corrosion has been recognised as being potentially detrimental to the integrity of a concrete member or structure. In view of the poor resistance of prestressing steel to corrosion, alternative materials which consisted of non-metallic high strength fibres have been used. These fibres include glass and synthetic fibres of aramids and carbons which are also stable in the highly alkaline environment within the concrete. The emergence of such materials has created a new area of interest in recent years although their application to prestressing has not been significant thus far.

Apart from using steel tendons or plastic composite tendons, Cousins, Johnston and Zia (1990, 1992) have also started promoting the use of epoxy coated strands. These tendons are expected to perform better in a corrosive environment than using steel alone but they probably do not perform as well as the plastic composite tendons.

Both the epoxy coated steel strands and the plastic composite tendons have the flexibility where the amount of grit (crushed glass or sand) can be varied on the surface of the tendons, thus varying the frictional resistance between the tendons and the concrete. They have tended to out-perform the standard uncoated seven-wire strand by invariably coming up with shorter transmission lengths when used in pretensioning works.

2.2.2 Concrete

Concrete consists of aggregates, cement, water and suitable admixtures. Some important properties imperative to prestressed concrete are:

(a) high compressive and tensile strengths to be able to disperse end zone stresses, reduce deflection and produce smaller member sizes.
(b) high early strength to allow rapid transfer hence speeding up the manufacturing process and increasing production and turnover.
(c) adequate consolidation and densification to improve its durability.
(d) able to restrict long term effects due to shrinkage and creep which influence the effective prestress.

2.3 End Zone Stresses In Pretensioned Prestressed Concrete Beams

Mechanical prestressing is the most common method of stressing steel and it requires positive grip on the tendon ends before stressing can be implemented. All of the following discussions relate to this prestressing technique.

In post-tensioned prestressed concrete, bearing plates are used to distribute large prestressing forces. The direct bearing stress under the anchor plate will not cause crushing of the concrete with proper design and construction. As the forces disperse away from the loading axis, equilibrating forces create transverse tensile stresses which act perpendicular to the axis of loading. The transverse tensile stresses act at the tendon depth but remote from the end of the beam. Such tensile stresses occur in a region called the "bursting zone" (Figure 2.1).

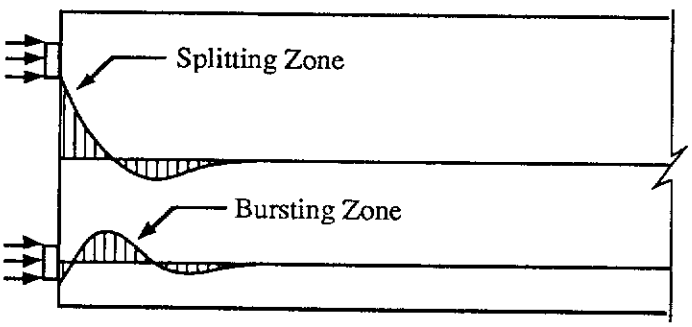

Figure 2.1 **Transverse Stresses in the End Zone of a Post-Tensioned Twin Anchorage Beam (from Figure 2.2 of Chandler (1984))**

When there are two anchorages used and they are spread wide apart, large transverse tensile stresses occur between the loading axes of the two anchorage points at the end of the beam. This zone also has the potential to crack and it is commonly referred to as the "splitting zone" (Figure 2.1).

Significant tensile stresses can also develop from shear lag effect of a large concentrated load. The concrete adjacent to the steel tendon will experience the effect of large stresses immediately but it takes shearing stresses to influence concrete at a greater distance away from the steel tendon, particularly in the top and bottom corners of the beam end. The

tensile stresses in these regions are called "spalling stresses" and may cause concrete to chip off.

Pretensioned prestressed concrete has a less severe problem with large transverse tensile forces since the transfer of force in pretensioning involves gradual load transfer with the load dispersing over a distance, hence decreasing the intensity of stress concentration.

The dispersion of forces from pretensioning steel into the concrete has been the focus of much research and has been and will remain a perplexing subject. Previous investigators have attempted to model the actual force transfer mechanism by proposing different postulations about the distribution of force at the steel-concrete interface. Most concepts have dealt with two-dimensional dispersion of force whereas a few have attempted to simulate the situation in three-dimensional space.

2.4 Transfer Of Prestress

When pretensioned steel is released, the transfer of force is gradually transferred into the concrete. This transfer occurs at the steel-concrete interface and is effected through 'bond stress'. Figure 2.2 indicates the actual behaviour of the steel tendon and concrete in terms of axial strain variation as the prestress force is transferred.

The tendon reduces in stress and strain as it is released. The tendon force increases from zero at the end of the beam to the full effective pretensioning force over a length called the ***transmission length***, or alternatively transfer length, anchorage length or development length.

There is conflicting usage of some of these terms. For example, Srinivasa Rao et al. (1977) argued that the 'bond length' was "*the length required for full transfer of prestressing force from the wire to surrounding concrete by bond*". The 'transmission length' was the length where "*prestressing force needs to be distributed over the entire concrete section and should be introduced into the member only when the concrete stresses exhibit a linear distribution over the section*". This contradicts the usage of terms by Chandler (1984) and other researchers who used transmission length instead of bond length and end zone length instead of

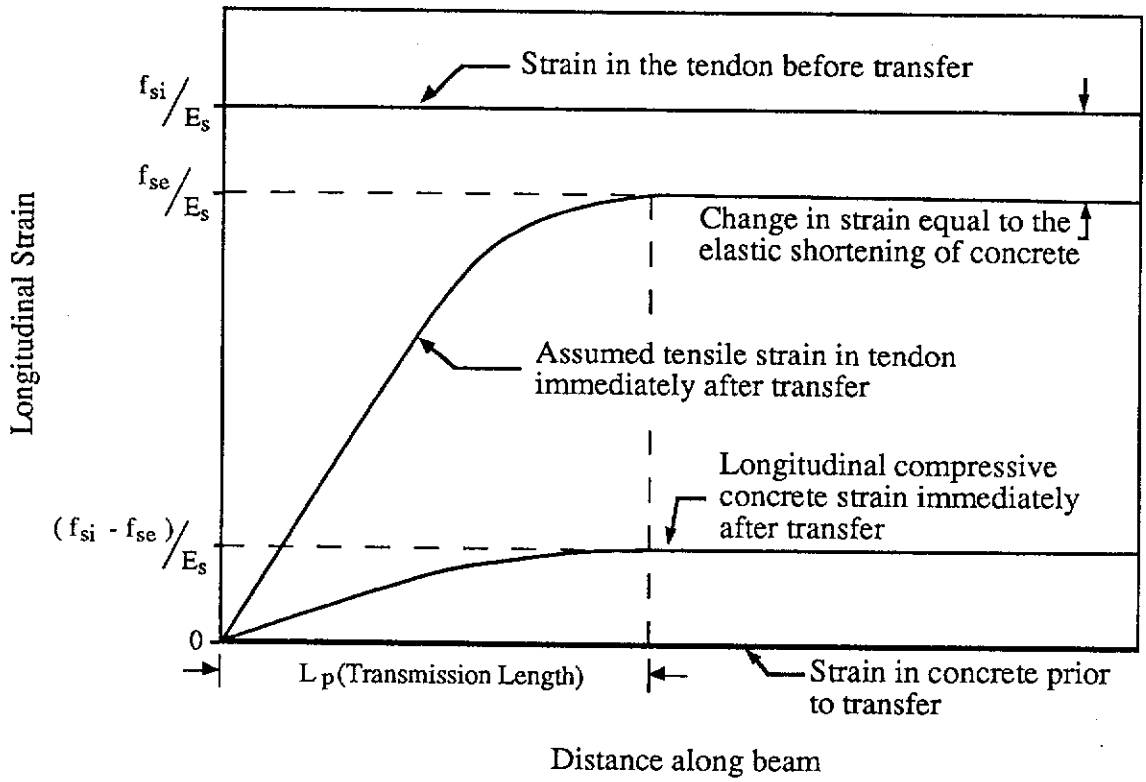

Figure 2.2 Longitudinal Strains in the End Zone Before and Immediately After Prestress Transfer (adapted from Figure 2.11 of Chandler (1984))

transmission length. For the purpose of this thesis, the term 'transmission length' (denoted as 'L_p') is adopted as the length required to reach the maximum prestress force and the 'end zone length' (denoted as 'a') represents the length to reach a linear stress distribution in accordance to the St. Venant's principle. The end zone length is slightly longer than the transmission length to allow for the dispersion of forces. However, for small beam sections, as in the case of this project, there is little difference between the two lengths and reference is only made to the transmission length.

Prestress builds up over the transmission length. As the steel strain curve flattens off, the full prestress is considered to have been transferred. However, since the concrete beam shortens elastically due to the large compressive force, the steel also shortens by an equivalent amount, consequently ending up with a smaller full effective prestress of f_{se} from an initial steel stress of f_{si}. Total loss of prestress occurs at the end face of the beam and this is consistent with the end boundary condition.

The concrete responds with a similar shaped stress-strain curve, with zero strain at the end face increasing to maximum compressive strain at the 'end' (referred to as 'inner end' in AS 3600 (1988)) of the transmission length. The magnitude of the maximum concrete strain is the same as the decrease in steel strain past the transmission length.

The steel and concrete strains versus longitudinal distance profile can be obtained by recording these strains before and after the load transfer. Various techniques which have been used to determine these strains include:

(a) a radiographic technique whereby minute lead markers were inserted into slots specially milled onto the steel tendon. The relative movements of adjacent markers would give the change in steel strains (Evans and Robinson (1955)).

(b) strain measurement on steel between drillholes made through the concrete cover to the tendon.

(c) using strain gauges attached to the 'inside' of a specially prepared hollow steel bar with leads extending out through the ends of the bar (Mains (1951)).

(d) using a demountable mechanical strain gauge (or "DEMEC" after Base (1955)) where stainless steel target discs were placed at constant intervals on the hardened concrete surface. This method remains the most practical and has been discussed by Morice and Base (1953), Base (1955) and Chandler (1984).

(e) strain measurement from electrical resistance strain gauges (ERSGs) placed on the tensioned steel tendon before concrete casting or placed on the hardened concrete surface after casting.

The X-ray radiographic method has many associated disadvantages. The primary restriction to this technique is the requirement for the specimen to be thin with steel placed close to the beam sides because of limited radiation penetration. It requires suitable radiographic conditions before a satisfactory film can be produced. The correct amount of radiation, the size of the specimen, the degree of filtration and shielding employed and the processing technique could all affect the quality of the film. In addition, changes in humidity cause shrinkage in the film and this affects the accuracy of the technique.

Another method involving making holes through the concrete to measure steel strains is also impractical. Only a limited number of points can be located for such measurements since bond stress is destroyed through concrete removal at the steel-concrete interface.

The method used by Mains (1951) was to slice a bar into two halves longitudinally and mill the inside of each half to provide a groove where strain gauges could be attached. This method avoided the problem of affecting the bonding characteristics but it had other disadvantages. With leads coming through the ends of the hollow bar, only a limited number of strain gauges could be used. It could not be applied to small diameter bars or wires and strands. As a large proportion of steel is removed, the amount of prestress applied has to be decreased. Hence, the prestress used is no longer consistent with the size of the bar.

Measuring strain between pairs of demec target points seems to be the universally accepted method of strain measurement on hardened concrete. This method requires measurements to be made manually which can increase the likelihood of making errors in either reading or recording the results. It is important to note that demec readings actually show the concrete response at the surface but they are used to interpret the behaviour of internal force transfer.

In reality, the demec strain readings predict the end zone length rather than the actual transmission length. Should tendons be closely and uniformly spread over the beam cross-section, the end zone length would reduce to the transmission length as constant force distribution is achieved almost immediately past the end of the transmission length.

In its practical application, the demec gauge method has been assumed to measure L_p instead of 'a'. The difference is normally small enough to permit such an approximation. In most cases, tendons will be near to the concrete faces allowing demec points to be placed close to the tendon. The major advantage of this method is that it does not affect the transfer of prestress as apparent in most other techniques. It also allows the investigator the freedom of having more data points without jeopardising the accuracy of the results.

A final alternative for measuring strains is by using electrical resistance strain gauges either attached to the tendon before concrete casting or mounting the gauges onto the hardened concrete surface. Attaching gauges to the steel requires the gauges and leads to be connected properly so that concrete pouring will not render the gauges unserviceable. The attachments also reduce the steel area available for concrete bond and only limited number of gauges can be placed. Gauges fixed to the concrete surfaces require more care than attaching demec targets as the alignment of the gauges is important. The gauges are also more costly than demec discs and less can be used. If cracking occurs across the strain gauge, it may be destroyed whereas the demec measuring technique would pick up the sudden change in the strain distribution due to the opening of the crack.

The electrical resistance strain gauges tend to outperform demec gauges in terms of consistency, maybe due to inconsistencies associated with the pressure applied when handling the demec gauge. Recent tests on strand transfer lengths by Shahawy et al. (1992) found ERSGs to be superior compared to the demec gauges.

2.4.1 The Nature of Bond Stress

In pretensioned prestressed concrete members, the transfer of the prestress force occurs through the development of bond stress which is generated from the resistance between steel and concrete.

Expanding on Janney's (1954) postulation, Evans and Robinson (1955) proposed that the bond stress mechanism was actually made up of the following:

(a) adhesion between the steel and concrete - it was proposed that it could only exist with slip, but only to an infinitesimal amount. It was suggested that such small relative movement provided resistance from the micromechanical locking of fine concrete particles in micro-indentations on the steel surface. In any case, the amount of resistance due to this particular mechanism was negligible when appreciable slip occurred in the end zone.

(b) macro-mechanical interlocking - this was a similar concept to micromechanical locking but to a larger scale. Indentations or deformations provided on the pretensioning tendons improved the bond with concrete. In prestressing strands, the 'cusps' between adjacent wires provide similar but better bond capability. Therefore, surface condition was important with respect to bond transfer.

(c) frictional resistance - this was achieved as the tendon was released; the steel at the end face lost all prestress and had a tendency to expand radially. The expanded end acted as a 'wedge', hence providing some form of end anchorage. This is known as the Hoyer's effect (Figure 2.3). The expansion also induced normal compressive forces on the steel-concrete interface. Frictional resistance was then attained as the tendon slipped into the concrete; the frictional force being the product of the normal reaction force from the confining concrete acting on the steel surface and the steel-concrete frictional coefficient.

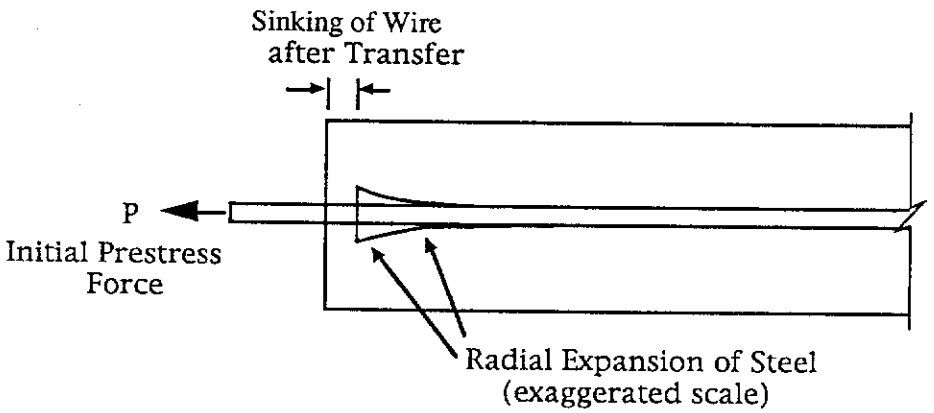

Figure 2.3 Hoyer's Effect in the End Zone

(d) dilatancy - the resistance against slip due to wedging of concrete particles at the steel-concrete interface produced after initial slip.

There are differences between various pretensioning wires. A plain wire having no deformations impressed on its surface tends to slip more freely than an indented wire. The indented wire has extra resistance from cement paste filled in the pockets of indentations which are normally spaced regularly in two or more lines along the length of the wire. Even

when the cement paste 'wedges' shear off along the circumference of the tendon, the rough surfaces from the shearing off still provide resistance to slip.

Different patterns such as simple round dimple (Belgian pattern), rhomboidal shape (Chevron pattern), oval and rectangular shapes have been used. The emphasis on the effectiveness of such indentations has been attributed to the size and depth of these indentations, giving less attention the shape of the indentation. Should the indentations be of insufficient depth or definition in the imprint as a result of worn manufacturing equipment, then the wires would tend to behave more like plain wires.

Since plain wires are expected to be unreliable in the transfer of prestress compared to indented wires, AS 3600 (1988) has excluded these wires from being used in pretensioned prestressed concrete.

Crimped wire has also been used to improve transfer bond. The wire is set into a helical spiral with a very small eccentricity from the longitudinal axis of the wire. However, there are problems in providing anchorage for the wire when stressing.

Prestressing strand has undisputably better bond characteristics than wires. Other than having cement paste adhering to the steel within the cusps, Chandler (1984) also suggested that the pitch shortens as the strand is detensioned. The increases in the pressure at the steel-concrete interface coupled with the shortening enhances the frictional resistance to slip. It was also noticed that when strands were released, it had a tendency to rotate. Preswalla and Preston (1990) had shown analytically and experimentally that as a strand is tensioned, a torque to tighten the spiral tends to occur. The reverse argument could be applied when detensioning, where the strand is expected to have an unwinding torque as it is released. The contact pressures will increase, thus increasing the frictional resistance.

The complexity involved in determining the bond stress and the improbability of actually being able to measure it physically had inspired the origination of many hypotheses about the bond stress distribution along the transmission length. Any attempt to physically determine the

strains and stresses at the interface, such as through the use of ERSGs as explained earlier, caused interaction between the measuring equipment and the bond stress, thus defeating the purpose of the tests.

Four bond stress distributions had been described by Chandler (1984) as shown in Figure 2.4. The distributions by Guyon (1953) or Marshall (1949) assumed a decaying exponential function whereas Leonhardt advocated a distribution of the shape of a Poisson's distribution. Other more simplified distributions were the triangular and rectangular distributions.

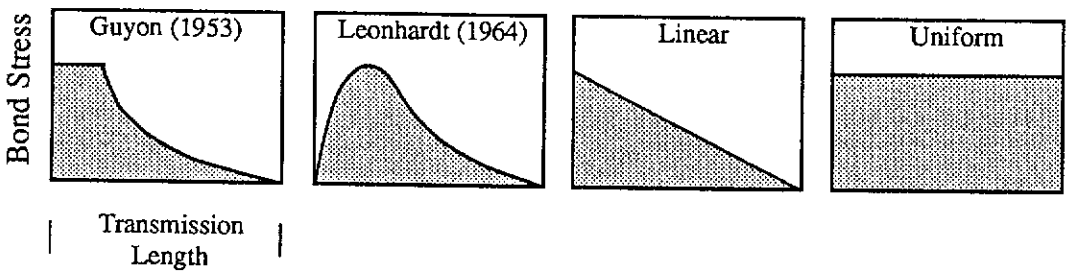

Figure 2.4 Bond Stress Distributions (adapted from Figure 2.5 of Chandler (1984))

Guyon's bond stress distribution may or may not have a section of constant bond stress (u) near the end of the beam as the distribution depended on whether the maximum bond stress had been reached. Bond stress was found to be directly proportional to slip for small slip values but reached a limiting value, u_{max}, as slip increased as shown in Figure 2.5.

Guyon explained how four different zones at the beam end were simplified into two zones by collapsing the elastic and elasto-plastic zones, and the friction and plastic zones. The bond stress in the plastic zone would have a ceiling value of u_{max} whereas the elastic zone bond stress varied linearly with slip (as long as the displacements were minute, the bond stress was proportional to the displacement, according to Figure 2.5 (a)). The simplified distribution of the bond stress can be seen in Figure 2.6.

Cousins, Johnston and Zia (1990) extended Guyon's concept using the model in Figure 2.6 to cater for uncoated and epoxy-coated strands. Thus, they had effectively ended up with a bond stress distribution model which was a combination of the simplified linear triangular and uniform rectangular distributions.

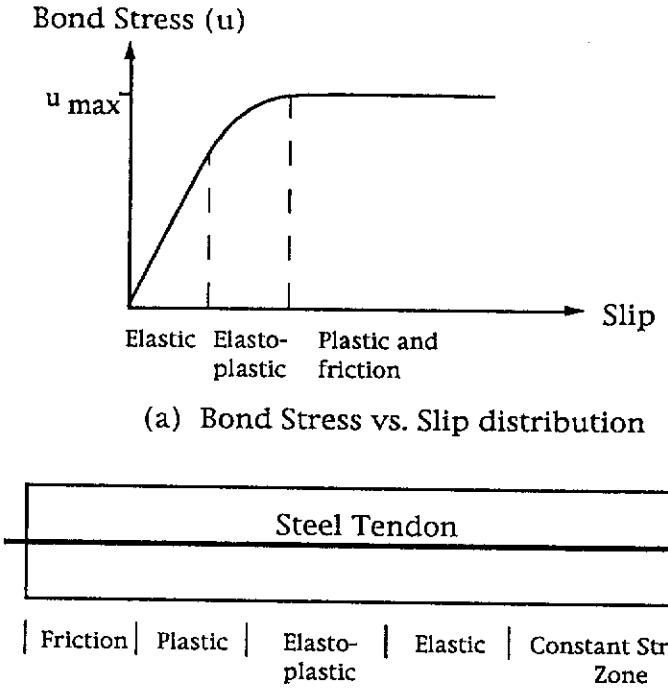

Figure 2.5 **Bond Stress Along the End Zone of a Pretensioned Prestressed Concrete Beam (adapted from Guyon (1953))**

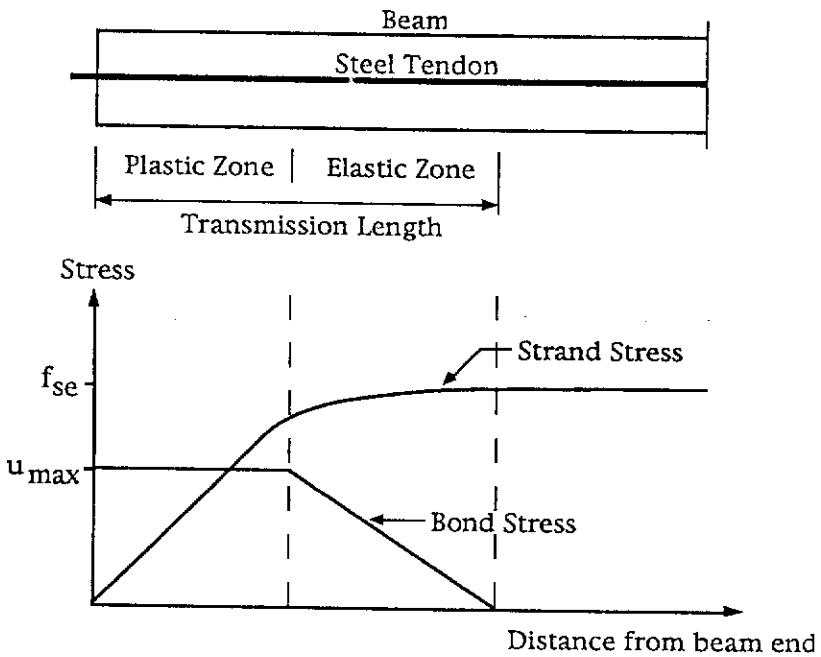

Figure 2.6 **Elastic-Plastic Zones and Bond Stress Model (adapted from Figure 2 of Cousins, Johnston and Zia (1990))**

Chandler (1984) pointed out that since the whole concept of bond stress was based upon hypothetical model distributions, the use of Guyon's distribution or similar was not necessary and could be dispensed with. The shape function had to be assumed and constants (such as u_{max}) were approximated from a finite number of tests. This could lead to a misconception of the accuracy of formulae obtained. When properly considered, the whole concept of bond stress serves no other purpose than to allow the designer to determine the transmission length. Simpler approximations can be used to provide values of transmission length which are just as reasonable as those found by the bond stress approach.

The steel stress distribution reaches a limiting value at the end of the transmission length and bond stress is zero past the transmission length. This holds true during prestress transfer but not when the beam is loaded flexurally. Once the member goes into bending, the steel tendon stress will begin to increase. The increase is small prior to cracking but as cracks set in, the adjacent steel stress will increase sharply (Figure 2.7).

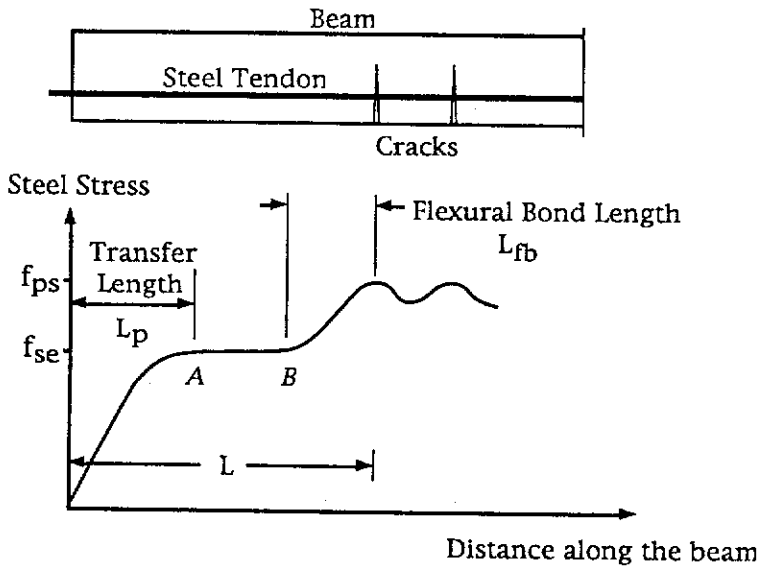

Figure 2.7 Flexural Bond Length Extending into the Transfer Length Zone (from Figure 7-21 of Lin and Burns (1981))

The additional tension in the tendon induces extra bond stress required to counter the increase in steel stress to a maximum value of f_{ps}. The extra length required for bonding is called the 'flexural bond length' (L_{fb}). As cracks progress towards the end of the beam, the flexural bond length also moves towards the end like a "wave", hence decreasing the distance

between the end of L_p and the beginning of L_{fb} (ie. the distance between points *A* and *B* in Figure 2.7).

2.4.2 The Determination of the Transmission Length

A few methods for determining the transmission length has already been discussed earlier. A brief review of literature showed that previous investigators have used four main procedures for determining the transmission length (Srinivasa Rao et al. (1977)):

(a) examination of build-up strains along the longitudinal sides of pretensioned prestressed members due to transfer.
(b) measuring the pull-in or end-slip of tendons into the concrete at the time of transfer and relating this to the transmission length.
(c) theoretical calculations based on bond-slip relationships using models of bond stress distribution.
(d) semi-empirical formulae based on the friction-bonding characteristics of the tendons.

For the purpose of this project, the first and second methods were used. As explained earlier, bond-slip and friction-bond models are not considered realistic for determining the transmission length.

Demec discs are generally spaced at regular intervals along a line where the strains are to be measured. Figure 2.8 shows the target discs at 25 mm spacing (50 mm is also commonly used) and a 200 mm long mechanical strain gauge (100 mm strain gauge is also available) is used to measure strain between target points 200 mm apart.

Some practical considerations in using the mechanical strain gauge had been raised by Morice and Base (1953). A reasonable amount of care should be exercised when fixing discs to the surface of the concrete. Flatness on the concrete surface was achieved by grinding off irregularities before attaching discs on it. Consistency of results was enhanced by having a single operator when taking the results. A reference in the form of an Invar bar allowed temperature effects to be taken into account.

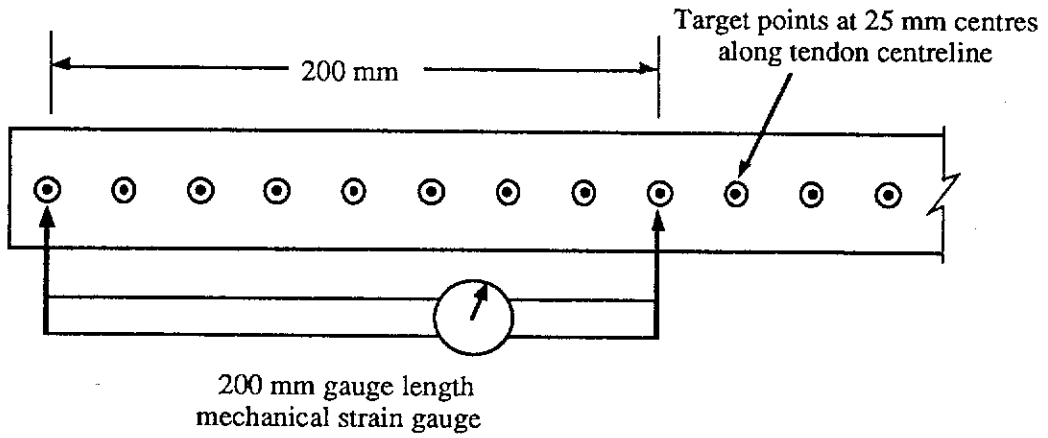

Figure 2.8 A 200 mm Mechanical Strain Gauge Used to Determine Longitudinal Strains Between Demec Target Points Set on a Beam

Chandler (1984) expressed some pertinent problems associated with this method of surface strain measurement for determining the transmission length and they are summarised as follows:

(a) deficient number of measurements - an insufficient number of points will create difficulty in trying to estimate the first instance when the strain versus distance curve flattens off horizontally. Only with many strain readings will this point be more accurately pin-pointed. A spacing of 25 mm was considered to be practical. Errors can occur in reading and some of these which cannot be accounted for will be discarded. Should the loss of data points happen near the end of the transmission length, then the accuracy of determining the transmission length can be affected.

(b) difficulty in identifying the end point for the transmission length - even with adequate number of data points, the determination of the end point is impossible when the curve does not flatten off but continues to rise monotonically without a sharp change in the curvature of the strain versus distance plot.

(c) location of measurements on the concrete surface - measurements of strain on the surface actually show the lag effect of stresses dispersed across the concrete between the tendon and the surface of the beam. However, not only does concrete cover influence the

strains but the location of the discs also has a significant effect. For example, strains can be obtained at the top flange, web and bottom flange levels of an I-beam (Figure 2.9). Upon transfer of prestress, the top flange strains (line A) would be small and the error associated with the technique of measurement would swamp the results. Measuring along the neutral axis B should give strains consistent with the $\left(\frac{P}{A_c}\right)$ effect but this depends on the stresses having reached this beam depth from the tendons. The distance between the end of L_p and the end of 'a' (end zone length) allows for the dispersion of stresses.

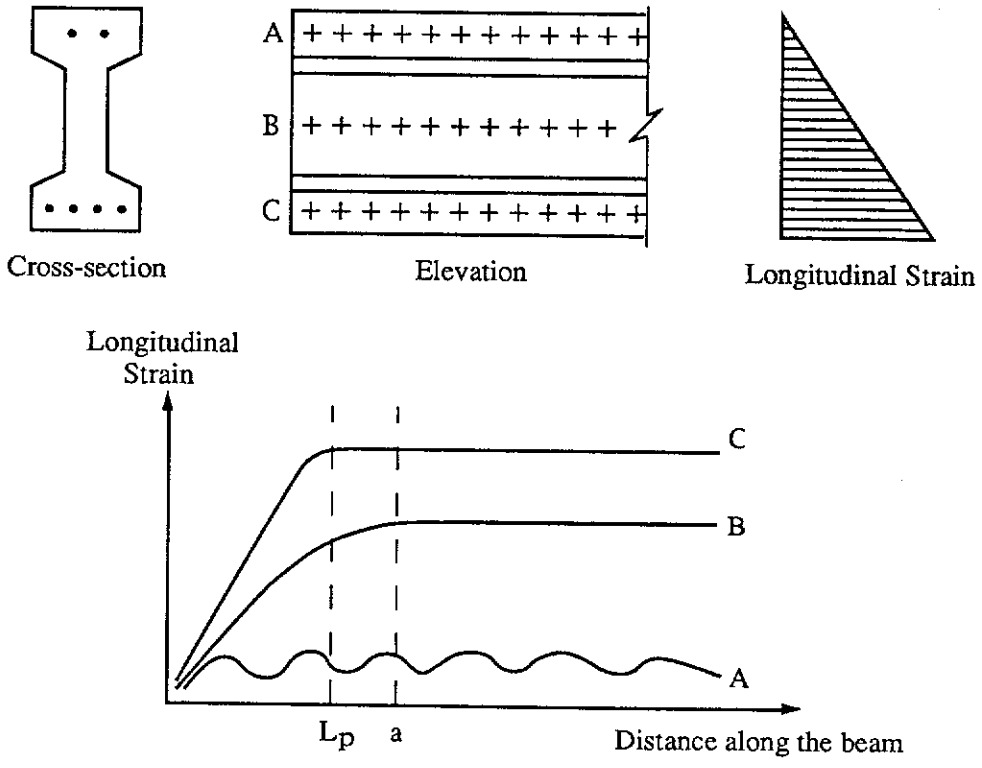

Figure 2.9 Longitudinal Strain versus Distance Plot for Various Levels on an I-beam (adapted from Figure 2.10 of Chandler (1984))

Curve C, which gives a shorter length to first flattening compared to curve B, had been viewed by Chandler as being the transmission length of the tendons in the bottom flange only and cannot be generalised for all other tendons within the same beam. With an eccentric prestress force, curve C is the resultant of a concentric $\left(\frac{P}{A_c}\right)$ effect and a bending $\left(\frac{Pey}{I}\right)$ effect.

(d) grouping of tendons - when more than one tendon is used, the stress flow superimposes for every tendon and the compressive strains at the concrete surface are not representative of the transmission length for one particular tendon only. When there are different strain build up rates, the transmission lengths are masked by the combination of force transfers.

2.5 Formulae For Determining The Transmission Length And Pull-in

The many existing theories on transfer of prestress have resulted in numerous mathematical equations for the determination of the transmission length and pull-in. This section gives a brief summary of equations used by other researchers to determine L_p and Δ_o. It is noted that most of the formulae discussed are related to pretensioning work using wire tendons. There are many more relationships available in literature which deal with strands or other types of tendons but they are not included here. A comprehensive discussion on these formulae was presented in Chandler (1984).

2.5.1 Guyon (1953)

The equation developed was purely theoretical. Guyon estimated the 'anchorage length' (equivalent to the transmission length in the context of this thesis) using two different assumptions. These two different assumptions have had far reaching consequences on the concept of bond stress in succeeding work by other contemporary researchers in the early history of pretensioned prestressed concrete. The two assumptions are summarised briefly as follows:

First assumption: the bond was considered to be perfectly elastic and the bond stress in the tendon (τ) varied along the length x, according to an exponential law:

$$\tau = \tau_{max}\, e^{-x/\lambda} \qquad \text{Equation 2.1}$$

where, τ_{max} = the maximum bond stress at the end of the beam

With this assumption, the 'characteristic length', λ, worked out to be:

$$\lambda = \frac{E_p}{f_{si}} \Delta_o \qquad \text{Equation 2.2}$$

where, E_p = the elastic modulus of prestressing tendon

f_{si} = the initial steel stress

Marshall and Krishnamurthy (1969) and Guyon explained how the characteristic length due to elastic bond was λ. At a distance of 3λ from the end of the wire, Guyon's model estimated 95% of the prestress would be transferred. For practical purposes, the transmission length (L_p) was taken as 3λ.

$$L_p = 3\lambda = \frac{3E_p \Delta_o}{f_{si}} \qquad \text{Equation 2.3}$$

where, Δ_o = the pull-in of the tendon

Second assumption: the above bond stress equation was difficult to deal with and Guyon simplified it by assuming the bond to be entirely plastic (ie. uniform bond stress) and the tension in the wire tendon varied linearly. Marshall and Krishnamurthy (1969) stated the equation which gave approximately the same bonding force per unit length (t) and the same developed total force (P) compared to the exponential law distribution, and it is as follows:

$$t = \frac{P\left(1 - \frac{x}{2\lambda}\right)}{\lambda} \qquad \text{Equation 2.4}$$

Using this assumption, the anchorage length found was:

$$L_p = 2\lambda = \frac{2E_p}{f_{si}} \Delta_o \qquad \text{Equation 2.5}$$

The equation using the first assumption related transmission length to the pull-in by a factor of $\frac{3E_p}{f_{si}}$. Chandler (1984) referred to this as the K_o factor and it was found to vary between $\frac{3E_p}{2f_{si}}$ and $\frac{4E_p}{f_{si}}$. It will be shown in Section 2.6 that K_o is dependent on the differential strain curve but the derivation by the author was a departure altogether from Guyon's concepts.

To allow Guyon's theoretical equation to be compared to results from the current tests (Chapter 4), the author substituted appropriate test values into the variables in Equation 2.3. With initial steel stress of about 1200 MPa and E_p of 200 GPa, the predicted transmission length is:

$$L_p = 500\,\Delta_o \qquad \text{Equation 2.6}$$

2.5.2 Janney (1954)

Janney considered the expansion of a wire tendon as it was released. The concrete section was considered to be large in comparison to the wire and thick-walled cylinder theory was adopted. The equation which resulted from his work was:

$$\log_e \frac{f_{se} - f_s}{f_{se}} = - \frac{2\,\mu\,\nu_s\,x}{r_w \left[1 + (1+\nu_c)\,\frac{E_p}{E_c}\right]} \qquad \text{Equation 2.7}$$

where,

ν_c , ν_s = Poisson's ratios for concrete and steel

E_c , E_p = moduli of elasticity for concrete and steel tendon

μ = coefficient of friction between concrete and steel

r_w = radius of the prestressing wire

x = distance from the beam end

f_{se} = effective pretension stress in the wire

f_s = tensile stress in the wire at point x

However, no formula was actually derived for determining the transmission length. Instead, Equation 2.7 was only used for estimating stress in the wire along the length of a beam.

Janney also provided an equation for determining the longitudinal compressive strain in concrete due to full prestress transfer (ε_{co}), as follows:

$$\varepsilon_{co} = \frac{f_{si}\,A_p}{A_p\,E_p + A_c\,E_c} \qquad \text{Equation 2.8}$$

where,

A_p = cross-sectional area of the prestressing tendon

A_c = cross-sectional area of the concrete beam

2.5.3 Evans and Robinson (1955)

Evans and Robinson found that the slip along a wire tendon decayed exponentially from a maximum pull-in value at the end of a beam. From their derivations, they assumed that the slip at the end of the transmission length was $\frac{1}{40}$ of Δ_o. This arbitrary ratio seems to be based on comparison between measured and calculated transmission lengths for two columns only (Columns G1 and K with 2 mm and 5 mm dia. wires respectively, given in Table 5 of reference). There was no justification as to how such a small sample size could be used to develop a generalised equation such as (in S.I. units):

$$L_p = \frac{0.14\Delta_o}{\varepsilon_{si}-\varepsilon_{se}} \qquad \text{Equation 2.9}$$

where, ε_{si} = strain in steel before release of prestress

ε_{se} = strain in steel beyond the transmission length after transfer

The effective strain in the tendon, ε_{se}, can be estimated by subtracting the concrete compressive strain, ε_{co}, from the initial steel strain of ε_{si}:

$$\varepsilon_{se} = \varepsilon_{si} - \varepsilon_{co} \qquad \text{Equation 2.10}$$

The author combined Equations 2.8 and 2.10 with Equation 2.9, giving:

$$L_p = \frac{0.14\Delta_o}{\varepsilon_{co}} = \frac{0.14(A_p E_p + A_c E_c)}{f_{si} A_p} \Delta_o \qquad \text{Equation 2.11}$$

Substituting values of A_c with 5000 mm^2, A_p with 80 mm^2 and E_c ranging from 22.6 to 40.8 GPa (corresponding to concrete strengths of 20 to 65 MPa (AS 3600)), the prediction for the transmission length is:

$$L_p = 188\,\Delta_o \text{ to } 321\,\Delta_o \quad \text{(for 20 to 65 MPa respectively)} \qquad \text{Equation 2.12}$$

The smaller K_o coefficient for the lower concrete strength does not mean that transmission length is shorter for lower concrete strength since Δ_o for concrete of lower strength is expected to be much greater than that for higher concrete strength.

2.5.4 Arthur and Ganguli (1965)

The theoretical equation by Arthur and Ganguli was a modified version of Janney's expression and it is as follows:

$$L = d_b \left[\frac{1 + (1+\nu_c) \frac{E_p}{E_c}}{2 \mu \nu_s} \right] \qquad \text{Equation 2.13}$$

where, d_b = diameter of the prestressing wire

They indicated that Marshall (1966) suggested 'L' as the length of the anchorage zone after Guyon but in actual fact, the right hand side of the above equation was taken from Janney's work. It should be noted that Janney's original equation did not use the tendon diameter (d_b) but instead the radius of the wire (r_w) as a variable. It can only be presumed that Arthur and Ganguli had assumed Guyon's anchorage length to be 2λ (where Marshall argued that $\lambda = r_w \left[\frac{1 + (1+\nu_c) \frac{E_p}{E_c}}{2 \mu \nu_s} \right]$). This allowed a factor of 2 to be multiplied to r_w to give d_b in Equation 2.13.

A debatable issue is the correct values to be used for ν_c, ν_s and μ. The Poisson's ratios are less variable but the coefficient of friction can have different magnitude depending on the surface condition of the wire. Janney (1954) and Hognestad and Janney (1954) stated that μ could be from 0.2 to 0.6. Marshall (1966) explained that μ = 0.6 represented "*a very rough wire*". Ganguli (1966) used a nominal value of μ = 0.3 in Janney's equation. Srinivasa Rao et al. (1977) also selected a value of 0.3 for the friction coefficient. The author used this nominal value in conjunction with Equation 2.13.

By substituting E_c with 22.6 to 40.8 MPa, E_p with 200 GPa, ν_c with 0.2, ν_s with 0.3 and μ with 0.3, the range of transmission length predicted by Equation 2.13 is as follows:

$L_p = 38\ d_b$ to $65\ d_b$ (for 65 to 20 MPa respectively)
(Note: $L_p = 52\ d_b$ (for 32 MPa)) Equation 2.14

Theoretically, for the same wire size, the transmission length is expected to be longer for lower concrete strength than for higher concrete strength. This issue will be treated more thoroughly when the practical results are presented in Section 4.10.

2.5.5 Ganguli (1966)

Ganguli cited Hoyer's (1939) theoretical equation for calculating the transmission length based on radial expansion of a wire tendon:

$$L_p = \frac{d_b}{2\mu}(1 + \nu_c)\left(\frac{m}{\nu_s} - \frac{f_{s\,i}}{E_c}\right)\frac{f_{s\,e}}{2f_{si} - f_{s\,e}} \qquad \text{Equation 2.15}$$

where m is the modular ratio of steel over concrete. The effective stress (f_{se}) was:

$$f_{se} = (\varepsilon_{si} - \varepsilon_{co})\,E_p = f_{si} - \frac{f_{si}\,A_p}{A_p\,E_p + A_c\,E_c}\,E_p \qquad \text{Equation 2.16}$$

Using values related to the current tests for the various parameters in Equation 2.15, L_p can be found as:

$L_p = 28\ d_b$ to $46\ d_b$ (for 65 to 20 MPa respectively)

(Note: $L_p = 38\ d_b$ (for 32 MPa)) Equation 2.17

2.5.6 Marshall and Krishnamurthy (1969)

Marshall and Krishnamurthy used Equation 2.4 (given above) from Guyon's second assumption and Equation 2.7 from Janney's formula for steel distribution along a wire, to come up with a solution for the characteristic length λ as follows (same equation was also given in Marshall (1966)):

$$\lambda = r_w\left[\frac{1 + (1+\nu_c)\frac{E_p}{E_c}}{2\,\mu\,\nu_s}\right] \qquad \text{Equation 2.18}$$

And,

$$L_p = 3r_w\left[\frac{1 + (1+\nu_c)\frac{E_p}{E_c}}{2\,\mu\,\nu_s}\right] \qquad \text{Equation 2.19}$$

The values for the transmission length (Equation 2.20) were 1.5 times the values estimated by Arthur and Ganguli (ie. ratio of 3λ to 2λ according to Guyon's first and second assumptions). The anchorage length of 3λ seems to be more widely accepted and was used in Section 2.5.1. It is reasonable to expect Equation 2.20 to be a better predictor of the transmission length than Equation 2.14.

$L_p = 57\ d_b$ to $98\ d_b$ (for 65 to 20 MPa respectively)

(Note: $L_p = 78\ d_b$ (for 32 MPa)) Equation 2.20

Marshall and Krishnamurthy did develop an equation of their own and this was in the form of:

$$L_p = \sqrt{\frac{\Delta_o}{K}} \qquad \text{Equation 2.21}$$

where K was a constant dependent on the type of tendon (strand or wire) and the tendon size used. The pull-in (Δ_o) was in inches. For 5 mm and 7 mm dia. wires, K was reported to be 90 x 10^{-6} (Krishnamurthy (1969, 1970)) (but it was inconsistently stated as 35 x 10^{-6} for 5 mm dia. wire in Krishnamurthy (1973)). Converting to S.I. units (Δ_o in mm), with K = 90 x 10^{-6} for both 5 mm and 7 mm dia. wires (which were used in this project), the estimated transmission length is:

$$L_p = 25.4 \sqrt{\frac{\Delta_o}{25.4\ K}} \quad \text{(mm)} \qquad \text{Equation 2.22}$$

giving:

$$L_p = 531 \sqrt{\Delta_o} \qquad \text{Equation 2.23}$$

Alternatively, they also had a relationship between transmission length and concrete strength given as follows (original equation):

$$L_p = \sqrt{\frac{\sqrt{u_t} \times 10^{-3}}{C\ K}} \qquad \text{Equation 2.24}$$

where u_t was the concrete cube strength at transfer (in lb/in^2) and C was another constant (C = 2 for 5 mm dia. wire and C = 1.5 for 7 mm dia. wire). In S.I. units (mm), the equation gives:

$$L_p\ (5\ \text{mm}\varnothing) = \sqrt{\frac{\sqrt{\frac{f_{cp}}{1.04 \times 0.8 \times 6.897 \times 10^{-3}}} \times 10^{-3}}{C\ K}} \times 25.4$$

$$L_p\ (5\ \text{mm}\varnothing) = 218 \sqrt[4]{f_{cp}} \qquad \text{Equation 2.25}$$

$$L_p\ (7\ \text{mm}\varnothing) = 251 \sqrt[4]{f_{cp}} \qquad \text{Equation 2.26}$$

where f_{cp} = the concrete compressive cylinder strength at transfer (MPa), the factor of $\frac{1}{(1.04 \times 0.8)}$ converts concrete compressive strength for 100 mm dia. x 200 mm cylinder to standard cube strength (Section 2.8) and $\frac{1}{(6.897 \times 10^{-3})}$ is the conversion factor from MPa to lb/in^2.

Marshall and Krishnamurthy had intended to indicate that the effect of concrete strength was less apparent for higher strength than for lower strength. The fourth root equation definitely has this trend but they failed to justify the fact that the estimated transmission length ***increased***

with higher concrete strength (expressed graphically in Figure 2.13 of Section 2.5.12). Most researchers expounded that higher concrete strength should give smaller transmission length. Chandler (1984) refuted the equation and rightly did so. The relationship between L_p and f_{cp} was dependent on a correlation made between Δ_o and $\sqrt{u_t}$ (given in Table 3 of Marshall and Krishnamurthy (1969)) but the correlation coefficient was only 0.39 according to Chandler (1984). Therefore, the validity of Equations 2.24 to 2.26 is doubtful.

2.5.7 Anderson and Anderson (1976)

Anderson and Anderson developed a formula based on the assumption of linear differential change in longitudinal strain between concrete and strand tendon. The equation provided an estimate for the pull-in without having to rely on the transmission length. The formula (from Chandler (1984)) in S.I. units is:

$$\Delta_o = 0.024 \left(\frac{f_{se}\, f_{si}}{E_p}\right) d_b \quad \text{(mm)} \qquad \text{Equation 2.27}$$

Substituting for f_{se}, f_{si} and E_p:

$$\Delta_o = 0.15\, d_b \text{ to } 0.16\, d_b \text{ (for 65 to 20 MPa respectively)} \qquad \text{Equation 2.28}$$

Although this equation was developed for strands, a similar equation could be applicable for wires. It is noted that the original equation by Anderson and Anderson was $\Delta_o = \left(\frac{f_{se}}{3} d_b\right)\left(\frac{f_{si}}{2\, E_p}\right)$, where the first part of the equation was a prediction of L_p according to the American Concrete Institute (ACI) code while the second part estimated the average strain over L_p.

2.5.8 Bruggeling (1986)

The formulae established by Bruggeling were based on European pretensioning work and the bond stress concept was the crux of the derivations. The formulation treated both wires and strands in a similar manner by considering the nominal diameters of these tendons. The tensile force in a tendon was equated to the total bond force within the transmission length (effective steel stress x cross-sectional steel area = 'average' bond stress x perimeter x transmission length), giving:

$$f_{se}\, A_p = s_\tau\, \tau_{cp}\, \Phi\, L_p \qquad \text{Equation 2.29}$$

where, τ_{cp} = maximum bond stress on the tendon

s_τ = ratio of the area under the bond stress curve compared to an enclosing rectangular area of ($\tau_{cp}\, L_p$) (shown in Figure 2.10)

Φ = circumference of the tendon

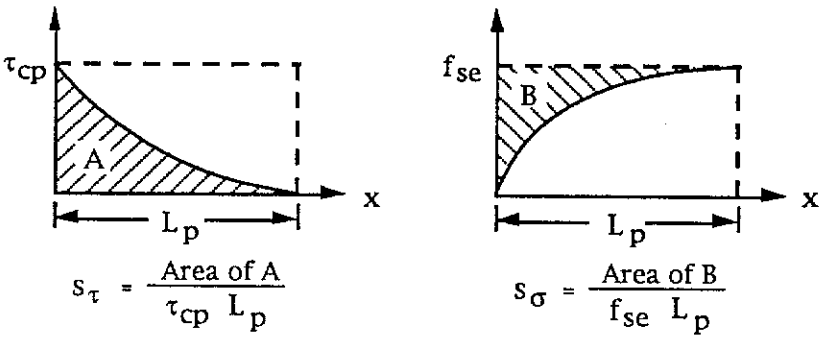

$$s_\tau = \frac{\text{Area of A}}{\tau_{cp}\, L_p} \qquad s_\sigma = \frac{\text{Area of B}}{f_{se}\, L_p}$$

Figure 2.10 Ratios of Areas (s_τ and s_σ) (from Figure 1 of Bruggeling (1986))

From the above equation, Bruggeling was able to develop the following:

$$L_p = \frac{f_{se}\, d_b}{4\, s_\tau\, \tau_{cp}} \qquad \text{Equation 2.30}$$

The factor of s_τ was stated as being equal to $\frac{1+N}{1-N}$ where N was from the work of Noakowski and tests by RILEM/CEB/FIP on reinforcement bars in normally reinforced concrete with the bond stress-slip relationship of:

$$\tau_x = C_0\, \Delta_x^N \qquad \text{Equation 2.31}$$

where, C_0 = constant in the equation

τ_x = bond stress at a distance x from the beam end

Δ_x = slip at a distance x from the beam end

The author believes the given ratio of $\frac{1+N}{1-N}$ is incorrect as s_τ would be greater than 1.0 for positive values of N, which is not possible. The correct ratio should have been $\frac{1-N}{1+N}$ after analysing other related equations.

Bruggeling contended that "*in case of indented wires there is no reason to doubt that the results of this test method* (which is used for reinforcing bars) *can be used, because the surface conditions of the prestressing steel*

wires are comparable with those of the reinforcing steel bars". The author believes that this is not true since a pretensioning wire exerts radial pressure on the concrete and expands radially when destressed but a steel bar does not. Furthermore, the transfer of bond for a reinforcing bar depends on its steel ribs but a wire does not have these.

An equation relating pull-in to transmission length was given as:

$$\Delta_o = \frac{f_{se}}{E_p} s_\sigma L_p \qquad \text{Equation 2.32}$$

where, s_σ = ratio of the area above the steel stress curve compared to an enclosing rectangular area of (f_{se} L_p) (shown in Figure 2.10)

$$s_\sigma = \frac{1-N}{2}$$

Substituting L_p (from Equation 2.30), s_σ and s_τ into the Δ_o-L_p equation, the final formula for the pull-in was:

$$\Delta_o = \left[\frac{f_{se}^{\,2}}{C_o E_p} \frac{1+N}{2} \frac{d_b}{4} \right]^{\frac{1}{1+N}} \qquad \text{Equation 2.33}$$

The equation for the transmission length was:

$$L_p = \frac{2 E_p}{(1-N) f_{se}} \Delta_o \qquad \text{Equation 2.34}$$

The values for N and C_o were from pull-out tests of indented wires (indentations according to Euronorm EU 138), and they were:

$C_o = 0.17 f_{cu}$ and $N = 0.32$ (assumed for wires)

where, f_{cu} = mean value of 150 mm concrete cube strength

The predictions for the transmission length and pull-in according to this technique were:

$$L_p = 490 \Delta_o \qquad \text{Equation 2.35}$$

$$\Delta_o = 0.14 d_b^{0.76} \text{ to } 0.31 d_b^{0.76} \quad \text{(for 65 to 20 MPa respectively)} \qquad \text{Equation 2.36}$$

2.5.9 ACI 318/318R (1989)

There is no guidance given in this code on the usage of pretensioning wires. Most of the research work undertaken was biased towards the use of strands. The equation for estimating the transmission length of strand was (S.I. units):

$$L_p = 0.05\, f_{se}\, d_b \qquad \text{Equation 2.37}$$

Equation 2.37 is actually $L_p = \frac{f_{se}}{f_c'}\, d_b$ (imperial units) with an assumed concrete strength of 20 MPa (Chandler (1984)). This equation was not used for comparisons with results from the current tests since its derivation was based on strands.

In Section 4.13, formulae based on current and previous test data were derived for wire tendons where L_p was related to f_{si}, f_{cp}, A_p, A_c and d_b.

2.5.10 BS 8110:Part 1:1985

In Section 4 of BS 8110, a caution on the variability of transmission length had been aptly included. Site experience had shown that L_p varied between 50 and 160 d_b. However, this code also gives an equation for evaluating the transmission length and it is as follows:

$$L_p = \frac{K_t\, d_b}{\sqrt{f_{ci}}} \qquad \text{Equation 2.38}$$

where, K_t = 600 for plain or indented wire (including crimped wire with small wave height)

f_{ci} = the concrete cube strength at transfer (MPa)

$$f_{ci} = \frac{f_{cp}}{(0.8 \times 1.04)}$$

which can be converted to:

$$L_p = \frac{547\, d_b}{\sqrt{f_{cp}}} \qquad \text{Equation 2.39}$$

thus, L_p = 68 d_b to 122 d_b (for 65 to 20 MPa respectively)

(Note: L_p = 97 d_b (for 32 MPa)) Equation 2.40

and

$$L_p\ (5\ \text{mm}\varnothing) = \frac{2740}{\sqrt{f_{cp}}} \qquad \text{Equation 2.41}$$

$$L_p\ (7\ \text{mm}\varnothing) = \frac{3830}{\sqrt{f_{cp}}} \qquad \text{Equation 2.42}$$

2.5.11 AS 3600 (1988)

The Australian Standard AS 3600 (1988) treats the estimation of L_p by considering two categories of concrete, one with transfer strength $f_{cp} \geq 32$ MPa and the other with $f_{cp} < 32$ MPa. The 32 MPa concrete is one of the grades of concrete used in the Australian industry (grades in MPa are 20, 25, 32, 40 and 50 or higher). There is no clear demarcation which separates an actual 31 MPa mix from a 33 MPa mix. Since AS 3600 does not permit the use of plain wires, the transmission length for an indented wire can be estimated as follows ("*in the absence of substantiated data*", Clause 13.3.2):

$L_p = 100\ d_b$ (for $f_{cp} \geq 32$ MPa concrete) Equation 2.43

$L_p = 175\ d_b$ (for $f_{cp} < 32$ MPa concrete) Equation 2.44

The above values would increase with sudden (or shock) release but no specific values were given.

For a tendon at the top of a concrete member, AS 3600 cautions that the transmission length may be doubled. AS 1481 (1978) suggests that this may occur when the tendon is located more than 200 mm above the base of the concrete beam. Stocker and Sozen (1970) found the transmission lengths for 11 mm dia. strands with 250 mm of concrete below them were 30% longer than for strands with 50 mm of concrete below. Base (1958) confirmed this trend in 5 mm dia. wires near the top of pretensioned prestressed members tested. Warner and Faulkes (1988) attributed this phenomenon to the 'water gain' effect where consolidation of concrete tended to "*create a film of water at the underside of the bar ...*".

2.5.12 Summary of Existing Theoretical Formulae

Existing formulae for estimating the transmission length and pull-in are summarised in Table 2.1. Note that these equations have been simplified using values for parameters that are relevant to the current laboratory tests. The equations given in Table 2.1 are plotted in Figures 2.11 to 2.14 for L_p versus d_b, L_p versus Δ_o, L_p versus f_{cp} and Δ_o versus d_b respectively.

Table 2.1 Summary of Formulae for Determining L_p and Δ_o

Source	Equation
Guyon (1953)	$L_p = 500\ \Delta_o$
Evans and Robinson (1955)	$L_p = 188\ \Delta_o$ to $321\ \Delta_o$ (for 20 to 65 MPa)
Arthur and Ganguli (1965) (modified Janney's equation)	$L_p = 38\ d_b$ to $65\ d_b$ (for 65 to 20 MPa)
Ganguli (1966) (Hoyer's equation)	$L_p = 28\ d_b$ to $46\ d_b$ (for 65 to 20 MPa)
Marshall and Krishnamurthy (1969) (Guyon and Janney's equations)	$L_p = 57\ d_b$ to $98\ d_b$ (for 65 to 20 MPa)
Marshall and Krishnamurthy (1969) and Krishnamurthy (1970 to 1973)	L_p (5 & 7 mmØ) $= 531\sqrt{\Delta_o}$ (Δ_o in mm) L_p (5 mmØ) $= 218\sqrt[4]{f_{cp}}$ (f_{cp} in MPa) and L_p (7 mmØ) $= 251\sqrt[4]{f_{cp}}$
Anderson and Anderson (1976)	$\Delta_o = 0.15\ d_b$ to $0.16\ d_b$ (for 65 to 20 MPa)
Bruggeling (1986)	$L_p = 490\ \Delta_o$ $\Delta_o = 0.14\ d_b^{0.76}$ to $0.31\ d_b^{0.76}$ (for 65 to 20 MPa)
BS 8110:Part 1:1985	$L_p = 68\ d_b$ to $122\ d_b$ (for 65 to 20 MPa) L_p (5 mmØ) $= \frac{2740}{\sqrt{f_{cp}}}$ L_p (7 mmØ) $= \frac{3830}{\sqrt{f_{cp}}}$
AS 3600 (1988)	$L_p = 100\ d_b$ (for $f_{cp} \geq 32$ MPa) $L_p = 175\ d_b$ (for $f_{cp} < 32$ MPa)

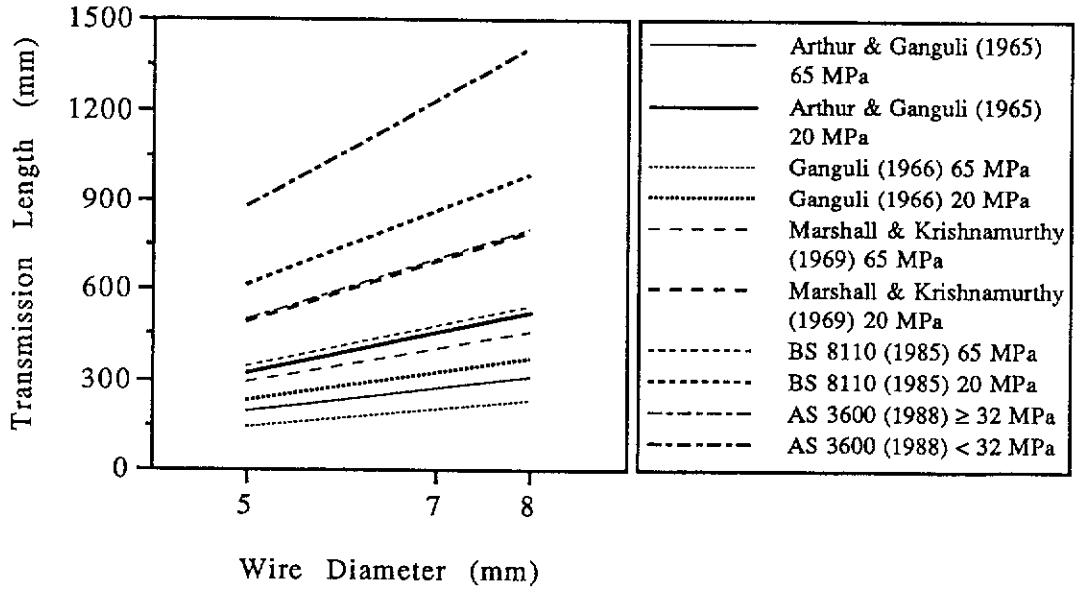

Figure 2.11 Proposed Relationships for Transmission Length as a Function of Wire Diameter

There is agreement from all the sources in Figure 2.11 that greater concrete strength would give shorter L_p. The range of the smallest L_p values is given by Ganguli (1966) whereas the range of the largest values is proposed by AS 3600 (1988). AS 3600 seems conservative in this respect.

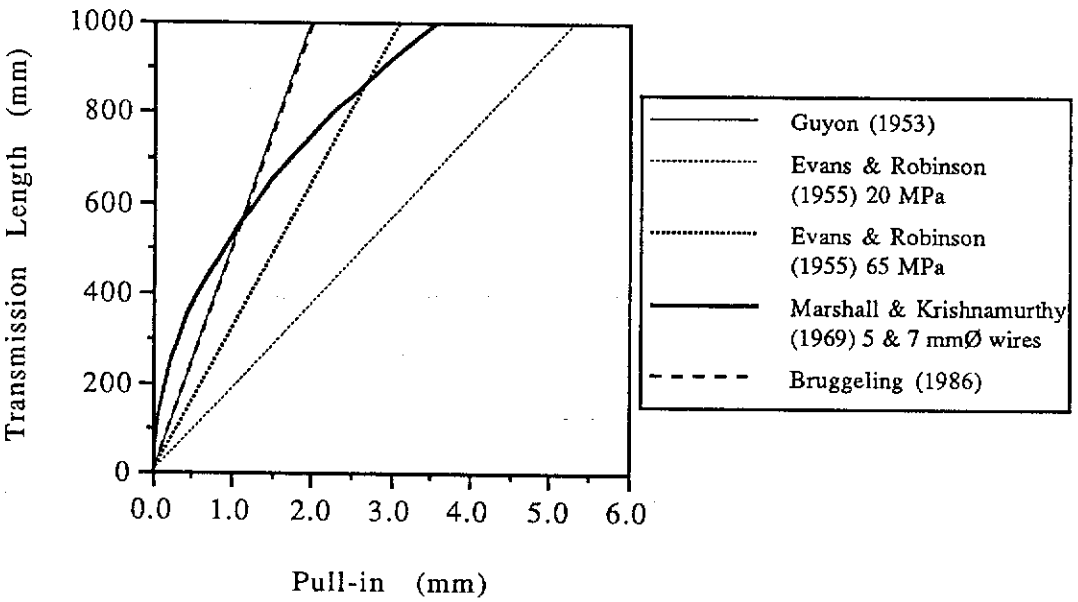

Figure 2.12 Proposed Relationships Between Transmission Length and Pull-in

In Figure 2.12, all the formulae are linear except the one proposed by Marshall and Krishnamurthy. The relationship by Evans and Robinson indicates that the L_p-Δ_o relationship depends on the transfer strength (K_o which controls the slope of the linear equation can vary significantly).

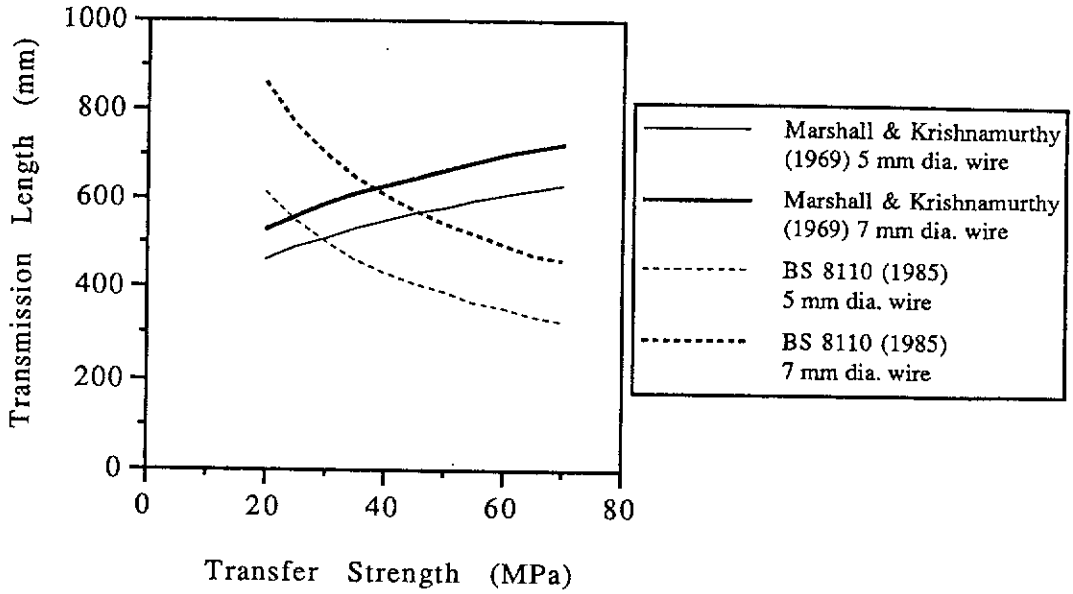

Figure 2.13 Proposed Relationships Between Transmission Length and Concrete Strength at Transfer

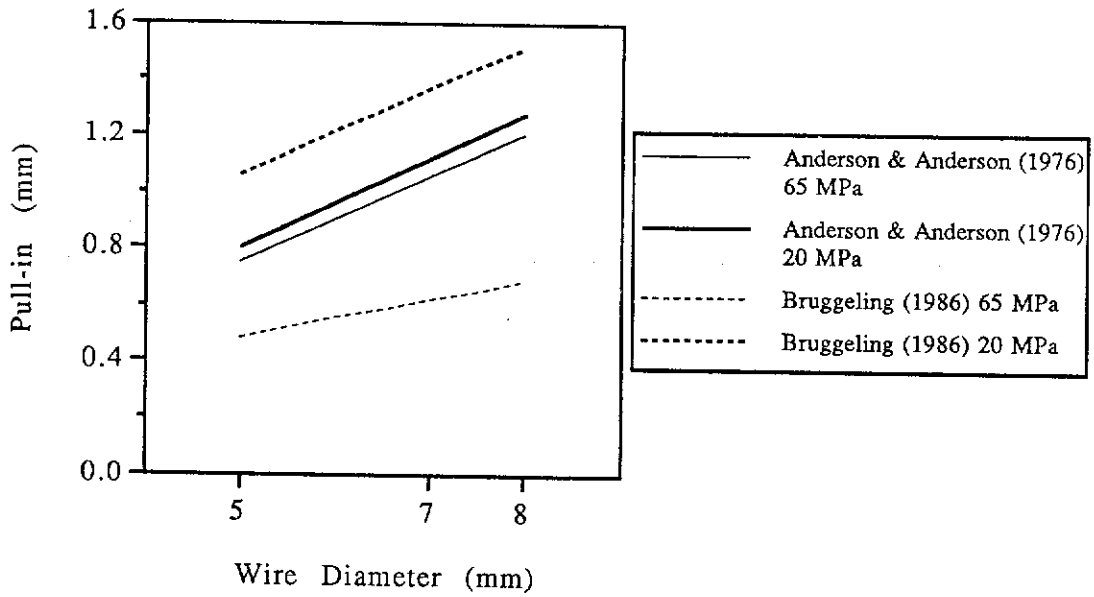

Figure 2.14 Proposed Relationships for Pull-in as a Function of Wire Diameter

In Figure 2.13, the inconsistency in Marshall and Krishnamurthy's (1969) equation is apparent. It gives unexpected increase in the transmission length with an increase in the transfer strength. On the other hand, BS 8110 (1985) gives a more realistic prediction of the L_p-f_{cp} relationship.

Anderson and Anderson (1976) and Bruggeling (1986) predicted that pull-in would increase with larger wire diameter (Figure 2.14). There is a small range in Anderson and Anderson's curves but Bruggeling's equations gave significant differences in pull-in for 20 and 65 MPa concrete. The linear equations by Anderson and Anderson seem to be more realistic than those proposed by Bruggeling because of the smaller deviations in the pull-in for any particular wire diameter.

2.6 Simplified Method For Determining The Transmission Length

Different methods have been discussed pertaining to the determination of transmission lengths in pretensioned prestressed concrete beams. In research work by Chandler (1984), it was discovered that there was a strong correlation between the transmission length and pull-in of multi-wire strands. Chandler (1984, 1990) subsequently proposed the use of pull-in to indirectly predict the actual transmission length.

Measuring the pull-in was used as an approximate method for checking the transmission length. *"Such measurements are much quicker and simpler to obtain, making the recording of these a viable approach to quality assurance of the transmission lengths ..."* (Chandler (1990)).

Pull-in is the cumulative effect of small movement or slip of the tendon relative to the concrete when the tendon is released. It is the integral of the differential longitudinal strain between concrete and steel:

$$\Delta_o = \int_0^{L_p} \delta\varepsilon \, dx \qquad \text{Equation 2.45}$$

This equation reduces to a relationship between L_p and Δ_o:

$$L_p = K_o \cdot \Delta_o \qquad \text{Equation 2.46}$$

The value of K_o is quite subjective but is normally considered to be a constant which makes the method of predicting the transmission length simple and straightforward. The derivation from Equation 2.45 to 2.46 is based on certain assumptions leading to the determination of K_o. The following is a simplified interpretation of the concept and assumptions used.

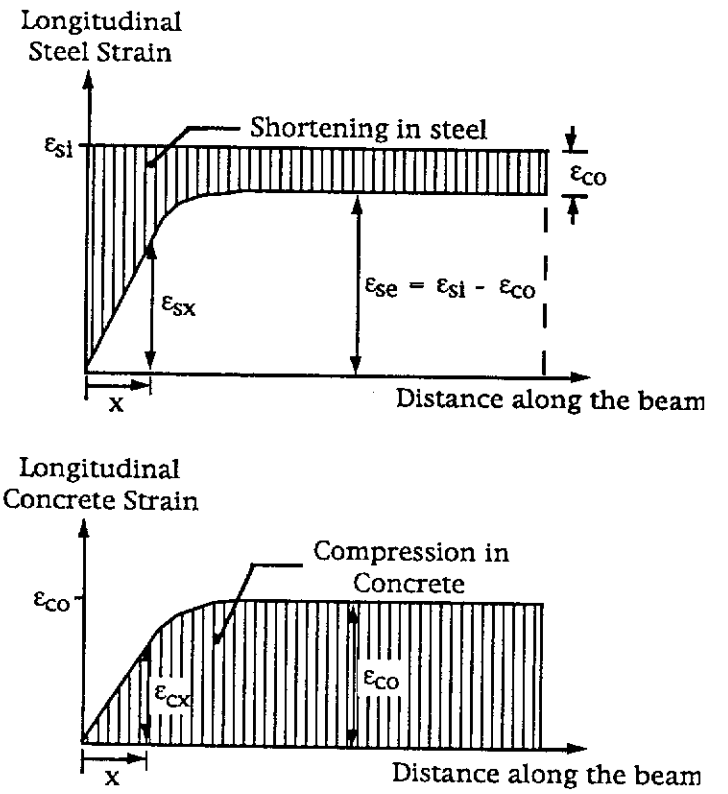

Figure 2.15 Longitudinal Strains in Steel Tendon and Concrete at the End of a Pretensioned Prestressed Beam During Transfer

Each steel strain value at a distance x (from the beam end) in the steel strain-distance curve is assumed to correspond to a concrete strain value at the same distance x in the concrete strain-distance curve, ie. plane sections' concept is used although this is not strictly true.

Steel strain change at distance x from the end face after transfer = $\varepsilon_{si} - \varepsilon_{sx}$
Concrete strain at distance x from the end face after transfer = ε_{cx}
Relative change in strain between steel and concrete = $(\varepsilon_{si} - \varepsilon_{sx}) - \varepsilon_{cx}$

Both the steel and concrete strain curves are assumed to have the same shape where one is the multiple of the other.

$$\varepsilon_{sx} = \frac{\varepsilon_{si} - \varepsilon_{co}}{\varepsilon_{co}} \varepsilon_{cx} \qquad \text{Equation 2.47}$$

The relative change in strain between steel and concrete at distance x is:

$$\delta\varepsilon = \varepsilon_{si} - \frac{\varepsilon_{si} - \varepsilon_{co}}{\varepsilon_{co}} \varepsilon_{cx} - \varepsilon_{cx} = \varepsilon_{si} - \frac{\varepsilon_{si}\,\varepsilon_{cx}}{\varepsilon_{co}}$$

$$\delta\varepsilon = \frac{\varepsilon_{si}}{\varepsilon_{co}} (\varepsilon_{co} - \varepsilon_{cx}) \qquad \text{Equation 2.48}$$

The change in slip over the distance from x to x+dx = $d\Delta = \delta\varepsilon . dx$

$$d\Delta = \frac{\varepsilon_{si}}{\varepsilon_{co}} (\varepsilon_{co} - \varepsilon_{cx})\, dx \qquad \text{Equation 2.49}$$

The pull-in at the end face (Δ_o) over $L_p = \int_{\Delta_o}^{0} d\Delta$ and this gives:

$$\Delta_o = \int_0^{L_p} \frac{\varepsilon_{si}}{\varepsilon_{co}} (\varepsilon_{co} - \varepsilon_{cx})\, dx = \int_0^{L_p} \varepsilon_{si}\, dx - \int_0^{L_p} \frac{\varepsilon_{si}\,\varepsilon_{cx}}{\varepsilon_{co}}\, dx$$

$$\Delta_o = \varepsilon_{si} L_p - \frac{\varepsilon_{si}}{\varepsilon_{co}} \int_0^{L_p} \varepsilon_{cx}\, dx$$

$$\Delta_o = \varepsilon_{si} L_p - \frac{\varepsilon_{si}}{\varepsilon_{co}} \{\text{Area under conc. strain curve for } 0 < x \leq L_p\}$$

Equation 2.50

This relationship indicates that L_p needs to be known before Δ_o can be estimated. The end zone (and L_p) has to be defined before the area under the concrete strain curve within this end zone can be worked out. An additional simplifying assumption made by the author was to consider both the steel strain and concrete strain versus distance curves as being linear within L_p.

Therefore, area under concrete strain curve = $\frac{1}{2} \varepsilon_{co} L_p$

and, $$\Delta_o = 0.5\, \varepsilon_{si} L_p = 0.5 \frac{f_{si}}{E_p} L_p \qquad \text{Equation 2.51}$$

From the above relationship, the transmission length can be estimated if the pull-in is known:

$$L_p = \frac{2E_p}{f_{si}} \cdot \Delta_o \qquad [K_o = \frac{2E_p}{f_{si}}] \qquad \text{Equation 2.52}$$

Different assumptions with respect to the shape of the curve in the concrete strain versus distance plot within the end zone were considered by Chandler (1984); apart from a linear curve, convex and concave parabolic curves were also examined. Hence, a range of K_o values resulted depending on the shape of the model curve. For the linear, concave down and concave up curves, the K_o values were 280, 200 and 533 respectively (Chandler (1990)) for strands with E_p = 195 GPa and f_{si} = 1380 MPa.

From tests performed by Chandler (1984), a value of K_o = 400 was recommended for both 12.7 and 15.2 mm diameter strands. Similar relationships were developed for different wires used in this project and they are presented in Section 4.9.

2.7 Factors Affecting The Transmission Length

Factors which influence the prestress transfer and hence the transmission length are given as follows:

(a) type of tendon - wires or strands can be with or without indentations. Codes of practice are mainly interested with the length, pitch and depth of these indentations (ASTM A886/A886M (1988), ASTM A864/864M (1987) and AS 1310 (1987)). In fact, AS 1310 is more flexible as Clause 8.3 provides that "*the shape and configuration of the indents are subject to agreement between the purchaser and manufacturer...*", with major control based on the depth and mass to length ratio criteria.

Ratz, Holmjanski and Kolner (1958) found that by indenting wire tendons, it was possible to change the bond between the steel and the concrete to a greater extent than by changing the wire diameter. Austrak (1993) found that the profile and type of indentation used can significantly influence the transmission length. Austrak considered the sharpness of the indentation as being crucial to the bond transfer mechanism.

(b) size of the tendon - previous research has shown that the transmission length is related to the size of the tendon, with an almost linear correlation. The ACI code recommends $L_p = \frac{f_{se}}{3} d_b$ for determining the transmission length for strand tendons. Using f_{se} of approximately 0.75 f_p, the ACI code gives roughly 60 d_b for the transmission length of a 12.5 mm diameter strand and this agrees with AS 3600 (1988).

Table 2.1 (in Section 2.5.12) has several equations which clearly indicate that the transmission length can be correlated to the wire diameter.

(c) tendon stress - researchers such as Hanson and Kaar (1969) found the transmission length to be proportional to the tendon stress and this is reflected in the ACI 318/318R (1989) code. However, no specific guidance is given in AS 3600 (1988) with respect to this.

(d) surface condition of the steel tendon - contaminants and excessive rust can have adverse effects on the transfer of prestress. Grease, oil, dirt or residue of cleaning solvent can cause greater slippage as frictional resistance is reduced.

With light rusting, prestressing steel tendons are claimed to have shorter transmission lengths. Clause 8.6 of ASTM A421 (1985) permits the acceptance of slightly rusted steel as long as there is no pitting "*visible to the naked eye*". Similarly Clause 8.3 of CP 110 Part 1 (1972) (or BS 8110:Part 1:1985) states that "*a film of rust is not necessarily harmful and may improve bond*". Clause 19.3.4.3 of AS 3600 (1988) holds the same view on this matter.

Sason (1992) presented a procedure for classifying the degree of rust that occurs on prestressing strand and proposed a visual inspection technique which can be employed to identify the degree of corrosion in terms of pitting; thus giving a better basis for accepting or rejecting tendons. The main concern of pitted or heavily corroded tendons lies with the fact that pits can act as "*stress-raisers which serve as initiation sites for fatigue failures*" (Sason (1992)). The codes of practice prohibit the use of such tendons for all prestressing works.

2.7.1 Concrete Properties

There are a few ways in which concrete properties can affect the transmission length and they are detailed as follows:

(a) compressive strength of the concrete - this is a subjective variable which has brought about conflicting views. Janney (1954) made the hypothesis that increased concrete strength has less significant impact on the bond transfer characteristic than it would have on the ability of the concrete to sustain radial pressure due to Hoyer's effect. Kaar, LaFraugh and Mass (1963) found concrete strengths of 11 to 35 MPa at transfer had little influence on the transmission length of clean 7-wire strands up to 12.5 mm in diameter.

Ratz, Holmjanski and Kolner (1958) used eighteen types of prestressing wires for their tests. Although no measurement of transmission length was made, the pull-in and steel stress were monitored and they found that bond transfer depended significantly upon the concrete strength used. Different mixes of concrete varied from 19.6 to 49.1 MPa.

Marshall and Krishnamurthy (1969) proposed the relationship where L_p was directly proportional to the fourth root of the concrete strength (Section 2.5.6). However, there is no reason why the transmission length should increase with greater concrete strength. Moreover, Krishnamurthy (1970) admitted that increased concrete strength would reduce L_p.

Zia and Mostafa (1977) came up with a more realistic equation where L_p was inversely proportional to the concrete strength.

A more recent development of an equation relating concrete strength to L_p was proposed by Cousins, Johnston and Zia (1990). The two part equation was developed for uncoated and epoxy coated strands (S.I units, in mm):

$$L_p = 41.6\left(\frac{U_t' \sqrt{f'_{ci}}}{B}\right) + 12.0\left(\frac{f_{se}\, A_p}{\pi\, d_b\, U_t' \sqrt{f'_{ci}}}\right) \qquad \text{Equation 2.53}$$

where, f'_{ci} = concrete compressive strength at transfer (MPa)

U_t = uniform plastic bond stress

$U'_t = \frac{U_t}{\sqrt{f'_{ci}}}$ (constants given by Cousins, Johnston and Zia are used although derived from imperial units. Equation 2.53 takes this into account.)

B = bond modulus (assumed as a constant slope) (kPa/mm)

An increase in the concrete strength would cause the first term to increase and the second term to decrease. However, the overall effect sees a decrease in the calculated L_p with increasing concrete strength (Tables 2a and 2b of Cousins, Johnston and Zia (1990)).

Two other factors which can be more significant are cracking in the concrete and poor consolidation (as discussed below).

(b) tensile strength of the concrete - cracking can occur in the bursting, spalling or splitting zones if the concrete tensile strength is exceeded. Cracking in the bursting zone is undesirable as the crack propagates along the tendon. The transmission length increases as the concrete hoop tension near the end of the beam is destroyed by cracks and the tendon slips further into the concrete. Chandler (1984) quantified the effect of cracking in the bursting zone on the transmission lengths of strands.

(c) consolidation or compaction of concrete - Guyon (1953) had established that transfer bond was dependent on the quality of the concrete and this was governed by factors such as workmanship, casting procedures and consolidation of concrete. Base (1958) recommended that adequate compaction at the ends of a beam was of greater importance than the concrete strength. Poor compaction may result in voids trapped within the concrete, more significantly under and around the tendons. The gap between the steel tendon and concrete caused by the accumulation of pockets of water and air affects bonding since there is no resistance to the radial expansion of the tendon when it is released. There is also a loss of 'hoop tension' of the concrete surrounding the tendon according to Chandler (1984) and this does not allow the tendon to be tightly bonded.

(d) maturity of the concrete - the transmission length is affected by maturity through the strength of the concrete at different ages. It is not known whether beams from two different concrete mixes at different maturities but having the same strength would perform the same. Differences in L_p for concrete units made from a single mix but prestressed at different maturities has also never been addressed.

Maturity can be understood as being a function of time and temperature, both of which affects the curing of the concrete. The combined effects may be numerically represented as the sum of the product between elapsed time and temperature (Chengju (1989)):

$$M_s = \sum_{0}^{t} (T-T_o)\,\Delta t \qquad \text{Equation 2.54}$$

where, M_s = maturity of the concrete (°C.hr)

T = average temperature of the concrete during the time interval of Δt (°C)

Δt = time interval of the hardening process (hr)

T_o = a suitably chosen reference temperature (°C)

Concrete strength was related to the maturity of the concrete by:

$$f_{cp} = a_1 + a_2 \log (M_s) \qquad \text{Equation 2.55}$$

where, a_1, a_2 = constants

Both maturity and concrete strength increase with the progression of time and the transmission length is expected to decrease.

(e) low pressure steam curing - the objective of utilising this method of curing concrete is to attain high early strength. The commencement of the steam curing process has to be preceded by a 'delay period' after placing the concrete. The strength gain during this period is referred to as the 'initial maturity' of the concrete. Steam applied too quickly after placing the concrete may cause appreciable internal stresses as a result of large thermal gradients. Microcracking may follow having a detrimental effect on the strength of the concrete. Australian experience indicates that a minimum initial maturity of 40 °C.hr (standard 2-hour delay at 20 °C) is required to control internal microcracking (Merretz, Stevens and Egan (1984)).

Apart from the initial maturity, the complete thermal action occurring until the end of the curing period is important in the development of strength in the concrete; the remaining part of the steam curing cycle includes periods of:

(i) constant rate of temperature rise.
(ii) maintained maximum curing temperature.
(iii) cooling down period.

The AS 1481-Appendix A (1978) specifies a maximum increase in temperature of 24°C per hour and a maximum curing temperature of 80°C for normal-weight concrete. In general, the maximum temperature does not exceed 70°C. In practice, the concrete pretensioned precast components are kept at the maximum curing temperature for 6 to 12 hours in a 24-hour production cycle. Some manufacturers have brought the steaming period down to 3 hours before releasing the prestress. At the end of the steaming process, the concrete has to be brought to ambient temperature.

Two uncertainties drawn from the steam curing technique are:

(i) whether releasing the prestress into a steam cured concrete beam at a young age gives the same L_p as releasing the prestress at a later age.
(ii) whether the steel can be released immediately after the completion of the steaming period. AS 1481 (1978) permits prestress release prior to cooling as long as there is no "... *visible evidence that any steam cured element or product may be damaged by thermal shock or differential cooling* ...".

2.7.2 Geometry of the End Zone Section

The geometry of the beam ends can affect the transfer of the prestress force significantly. The factors which are considered to influence prestress transfer are:

(a) the end cross-sectional shape of the beam.
(b) the location and spacing of steel tendons.
(c) the amount of concrete surrounding the tendons.
(d) the amount of reinforcing steel provided to control cracks.

2.7.3 Release of Prestressing Force

The prestressing force can be transferred into the concrete section by gradual, sudden or shock releases. Sudden and shock releases (referred to collectively by the author as ***rapid*** releases) generally cause a tendon to slip further into the concrete. This could be due to the sudden inertial force which acts as impact force in addition to the applied prestress load. Shock release is generally carried out by angle grinding the tendons. Sudden release is slightly more gradual than shock release and it is achieved by methods such as quick release of hydraulic jacks.

Kaar, LaFraugh and Mass (1963), Hanson (1969), Zia and Mostafa (1977), and Schupack and Mizuma (1979) have found increases in the transmission length for strands and bars when sudden release of the pretensioning load occurred. Chandler (1984) propounded that shock can reduce the rate of prestress transfer, hence creating a concave up concrete strain curve and a length of unstressed concrete in the end zone.

2.7.4 Time Dependent Factors

Evans and Robinson (1955) postulated that the transmission length increased at a decreasing rate with time due to time effects such as shrinkage and creep. The whole end zone would shift into the concrete, leaving an unloaded zone near the end face and giving a longer transmission length.

Base (1957, 1958) asserted that the transmission length changed slightly with time and there may be a short length of the beam near the end which became unstressed due to the effects of shrinkage. Base also indicated that an increase of up to 75 mm in the transmission length for 5 mm dia. plain wires may occur with time but there was "*no significant continuation of pull-in after transfer*".

AS 3600 (1988) indicated that there may be an unstressed length at a beam end of $0.1L_p$ but there was to be no change in the position of the inner end of the transmission length with time.

2.8 Comparisons Of Concrete Compressive Cylinder And Cube Strengths

Since the results from the tests in this project were compared to those obtained by other researchers, the concrete crushing strength for all investigations had to be compatible. For the current tests, concrete cylinder strength was used according to the Australian practice, but many of the tests done previously involved the use of concrete cube strength.

The previously used standard cylinder size was 150 mm dia. x 300 mm high, but the 100 mm dia. x 200 mm cylinder is more commonly used in recent times, particularly for research purposes. On the other hand, the standard cube has 150 mm sides. Other cube sizes which have been used were the 100 mm and 200 mm cubes.

For cylinders, there seems to be a small difference in the compressive strength between the small and large cylinder sizes. As long as the height to diameter ratio remains at 2, the end effects of the loading platens will be comparable. The compressive strength for the 100 mm dia. x 200 mm cylinder is about 104% of that for the 150 mm dia. x 300 mm standard cylinder according to Figure 27.5 of Murdock and Brook (1979) (Cement and Concrete Association (1993) also confirmed this).

In the current tests, both sizes of 100 mm dia. x 200 mm and 150 mm dia. x 300 mm cylinders were used. For the purpose of analysis within this thesis, the compressive strength for the 150 mm dia. x 300 mm cylinder was multiplied by 1.04 to convert to the equivalent 100 mm dia. x 200 mm cylinder strength.

Avram et al. (1981) explained how friction between the loading steel platen and the concrete cube could enhance the strength of the concrete due to secondary lateral confinement of the concrete. With all other conditions being equal, the compressive strength increased with decreasing cube dimensions. For the 100 mm cube, Murdock and Brook (1979) stated a 4% increase in strength compared to the standard 150 mm cube, but the 200 mm cube was approximately 8% weaker.

The most important difference comes in the cross comparison between the cylinders and the cubes. It is obvious that cube strength is greater than cylinder strength but there are different opinions as to the relationship

between the two types of control specimens. Avram et al. (1981) highlighted a scale factor between 0.80 and 0.85 when obtaining cylinder strength from cube strength. Murdock and Brook (1979) quoted a correction factor from BS 1881:Part 4:1970 which was applied to 150 mm dia. x 300 mm cylinder or core (with various height to diameter (H/D) ratios) strength for determining the equivalent standard cube strength. The correction factor multiplied to the cylinder strength was expressed as:

$$C' = \frac{H}{10D} + 1.05 \qquad \text{Equation 2.56}$$

where, C' = factor to convert the 150 mm dia. x 300 mm cylinder strength to the equivalent standard cube strength

This factor was adopted for the conversion of cube strengths used in previous research work in order to compare them with the current results. For H/D of 2, C ' equals 1.25 and hence, the conversion factor from standard cube strength to the 150 mm dia. x 300 mm cylinder strength is $\frac{1}{1.25}$, or 0.80. A factor of 1.04 was included to convert from the 150 mm dia. x 300 mm cylinder to the 100 mm dia. mm x 200 mm cylinder (100 mm dia. x 200 mm cylinder was considered as the standard). Additional correctional factors were used if 100 mm or 200 mm cubes were used, the factors being $\frac{1}{1.04}$ (=0.96) and $\frac{1}{0.92}$ (=1.09) respectively. The conversion factors are:

For 100 mm cube, factor = 0.80 x 1.04 x 0.96 = 0.799
For 150 mm cube, factor = 0.80 x 1.04 x 1.00 = 0.832 (standard cube)
For 200 mm cube, factor = 0.80 x 1.04 x 1.09 = 0.907

2.9 Statistical Analysis

A brief discussion on statistical approaches used for comparing results obtained for transmission length and pull-in is presented in this section.

According to Walpole (1982), statistical methods are divided into two major areas, known as *descriptive statistics* and *statistical inference*. Descriptive statistics are those methods which provide information for the group and range of data collected only, and in no way predict or draw conclusion concerning a larger population. A population is the entirety or totality of the observations that are ever conceivable.

In many cases, it is not possible to know the limits of this population set (it could be finite or infinite). For this reason, a subset or a 'sample' of the population is collected and used to make inferences or predictions about the population. This second type of statistical methods is called statistical inference.

For inferences made from the collected samples concerning the populations to be accurate, the samples obtained must be representative of the population. Such simple random samples are independent of bias and every subset observation is expected to have the same probability of occurring. The test data observed from the current laboratory exercises is expected to be representative of the different population conditions set for each separate test, which include varying the concrete strength, using different wire types and sizes, and the use of rapid and gradual releases.

Regression analysis restricted to its data range is descriptive statistics whereas hypothesis testing is part of statistical inference methods. These two methods were used to analyse test data to provide evidence for substantiating proposed arguments and conclusions.

2.9.1 Regression Analysis

This was used to determine whether two or more variables were dependent on each other. Regression analyses were performed between:

(a) transmission length and pull-in.

(b) ratios of $\left(\frac{L_p}{d_b}\right)$ and $\left(\frac{f_{si}.A_p}{f_{cp}.A_c}\right)$

Results of these analyses are presented in Chapter 4 (in Sections 4.9 and 4.13 respectively). Details of the regression analysis method is well known and will not be pursued here.

2.9.2 Hypothesis Testing

A statistical hypothesis is a conjecture or speculation which results when comparing two or more populations. Samples from these populations are used to predict the actual characteristics of the real populations.

The essence of hypothesis testing are to:

(a) formulate a hypothesis H_0 (called the 'null hypothesis') and an alternative hypothesis H_a.

(b) select a suitable test statistic to compare between populations (generally the population means, μ_1 and μ_2, are considered; if these two populations are different, then the sample means, $\bar{x}_1$ and $\bar{x}_2$, will reflect this).

(c) select the level of confidence deemed to be acceptable.

(d) calculate the values of the experimental and test statistics.

(e) reject or accept the postulated hypothesis.

The various sets of laboratory test data were obtained from small statistical sample sizes. The sample mean $\bar{x}$ was used to estimate the population mean μ and the sample variance s^2 was used to estimate the population variance σ^2, since both μ and σ^2 were not known. These approximations introduced greater variability into the statistical inference method, thus the t-distribution was suitably selected for calculating the test statistic.

The standard deviation *per se*, does not indicate the variability of a set of data. A better estimate of scatter in a sample is given by the coefficient of variation (V), which is the ratio of standard deviation over the sample mean:

$$V = \frac{s}{\bar{x}} \qquad \text{Equation 2.57}$$

For the t-distribution, confidence intervals ($t_{1-\alpha/2}$ and $t_{\alpha/2}$) has to be chosen for the hypothesis test (Figure 2.16). The area under the curve between the confidence intervals is known as the confidence coefficient. The term 'level of confidence' (or 'confidence level', denoted as 'C.L.') is frequently used to describe the percentage of area in the acceptance region compared to the total area under the curve. If the test statistic of the experimental data (t_{test}) fell within the confidence intervals, H_0 would be accepted.

For a two-tailed test, one half of the critical region falls to the right end of the curve and the other to the left end. In Figure 2.16, the area in the critical region at one end is assigned a value of $\frac{\alpha}{2}$. The total area in these critical regions is called the level of significance (α). On the other hand, 'one-tailed' tests have the critical region at one end of the curve only.

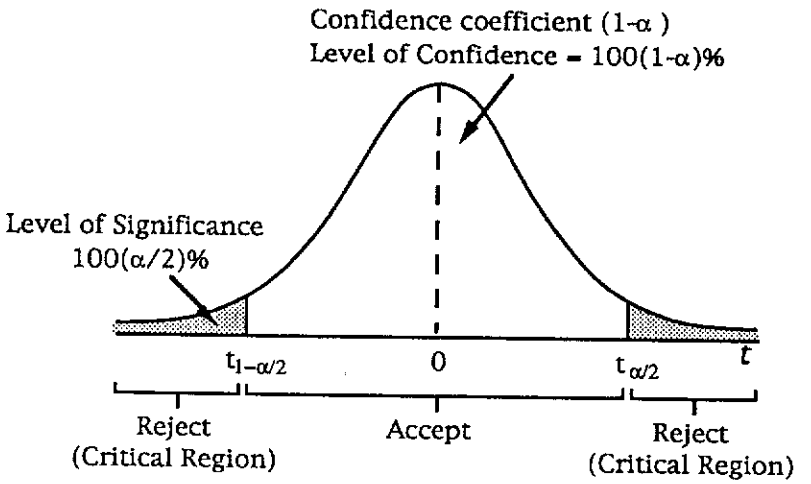

Figure 2.16 The t-Distribution Curve

When the experimental statistic is accepted, it does not mean that H_o is true. It only means that the experimental results supported the postulated hypothesis and there was insufficient evidence to doubt it. Similarly, when H_o is rejected, it only means that the data was inconsistent with this hypothesis, ***not*** necessarily that it is false. It is preferable to choose a high level of confidence to be more confident in rejecting H_o. As a consequence, choosing the 'right' level of confidence is not a straightforward matter as it will influence the acceptance or rejection criterion. Therefore, it was decided to check the tests at 90.0, 95.0, 99.0, 99.5, 99.9 and 99.99% levels of confidence and to adopt the highest level where rejection occurred.

Two sample tests were conducted on the transmission lengths in conjunction with the use of the t-distribution. The sample sizes being compared were from 4 to 32 and obviously constituted small statistical sample sizes. It was assumed that the population means were unknown and the variances were unknown and unequal. Walpole (1982) gave the test statistics as:

$$t_{test} = \frac{(\bar{x}_1 - \bar{x}_2)}{\sqrt{(s_1^2/n_1) + (s_2^2/n_2)}} \qquad \text{Equation 2.58}$$

$$\nu = \frac{\left(s_1^2/n_1 + s_2^2/n_2 \right)^2}{\frac{(s_1^2/n_1)^2}{n_1 - 1} + \frac{(s_2^2/n_2)^2}{n_2 - 1}} \qquad \text{Equation 2.59}$$

where,

ν = the degrees of freedom, rounded to the nearest integer

n_1, n_2 = the sample sizes for the two samples

s_1^2, s_2^2 = the sample variances

Hypothesis testing was also performed on pull-in values and where the statistical sample sizes were small, the t-distribution was used. Where sample sizes n_1 and n_2 were both greater than 30, the Gaussian normal distribution was used instead, with the test statistic of:

$$z_{test} = \frac{(\bar{x}_1 - \bar{x}_2)}{\sqrt{(\sigma_1^2/n_1) + (\sigma_2^2/n_2)}} \qquad \text{Equation 2.60}$$

Using the z_{test}, the degree of confidence is exact when samples are selected from two normal populations. For non-normal populations, the confidence interval is still a good estimate when both n_1 and n_2 are greater than 30. An additional assumption is that σ_1^2 and σ_2^2 may be replaced by s_1^2 and s_2^2 when the samples are sufficiently large without adversely affecting the confidence interval.

CHAPTER 3

Experimental Investigation

3.1 Introduction

The objective of the experimental investigation was to determine the effects of factors influencing the transfer of prestress from tensioned steel to its concrete surrounding. The transfer behaviour was examined for small rectangular concrete beams with pretensioned wires.

The quality of the prestress transfer was dependent on the bond stress developed at the interface between the steel tendon and concrete. However, it was not possible to determine the bond stress distribution and instead, the quality of transfer was monitored in two ways: by recording strain readings at the top surface of a beam and by taking pull-in reading for each wire with respect to the adjacent beam end face. From these measurements, the transmission length and average pull-in for each end of the test beams were evaluated.

The experimental programme contained tests which were tailored to investigate certain factors which affected the transmission length.

Concrete strength was believed to have an influence on the transmission length but its significance was not clear from previous research. Beams in current tests had various concrete strengths where prestress transfer

generally took place at 7 days. In one of the tests, four beams each were prestressed at 2 and 7 days, and the issue of maturity was considered.

The use of plain pretensioning wires is specifically discouraged by AS 3600 (1988). The effect of indentation on wire tendons was considered through comparative tests carried out with plain and indented wire pretensioned prestressed concrete beams.

Three types of prestress releases were used in the laboratory tests; namely gradual, sudden and shock releases.

The experimental study was planned and implemented with the collection of long term data for concrete strains and wire pull-ins over a six-month period. The accumulated data enabled the author to determine the changes in the transmission length and pull-in over the monitoring period.

An existing testing frame in the concrete testing laboratory of the Civil Engineering Department at Curtin University of Technology was available for the tests. Seven sets of beams were cast for the complete project, with the first test used as a trial run to familiarise with the procedure required to produce the test beams.

3.2 Prestressing Frame

3.2.1 Overview of the Prestressing Frame

The prestressing frame used was designed and constructed by Bailey (1989) for a capacity of 700 kN. It adequately catered for the prestressing forces used in each of the tests. A total force of approximately 350 kN was sustained by the frame in each test.

For this project, the testing frame was set up with its length orientated in the East-West direction. It consisted of an existing movable crosshead at the live end (West) and a fixed crosshead at the dead end (East) (Figure 3.1).

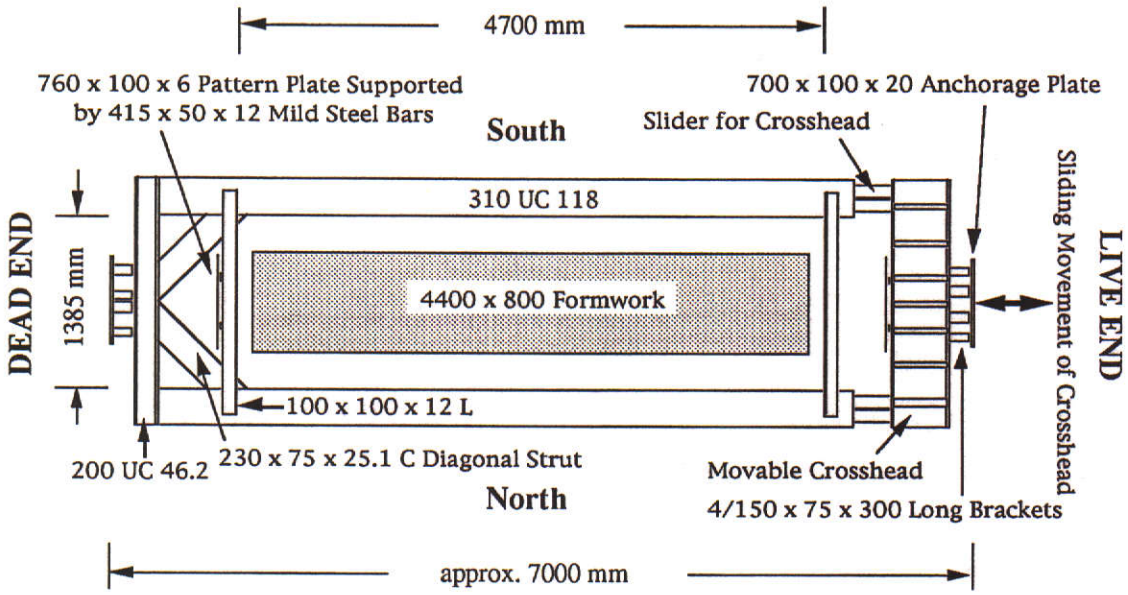

(a) Plan View of the Prestressing Frame (Scale 1:60)

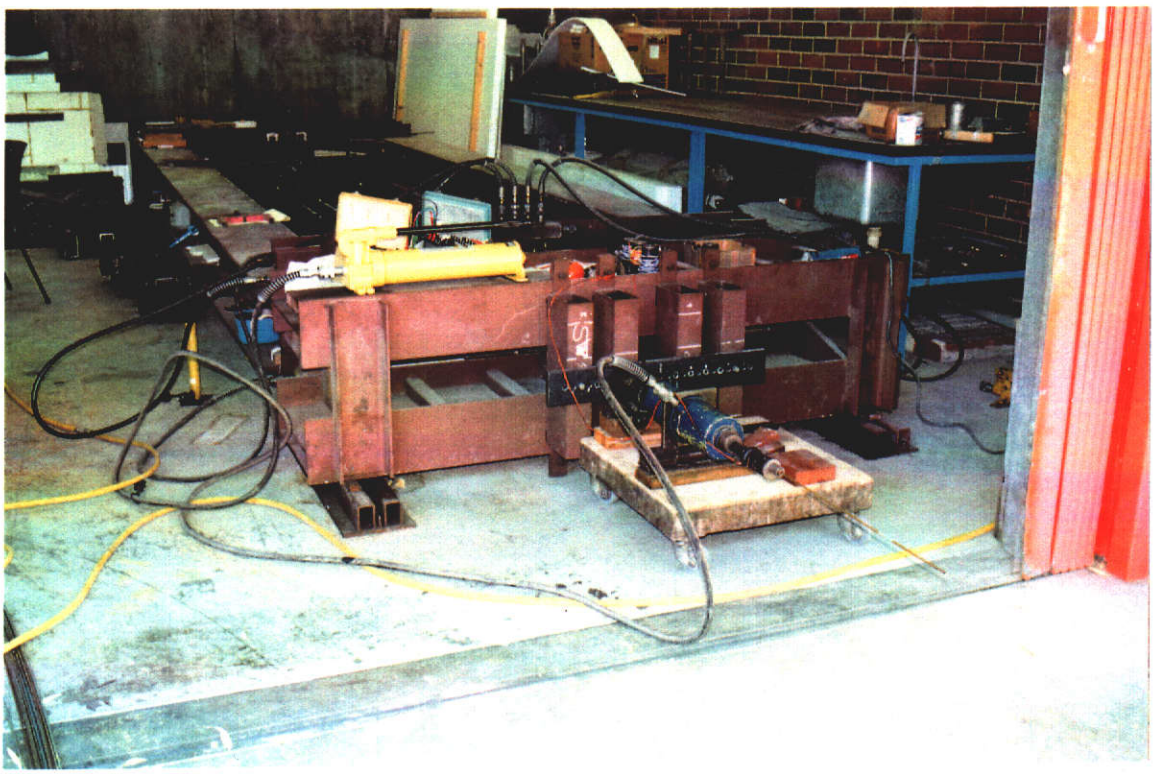

(b) Perspective View of the Prestressing Frame

Figure 3.1 Prestressing Frame

3.2.2 Details of Standard Operation

The movable crosshead which was supported on rollers allowed the destressing process to be carried out gradually. This permitted recordings to be taken as the beams were prestressed incrementally. The transfer was effected through the removal of two steel blockouts supporting the crosshead after slightly overstressing the tendons.

Figure 3.2 shows how the load could then released by retracting four jacks connected to a common manifold. A steel blockout (in red) had been removed from between the two jacks in the photograph's foreground.

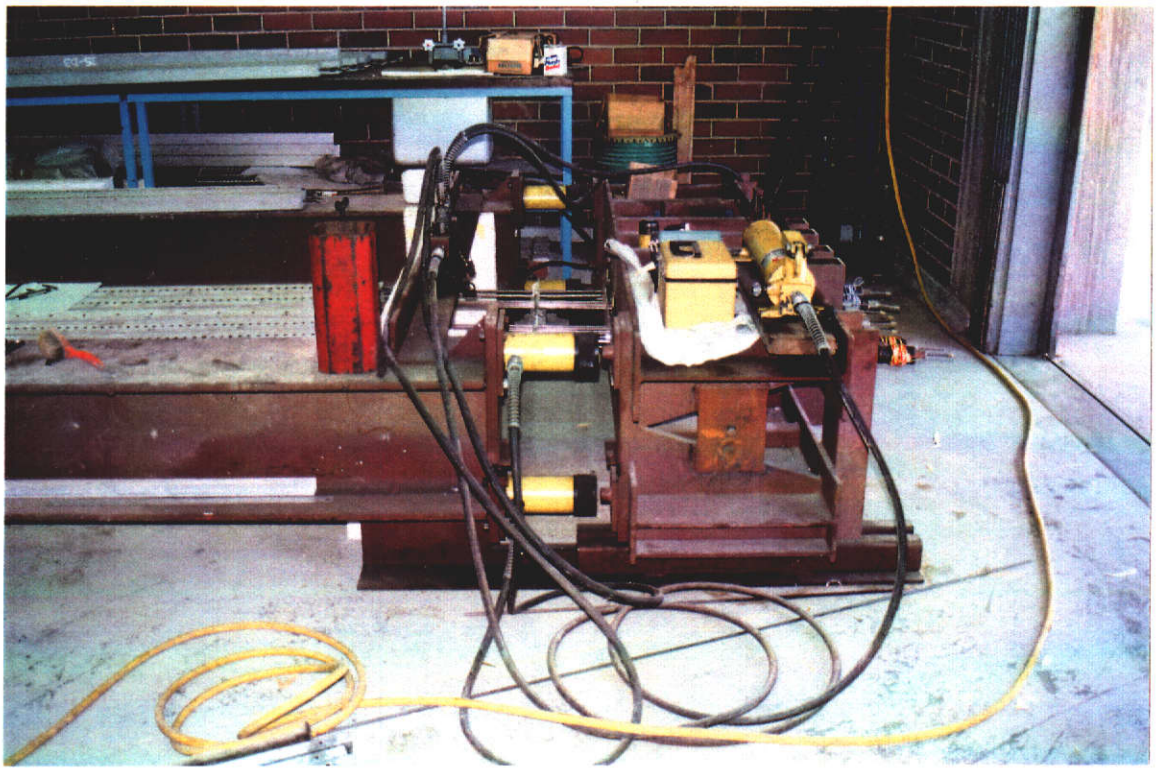

Figure 3.2 Destressing Using the Movable Crosshead

3.2.3 Modified Use of the Testing Frame

3.2.3.1 Anchorage brackets and anchorage plate

Four existing anchorage brackets were attached to the face of the movable crosshead. A 20 mm thick anchorage plate was laid across these brackets

and it provided the base for locking off the stressed tendons (Figure 3.3). Since the tendons had to be spaced 50 mm apart to allow for a combined system of threaded adjuster, barrel and wedges and load cell to work properly, the tendons had to be splayed at the crosshead. The maximum deviation in the horizontal alignment of the wires was kept below 8° from the intended alignment parallel to the length of the testing frame. The loss of load due to the small deviation in the tendons was negligible.

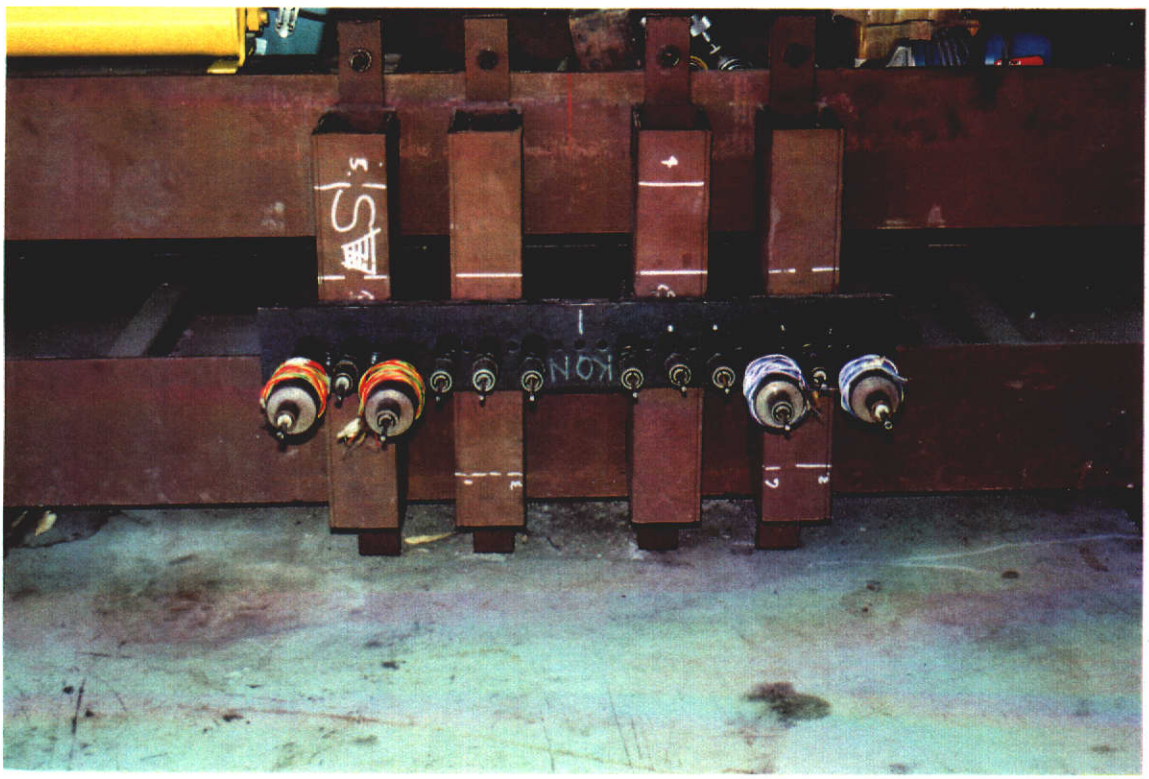

Figure 3.3 Anchorage Brackets and Anchorage Plate

The anchorage brackets and plate were fixed to the movable crosshead as shown in Figure 3.3 and all the wires were locked off on the anchorage plate. This meant that the movable crosshead could only detension all the wires simultaneously. When this crosshead slid towards the dead end, the tendons should see a uniform decrease in their forces. The previously mentioned common manifold supplied equal jacking force to each of the four jacks which support the crosshead.

A similar arrangement for the anchorage brackets and plate was set up at the dead end face of the prestressing frame (Figure 3.1 (a)).

3.2.3.2 Pattern plate

To ensure that the steel wires were spaced out parallel when passing through the beams, two pattern plates (or locator plates) with drilled holes at the required spacings were utilised. One was connected to the back face of the movable crosshead and the other to the dead end of the testing frame (Figures 3.1 (a) and 3.4).

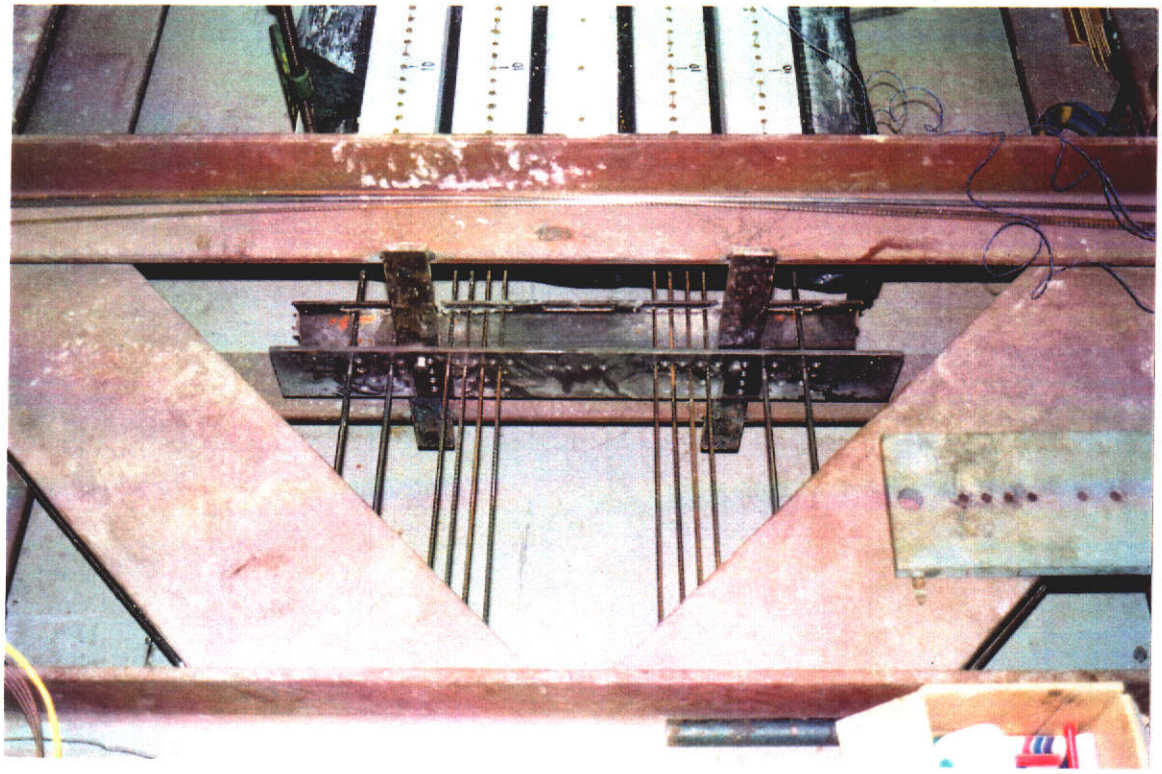

Figure 3.4 Pattern Plate at the Dead End of the Prestressing Frame

3.3 Formwork And Formwork System

The existing formwork by Bailey (1989) consisted of a base of two thicknesses of 17 mm formply which were 800 mm wide and 4000 mm long, with sides made from cold formed steel channel sections. The timber formply was stiffened by two 51 mm x 51 mm angle sections which ran the length of the formwork (Figure 3.5).

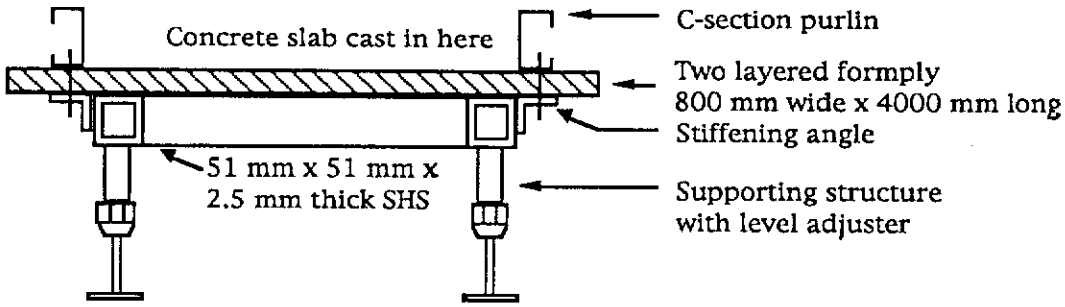

Figure 3.5 Existing Formwork Cross-section from Bailey (1989)

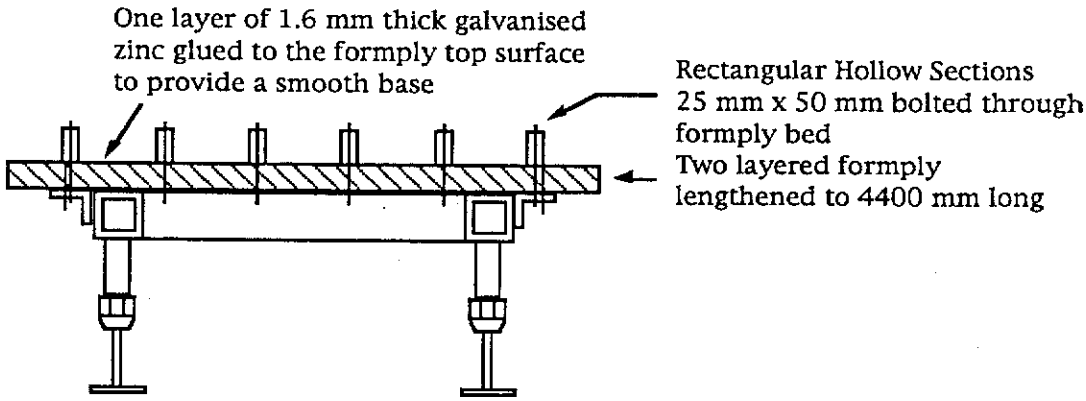

Figure 3.6 Modified Formwork Cross-section for Current Tests

The formwork system was modified to accommodate for the production of ten 50 mm deep x 100 mm wide beams for each casting (the use of this size for the beams will be discussed in Section 3.4.2). The formply bed was extended to a maximum possible length of 4400 mm but the width remained unchanged. The C-section purlins were substituted with rectangular hollow sections (RHS) which were 50 mm high, 25 mm wide and had a wall thickness of 1.0 mm. Six RHS's were bolted through their widths to the formply parallel to each other along the length of the form bed. These sections were spaced at 125 mm centre to centre, providing clear spacings of 100 mm between them where concrete beams were cast. The RHS's acted as dividers which could be removed easily after casting. The depth of the concrete beams was controlled by a screed finish flush with the top of the steel hollow sections.

The 4.4 m long formwork permitted two beams to be cast along the length of the prestressing bed. Each beam was 2.1 m long and a 200 mm blockout section was incorporated between each pair of live and dead end beams to

ensure that there was enough space for fixing attachments to measure the pull-in of each wire and for cutting the wires after destressing so as to allow the beams to be removed individually from the prestressing bed.

At the extreme beam ends, that is at the live ends of the live end specimens and the dead ends of the dead end specimens, end forms made of 51 mm x 51 mm x 3.0 mm equal angles were used. Slots were provided for the tendons to pass through during stressing.

Since it was important to fully transfer the prestress force into the concrete beams, friction between the concrete beams and the formwork had to be minimised. This was achieved by placing two layers of 100 μm thick damp proof membrane over the form zinc surface (which was glued to the top surface of the formply) before the RHS's were bolted into position. The membrane allowed the beams to slide unrestrained as prestress was transferred and the beams were noticeably pulled towards the dead end of the testing frame. In addition, the RHS's were removed before destressing.

3.4 Outline Of Test Procedure

There were seven sets of tests performed during the period of this project. Although the tests were different from one to another, the basic test procedure was the same. The following will elaborate on this test procedure and where significant differences occurred, they are pointed out.

3.4.1 Investigation of Factors Influencing L_p

The test procedure was designed to determine the effect of the following factors on the transmission length and pull-in of wire pretensioned prestressed beams:

(a) different concrete strengths for different mixes with the same age at transfer.

(b) reasonably similar concrete strengths at transfer for different mixes.

(c) indentations on the pretensioning wires.

(d) method of release - gradual, sudden or shock.

(e) different sizes of wire tendons.

(f) long term effects due to shrinkage and creep.

When testing for each of the above, the effects of other factors were controlled as much as possible to ensure that the data obtained reflected the factor being tested for.

3.4.2 Details of the Test Beams

The magnitude of prestress force used in a prestressed beam depends on the beam cross-sectional area and the concrete strength at the time of release. The geometry of the beams was the same throughout all the laboratory tests but the concrete strength varied. The initial prestress force for each of the beams was kept close to a constant value although it could have been varied to match different concrete strengths. However, the prestress force was not varied since the exact strength value was not known until the time of testing. Moreover, the author selected to use a constant precompression stress $\left(\frac{P}{A_c}\right)$ for all the beams.

Four types of wires were used, namely 5 mm dia. Plain, 5 mm dia. Chevron, 7 mm dia. Plain and 7 mm dia. Belgian wires. The 5 mm dia. Chevron wire was donated by Austrak Pty. Ltd.. The 5 mm dia. Plain wire was obtained through arrangements between Austrak Pty. Ltd. and BHP Co. Ltd.. The 7 mm dia. Plain and Belgian wires were obtained from available stock within the Civil Engineering Department.

The ratio of the cross-sectional area of a 7 mm dia. wire to the cross-sectional area of a 5 mm dia. wire is approximately two times. For this reason, the beams were concentrically loaded using either two 7 mm dia. wires or four 5 mm dia. wires. The ratio of total force was then approximately 1:1 between the beams with 5 mm and 7 mm dia. wires. The wires were stressed up to approximately 70% of the ultimate strength (f_p) which was acceptable according to AS 3600 (1988). A limit of 0.8 $f_p A_p$ was stipulated for the jacking force (Clause 19.3.4.6 (a)).

It is generally accepted that concrete should not be precompressed with a stress greater than 0.5 f_{cp} (50% of the compressive strength at transfer). Prior to doing the tests, the anticipated general concrete strength at transfer was expected to be about 30 to 40 MPa. Consequently, the beam size was chosen as 50 mm high x 100 mm wide. Each beam was then prestressed with approximately 88 kN using two 7 mm dia. wires or four 5 mm dia. wires, which gave 0.5 f_{cp} for 35 MPa at transfer.

The 5 mm and 7 mm dia. wires were all stressed in single layers as this fitted in well with the set up of the existing testing frame. Opting for a multi-layered tendon layout pattern would have required substantial modifications to be made to the formwork system and testing frame. The latter option was dismissed.

It is noted that the spacing between the 7 mm dia. wires in a beam was 5.1 d_b. The beams with four 5 mm dia. wires had wire spacings of 3.5 d_b. It is appreciated that all the wires placed in a single plane would have generated appreciable shearing stresses.

3.4.3 Layout of the Tests

Each casting consisted of five pairs of beams, with five of them at the dead end side and five duplicates at the live end side of the testing frame (Figure 3.7). The central beams on both the dead and live ends (ie. 1S-D3 and 1S-L3) were used as full size shrinkage specimens whereas the remaining beams were prestressed.

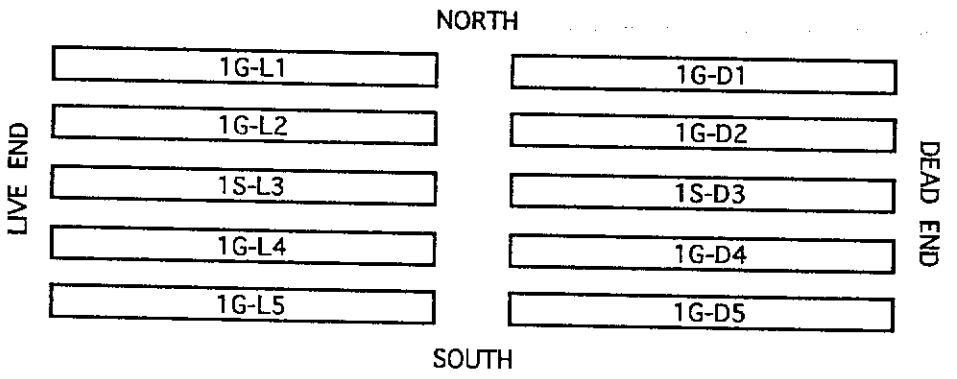

Figure 3.7 Layout of the Test Beams

The beams and wires were coded in a special manner to distinguish each of them. In general, all the alphanumeric assignments had digits increasing and alphabets ascending from North to South. The following explains the method of assignment used:

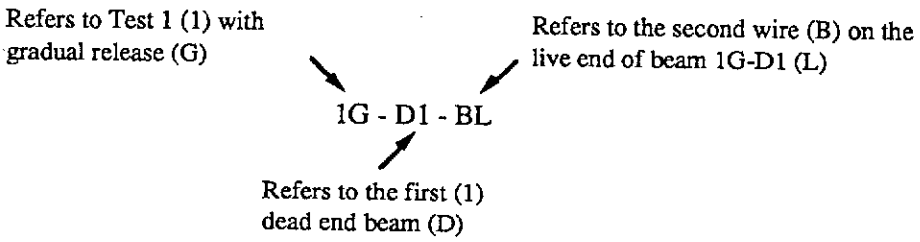

The first digit in the string refers to the test number, in this case it is the first test. The following alphabet can be either G, R or S, respectively referring to ***gradual*** release, ***rapid*** release (sudden or shock), or ***shrinkage*** specimens which were unstressed.

The middle portion of the code has one letter which can be either D or L representing the ***dead*** or ***live*** end beam (live end beams were adjacent to the movable head which released the prestress force), and the digit refers to the beam position numbered from North to South.

The last two letters refer to the wire location (B is the second wire from North), which can be at the dead end or live end (L refers to the ***live*** end).

Each individual beam may be uniquely defined by omitting the last portion of the above code, in this case reference is made to beam 1G-D1 and the beam location is shown in Figure 3.7.

3.4.4 Examining the Surface Condition of Wire Tendons

The wires were checked for rusting and contaminants on their surfaces. Corrosion tended to occur in a non-uniform manner. Coiled wires had outer exposed wires covered with rust while those of the inner coils only had minor surface rust. Wires used for the first set of test were not cleaned of rust as they were only slightly rusted. From the second test onwards, all the wires used had rust removed using emery paper. All the wires were also checked for pitting but this was not a problem.

3.4.5 Stressing the Wire Tendons

A schematic diagram of the stressing process is shown in Figure 3.8 (a). The movable crosshead at the live end was held stationary by two steel rectangular hollow section blockouts during the stressing of the tendon.

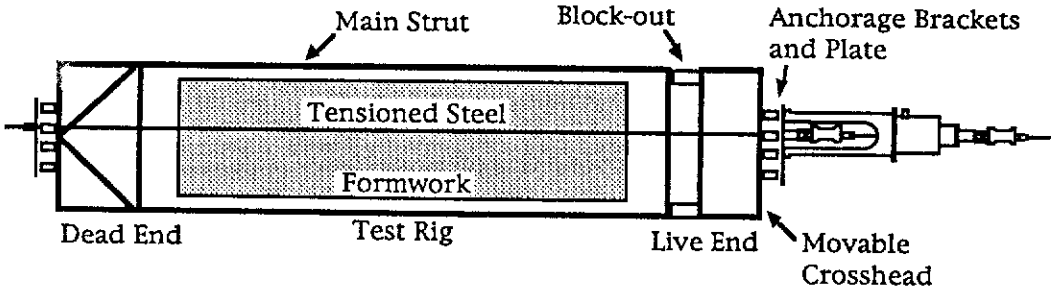

(a) Plan view of test rig with hollow ram jack used for stressing (Not to scale)

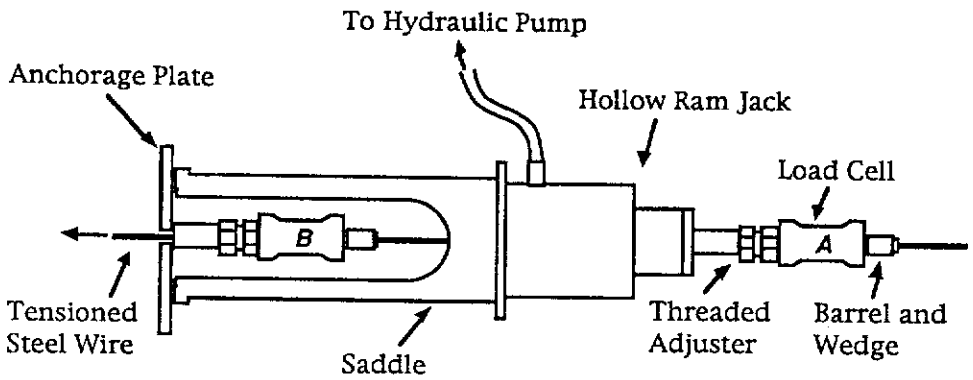

(b) Schematic diagram of the tensioning of a steel wire

Figure 3.8 Tensioning of the Prestressing Wires Using the Hollow Ram Jack

Each steel wire was pulled through from the live end to the dead end of the testing frame and also through the prepared formwork. The dead end was anchored with a set of barrel and wedges appropriate for the diameter of wire used. At the live end, the wire was fed through a hollow ram jack secured to a saddle which reacted off the anchorage plate and brackets connected to the front face of the movable crosshead. The wire was subsequently anchored past the ram of the jack before stressing was carried out.

A system consisting of a threaded adjuster, a load cell and a set of barrel and wedges was located in front of the hollow ram to allow for the anchoring of the wire (indicated as ***A*** in Figure 3.8 (b)). The two pieces of conical wedges were self-locking as they jammed into the barrel, thus creating a positive anchorage for the wire. Strain gauges attached to the load cell enabled the load applied to the steel tendon to be determined. All the load cells were calibrated prior to the running of the tests. The threaded adjuster was utilised to reduce excessive slackness in the wire (so that less ram travel was required to stress the wire) or conversely, to add to the slackness in the wire (useful when removing the barrel and wedges).

A similar system of threaded adjuster, load cell and barrel and wedges (***B***) was also placed in front of the supporting anchorage plate where the wire was to be locked off.

The stressing operation consisted of tensioning the wire using system ***A*** and then securing it on system ***B***. Once the wire had been pulled to the correct tension on ***A***, the wedges were fixed into the barrel in ***B***. The force was released from ***A*** and transferred to ***B***. However, the load transferred would be less than that in ***A*** due to snug tight slackness in ***B*** and the sinking of the wedges into the barrel in ***B***. To overcome this problem, the wire was stressed to the required tension on system ***A*** again and the slackness in system ***B*** was removed by tightening the threaded adjuster to finger-tightness. This procedure was repeated at least once more to ensure the maximum possible load had been transferred before system ***A*** was removed and the wire cut off a short length beyond the anchoring point of the barrel and wedges in system ***B***. Obviously, the effectiveness of the transfer depended on the tightness of the adjuster. The improbability of achieving the same tightness for every wire gave a range of values for the transferred prestress force. The discrepancies of these sustained loads from the intended load value were minimised.

Since lock-off tension was less than the jacking tensile force, it was necessary to stress the wires with larger forces in order to achieve the appropriate pretensioning forces. Experience in the laboratory indicated that the stressing operations attained 91-95% of the jacking loads. The jacking loads for the 5 mm and 7 mm dia. wires were about 24 kN and 48 kN respectively and the tendon stresses were below 0.8 f_p.

Four load cells were available for monitoring loads transferred to system *B* in four wires. Therefore, one load cell each was assigned to the four pairs of beams in each casting (ie. one load cell for a dead end beam and its corresponding live end duplicate). More load cells were not available and in any case, the anchorage plate was congested with barrels and wedges from anchoring four pairs of beams (12 wires altogether from North to South).

3.4.6 Preparation for the Concreting Works

Before concrete could be placed into the formwork, additional preparatory work had to be performed. These included adjusting the formwork, sealing the formwork, inserting block-out forms, coating the formwork with form oil and cleaning the wires.

Once the wires had been tensioned, the formwork was adjusted laterally and vertically before being held in position using G-clamps and steel sections fixed to the main struts of the testing frame. Blocks of jarrah timber cut to the correct depths were used to gauge whether the base of the formwork was at the correct depth from the underside of the wires.

Small holes were sealed with silicon sealant to prevent losing cement paste which would leave a bony concrete structure. The sealing was particularly important at the ends of the beams as this was the location where the bond transfer would occur.

The space between each pair of dead and live end beams had to be filled with timber and foam to act as block-out. Proper sealing also had to be achieved at this location.

Where possible, most parts of the steel RHS dividers were coated with mould oil before stressing the wires. After stressing, the oil was applied to the uncoated portions of the RHS's near the beam ends after sealing had been completed.

Even with care, oil could sometimes get on the surfaces of the wires. While pulling the wires through the formwork during stressing, they could come in contact with oil from the oil-coated dividers. Disregarding the

fact that special care had been taken and the wires had been cleaned before stringing them through the formwork, they were subsequently cleaned two more times with the X55 solvent before concrete casting.

3.4.7 Casting the Concrete Beams

Concreting generally took place two days after the stressing of the tendons to allow for the preparatory works. There was no discernible decrease in the wire tension due to relaxation over such a short period of time.

Ten beam specimens were cast for each set of tests. The number of concrete cylinders used for the compression and Brazilian tests varied depending on the availability of cylinder moulds and the length of monitoring for the particular set of beams.

Where the beams were to have one single strength mix, concrete was placed from the live end to the dead end. When half the beams in any set was to have a different strength mix, pouring of the first concrete mix was performed taking precautions to cover the remaining parts of the mould. The first mix was always placed for the two Southern pairs of beams (ie. D4, L4 and D5, L5) and the live end unreinforced beam (L3). The second mix filled the remaining parts of the mould. Unreinforced beams L3 and D3 were used for estimating shrinkage in the beams for the first and second mixes respectively. Tests 2, 3 and 5 had two concrete mixes.

In all of the castings, a poker vibrator was used to compact the concrete. The poker vibrator could puncture the two layers of damp proof membrane used. Therefore, direct contact with the plastic sheetings was avoided. As the beams had a small depth, excess concrete was piled on top of the specimens so that the vibrator could be immersed into the concrete mass in order to provide effective consolidation. The extra concrete was then removed by screeding it off the surface. Care was taken in screeding the top surfaces of the beams when there were different concrete mixes to avoid mixing.

The initial finishing of the top surfaces was done using an aluminium screed. When the concrete had set and began to harden, the final smoothing was carried out. With the bleed water evaporated and the

concrete colour changed from a sheeny grey to a dull grey shade, the surfaces were worked back to give a smooth, flat and hard surface on which demec target points were attached. The re-working was done using a steel trowel.

The concrete test cylinders were stripped the day after the casting operation. At the same time, the moulds were cleaned and coated with oil ready for the successive test.

The steel RHS's acting as side moulds for the concrete beams could not be removed too early in order to avoid damage. They were removed only on the second day after each casting.

3.4.8 Instrumentation for the Tests

3.4.8.1 Determination of the longitudinal concrete strains

Brass discs with punched holes were used throughout this project as the reference points for the demec gauge. Tests at Curtin University of Technology had shown that they gave as consistent results as steel discs with drilled holes.

A scapula was used to remove irregular protrusions on the concrete beam surfaces and a wire brush cleared the surfaces of rich hardened cement paste along the lines where demec discs were to be attached. The discs could then be firmly implanted on the concrete instead of being seated on a superficial layer of cement paste.

Each of the beams were then marked for the positions where the discs were to be fixed. In general, there was only one line of demec discs at 25 mm centres along the length of each beam (starting and ending 25 mm from both ends) and it was located centrally across the width. The only exceptions were all the shrinkage beams and beams in Test 1.

Shrinkage beams for all the tests had the first and last demec points 50 mm from the beam ends and other points in between were spaced at 100 mm.

Beams 1G-D1 and 1G-L1 had two rows of demec points, each directly above a 7 mm dia. plain wire whereas all other beams in Test 1 had a single central row of demec points. The twin rows used were to check if there was any difference between strain readings taken for the two rows and also to compare with other beams having single rows. The spacings of demec points for prestressed beams in Test 1 were different from other tests. The first and last discs were 25 mm from the beam ends. Two 450 mm sections of discs spaced at 50 mm centres straddled both ends of a 1150 mm central section where discs were spaced at 25 mm centres.

All the discs were glued to the clean concrete surfaces using commercially available Araldite epoxy resins (5 minute and 24 hour Araldite were used). Releasing the prestress at 7 days was found to be reasonable as it was necessary to allow time for the concrete to harden sufficiently, for attaching the demec discs and for the Araldite resin to harden.

A 200 mm setting out bar was used to position each of the discs and this was done consistently from the dead end to the live end of each beam.

A 200 mm gauge length demountable mechanical strain gauge (DEMEC, Base (1955)) was used to determine the strain reading between discs and all the readings were taken starting from the dead end of each beam. Recordings were made before and after destressing, and the difference in the readings multiplied by a gauge factor of 8.1 x 10^{-6} gave the longitudinal concrete strains due to prestress transfer.

3.4.8.2 Determination of the pull-ins

In order to determine the amount of pull-in or end-slip (Δ_o) that occurred in the end zones, a unique measuring technique was used. Figure 3.9 shows a clip or wall tube attached firmly to a wire tendon with Araldite resin about 40 mm from the end face of the concrete beam. Metal foldback clips were initially used as attachments for Test 1 where all the tendons were 7 mm dia. Plain wires. For Test 2 onwards, slit plastic wall tubes were used on 5 mm dia. wires. A pair of specially calibrated callipers (Westoby, 1991) was used to measure the distance between the end face of the concrete beam and the near face of the attachments in order to monitor the pull-in. As the wire tendon was detensioned, the monitored gauge

length shortened. This shortening was due to the wire slipping into the concrete and due to the 40 mm gauge length regaining its original length with the decrease in the prestressing force. Correction was made for the shortening when the data was analysed. Both types of attachments were checked for repeatability of results and were found to be satisfactory.

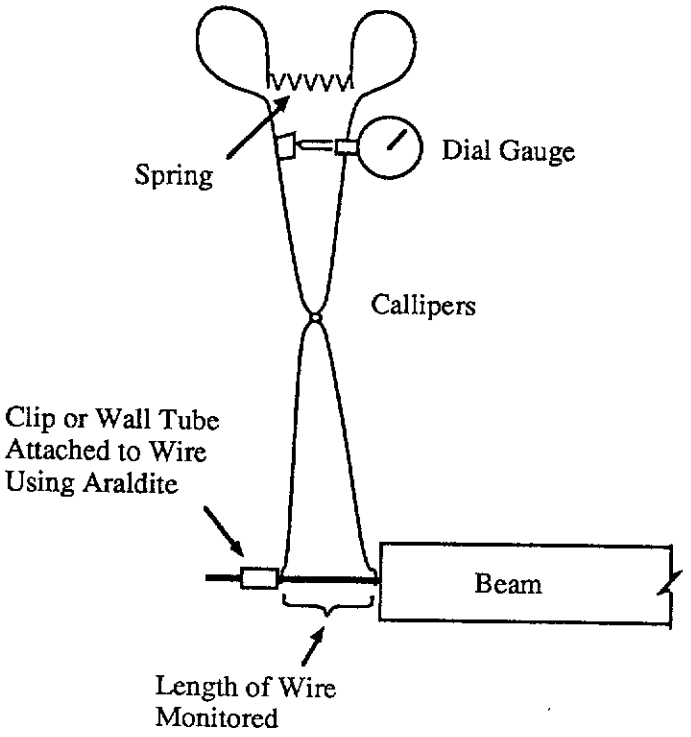

Figure 3.9 Determining Pull-in Using Calibrated Callipers

3.4.8.3 Determination of concrete temperature

Thermocouples were used in Tests 1 to 3 for monitoring the temperature in the concrete. Type K thermocouple wires were crimped together at the sensoring end and a temperature measuring micrometer was used to determine the temperature in the concrete beams. After Test 3, the temperature within the concrete was not monitored as there was very little difference between the temperatures within and without the concrete beams (maximum difference was 2 °C and the measuring equipment could only be read to the nearest degree accuracy).

The measuring points were located in the second dead end beams for each of Tests 1 to 3 (ie. 1G-D2, 2G-D2 and 3R-D2). In Test 1, thermocouples were attached to the Northern wire (1G-D2-A) at 50 mm, 500 mm and 1050 mm

from the dead end. Only a small amount of Araldite was used at each point to avoid interference with the bond transfer. For Test 2, again three locations with the same distances from the dead end were used but the thermocouple measurement junctions were all attached to the second wire from the North (2G-D2-B). For the third test, only one measuring point was located on the second wire from North in the middle of beam 3R-D2.

The small increase in the temperature within the concrete above ambient was due to the small size of the beam and the ease of dissipation of energy released during the hydration process. The beams had a very small cross-sectional area and the heat of hydration was quickly lost to the surroundings. In addition, the steel dividers separating the beams, the zinc sheeting on the formwork base and the wire tendons running through the beams would have contributed to the heat loss.

3.4.9 Destressing Process

The four load cells previously described in Section 3.4.5 were used to determine the tension just before and during the detensioning of the wires. As detensioning was done incrementally (roughly every 10% of the "initial" force), the load cells were used to monitor the detensioning process. When the jacks were retracted slowly, the movable head did not necessarily move uniformly. Due to unequal friction on the supporting rollers, the movable crosshead would slide in a skewed manner. This was initially controlled by tapping on the side of the crosshead which was slow to respond to the retraction of the jacks. From Test 5 to Test 7, an additional jack was used to restrain the side of the movable crosshead that was retracting too quickly and this resulted in well controlled uniform releases.

The author attempted to improve the rolling mechanism by removing the crosshead from the testing frame and cleaning the bar rollers. They were then replaced and properly aligned to ease the sliding action of the crosshead. Little improvement was experienced after this exercise.

In order to effectively identify skewness in the movable crosshead, two of the outer load cells were located as far apart from each other as possible and were positioned symmetrically about the centre-line. Figure 3.10 shows the general locations of the four load cells used.

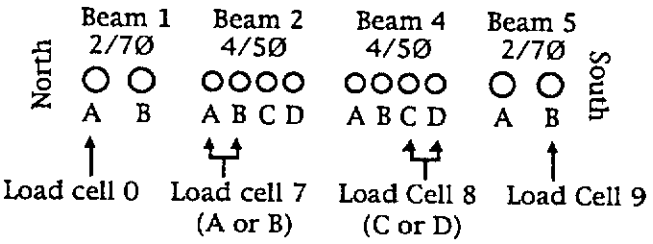

Figure 3.10 Load Cell Locations Viewing at the Wires from the Live End

Load cells 0 and 9 were placed on the two outermost wires (beam 1 wire A and beam 5 wire B). The load cells on beams 2 and 4 were not as crucial; in Tests 2 to 5 load cell 7 was placed on wire A and load cell 8 was placed on wire D but in the Tests 6 and 7, load cell 7 was placed on wire B and load cell 8 was placed on wire C.

3.4.10 Types of Prestress Release

Three types of releases were used for the tests:

(a) the most common method was the hydraulically controlled gradual release. Detensioning was done in approximately 10% decrements of the original forces. After each decrement, a full set of pull-in recordings were taken. Recording of the demec readings was done prior to any force release and after 100% force transfer. In Tests 1, 2 and 4, readings were also taken for some of the beams at 50% force transfer. Gradual release was performed for Tests 1, 2, 4, 5, 6, and half of the beams in Test 7 (7G-D2, 7G-L2, 7G-D5 and 7G-L5). It is noted that the beams in Test 7 were gradually released in one increment instead of the ten (10%) increments. This was achieved by slowly releasing the jacks in one step. All the other tests had incremental transfer.

(b) Test 3 experienced sudden release, where the valve on the pump was instantaneously cracked open, releasing all the prestressing wires at once. This type of release is rated to be between a gradual release and a shock release.

(c) Beams 7R-D1, 7R-L1, 7R-D4 and 7R-L4 were shock released by using an angle grinder to cut the wires. The cuts were executed between the live and dead end specimens. This meant that the live ends of the dead specimens (7R-D1-L and 7R-D4-L) and dead ends of the live specimens (7R-L1-D and 7R-L4-D) all received direct shock from the cutting.

In concluding Section 3.4 on the outline of the test procedure, a summary of the variables used in the seven tests is given in Table 3.1.

Table 3.1 Summary of the Different Variables Used in the Laboratory Tests

Test No.	Beam No.	Size/Type of Wire	Type of Release
1	1, 2, 4 & 5	7 mm dia. Plain	Gradual (10% inc.)
2	1 & 5 2 & 4	7 mm dia. Plain 5 mm dia. Chevron	Gradual (10% inc.) "
3	1 & 5 2 & 4	7 mm dia. Plain 5 mm dia. Chevron	Sudden (1 step) "
4	1 2 4 5	7 mm dia. Plain 5 mm dia. Plain 5 mm dia. Chevron 7 mm dia. Belgian	Gradual (10% inc.) " " "
5	1 & 5 2 & 4	7 mm dia. Plain 5 mm dia. Chevron	Gradual (10% inc.) "
6	1 2 4 5	7 mm dia. Plain 5 mm dia. Plain 5 mm dia. Chevron 7 mm dia. Belgian	Gradual (10% inc.) " " "
7	1 2 4 5	7 mm dia. Plain 5 mm dia. Chevron 5 mm dia. Chevron 7 mm dia. Plain	Shock (1 step) Gradual (1 step) Shock (1 step) Gradual (1 step)

3.5 Dimensional Tolerances

The depths of indents on a 5 mm dia. Chevron wire sample were determined using the Hilger Watts Optical Projector which magnified the silhouette profile of the wire. As the indents were of a rhomboidal pattern, the length could not be accurately measured as it depended on the angle which the wire was orientated with respect to the axis of the incident light beam. One wire sample had three of its indents measured and the depths were 0.091, 0.135 and 0.145 mm. For a nominal diameter of indented wire equal to or greater than 5 mm but less than 7 mm, the lower and upper limits of acceptable depths of indentation are 0.05 and 0.20 mm according to AS 1310 (1987). There seems to be a large range between these limits. For 7 mm dia. indented wires, the limits are 0.10 and 0.30 mm. Whether there is significant difference between small and large depths remains unknown as further work on this issue was not pursued.

The indents for the sample used also had rounded corners indicating that the die imprinting these indents could be wearing out. There was no guidance on this matter within AS 1310.

3.6 Wire Tension Tests

Tensile tests were performed for the 5 mm dia. Plain, 5 mm dia. Chevron and 7 mm dia. Plain wires. Tensile test was not performed for the 7 mm dia. Belgian wire as there was only enough length for prestressing the beams.

The wires tested sustained large loads before failing and it was difficult to use the existing testing machine gripping jaws to hold on to the wires without slipping. A testing method was devised to overcome this problem but the wires were only tested for their ultimate tensile strengths.

Testing was carried out in accordance to AS 1391 (1991). However, there was no flaring out to a larger cross-section at the gripping ends for pretensioning wires, as required in AS 1391 for standard tensile specimens. The specimens used were continuously parallel all along their lengths. AS 1310 (1987) required a minimum gauge length of 250 mm to determine the elongation of a wire. Although the tests done were not

geared at determining the elongation of the wires, a gauge length of approximately 260 mm was used for all the tensile tests.

Two 152 x 102 x 6.5 mm RHS's were employed for connecting a wire sample to 17 mm dia. mild steel bars (Figure 3.11). The bars were then clamped on to the gripping jaws of the testing machine.

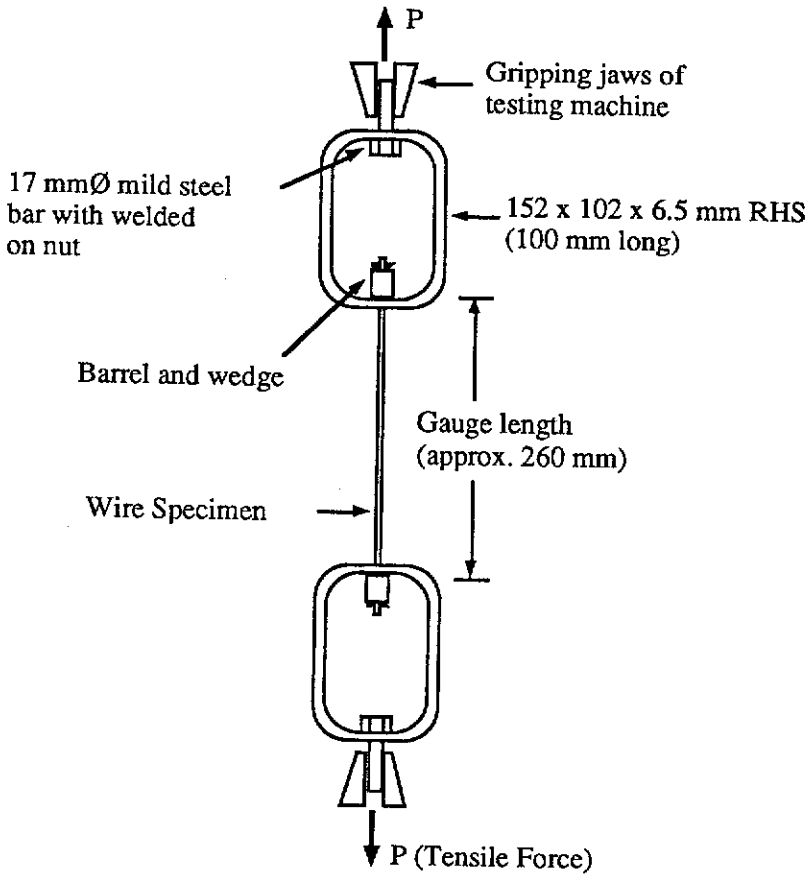

Figure 3.11 Tensile Testing of Pretensioning Wires

An Instron 3710-016 tensile testing machine was used for the tests. The standard strain rate suggested in AS 1391 was the target value of 800 με per second within a range of 250 to 2500 με per second. The actual gripping jaw displacement rate was 10 mm/min. over the gauge length of about 260 mm, which was equivalent to a strain rate of 640 με per second.

The results of the tensile tests for the 5 mm dia. Plain, 5 mm dia. Chevron and 7 mm dia. Plain wires are given in Table 3.2.

Table 3.2 Tensile Test Results for the Prestressing Wires Used

Specimen Designation	Type of Wire	Failure (kN)	Ultimate Strength (MPa)	Failure Location in Specimen
PW-7P-A	7 mm dia. Plain	68.4	1780	In grip
PW-7P-B	"	66.9	1740	"
PW-7P-C	"	65.5	1700	"
PW-5C-A	5 mm dia. Chevron	35.9	1830	Remote from ends
PW-5C-B	"	35.8	1820	
PW-5C-C	"	35.8	1820	"
PW-5P-A	5 mm dia. Plain	36.2	1840	Remote from ends
PW-5P-B	"	36.3	1850	
PW-5P-C	"	36.2	1840	"

The wedges (in the barrel and wedge grip) used for testing the 7 mm dia. Plain wires could have caused the failures to precipitate near the ends. However, at failure, all the wires had strengths exceeding 1700 MPa which is the minimum required characteristic ultimate strength for prestressing wires according to AS 3600 (1988). Therefore, it was reasonable to assume 1700 MPa as the failure stress for the wires.

3.7 Calibrating The Load Cells

The load cells were connected to a Vishay switch and balance unit (serial no. 007593) which was in turn connected to a strain indicator (serial no. 50837). The gauge factor on the strain indicator was set to 2.401. With this setting, the actual load was roughly 0.10 times the strain indicator reading. Total prestress force applied to each beam was in general slightly greater than the nominal 88 kN because the calibration factor for the load cells was up to 3% greater than the adopted working value of 0.10.

For calibration, each of the load cells was loaded in an Avery testing machine. Readings were taken from the dial of the testing machine and also from the strain indicator. The maximum load reached was 200 kN and after unloading, each of the zero readings was checked. Regression analysis was then used to fit a line of best fit for each set of readings.

3.8 Calibrating The Pull-in Callipers

The pair of callipers used for monitoring the pull-ins of wires had a 5 mm ± 0.01 mm travel dial gauge attached to it as shown in Figure 3.9. The relative displacement between the measuring ends of the callipers was a magnification of the dial gauge reading.

For the calibration, a straight wire was first set in a vertical drilling machine. The callipers' dial gauge was set to zero for maximum separation of the callipers' ends and it was subsequently placed on the wire to measure the distance between the tip of the chuck and the top of the machine's base plate table. This distance was decreased to the point where it equalled the maximum separation for the callipers. The initial gauge length between the chuck and the base plate was measured using a vernier scale. As the base plate was moved towards the chuck, readings from a separate dial gauge determined the displacements of the chuck. Readings from the callipers' dial gauge were also read. Calibration was done for the callipers' dial gauge reading from 0.00 to 4.50 mm in steps of 0.25 mm. With this information, regression analysis was applied to establish a relationship between the absolute separation of the callipers' ends and the callipers' dial gauge reading. This yielded a linear best fit equation of:

Absolute gauge length (mm) = 35.050 + 1.9767 x Calliper reading
(Correlation coefficient r = 1.000) Equation 3.1

To allow for the shortening of the gauge length as detensioning took place, the correction was calculated as follows:

$$\text{Correction (mm)} = \frac{\Delta P_i}{A_p E_p} \times \text{(Initial gauge length)} \qquad \text{Equation 3.2}$$

where, ΔP_i = decrease in prestress force from the initial value (kN)

3.9 Concrete Mix Design

Commercial concrete mixes obtained from Readymix Pty. Ltd. were used in beams 2G-D1, 2G-L1, 2G-D2 and 2G-L2 of Test 2, and all of Test 6 beams. All other beams had concrete mixes which were cast in-situ.

For Test 1, 20 mm aggregate was used but this was found to be difficult to work with since the beams were small and the wires closely spaced (all prestressed beams had 50 mm centre to centre spacing between the 7 mm dia. wires used). From Test 2 onwards, the in-situ and Readymix mixes contained maximum aggregate size of 10 mm. Details of the concrete mixes are given in Table 3.3. Concrete strengths are standardised to the 100 mm dia. x 200 mm cylinder strengths.

Table 3.3 Details of Concrete Mixes for Tests 1 to 7

Test No.	Mix No.	Agg/Cem ratio	w/c ratio	% of Aggregate				Compressive Strength (MPa)	
				20 mm	10 mm	7 mm	Sand	Transfer	28 days
1	1	3.5	0.40	40	25	10	25	49.0	59.7
2	1A	6.9	0.60	-	40	20	40	38.0	49.0
2	1B	5.87	0.60	-	40	20	40	33.5	45.8
2	2	-	-	-	-	-	-	48.7	56.1
3	1	6.0	0.60	-	40	20	40	33.8	41.4
3	2	3.4	0.40	-	40	25	35	53.1	64.7
4	1	3.5	0.40	-	40	25	35	48.7	62.7
5	1	3.8	0.70	-	40	20	40	26.8	32.2
5	*2*	***4.0***	***0.55***	-	***40***	***20***	***40***	***20.1***	-
6	1	-	-	-	-	-	-	65.1	88.6
7	1	3.6	0.38	-	40	25	35	53.9	59.0

For the aggregate combination of in-situ mixes; 40% of 10 mm aggregate, 20% of 7 mm aggregate and 40% of sand gave a reasonably good concrete mix when blended with Cockburn Type GP (General Purpose or previously Type A) cement and water. All mixes except for Test 1 had this proportioning or a slight variation of it. No additives were added to any of the in-situ mixes.

Details of the commercial mixes in Test 2 (Mix 2) and Test 6 are kept strictly confidential by the supplier. The former mix contained superplasticiser and the latter had superplasticiser and also silica fume.

The "Mix No." in Table 3.3 indicates concrete mixes with different proportion of constituents. Tests 1, 4, 6 and 7 were each made up of three batches but had exactly the same amount of weighed materials for each of the batches. The volume of concrete required to fill up the beam and control cylinder moulds was 0.21 m^3 (allowing for a small amount of waste). The pan mixer used had a capacity of 0.07 m^3, hence three equal mixes were needed to complete each job.

Mixes 1 and 2 in Tests 3 and 5 each had two batches of 0.50 m^3 each.

For Test 2, Mixes 1A and 1B were cast in-situ and should have been the same. The aggregate/cement ratio of 6.9 (Mix 1A) turned out to be quite high and the resulting mix was harsh. Immediate action was taken to improve workability by adding cement and water to Mix 1B. By keeping the w/c ratio constant and changing the aggregate/cement ratio, the difference in strengths was mimimised. When tested, the concrete strengths at transfer and at 28 days did have minor differences. These were ignored and the averages of the concrete strengths were used. In the beam moulds, mixes 1A and 1B were combined together but for the control cylinders the mixes were distinctly separate.

All the tests had the prestress transferred at 7 days except for Test 5 (Mix 2, shown in *italics* in Table 3.3). For Test 5, it was planned to cast Mix 1 first and then cast Mix 2 five days later. Both mixes were allowed to cure under similar conditions and the prestress was transferred at the same time for all the beams (ie. 7 days for Mix 1 and 2 days for Mix 2). The aim of the test was to achieve low strength concrete of about 25 MPa at transfer for all the beams but half the beams would have greater maturity being cured for a longer period of time. Trial mixes were used to determine the mixes for the actual casting. Unfortunately, Mix 2 (2 days) gave much lower strength but Mix 1 (7 days) had gained higher strength than anticipated from the trial mixes. The discrepancy was probably due to the small quantities used for the trial mixes. However, it could still be assumed that these two concrete mixes represented concrete of lower strength at transfer in the range of 20 to 30 MPa.

The single mix in Test 6 was workable initially for about 20 minutes with the large amount of superplasticiser used. It had 'collapsed' slump > 150 mm (definition according to Newbegin and Bruere [Ryan and Samarin (1992)]) when it reached the laboratory. However, with a large amount of added silica fume, the mix was very sticky and set fairly rapidly. Final finishing of the concrete surface with a steel trowel was difficult as a layer of gel-like crust covered the top of the beams as the concrete set. Attempts to smooth the surface broke this 'skin' and it adhered to the trowel leaving a rough surface behind. As a consequence, the surfaces had to be smoothened after the concrete had hardened.

The concrete control cylinders were submerged in a water tank and cured in a standard manner under full moisture saturation but the beams were air cured. Obviously, the cylinder strength did not truly represent the concrete in the beams due to different curing conditions, but there were already differences between the beams and cylinders in terms of size and shape. Air-cured beams (50 mm x 100 mm) would most likely experience different moisture loss compared to air-cured cylinders.

Sieve analysis was performed on the aggregate used in the in-situ mixes. Table 3.4 gives the results of this analysis:

Table 3.4 Percentage Mass Retained for the Sieve Analysis

Aggregate Type	20 mm	10 mm	7 mm	Sand
Size of Sieve	300 mm	200 mm	200 mm	200 mm
Mass of Sample	1293.30 g	583.00 g	563.80 g	201.50 g
Mass Retrieved	1293.26 g	582.79 g	563.38 g	201.46 g
Sieve Aperture Size (mm)				
19.0				
9.5	97.8	7.8		
4.75	2.0	89.2	49.0	
2.36	0.1	3.0	46.6	
1.18	0.0	0.0	3.5	0.1
0.600	0.1	0.0	0.3	18.7
0.300	0.0	0.0	0.2	61.7
0.150	0.0	0.0	0.1	18.2
0.075	0.0	0.0	0.1	1.2
Pan	0.0	0.0	0.2	0.1

3.10 Strain Corrections For Shrinkage And Creep

Shrinkage beams (D3 and L3) were used in each test to determine the shrinkage corrections for other beams within the same test. Although the shrinkage beams were unreinforced and experienced unrestrained shrinkage, the average shrinkage values along their lengths were used as the corrections for the prestressed beams. Theoretically, the ends of the beams would experience greater amount of shrinkage due to loss of moisture from the end faces of the beams as well as the top and side faces of the beams. However, differential shrinkage along the length was found to be negligible due to the small cross-sectional size of the beams.

Creep acts concurrently with shrinkage and relaxation and there is interdependence. Shrinkage and relaxation losses both reduce the stress in the tendon over time and they cause creep loss to decrease with time. In addition, there is also a decrease in creep caused by the increase in the modulus of elasticity of the concrete with increasing age.

The difference between strains at two periods of time (say between transfer strains and 28-day strains), gives the change in the concrete strains due to creep and shrinkage. By estimating shrinkage, the amount of creep can also be found (assuming thermal effects can be estimated or ignored if insignificant). These effects should be considered for long term monitoring of the transmission length.

Creep was made up of a proportion of the initial strain but it was not removed from strain distributions in the tests because any change in L_p would be mainly due to this, which was the interest of the long term monitoring. Shrinkage was also not corrected for in the determination of the transmission length since subtracting off a constant shrinkage value throughout the strain distribution of a beam would not change the length of L_p. Shrinkage correction was only important when a true strain distribution due to transfer and creep was required but not when determining the transmission length.

3.11 Strain Corrections For Curvature Effects

It was realised that most of the beams in the tests were slightly curved concave upwards. The curvature was not desirable but it could not be eradicated. This curvature may be attributed to a few factors:

(a) the depth of about 50 mm for the beams was small. A small variation in the depth along the beam could change the eccentricity of the wire. Eccentricity of 1.0 mm for the 7 mm dia. wires could cause a change in longitudinal strain of 100 $\mu\varepsilon$ (for concrete strength of 20 MPa).

(b) the wires were set to be at mid-depth of the beams using a timber spacer block to just fit into the space between the wire and the base surface of the formwork. Minor discrepancies could occur along the beams as the formwork was only adjusted to the correct height relative to the tensioned tendons at locations where the formwork had adjustable threaded support stands (Figure 3.5). In between these supports, the wire heights were still checked but there were slight unavoidable vertical misalignments.

(c) concrete towards the top of the beams was less compacted compared to the concrete at the base of the beams. Moreover, bleed water and paste ended up at the top of the beams. These contributed to differential stiffness between the top and bottom of the beams. With the base of the beam stiffer than the top, slight concave upward bending was not unexpected.

It had to be ascertained whether correcting for the curvature strains was necessary. Some of the beams were found to have both ends uplifted by as much as 8 mm at transfer. Assuming the beams had circular arc curvature, the corresponding estimated strain would be 360 $\mu\varepsilon$. Although some of the beams could have significant strains due to curvature compared to the strains due to the concentric prestress, the curvature in these beams were generally gradual and smooth. This inferred that there was fairly uniform curvature along the length of beams. Hence, the corrections would not have a significant effect on the location of the ends of the transmission lengths.

Two sets of strain distributions were determined for each beam in some of the early tests. One set of distributions was corrected for curvature strains while another set did not have any corrections. A method for working out the curvature strains is detailed as follows. Each beam was set on a flat steel section and markings were made at 150 mm spacings along the beam. A steel ruler was laid across the top of the beam at the markings and a vernier scale was used to read the distance between the ruler and the steel section. After taking these readings for all the marked points, the depth of the beam at each of the marked locations was measured. The difference between the two sets of readings gave the uplift displacements along the beam due to curvature. A suitable deflection equation (y) was fitted to these points and the curvature strains were evaluated from the product of the second derivative of this deflection equation (y") and half the depth of the beam $\{\varepsilon_{curv} = \kappa \frac{d}{2} = y'' \frac{d}{2}\}$. The curvature strains were then subtracted from the initial concrete strains. In some cases, curvature correction seemed to improve the process of interpreting the strain diagrams but in other instances it made it worse.

Apart from this, another method was established to obtain the deflection values. A straight-edge was fixed at an arbitrary distance from the beam tilted on its side. The distance between the straight-edge and the bottom face of the beam was measured for set intervals along the whole length of the beam. This also gave a deflection versus distance relationship but again the corrections did not consistently help in determining the transmission length. The reasons for this were probably due to:

(a) the beams had variations in depth not only along their lengths but also across their widths. Thus measurements made to the nearest 0.1 mm using a vernier scale would have been futile.

(b) there was the occasional protrusion or surface roughness which affected the accuracy of the readings.

(c) a fourth order polynomial was chosen for the deflection function to fit the deflection values. A second order equation would have yielded a constant curvature value (ie. y" = constant). Maybe either of these was appropriate for some beams but not others. It was impossible to know the exact deflection curve for every beam.

With these uncertainties, the original strain profiles were used without correcting for the curvature. Moreover, almost all transmission lengths for Tests 1 to 3 were found to be the same using either the curvature corrected or uncorrected strain profiles. Even when there was a difference, it was not more than 50 mm, which was assumed to be tolerable.

CHAPTER 4

Analysis and Discussion of Results

4.1 Introduction

The results and observations obtained from the experimental investigation are presented and discussed in this chapter. Results for transmission length (L_p) and pull-in (Δ_o) from previous research work done by other investigators are also considered with the intention of creating a better overall view concerning the effects of various factors on the transmission length and pull-in.

As a prelude to more in-depth discussions, problems encountered when determining the transmission lengths from longitudinal strain curves are revealed and ways of overcoming them are explained.

There were two or four pull-in values and occasionally more than one transmission length value evaluated for a beam end. Logically, there should be the same number of transmission lengths and pull-ins as the number of wires. Average values were used for the pull-ins and where there was more than a single transmission length, the average value was assigned to this end for analysis.

Concrete crushing and Brazilian tensile strengths obtained from cylinder tests are also presented in this chapter.

Comparisons of L_p and Δ_o for different surface conditions (plain or indented), wire sizes, types of releases (gradual, sudden or shock) and a range of concrete strengths were made using hypothesis tests as described in Chapter 2.

Relationships between L_p and Δ_o for the different wires used are established. The significance of such relationships is to allow for the determination of the transmission length by only measuring the pull-in occurring at the ends of pretensioned prestressed beams. If indeed such relationships exist, then there may not be a need to directly monitor beams for their transmission lengths. This would be extremely useful for quality control purposes as pull-ins are much easier and quicker to determine than transmission lengths but it is the transmission lengths which are of interest to the designer and not the pull-ins.

The subsequent issues addressed were the effects of concrete compressive strength on transmission length and pull-in. AS 3600 (1988) proposed 32 MPa at transfer as the minimum grade of concrete in order to attain good prestress transfer. This was considered in conjunction with the establishment of limiting values for both the transmission length and pull-in for each type of wire tested.

There are many factors which affect the transmission length as explained earlier. However, not all of these factors can be quantified. An attempt was made to use dimensional analysis to derive formulae for estimating the transmission lengths for plain and indented wires.

Finally, the chapter concludes with the comparisons of transmission lengths and pull-ins at 3 and 6 months to the corresponding measurements at transfer.

4.2 Evaluated Transmission Lengths And Measured Pull-ins

The transmission lengths were determined from strain profiles given in Appendix A and were complemented by plots of percentage load transfer versus pull-in provided in Appendix B. Since the determination of the transmission lengths was subject to personal interpretation of the

longitudinal concrete strain distributions, the values obtained from the tests were the best estimates that the author could comprehensively produce.

Unlike the transmission lengths, the pull-in readings were obtained directly from a pair of calibrated callipers (Westoby (1991)). The accuracy of the pull-ins were dependent on the accuracy of the measuring dial gauge mounted on the pull-in callipers. The gauge could be read to 0.01 mm. With a magnification of almost two times by the callipers (absolute gauge length (mm) = 35.05 + 1.9767 x Calliper reading), the accuracy of the device was to approximately 0.02 mm. The slip between the steel and concrete does not occur smoothly but takes place in minute intermittent movements, especially with indented wires. If after 10% of full load transfer, the wire tendon had not begun to slip, the callipers would only measure the decrement in the gauge length due to its shortening. The expected shortening for each 10% of load was about 0.02 mm or equivalent to one division accuracy on the dial gauge. Therefore, for the initial readings with small percentages of transfer (say 10-30%), the callipers may not measure the pull-in accurately. Pull-ins obtained for the tests were generally 0.40 mm or greater (265 out of 303 measured pull-ins at transfer were in the range of 0.40 to 3.65 mm), which meant an error of less than 5% in the measured pull-ins. It is appreciated that the error could be as large as 14% (for one pull-in only, 0.14 mm for 2G-D4-CD, ie. wire C at the dead end of beam 2G-D4).

Base (1957, 1958) used dial gauges accurate to 2.5 x 10^{-3} mm but they were fixed to the wires for the duration of monitoring. With the many pull-ins measured by the author for each of the current tests, it was not possible to attach a dial gauge to each individual wire. Hence, the pair of pull-in callipers was used. It was assumed that the accuracy to 0.02 mm was adequate for the technique. A very accurate dial gauge would not have given better results since there must have been inevitable minor differences in the actual placement of the callipers each time it was used to measure over a same gauge length. A dial gauge reading for any particular location was only recorded after two or more readings showed a single consistent value.

Ideally, there should be one transmission length and one pull-in for each wire transferring the prestress. Pull-ins were recorded for all the

individual wires but only single lines of demec points were used for determining the longitudinal concrete strain distributions (except beams 1G-D1 and 1G-L1). Naturally, one value of transmission length was obtained for each beam end. Assigning the same transmission length value to all the wires within one end would place extra confidence on the single transmission length value obtained, from a statistical point of view. Therefore, it was resolved to use a single transmission length value matched with an average pull-in value for each end of every test beam. However, there were a few instances where two transmission lengths were estimated from a single strain distribution (this will be discussed in Section 4.6). In each case, the mean of the transmission lengths was used.

There were 56 pretensioned prestressed concrete beam specimens altogether. With two transmission lengths for each beam, there were 112 results at transfer. Similarly, there were also 112 corresponding average pull-ins. Of these, 16 transmission lengths were approximated as the ends of the transmission lengths were not distinct, and 2 results (for beam 5G-L1) could have been affected by the overlapping of the end zones. As for the pull-ins, 4 results were not obtainable in Test 1 after transfer because the attached clips for monitoring the pull-ins were disturbed when storing the beams away. Also, pull-in readings for six beam ends in Test 7 could not be measured as the impact from the shock transfers either shattered or moved the pull-in measuring attachments.

The results for transmission lengths and pull-ins are summarised graphically in Figure 4.1. The full details of the results for the tests are given in Appendix C. It is obvious from both bar charts in Figure 4.1 that the transmission lengths and pull-ins obtained for the four types of wires used can vary significantly over large ranges of values. The large scatter within a set of transmission length or pull-in values for each type of wire is due partly to factors which affect the prestress transfer and partly to the inherent variability in concrete. It is also apparent that the 7 mm dia. Plain wire gave some of the largest transmission lengths and pull-ins. The 7 mm dia. Belgian wire performed better than the 7 mm dia. Plain wire but it was only used for gradual releases in beams with reasonably high concrete strengths. The 7 mm dia. Plain wire was used as for the 7 mm dia. Belgian wire, and it was also used in rapid releases and with low concrete strength. There was no indication of obvious difference between the 5 mm dia. Plain and 5 mm dia. Chevron wires.

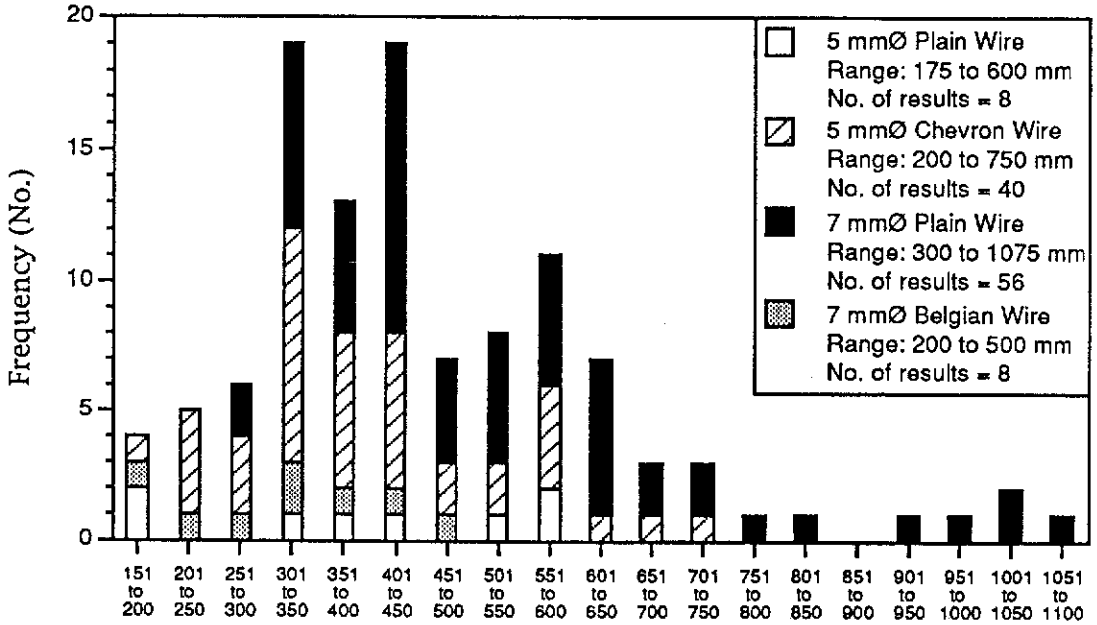

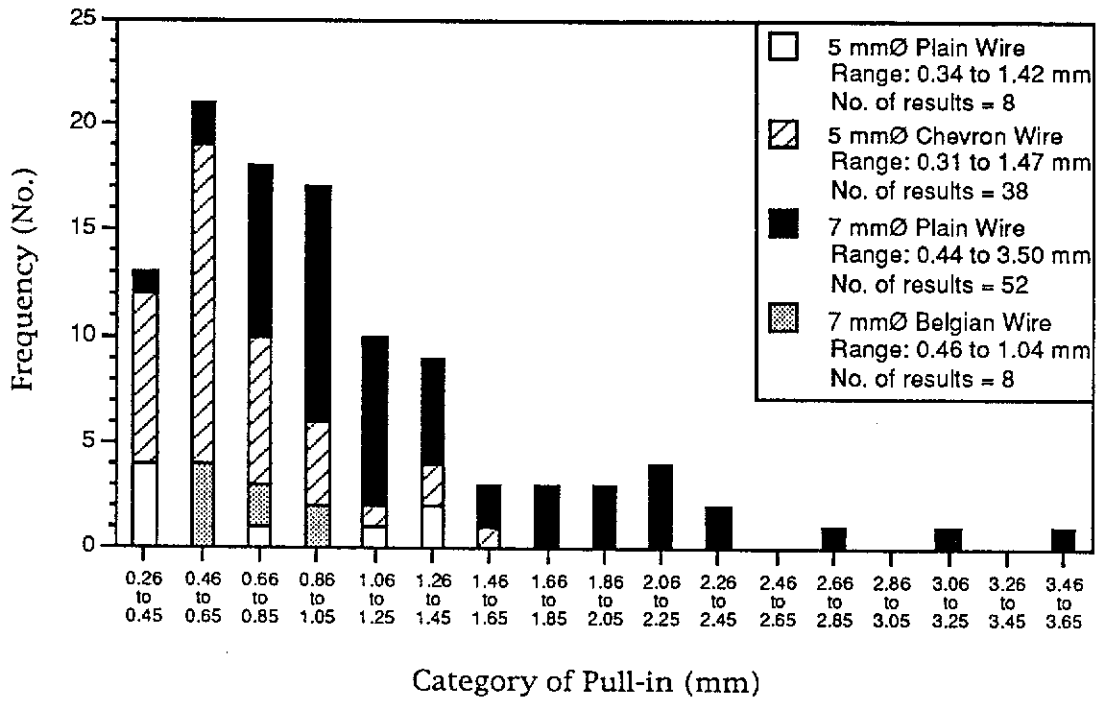

Figure 4.1 Summary of Transmission Lengths and Average Pull-ins for Beams in Current Tests

Due to time constraints, only Tests 1 and 2 have been monitored up to six months. Tests 3 to 6 were monitored for three-month periods whereas Test 7 only had readings taken at 7 and 28 days. All tests had transfers at 7 days except Test 5 where one half of the beams, 5G-D1, 5G-D2, 5G-L1 and 5G-L2, were loaded at 2 days. They were cast 5 days after beams 5G-D4, 5G-D5, 5G-L4 and 5G-L5 were cast with a different mix. The measurements for Test 5 were registered at 2 and 7 days (at time of transfer), at 23 and 28 days, and at 3 months after casting. The 5-day difference in age at about 3 months was considered to be insignificant and all the results were recorded as 3-month results.

4.3 Transmission Lengths And Pull-ins From Previous Investigations

To compare with the data obtained from the current laboratory tests, results from previous investigations were compiled. These results are represented by frequency bar charts in Figure 4.2, and the full summary of the results is given in Appendix D. Some researchers gave ranges for the transmission lengths and pull-ins instead of individual values and in such cases, single average values were used in plotting the charts.

A single transmission length of 2000 mm found by Marshall (1949) for 5 mm dia. Plain wire was not included in Figure 4.2 as it was badly affected by poor consolidation of concrete. The 5 mm dia. Plain and 5 mm dia. Belgian wires were the most common types of wire tendons used. Some of the previous investigators gave results for unknown or less well known wire types and these were generalised as "other types" of wires in simplifying the graphical representations.

There is greater scatter in transmission lengths for the 5 mm dia. Plain wire than for the 5 mm dia. Belgian wire. The scatter for the 5 mm dia. Plain wire was due to transmission lengths from the Cement and Concrete Association (Base (1958)) which had a range of 152-813 mm.

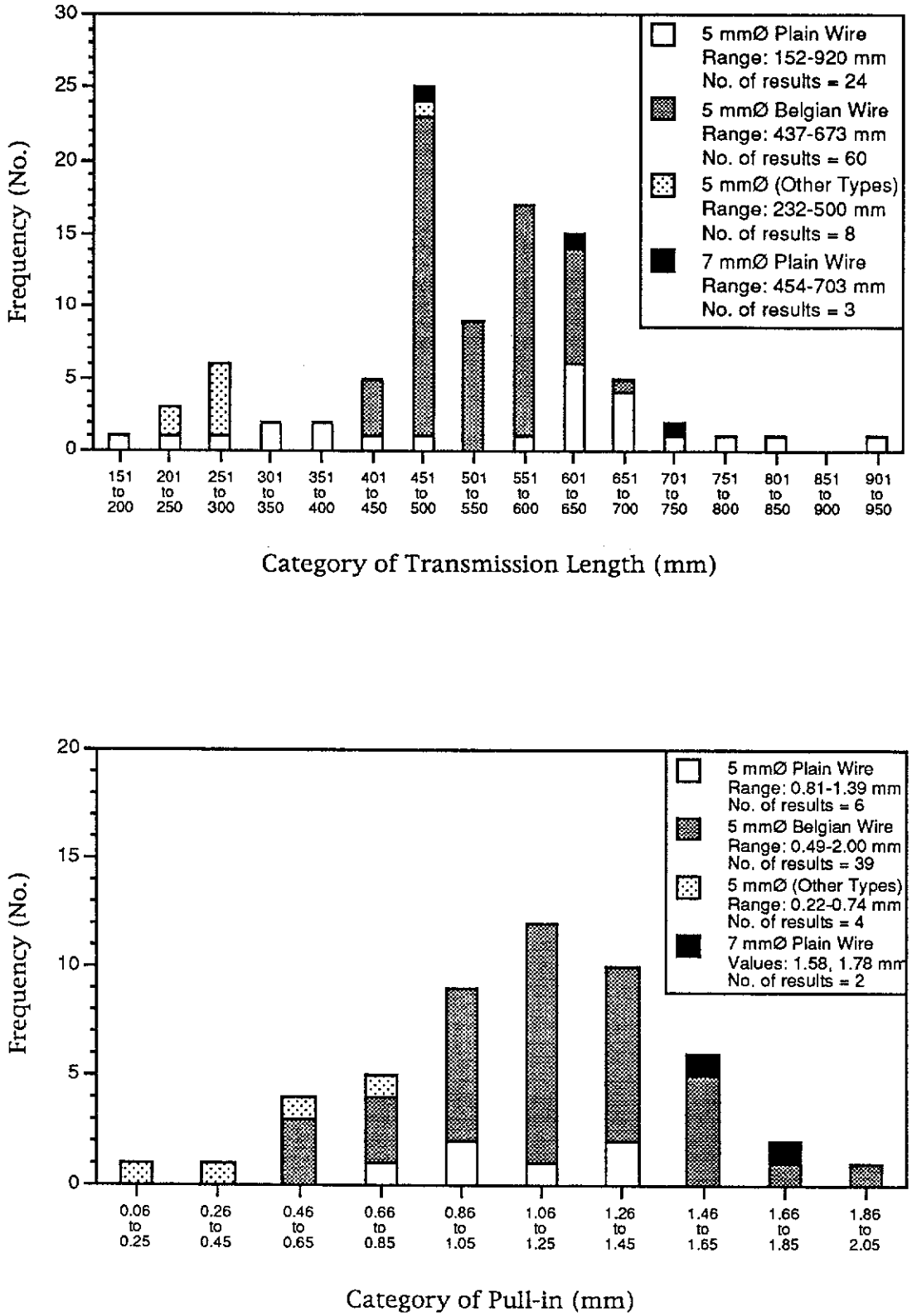

Figure 4.2 Summary of Transmission Lengths and Pull-ins from Previous Investigations

4.4 Dependence Of Transmission Length On The Location Of Measurement

Previous investigators tended to use a single transmission length for each beam, ie. the transmission length was the average for both ends of a beam. This was not adopted in the current tests. The author believes the two ends are uniquely separate although there is technically no major difference between them. There are four beam ends in one prestressing line of this experimental investigation, ie. the DD (dead end of the dead end beam), DL, LD and LL ends. For gradual release, the distribution of force should be the same at all of these four locations since there is negligible frictional force between the concrete beam and the base formwork. From the data obtained, there was no trend to suggest that the resulting transmission lengths were dependent on the location from which they were determined. However, there is a difference for the shock release cases.

Transmission lengths are given in Figure 4.3 for beams 7R-D1, 7R-L1, 7R-D4 and 7R-L4 which were shock released by angle grinding wire tendons between the dead and live end beams. For beams 7R-D1, 7R-D4 and 7R-L4, it is seen that the direct effect of shock had caused greater transmission lengths at the active ends compared to the passive ends. The transmission length at the live end of beam 7R-L1 was estimated from a strain distribution with an indistinct end to the transmission length (700 mm was assigned to this end but it could be as small as 550 mm). The associated uncertainty may explain for the seemingly smaller transmission length of 575 mm at the active end.

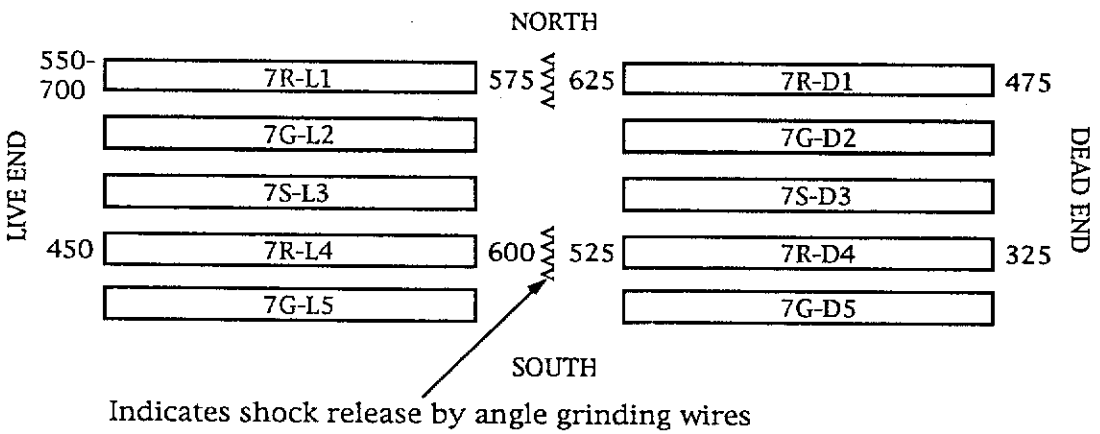

Figure 4.3 Transmission Lengths for Beams Shock Released in Test 7

4.5 Profiles Of Longitudinal Strain In Concrete

4.5.1 Expected and Experimental Strain Values

For simplicity, only the strain profiles at the time of transfer for the test beams will be considered in this section. The shapes of these profiles do vary from one beam to another. Theoretically, each profile should have a section of constant strain in the middle of the beam and two end zone sections of monotonically decreasing strains moving towards the beam ends. Figure 4.4 depicts a typical curve that illustrates this behaviour.

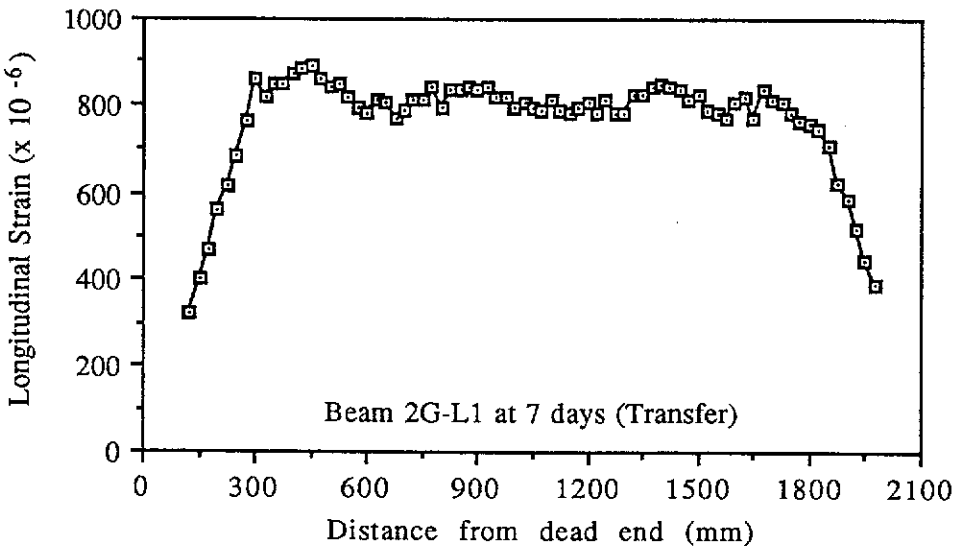

Figure 4.4 Typical Profile of Longitudinal Strain in the Test Concrete Beams

However, there were some profiles that had peculiar phenomena which were difficult to explain. Therefore, it was appropriate to provide a basis where these profiles could be checked for the reasonableness of the strain values. Since the force transferred could be estimated from a single load cell attached to one of the wires for each pair of live and dead end beams, the expected maximum constant longitudinal concrete strain could be estimated using Equation 4.1 (as an approximation, the prestressing steel area of 1.6% of A_c was ignored):

$$\text{Expected Strain} = \frac{P}{A_c E_c} \qquad \text{Equation 4.1}$$

where E_c is the modulus of elasticity of concrete. The mean secant modulus of elasticity of concrete at the appropriate age from Clause 6.1.2(a) of AS 3600 (1988), E_{cj}, was used to determine the modulus of elasticity of concrete.

It is noted that E_{cj} was calculated based on an assumed value of 2400 kg/m^3 for the density of concrete. AS 3600 actually covers concrete strength up to 50 MPa but it was used to determine the modulus of elasticity for the current tests with concrete strength up to 65.1 MPa. Apart from these assumptions, E_{cj} is only accurate to within ±20% of the actual value, which means that the expected strain can vary between -17% and +25%. For simplicity, it was assumed that the strains also had an error band of ±20%.

From the strain profiles, the experimental strain values at the inner ends of the two transmission lengths within each beam were evaluated and compared to the mean of the expected strain value. Table 4.1 gives a summary of the expected and experimental strains for the beams tested.

In the current tests, it can be seen that most of the actual strains from the strain profiles were greater than the expected strains estimated for the ideal concentric loading condition (out of 56 average strain values, there were only 7 which were within the given range of expected strains and another 25 which came within 100 με of the upper bounds of the expected strains). In particular, Tests 2, 3, 5 and 6 indicated that there can be strains much larger than those predicted by the calculated values. In two of the worst cases involving beams 6G-D5 and 6G-D1, the average of each pair of measured strains was 99% and 91% above the upper bounds of the expected strains. All other beams had less than 60% difference between the measured strains and the upper bounds of the expected strains. Some of the significant results are shown in ***italics*** in Table 4.1. In retrospect, the modulus of elasticity of concrete should have been determined experimentally in the compressive cylinder tests but this was not done as the significantly large discrepancies were not anticipated.

The large strains for beams 5G-D1, 5G-D2 and 5G-L2 in Test 5 could be attributed to small concrete strength of 20.1 MPa. The smaller stiffness of the concrete would have resulted in greater deformations compared to the 26.8 MPa concrete in beams 5G-D4, 5G-L4, 5G-D5 and 5G-L5.

In addition, beams 5G-D1 and 5G-L1 were loaded up to 89% of the concrete compressive strength (or 0.89 f_{cp}) and beams 5G-D2 and 5G-L2 were loaded to 0.88 f_{cp} (ie. large stress/strength ratios). A strength of approximately 25 MPa (0.7 f_{cp} with the same prestress load) was expected for the concrete but the actual strength at transfer turned out to be 20.1 MPa for these four beams. They were overloaded but there was no sign of any visible surface cracks (caused by bursting stress) for the duration of monitoring.

Table 4.1. Expected and Experimental Longitudinal Strains

Beam	f_{cp} (MPa)	E_{cj} (GPa)	P (kN)	Expected Strains (x 10^{-6}) (± 20% error)	Longitudinal Strain at Inner End of L_p (x 10^{-6})	
					Dead End	Live End
1G-D1	49.0	35.4	91.8	520 ± 100	750	620
1G-L1					600	660
1G-D2			89.2	500 ± 100	710	630
1G-L2					610	580
1G-D4			91.7	520 ± 100	730	620
1G-L4					710	730
1G-D5			91.8	520 ± 100	820	620
1G-L5					620	770
2G-D1	48.7	35.3	91.6	520 ± 100	660	620
2G-L1					850	780
2G-D2			88.0	500 ± 100	650	850
2G-L2					***920***	***850***
2G-D4	35.8	30.3	88.0	580 ± 120	820	720
2G-L4					780	670
2G-D5			90.4	600 ± 120	790	790
2G-L5					750	710
3R-D1	53.1	36.8	90.4	490 ± 100	550	750
3R-L1					670	690
3R-D2			89.6	490 ± 100	660	690
3R-L2					690	680
3R-D4	33.8	29.4	86.4	590 ± 120	***910***	***960***
3R-L4					***1000***	***830***
3R-D5			91.4	620 ± 120	***1070***	***850***
3R-L5					***940***	***990***
4G-D1	48.7	35.3	91.0	520 ± 100	740	750
4G-L1					770	730
4G-D2			90.8	510 ± 100	820	640
4G-L2					700	650
4G-D4			84.4	480 ± 100	760	670
4G-L4					680	600
4G-D5			87.2	490 ± 100	750	780
4G-L5					730	670
5G-D1	20.1	22.7	89.4	1130 ± 230*	***1500***	***1520***
5G-L1					1380	1340
5G-D2			85.6	1080 ± 220*	***1940***	***1730***
5G-L2					1070	***1460***
5G-D4	26.8	26.2	84.8	720 ± 140°	1000	790
5G-L4					750	900
5G-D5			90.2	770 ± 150°	710	680
5G-L5					890	870
6G-D1	65.1	40.8	93.6	460 ± 90	***1120***	***980***
6G-L1					***920***	740
6G-D2			91.2	450 ± 90	690	***1030***
6G-L2					830	720
6G-D4			92.4	450 ± 90	640	***1080***
6G-L4					820	660
6G-D5			88.6	430 ± 90	***990***	***1080***
6G-L5					790	650
7R-D1	53.9	37.1	91.0	490 ± 100	750	560
7R-L1					580	720
7G-D2			92.4	500 ± 100	630	560
7G-L2					640	660
7R-D4			90.4	490 ± 100	590	620
7R-L4					670	630
7G-D5			90.6	490 ± 100	580	640
7G-L5					710	730

Note: * indicates strain estimated using E_{cj} (from AS 3600 (1988)) with an incorporated 43% increase to correct for a stress/strength ratio of 0.89.

° indicates strain estimated using E_{cj} (from AS 3600 (1988)) with an incorporated 12% increase to correct for a stress/strength ratio of 0.67.

The prestress load was initially established such that a nominal 35 MPa concrete beam was loaded to 0.5 f_{cp}. This same total prestress force (88 kN) was used for all the tests in order to keep the tendon stress constant. The modulus of elasticity according to AS 3600 is actually the secant modulus for concrete at 50% of f_{cm} (Darvall (1989) and the Concrete Design Handbook (1991) referred to 0.5 f'_c whereas Warner, Rangan and Hall (1991) referred to 0.45 f'_c) and beyond this amount of stress, the modulus decreases significantly. With a decreased modulus of elasticity, the expected strains would be larger than those in Table 4.1. It also explains the large experimental strains in beams 5G-D1, 5G-D2 and 5G-L2.

Lydon (1979) stated a normalised stress-strain curve which was established by Baldwin and North (1969) as follows:

$$\frac{\sigma}{\sigma_{max}} = \frac{\varepsilon}{\varepsilon_o} e^{1-\varepsilon/\varepsilon_o} \qquad \text{Equation 4.2}$$

where, σ = stress in the concrete
σ_{max} = maximum stress reached in the concrete
ε = strain in the concrete
ε_o = strain corresponding to the maximum stress σ_{max}

By substituting a ratio of 0.89 for $\frac{\sigma}{\sigma_{max}}$ (as for beams 5G-D1 and 5G-L1) into Equation 4.2, the ratio of $\frac{\varepsilon}{\varepsilon_o}$ was 0.59. Similarly, a ratio of 0.23 for $\frac{\varepsilon}{\varepsilon_o}$ corresponded to 0.50 for $\frac{\sigma}{\sigma_{max}}$. Equation 4.2 can be rearranged to give:

$$\frac{\sigma}{\varepsilon} = \frac{\sigma_{max}}{\varepsilon_o} e^{1-\varepsilon/\varepsilon_o} = \text{secant modulus} \qquad \text{Equation 4.3}$$

Subsequently, the ratio of the secant modulus at x% of σ_{max} over the secant modulus at 50% of σ_{max} (AS 3600) can be found as:

$$\frac{E_{x\%}}{E_{50\%}} = e^{\varepsilon_{50\%}/\varepsilon_o - \varepsilon_{x\%}/\varepsilon_o} \qquad \text{Equation 4.4}$$

Using Equation 4.4, it was found that $\frac{E_{89\%}}{E_{50\%}}$ was 0.70 (Park and Paulay (1975) displayed a set of stress/strength versus concrete strain curves by Rusch (1955) and the ratio of $\frac{E_{89\%}}{E_{50\%}}$ was found to be 0.68 using the curve for concrete strength of about 22 MPa). The strains estimated using E_{cj} were factored by $\frac{1}{0.70}$ (=1.43).

Beams 5G-D4, 5G-L4, 5G-D5 and 5G-L5 with 26.8 MPa concrete were loaded up to 0.67 f_{cp}. The strains given for these beams include a 12% increase above the strain values estimated using E_{cj} ($\frac{\varepsilon_{67\%}}{\varepsilon_o} = 0.35$ and $\frac{E_{67\%}}{E_{50\%}} = 0.89$).

In conclusion to the issue of decreased modulus of elasticity, the expected concrete strains is likely increase by 43% and 12% above the calculated mean values of E_{cj} from AS 3600 for the beams in Test 5 with 20.1 and 26.8 MPa strengths respectively. These increases were included in the expected strains for these beams in Table 4.1 (indicated by * and ∘ respectively). The expected strains for all other beams were considered to be reasonably estimated using E_{cj} with no such correction applied since the stresses in these beams were 0.54 f_{cp} or less.

However, the decrease in E_{cj} does not account for a 41% increase in the average experimental concrete strain above the upper bound of the expected strain for beam 5G-D2. The author attributes the remaining increase in 5G-D2 to curvature and local effects.

Section 3.11 described how curvature of a prestressed beam (uplifted by 8 mm at each end) would give an increase in strain of 360 με at the top of the beam due to curvature. Although the end uplifts were not determined for beam 5G-D2 immediately after transfer, the average of these values were found to be 18 mm at 6 months after casting. Uplifts of 10 mm were estimated for 2-day transfer from the 6-month values using a factor of $\left(\frac{1+\emptyset_{cc.transfer}}{1+\emptyset_{cc.6month}} \cdot \frac{E_{c.6month}}{E_{c.transfer}}\right)$ involving creep effect (creep factors obtained from AS 3600) and the change in modulus of elasticity for concrete over time. This factor was multiplied to the 6-month average uplift to obtain the uplift at 2-day transfer. The 10 mm uplifts correspond to a curvature strain of 460 με. If the upper bound for the strains in beam 5G-D2 was 1300 με, then the concrete strain could reach 1760 με (= 1300 με + 460 με) but the largest measured strain for this beam was 1940 με (average for both ends was 1840 με). The remaining discrepancy may be attributed to local curvature effects due to change in stiffness of the concrete across the depth of the beam, variability of depth and differential strains due to eccentricity of tendon.

The following describes how the change in stiffness of concrete across the depth due to poorer consolidation of concrete at the top of the beams can occur. Figure 4.5 shows a portion of a concentrically loaded test beam undergo unequal straining at the top and bottom surfaces. The change in the modulus of elasticity of concrete from E_b at the bottom to E_t at the top was assumed to be linear across the depth.

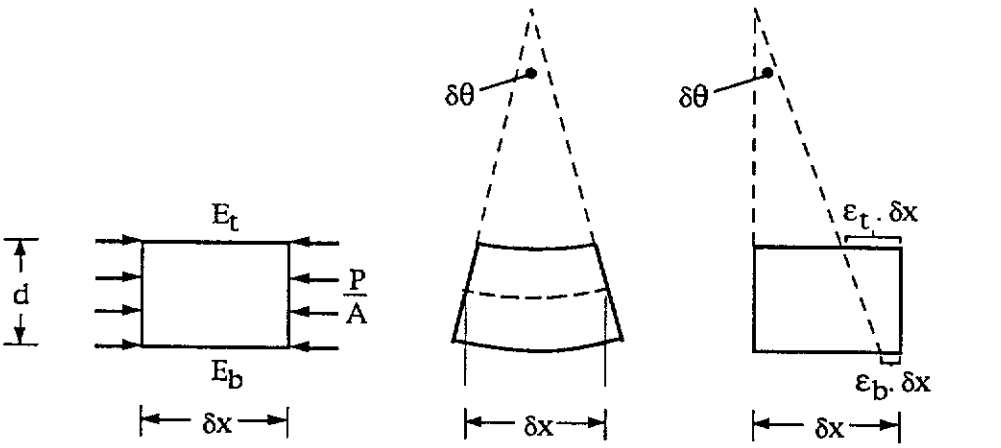

Figure 4.5 Deformations due to Unequal Concrete Stiffnesses Across the Depth of A Pretensioned Prestressed Test Beam (partially adapted from Figure 4.7 of Warner, Rangan and Hall (1991))

The curvature strain due to unequal stiffnesses is derived from an approximate strain state in the beam due to concentric prestress; the approach is similar to the derivation for flexural strains in reinforced concrete by Warner, Rangan and Hall (1991). The elemental length of δx shortens more at the top than at the bottom of the beam. The curvature κ can be expressed as:

$$\kappa = \frac{\delta\theta}{\delta x} \qquad \text{Equation 4.5}$$

The angular change $\delta\theta$ over the length of δx can be stated as:

$$\delta\theta = \frac{(\varepsilon_t\,\delta x - \varepsilon_b\,\delta x)}{d} \qquad \text{Equation 4.6}$$

where, ε_b = compressive strain at the bottom of the beam = $\dfrac{P}{A_c E_b}$

ε_t = compressive strain at the top of the beam = $\dfrac{P}{A_c E_t}$

It is assumed that E_t can be stated as a proportion ψ of E_b:

$$E_t = \psi . E_b \qquad \text{Equation 4.7}$$

By substituting Equations 4.6 and 4.7 into Equation 4.5, the curvature can be expressed as:

$$\kappa = \frac{P}{A_c d}\left(\frac{1}{\psi E_b} - \frac{1}{E_b}\right) \qquad \text{Equation 4.8}$$

The proportion of decrease in the modulus of elasticity from E_b to E_t resulting in the curvature of κ is:

$$\text{Proportion of decrease in } E_b = 1 - \psi = \left(\frac{\kappa E_b A_c d}{P + \kappa E_b A_c d}\right)$$

Equation 4.9

Non-destructive Schmidt rebound hammer test was performed on beam 5G-D2 to investigate whether there was change in stiffness across its depth. It is appreciated that the rebound number (R) is related to the hardness of concrete and is only indicative of the concrete strength to certain extent. A larger R value infers greater concrete strength and stiffness. The beam was laid with one side on a flat concrete floor and readings were taken near the top and bottom surfaces. The test could not be used to find absolute strength values because the readings would have been affected by the small beam size and also the rebound effect would be dependent on the concrete floor response. Results from the test are given in Table 4.2:

Table 4.2 Rebound Hammer Number

Location	Distance from the dead end (mm)																			
	100	200	300	400	500	600	700	800	900	1000	1100	1200	1300	1400	1500	1600	1700	1800	1900	2000
Top	21	26	27	31	32	32	29	28	26	26	30	27	25	24	25	25	27	26	28	27
Bottom	30	27	30	32	32	30	29	30	32	35	30	27	27	28	28	30	29	28	30	29

The top of the beam has an average R of about 27 whereas the bottom has an average of 30. There was greater variation in the top readings but in general, the top had smaller R values. This insinuates smaller stiffness at the top of the beam. Ratios of R values (top over bottom) are in the range of 0.70 to 1.06. Concrete strength has a linear relationship to the rebound value while modulus of concrete is related to the square root of the

strength. As a crude approximation, it is predicted that the ratio of modulus of elasticity at the top of the beam over the modulus of elasticity at the bottom of the beam could be as small as $\sqrt{0.70}$ (= 0.84).

Arbitrarily considering $E_t = 0.84\ E_b$ (ie. 16% decrease in the modulus of elasticity), a curvature strain of about 80 $\mu\varepsilon$ was calculated from Equation 4.9 (where $\varepsilon_{curv} = \kappa \frac{d}{2}$ and E_{cj} was assumed for E_b). Therefore, about 80 $\mu\varepsilon$ of the 460 $\mu\varepsilon$ due to curvature effects in beam 5G-D2 may be attributed to the difference in the modulus of elasticity of concrete across its depth.

Only beam 2G-L2 has a percentage difference between the average experimental strain and the upper bound expected strain greater than for beam 5G-D2 (with the exception of beams in Test 6). The 48% difference would have also been caused by curvature effects.

Curvature could have been reduced if a square cross-section was used instead of the adopted rectangular cross-section. It would have been even better to have used larger cross-sectional beams. Both these options were considered and dismissed before the tests were performed. A square cross-section would require multi-wire beams to have some wires stressed on top of other wires (ie. to have layered steel) instead of having all the wires aligned in one plane. A significant amount of alterations to the existing formwork and testing frame would have been necessary to implement this. Increasing the size of the beams would mean that more wires had to be used to be able to provide the concrete compression of 0.5 f_{cp}.

Curvature in all of the beams resulted in greater strains measured on the top surface and the curvature strain distributions varied along the length of the beams. Even if corrections were to be applied, the determination of the correction values was not straightforward. The most important factor for the correction was the selection of the 'deflection versus longitudinal distance' function which correctly represented the deformation of the beams before the curvature strains could be evaluated. It was impossible to know the exact relationship for each beam. To complicate the problem even more, the depth varied along the length of each beam due to construction inaccuracies and the wire tendons were not always perfectly located at mid-height of the beams. The attempts to correct for the curvature were abandoned as the author did not believe that the supposed corrections were justifiably accurate.

In Test 6, there were many transverse minute plastic shrinkage cracks along the top of the beams which resulted in some large strains as shown in Table 4.1. This explains why the strain values in Test 6 were some of the greatest compared to other tests despite the fact that the high strength concrete used should have given much lower strains. The average experimental strains were in the range of 37% to 99% above the corresponding upper bounds of the expected strains. The effect of these cracks will be elaborated in Section 4.5.5.

Carrasquillo, Nilson and Slate (1981) derived an empirical equation for determining the modulus of elasticity of concrete which was based on normal weight concrete with 28-day standard cylinder compressive strength in the range of 21 to 83 MPa:

$$E_c = 3320\sqrt{f_{cm}} + 6900 \quad \text{(MPa)} \qquad \text{Equation 4.10}$$

Using Equation 4.10, the moduli of elasticity for the medium strength concrete in Test 2 and high strength concrete in Test 6 were calculated as 30.1 and 33.7 GPa respectively. These values are much lower than those predicted by AS 3600. Assuming the values from Equation 4.10 to be correct, then the expected concrete strains are 17% and 21% greater than the values given in Table 4.1 for Tests 2 and 6. In fact, this equation consistently predicts smaller modulus of elasticity over the range of concrete strength where it is applicable compared to AS 3600.

There are a few incongruent strain profiles which evolved from the tests. Events which happened during the tests were used to rationally explain these disparities. The following sub-sections will demonstrate some of these inconsistencies.

4.5.2 Small Fluctuations in Strain Profiles

A well-conditioned and smooth strain profile is ideal but is rarely obtained from tests. Many of the test beams showed minor fluctuations in the strain readings from one end of the beam to the other (as shown previously in Figure 4.4).

Concrete being a heterogeneous material has properties which depend on the ingredients making up the mix. There can be local variations in the quality of the material and minor local changes in the stiffness have to be expected. This would account for most of the small fluctuations in the strain diagrams.

4.5.3 Large Fluctuations in Strain Profiles

Large fluctuations occurred in 6 of the 56 strain profiles. Beams 3R-D1, 3R-D2, 3R-D4 and 3R-D5 clearly exhibited this interesting phenomenon but not beams 3R-L1, 3R-L2, 3R-L4 and 3R-L5. Figure 4.6 shows a typical curve with the large fluctuations. The strain profile for 3R-D4 shows that the magnitude of the fluctuations could be up to 300 με, which would be 42% of the upper bound of the expected strain value. Other beams exhibiting this type of behaviour to a lesser extent were 5G-L2 and 7R-L4. The occurrence of this type of fluctuations in some beams and not others is perplexing.

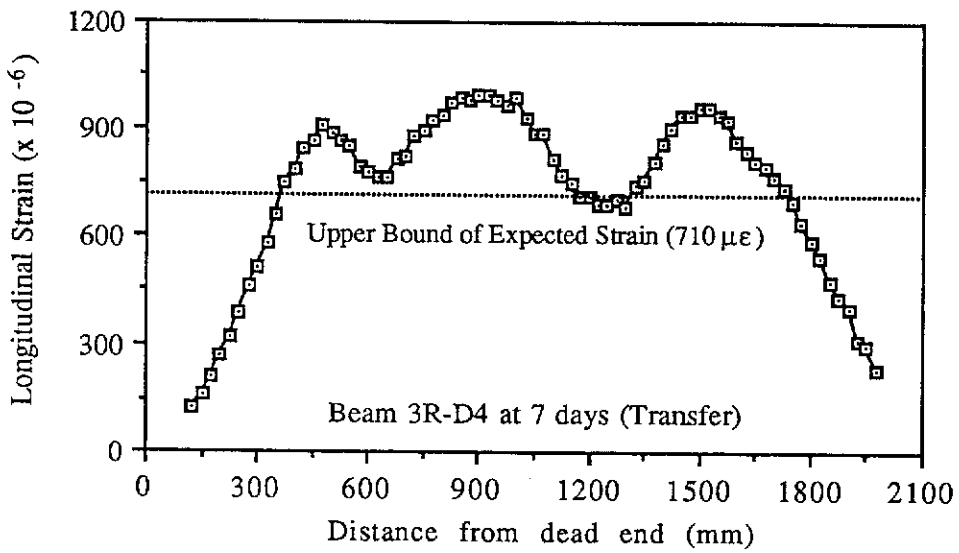

Figure 4.6 Example of Large Fluctuations in the Longitudinal Strain Distribution

The "waviness" in the profile suggests either there was a variation in the prestress force, radical local changes in curvature, or changes in the stiffness of the concrete along the length of the beam. It is not possible to have variation in the prestress force between the established end zones

within a beam. There was no detectable sudden change in curvature in the beams having the large fluctuations. It was also not possible for the change in stiffness alone to be able to cause such large variations in strains.

The casting procedure was scrutinized and the formwork inspected after Test 3. The consolidation of concrete was carried out by the author personally for every test and hence, there should not be any reason why other tests did not have this problem.

The anomaly to note is that all the dead end beams in Test 3 had the fluctuations. Logically, it should have also occurred in the live end beams since the prestress forces were the same and the consolidation and screeding procedures were the same. Perhaps the reason for the fluctuations was related to the location of the beam and the type of release. The transfer in Test 3 was implemented by instantaneously opening the control release valve such that the jacks supporting the movable head retracted immediately to destress the wires. The live end beams would see the rapid release of forces before the dead end beams. Whether this subtle difference contributed to the unusual behaviour in the dead end beams remains unanswered.

The average transmission lengths and pull-ins for the beams in Test 3 are given in Table 4.3.

Table 4.3 Average Transmission Lengths and Pull-ins at Transfer for Test 3 Concrete Beams

Dead End Beam Mark	Average Transmission Length (mm)	Average Pull-in (mm)	Live End Beam Mark	Average Transmission Length (mm)	Average Pull-in (mm)
3R-D1	450	0.92	3R-L1	438	0.94
3R-D2	425	0.41	3R-L2	363	0.47
3R-D4	525	1.11	3R-L4	544?	1.41
3R-D5	525	1.57	3R-L5	825?	2.02

Note: (?) indicates that there was uncertainty in determining the transmission length.

The dead end average pull-ins are less than those for the live end although the transmission lengths did not indicate this. There is no conclusive

evidence to prove that the dead end beams in Test 3 behaved differently compared to the duplicate live end beams under sudden prestress transfer.

The author did not find any other factor which may explain the large fluctuations in strain profiles for these beams.

4.5.4 Overlapping of Transmission Lengths

The strain profile for beam 5G-L1 indicates that the transfer of prestress force at one end of the beam interfered with the other end of the beam. When this occurred, there was significant slip along the whole tendon and the concrete strains at the inner ends of the end zone regions decreased. Strain profiles in Figure 4.7 illustrate the decrease in concrete strains but the peak value in beam 5G-L1 was the same as the strain value in the duplicate beam 5G-D1 at this location.

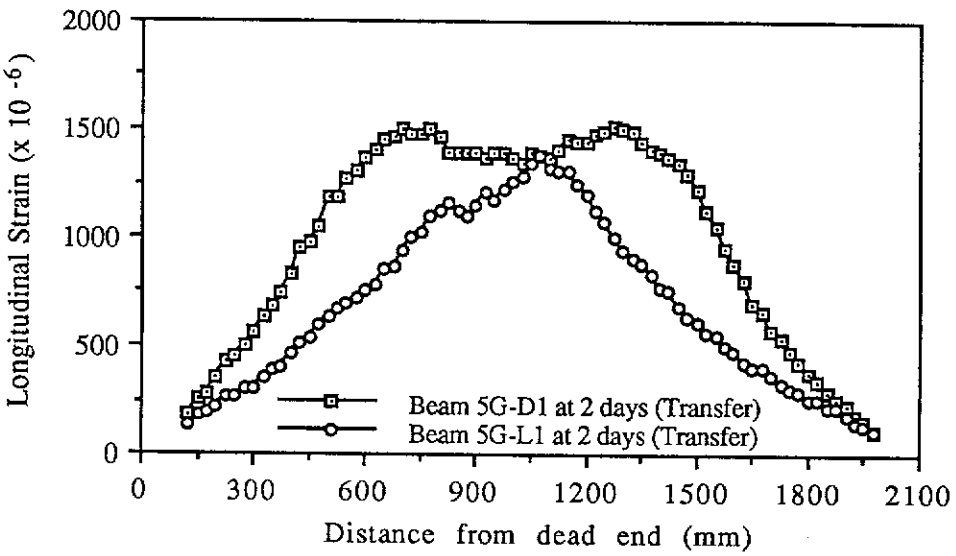

Figure 4.7 Longitudinal Strain Distributions for Beams 5G-D1 and 5G-L1 at Transfer

Beam 5G-D1 had maximum strain values in the range of 1340 to 1510 με. However, beam 5G-L1 seemed to have just reached the maximum prestress at one single point near the centre of the beam. The maximum value was 1380 με and it was assumed that the wire tendons had just attained the maximum prestress force. If the strains in beam 5G-L1 were much lower

than those in beam 5G-D1, then the strain profile could not be used to determine the transmission lengths of the beam. The two end zones had just overlapped into each other's region. Therefore, the results from this beam were recorded and used with caution. The transmission lengths were 1075 and 1025 mm for the dead and live ends respectively. Corresponding pull-ins were 2.23 and 2.35 mm for dead end, and 2.96 and 2.66 mm for the live end. The pull-ins suggest slightly better transfer at the dead end but the transmission lengths indicated otherwise. Despite this discrepancy, all the measurements of transmission lengths and pull-ins for beam 5G-L1 highlighted the fact that transfer was poor.

4.5.5 Inconsistent Strains Caused by Microcracking

Strain profiles in Test 6 were some of the worst for the whole of the laboratory testing programme. Instrumentation was the same and the demec discs used could not have been different since all of them were made in a single batch before the commencement of Test 1.

The results were checked to ensure that there was no blunder in data observation which had caused the inconsistencies. Long term monitoring was a way by which the strain profiles were checked. Generally, the shape of the curves changed little with time. The 28-day and 3-month curves showed similar characteristics as the 7-day curve and this confirmed the reality of the irregular behaviour in these beams. The strain curves which were most difficult to interpret were for beams 6G-D1, 6G-D2, 6G-D4 and 6G-D5. The strain curves for other beams in this set of test were more consistent. The strain curve for beam 6G-D4 in Figure 4.8 shows large erratic fluctuations in the strain values.

A high strength concrete mix with large quantities of silica fume and superplasticiser was used in Test 6. The silica fume accelerated the setting process and its high affinity for water resulted in little bleed water at the top surfaces of the beams. Hence, evaporation caused these surfaces to dry up and plastic shrinkage cracks to form. Upon inspection of the beams after casting and during the concrete hardening process, these hairline plastic shrinkage cracks were observed to be transverse to the lines of demec points used for strain measurement. Ropke (1982) suggested that

fine water spray applied to the surfaces would either close the cracks or at least reduce their penetration. In an attempt to control the development of these cracks, wet hessian bags were laid on top of the beams.

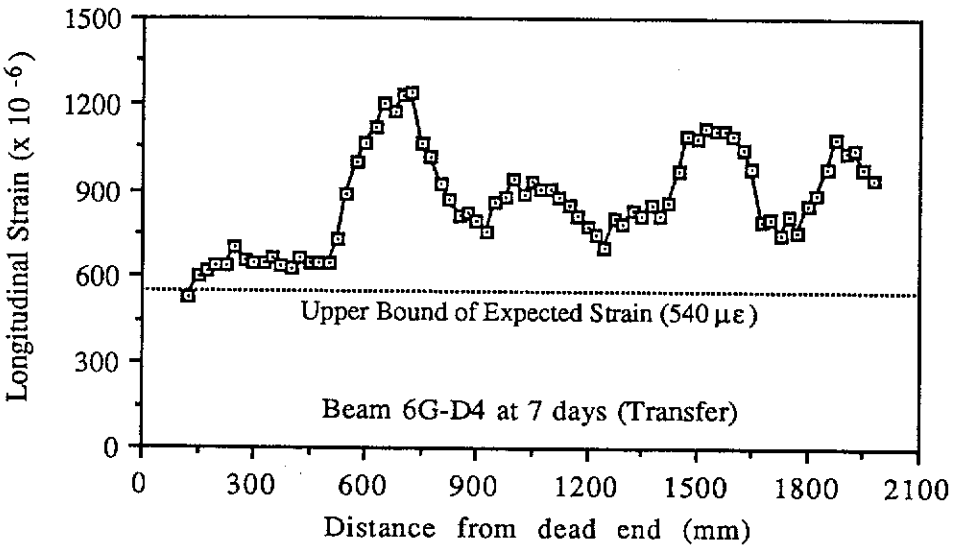

Figure 4.8 Longitudinal Strain Distribution for Beam 6G-D4 at Transfer

The existence of these cracks meant that the demountable mechanical gauge did not only measure the concrete compressive strains but also the closing up of a multitude of cracks between any two demec target points during transfer. Although there was no obvious large crack at any spot on any of the beams, the accumulation of many small cracks would amount to the same effect as a large crack.

The major protrusions in Figure 4.8 show the effect of these cracks. The maximum increase in strain due to cracking was estimated to be 400 με. Such a change in strain over a 200 mm gauge length infers a total crack width of 0.08 mm.

The obscurity in the strain profiles due to the presence of the cracks led to the difficult task of determining the correct transmission lengths for the beams. This problem was overcome by augmenting the information available from the strain curves by using the percentage load transfer versus pull-in diagrams (or simply referred to as 'pull-in diagrams'). These diagrams were also good indicators of the quality of prestress transfer and if used to complement the strain profiles, provide a very

powerful means of estimating the actual transmission lengths. In fact, all of the transmission lengths obtained from each and every strain profile were checked for the amount of pull-in related to the particular beam end. The plot of percentage load transfer versus pull-in for the dead end of beam 6G-D4 is presented in Figure 4.9.

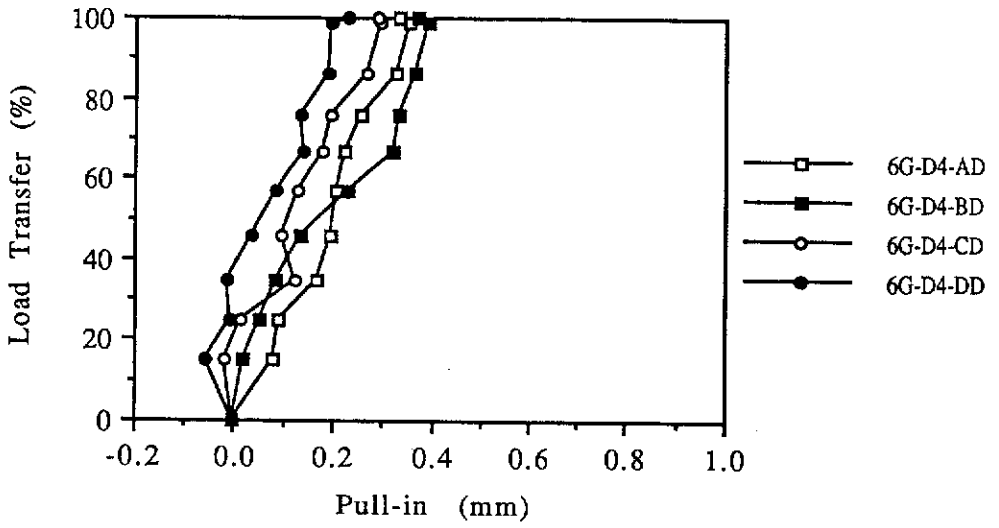

Figure 4.9 Plot of Load Transfer (%) vs. Pull-in (mm) for Wires at the Dead End of Beam 6G-D4 at Transfer

With user error from not handling the callipers perfectly the same every time a reading is taken for a particular location, small inaccuracies have to be expected and this explains for the negative readings in the pull-in diagrams. Negative values imply pull-out of the wire but in reality, this does not occur at transfer (although Base (1957, 1958) indicated 5 mm dia. wires can have small outward movements with respect to the end faces of prestressed beams over time).

From Figure 4.9, it is obvious that the pull-in values were small, lying in the range of 0.23 to 0.37 mm for full transfer of prestress. Hence, this information was used to enhance the prediction of the transmission lengths in Figure 4.8. The author estimated the transmission lengths of the dead and live ends to be 200 and 225 mm respectively, by comparing with other beams where pull-ins were similar.

The other beams within Test 6 which were affected by microcracking were analysed in a similar fashion to beam 6G-D4.

4.5.6. Sloping Strain Profiles

There were 13 out of 56 strain profiles which had a strain region in the centre of a beam clearly sloping towards either end of the beam. Figure 4.10 shows the central portion of the strain profile sloping downwards towards the live end of the beam.

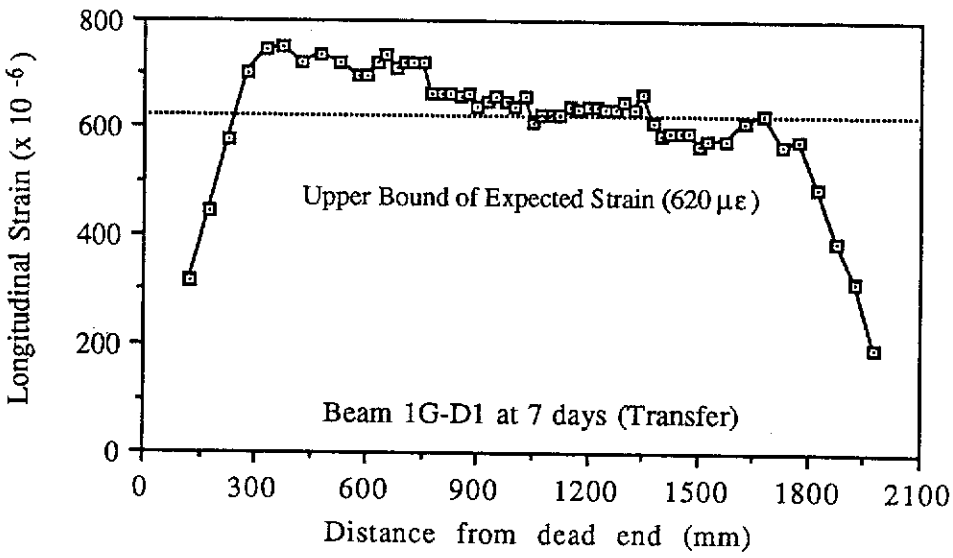

Figure 4.10 Longitudinal Strain Distribution for Beam 1G-D1 Sloping Downwards Towards Live End

Beams with relatively different maximum strains between both ends at transfer were 1G-D5, 1G-L5, 2G-D2, 3R-D1, 3R-D5, 3R-L4, 4G-D2, 5G-D2, 5G-D4, 5G-L2, 5G-L4 and 7R-D1 (150 to 220 με), and 5G-L2 (390 με). This type of behaviour could be caused by unequal curvature near the ends of the beams. If a beam was to curl more in the proximity of the dead end than at the live end due to greater change in concrete stiffness over the depth and due to eccentricity of the wires, then it would have larger strains at this end. Eccentricities of 1 mm above the neutral axis near the live end and 1 mm below the neutral axis near the dead end would account for about 200 με. In addition, inhomogeneity of concrete properties causing change in the modulus of elasticity between the dead and live ends could have contributed to the difference in strain. The 390 με difference in beam 5G-L2 was partly due to the fact that the beam had inexplicably large fluctuations as described in Section 4.5.3.

Some of the beams in Test 6 also had significant differences in strains at both ends but these discrepancies were attributed to microcracking.

4.6 Strain Profiles Affected By Unequal Pull-ins In Wires

For most of the beams, the pull-ins were similar for wires within the same end of a beam. However, there were beams where the pull-ins were different. This caused problems as one or more wires would transfer at a shorter length compared to the other wire(s) present. Chandler (1984) explained how unequal rates of transfer can cause 'masking' of a strain profile, thus resulting in obscure ends of transmission lengths.

Figure 4.11 depicts the combination of two transfer strain curves due to two wires. Strain curve 2 has a transmission length significantly greater than strain curve 1. Assuming there are only two wires in the beam considered, the strain readings taken from a line of demec points laid in the centre of the beam between the two wires would actually measure the effects of compression due to a combination of both the wires. The shorter transmission length tends to be 'masked' by the longer one. There should be a point on the resultant curve within the end zone section where there is a noticeable 'kink' which represents the end of the shorter

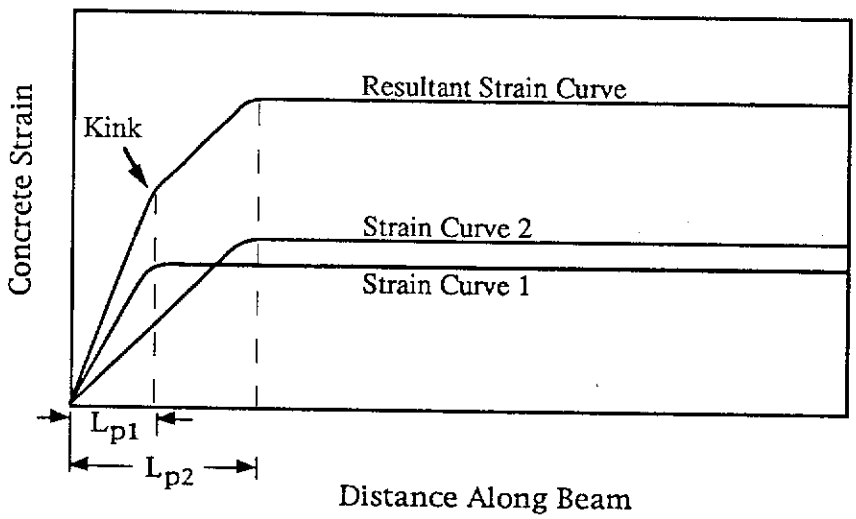

Figure 4.11 Combination of Two Strain Distributions Due to Wires Exhibiting Different Rates of Transfer

transmission length. If there are radically different values for the pull-ins of the wires, then it is only reasonable to assign L_{p2} to the larger pull-in value and L_{p1} to the smaller value. Theoretically, there should not be any difference in the transfer within the same beam but such unpredictable behaviour can be quite real. A set of strain and pull-in curves are given in Figure 4.12 (a) and (b) for beam 2G-D1, which exemplifies this behaviour.

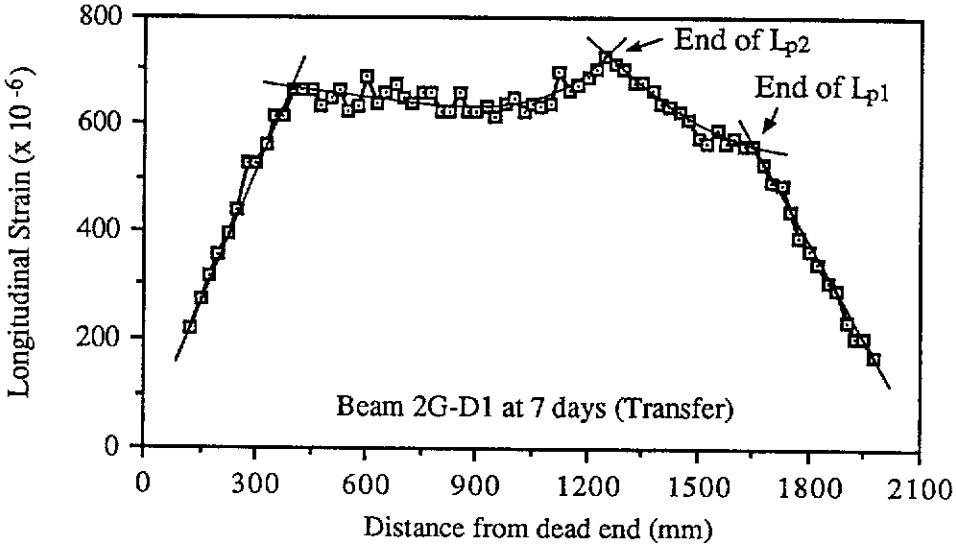

(a) Longitudinal Strain Distribution for Beam 2G-D1 At Transfer

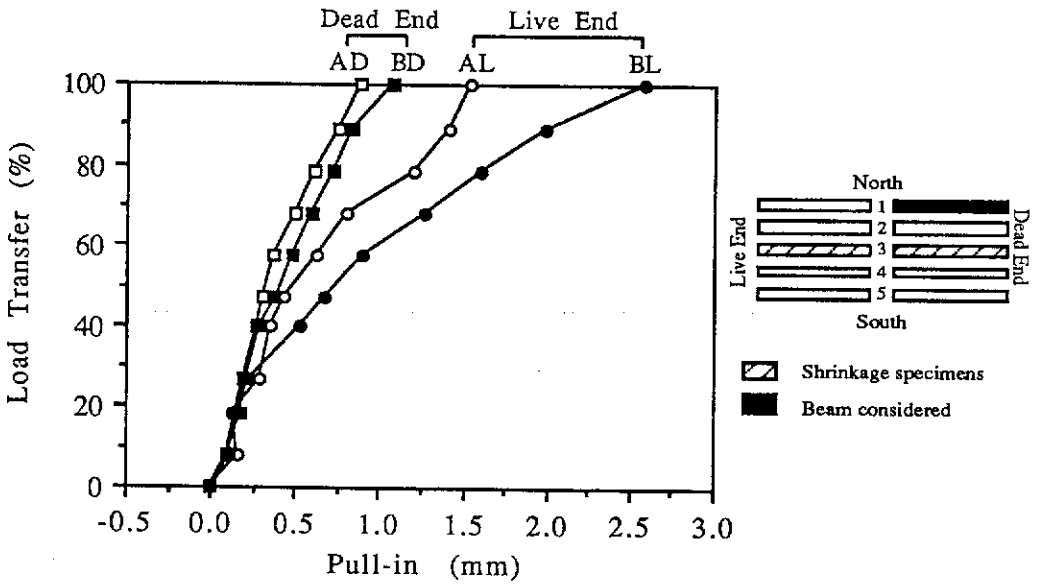

(b) Plot of Load Transfer (%) vs. Pull-in (mm) for Beam 2G-D1 At Transfer

Figure 4.12 The Longitudinal Strain Distribution and Pull-in Plot for Beam 2G-D1

The pull-ins for the two 5 mm dia. Plain wires at the live end were quite different, with 1.54 mm for wire A and 2.58 mm for wire B. The rate of prestress transfer was expected to be slower for wire B compared to wire A. The transmission lengths of L_{p1} and L_{p2} (from Figure 4.12 (a)) were estimated as 450 and 850 mm for wires A and B, respectively.

Beam ends such as 1G-L2 (L), 1G-L5 (D), 2G-L1 (D), 2G-L1 (L) and 3R-L4 (L) were also considered in a manner similar to 2G-D1 (L). It then becomes an arduous task trying to compare results as some beam ends have single transmission lengths whereas others have two to correspond to two or four pull-ins. As there were only single lines of demec points used for strain measurements, it became questionable whether it was possible to assign the same transmission length to each of the individual pull-in measurements. Practically, a single demec line should really produce only one result for each end of the beam. Since the accuracy of determining some of the transmission lengths was dubious, by assigning one value to multiple wires would over-rate the accuracy of the transmission length. This may place a false sense of confidence on the transmission lengths when applying statistical tests on small samples whose levels of confidence are dependent on the degrees of freedom (or the number of raw score). For this reason, average transmission lengths and pull-ins were used.

4.7 Concrete Strength

Both compressive and tensile strengths were determined from cylinder crushing and Brazilian tensile tests performed on a Farnell testing machine (Serial No. 12104/1000) which had a capacity of 2000 kN. The tests were carried out in accordance to AS 1012.9 (1986) and AS 1012.10 (1985) respectively and the results are summarised in Table 4.4. For further details of the individual test results, the reader is referred to Appendix E.

Table 4.4 Average Values for Concrete Cylinder Compressive and Tensile Strengths

Test No.	Beam Mark	Compressive Strength, f_{cm} (MPa)					Brazilian Tensile Strength, f_{ct} (MPa)				
		2 days	7 days	23 days	28 days	3 mths	2 days	7 days	23 days	28 days	3 mths
1	All beams		49.0		59.7	69.5		3.67		4.05	4.40
2	2G-D1, 2G-D2, 2G-L1, 2G-L2 and 2S-D3		48.7		56.1	65.8		3.33		4.03	4.80
	2G-D4, 2G-D5, 2G-L4, 2G-L5 and 2S-L3		35.8		47.4	48.6		3.17		3.39	3.55
3	3R-D1, 3R-D2, 3R-L1, 3R-L2 and 3S-D3		53.1		64.6	71.7		4.20		4.24	5.09
	3R-D4, 3R-D5, 3R-L4, 3R-L5 and 3S-L3		33.8		41.4	51.3		3.19		3.79	3.59
4	All beams		48.7		62.8	70.6		3.63		4.55	4.57
5	5G-D1, 5G-D2, 5G-L1, 5G-L2 and 5S-D3	20.1		39.2		45.3	2.29		3.36		3.47
	5G-D4, 5G-D5, 5G-L4, 5G-L5 and 5S-L3		26.8		32.2	37.3		2.33		2.69	2.70
6	All beams		65.1		88.6			4.95		4.95	
7	All beams		53.9		59.0			3.94		4.24	

4.8 Statistical Analysis On Current Test Data

Transmission lengths and pull-ins were compared for beams with different factors which affect the transfer of prestress from the steel tendons to the concrete. The following details the results of hypothesis tests done. Only two-sample tests in conjunction with t- or z-distributions were used in the statistical inference tests. The alternative hypothesis chosen was based on the assumption that the mean of the transmission lengths (or pull-ins) for one population was significantly different from the mean of another population (one-tailed test was used unless noted otherwise). The null hypothesis proposed that the mean values were the same. The t or z statistic was checked to find out the level of confidence at which the null hypothesis could be rejected. Confidence levels (C.L.) were

considered at 99.99, 99.9, 99.5, 99.0, 95.0 and 90.0%. Rejection of the null hypothesis at 99.99% C.L. would indicate that the data values of the two samples were strongly inconsistent with the null hypothesis. Acceptance of the null hypothesis at 90% C.L. would imply that there is insufficient evidence from the samples to dispute the possibility of the null hypothesis.

In the following sub-sections, when the null hypothesis was accepted, the populations compared were considered to be the same; hence, the use of the equal ('=') sign. Otherwise, data values of one population were considered greater than ('>'), less than ('<') or unequal to ('≠') the data values from the other population. Appendix F presents the full details of the statistical inference tests. Concrete strengths considered were at the time of transfer.

4.8.1 Comparisons of L_p and Δ_o for Plain Wires with L_p and Δ_o for Indented Wires (Gradual Release Only)

These comparisons were to determine whether there was any significant difference between plain wires and wires which had either Belgian or Chevron pattern indentations. There were four sets of comparisons carried out and the outcomes were as follows (the sample size, mean value (mm) and standard deviation (mm) are given in brackets {} for each set of data):

(A) Test 4 only (48.7 MPa concrete)

(i) 7 mm dia. Plain wire vs. 7 mm dia. Belgian wire

L_p (Plain) = L_p (Belgian) 90% C.L.

$\{n = 4, \bar{L}_p = 519, s = 143\}$, $\{n = 4, \bar{L}_p = 413, s = 78\}$

Δ_o (Plain) > Δ_o (Belgian) 99% C.L.

$\{n = 8, \bar{\Delta}_o = 1.44, s = 0.46\}$, $\{n = 8, \bar{\Delta}_o = 0.90, s = 0.09\}$

(ii) 5 mm dia. Plain wire vs. 5 mm dia. Chevron wire

L_p (Plain) > L_p (Chevron) 90% C.L.

$\{n = 4, \bar{L}_p = 519, s = 118\}$, $\{n = 4, \bar{L}_p = 400, s = 35\}$

Δ_o (Plain) > Δ_o (Chevron) 99.99% C.L.

$\{n = 16, \bar{\Delta}_o = 1.18, s = 0.30\}$, $\{n = 16, \bar{\Delta}_o = 0.59, s = 0.09\}$

(B) Test 6 only (65.1 MPa concrete)

(i) 7 mm dia. Plain wire vs. 7 mm dia. Belgian wire

L_p (Plain) > L_p (Belgian) 95% C.L.

$\{n = 4, \bar{L}_p = 363, s = 43\}$, $\{n = 4, \bar{L}_p = 269, s = 55\}$

Δ_o (Plain) > Δ_o (Belgian) 99.5% C.L.

$\{n = 8, \bar{\Delta}_o = 0.74, s = 0.16\}$, $\{n = 8, \bar{\Delta}_o = 0.51, s = 0.08\}$

(ii) 5 mm dia. Plain wire vs. 5 mm dia. Chevron wire

L_p (Plain) = L_p (Chevron) 90% C.L.

$\{n = 4, \bar{L}_p = 294, s = 125\}$, $\{n = 4, \bar{L}_p = 281, s = 83\}$

Δ_o (Plain) > Δ_o (Chevron) 99.9% C.L.

$\{n = 16, \bar{\Delta}_o = 0.40, s = 0.07\}$, $\{n = 16, \bar{\Delta}_o = 0.32, s = 0.06\}$

(C) Test 2 (48.7 MPa) and Test 4 (48.7 MPa)

(i) 7 mm dia. Plain wire vs. 7 mm dia. Belgian wire

L_p (Plain) = L_p (Belgian) 90% C.L.

$\{n = 8, \bar{L}_p = 481, s = 137\}$, $\{n = 4, \bar{L}_p = 413, s = 78\}$

Δ_o (Plain) > Δ_o (Belgian) 99% C.L.

$\{n = 16, \bar{\Delta}_o = 1.32, s = 0.53\}$, $\{n = 8, \bar{\Delta}_o = 0.90, s = 0.09\}$

(ii) 5 mm dia. Plain wire vs. 5 mm dia. Chevron wire

L_p (Plain) > L_p (Chevron) 95% C.L.

$\{n = 4, \bar{L}_p = 519, s = 118\}$, $\{n = 8, \bar{L}_p = 341, s = 71\}$

Δ_o (Plain) > Δ_o (Chevron) 99.99% C.L.

$\{n = 16, \bar{\Delta}_o = 1.18, s = 0.30\}$, $\{n = 32, \bar{\Delta}_o = 0.58, s = 0.10\}$

(D) Test 1 (49.0 MPa), Test 2 (48.7 MPa) and Test 4 (48.7 MPa)

(i) 7 mm dia. Plain wire vs. 7 mm dia. Belgian wire

L_p (Plain) > L_p (Belgian) 90% C.L.

$\{n = 24, \bar{L}_p = 489, s = 109\}$, $\{n = 4, \bar{L}_p = 413, s = 78\}$

Δ_o (Plain) > Δ_o (Belgian) 99.99% C.L.

$\{n = 48, \bar{\Delta}_o = 1.19, s = 0.42\}$, $\{n = 8, \bar{\Delta}_o = 0.90, s = 0.09\}$

The above comparisons were made such that transmission lengths or pull-ins used within a statistical test had similar or very close concrete compressive strength. The comparisons were to ascertain whether there was a difference between plain and indented wires and the results should not be affected by variation in concrete strength.

Set A only compared the transmission lengths and pull-ins obtained for beams in Test 4 only. Set B had similar comparisons for Test 6, which had transfer strength of 65.1 MPa. Since half of the beams in Test 2 and all the beams in Test 4 had transfer strength of 48.7 MPa, set C comparisons took advantage of the extra data from Test 2. Finally, Test 1 had a transfer strength of 49.0 MPa which was similar to the 48.7 MPa mixes in Tests 2 and 4. Set D was a combination of results from Tests 1, 2 and 4 for making comparisons for the 7 mm dia. Plain wire.

The results above show that in some instances, there is not much difference between the transmission lengths for plain wires and Belgian or Chevron indented wires (ie. insufficient evidence in these cases to disprove H_0: L_p (Plain) = L_p (Chevron or Belgian)). The confidence levels considered were the lower levels of 90.0% or 95.0% (from the range of 90.0% - 99.99%) and three of the comparisons indicate that there is not enough evidence to show any difference between plain and indented wires. There was significant scatter in those results and coefficients of variation $\left(V = \frac{\text{standard deviation}}{\text{mean}} \right)$ were in the range of 19% to 42% for L_p comparisons in (A)(i), (B)(ii) and (C)(i), which were large compared to all other comparisons which had coefficients of variation smaller than 23%.

On the other hand, the comparisons of the pull-ins provided a more positive picture. All the comparisons showed that the pull-in for plain wires were greater than for indented wires and the confidence levels were at 99.0% to 99.99%, where the rejection of the null hypotheses occur. It can be seen from Equation 2.58 that the test statistic (t_{test}) gives a critical value when the difference between the sample means is large, the sample standard deviations are small and/or the sample sizes (n_1 and n_2) are large. There were always less number of transmission lengths than pull-ins available for comparison (eg. comparison (A)(i) had 4 pairs of transmission lengths and 8 pairs of pull-ins). With large standard deviations and small sample sizes, the tests on the transmission lengths may not be sensitive enough to show the difference that the tests on the pull-ins indicate.

AS 3600 clearly prohibits the use of plain wires as they are expected to give long transmission lengths - an outcome not evident in these laboratory tests. It must be highlighted that all the statistical comparisons

made between plain and indented wires involved concrete strength in the range of 48.7 to 65.1 MPa. No comparisons could be made with smaller concrete strength at transfer. Transmission lengths obtained from Test 5 for concrete of 20-30 MPa were large compared to the rest of the other wires. The difference between transmission lengths for plain and indented wires with low concrete strength is expected to be relatively greater compared to those with high concrete strength. Further consideration of the difference between the plain and indented wires is given in Section 4.9.

Considering the comparisons of transmission lengths and pull-ins, indentations seem to have more impact on the rate of transfer than the overall length of L_p. There is evidence in the pull-in comparisons indicating it is better to use indented wires instead of plain wires for pretensioning. However, there is no specific guidance in the Australian Standards (AS 1310) with respect to the types of indentations which are acceptable.

4.8.2 Comparisons of L_p and Δ_o for Different Wire Sizes (Gradual Release Only)

Larger wire sizes generally produce greater transmission lengths and pull-ins. Fundamentally, only 5 mm and 7 mm dia. Plain wires could be compared to determine the effect of wire size since Chevron pattern was restricted to 5 mm dia. wire and Belgian pattern was available for 7 mm dia. wire only. However, if the significance of the type of indentation was ignored, then the results for the 5 mm dia. Chevron wire could be compared with those for the 7 mm dia. Belgian wire. The results of the statistical tests are given as follows:

(A) Test 4 only (48.7 MPa concrete)

(i) 5 mmØ Plain wire vs. 7 mmØ Plain wire

L_p (5 mmØ) = L_p (7 mmØ) 90% C.L.

$\{n = 4, \bar{L}_p = 519, s = 118\}$, $\{n = 4, \bar{L}_p = 519, s = 143\}$

Δ_o (5 mmØ) < Δ_o (7 mmØ) 90% C.L.

$\{n = 16, \bar{\Delta}_o = 1.18, s = 0.30\}$, $\{n = 8, \bar{\Delta}_o = 1.44, s = 0.46\}$

(ii) 5 mmØ Chevron wire vs. 7 mmØ Belgian wire

L_p (5 mmØ) = L_p (7 mmØ) 90% C.L.

$\{n = 4, \bar{L}_p = 400, s = 35\}$, $\{n = 4, \bar{L}_p = 413, s = 78\}$

Δ_o (5 mmØ) < Δ_o (7 mmØ) 99.99% C.L.

$\{n = 16, \bar{\Delta}_o = 0.59, s = 0.09\}$, $\{n = 8, \bar{\Delta}_o = 0.90, s = 0.09\}$

(B) Test 6 only (65.1 MPa concrete)

(i) 5 mmØ Plain wire vs. 7 mmØ Plain wire

L_p (5 mmØ) = L_p (7 mmØ) 90% C.L.

$\{n = 4, \bar{L}_p = 294, s = 125\}$, $\{n = 4, \bar{L}_p = 363, s = 43\}$

Δ_o (5 mmØ) < Δ_o (7 mmØ) 99.9% C.L.

$\{n = 16, \bar{\Delta}_o = 0.40, s = 0.07\}$, $\{n = 8, \bar{\Delta}_o = 0.74, s = 0.16\}$

(ii) 5 mmØ Chevron wire vs. 7 mmØ Belgian wire

L_p (5 mmØ) = L_p (7 mmØ) 90% C.L.

$\{n = 4, \bar{L}_p = 281, s = 83\}$, $\{n = 4, \bar{L}_p = 269, s = 55\}$

Δ_o (5 mmØ) < Δ_o (7 mmØ) 99.99% C.L.

$\{n = 16, \bar{\Delta}_o = 0.32, s = 0.06\}$, $\{n = 8, \bar{\Delta}_o = 0.51, s = 0.08\}$

The pull-ins consistently showed smaller values for smaller wires but there was no such evidence for the transmission length (ie. there was insufficient evidence from the transmission lengths to disprove H_o: L_p (5 mm dia.) = L_p (7 mm dia.)). All the wires were stressed to an initial stress of about 1200 MPa, therefore longer transmission lengths were expected for the 7 mm dia. wire. There were only four pairs of values available for each of the above L_p comparisons and the coefficients of variation were generally large (eg. V = 42% for 5 mm dia. Plain wire in (B)(i)).

Pull-ins compared had 8 or 16 values for each set of data and gave more reliable results. There is no doubt that the size of the wire affects the transfer of prestress by giving greater pull-ins for the larger wire.

It is the variability of the transmission lengths and the small amount of data available which are the main reasons for the insensitivity of the statistical tests on L_p.

4.8.3 Comparisons of L_p and Δ_o for Gradual, Sudden and Shock Releases

Three sets of comparisons were performed to determine whether there was significant difference in the transmission lengths and pull-ins when the wires experienced gradual, sudden or shock releases.

(A) Test 2 Gradual Release (48.7 and 35.8 MPa) vs. Test 3 Sudden Release (53.1 and 33.8 MPa)

(i) 7 mm dia. Plain wire (Test 2-48.7 MPa vs. Test 3-53.1 MPa)

L_p (Gradual) = L_p (Sudden) 90% C.L.

$\{n = 4, \bar{L}_p = 444, s = 139\}$, $\{n = 4, \bar{L}_p = 444, s = 123\}$

Δ_o (Gradual) > Δ_o (Sudden) 90% C.L. (anomalous result)

$\{n = 8, \bar{\Delta}_o = 1.21, s = 0.60\}$, $\{n = 8, \bar{\Delta}_o = 0.93, s = 0.39\}$

(ii) 7 mm dia. Plain wire (Test 2-35.8 MPa vs. Test 3-33.8 MPa)

L_p (Gradual) < L_p (Sudden) 90% C.L.

$\{n = 4, \bar{L}_p = 450, s = 82\}$, $\{n = 4, \bar{L}_p = 675, s = 201\}$

Δ_o (Gradual) < Δ_o (Sudden) 99% C.L.

$\{n = 8, \bar{\Delta}_o = 1.12, s = 0.21\}$, $\{n = 8, \bar{\Delta}_o = 1.79, s = 0.55\}$

(iii) 5 mm dia. Chevron wire (Test 2-48.7 MPa vs. Test 3-53.1 MPa)

L_p (Gradual) < L_p (Sudden) 95% C.L.

$\{n = 4, \bar{L}_p = 281, s = 31\}$, $\{n = 4, \bar{L}_p = 394, s = 90\}$

Δ_o (Gradual) > Δ_o (Sudden) 90% C.L. (anomalous result)

$\{n = 16, \bar{\Delta}_o = 0.58, s = 0.11\}$, $\{n = 16, \bar{\Delta}_o = 0.44, s = 0.08\}$

(iv) 5 mm dia. Chevron wire (Test 2-35.8 MPa vs. Test 3-33.8 MPa)

L_p (Gradual) < L_p (Sudden) 99.5% C.L.

$\{n = 4, \bar{L}_p = 300, s = 58\}$, $\{n = 4, \bar{L}_p = 534, s = 87\}$

Δ_o (Gradual) < Δ_o (Sudden) 99.99% C.L.

$\{n = 16, \bar{\Delta}_o = 0.48, s = 0.14\}$, $\{n = 16, \bar{\Delta}_o = 1.25, s = 0.30\}$

(B) Test 7 Gradual Release vs. Shock Release (53.9 MPa)

(i) 7 mm dia. Plain wire

L_p (Gradual) < L_p (Shock) 95% C.L.

$\{n = 4, \bar{L}_p = 413, s = 97\}$, $\{n = 4, \bar{L}_p = 594, s = 94\}$

Δ_o (Not available for comparison)

(ii) 5 mm dia. Chevron wire

L_p (Gradual) < L_p (Shock) 90% C.L.

$\{n = 4, \bar{L}_p = 344, s = 63\}$, $\{n = 4, \bar{L}_p = 475, s = 117\}$

Δ_o (Gradual) = Δ_o (Shock) 90% C.L.

$\{n = 16, \bar{\Delta}_o = 0.52, s = 0.10\}$, $\{n = 7, \bar{\Delta}_o = 0.55, s = 0.21\}$

(C) Test 3 Sudden Release (53.1 MPa) vs. Test 7 Shock Release (53.9 MPa)

(i) 7 mm dia. Plain wire

L_p (Sudden) < L_p (Shock) 90% C.L.

$\{n = 4, \bar{L}_p = 444, s = 123\}$, $\{n = 4, \bar{L}_p = 594, s = 94\}$

Δ_o (Not available for comparison)

Set A were comparisons made between wires with gradual and sudden releases. Test 2 had two concrete mixes of 35.8 and 48.7 MPa and it was intended to have concrete mixes with similar strengths for Test 3. The actual transfer strengths for Test 3 turned out to be 33.8 and 53.1 MPa, these were assumed to be reasonably close to the strength values in Test 2.

The second set of comparisons, B, involved results from Test 7 only; for the 7 mm dia. Plain wires, the pull-ins were not obtainable as the clips used for monitoring pull-in readings were shattered or displaced from the impact of the shock release. Finally, set C compared transmission lengths and pull-ins for sudden and shock releases.

Four out of six comparisons for L_p show that gradual release gave shorter transmission lengths than sudden or shock releases at 90% or 95% C.L.. Another comparison indicates a similar trend but at 99.5% C.L.. In contrast, only two pull-in comparisons indicate smaller pull-ins from using gradual transfer. Two comparisons even demonstrate that gradual release gave greater pull-ins than sudden release. Upon checking the coefficients of variability for these sets of data, they were found to be very large (in the range of 19% to 50%) which would have caused the results to be reversed.

Shock release gave greater transmission lengths than sudden release. In brief, it can be said that shock release by angle grinding gave the largest transmission lengths followed by sudden release and then gradual release.

Pull-ins are expected to have the same kind of trend. The anomalies experienced in A(i) and A(iii) for Δ_o comparisons can only be explained by the possibility of diverse behaviour when it came to sudden release, thus giving large scatter in the resulting pull-ins. Pull-ins were not available from Test 7 to confirm such a behaviour.

4.8.4 Comparisons of L_p and Δ_o for Different Concrete Strengths

The following are results of inference tests made on transmission lengths and pull-ins for the different concrete compressive strengths available from the laboratory tests.

(A) Test 2 Gradual Release (35.8 vs. 48.7 MPa)

(i) 7 mm dia. Plain wire

L_p (35.8 MPa) = L_p (48.7 MPa) 90% C.L.

$\{n = 4, \bar{L}_p = 450, s = 82\}$, $\{n = 4, \bar{L}_p = 444, s = 139\}$

Δ_o (35.8 MPa) = Δ_o (48.7 MPa) 90% C.L.

$\{n = 8, \bar{\Delta}_o = 1.12, s = 0.21\}$, $\{n = 8, \bar{\Delta}_o = 1.21, s = 0.60\}$

(ii) 5 mm dia. Chevron wire

L_p (35.8 MPa) = L_p (48.7 MPa) 90% C.L.

$\{n = 4, \bar{L}_p = 300, s = 58\}$, $\{n = 4, \bar{L}_p = 281, s = 31\}$

Δ_o (35.8 MPa) < Δ_o (48.7 MPa) 90% C.L. (anomalous result)

$\{n = 16, \bar{\Delta}_o = 0.48, s = 0.14\}$, $\{n = 16, \bar{\Delta}_o = 0.58, s = 0.11\}$

(B) Test 3 Sudden Release (33.8 vs. 53.1 MPa)

(i) 7 mm dia. Plain wire

L_p (33.8 MPa) > L_p (53.1 MPa) 90% C.L.

$\{n = 4, \bar{L}_p = 675, s = 201\}$, $\{n = 4, \bar{L}_p = 444, s = 123\}$

Δ_o (33.8 MPa) > Δ_o (53.1 MPa) 99% C.L.

$\{n = 8, \bar{\Delta}_o = 1.79, s = 0.55\}$, $\{n = 8, \bar{\Delta}_o = 0.93, s = 0.39\}$

(ii) 5 mm dia. Chevron wire

L_p (33.8 MPa) > L_p (53.1 MPa) 95% C.L.

$\{n = 4, \bar{L}_p = 534, s = 87\}$, $\{n = 4, \bar{L}_p = 394, s = 90\}$

Δ_o (33.8 MPa) > Δ_o (53.1 MPa) 99.99% C.L.

$\{n = 16, \bar{\Delta}_o = 1.25, s = 0.30\}$, $\{n = 16, \bar{\Delta}_o = 0.44, s = 0.08\}$

(C) Test 5 Gradual Release (20.1 MPa at 2 days vs. 26.8 MPa at 7 days) - Two-tailed tests used

(i) 7 mm dia. Plain wire

L_p (20.1 MPa) = L_p (26.8 MPa) 90% C.L.

$\{n = 4, \bar{L}_p = 906, s = 175\}$, $\{n = 4, \bar{L}_p = 894, s = 156\}$

Δ_o (20.1 MPa) $\neq \Delta_o$ (26.8 MPa) 95% C.L.

$\{n = 8, \bar{\Delta}_o = 2.26, s = 0.42\}$, $\{n = 8, \bar{\Delta}_o = 2.86, s = 0.59\}$

(ii) 5 mm dia. Chevron wire

L_p (20.1 MPa) $\neq L_p$ (26.8 MPa) 90% C.L.

$\{n = 4, \bar{L}_p = 456, s = 80\}$, $\{n = 4, \bar{L}_p = 625, s = 124\}$

Δ_o (20.1 MPa) $\neq \Delta_o$ (26.8 MPa) 99.99% C.L.

$\{n = 16, \bar{\Delta}_o = 0.80, s = 0.06\}$, $\{n = 16, \bar{\Delta}_o = 0.99, s = 0.13\}$

(D) Test 4 Gradual Release (48.7 MPa) vs. Test 6 Gradual Release (65.1 MPa)

(i) 7 mm dia. Plain wire

L_p (48.7 MPa) > L_p (65.1 MPa) 90% C.L.

$\{n = 4, \bar{L}_p = 519, s = 143\}$, $\{n = 4, \bar{L}_p = 363, s = 43\}$

Δ_o (48.7 MPa) > Δ_o (65.1 MPa) 99% C.L.

$\{n = 8, \bar{\Delta}_o = 1.44, s = 0.46\}$, $\{n = 8, \bar{\Delta}_o = 0.74, s = 0.16\}$

(ii) 7 mm dia. Belgian wire

L_p (48.7 MPa) > L_p (65.1 MPa) 95% C.L.

$\{n = 4, \bar{L}_p = 413, s = 78\}$, $\{n = 4, \bar{L}_p = 269, s = 55\}$

Δ_o (48.7 MPa) > Δ_o (65.1 MPa) 99.99% C.L.

$\{n = 8, \bar{\Delta}_o = 0.90, s = 0.09\}$, $\{n = 8, \bar{\Delta}_o = 0.51, s = 0.08\}$

(iii) 5 mm dia. Plain wire

L_p (48.7 MPa) > L_p (65.1 MPa) 95% C.L.

$\{n = 4, \bar{L}_p = 519, s = 118\}$, $\{n = 4, \bar{L}_p = 294, s = 125\}$

Δ_o (48.7 MPa) > Δ_o (65.1 MPa) 99.99% C.L.

$\{n = 16, \bar{\Delta}_o = 1.18, s = 0.30\}$, $\{n = 16, \bar{\Delta}_o = 0.40, s = 0.07\}$

(iv) 5 mm dia. Chevron wire

L_p (48.7 MPa) > L_p (65.1 MPa) 95% C.L.

$\{n = 4, \bar{L}_p = 400, s = 35\}$, $\{n = 4, \bar{L}_p = 281, s = 83\}$

Δ_o (48.7 MPa) > Δ_o (65.1 MPa) 99.99% C.L.

$\{n = 16, \bar{\Delta}_o = 0.59, s = 0.09\}$, $\{n = 16, \bar{\Delta}_o = 0.32, s = 0.06\}$

(E) Test 5 Gradual Release (20.1 and 26.8 MPa) vs. Tests 1, 2, 4, 6 and 7 (33.8 to 65.1 MPa)

(i) 7 mm dia. Plain wire

L_p (20.1 and 26.8 MPa) > L_p (33.8 to 65.1 MPa) 99.99% C.L.

$\{n = 8, \bar{L}_p = 900, s = 154\}$, $\{n = 36, \bar{L}_p = 465, s = 107\}$

Δ_o (20.1 and 26.8 MPa) > Δ_o (33.8 to 65.1 MPa) 99.99% C.L.

$\{n = 16, \bar{\Delta}_o = 2.56, s = 0.58\}$, $\{n = 72, \bar{\Delta}_o = 1.10, s = 0.39\}$

(ii) 5 mm dia. Chevron wire

L_p (20.1 and 26.8 MPa) > L_p (33.8 to 65.1 MPa) 99.9% C.L.

$\{n = 8, \bar{L}_p = 541, s = 132\}$, $\{n = 20, \bar{L}_p = 321, s = 69\}$

Δ_o (20.1 and 26.8 MPa) > Δ_o (33.8 to 65.1 MPa) 99.99% C.L.

$\{n = 32, \bar{\Delta}_o = 0.90, s = 0.14\}$, $\{n = 80, \bar{\Delta}_o = 0.50, s = 0.14\}$

Test 2 had specimens with two different concrete strengths and comparisons in set A were to investigate the differences in the transmission lengths and pull-ins for the two mixes. Similar comparisons were made for Test 3 in set B.

Test 5 was initially designed to have similar concrete strengths achieved at different ages. However, the actual concrete mixes had greater discrepancy than the trial mixes. At the time of transfer, Mix 1 had a cylinder strength of 26.8 MPa (7 days) whereas Mix 2 had a strength of 20.1 MPa (2 days). Mix 1 was cast as a lower strength mix compared to Mix 2 (if considered at the same age) but it had greater maturity and strength at the time of transfer and this made it difficult to predict which mix should perform better in terms of transferring the prestress force. For this reason, two-tailed tests were used in the comparisons in set C.

Tests 4 and 6 in set D were identical except the former had an insitu mix of 48.7 MPa at transfer and the latter had a commercial high strength mix of 65.1 MPa at transfer. Cross comparisons between Tests 4 and 6 were made for the four different wires used.

Finally, comparisons were made between results from Test 5 and the results from all other tests (except Test 3 and shock released beams in Test 7). It was apparent that transmission lengths and pull-ins obtained for Test 5 were significantly greater than those from other tests.

Set A indicates there is not much difference in transmission lengths and pull-ins for concrete strengths of 35.8 and 48.7 MPa in Test 2. Set B indicates otherwise. Comparisons of L_p and Δ_o in set A generally had small differences between sample means tested and V ranged from 11% to 50%. On the other hand, similar comparisons in set B had large differences between the means, and V values were less than 30%. These reasons may explain for the dissimilar outcomes for sets A and B. There is an implication that concrete strength affects L_p to a greater extent for sudden transfer than for gradual transfer.

Three out of four comparisons in set C show that the 20.1 MPa mix performed slightly better than the 26.8 MPa mix. This contradicts the fact that transmission length should be smaller for greater concrete strength. However, it is important to note that the greater concrete strength in Mix 1 was achieved from a lower grade mix over a longer period of time after casting. There is indication that the quality of the concrete mix is just as important as strength. The strengthwise weaker 20.1 MPa mix loaded at two days generally gave smaller transmission lengths and pull-ins compared to the 26.8 MPa mix loaded at seven days. Hence, concrete strength alone does not dictate the behaviour at transfer. These results support the possibility of transferring prestress at earlier ages but with the use of good quality higher grade concrete.

Comparisons in set D undoubtedly prove that transmission length and pull-in decrease for greater concrete strength.

In set E, the transmission lengths and pull-ins were found to be exceptionally larger for Test 5 compared to all other tests. There are a few reasons which can explain for this. It can be argued that the beams were overloaded but there were no visible cracks on the beams although internal cracking could be possible. In general, concrete for Test 5 were made of lower strength mixes compared to the other tests and this is the main factor causing the poor performance.

In brief, greater concrete strength gave smaller transmission lengths and pull-ins. Prestress transfer also depended on the quality of concrete used. Transfer can be achieved for a higher strength mix at an early age and still give smaller transmission lengths and pull-ins compared to a lower strength mix loaded at greater maturity. The concrete mixes of 20.1 and

26.8 MPa had much longer transmission lengths and larger pull-ins compared to all other tests with transfer strengths of at least 33.8 MPa.

4.9 Relationship Between Transmission Length And Pull-in

A relationship between transmission length and pull-in is important as it allows the transmission length to be predicted from measured pull-in. Data was plotted for L_p versus Δ_o for the four different wires used in the seven tests and these graphs are shown in Figures 4.13 and 4.14.

There were limited results for the 5 mm dia. Plain and 7 mm dia. Belgian wires. Conversely, the graphs for 5 mm dia. Chevron and 7 mm dia. Plain wires show that regression lines could be fitted to the data:

$L_p = 310\,\Delta_o + 200$ $(r = 0.71)$ (5 mm dia. Chevron) Equation 4.11

$L_p = 280\,\Delta_o + 170$ $(r = 0.93)$ (7 mm dia. Plain) Equation 4.12

Both these sets of data indicate a linear relationship between L_p and Δ_o. It is interesting to note that there is greater scatter in the graph for the Chevron wires than for the plain wires. Perhaps changes in the dimensions and sharpness of the indentations on the Chevron wires caused this whereas the plain wires were more consistent in their behaviour as the cross-section and circumference were the same throughout every wire.

There was no other data available from previous research to add to the graph for the 5 mm dia. Chevron wire. This was also the case for the 7 mm dia. Belgian wire. However, there were results for 5 mm dia. Plain, 5 mm dia. Belgian and 7 mm dia. Plain wires from previous research work.

For the 7 mm dia. Plain wire, two outlying data points away from the line of best fit in Figure 4.14 had uncertain transmission lengths and were removed from the plot (viz. (i) Δ_o = 2.14 mm and L_p = 925 mm from Test 3; and (ii) Δ_o = 2.29 mm and L_p = 1075 mm from Test 5). On the other hand, one result each from Evans and Robinson (1955), and Evans and Williams (1957) were included in the graph, as shown in Figure 4.15.

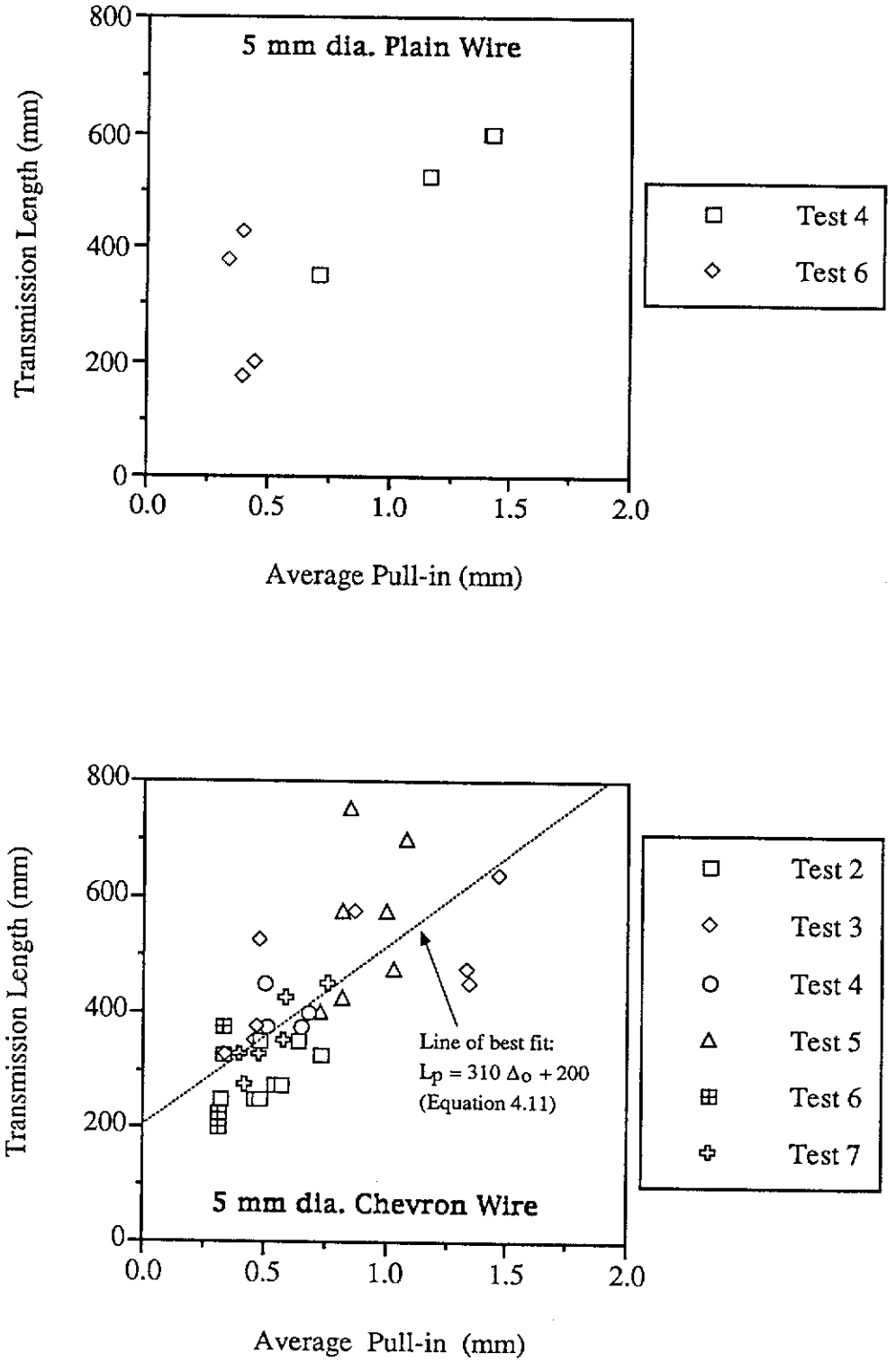

Figure 4.13 Plots of L_p vs. Average Δ_o for 5 mm dia. Plain and 5 mm dia. Chevron Wires (Current Test Data)

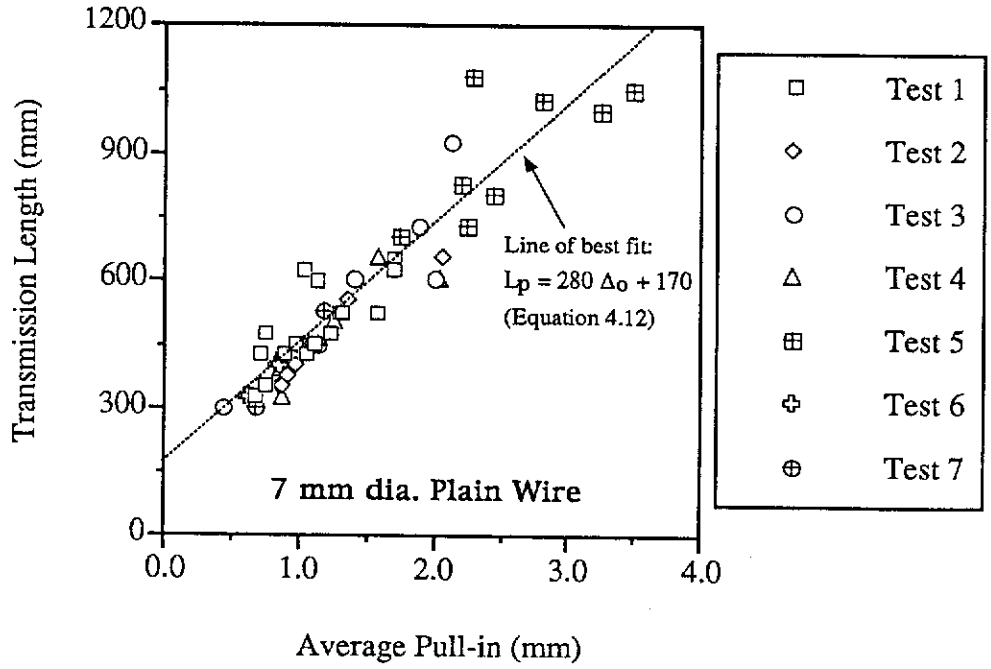

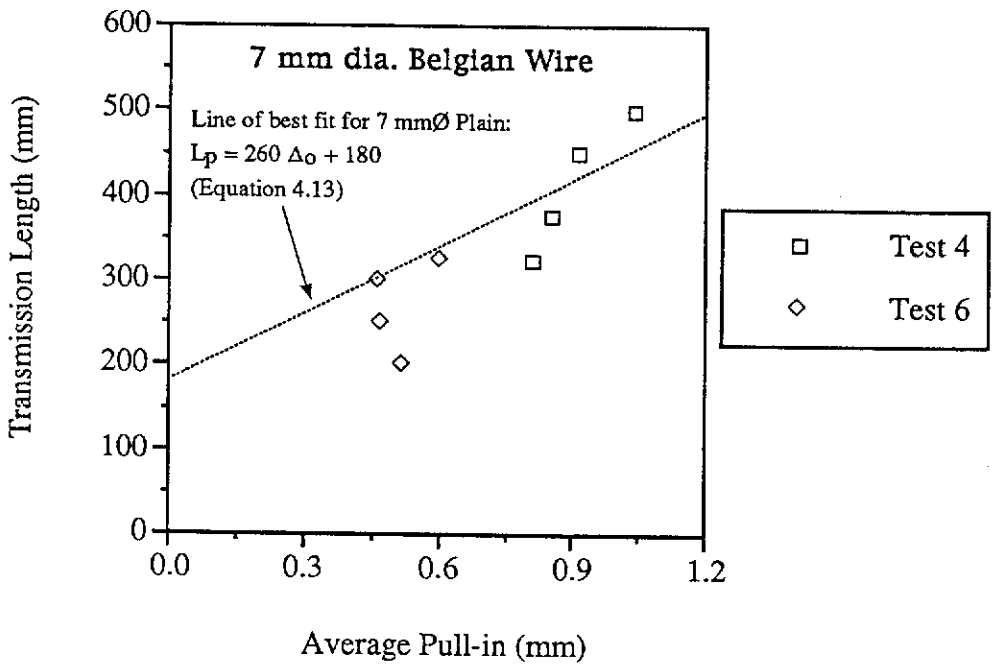

Figure 4.14 Plots of L_p vs. Average Δ_o for 7 mm dia. Plain and 7 mm dia. Belgian Wires (Current Test Data)

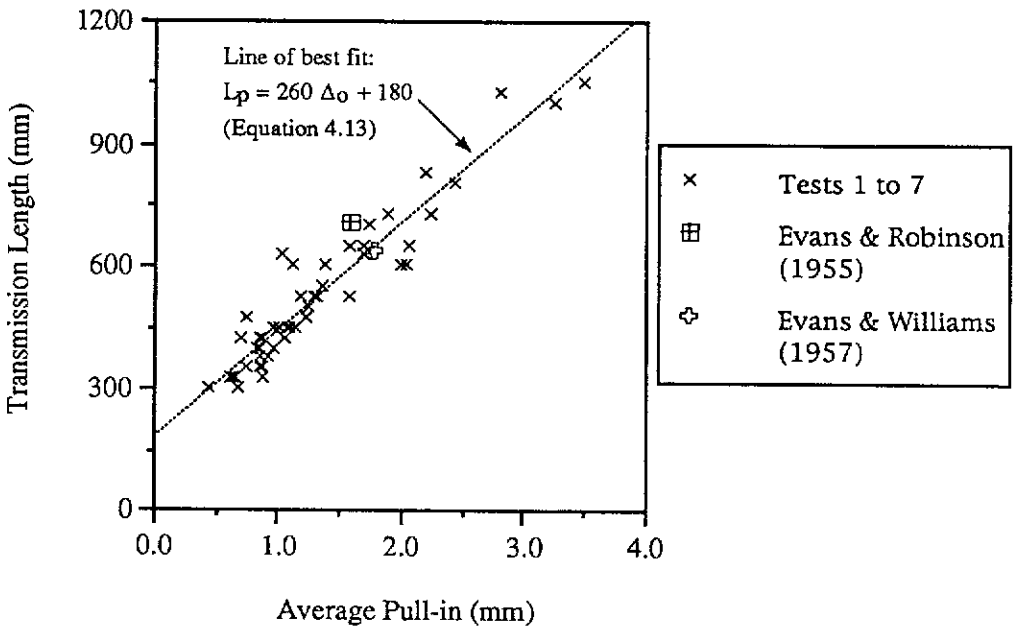

Figure 4.15 Plot of L_p vs. Average Δ_o for 7 mm dia. Plain Wire (Combined Test Data)

By trimming the two outliers, there is slightly less scatter in the graph (Figure 4.15). The additional data points from previous investigations fitted well into the general trend of the current tests. The relationship between the transmission length and pull-in which had a marginally enhanced correlation coefficient is as follows:

$$L_p = 260\,\Delta_o + 180 \quad (r = 0.95) \quad \text{(7 mm dia. Plain)} \qquad \text{Equation 4.13}$$

Although there were no extra data points added to the graph for the 5 mm dia. Chevron wire, the scatter was improved by removing outlying points (viz. (i) Δ_o = 0.48 mm, L_p = 525 mm from Test 3; (ii) Δ_o = 0.50 mm, L_p = 450 mm from Test 4; (iii) Δ_o = 0.86 mm, L_p = 750 mm and (iv) Δ_o = 1.09 mm, L_p = 700 mm from Test 5; and (v) Δ_o = 0.33 mm, L_p = 375 mm from Test 6). Even though the transmission lengths had distinct ends, points (i), (iii) and (v) were removed as there were local changes in strain near the end zones which may have affected the determination of L_p (L_p may be as small as 375, 450 and 275 mm for these respective points). It is also noted that L_p for (i) was obtained from strain profile of beam 3R-D2 which had large fluctuations. Points (ii) and (iv) were removed as they had uncertain transmission lengths. Figure 4.16 shows the graph after removing these points.

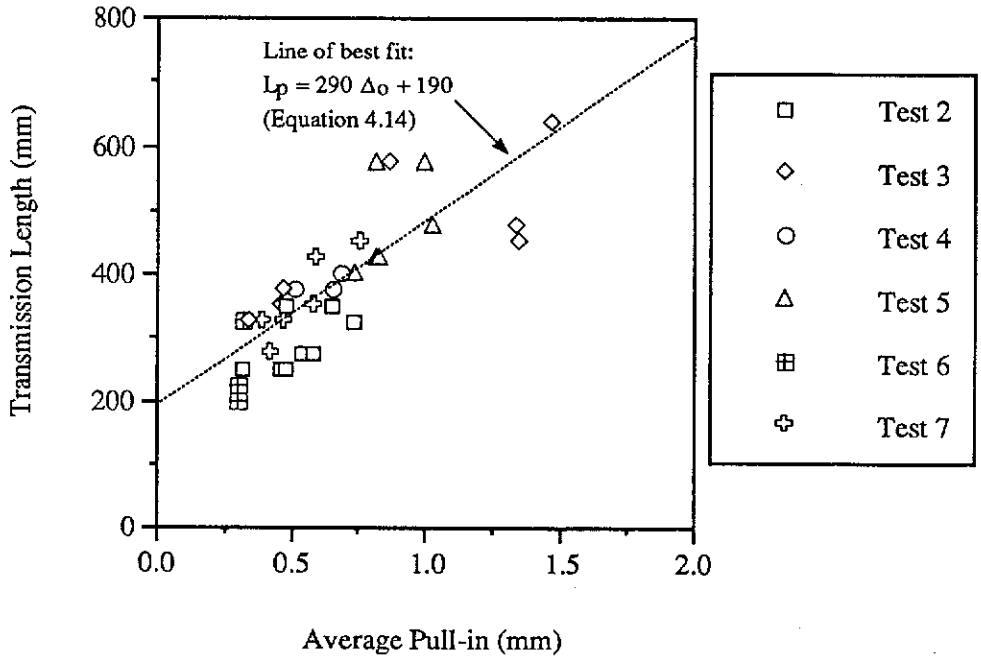

Figure 4.16 Plot of L_p vs. Average Δ_o for 5 mm dia. Chevron Wire (Outliers Removed)

The relationship between L_p and Δ_o is:

$L_p = 290\,\Delta_o + 190$ ($r = 0.81$) (5 mm dia. Chevron) Equation 4.14

Results from previous investigations were included into the graph for the 5 mm dia. Plain wire in Figure 4.13 to establish a similar relationship for this wire. One suspect result was removed (viz. Δ_o = 1.39 mm, L_p = 920 mm from Srinivasa Rao, Kalyanasundaram and Fazlullah Sharief (1977)) and the best fit equation obtained in Figure 4.17 is:

$L_p = 350\,\Delta_o + 190$ ($r = 0.77$) (5 mm dia. Plain) Equation 4.15

The equations for the 5 mm dia. Plain, 5 mm dia. Chevron and 7 mm dia. Plain wires indicate the vertical intercept to be L_p = 180 to 190 mm. This means that all the equations have about the same arbitrary base L_p value when Δ_o = 0. However, it is never possible to have zero pull-in. From the current test data, it was found that pull-in was generally greater than 0.30 mm and this value gives a transmission length of about 300 mm (assuming an approximation of $L_p = 300\,\Delta_o + 200$ for all the wires).

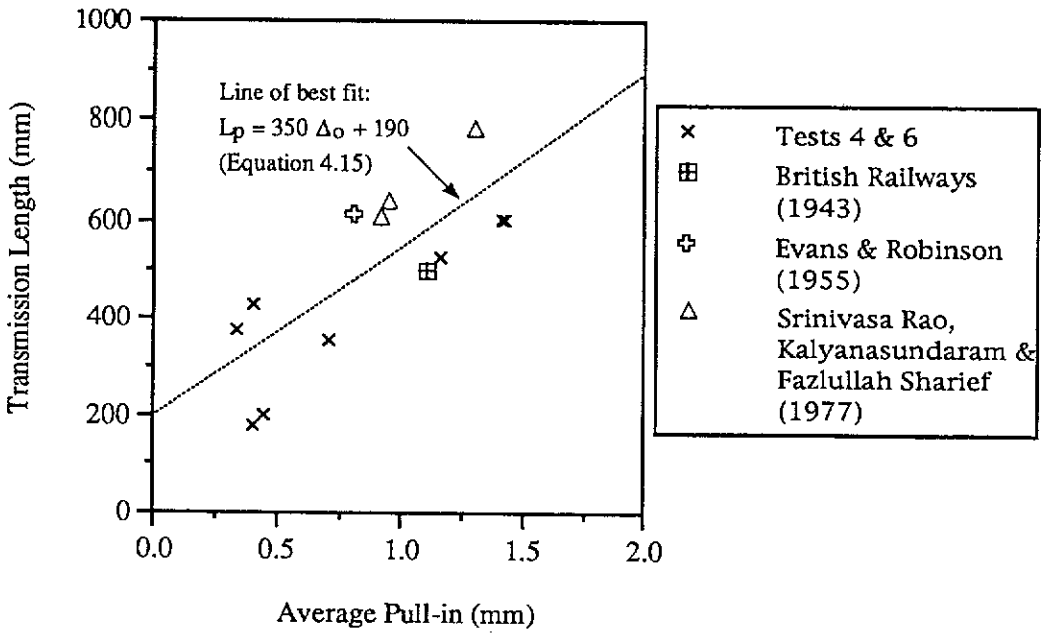

Figure 4.17 Plot of L_p vs. Average Δ_o for 5 mm dia. Plain Wire (Combined Test Data)

Considering equations 4.13 to 4.15, the greater the K_o value, the greater will be the rate of increase in transmission length with respect to increase in pull-in. The K_o values for 5 mm dia. Plain and 5 mm dia. Chevron wires (K_o = 350 and 290) are larger than that for the 7 mm dia. Plain wire (K_o = 260). The transmission lengths for the 7 mm dia. Plain wire were generally large but the corresponding pull-ins were also large. This explains why K_o can be smaller for the 7 mm dia. Plain wire compared with the 5 mm dia. wires.

Re-addressing the issue of comparison between plain and indented wires which was first raised in Section 4.8.1, the inference tests on pull-ins convincingly proved the difference between plain and indented wires but not the tests on transmission lengths. The 5 mm dia. Plain wire has an average pull-in of 0.8 mm whereas the 5 mm dia. Chevron wire has 0.5 mm (Equations 4.19 (a) and (b)). Equations 4.15 and 4.14 predict transmission lengths of 470 and 340 mm respectively. The pull-in for the 5 mm dia. Plain wire is 60% above that for the 5 mm dia. Chevron wire while the transmission length is only 38% greater. The transformation from the pull-ins to the transmission lengths according to the L_p-Δ_o equations showed smaller relative change in the transmission length. This contributes to explain why any difference between transmission lengths for these wires is not readily detected by statistical tests compared to the pull-ins.

In Section 4.8.2, the inference tests on Δ_o consistently indicated that there was a difference between wires of different sizes (ie. 5 mm vs. 7 mm dia.) but not the tests on L_p. Hypothetically assuming that the two wire sizes give exactly the same L_p value, the L_p-Δ_o relationships predict larger Δ_o for the 7 mm dia. wire. Therefore, the difference in L_p between the two sizes of wire may be small (the 7 mm dia. wires have transmission lengths slightly longer than the 5 mm dia. wires) but the unequal K_o values cause relatively greater difference between their pull-ins.

A comparison between the 7 mm dia. Plain and 7 mm dia. Belgian wires could not be made as there were not enough data points for the 7 mm dia. Belgian wire to establish a L_p-Δ_o relationship. In Figure 4.14, the line of best fit for the 7 mm dia. Plain wire was superimposed on the data points for the 7 mm dia. Belgian wire. The linear equation does not seem to be a good predictor of the relationship between the transmission length and pull-in for the 7 mm dia. Belgian wire although the correlation coefficient using this imposed line is 0.80 ($r = 0.90$ from the data set for the 7 mm dia. Belgian wire alone but there are insufficient number of points to justify the formulation of an L_p-Δ_o equation of its own).

In Figure 4.18, some of the formulae obtained from previous research work (given in Chapter 2) are superimposed on the graph for the 5 mm dia. Chevron wire. None of the curves provide good prediction of the transmission length from the average pull-in. Evans and Robinson's (1955) two formulas underestimate the actual transmission lengths. The parabolic trend proposed by Marshall and Krishnamurthy (1969) in Section 2.5.6 was disregarded since the equation was fundamentally wrong.

Figure 4.19 contains current and previous test data points as given in Figure 4.15 for the 7 mm dia. Plain wire. Again the same equations due to previous research work were plotted on the graph. The equations by Guyon and Bruggeling overestimate L_p for large Δ_o while the equations by Evans and Robinson generally underestimate L_p.

Combining the test data, Figure 4.20 show the data points for all the 5 mm and 7 mm dia. wires. Relationships from previous investigations were also included in these graphs.

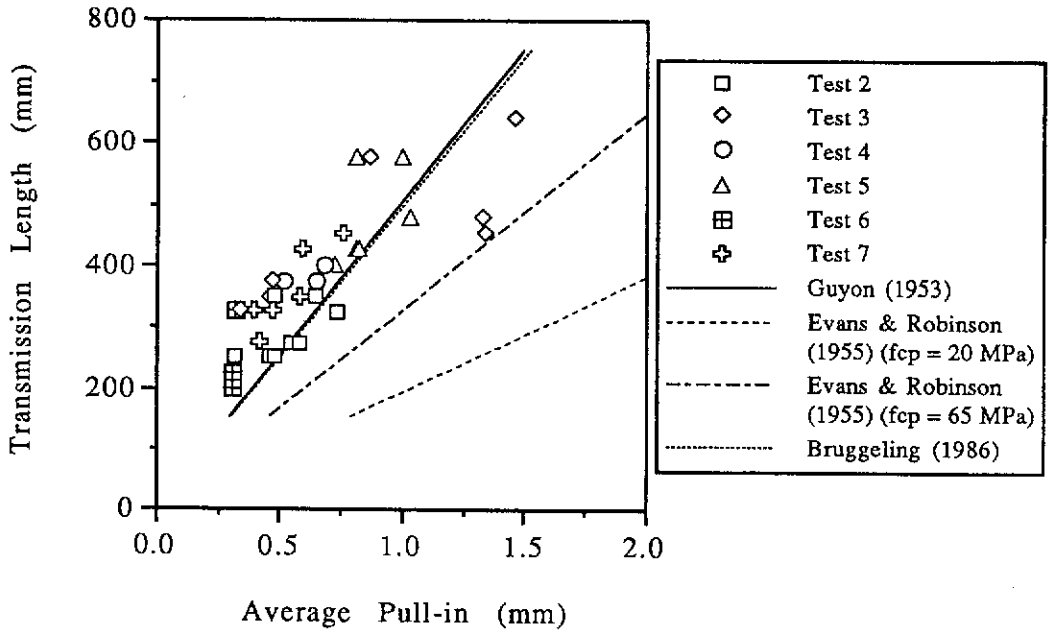

Figure 4.18 **Plot of L_p vs. Average Δ_0 for 5 mm dia. Chevron Wire (Current Test Data and Relationships from Previous Investigators)**

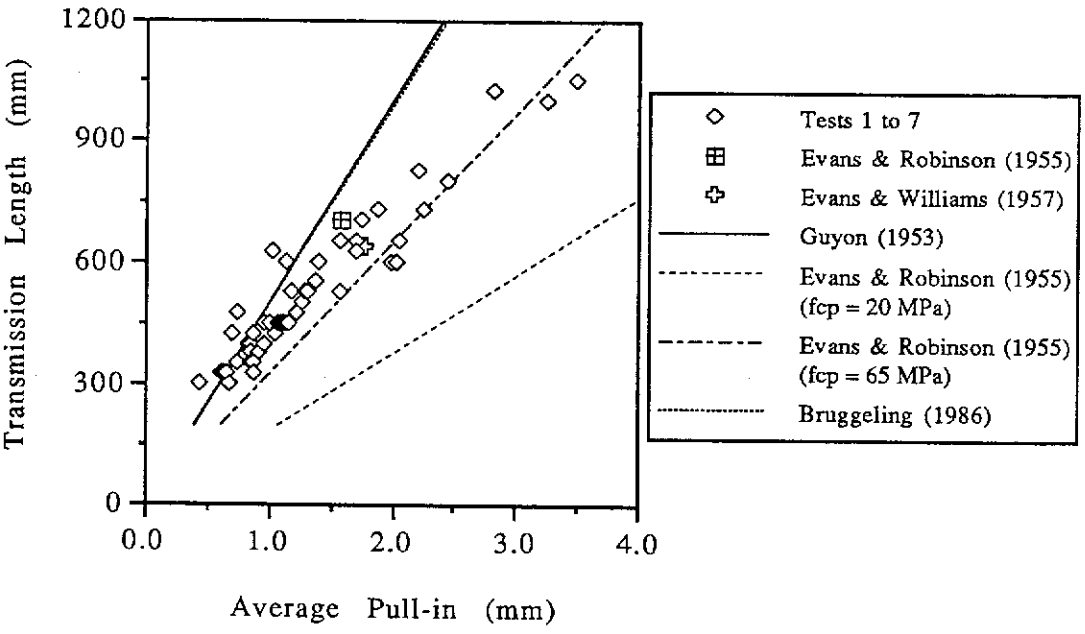

Figure 4.19 **Plot of L_p vs. Average Δ_0 for 7 mm dia. Plain Wire (Combined Test Data and Relationships from Previous Investigators)**

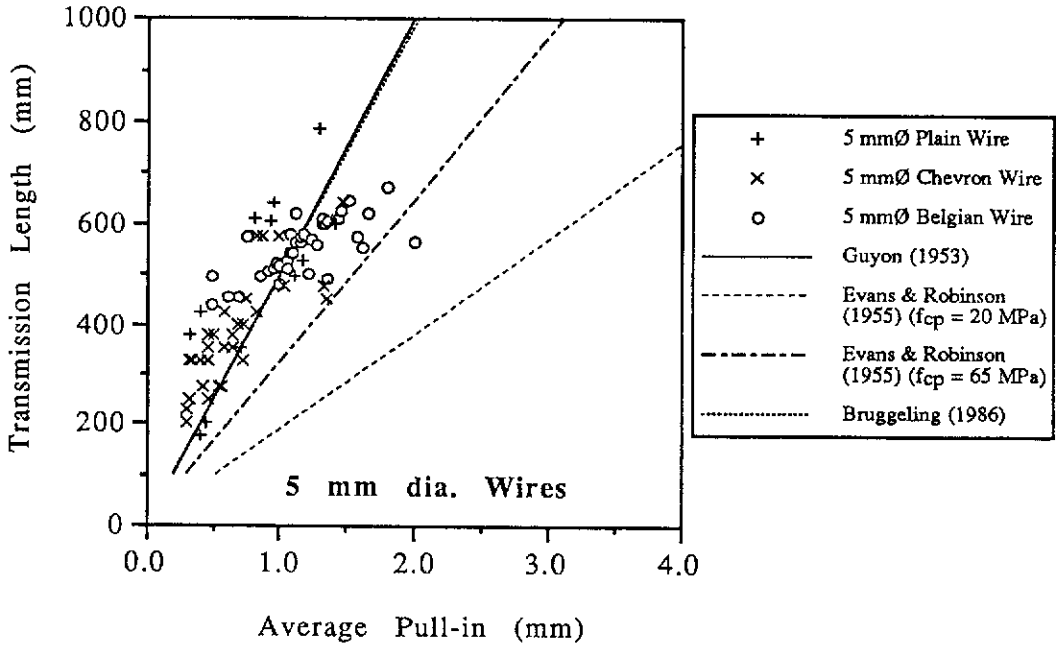

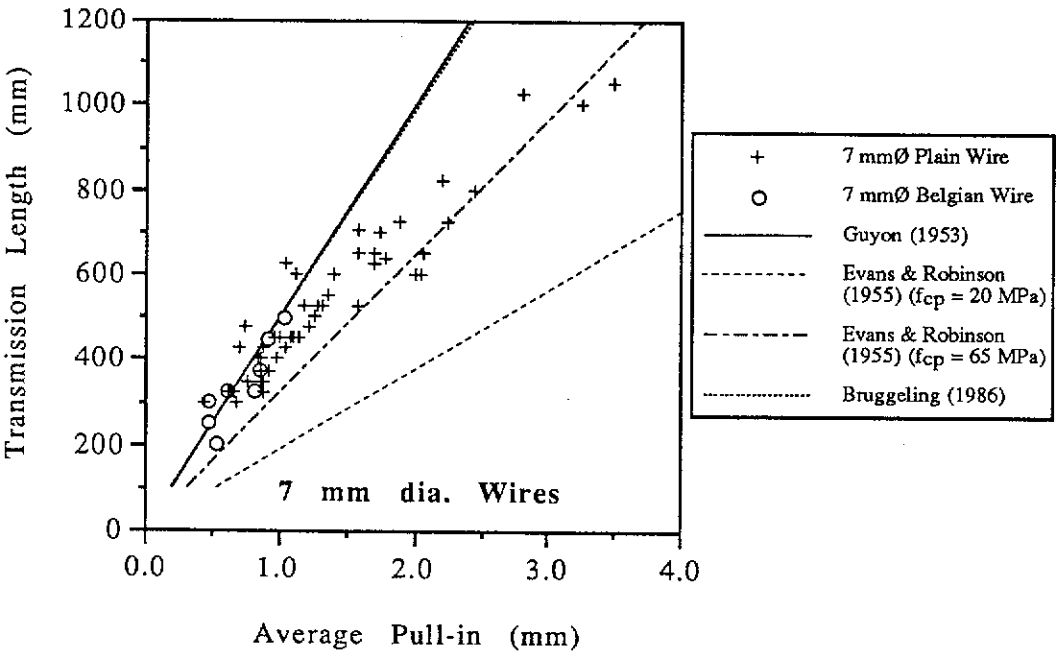

Figure 4.20 Plots of L_p vs. Average Δ_0 for All 5 mm and 7 mm dia. Wires (Combined Test Data and Relationships from Previous Investigators)

The 7 mm dia. Belgian wire tends to follow the trend for the 7 mm dia. Plain wire but this is not the case for the 5 mm dia. Belgian and 5 mm dia. Plain wires. There is even a possibility that the 7 mm dia. wires have a bilinear L_p-Δ_o relationship but there are not enough data points to check this.

It is recommended that the different equations developed by the author (Equations 4.13, 4.14 and 4.15) are more appropriate for determining the transmission lengths for the 5 mm and 7 mm dia. wires compared to the equations given by previous researchers since there is appreciable scatter in the combined data set.

4.10 Relationship Between Concrete Compressive Strength At Transfer And Transmission Length

Graphs plotted for concrete strength at transfer (f_{cp}) versus transmission length (L_p) are shown in Figures 4.21 to 4.23. The graphs only include data points for gradual releases in current and previous tests. There is a general trend for the 5 mm dia. Plain, 5 mm dia. Chevron and 7 mm dia. Plain wires where the transmission lengths were shorter for higher concrete strength at transfer. All the three graphs showed large scatter and it was pointless to fit equations through them. However, by plotting a demarcation line of 32 MPa (AS 3600 (1988) suggests Grade 32 MPa concrete or better for short transmission lengths) on each of these scattergraphs, the data points can generally be grouped. Vertical separation lines were also drawn in to estimate the upper limits for acceptable transmission lengths. The selection of such lines was based on visual examination of the plots.

There are points where the transmission lengths are shorter than expected for concrete strength of less than 32 MPa. Three data points by the Building Research Station and one data point by the Cement and Concrete Association are found in the region of {small f_{cp}-small L_p} or {f_{cp} < 32 MPa and L_p < 605 mm} in the plot for the 5 mm dia. Plain wire. Similarly, three and one such data points can be seen in the plots for the 5 mm dia. Chevron (2 identical points with f_{cp} = 20.1 MPa, L_p = 425 mm) and 7 mm dia. Plain wires respectively. These results are not a problem as they indicate better transfer than expected.

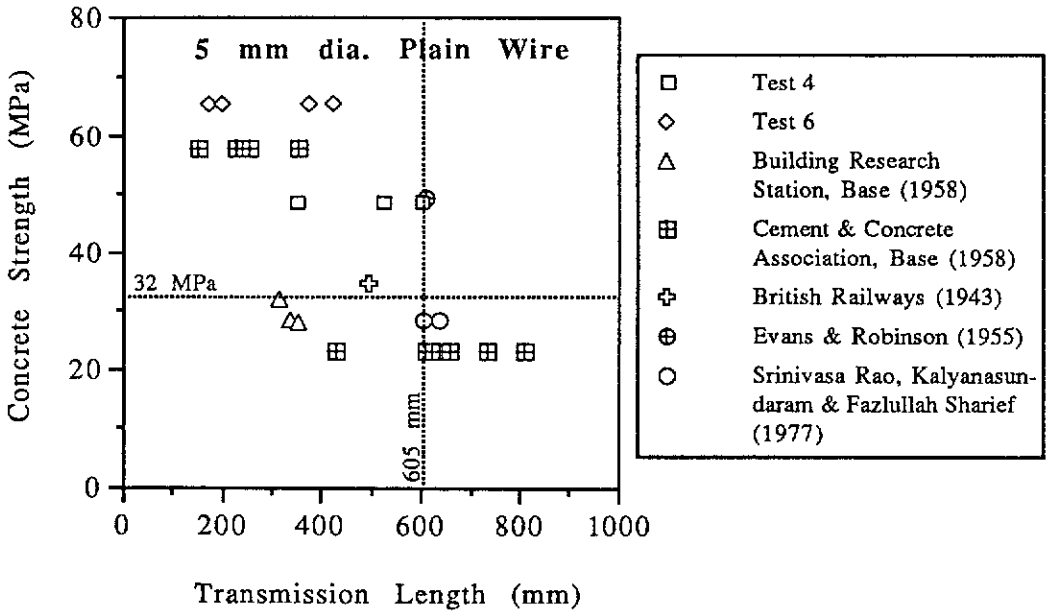

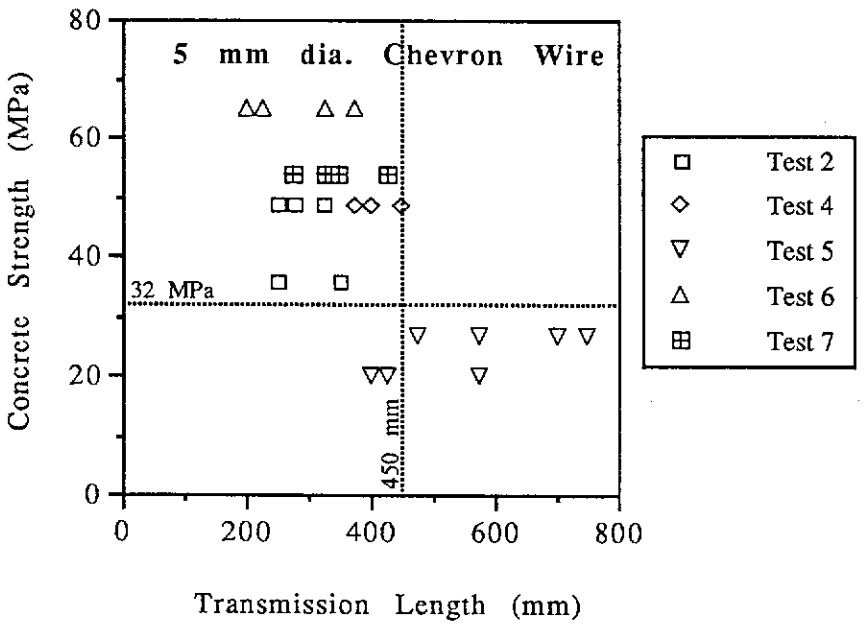

Figure 4.21 Plots of f_{cp} vs. L_p for 5 mm dia. Plain and 5 mm dia. Chevron Wires

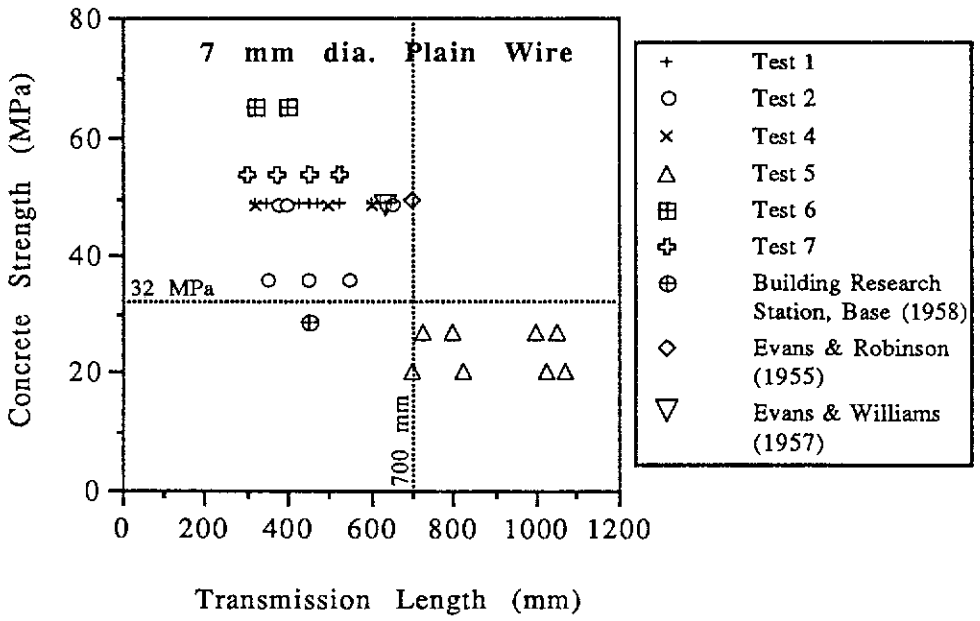

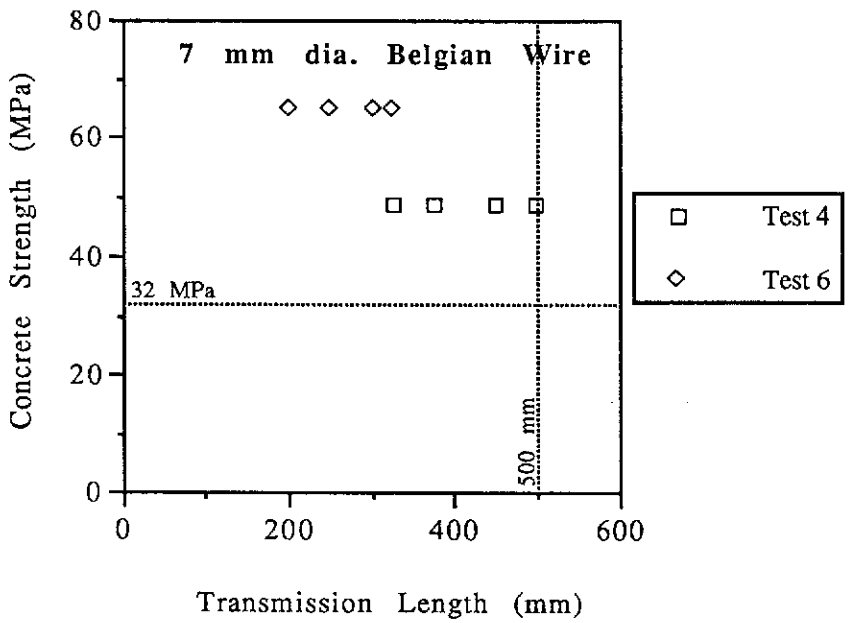

Figure 4.22 Plots of f_{cp} vs. L_p for 7 mm dia. Plain and 7 mm dia. Belgian Wires

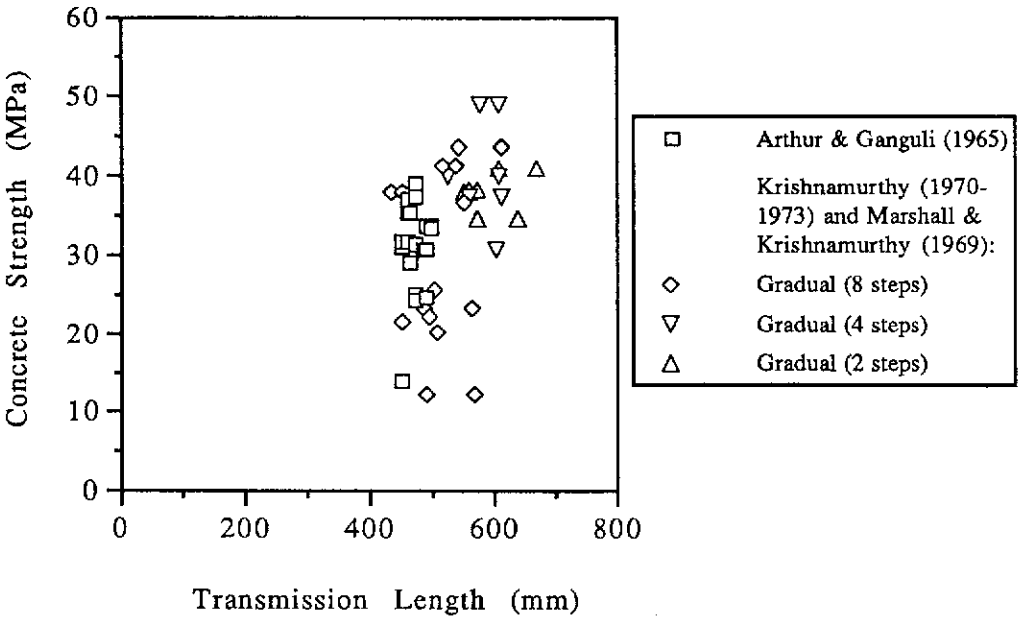

Figure 4.23 Plot of f_{cp} vs. L_p for 5 mm dia. Belgian Wire

In contrast, there was only one data point each in the plots for the 5 mm dia. Plain and 7 mm dia. Plain wires where the transmission lengths were slightly greater than the respective demarcation values (f_{cp} = 49.3 MPa, L_p = 609 mm and f_{cp} = 49.3 MPa, L_p = 703 mm for 5 mm dia. Plain and 7 mm dia. Plain wires respectively; both data points were given by Evans and Robinson (1955)). The small differences between L_p and the demarcation values were ignored.

The plot for 7 mm dia. Belgian wire has only 8 data points and the demarcation value for L_p was an estimate based on available information.

As for the 5 mm dia. Belgian wire in Figure 4.23, there is no trend showing decreased transmission length for transfer strength greater than 32 MPa. For this reason, no demarcation lines were plotted in this graph. The results fell into a band between 400 and 700 mm for strengths of 11.5 to 43.9 MPa. The obvious impression is that the transmission lengths were independent of the concrete transfer strengths. However, there are a few factors which may have led to this.

In the investigations by Arthur and Ganguli, and Marshall and Krishnamurthy, the transmission lengths were determined for I-section beams from longitudinal strain distributions obtained at the top and

bottom flanges and also at mid-depth in the web. The transmission lengths in the web would indicate delayed effects from the prestress and are not effective in picking up the end of the transmission length. In addition to this, 13 out of the 19 beams tested by Arthur and Ganguli had cracks in the splitting zone at either one or both ends. In most cases, web cracking was reported to occur after 30% to 55% of full prestress transfer. The longitudinal strain readings at the web level would be affected and should not be used for determining the transmission length.

Marshall and Krishnamurthy produced results for transmission lengths based on the formula $L_p = 1.35\ L_{80\%}$, where $L_{80\%}$ was the length between the end face of a beam and a location along the beam such that 80% of the maximum concrete strain was achieved (according to the German specification DIN-4227-1953). This method assumed an exponential law for the strain distribution and the length needed for complete transfer was theoretically infinite. The author does not believe in the logic of such an argument because L_p should be determined by identifying the point of first flattening in the strain distribution. The transmission lengths were accepted with reservations placed on their degree of accuracy.

The total prestress force was kept constant in each investigation by Arthur and Ganguli, and Marshall and Krishnamurthy. However, there was a great range of concrete strengths at transfer. Arthur and Ganguli had concrete strengths in the range of 14.1 to 38.8 MPa (equivalent 100 mm dia. x 200 mm cylinder strengths). Marshall and Krishnamurthy had concrete strengths of 12.0 to 48.7 MPa. It was necessary to consider the concrete strength concurrent with the applied prestress force. Figure 4.24 is a plot of stress/strength ratio or $\left(\frac{P/A_c}{f_{cp}}\right)$ versus the transmission length. However, this graph did not provide any further insight into the behaviour of the 5 mm dia. Belgian wire.

In brief, some of the results obtained from the above plots for transfer strength equal to or better than 32 MPa are given as follows:

(a) 5 mm dia. Plain wire $L_p \leq 600$ mm (120 d_b)

(b) 5 mm dia. Chevron wire $L_p \leq 450$ mm (90 d_b)

(c) 7 mm dia. Plain wire $L_p \leq 700$ mm (100 d_b)

(d) 7 mm dia. Belgian wire $L_p \leq 500$ mm (70 d_b)

(e) 5 mm dia. Belgian wire $L_p \leq 700$ mm (140 d_b)

Equations 4.16 (a)-(e)

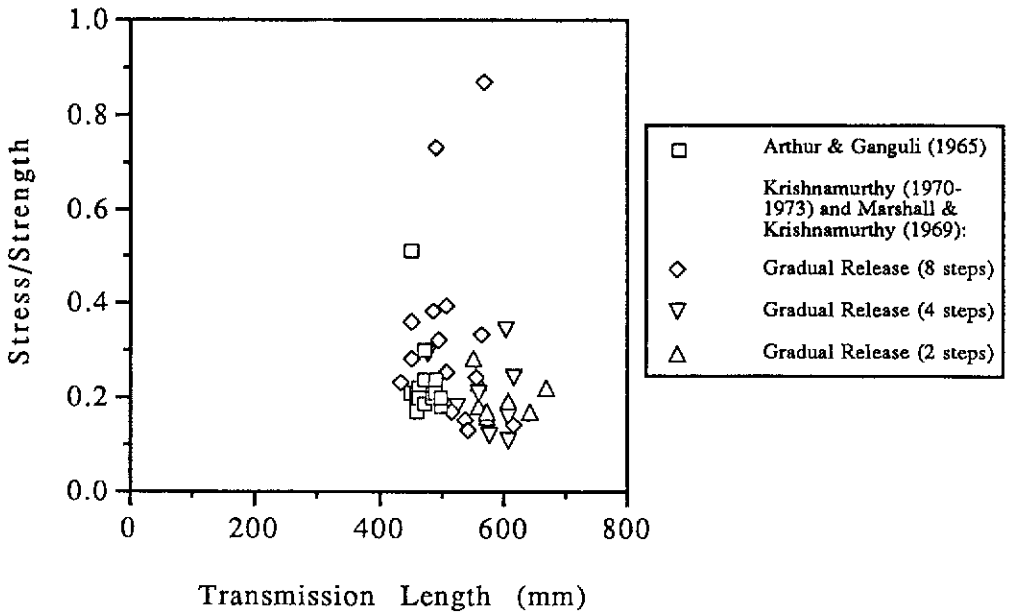

Figure 4.24 Plot of Stress/Strength vs. Transmission Length for 5 mm dia. Belgian Wire

The above limits are the maximum transmission lengths experienced for beams prestressed with the five types of wires considered and with transfer strength equal to or greater than 32 MPa. They were obtained from existing test data in current and previous investigations. The value given for the 7 mm dia. Belgian is based on a limited number of observations.

It can be seen that transmission lengths for the indented 5 mm dia. Chevron and 7 mm dia. Belgian wires were shorter than those for the 5 mm dia. Plain and 7 mm dia. Plain wires respectively. The only inconsistency is that the 5 mm dia. Belgian wire indicates worse transmission lengths than for the 5 mm dia. Plain wire; but the data for the former has already been noted as being suspect from investigations carried out by Arthur and Ganguli, and Marshall and Krishnamurthy.

Predictions for the maximum transmission length for beams with strength less than 32 MPa were not obtained.

From a different perspective, bar charts were drawn for transmission length versus concrete strength categories. For arbitrarily chosen strength categories of 20-30, 30-40, 40-50, 50-60 and 60-70 MPa, the mean

and standard deviation bars for transmission lengths were plotted for the results of each type of wire (Figures 4.25 and 4.26), except for the 5 mm dia. Belgian wire. However, transmission length is not only influenced by the concrete strength alone but it is also affected by the amount of prestress in the concrete, $\left(\frac{P}{A_c}\right)$. Therefore, stress/strength or $\left(\frac{P/A_c}{f_{cp}}\right)$ ratios were evaluated in categories of 0.88-0.59, 0.59-0.44, 0.44-0.35, 0.35-0.29 and 0.29-0.25, to correspond to the above-mentioned strength categories respectively (the nominal $\left(\frac{P}{A_c}\right)$ concrete stress was 17.6 MPa for all the beams in the current tests, but the actual values ranged from 16.9 to 18.7 MPa). Results from current and previous investigations were checked to ensure each L_p value was entered into the same related categories of f_{cp} and $\left(\frac{P/A_c}{f_{cp}}\right)$ in the bar charts. Table 4.5 shows experimental f_{cp} and $\left(\frac{P/A_c}{f_{cp}}\right)$ values from the various sources.

When the stress $\left(\frac{P}{A_c}\right)$ was small (much less than 17.6 MPa), there was indication that an L_p value would be assigned to categories of f_{cp} and $\left(\frac{P/A_c}{f_{cp}}\right)$ which were unrelated (these results are in ***italics*** in Table 4.5). Two of these concrete strength results were from the Building Research Station, Base (1958) and one was from Srinivasa Rao, Kalyanasundaram and Fazlullah Sharief (1977).

Data not considered in the bar charts include:

(a) data where the concrete stress $\left(\frac{P}{A_c}\right)$ was not known.

  (i) British Railways (1943).

  (ii) Evans and Williams (1957).

(b) outlying data points for the 5 mm dia. Plain, 5 mm dia. Chevron and 7 mm dia. Plain wires in Figures 4.21 and 4.22. Four data points were not considered for the 5 mm dia. Plain wire (f_{cp} = 27.9 MPa, L_p = 356 mm, f_{cp} = 28.5 MPa, L_p = 340 mm and f_{cp} = 31.8 MPa, L_p = 318 mm by the Building Research Station, Base (1958); and f_{cp} = 23 MPa, L_p = 432 mm by the Cement and Concrete Association, Base (1958)). Similarly, three points were ignored for the 5 mm dia. Chevron wire (f_{cp} = 20.1 MPa, L_p = 425 mm (2 points) and L_p = 400 mm (1 point) from Test 5) and one point for the 7 mm dia. Plain wire (f_{cp} = 28.5 MPa, L_p = 454 mm).

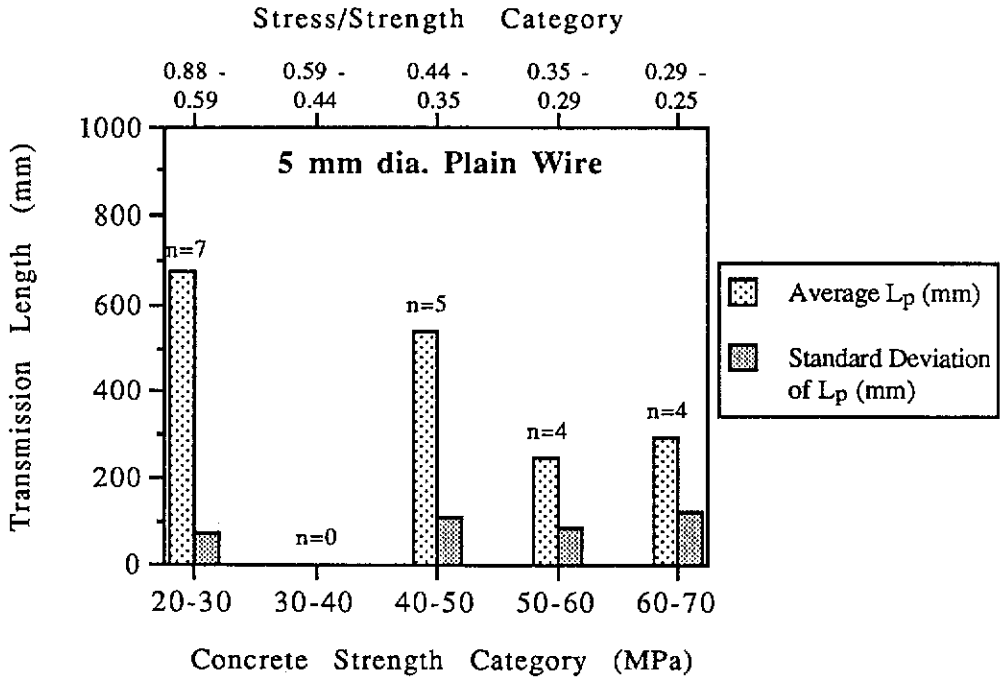

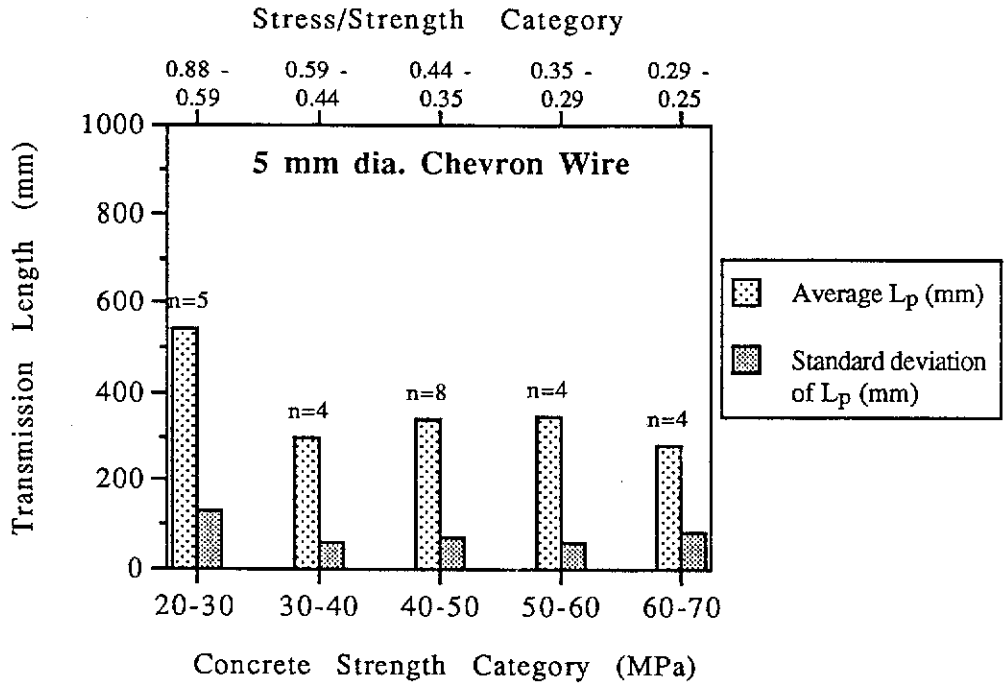

Figure 4.25 Bar Charts of L_p vs. f_{cp} and $\left(\frac{P/A_c}{f_{cp}}\right)$ Categories for 5 mm dia. Plain and 5 mm dia. Chevron Wires

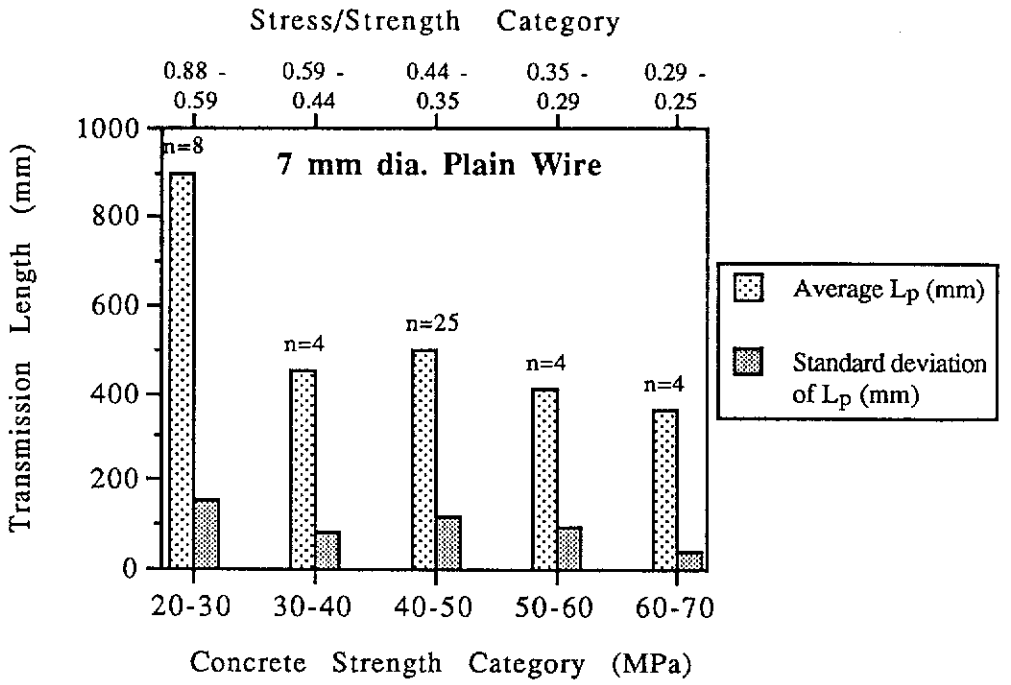

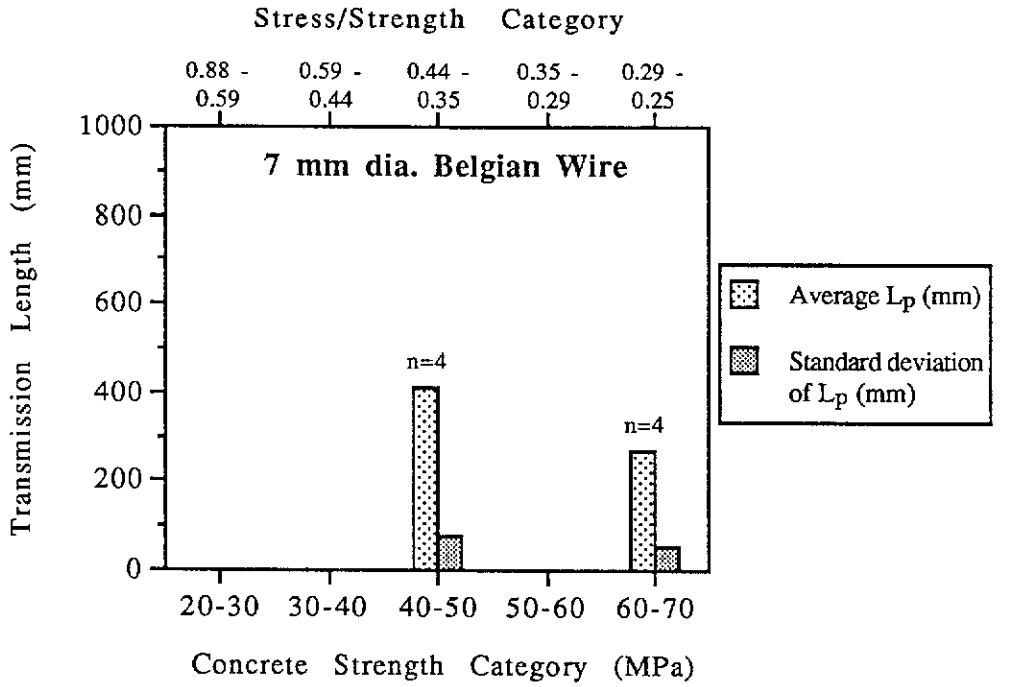

Figure 4.26 Bar Charts of L_p vs. f_{cp} and $\left(\frac{P/A_c}{f_{cp}}\right)$ Categories for 7 mm dia. Plain and 7 mm dia. Belgian Wires

Table 4.5 Concrete Strength (f_{cp}) and Stress/Strength $\left(\frac{P/A_c}{f_{cp}}\right)$ Categories

Source of L_p and f_{cp}	$\frac{P}{A_c}$ (MPa)	Experimental Values									
		f_{cp} Category (MPa)					$\left(\frac{P/A_c}{f_{cp}}\right)$ Category				
		1*	2*	3*	4*	5*	1°	2°	3°	4°	5°
		20-30	30-40	40-50	50-60	60-70	0.88 - 0.59	0.59 - 0.44	0.44 - 0.35	0.35 - 0.29	0.29 - 0.25
Test 1	18.4-17.8			49.0					0.38-0.36		
Test 2	18.3			48.7					0.38		
	17.6			48.7					0.36		
	17.6		35.8					0.49			
	18.1		35.8					0.51			
Test 3	18.1				53.1					0.34	
	17.9				53.1					0.34	
	17.3		33.8					0.51			
	18.3		33.8					0.54			
Test 4	18.2-16.9			48.7					0.37-0.35		
Test 5	17.9	20.1					0.88				
	17.1	20.1					0.85				
	17.0	26.8					0.63				
	18.0	26.8					0.67				
Test 6	18.7-17.7					65.1					0.29-0.27
Test 7	18.5-18.1				53.9					0.34	
Building Res. Stn., Base (1958)											
5 mmØ Plain	13.8		*31.8*						*0.43*		
5 & 7 mmØ Plain	13.8	*28.5*						*0.48*			
Cem. & Conc. Association, Base (1958)											
5 mmØ Plain	13.8-16.6	23.0					0.60-0.72				
	16.6				57.4					0.29	
Evans & Robinson (1955)											
5 & 7 mmØ Plain	20.7			49.3					0.42		
Srinivasa Rao et al. (1977)											
5 mmØ Plain	10.0		*28.4*						*0.35*		

Note: Categories 1* to 5* correspond to categories 1° to 5° respectively.

(c) points with inconsistent categories of f_{cp} and $\left(\frac{P/A_c}{f_{cp}}\right)$. Two data points each from the Building Research Station and Srinivasa Rao, Kalyanasundaram and Fazlullah Sharief (1977) were omitted (for Srinivasa Rao et al., both sets of results had the same concrete strength of 28.4 MPa).

The first three of the four graphs in Figures 4.25 and 4.26 show that transmission lengths for the 20-30 MPa category were significantly longer than for other categories. The statistical hypothesis tests in Section 4.8.4 also found this to be prevalent (L_p for 20.1 and 26.8 MPa concrete > L_p for 33.8 to 65.1 MPa concrete). The stress/strength $\left(\frac{P/A_c}{f_{cp}}\right)$ ratio for this category is 0.88 to 0.59 corresponding to 20 and 30 MPa respectively. The long transmission lengths may be attributed to low concrete strengths and large stress/strength ratios.

The transmission lengths for the strength category of 60-70 MPa are generally shorter than transmission lengths in the range of 30-60 MPa. This is most likely due to the combined effects of high concrete strength and small stress/strength ratio.

Furthermore, the transmission lengths were grouped into two major categories of 20-30 and 30-70 MPa. From these groupings, the results in Table 4.6 were obtained.

For the 5 mm dia. Plain, 5 mm dia. Chevron and 7 mm dia. Plain wires, the average of the measured transmission lengths for f_{cp} between 20 and 30 MPa is about twice that measured for f_{cp} between 30 and 70 MPa.

The estimates for L_p with transfer strength equivalent to or better than 32 MPa are as follows:

(a)	$L_p = 70\ d_b \pm 50\ d_b$	(5 mm dia. Plain wire)
(b)	$L_p = 60\ d_b \pm 30\ d_b$	(5 mm dia. Chevron wire)
(c)	$L_p = 70\ d_b \pm 30\ d_b$	(7 mm dia. Plain wire)
(d)	$L_p = 60\ d_b \pm 10\ d_b$ (?)	(7 mm dia. Belgian wire)

Equations 4.17 (a)-(d)

Considering Equations 4.17 (a)-(d), the suggestions to use L_p = 38-52 d_b (f_{cp} = 65 to 32 MPa) and L_p = 28-38 d_b (f_{cp} = 65 to 32 MPa) by Arthur and Ganguli (1965) and Ganguli (1966) underestimate the transmission length. The range of L_p = 50-160 d_b cautioned by BS 8110:Part 1:1985 with formula-based estimates of L_p = 68-97 d_b (f_{cp} = 65 to 32 MPa) portray greater realism towards predicting the actual transmission lengths.

Table 4.6 Transmission Lengths of Various Wires for Concrete Strength Categories of 20-30 and 30-70 MPa

Type of Wire	f_{cp} (MPa)	Average L_p (mm)	Standard deviation of L_p (mm)	Range of L_p (mm)	L_p as function of d_b	Remarks
5 mmØ Plain	20-30 30-70	679 373	72 168	610-813 152-609	140 d_b ± 30 d_b 70 d_b ± 50 d_b	Seven data points removed; 3 points from Bldg. Res. Stn. and 1 point from Cem. & Conc. Ass., Base (1958); 1 point from British Railways (1943); and 2 points from Srinivasa Rao et al. (1977).
5 mmØ Chevron	20-30 30-70	615 321	110 69	475-750 200-450	120 d_b ± 30 d_b 60 d_b ± 30 d_b	Data points from current tests used. Three outliers removed; f_{cp} = 20.1 MPa, L_p = 400 mm (1 pt.) and L_p = 425 mm (2 pts.) from Test 5.
7 mmØ Plain	20-30 30-70	900 468	154 112	700-1075 300-703	130 d_b ± 30 d_b 70 d_b ± 30 d_b	Two outlying data points removed; f_{cp} = 28.5 MPa, L_p = 454 mm from Bldg. Res. Stn., Base (1958); and f_{cp} = 48.6 MPa, L_p = 635 mm from Evans and Williams (1957).
7 mmØ Belgian	40-50 60-70	413 269	78 55	325-500 200-325	60 d_b ± 10 d_b 40 d_b ± 10 d_b	Only four results for each of the two categories.

The transmission length limits for the 5 mm and 7 mm dia. indented wires with $f_{cp} \geq 32$ MPa were 90 d_b and 70 d_b, and both were less than the design value of 100 d_b suggested in AS 3600 (1988). It must stressed that the experimental limits given in Equations 4.16 (a)-(e) and the ranges of transmission lengths in Table 4.6 were obtained under controlled laboratory conditions and more diverse results can be expected for field

conditions. The laboratory data on its own had already exhibited reasonable scatter. However, AS 3600 did not give any guidance with respect to the variability of transmission lengths under unchanging conditions. The transmission lengths cannot be aptly represented by 100 d_b or any other single value. It is proposed that ranges of transmission lengths such as those given in Equations 4.17 (a)-(d) be used, in order to indicate characteristic variability associated with the transmission length. The upper and lower limits are both important because long transmission lengths cause undesirable loss in prestress near beam ends whereas short transmission lengths cause high concentration of force in the end zone which may initiate cracking. The actual ranges of L_p in Table 4.6 may be more appropriate than Equations 4.17 (a)-(d) for predicting the upper and lower limits.

In contrast, the 5 mm and 7 mm dia. Plain wires had limits of 120 d_b and 100 d_b respectively, which prove that plain wires can have transmission lengths of at least 100 d_b. This consolidates the exclusion of plain wires from being used in pretensioning works according to AS 3600.

4.11 Relationship Between Concrete Compressive Strength At Transfer And Pull-in

Pull-ins were also compared for the different categories of concrete strength at transfer. Figures 4.27 to 4.29 are plots of f_{cp} versus average Δ_o for the different types of wires considered.

The plot for the 5 mm dia. Plain wire shows that all the pull-ins were less than 1.42 mm. Four pull-ins from Srinivasa Rao, Kalyanasundaram and Fazlullah Sharief (1977) with f_{cp} < 32 MPa were also less than the demarcation value.

There was only one data point for the 7 mm dia. Plain wire with f_{cp} < 32 MPa which had a pull-in less than the demarcation value of 2.06 mm.

Just as for the f_{cp}-L_p plot, there were only eight f_{cp}-Δ_o data points available for the 7 mm dia. Belgian wire. The demarcation value was taken as the maximum pull-in in the data set obtained for Tests 4 and 6 where the transfer strengths were greater than 32 MPa.

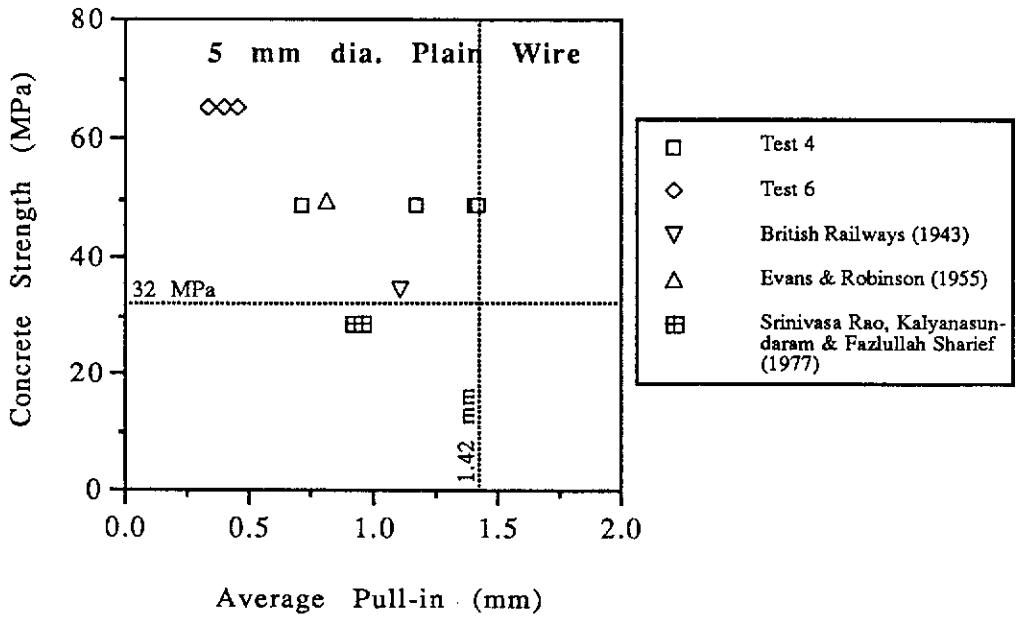

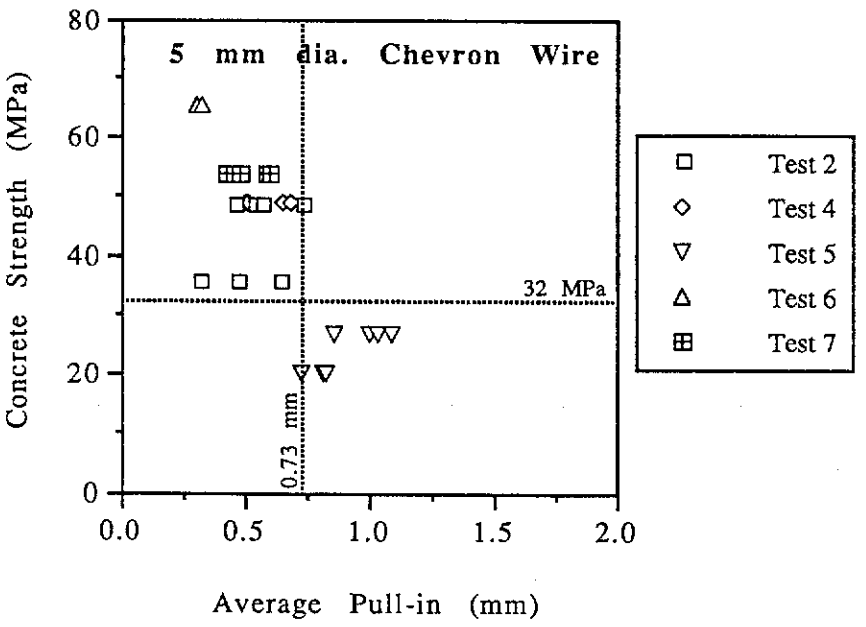

Figure 4.27 Plots of f_{cp} vs. Average Δ_o for 5 mm dia. Plain and 5 mm dia. Chevron Wires

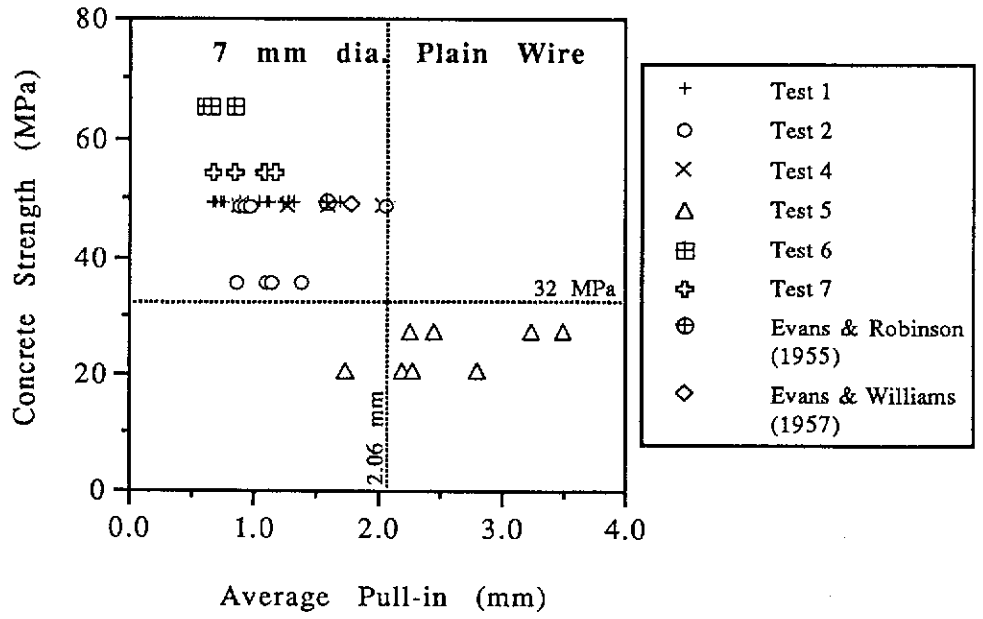

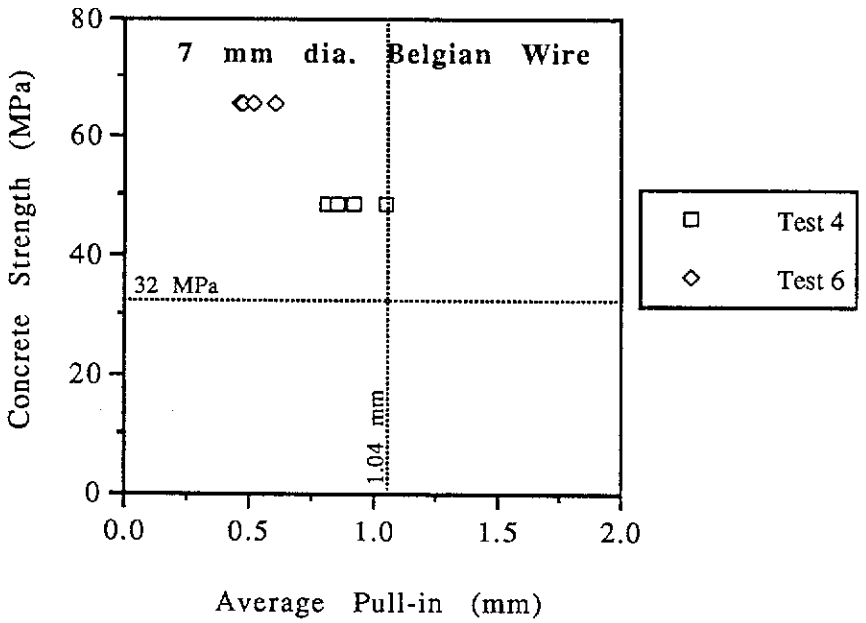

Figure 4.28 Plots of f_{cp} vs. Average Δ_0 for 7 mm dia. Plain and 7 mm dia. Belgian Wires

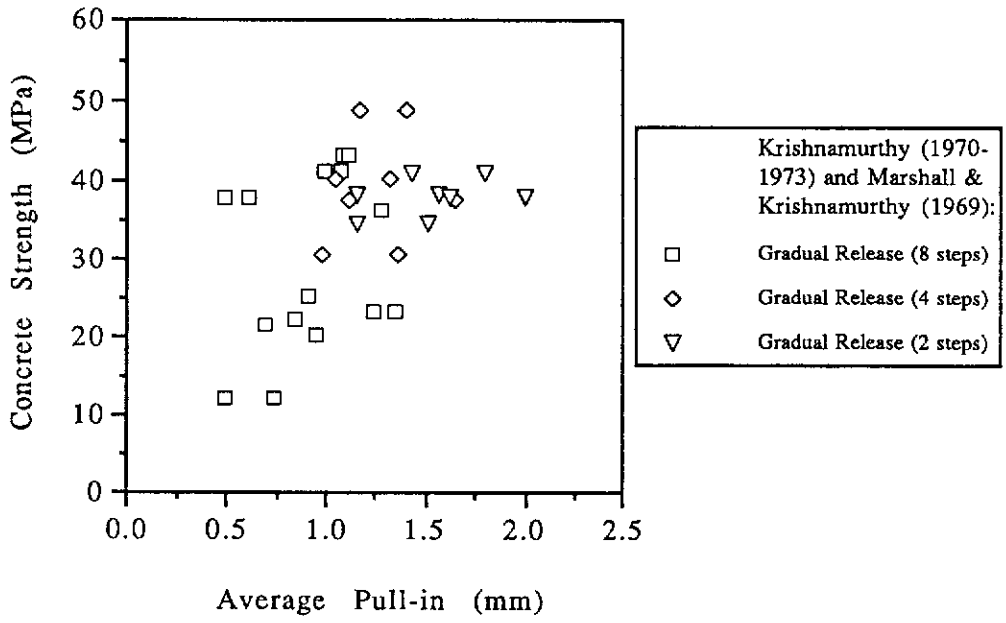

Figure 4.29 Plot of f_{cp} vs. Average Δ_o for 5 mm dia. Belgian Wire

In contrast, the plot for the 5 mm dia. Belgian wire did not indicate the trend found in the other four f_{cp}-Δ_o plots where the data points were generally located in either region of {large f_{cp}-small L_p} or {small f_{cp}-large L_p}. The graph in Figure 4.30 is the stress/strength versus pull-in plot for the 5 mm dia. Belgian wire. Neither Figure 4.29 nor 4.30 gives an indication of segregation in the data points.

The pull-ins obtained for concrete transfer strength equal to or better than 32 MPa had the following upper limits:

(a) 5 mm dia. Plain wire $\Delta_o \leq 1.42$ mm (0.28 d_b)
(b) 5 mm dia. Chevron wire $\Delta_o \leq 0.73$ mm (0.15 d_b)
(c) 7 mm dia. Plain wire $\Delta_o \leq 2.06$ mm (0.29 d_b)
(d) 7 mm dia. Belgian wire $\Delta_o \leq 1.04$ mm (0.15 d_b)
(e) 5 mm dia. Belgian wire $\Delta_o \leq 2.00$ mm (0.40 d_b)

Equations 4.18 (a)-(e)

The benefit of using indented wires is obvious from comparing results for the 5 mm dia. Plain wire with those for the 5 mm dia. Chevron wire, and results for the 7 mm dia. Plain wire with those for the 7 mm dia. Belgian wire. In both cases, the indented wires gave limits which were about one-half of those for plain wires.

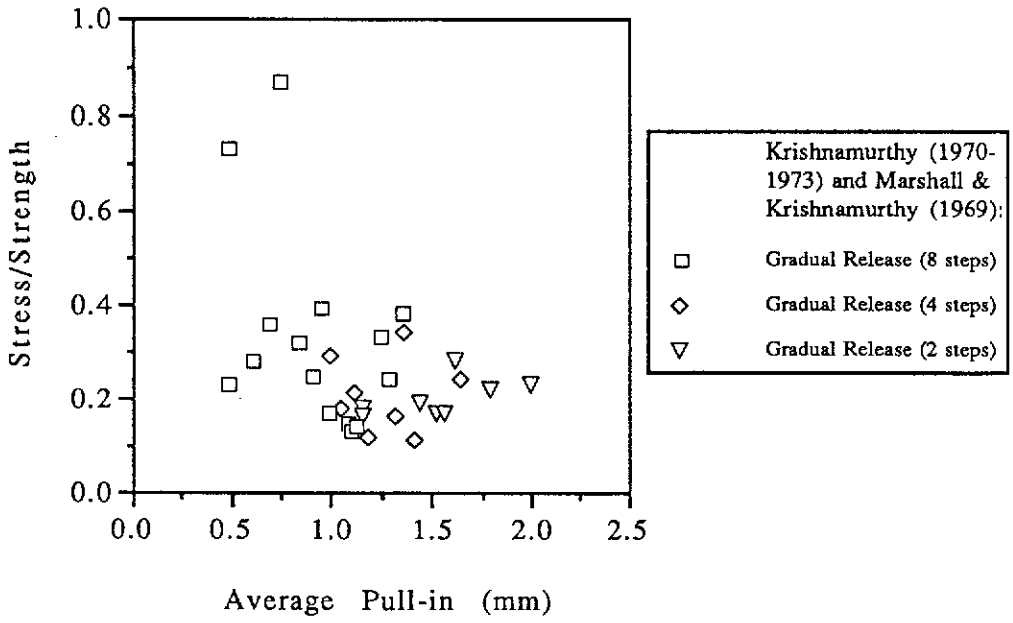

Figure 4.30 Plot of Stress/Strength vs. Average Pull-in for 5 mm dia. Belgian Wire

Anderson and Anderson (1976) suggested 0.15 d_b to 0.16 d_b for pull-in in strands (f_{cp} = 65 and 20 MPa respectively). On the contrary, pull-in for a 12.7 mm or 15.2 mm dia. strand of 0.14 d_b was considered by Chandler (1984) to indicate "*poor transfer bonding of the strand and/or the presence of cracks in the bursting zone in the surrounding concrete*". The comparison of the limits for the indented wires and the strands tends to suggest that the pull-in behaviour of the indented wire may be comparable to those for the strands. It must be stressed that although the limits are fairly similar, it does not mean that the actual bond transfer mechanisms are the same.

Figures 4.31 and 4.32 show bar charts of mean and standard deviation of Δ_0 versus categories of f_{cp} and $\left(\frac{P/A_c}{f_{cp}}\right)$ for the various types of wires.

Data not considered in these bar charts include:

(a) data where the concrete stress $\left(\frac{P}{A_c}\right)$ was not known.

(b) outlying data points for the 5 mm dia. Plain and 7 mm dia. Plain wires in Figures 4.27 and 4.28.

(c) points with inconsistent categories of f_{cp} and $\left(\frac{P/A_c}{f_{cp}}\right)$ as explained earlier.

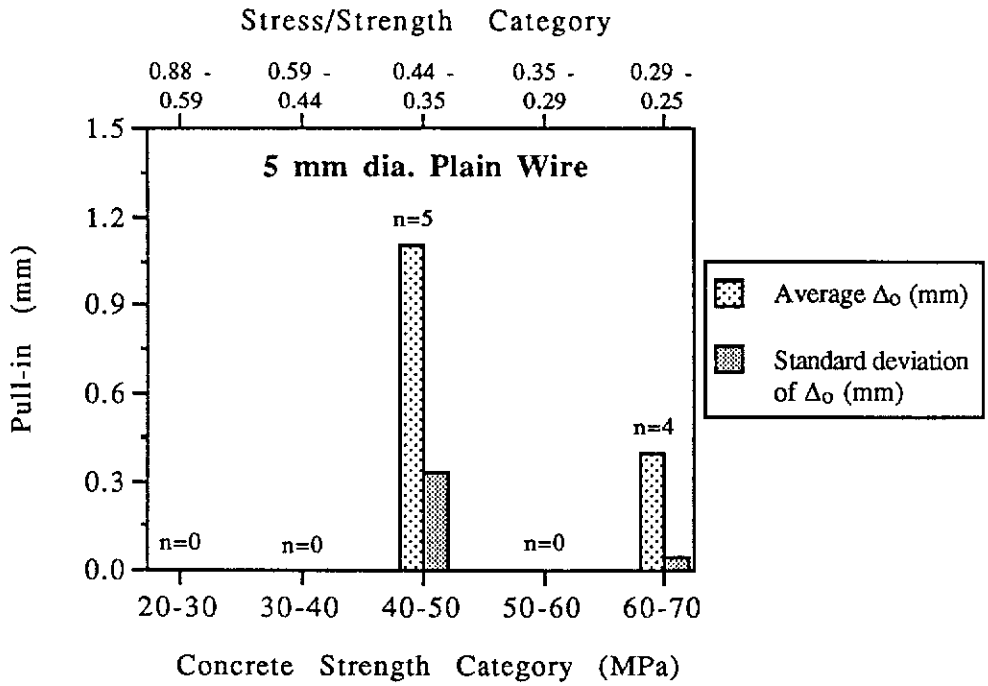

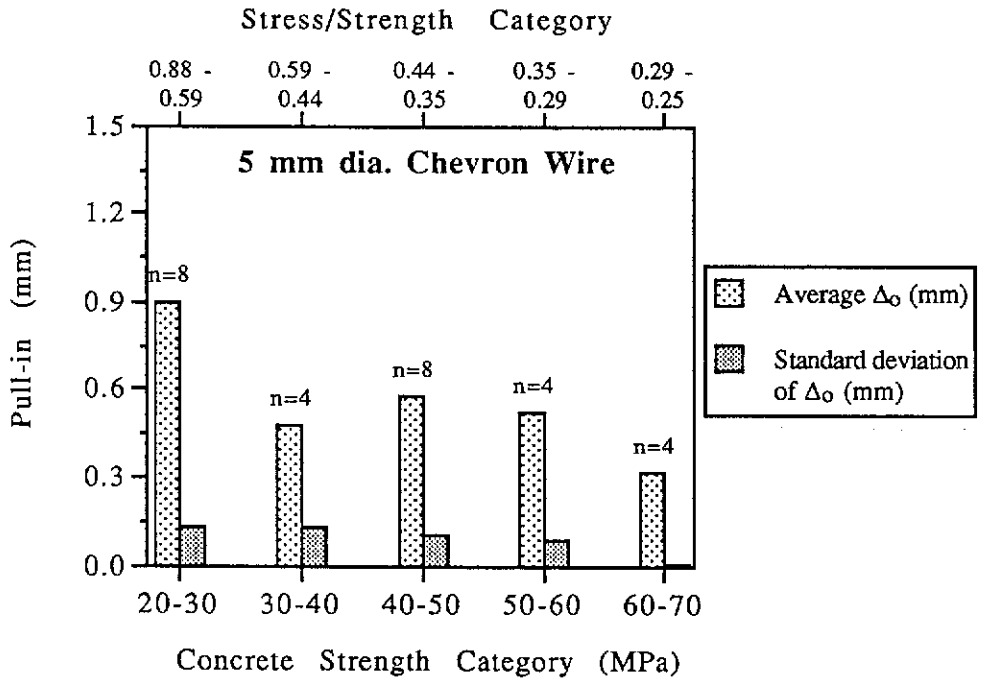

Figure 4.31 Bar Charts of Δ_o vs. f_{cp} and $\left(\frac{P/A_c}{f_{cp}}\right)$ Categories for 5 mm dia. Plain and 5 mm dia. Chevron Wires

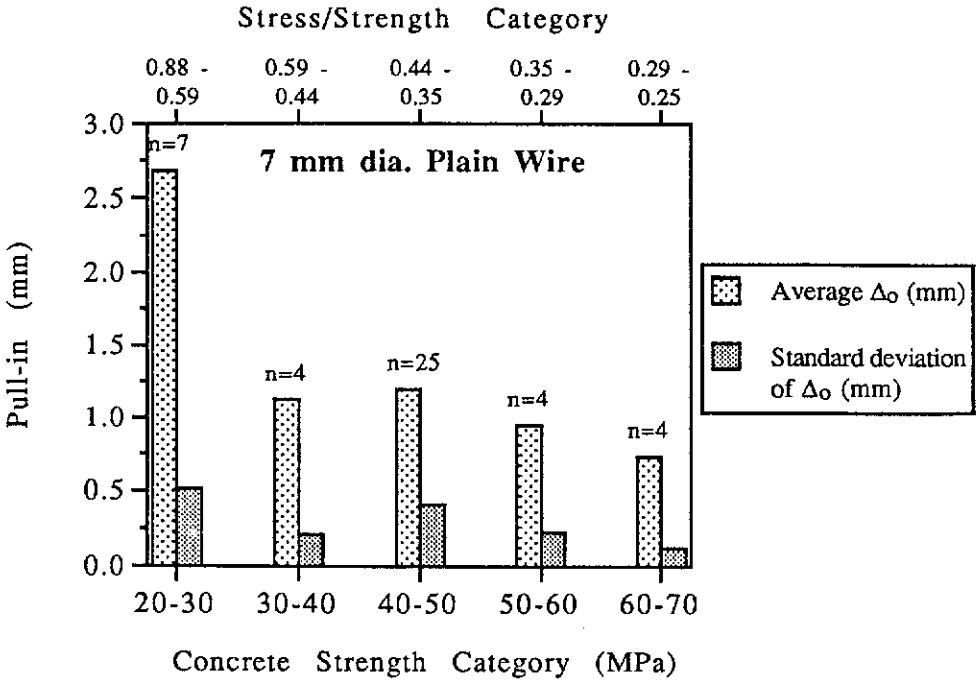

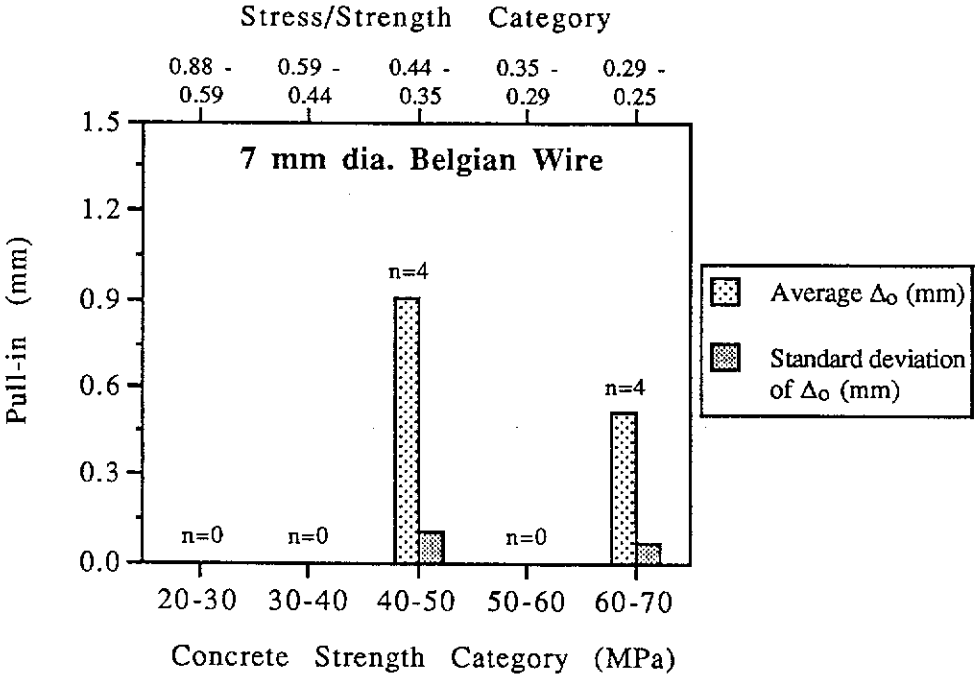

Figure 4.32 Bar Charts of Δ_o vs. f_{cp} and $\left(\frac{P/A_c}{f_{cp}}\right)$ Categories for 7 mm dia. Plain and 7 mm dia. Belgian Wires

Pull-ins obtained for concrete transfer strength of 60-70 MPa were smaller than pull-ins obtained for concrete with lower strength for every type of wire. However, there is insufficient data to establish if this is statistically significant. Furthermore, the smaller pull-ins may be the result of high concrete strength and small stress/strength ratio.

Data was not available for concrete strength categories of 20-30, 30-40 and 50-60 MPa for both the 5 mm dia. Plain and 7 mm dia. Belgian wires. A summary of the results with respect to the bar charts is given in Table 4.7.

Table 4.7 Pull-ins for Various Wires According to Concrete Strength Categories of 20-30 and 30-70 MPa

Type of Wire	f_{cp} (MPa)	Average Δ_o (mm)	Standard deviation of Δ_o (mm)	Range of Δ_o (mm)	Δ_o as function of d_b	Remarks
5 mmØ Plain	20-30	-	-	-	-	Three points removed; 2 pts. from Srinivasa Rao et al. (1977) and 1 pt. from British Railways (1943).
	30-70	0.79	0.44	0.34-1.42	$0.16\ d_b \pm 0.13\ d_b$	
5 mmØ Chevron	20-30	0.90	0.13	0.73-1.09	$0.18\ d_b \pm 0.04\ d_b$	Data points from current tests used .
	30-70	0.50	0.13	0.31-0.73	$0.10\ d_b \pm 0.05\ d_b$	
7 mmØ Plain	20-30	2.68	0.52	2.20-3.50	$0.38\ d_b \pm 0.12\ d_b$	Two points removed; f_{cp} = 20.1 MPa, Δ_o = 1.75 mm from Test 5 and 1 pt. from Evans & Williams (1957) .
	30-70	1.11	0.38	0.62-2.06	$0.16\ d_b \pm 0.14\ d_b$	
7 mmØ Belgian	40-50	0.90	0.10	0.81-1.04	$0.13\ d_b \pm 0.02\ d_b$	Four results for each of the two categories.
	60-70	0.51	0.06	0.46-0.52	$0.07\ d_b \pm 0.01\ d_b$	

The estimates for Δ_o with transfer strength equivalent to or better than 32 MPa are as follows:

(a) $\Delta_o = 0.16\ d_b \pm 0.13\ d_b$ (5 mm dia. Plain wire)

(b) $\Delta_o = 0.10\ d_b \pm 0.05\ d_b$ (5 mm dia. Chevron wire)

(c) $\Delta_o = 0.16\ d_b \pm 0.14\ d_b$ (7 mm dia. Plain wire)

(d) $\Delta_o = 0.13\ d_b \pm 0.02\ d_b$ (7 mm dia. Belgian wire)

Equations 4.19 (a)-(d)

The upper pull-in limits for the 5 mm dia. Plain and 7 mm dia. Plain wires are 0.29 d_b and 0.30 d_b and these are about twice the pull-in limit of 0.15 d_b for both the 5 mm dia. Chevron and 7 mm dia. Belgian wires. It can also be seen that the ranges are consistently greater for the plain wires compared to the indented wires.

4.12 Limits To The Transmission Length Versus Pull-in Equations

For each type of wire used, there were limits given for the transmission length and pull-in. However, there were also relationships developed for L_p versus Δ_o. The following will establish suitable upper limits of $\hat{L}_p$ and $\hat{\Delta}_o$ for the transmission length and pull-in.

The L_p-Δ_o relationships for the 5 mm dia. Plain, 5 mm dia. Chevron and 7 mm dia. Plain wires were given in Section 4.9 and the limits for transmission length and pull-in were given in Equations 4.16(a)-(c) and 4.18 (a)-(c); with gradual release and $f_{cp} \geq 32$ MPa. The matched pairs of limiting values are:

(a) $\hat{L}_p = 600$ mm and $\hat{\Delta}_o = 1.42$ mm; (5 mm dia. Plain)

(b) $\hat{L}_p = 450$ mm and $\Delta_o = 0.50$ mm, (5 mm dia. Chevron)
$\hat{\Delta}_o = 0.73$ mm and $L_p = 325$ mm;

(c) $\hat{L}_p = 700$ mm and $\Delta_o = 1.58$ mm, (7 mm dia. Plain)
$\hat{\Delta}_o = 2.06$ mm and $L_p = 650$ mm.

The $\hat{L}_p$ was used to predict a corresponding $\hat{\Delta}_o$ using the linear equations and vice versa. The pairs of $\hat{L}_p$ and $\hat{\Delta}_o$ with the largest values were then adopted as the upper bounds for estimating the maximum transmission lengths and pull-ins for these three types of wires according to the existing data. Figure 4.33 shows the L_p versus Δ_o linear equation and two sets of the actual and predicted limits for the 5 mm dia. Plain wire.

From suitable calculations made, the upper limits found for the current and previous test data were found as follows:

$\hat{L}_p = 690$ mm and $\hat{\Delta}_o = 1.42$ mm (5 mm dia. Plain)

$\hat{L}_p = 450$ mm and $\hat{\Delta}_o = 0.90$ mm (5 mm dia. Chevron)

$\hat{L}_p = 720$ mm and $\hat{\Delta}_o = 2.06$ mm (7 mm dia. Plain)

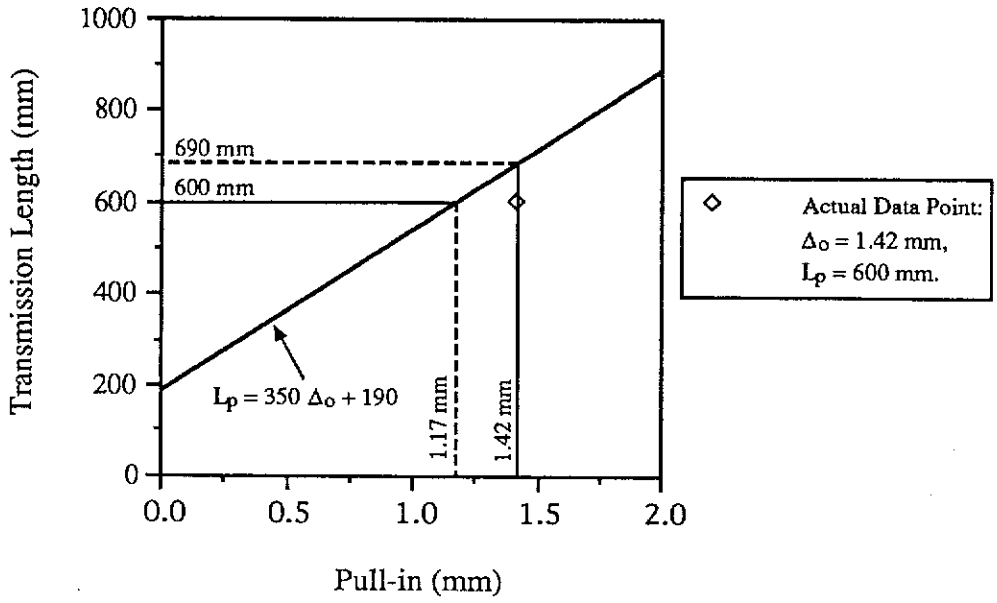

Figure 4.33 L_p vs. Δ_o Relationship and Limits of $\hat{L}_p$ and $\hat{\Delta}_o$ for 5 mm dia. Plain Wire

4.13 Formulae For Determining Transmission Length Using Dimensional Analysis

The preceding sections have considered how the transmission length and pull-in were affected by variable concrete strength. There are other factors which can affect L_p and Δ_o, such as:

(a) type of tendon (plain or indented).
(b) surface condition.
(c) diameter of wire.
(d) method of release.
(e) cracking and tensile capacity in concrete.
(f) tendon stress.
(g) compaction of fresh concrete.
(h) maturity of concrete.
(i) geometry of beam cross-section.
(j) stress level in concrete.
(k) time effects.

The only variables which can be quantitatively taken into account are the concrete strength (f_{cp}), cross-sectional area of the specimen (A_c), the

initial tendon stress (f_{si}) and diameter of the wire (d_b). Practically all the wires were de-rusted before use but this could not be measured. Only data for gradual releases was considered in attempting to establish a formulae for the transmission length. Therefore, cracking was not a problem as it only occurred in sudden or shock released beams. The degree of compaction could not be measured but care had been taken to provide uniform and good consolidation to the concrete mixes during placing.

Dimensional analysis was carried out assuming that the transmission length was a function of d_b, f_{si}, A_c and f_{cp}. There is no doubt that L_p is a function of wire diameter and tendon stress, as purported by reseachers such as Guyon (1953) and Ganguli (1966). The ACI 318-89 standard uses the effective tendon stress (f_{se}) to evaluate the transmission length instead of f_{si}:

$$L_p = \frac{f_{se}}{f_{cp}} d_b \qquad \text{Equation 4.20}$$

However, the ACI 318-89 equation does not take into account the variation in the concrete cross-sectional area. The author believes that the longitudinal axial concrete stress, $\sigma_{co} \left(= \frac{f_{si}.A_p}{A_c}\right)$, is more appropriate than f_{se} since it also takes into account the ratio of steel area to concrete area. The outcome of the dimensional analysis is an equation of the form:

$$\left(\frac{L_p}{d_b}\right) = \beta \left(\frac{\sigma_{co}}{f_{cp}}\right)^{\gamma} = \beta \left(\frac{f_{si}.A_p}{f_{cp}.A_c}\right)^{\gamma} \qquad \text{Equation 4.21}$$

$$\text{or} \quad \log\left(\frac{L_p}{d_b}\right) = \gamma \log\left(\frac{f_{si}.A_p}{f_{cp}.A_c}\right) + \log\beta \qquad \text{Equation 4.22}$$

where, β and γ are coefficients of the equation.

The data was checked to see if there was a linear relationship between $\log\left(\frac{L_p}{d_b}\right)$ and $\log\left(\frac{f_{si}.A_p}{f_{cp}.A_c}\right)$. It can be seen that $\left(\frac{f_{si}.A_p}{f_{cp}.A_c}\right)$ is the stress/strength ratio or $\left(\frac{P/A_c}{f_{cp}}\right)$. Data from previous investigations was omitted if the stress σ_{co} or $\left(\frac{P}{A_c}\right)$ was not known.

A reasonable linear equation with a correlation coefficient of 0.69 was obtained for the 5 mm and 7 mm dia. Plain wires, as shown in Figure 4.34.

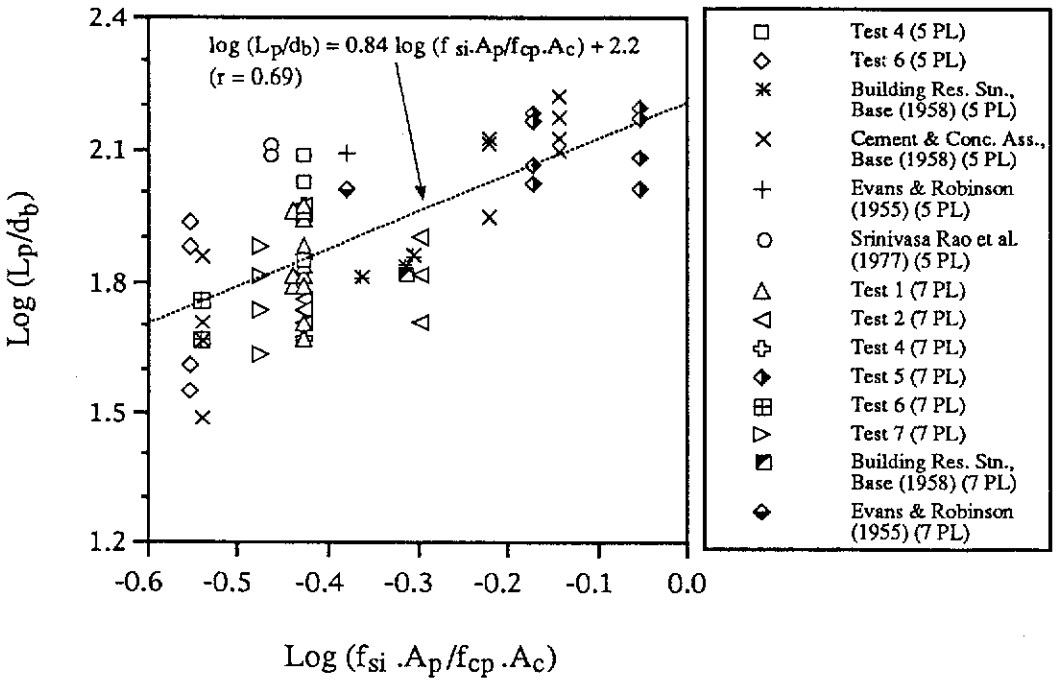

(Note: 5 PL = 5 mm dia. Plain wire and 7 PL = 7 mm dia. Plain wire)

Figure 4.34 Plot of Log $\left(\frac{L_p}{d_b}\right)$ vs. Log $\left(\frac{f_{si}.A_p}{f_{cp}.A_c}\right)$ for 5 mm and 7 mm dia. Plain Wires

The regression analysis gave the following:

$$\gamma = 0.84 \quad \text{and} \quad \log \beta = 2.20$$

which gave,

$$\left(\frac{L_p}{d_b}\right) = 158 \left(\frac{f_{si}.A_p}{f_{cp}.A_c}\right)^{0.84} \qquad \text{Equation 4.23}$$

The more significant deviations of the actual L_p values from predicted values using Equation 4.23 occur for small L_p values (towards the left hand end of the graph). Two points scattered furthest away above and below this curve are:

(a) $\left(\frac{P}{A_c}\right)$ = 9.8 MPa, f_{cp} = 28.4 MPa and L_p = 638 mm

(Beam 5P-3-1 by Srinivasa Rao et al. (1977)) - above

(b) $\left(\frac{P}{A_c}\right)$ = 16.6 MPa, f_{cp} = 57.4 MPa and L_p = 152 mm

(Beam P4(3) by the Cement and Concrete Ass., Base (1958)) - below

The predicted transmission lengths were (a) 320 mm and (b) 280 mm respectively. The deviation of the actual transmission lengths from the predicted values were -99% and +46% respectively. However, it seems that

the transmission lengths by Srinivasa Rao et al. were much greater than expected, especially for the small axial prestress of 9.8 MPa. The two beams (5P-3-1 and 5P-3-2) were both prestressed with four 5 mm dia. plain wires each and gradual release was implemented. Transmission lengths were 638 and 605 mm which are very large. The method used for determining L_p was through using the equation $L_p = 1.35\ L_{80\%}$. The author considered these points to be unreliable and they were disregarded. This meant that the next data point with the greatest deviation above the predicted values was considered:

(c) $\left(\frac{P}{A_c}\right)$ = 18.2 MPa, f_{cp} = 48.7 MPa and L_p = 600 mm

(from 4G-D2 (L) in Test 4)

The equation for determining L_p for plain wires with the range covering all the data points, including point (c) above, is given by the following:

$$L_p = 158\, d_b \left(\frac{f_{si}.A_p}{f_{cp}.A_c}\right)^{0.84} \pm 71\% \qquad \text{Equation 4.24}$$

A similar plot in Figure 4.35 was made for 5 mm and 7 mm dia. Indented wires, assuming that the different types of indented wires could be grouped together. The scatter for the indented wires is comparable to that for the plain wires in Figure 4.34. The regression analysis yielded (r = 0.69):

$$\gamma = 0.70 \quad \text{and} \quad \log \beta = 2.08$$

which gave,
$$\left(\frac{L_p}{d_b}\right) = 120 \left(\frac{f_{si}.A_p}{f_{cp}.A_c}\right)^{0.70} \qquad \text{Equation 4.25}$$

Data from Arthur and Ganguli (1965), Krishnamurthy (1970-1973) and, Marshall and Krishnamurthy (1969) for the 5 mm dia. Belgian wire was not included as there was great scatter in these plotted points. Furthermore, these results were dubious as explained earlier.

Data points above and below the line of best fit giving the largest deviations were:

(a) $\left(\frac{P}{A_c}\right)$ = 17.0 MPa, f_{cp} = 26.8 MPa and L_p = 750 mm

(from 5G-D4 (D) in Test 5) - above

(b) $\left(\frac{P}{A_c}\right)$ = 17.7 MPa, f_{cp} = 65.1 MPa and L_p = 200 mm

(from 6G-D5 (L) in Test 6) - below

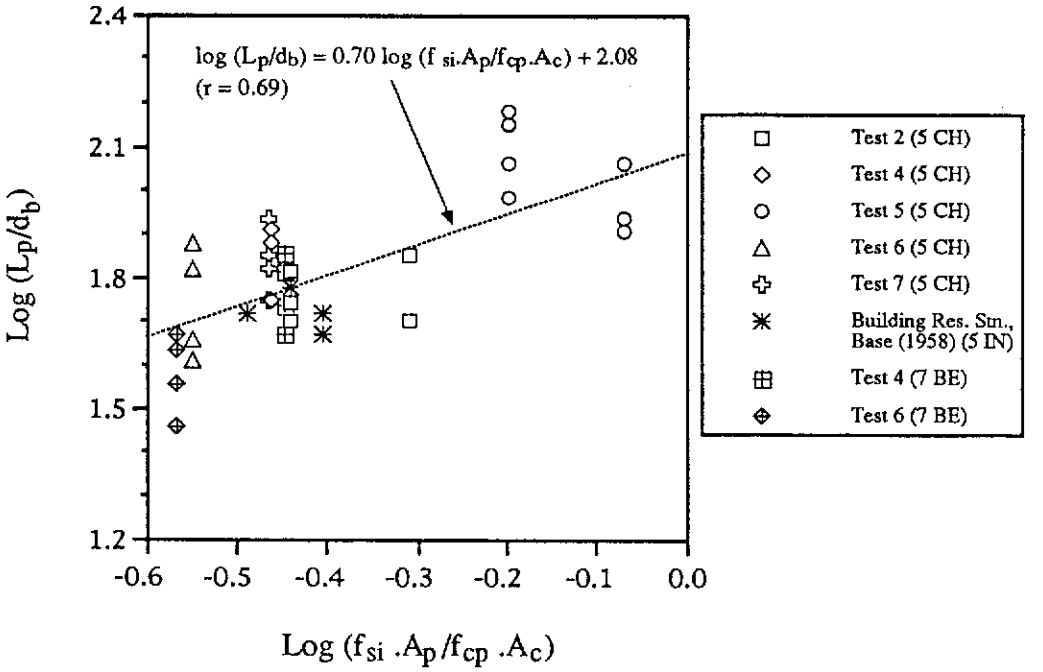

(Note: 5 CH = 5 mm dia. Chevron wire, 5 IN = 5 mm dia. Indented wire (type unknown), and 7 BE = 7 mm dia. Belgian wire)

Figure 4.35 Plot of Log $\left(\frac{L_p}{d_b}\right)$ vs. Log $\left(\frac{f_{si}.A_p}{f_{cp}.A_c}\right)$ for 5 mm and 7 mm dia. Indented Wires

The predicted transmission lengths were (a) 440 mm and (b) 340 mm and the corresponding percentages of deviation were -70% and +41% respectively. The equation can be re-stated with a range covering all the data points as follows:

$$L_p = 120\, d_b \left(\frac{f_{si}.A_p}{f_{cp}.A_c}\right)^{0.70} \pm 70\% \qquad \text{Equation 4.26}$$

Both the equations for the plain and indented wires are not particularly accurate in predicting the transmission length and the large percentage errors highlight this. However, it may be helpful to be able to roughly estimate L_p while appreciating the fact that there can be great variation in the actual values obtained. Estimates of the transmission lengths from Equations 4.24 and 4.26 were compared with experimental values from Table 4.6. The associated errors of 71% and 70% were ignored since they are applicable to results with the greatest deviations. The ranges for L_p are given in Table 4.8 (it was assumed that $\left(\frac{P}{A_c}\right)$ = 17.6 MPa):

Table 4.8 Ranges of Experimental L_p from Table 4.6 and Predicted L_p from Equations 4.24 and 4.26

Type of Wire	f_{cp} (MPa)	Ranges of Experimental L_p	Ranges of Predicted L_p
5 mm dia. Plain	20 - 30	110 - 170 d_b	100 - 140 d_b
	30 - 70	20 - 120 d_b	50 - 100 d_b
5 mm dia. Chevron	20 - 30	90 - 150 d_b	80 - 110 d_b
	30 - 70	30 - 90 d_b	50 - 80 d_b
7 mm dia. Plain	20 - 30	100 - 160 d_b	100 - 140 d_b
	30 - 70	40 - 100 d_b	50 - 100 d_b
7 mm dia. Belgian	30 - 70	50 - 70 d_b	50 - 80 d_b

The ranges of predicted transmission lengths are fairly close to the experimental ranges for both the 7 mm dia. wires but tend to be slightly smaller for the 5 mm dia. wires. The given formulae can be expected to give reasonable estimates of transmission lengths for plain and indented wires.

Given the large errors in these equations, it is fair to argue that the less complex {L_p = "constant" x d_b ± error} relationships previously given in Section 4.10 are more appropriate for determining the transmission lengths. Comparing the more simplified L_p-d_b equations to Equations 4.24 and 4.26, the "constants" in the simpler equations seem to be equivalent to functions of the stress/strength $\left(\frac{f_{si}.A_p}{f_{cp}.A_c}\right)$ ratio in the more complex equations. However, the stress/strength ratio did not remain constant for the different tests. The concrete strengths (f_{cp}) varied even though the stresses $\left(\frac{P}{A_c}\right)$ were kept close to the nominal 17.6 MPa. The scatter in the data made it difficult to determine whether the transmission length can be stated as a function of f_{cp}. More tests are required to determine whether Equations 4.24 and 4.26 are true for other conditions, especially with varying geometry and $\left(\frac{P}{A_c}\right)$.

4.14 Time Dependent Effects On The Transmission Length And Pull-in

Tests 1 and 2 had transmission lengths and pull-ins monitored for up to 6 months after casting the concrete specimens whereas Tests 3, 4, 5 and 6 were monitored up to 3 months only. The last set of beams in Test 7 had measurements taken during transfer at 7 days and also at 28 days after casting. For determining whether L_p and Δ_o have changed over time, two comparisons were made:

(a) L_p and Δ_o at transfer versus L_p and Δ_o at 3 months (Tests 1-6)

(b) L_p and Δ_o at transfer versus L_p and Δ_o at 6 months (Tests 1 & 2)

The changes in transmission lengths and pull-ins were grouped into categories for each type of wire used in order to ease the presentation of these results, this will be obvious in the following sub-sections of 4.14.1 and 4.14.2.

4.14.1 Transmission Lengths and Pull-ins at 3 Months

Changes in the transmission lengths over three months were grouped into ten categories with mid-values of -50, -25, 0, 25, 50, 75, 100, 125, 150 and 175 mm.

Likewise, eleven arbitrary categories were chosen for grouping changes in the pull-ins over time and they have mid-values of -0.20, -0.10, 0.00, 0.10, 0.20, 0.30, 0.40, 0.50, 0.60, 0.75 and 0.96 mm. The frequencies of occurrence for the changes in the transmission lengths and pull-ins were plotted in bar charts given in Figures 4.36 and 4.37.

It was found that both the transmission lengths and pull-ins obtained at three months could be greater than, equal to or less than those at transfer, hence there were results with negative values. Transmission lengths were dependent on strain profiles and their decrease could be caused by small fluctuations in these profiles. The change of -50 mm for the 5 mm dia. Chevron wire in beam end 2G-D4 (L) was reasonable. Theoretically, transmission lengths are expected to remain constant or lengthen but not shorten with time.

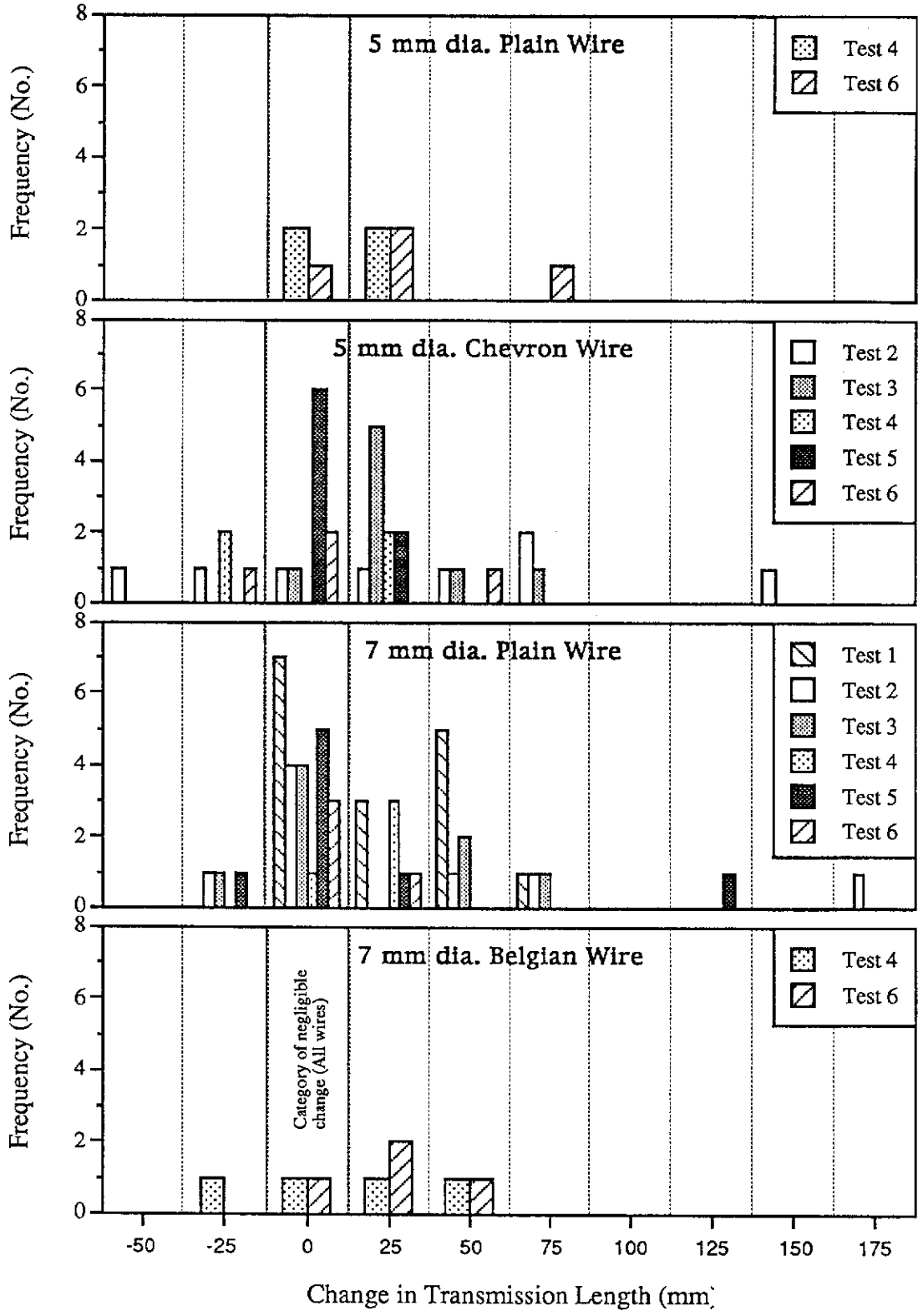

Figure 4.36 Bar Charts of Frequency vs. Category for Change in Transmission Length (At 3 months Relative to Transfer)

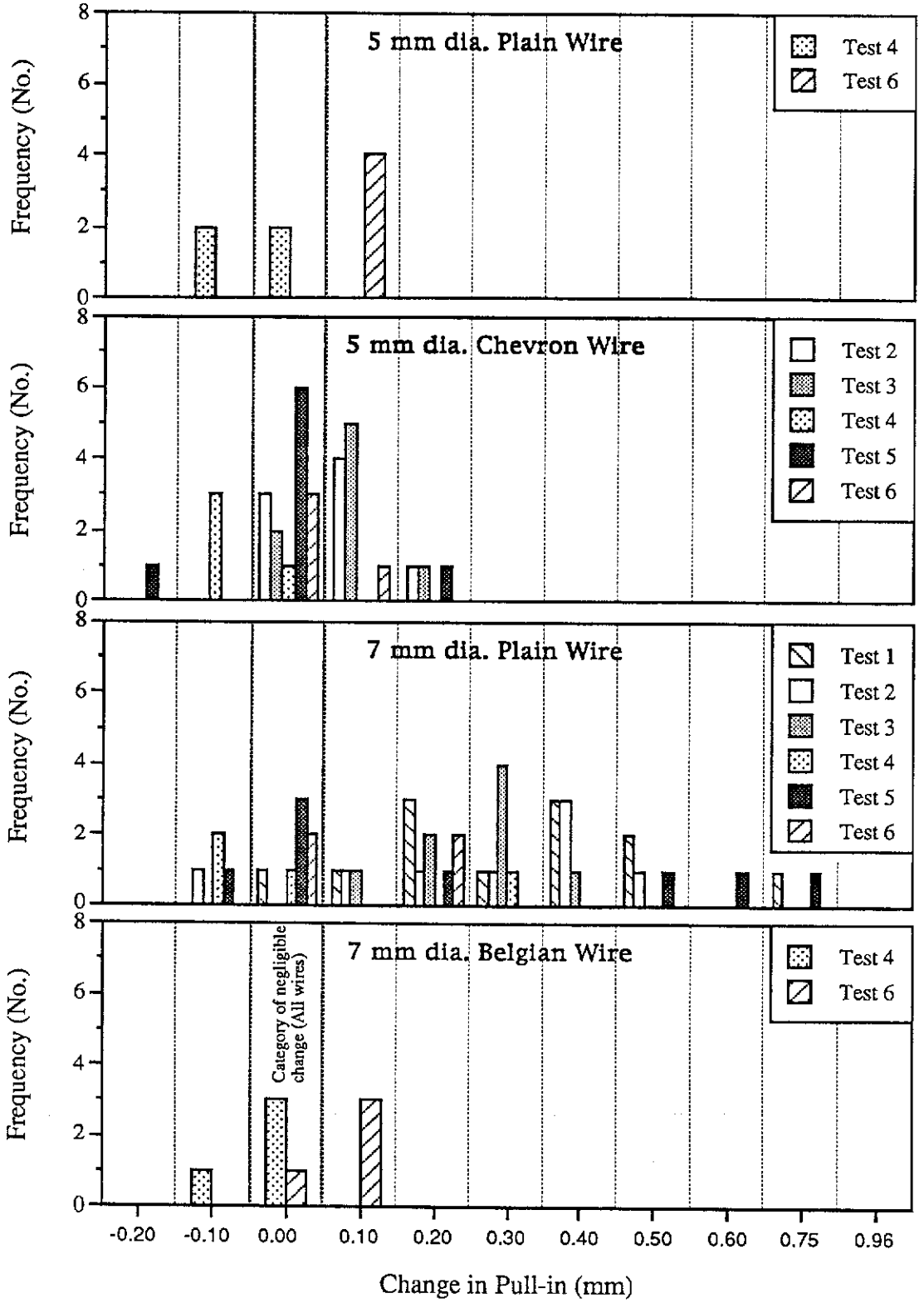

Figure 4.37 Bar Charts of Frequency vs. Category for Change in Pull-in (At 3 months Relative to Transfer)

Negative pull-ins implied "pull-outs". Small negative values may have been caused by inaccuracies when taking the pull-in readings. However, the change of -0.23 mm in beam end 5G-L4 (D) was unexpected. Its occurrence cannot be explained but it is possible that either the face of this beam end or the pull-in attachment was disturbed. It is noted that the change in pull-in between 28 days and transfer was only +0.01 mm.

Charts in Figures 4.36 show that only 9 results at 3 months fell into the negative value categories. Most of the results were between the categories with mid-values of 0 and 75 mm (only one result for the 5 mm dia. Chevron wire and two results for the 7 mm dia. wire were beyond this range). At 3 months, 75 mm seemed a reasonable value of maximum increase in the transmission length to be expected, with the exceptions that the 5 mm dia. Chevron and 7 mm dia. Plain wires increased by as much as 150 mm and 175 mm respectively. The different concrete strengths at 3 months or the different types of tests performed did not seem to have an effect on the distribution of the change in transmission length.

Just as for the transmission lengths, the changes in pull-ins at 3 months after casting generally increased (Figure 4.37). For the 5 mm dia. Plain and 7 mm dia. Belgian wires, the upper bound category for the current tests was 0.06 mm to 0.15 mm. The corresponding category for the 5 mm dia. Chevron wire was 0.16 mm to 0.25 mm. The 7 mm dia. Plain wire had much greater pull-ins than the other wires; the maximum increase in pull-in was 0.75 mm at 3 months.

A summary of the changes in the transmission lengths and pull-ins (δL_p and $\delta \Delta_o$ respectively) found for each type of wire used in the current tests is given in Table 4.9.

On the average, there are increases in both transmission length and pull-in. The average δL_p fell into a tight range of 19 mm to 23 mm, with greater values for the plain wires. The average $\delta \Delta_o$ did not behave as such. Compared to the indented wires, the 7 mm dia. Plain wire had large increases in the pull-ins but this was not the case for the 5 mm dia. Plain wire. A more objective approach is to consider the changes as a fraction of the initial transmission lengths and pull-ins at the time of transfer,

Table 4.9 Changes in the Transmission Lengths and Pull-ins at 3 Months Relative to Transfer

Type of Wire	Range of δL_p (mm)	Average of δL_p (mm)	Standard Deviation of δL_p (mm)	Range of $\delta \Delta_o$ (mm)	Average of $\delta \Delta_o$ (mm)	Standard Deviation of $\delta \Delta_o$ (mm)
5 mm dia. Plain	0 to 75	22	25	-0.12 to 0.14	0.03	0.10
5 mm dia. Chevron	-50 to 150	20	39	-0.23 to 0.18	0.04	0.09
7 mm dia. Plain	-25 to 175	23	38	-0.13 to 0.75	0.24	0.20
7 mm dia. Belgian	-25 to 50	19	26	-0.08 to 0.13	0.05	0.07

ie. $\frac{\delta L_p}{L_{pi}}$ and $\frac{\delta \Delta_o}{\Delta_{oi}}$, where L_{pi} and Δ_{oi} are the initial values. The percentages of change are given in Table 4.10, with the results segregated by the concrete strength at transfer of 32 MPa (stress/strength ratio equals 0.55).

Table 4.10 Percentages of Change in the Transmission Lengths and Pull-ins at 3 months Relative to Transfer

Type of Wire	f_{cp} (MPa)	No. of Results for $\frac{\delta L_p}{L_{pi}}$	Range of $\frac{\delta L_p}{L_{pi}}$ (%)	Average of $\frac{\delta L_p}{L_{pi}}$ (%)	Standard Deviation of $\frac{\delta L_p}{L_{pi}}$ (%)	No. of Results for $\frac{\delta \Delta_o}{\Delta_{oi}}$	Range of $\frac{\delta \Delta_o}{\Delta_{oi}}$ (%)	Average of $\frac{\delta \Delta_o}{\Delta_{oi}}$ (%)	Standard Deviation of $\frac{\delta \Delta_o}{\Delta_{oi}}$ (%)
5 mm dia. Plain	≥ 32	8	4 to 38	8	13	8	-17 to 35	10	19
5 mm dia. Chevron	≥ 32	24	-14 to 43	8	14	24	-20 to 44	10	16
	< 32	8	0 to 6	1	2	8	-22 to 17	1	11
7 mm dia. Plain	≥ 32	40	-3 to 50	6	10	36	-15 to 82	24	22
	< 32	8	-3 to 12	1	4	8	-3 to 22	7	9
7 mm dia. Belgian	≥ 32	8	-7 to 15	6	8	8	-9 to 28	9	13

The average values of the percentage changes in the transmission lengths suggest that there is not much difference for the different types of wires where the concrete strengths at transfer were greater than 32 MPa. There is indication from the average percentages of $\frac{\delta L_p}{L_{pi}}$ for 5 mm dia. Chevron and 7 mm dia. Plain wires that there can be smaller increases of $\frac{\delta L_p}{L_{pi}}$ for concrete strength less than 32 MPa (both 1%) compared to those for

concrete strength of at least 32 MPa (8% and 6%). The smaller relative increases were due to the large initial values.

A similar deduction can be drawn from the percentages of change in the pull-ins (ie. compare 10% and 24% (≥ 32 MPa) to 1% and 7% (< 32 MPa) for the 5 mm dia. Chevron and 7 mm dia. Plain wires).

All except one result (viz. average of $\frac{\delta\Delta_o}{\Delta_{oi}}$ = 24%) indicated that there was little difference between the average percentages of change in the transmission lengths and pull-ins for plain and indented wires at three months.

4.14.2 Transmission Lengths and Pull-ins at 6 Months

The bar charts in Figures 4.38 and 4.39 are plots of frequency versus changes in transmission lengths or pull-ins for the 5 mm dia. Chevron and 7 mm dia. Plain wires at 6 months relative to these two parameters at the time of transfer. They were obtained from Tests 1 and 2 which only had these two types of wires.

The average changes in the transmission lengths and pull-ins for the 5 mm dia. Chevron and 7 mm dia. Plain wires at 6 months are given in Table 4.11.

Table 4.11 Changes in the Transmission Lengths and Pull-ins at 6 Months Relative to Transfer

Type of Wire	Range of δL_p (mm)	Average of δL_p (mm)	Standard Deviation of δL_p (mm)	Range of $\delta\Delta_o$ (mm)	Average of $\delta\Delta_o$ (mm)	Standard Deviation of $\delta\Delta_o$ (mm)
5 mm dia. Chevron	-50 to 125	31	59	-0.02 to 0.22	0.11	0.06
7 mm dia. Plain	-13 to 175	37	47	-0.06 to 1.06	0.53	0.24

All the average values are greater than those at 3 months. The percentages of increase above the 3-month average δL_p values are 55% and 61% for the 5 mm dia. Chevron and 7 mm dia. Plain wires respectively. The corresponding increases in the pull-ins are 175% and 121%. These

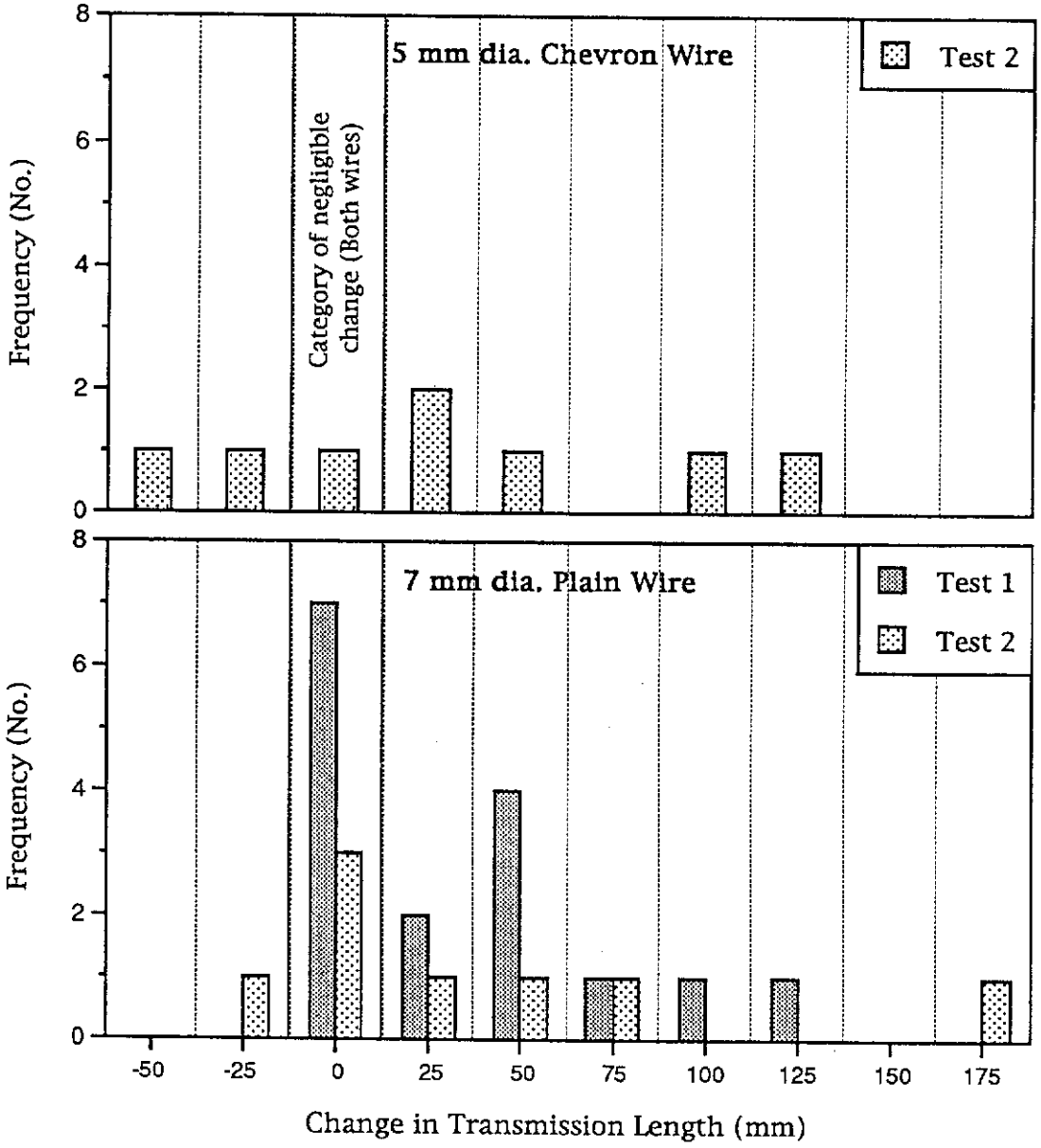

Figure 4.38 Bar Chart of Frequency vs. Category for Change in Transmission Length (At 6 months Relative to Transfer)

percentage increases are viewed with caution as the number of results at 6 months are much less than those for 3 months. From the existing results, it can be said that the transmission lengths and pull-ins generally increased with the progression of time. In fact, the 6-month period of monitoring was not long enough. Ideally, the time of monitoring should have been extended to two years.

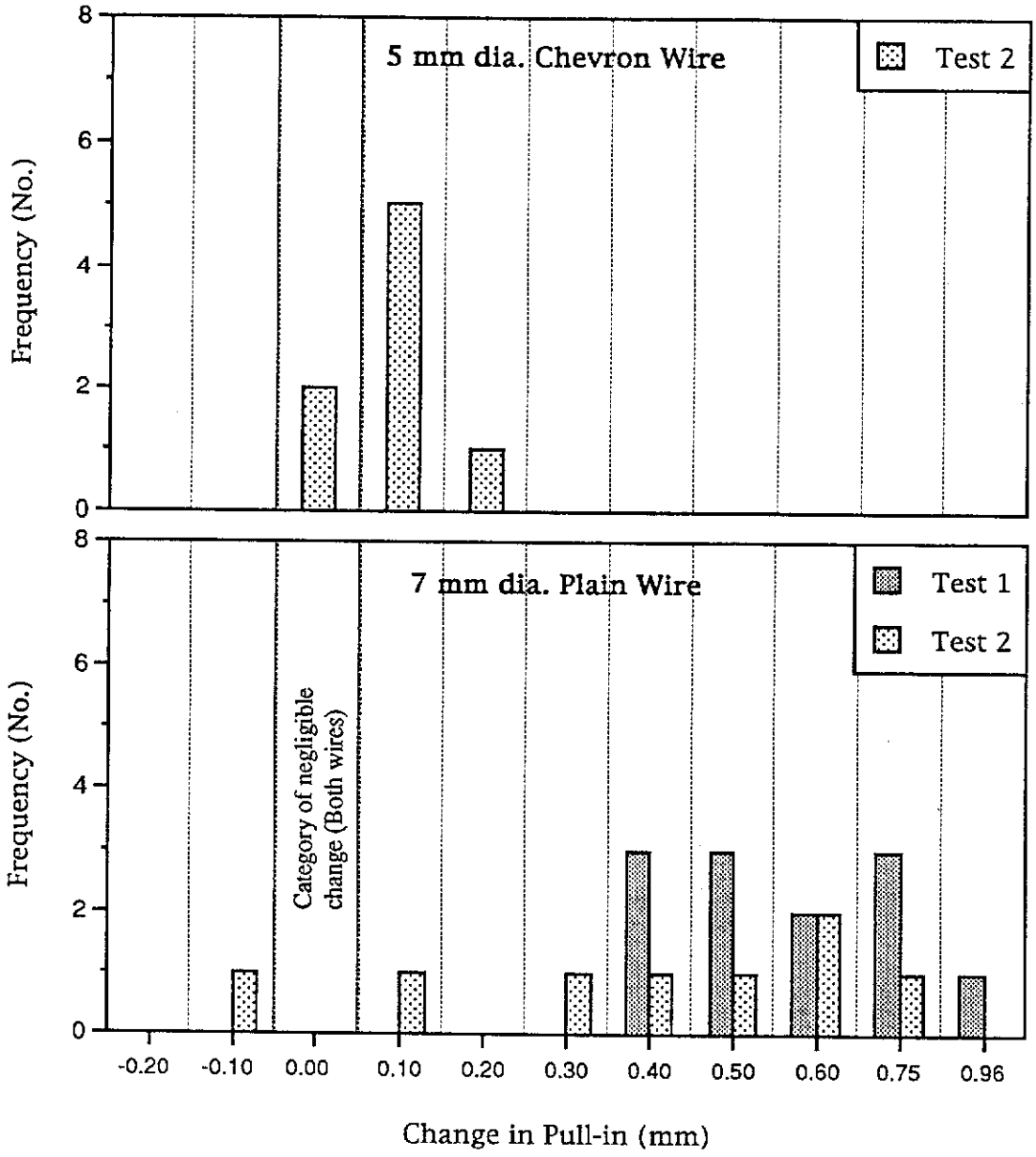

Figure 4.39 Bar Chart of Frequency vs. Category for Change in Pull-in (At 6 months Relative to Transfer)

Base suggested a possible increase of 75 mm to the transmission length for 5 mm dia. Plain wire (obtained from tests by the Building Research Station within 10 days after transfer). The changes in the transmission lengths of up to 125 mm and 175 mm for the 5 mm dia. Chevron and 7 mm dia. Plain wires render Base's prediction as an underestimation for these wires (it is appreciated that the 75 mm increase was not meant to be applicable to wires other than the 5 mm dia. Plain wire but the increase in the 5 mm dia. Chevron wire should have been smaller). Most likely, there are still small increases after 6 months.

The percentage increases for the pull-ins and transmission lengths are presented in Table 4.12. The average percentage increases $\frac{\delta L_p}{L_{pi}}$ are 3% greater than those at 3 months for both wires. In contrast, $\frac{\delta \Delta_o}{\Delta_{oi}}$ increased by 12% and 25% for the 5 mm dia. Chevron and 7 mm dia. Plain wires above the 3-month percentages. Time seemed to have affected the pull-ins more than the transmission lengths.

Table 4.12 Percentages of Change in the Transmission Lengths and Pull-ins at 6 months Relative to Transfer

Type of Wire	f_{cp} (MPa)	No. of Results for $\frac{\delta L_p}{L_{pi}}$	Range of $\frac{\delta L_p}{L_{pi}}$ (%)	Average of $\frac{\delta L_p}{L_{pi}}$ (%)	Standard Deviation of $\frac{\delta L_p}{L_{pi}}$ (%)	No. of Results for $\frac{\delta \Delta_o}{\Delta_{oi}}$	Range of $\frac{\delta \Delta_o}{\Delta_{oi}}$ (%)	Average of $\frac{\delta \Delta_o}{\Delta_{oi}}$ (%)	Standard Deviation of $\frac{\delta \Delta_o}{\Delta_{oi}}$ (%)
5 mm dia. Chevron	≥ 32	8	-14 to 36	11	19	8	3 to 44	22	12
7 mm dia. Plain	≥ 32	24	-2 to 50	9	12	20	-5 to 86	49	24

4.14.3 Normalised Distributions of Longitudinal Strain

Normalising longitudinal strains allowed strain distributions at different ages to be compared. The normalised strain distributions were obtained at the ages of 7 and 28 days, and 3 and 6 months. Two typical normalised longitudinal strain curves are given in Figure 4.40. Appendix G has all the normalised curves up to 6 months for Tests 1 and 2.

It is noted that original strain distributions without correcting for shrinkage or creep were used to determine transmission lengths for all the current tests. Shrinkage strains obtained from shrinkage beams were fairly uniform along each of the test beams and a constant shrinkage value was assigned to each beam. Beams 1S-D3, 1S-L3, 2S-D3 and 2S-L3 had average shrinkage strains of 230, 220, 390 and 320 $\mu\varepsilon$ respectively, which occurred during the first 6 months after transfer. These shrinkage strains were not corrected for when determining L_p because subtracting a constant shrinkage strain value from an entire strain distribution will not change the location of the inner end of the transmission length.

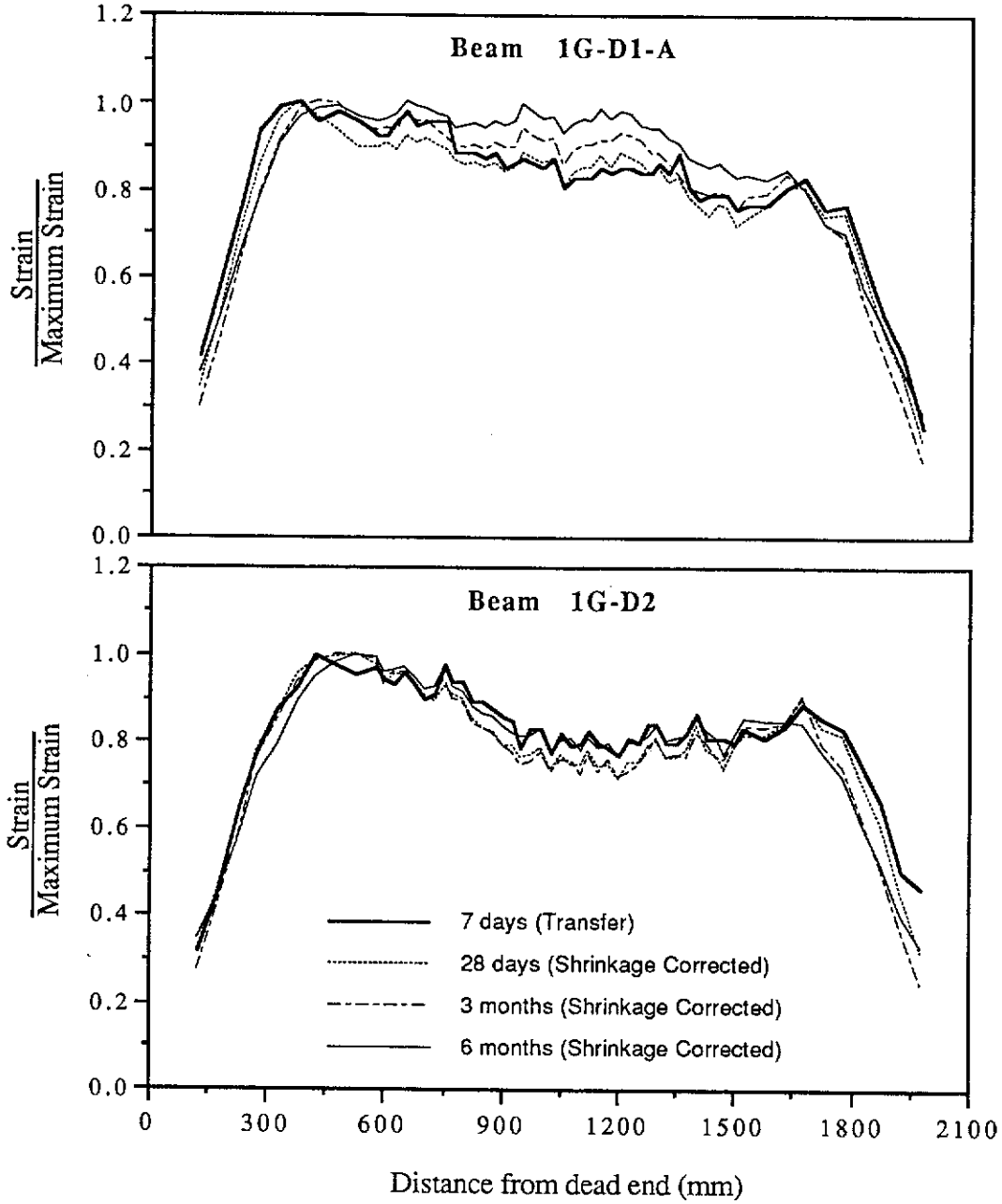

Figure 4.40 Normalised Longitudinal Strain Curves for Beams 1G-D1-A and 1G-D2

However, for the normalisation of the strain curves the shrinkage strains were subtracted off. After correcting for shrinkage, creep mainly accounted for the difference in the strain values between a distribution at transfer and the corresponding distribution at a later age. Although there is negligible difference to the shape of a normalised strain curve with or without the shrinkage correction, the shrinkage strains were removed so that only the combined strains due to prestress transfer and creep were

normalised. Creep had a major influence on the behaviour of the strain distributions in some of the test beams.

With only the transfer and creep strains, the ends of a normalised curve would be directed towards the ends of the beam. However, shrinkage causes a loss of precompression strain in concrete and this also affects the steel strain. The steel strain curve (such as that given in Figure 1 of Base (1957)) will exhibit a loss of prestress at the end of a beam. Consequently, the loss of the prestress force in this location will result in an unstressed length of concrete. It is important to differentiate between the steel and concrete strain curves. Theoretically, if the steel strains could be measured, then the location where zero strain occurred due to the shrinkage effect could be found. This should also be reflected in the concrete strain curve but it may not be obvious since the strains were read over 200 mm gauge lengths which may include lengths of stressed and unstressed concrete. The ability to locate this unstressed zone on the concrete strain curve also depends on the recovery of concrete strain as the tendon loses its prestress.

The recommendations in AS 3600 (1988) which reflect Base's work with respect to the effect of time on the outer and inner ends of the transmission length are given as follows:

(a) *"it shall be assumed that no change in the position of the inner end of the transmission length occurs with time but that . . .*

(b) *a completely unstressed zone of length $0.1L_p$ develops at the end of the tendon."*

Both the plots in Figure 4.40 indicate that the inner ends of the transmission lengths may move inwards from the beam ends. Out of 32 beam ends monitored for 6 months (Tests 1 and 2), there were 19 which showed increases in the transmission lengths of up to 175 mm. This fact contradicts suggestion (a) above.

On the other hand, the outer ends (or starting points) of the transmission lengths which were near the beam ends did not seem to have moved inwards. The largest transmission length for beams 1G-D1 and 1G-D2 was 450 mm. Therefore, the predicted length of unstressed zone according to AS 3600 would be 45 mm. It was not possible to determine the location along the beam where the strain was zero since the first reading

from the 200 mm gauge length demec mechanical gauge used determined the average strain for a location 125 mm from the beam end.

Comparing normalised curves at transfer and at 6 months, there is only 1 beam end out of 32 which may have this shift (ie. 2G-D1 (L)). It was uncertain since the end of L_p had shifted. The transmission length of 650 mm was one of the longest for beams from Tests 1 and 2.

In concluding, there is evidence from the current tests to show that transmission length increases with time. There seems to be negligible movement to the starting points of transmission lengths for beams tested and monitored over 6 months but it was not possible to confirm the $0.1L_p$ length of unstressed zone at the ends of pretensioned prestressed beams as suggested by AS 3600.

CHAPTER 5

Conclusions and Recommendations

5.1 Introduction

This chapter summarises the assessments and findings of this project with respect to the behaviour of prestressed concrete beams with pretensioned wire tendons during and after the transfer of prestress.

The transfer mechanism which occurs in the end zones of the beams is undoubtedly complex and is influenced by many factors. Only a few of these factors were studied during the course of this research project; namely, variable concrete strengths, different sizes and types of wires, and different methods of prestress transfer.

The quality of prestress transfer was assessed by determining the transmission lengths and pull-ins for the wire tendons. There were inconsistencies in the strain distributions which made the determination of the transmission lengths less straightforward.

Changes in the transmission lengths and pull-ins were monitored up to six months to ascertain the long term effect of time on these parameters.

Recommendations for further research into certain specific areas concerning the transfer of prestress are also presented.

5.2 Conclusions From The Present Study

5.2.1 Evaluated Transmission Lengths and Pull-ins

Fifty six pretensioned prestressed beam specimens tested in the current investigation yielded 112 transmission lengths and 106 average pull-ins at transfer. The transmission lengths had the following ranges:

5 mm dia. Wires:

Plain	175 - 600 mm
Chevron	200 - 750 mm

7 mm dia. Wires:

Plain	300 - 1075 mm
Belgian	200 - 500 mm

The average pull-ins for the beam ends ranged between the values of:

5 mm dia. Wires:

Plain	0.34 - 1.42 mm
Chevron	0.31 - 1.47 mm

7 mm dia. Wires:

Plain	0.44 - 3.50 mm
Belgian	0.46 - 1.04 mm

There were large scatters in both the measured transmission lengths and pull-ins. The 7 mm dia. Plain wire gave the largest transmission lengths and pull-ins compared to the other types of wires used in the tests.

5.2.2 Dependence of Transmission Length on the Location of Measurement

From the available data, there was no indication of dependence of the transmission length on the location of measurement along a single prestressing line; the four locations being the dead and live ends of the dead end beam (DD and DL) and the dead and live ends of the live end beam (LD and LL).

The only exception was when shock release was applied. Test 7 had two pairs of beams, 7R-D1 and 7R-L1, and 7R-D4 and 7R-L4, prestressed by wire

tendons which were cut using an angle grinder. The active beam ends adjacent to the locations of shock releases showed larger transmission lengths compared to the passive ends. It can be concluded that shock release did increase the transmission length.

5.2.3 Expected and Experimental Strain Values

The estimated expected strains were greater than the actual experimental strains. The larger strains were attributed to the following reasons:

(a) low concrete strengths in Test 5 (20.1 and 26.8 MPa) combined with large stress/strength ratio of about 0.90 rendered the modulus of elasticity (E_{cj}) from AS 3600 (1988) to be inappropriate since it is based on the secant modulus at 50% of the concrete crushing strength.

(b) the E_{cj} formula consistently gave larger values of modulus of elasticity compared to an equation by Carrasquillo, Nilson and Slate ($E_c = 3320 \sqrt{f_{cm}} + 6900$).

(c) the variation of ±20% in the modulus of elasticity, E_{cj}, explained partly for the discrepancies between expected and experimental strains.

(d) the concrete beams had unequal stiffness across their depths. Beam 5G-D2 was checked using the Schmidt rebound hammer test. A possible 16% decrease in the modulus of elasticity at the top of the beam compared to the bottom of the beam was postulated.

5.2.4 Inconsistencies in Strain Profiles

There were many longitudinal strain distributions which did not behave like the ideal curve. In addition, these distributions for beams cast under the same controlled conditions differed significantly, prompting the strong suggestion that there is inherent variability in the transfer of force between steel and concrete.

Inadequate consolidation of concrete was not a problem for any of the beams. However, the most disturbing issue stemmed from the existence of plastic shrinkage cracks on the top surfaces of beams in Test 6 where commercial high strength concrete was used. The strain distributions

were affected by these cracks making the determination of the transmission lengths a formidable task. It is understood that a substantial quantity of superplasticiser was used and this would have led to the development of the surface microcracks.

Anomalous strain distributions included profiles which showed uncharacteristic effects due to microcracking (400 $\mu\varepsilon$), small and large fluctuations (large fluctuations up to 300 $\mu\varepsilon$ in dead end beams of Test 3), and reasonably unequal maximum strains at the inner ends of the two end zones within a single beam (differences mainly 150 to 220 $\mu\varepsilon$). The strain distribution for beam 5G-L1 illustrated a classic example of overlapping end zones.

For each of the above atypical strain distributions, a corresponding plot of percentage load transfer versus pull-in for wire tendons loading the particular beam was used to complement the interpretation of the strain distribution and to estimate the end points of the transmission lengths.

5.2.5 Statistical Inference Tests

5.2.5.1 Comparisons of L_p and Δ_0 for plain wires with L_p and Δ_0 for indented wires

Statistical analysis which was employed to compare transmission lengths and pull-ins revealed a difference between plain and indented wires. Although the comparison of transmission lengths could not definitively prove beyond doubt that indented wires were superior to plain wires, pull-ins turned out to be significantly smaller for indented wires than for plain wires (99.0% to 99.99% confidence levels).

In general, it can be said that the indented wires performed better than the plain wires, not so much in producing shorter transmission lengths but more evidently in giving smaller pull-ins. Therefore, it is advisable to use indented wires instead of plain wires as suggested by AS 3600 (1988). However, there is no guidance in AS 1310 with respect to the acceptable type of indentation.

5.2.5.2 Comparisons of L_p and Δ_0 for different wire sizes

There was only a small number of results available for these comparisons (only 5 mm versus 7 mm dia. Plain wires), but they positively indicated that larger wires gave larger pull-ins. The transmission length comparisons did not substantiate the common believe that larger wires will also give longer transmission lengths.

5.2.5.3 Comparisons of L_p and Δ_0 for gradual, sudden and shock releases

Comparisons made for the various techniques of releasing the prestress consolidated the fact that shock release gave considerably larger transmission lengths than gradual or sudden releases. Sudden release by instantaneously and hydraulically backing off the movable head seemed to be better than direct shock release effected by cutting tendons with a rotary angle grinder. However, gradual release was only marginally better than sudden release (four out of six comparisons on L_p and Δ_0 had 90% to 99% confidence levels).

5.2.5.4 Comparisons of L_p and Δ_0 for different concrete strengths

It was found that beams with concrete strength at transfer of 20.1 and 26.8 MPa from Test 5 had larger transmission lengths and pull-ins compared to all other beams with concrete strength in the range of 33.8 to 65.1 MPa (all comparisons were at 99.99% confidence level). For the 7 mm dia. Plain wire, the mean transmission length and pull-in for low concrete strength ($f_{cp} < 32$ MPa) were 900 mm and 2.56 mm compared to 470 mm and 1.10 mm for higher concrete strength ($f_{cp} \geq 32$ MPa). Similarly, the 5 mm dia. Chevron wire yielded the mean transmission lengths and pull-ins of 540 mm and 0.90 mm for low concrete strength compared to 320 mm and 0.50 mm for higher strength.

The beams in Test 5 were highly loaded but there was no sign of cracking to indicate distress. The use of a grade of concrete (at transfer) of at least 32 MPa is advocated for all pretensioned prestressed concrete works to

avoid overloading green concrete and ending up with poor prestress transfer.

Greater concrete strength did promote smaller transmission lengths and pull-ins and this was particularly obvious for the 65.1 MPa mix used in Test 6. Another advantage of a higher grade of concrete is that it allows for earlier release.

5.2.6 Relationship Between Transmission Length and Pull-in

Formulae between transmission length and pull-in were established for the different types of wire tendons used (except for the 7 mm dia. Belgian wire). The formulae were established for transmission lengths and pull-ins at transfer and they are as follows:

$L_p = 350\,\Delta_o + 190$ **5 mm dia. Plain Wire**

$L_p = 290\,\Delta_o + 190$ **5 mm dia. Chevron Wire**

$L_p = 260\,\Delta_o + 180$ **7 mm dia. Plain Wire**

These equations are applicable with pull-in of at least 0.30 mm and within the ranges of pull-ins for which they were derived.

It was found that there can be greater percentage change in the pull-in compared to the corresponding percentage change in the transmission length according to these equations. This partially explained for the success of inference tests in confirming the difference between plain and indented wires, and the difference between wires of 5 mm and 7 mm dia. when comparing pull-ins; but not when comparing transmission lengths.

These L_p-Δ_o formulae are particularly useful in predicting transmission lengths from the measurements of pull-in on wire tendons. They provide an easier and less complicated way of assessing the quality of force transfer in pretensioned prestressed beams. None of the relationships given by previous researchers fitted well to the data points for the plots of transmission length versus pull-in.

5.2.7 Upper Limits for Transmission Lengths and Pull-ins

The upper limits determined for transmission lengths and pull-ins found from current and previous test data for various types of wires used where $f_{cp} \geq 32$ MPa are:

5 mm dia. Wires:

Plain $L_p \leq 600$ mm (120 d_b) ; $\Delta_o \leq 1.42$ mm (0.28 d_b)

Chevron $L_p \leq 450$ mm (90 d_b) ; $\Delta_o \leq 0.73$ mm (0.15 d_b)

7 mm dia. Wires:

Plain $L_p \leq 700$ mm (100 d_b) ; $\Delta_o \leq 2.06$ mm (0.29 d_b)

Belgian $L_p \leq 500$ mm (70 d_b) ; $\Delta_o \leq 1.04$ mm (0.15 d_b)

The transmission lengths and pull-ins were also grouped according to different categories of transfer strength and the following have been found to represent them for $f_{cp} \geq 32$ MPa (in actual groupings, 30 MPa was used as the separation value for the categories of 20-30 MPa and 30-70 MPa):

5 mm dia. Wires:

Plain $L_p = 70\ d_b \pm 50\ d_b$; $\Delta_o = 0.16\ d_b \pm 0.13\ d_b$

Chevron $L_p = 60\ d_b \pm 30\ d_b$; $\Delta_o = 0.10\ d_b \pm 0.05\ d_b$

7 mm dia. Wires:

Plain $L_p = 70\ d_b \pm 30\ d_b$; $\Delta_o = 0.16\ d_b \pm 0.14\ d_b$

Belgian $L_p = 60\ d_b \pm 10\ d_b$; $\Delta_o = 0.13\ d_b \pm 0.02\ d_b$

Since there was less information for the 7 mm dia. Belgian wire, the given equations for this wire have to be accepted with a certain degree of uncertainty.

From these simple equations, it can be concluded that plain wires did give larger transmission lengths and pull-ins. They also had greater ranges as the equations evidently show.

The design value of 100 d_b for transmission length, where $f_{cp} \geq 32$ MPa, as suggested by AS 3600 (1988) predicted transmission lengths longer than the experimental values for the 5 mm dia. Chevron and 7 mm dia. Belgian wires from current laboratory tests. Plain wires tested indicated that their transmission lengths could be longer than 100 d_b, which supports the rejection of the use of these wires by the standard.

However, AS 3600 failed to address the fact that transmission lengths do vary significantly even when all the conditions which affect prestress transfer are made equal. Despite testing under well-controlled laboratory conditions, reasonably diverse ranges of results were still obtained within each test in this project. The ranges of the transmission lengths and pull-ins given above serve better to indicate the variability associated with the actual behaviour of prestress transfer.

Furthermore, by considering the above-mentioned limits for L_p and Δ_o together with formulae developed between transmission length and pull-in, the following upper bound limits were obtained for current and previous tests:

$\hat{L}_p$ = 690 mm and $\hat{\Delta}_o$ = 1.42 mm	**5 mm dia. Plain Wire**
$\hat{L}_p$ = 450 mm and $\hat{\Delta}_o$ = 0.90 mm	**5 mm dia. Chevron Wire**
$\hat{L}_p$ = 720 mm and $\hat{\Delta}_o$ = 2.06 mm	**7 mm dia. Plain Wire**

5.2.8 Dimensional Analysis

Dimensional analysis was employed to establish relationships for evaluating transmission lengths based on concrete strength at transfer, total prestress force, cross-sectional area of the beam and diameter of the wire. The following equations gave estimates of transmission lengths for 5 mm and 7 mm dia. Plain wires, and 5 mm and 7 mm dia. Indented wires for transfer strength of 20-70 MPa:

5 mm and 7 mm dia. Plain Wires

$$L_p = 158\, d_b \left(\frac{f_{si}.A_p}{f_{cp}.A_c} \right)^{0.84} \pm 71\%$$

5 mm and 7 mm dia. Indented Wires

$$L_p = 120\, d_b \left(\frac{f_{si}.A_p}{f_{cp}.A_c} \right)^{0.70} \pm 70\%$$

These formulae can only be used to give rough estimates of the transmission lengths in view of the large variation band. The large errors are associated with predicted small transmission lengths.

5.2.9 Changes in Transmission Length and Pull-in Over Time

Transmission length and pull-in did have tendencies to increase over time. Some of the average increases after 6 months are given as follows (S.D. is the standard deviation):

5 mm dia. Chevron Wire:

δL_p : Ave. = 31 mm, S.D. = 59 mm, Range (-50 to 125 mm)

$\delta \Delta_o$: Ave. = 0.11 mm, S.D. = 0.06 mm, Range (-0.02 to 0.22 mm)

7 mm dia. Plain Wire:

δL_p : Ave. = 37 mm, S.D. = 47 mm, Range (-13 to 175 mm)

$\delta \Delta_o$: Ave. = 0.53 mm, S.D. = 0.24 mm, Range (-0.06 to 1.06 mm)

The pull-ins increased more significantly than the transmission lengths. Average percentages of increase in the pull-ins were 22% and 49% for the 5 mm dia. Chevron and 7 mm dia. Plain wires respectively. The corresponding percentages for the transmission lengths were 11% and 9% respectively.

Normalised strain distributions with shrinkage corrections did not indicate that the inner ends of the transmission lengths would remain unchanged with time as postulated by AS 3600 (1988). This is evident from the small increases in transmission lengths given above. Most of these curves (31 out of 32) did not indicate unstressed zones at the beam ends. The unstressed lengths of $0.1L_p$ suggested by AS 3600 due to shrinkage effect were expected but the measurement of longitudinal strains using a 200 mm gauge length demec mechanical gauge could not detect these lengths. The unstressed lengths are short and can be considered as negligible for practical purposes, unless they are associated with long transmission lengths.

5.3 Recommendations For Further Work

Obviously there are still many aspects of pretensioning with wire tendons which has yet to be fully understood. The following is a list of the possible areas where future expedient research may be directed:-

(a) steam curing is being universally used in pretensioning works with the intention of decreasing the time taken before transfer can be effected. Tests can be carried out to ascertain whether there is any problem associated with releasing wire tendons into green concrete when the required strength has been reached at a very early age after casting. Furthermore, release can be done with or without allowing for a cooling period. It is generally accepted that this cooling process is to be provided but there are arguments that releasing the wires without cooling diminishes the likelihood of cracking due to thermal gradients.

(b) the actual effect of indentations still remains vague. Different shapes of indentations may not necessarily provide the same rate of bond transfer. Also, the sharpness of these indentations was not studied. Their depths seem to be the main criteria with little concern given to the pitch, length and percentage circumferential area covered. The tolerances on the depths are quite flexible according to the Australian Standards AS 1310 (1987).

(c) more tests should be done to compare the transmission lengths for different sizes of wires. The comparisons within the tests performed did not prove that larger wires would give longer transmission lengths.

(d) since AS 3600 only condones gradual release for pretensioned prestressed units, this project was geared towards studying beams with this type release. There may be scope for considering the use of shock release in the industry for obvious reasons.

(e) the 6-month monitoring period was inadequate for establishing the increases which can occur in the transmission length and pull-in over time. The results were not conclusive and more tests should be done to address the issue of long term effects.

(f) field measurements should be obtained in practice to verify the considerable ranges in the transmission length and pull-in. These can also be compared to the existing laboratory test results.

(g) high strength concrete should be tested at large stress values (or large stress/strength ratios), eg. σ_{co} of 60%-80% of f_{cp}. Also, beams should be tested with different geometry and stress/strength ratios.

Bibliography

(Note: • is assigned to publications or sources of information which were referred to within the main text of this thesis. Other sources merely served as supplementary information.)

Abeles, P.W. and Turner, F.H. (1962)
Prestressed Concrete Designer's Handbook.
Concrete Publications Limited, Great Britain.

Abrishami, H.H. and Mitchell, D. (1992)
Simulation of Uniform Bond Stress.
A.C.I. Materials Journal, Vol. 89, No. 2, March - April, pp. 161-168.

• A.C.I. Committee 318 (1989)
Building Code Requirements for Reinforced Concrete (ACI 318-89).
American Concrete Institute, Detroit.

A.C.I. Committee 517 (1980)
Accelerated Curing of Concrete at Atmospheric Pressure - State of the Art.
A.C.I. Journal, Vol. 77, No. 6, November - December, pp. 429-457.

Al-Obaid, Y.F. (1989)
The Automated Analysis of Prestressed Concrete Poles for Street Lighting.
Journal of Engineering Fracture Mechanics, Vol. 34, No. 5-6, pp. 1031-1040.

• Anderson, A.R. and Anderson, R.G. (1976)
An Assurance Criterion for Flexural Bond in Pretensioned Hollow Core Units.
A.C.I. Journal, Proc. Vol. 73, No. 8, August, pp. 457-464.

Anza, G. (1990)
Effect of Tendon Spacing on Transmission Length in Pretensioned Prestressed Concrete.
Civil Engineering Project Report, Curtin University of Technology.

• Arthur, P.D. and Ganguli, S. (1965)
Tests on End-Zone Stresses in Pre-Tensioned Concrete I Beams.
Magazine of Concrete Research, Vol. 17, No. 51, June, pp. 85-96.

• AS 1012, Part 8 (1986)
Method for Making and Curing Concrete Compression, Indirect Tensile and Flexure Test Specimens in the Laboratory or in the Field.
Standards Association of Australia, Sydney.

• AS 1012, Part 9 (1986)
Determination of Compressive Strength of Concrete Specimens.
Standards Association of Australia, Sydney.

• AS 1012, Part 10 (1985)
Method for the Determination of Indirect Tensile Strength of Concrete Cylinders ('Brazil' or Splitting Test).
Standards Association of Australia, Sydney.

AS 1012, Part 13 (1970)
Method for the Determination of the Drying Shrinkage of Concrete - Metric.
Standards Association of Australia, Sydney.

AS 1012, Part 19 (1988)
Method of Testing Concrete - Method 19: Accelerated Curing of Concrete Compression Test Specimens (Laboratory or Field) - Hot Water and Warm Water Methods.
Standards Association of Australia, Sydney.

• AS 1310 (1987)
Steel Wire for Tendons in Prestressed Concrete.
Standards Association of Australia, Sydney.

AS 1311 (1987)
Steel Tendons for Prestressed Concrete - 7-Wire Stress-Relieved Steel Strand for Tendons in Prestressed Concrete.
Standards Association of Australia, Sydney.

• AS 1391 (1991)
Methods for Tensile Testing of Metals.
Standards Association of Australia, Sydney.

• AS 1481 (1978)
Prestressed Concrete Code - Metric.
Standards Association of Australia, Sydney.

AS 2758.1 (1985)
Aggregates and Rock for Engineering Purposes.
Standards Association of Australia, Sydney.

• AS 3600 (1988)
Concrete Structures.
Standards Association of Australia, Sydney.

• AS 3600 - Supp. 1 (1990)
Concrete Structures - Commentary (Supplement to AS 3600 - 1988).
Standards Association of Australia, Sydney.

A.S.T.M. A 416 - 88b (1988)
Standard Specification for Steel Strand, Uncoated Seven-Wire Stress-Relieved for Prestressed Concrete.
1992 Annual Book of A.S.T.M. Standards, Section 1, Vol 01.04, pp. 262-265.
American Society for Testing and Materials, Philadelphia.

• A.S.T.M. A 421 - 91 (1991)
Standard Specification for Uncoated Stress-Relieved Steel Wire for Prestressed Concrete.
1992 Annual Book of A.S.T.M. Standards, Section 1, Vol 01.04, pp. 266-268.
American Society for Testing and Materials, Philadelphia.

• A.S.T.M. A 864/A 864M (1987)
Standard Specification for Steel Wire, Deformed, for Prestressed Concrete Railroad Ties.
1992 Annual Book of A.S.T.M. Standards, Section 1, Vol 01.04, pp. 609-611.
American Society for Testing and Materials, Philadelphia.

• A.S.T.M. A 886/A 886M (1988)
Standard Specification for Steel Strand, Indented, Seven-Wire Stress-Relieved for Prestressed Concrete.
1992 Annual Book of A.S.T.M. Standards, Section 1, Vol 01.04, pp. 626-629.
American Society for Testing and Materials, Philadelphia.

• Austrak Pty. Ltd. (1993)
Private Communication on the Subject of Pretensioned Prestressed Concrete Railway Sleepers in the Civil Engineering Concrete Laboratory, Curtin University of Technology.

• Avram, C., Facaoaru, I., Filimon, I., Mirsu, O. and Tertea, I. (1981)
Concrete Strength and Strains.
Elsevier Scientific Publishing Company, Amsterdam.

• Bailey, T.C. (1989)
Effect of Tendon Spacing on Transmission Length in Pretensioned Prestressed Concrete.
Civil Engineering Project Report, Curtin University of Technology.

Balazs, G.L. (1992)
Transfer Control of Prestressing Strands.
P.C.I. Journal, Vol. 37, No. 6, November - December, pp. 60-69.

Balazs, G.L. (1993)
Transfer Length of Prestressing Strand as a Function of Draw-in and Initial Prestress.
P.C.I. Journal, Vol. 38, No. 2, March - April, pp. 86-93.

• Base, G.D. (1955)
Further Notes on the Demec, A Demountable Mechanical Strain Gauge for Concrete Structures.
Magazine of Concrete Research, Vol. 7, No. 19, March, pp. 35-38.

• Base, G.D. (1957)
Some Tests on the Effect of Time on Transmission Length in Pretensioned Concrete.
Magazine of Concrete Research, Vol. 9, No. 26, August, pp. 73-82.

• Base, G.D. (1958)
An Investigation of Transmission Length in Pretensioned Concrete.
Third Congress of F.I.P. Berlin, Volume 1 (Papers), pp. 603-623.

• Bruggeling, A.S.G. (1986)
Transmission Length of Pretensioned Prestressing Steel.
Betonwerk Fertigteil Technik, Vol. 52, No. 5, May, pp. 298-302.

• BS 1881:Part 4:1970
Methods of Testing Concrete - Methods of Testing Concrete for Strength.
British Standards Institution, London.

BS 1881:Part 108:1983
Methods of Testing Concrete - Method for Making Test Cubes from Fresh Concrete.
British Standards Institution, London.

BS 1881:Part 116:1983
Methods of Testing Concrete - Method for Determination of Compressive Strength of Concrete Cubes.
British Standards Institution, London.

• BS 8110:Part 1:1985
Standard for the Structural Use of Concrete - Part 1 Code of Practice for Design and Construction.
British Standards Institution, London.

• Carrasquillo, R.L., Slate, F.O. and Nilson, A.H. (1981)
Properties of High Strength Concrete Subject to Short-Term Loads.
A.C.I. Journal, Proc. Vol. 78, No. 3, May - June, pp. 171-178.

Carrasquillo, R.L., Slate, F.O. and Nilson, A.H. (1981)
Microcracking and Behaviour of High Strength Concrete Subject to Short - Term Loading.
A.C.I. Journal, Proc. Vol. 78, No. 3, May - June, pp. 179-186.

• Cement and Concrete Association of Australia (1991)
Concrete Design Handbook (in accordance with AS 3600).
Cement and Concrete Association of Australia, Sydney.

Cement and Concrete Association of Australia (1993)
Private Communication on the Subject of Concrete Strengths Obtained from 100 mm dia. x 200 mm and 150 mm dia. x 300 mm Cylinders, Perth.

Chandler, I.J. and Hoadley, P.J. (1975)
End Zone Stresses in Pretensioned Prestressed Concrete Beams.
Fifth Australasian Conference on the Mechanics of Structures and Materials, Melbourne.

• Chandler, I.J. (1984)
End Zones of Pretensioned Prestressed Concrete Beams.
Doctor of Philosophy Thesis, University of Melbourne.

• Chandler, I.J. (1990)
Transmission Lengths of Pretensioned Tendons from Measurements of Pull-in.
Second National Structural Engineering Conference, Adelaide, Australia. The Institution of Engineers, Australia; National Conference Publication No. 90/10, pp. 131-135.

• Chengju, G. (1989)
Maturity of Concrete: Method for Predicting Early-Stage Strength.
A.C.I. Materials Journal, Vol. 86, No. 4, July - August, pp. 341-353.

Christodoulides, S.P. (1955)
A Two Dimensional Investigation of the End Anchorages of Post-Tensioned Concrete Beams.
The Structural Engineer, Vol. 33, No. 4, April, pp. 120-133.

Cousins, T.E., Badeaux, M.H. and Moustafa, S. (1992)
Proposed Test for Determining Bond Characteristics of Prestressing Strand.
P.C.I. Journal, Vol. 37, No. 1, January - February, pp. 66-73.

• Cousins, T.E., Johnston, D.W. and Zia, P. (1990)
Transfer Length of Epoxy Coated Prestressing Strand.
A.C.I. Materials Journal, Vol. 87, No. 3, May - June, pp. 193-203.

• Cousins, T.E., Johnston, D.W. and Zia, P. (1990)
Development Length of Epoxy Coated Prestressing Strand.
A.C.I. Materials Journal, Vol. 87, No. 4, July - August, pp. 309-318.

• Cousins, T.E., Johnston, D.W. and Zia, P. (1990)
Transfer and Development Length of Epoxy Coated and Uncoated Prestressing Strand.
P.C.I. Journal, Vol. 35, No. 4, July - August, pp. 92-103.

• CP 110:1972
Code of Practice for the Structural Use of Concrete.
British Standards Institution, London.

Dardare, J. (Chairman) et al. (Year Unknown)
Guide to Good Practice - Acceleration of Concrete Hardening by Thermal Curing.
Guide from the Cement and Concrete Association (W. Australia): Prepared by Dardare, J., CERIB, Boite Postale 42, 28230 Epernon, France.

• Darvall, P. LeP. (1989)
Reinforced and Prestressed Concrete.
The MacMillan Company of Australia Pty. Ltd., Australia.

den Uijl, J.A. (1985)
Bond Properties of Strands in Connection with Transmission Zone Cracks.
Betonwerk Fertigteil Technik, Vol. 51, No. 1, January, pp. 28-36.

Dilger, W.H. and Ghali, A. (1986)
Response of Spun Cast Concrete Poles to Vehicle Impact.
P.C.I. Journal, Vol. 31, No. 1, January - February, pp. 62-82.

Dolan, C.W. (1990)
Developments in Non-Metallic Prestressing Tendons.
P.C.I. Journal, Vol. 35, No. 5, September - October, pp. 80-88.

El-Mezaini, N. and Citipitioglu, E. (1991)
Finite Element Analysis of Prestressed and Reinforced Concrete Structures.
Journal of Structural Engineering, Vol. 117, No. 10, October, pp. 2851-2864.

• Evans, R.H. and Robinson, G.W. (1955)
Bond Stresses in Prestressed Concrete from X-Ray Photographs.
Proc. Inst. of Civil Engineers, Part 1, Vol. 4, No. 2, March, pp. 212-235.

• Fogarasi, G. (1986)
Prestressed Concrete Technology.
Akademiai Kiado, Budapest, Hungary.

• Ganguli, S. (1966)
Transmission Length in Pretensioned Prestressed Concrete.
The Indian Concrete Journal, Vol. 40, No. 1, January, pp. 13-16.

Gergely, P. and Sozen, M.A. (1967)
Design of Anchorage Zone Reinforcement in Prestressed Concrete Beams.
P.C.I. Journal, Vol. 12, No. 2, April, pp. 63-75.

Ghosh, S.K. and Fintel, M. (1986)
Development Length of Prestressing Strands, including Debonded Strands, and Allowable Concrete Stresses in Pretensioned Members.
P.C.I. Journal, Vol. 31, No. 5, September - October, pp. 38-57.

• Guyon, Y. (1953)
Prestressed Concrete, Volume 1.
Contractors Record and Municipal Engineering, London.

Guyon, Y. (1963)
Prestressed Concrete, Volume 1.
Asia Publishing House, Bombay.

Hanna, A.N. (1979)
Prestressed Concrete Ties for North American Railroads.
P.C.I. Journal, Vol. 24, No. 5, September - October, pp. 32-61.

Hanson, J. A. (1963)
Optimum Steam-Curing Procedure in Precasting Plants.
A.C.I. Journal, Proc. Vol. 60, No. 1, January, pp. 75-100.

• Hanson, N.W. (1969)
Influence of Surface Roughness of Prestressing Strand on Bond Performance.
P.C.I. Journal, Vol. 14, No. 1, February, pp. 32-45.

• Hanson, N.W. and Kaar, P.H. (1959)
Flexural Bond Tests of Pretensioned Prestressed Beams.
A.C.I. Journal, Proc. Vol. 55, No. 7, January, pp. 783-802.

Hawkins, N.M. (1966)
The Behaviour and Design of End Blocks for Prestressed Concrete Beams.
Civil Eng. Trans. I.E. Aust., Vol. CE 8, No. 2, October, pp. 193-202.

Herbert, D.A. (1976)
The Application of Statics to End Zones of Prestressed Beams.
Civil Eng. Trans. I.E. Aust., Vol. CE 18, No. 2, pp. 117-124.

Discussion of the Application of Statics to End Zones of Prestressed Beams by Herbert, D.A. (1976)
Civil Eng. Trans. I.E. Aust., Vol. CE 18, No. 2, pp. 125-126.

Holland, E.P. (1976)
T.Y. Lin - "Mr. Prestressed Concrete".
P.C.I. Journal, Vol. 21, No. 5, September - October, pp. 18-21.

Iyengar, K.T.S.R. (1962)
Two Dimensional Theories of Anchorage Zone Stresses in Post-Tensioned Prestressed Beams.
A.C.I. Journal, Proc. Vol. 59, No. 10, October, pp. 1443-1465.

• Janney, J.R. (1954)
Nature of Bond in Pretensioned Prestressed Concrete.
A.C.I. Journal, Proc. Vol. 50, No. 9, May, pp. 717-736.

• Kaar, P.H., LaFraugh, R.W. and Mass, M.A. (1963)
Influence of Concrete Strength on Strand Transfer Length.
P.C.I. Journal, Vol. 8, No. 5, October, pp. 47-67.

Kalyanasundaram, P., Krishnamoorthy, C.S. and Srinivasa Rao, P. (1976)
End Zone Stresses in Pre-Tensioned Prestressed Concrete Beams.
The Indian Concrete Journal, Vol. 50, No. 10, October, pp. 303-307.

Kong, F.K. and Evans, R.H. (1977)
Reinforced and Prestressed Concrete.
Thomas Nelson (Australia) Ltd., Victoria, Australia.

Kripanarayanan, K.M. and Meyers, B.L. (1972)
Transfer Stress Distribution of Fully Bonded Pretensioned Wires Using the Finite Element Method.
Proc. Conference on Finite Element Method in Civil Engineering, McGill University, Montreal, Quebec, June.

• Krishnamurthy, D. (1970)
The Effect of the Method of Transfer on the End Zone Stresses and Transmission Length in Pretensioned Concrete Members.
The Indian Concrete Journal, Vol. 44, No. 3, March, pp. 110-116, 128.

• Krishnamurthy, D. (1971)
A Method for Determining the Tensile Stresses in the End Zones of Pretensioned Beams.
The Indian Concrete Journal, Vol. 45, No. 7, July, pp. 286-297, 315.

• Krishnamurthy, D. (1972)
Relationship between Transmission Length and Diameter of Prestressing Tendons.
Journal of Institution of Engineers (India), Civil Engineering Division, Vol. 52, No. 9, Part CI 5, May, pp. 243-247.

• Krishnamurthy, D. (1973)
A Theory for the Transmission Length of Prestressing Tendons.
The Indian Concrete Journal, Vol. 47, No. 2, February, pp. 73-80.

Lenschow, R.J. and Sozen, M.A. (1965)
Practical Analysis of the Anchorage Zone Problem in Prestressed Beams.
A.C.I. Journal, Proc. Vol. 62, No. 11, November, pp. 1421-1439.

• Leonhardt, F. (1964)
Prestressed Concrete - Design and Construction.
Wilhelm Ernst and Sohn, Berlin.

Libby, J.R. (1977)
Modern Prestressed Concrete - Design Principles and Construction Methods (2nd Ed.).
Van Nostrand Reinhold Co., New York.

Lin, T.Y. (1976)
The Future of Prestressed Concrete - A Long Look Ahead.
P.C.I. Journal, Vol. 21, No. 5, September - October, pp. 204-214.

• Lin, T.Y. and Burns, N.H. (1981)
Design of Prestressed Concrete Structures (3rd Ed.).
John Wiley and Sons, New York.

• Lydon, F.D. (1979)
Developments in Concrete Technology - 1.
Applied Science Publishers Ltd., London.

Magnel, G. (1949)
Design of the Ends of Prestressed Concrete Beams.
Concrete and Construction Eng., Vol. 44, No. 5, May, pp. 141-148.

Magnel, G. (1954)
Prestressed Concrete (3rd Ed.).
Concrete Publications Limited, London, England.

• Mains, R.M. (1951)
Measurement of the Distribution of Tensile and Bond Stresses Along Reinforcing Bars.
A.C.I. Journal, Vol. 23, November, pp. 225.

• Marshall, G. (1949)
End Anchorage and Bond Stress in Prestressed Concrete.
Magazine of Concrete Research, Vol. 1, No. 3, December, pp. 123-127.

Marshall, W.T. (1966)
A Theory for End Zone Stresses in Pretensioned Concrete Beams.
P.C.I. Journal, Vol. 11, No. 2, April, pp. 45-51.

• Marshall, W.T. and Krishnamurthy, D. (1969)
Transmission Length of Prestressing Tendons from Concrete Cube Strengths at Transfer.
The Indian Concrete Journal, Vol. 43, No. 7, July, pp. 244-253, 257.

Marshall, W.T. and Krishnamurthy, D. (1970)
The Design of End Zone Reinforcement for Pretensioned Prestressed Concrete Beams.
Sixth Congress of Federation Internationale de la Precontrainte, Prague.

Marshall, W.T. and Mattock, A.H. (1962)
Control of Horizontal Cracking in the Ends of Pretensioned Prestressed Concrete Girders.
P.C.I. Journal, Vol. 7, No. 5, October, pp. 56-74.

Martin, L.D. and Scott, N.L. (1976)
Development of Prestressing Strand in Pretensioned Members.
A.C.I. Journal, Proc. Vol. 73, No. 8, August, pp. 453-456.

Mayfield, B., Davies, G. and Kong, F.K. (1970)
Some Tests on the Transmission Length and Ultimate Strength of Pretensioned Concrete Beams Incorporating Dyform Strand.
Magazine of Concrete Research, Vol. 22, No. 73, December, pp. 219-226.

• Merretz, W.E., Stevens, B. and Egan, D.E. (1984)
Low Pressure Steam Curing.
Concrete Institute of Australia, Current Practice Note 18, December.

Mindess, S. and Young J.F. (1981)
Concrete.
Prentice-Hall Inc., Englewood Cliffs, New Jersey.

Mohan Rao, S.V.K. and Dilger, W.H. (1992)
Control of Flexural Crack Width in Cracked Prestressed Concrete Members.
A.C.I. Structural Journal, Vol. 89, No. 2, March - April, pp. 127-138.

Monfore, G.E. and Verbeck, G.J. (1960)
Corrosion of Prestressed Wire in Concrete.
A.C.I. Journal, Vol. 32, No. 5, November, pp. 491-515.

• Morice, P.B. and Base, G.D. (1953)
The Design and Use of a Demountable Mechanical Strain Gauge for Concrete Structures.
Magazine of Concrete Research, Vol. 5, No. 13, August, pp. 37-42.

• Murdock, L.J. and Brook, K.M. (1979)
Concrete Materials and Practice (5th Ed.).
Edward Arnold (Publishers) Ltd., London.

M180: Introduction to Statistics (Lecture Notes) (1992)
Murdoch University Mathematics Programme.
Murdoch University, Western Australia.

Nanni, A., Utsunomiya, T., Yonekura, H. and Tanigaki, M. (1992)
Transmission of Prestressing Force to Concrete by Bonded Fibre Reinforced Plastic Tendons.
A.C.I. Structural Journal, Vol. 89, No. 3, May - June, pp. 335-344.

Navaratnarajah, V. (1967)
An Analysis of Stresses during Steam Curing of Pretensioned Concrete.
Constructional Review, Vol. 40, No. 12, December, pp. 18-25.

Neville, A.M. (1981)
Properties of Concrete (3rd Ed.).
Pitman Publishing Pty. Ltd., Melbourne.

Nilson, H.N. (1978)
Design of Prestressed Concrete.
John Wiley and Sons, New York.

Oluokun, F.A., Burdette, E.G. and Deatherage, J.H. (1990)
Early-Age Concrete Strength Prediction by Maturity - Another Look.
A.C.I. Materials Journal, Vol. 87, No. 6, November - December, pp. 565-572.

Over, S.R. and Au, T. (1965)
Prestress Transfer Bond of Pretensioned Strands in Concrete.
A.C.I. Journal, Proc. Vol. 62, No. 11, November, pp. 1451-1459.

• Park, R. and Paulay, T. (1975)
Reinforced Concrete Structures.
John Wiley and Sons, New York.

• Presswalla, H. and Preston, H.K. (1990)
Torque in Tensioned Strand.
P.C.I. Journal, Vol. 35, No. 2, March - April, pp. 78-81.

Preston, H.K. (1990)
Handling Prestressed Concrete Strand.
P.C.I. Journal, Vol. 35, No. 6, November - December, pp. 68-71.

Ramaswamy, G. S. (1976)
Modern Prestressed Concrete Design.
Pitman Publishing Ltd., Australia.

• Ratz, E.H., Holmjanski, M.M. and Kolner, V.M. (1958)
The Transmission of Prestress to Concrete by Bond.
Third Congress of Federation Internationale de la Precontrainte (F.I.P.) Berlin, Vol. 1 (Papers), pp. 624-640.

• Ropke, J.C. (1982)
Concrete Problems - Causes and Cures.
McGraw-Hill, Inc., United States of America.

Rowe, R.E. (1963)
End Block Stresses in Post-Tensioned Concrete Beams.
The Structural Engineer, Vol. 41, No. 2, February, pp. 54-68.

• Ryan, W.G. and Samarin, A. (1992)
Australian Concrete Technology.
Longman Cheshire Pty. Ltd., Australia.

Rydzewski, J.R. and Whitbread, F.J. (1963)
Short End Blocks for Prestressed Beams.
The Structural Engineer, Vol. 41, No. 2, February, pp. 43-53.

• Sason, A.S. (1992)
Evaluation of Degree of Rusting on Prestressed Concrete Strand.
P.C.I. Journal, Vol. 37, No. 3, May - June, pp. 25-30.

• Schupack, M. and Mizuma, K. (1977)
Bond Properties of High Strength, Low Carbon Bars with Drawn-In Helical Deformation for Use in Pretensioning and as Special Normal Reinforcement.
A.C.I. Journal, Vol. 76, No. 2, Symposium on Interaction between Steel and Concrete at the American Concrete Institute (ACI) Annual Conference, San Diego, California, March 13-18, Publ. 1978, pp. 249-275.

Scott, R.H. and Gill, P.A.T. (1987)
Measurement of Internal Concrete Strains Using Embedment Strain Gauges.
Magazine of Concrete Research, Vol. 39, No. 139, June, pp. 109-112.

• Sengupta, B. and Som, P.K. (1976)
An Experimental Study of the Transverse Tensile Stress in the Anchorage Zone of Pre-Tensioned Members.
The Indian Concrete Journal, Vol. 50, No. 12, December, pp. 378-383.

• Shahawy, M.A., Issa, M. and deV Batchelor, B. (1992)
Strand Transfer Lengths in Full Scale AASHTO Prestressed Concrete Girders.
P.C.I. Journal, Vol. 37, No. 3, May - June, pp. 84-96.

• Srinivasa Rao, P., Kalyanasundaram, P. and Fazlullah Sharief, M. (1977)
Transmission Length of Ribbed Bars in Pre-Tensioned Concrete.
The Indian Concrete Journal, Vol. 51, No. 5, May, pp. 149-153, 159.

Stocker, M.F. and Sozen, M.A. (1970)
Bond Characteristics of Prestressing Strand.
University of Illinois, Engineering Bulletin No. 503, August.

Tay, C.J. (1986)
Performance Tests of Precast Prestressed Hollow Core Slabs.
Jurnal Institusi Jurutera Malaysia, Bil. 40, KDN PP 1/8/86, ISSN 0126-513X, pp. 41-50.

Uren, J.G. (1988)
Deflection Controlled Precast Prestressed Concrete Planks.
Master of Engineering Science Thesis, University of Western Australia.

• Walpole, R.E. (1982)
Introduction to Statistics (3rd Ed.).
Macmillan Publishing Co., New York.

• Warner, R.F. and Faulkes, K.A. (1989)
Prestressed Concrete (2nd Ed.).
Longman Cheshire Ltd., Australia.

• Warner, R.F., Rangan, B.V. and Hall, A.S. (1991)
Reinforced Concrete (3rd Ed.).
Longman Cheshire Ltd., Australia.

• Westoby, S. (1991)
Spun Poles (Clough).
Civil Engineering Project Report, Curtin University of Technology.

Yettram, A.L. and Robbins, K. (1969)
Anchorage Zone Stresses in Axially Post-Tensioned Members of Uniform Rectangular Section.
Magazine of Concrete Research, Vol. 21, No. 62, pp. 103-112.

• Zia, P. and Mostafa, T. (1977)
Development Length of Prestressing Strands.
P.C.I. Journal, Vol. 22, No. 5, September - October, pp. 54-65.

Discussion of the Development Length of Prestressing Strands by Zia, P. and Mostafa, T. (1978)
P.C.I. Journal, Vol. 23, No. 4, July - August, pp. 97-106.

Zollman, C.C. (1978)
Magnel's Impact on the Advent of Prestressed Concrete (Part 1).
P.C.I. Journal, Vol. 23, No. 3, May - June, pp. 22-48.

APPENDIX A

Longitudinal Strain Distributions

The longitudinal strain distributions for all the tests are given in this Appendix. The profiles for beams in Tests 1 and 2 have curves at 7 days (transfer), 28 days, 3 months and 6 months. Tests 3 to 6 have distributions at transfer (only beams 5G-D1, 5G-D2, 5G-L1 and 5G-L2 were transferred at 2 days whereas all the other beams had prestress transferred at 7 days), 28 days, 3 months and 6 months.

These curves give the actual strain values at various instances in time and they are not corrected for long term and curvature effects.

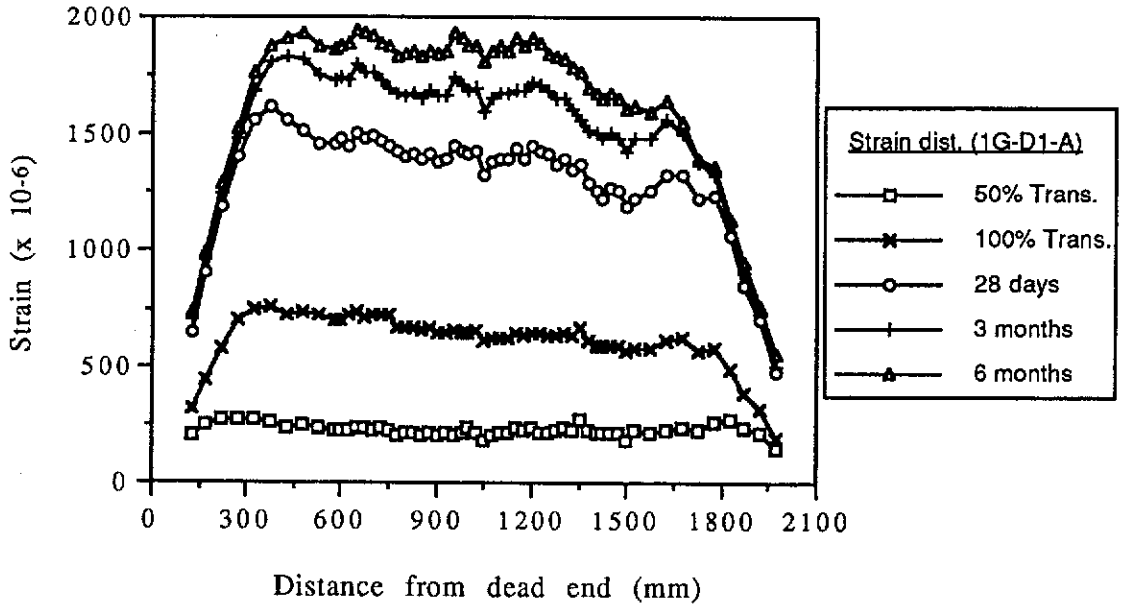

Figure A.1 Longitudinal Strain Distributions for Beam 1G-D1 (Wire A, Northern Wire)

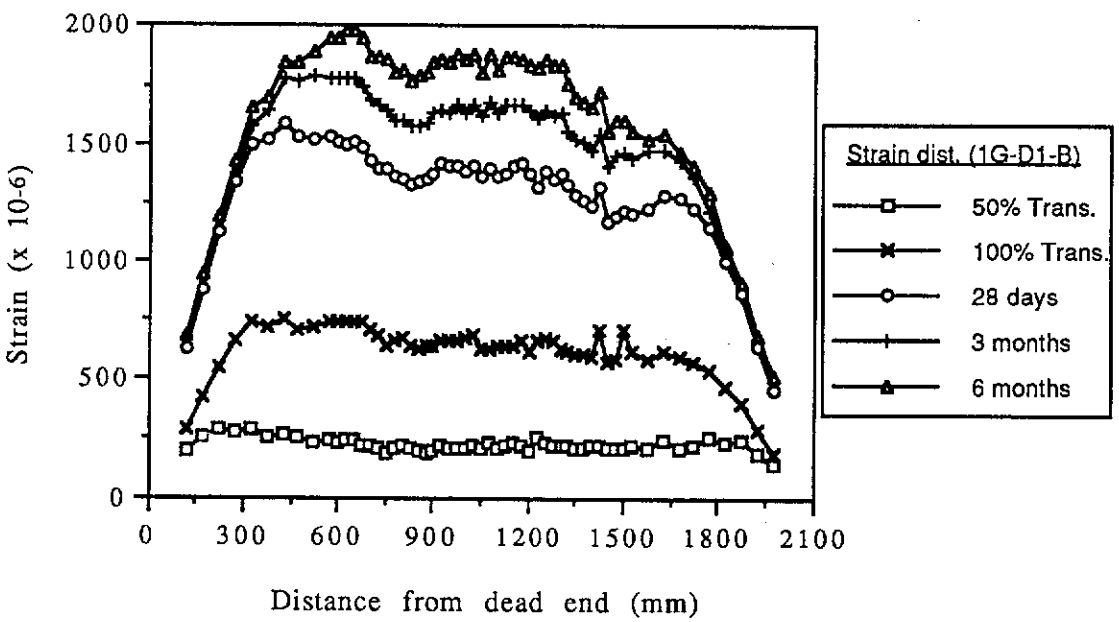

Figure A.2 Longitudinal Strain Distributions for Beam 1G-D1 (Wire B, Southern Wire)

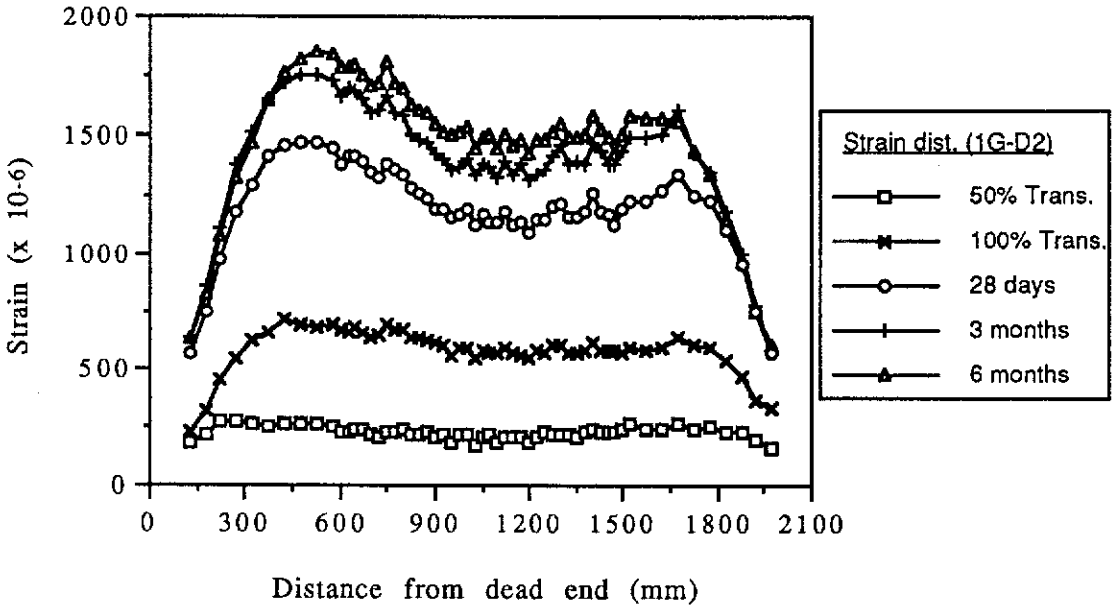

Figure A.3 Longitudinal Strain Distributions for Beam 1G-D2

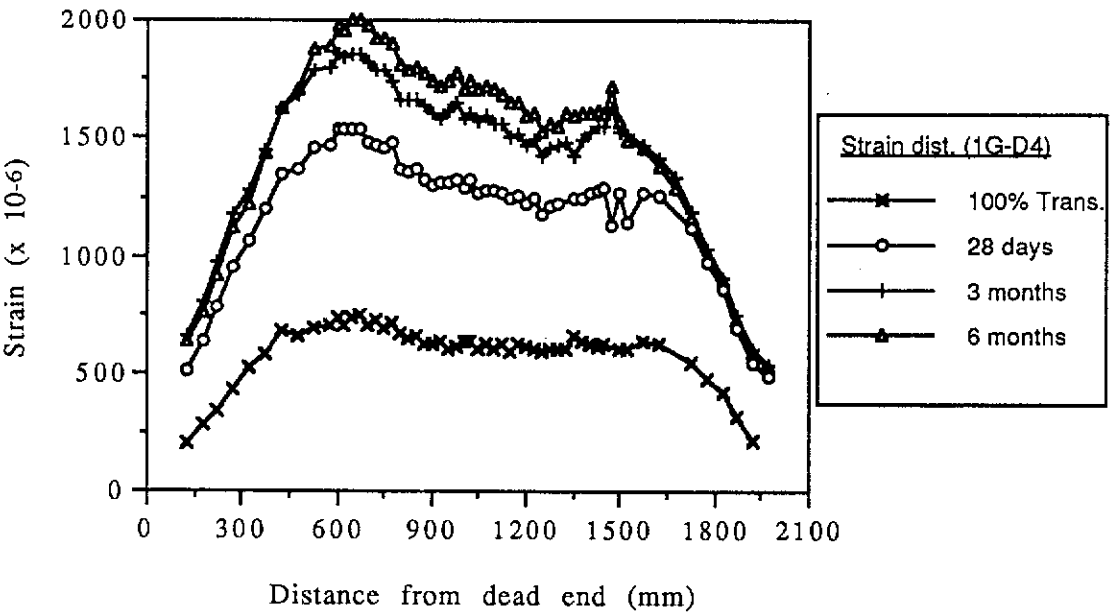

Figure A.4 Longitudinal Strain Distributions for Beam 1G-D4

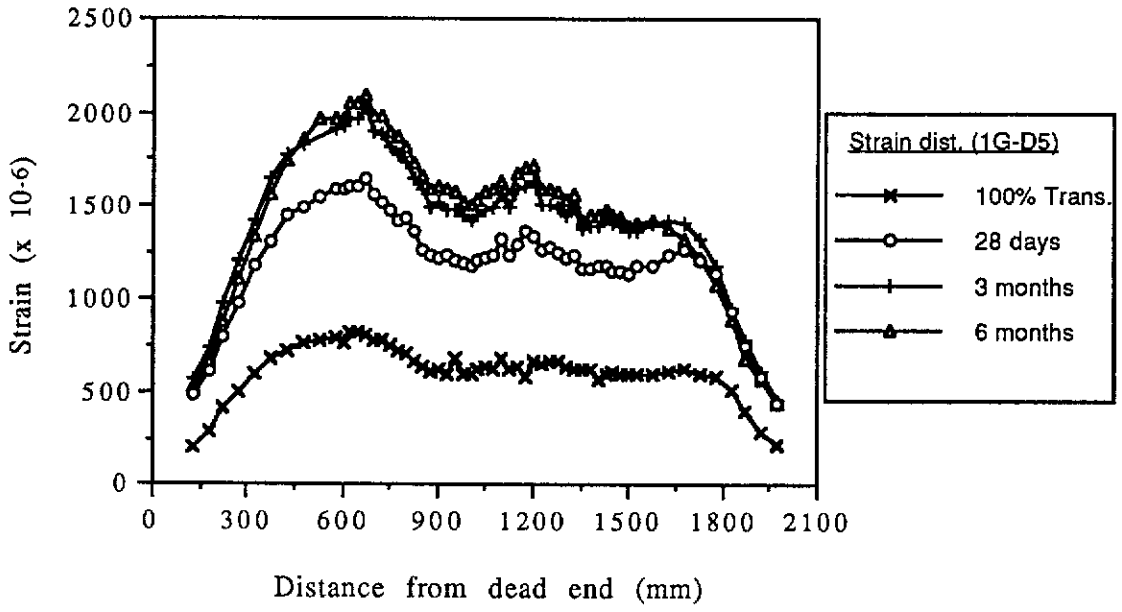

Figure A.5 Longitudinal Strain Distributions for Beam 1G-D5

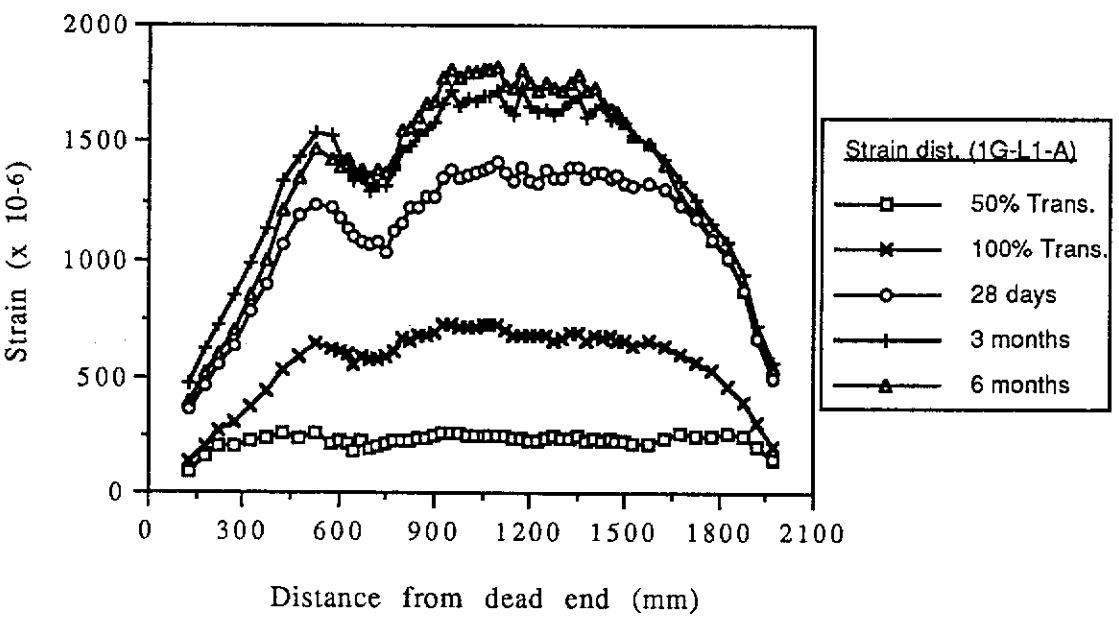

Figure A.6 Longitudinal Strain Distributions for Beam 1G-L1 (Wire A, Northern Wire)

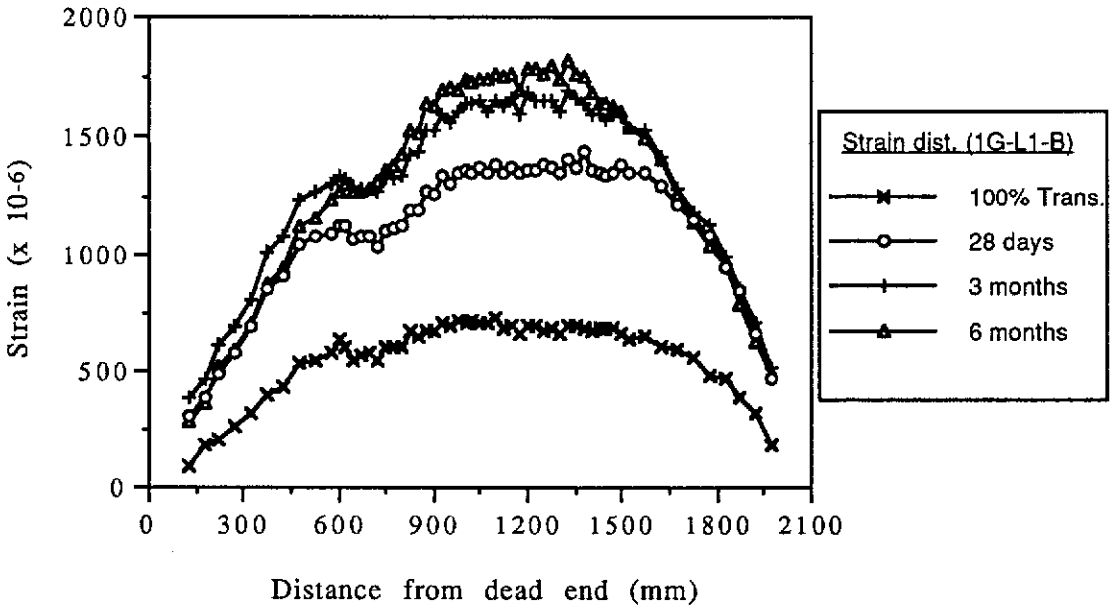

Figure A.7 Longitudinal Strain Distributions for Beam 1G-L1 (Wire B, Southern Wire)

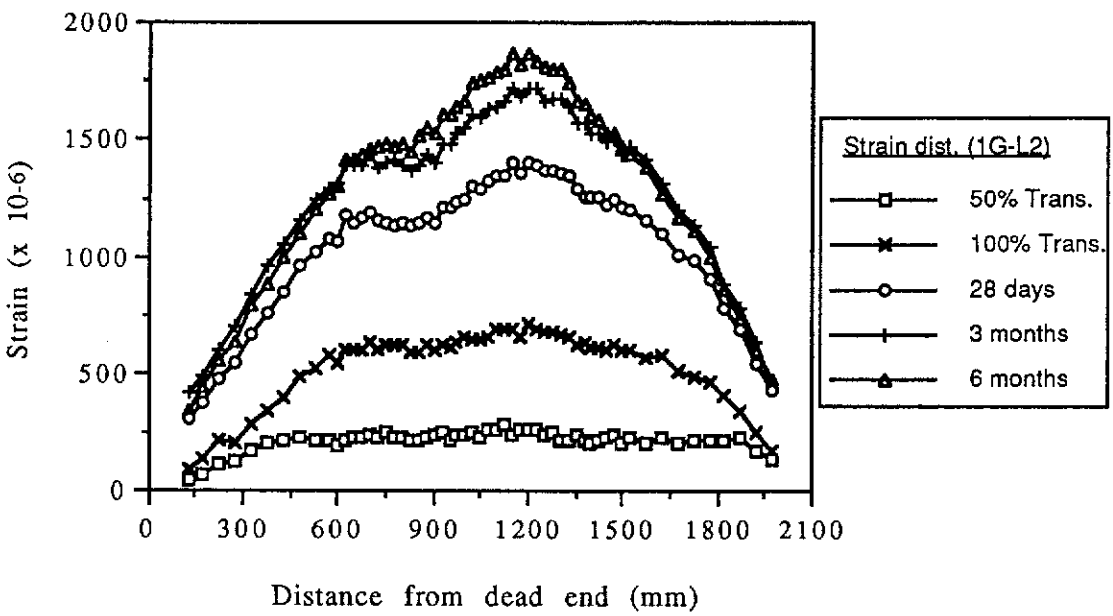

Figure A.8 Longitudinal Strain Distributions for Beam 1G-L2

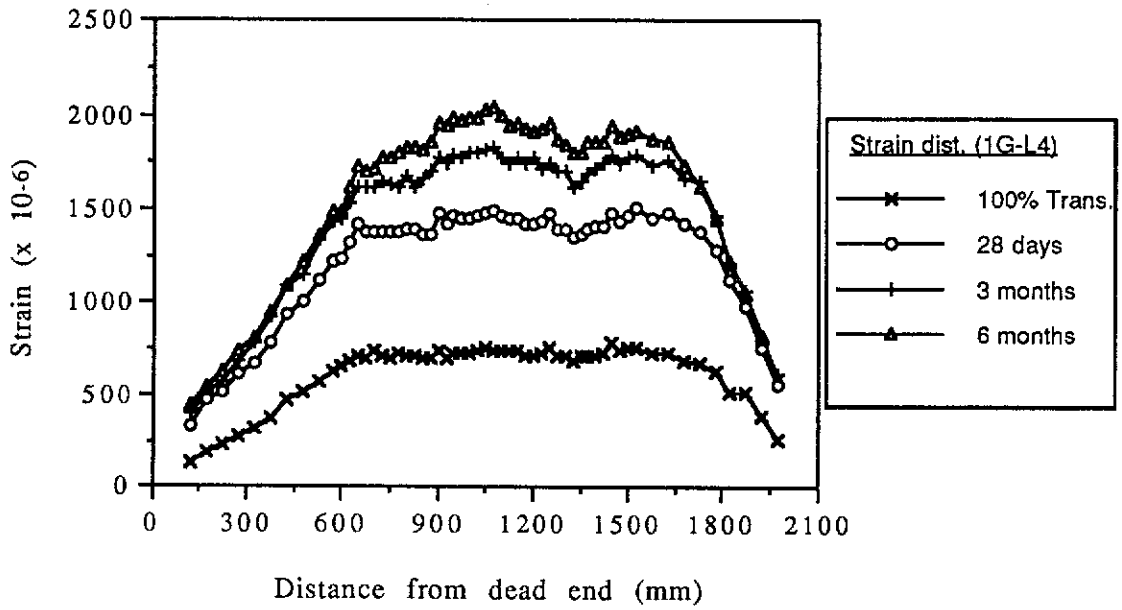

Figure A.9 Longitudinal Strain Distributions for Beam 1G-L4

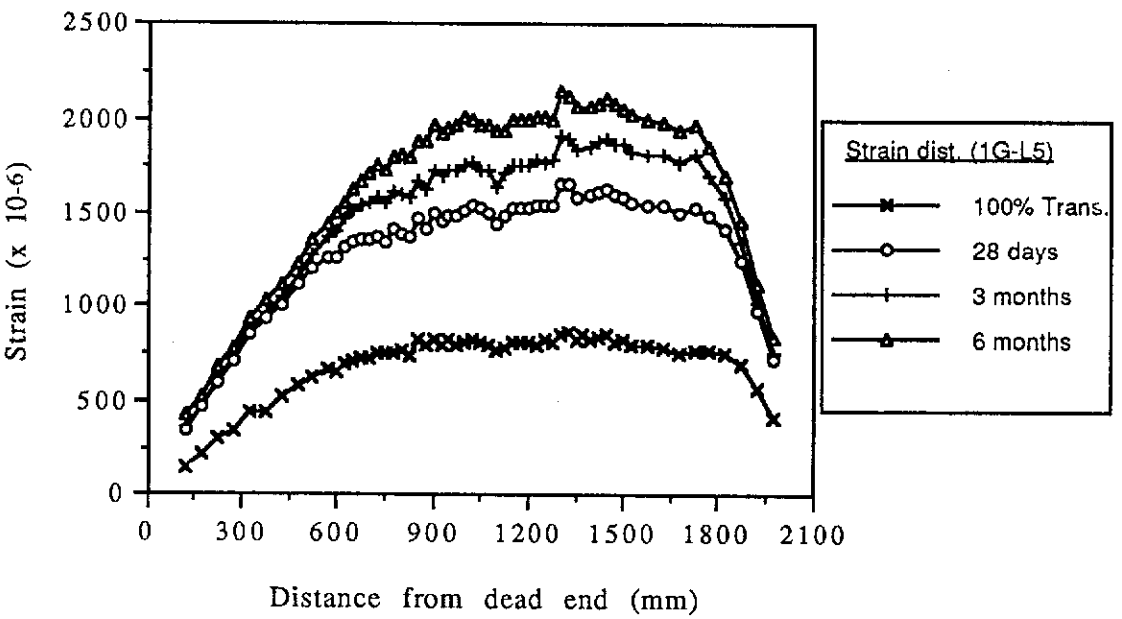

Figure A.10 Longitudinal Strain Distributions for Beam 1G-L5

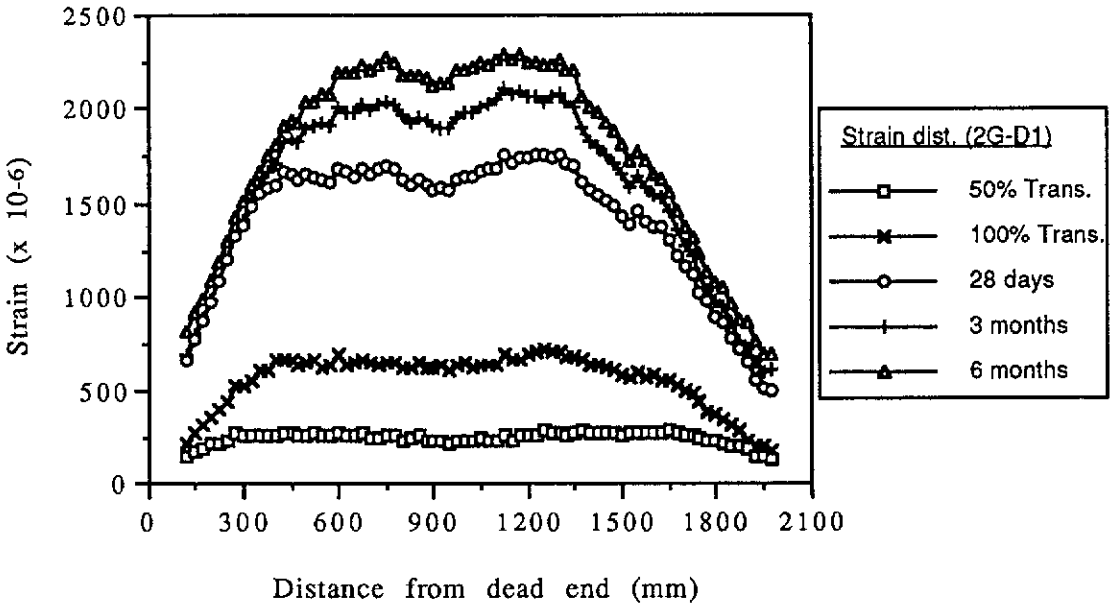

Figure A.11 Longitudinal Strain Distributions for Beam 2G-D1

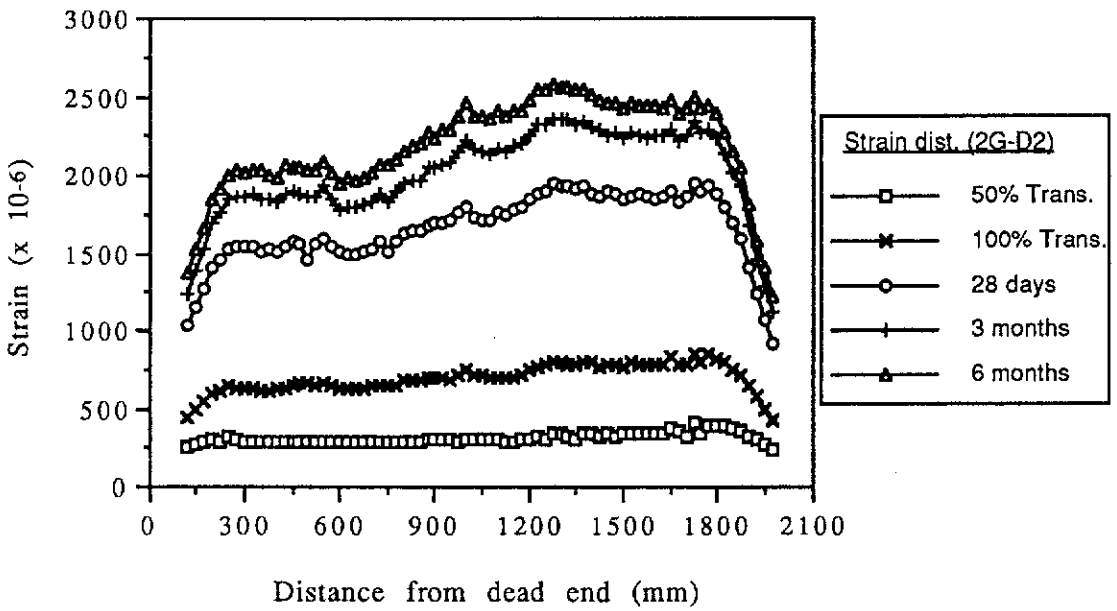

Figure A.12 Longitudinal Strain Distributions for Beam 2G-D2

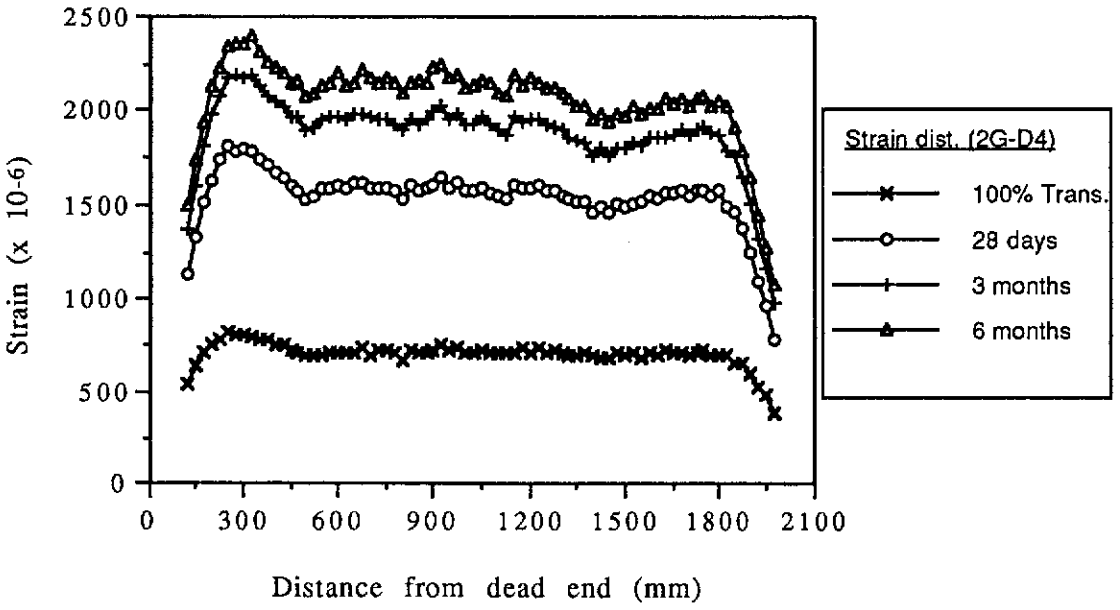

Figure A.13 Longitudinal Strain Distributions for Beam 2G-D4

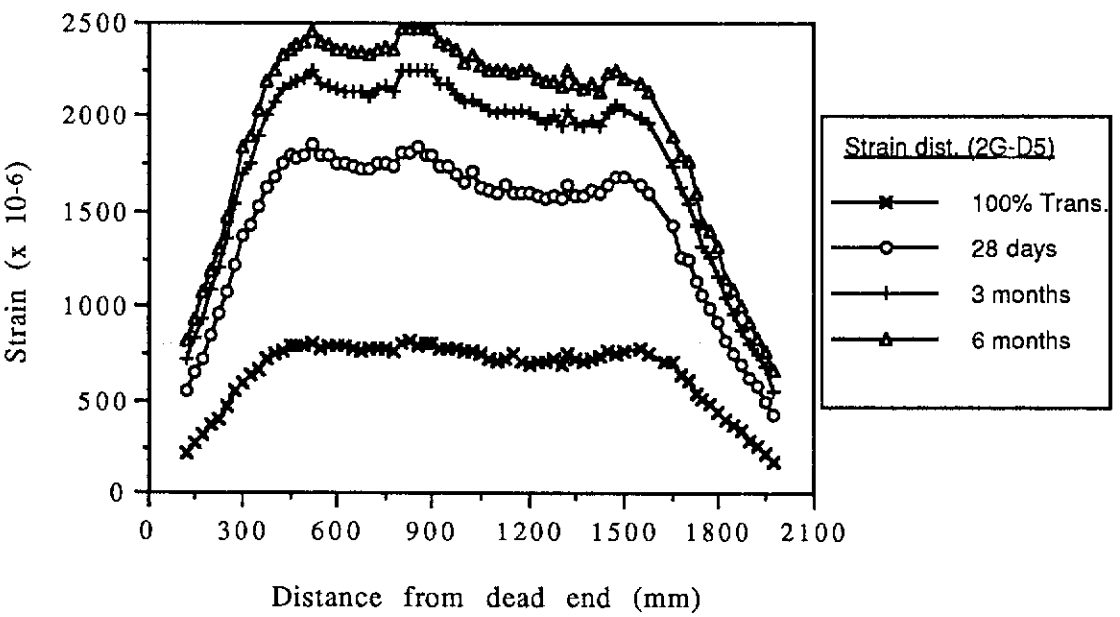

Figure A.14 Longitudinal Strain Distributions for Beam 2G-D5

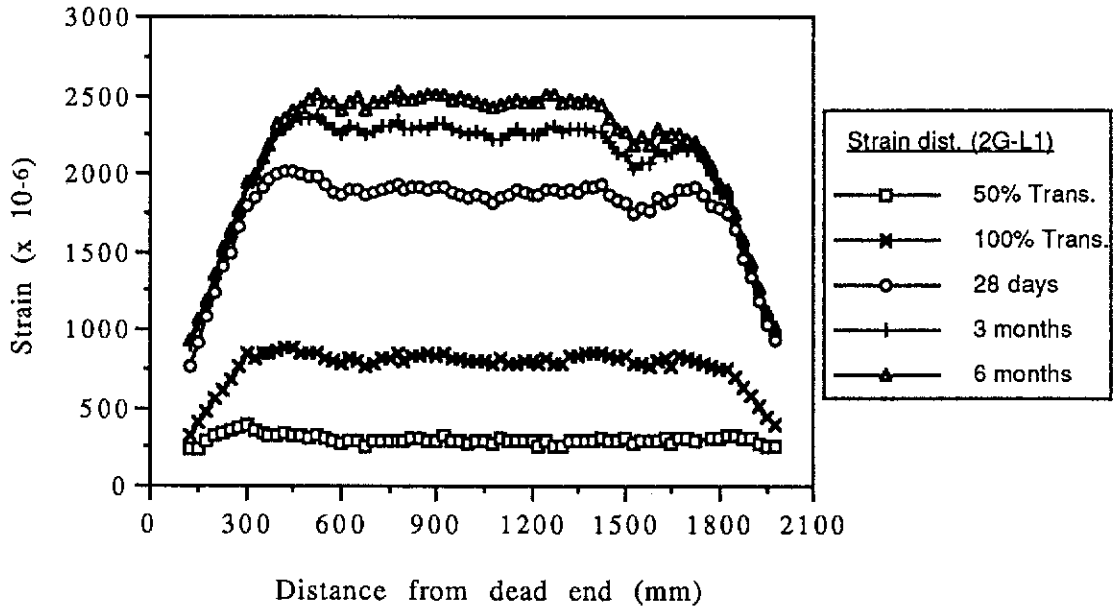

Figure A.15 Longitudinal Strain Distributions for Beam 2G-L1

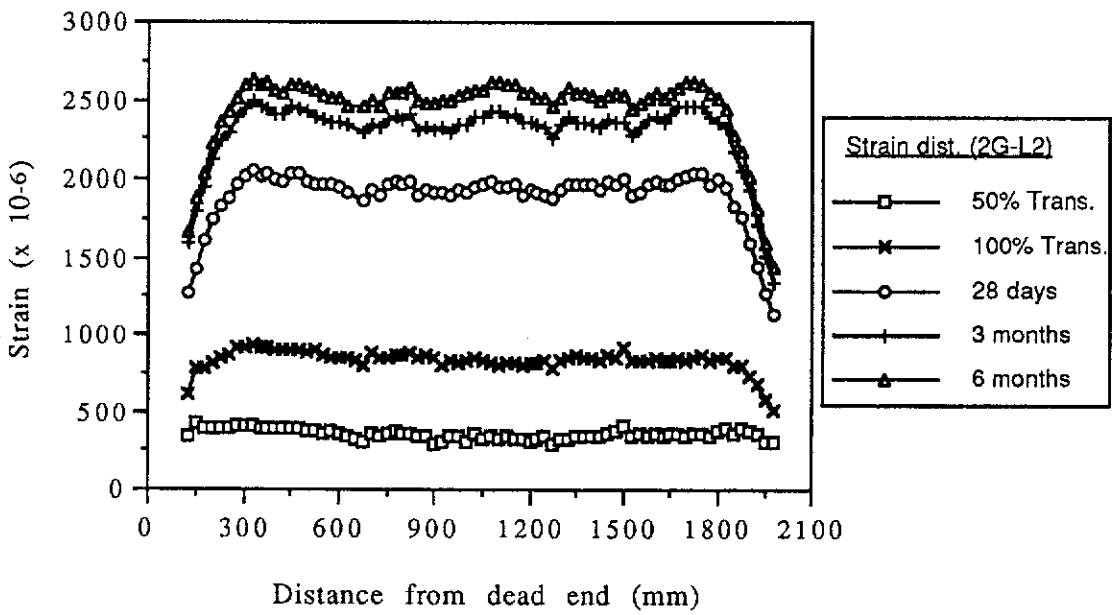

Figure A.16 Longitudinal Strain Distributions for Beam 2G-L2

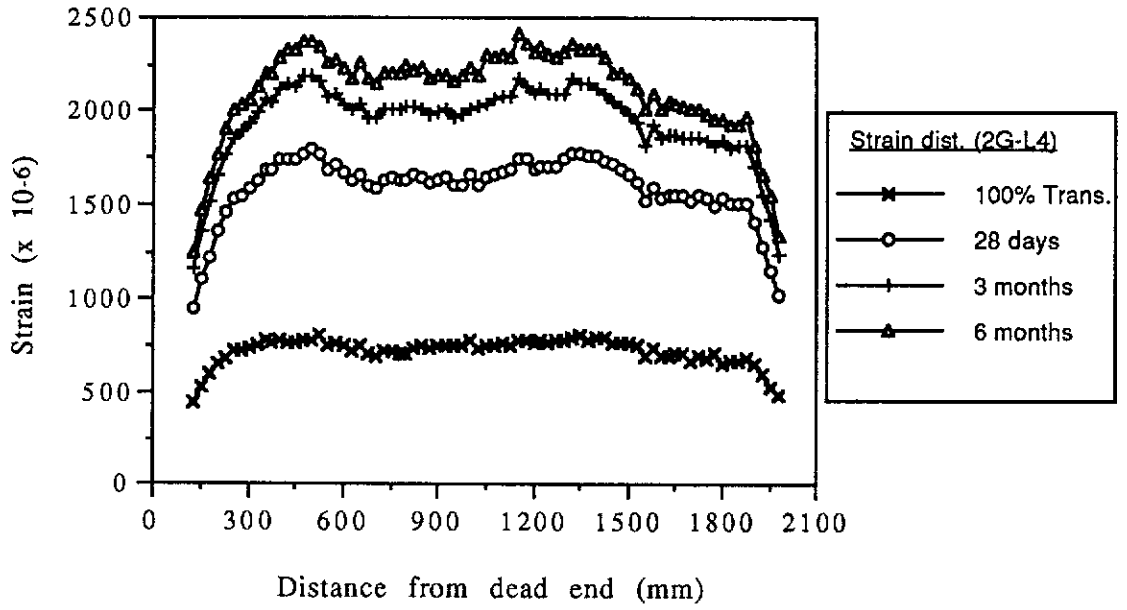

Figure A.17 Longitudinal Strain Distributions for Beam 2G-L4

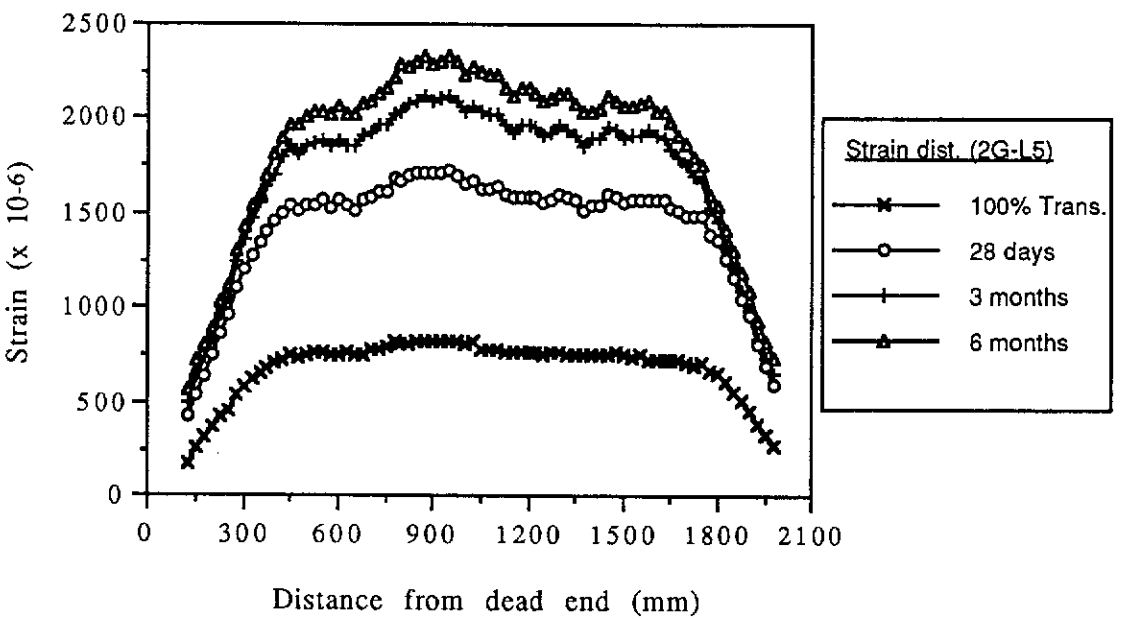

Figure A.18 Longitudinal Strain Distributions for Beam 2G-L5

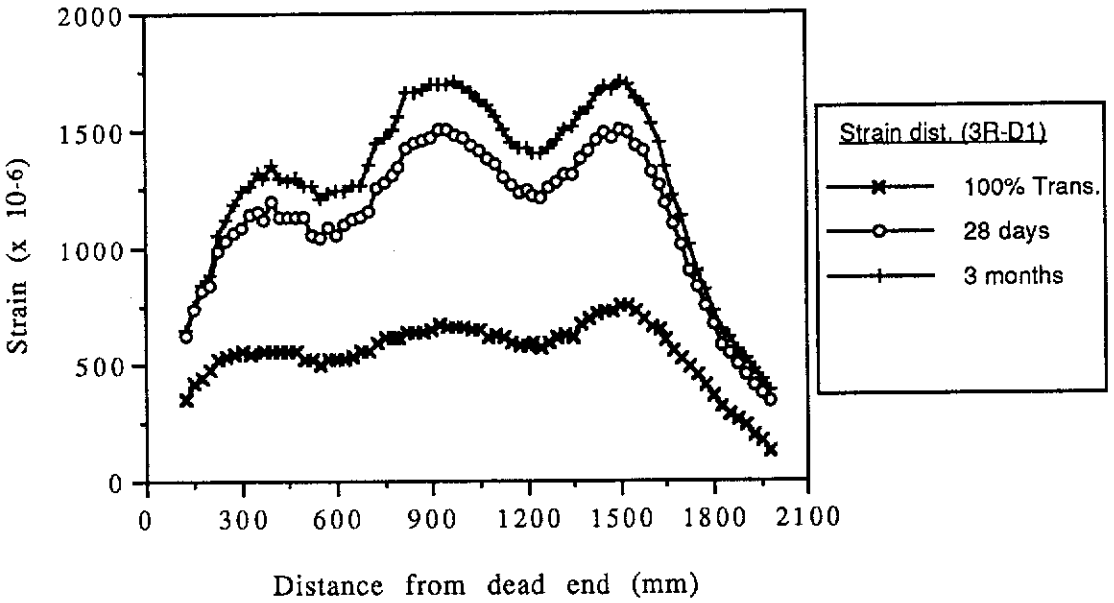

Figure A.19 Longitudinal Strain Distributions for Beam 3R-D1

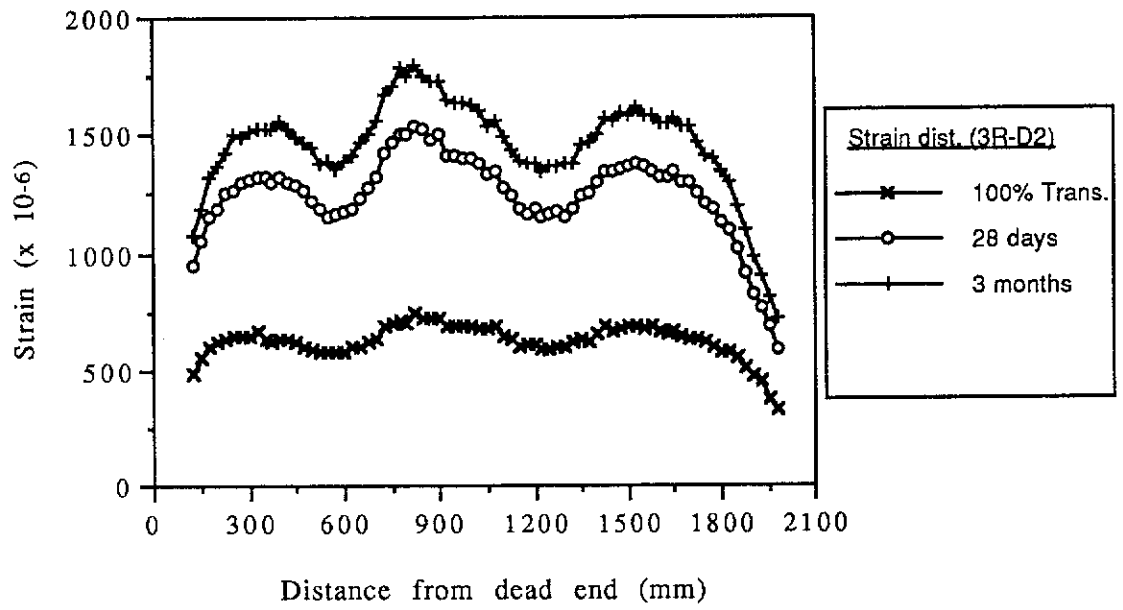

Figure A.20 Longitudinal Strain Distributions for Beam 3R-D2

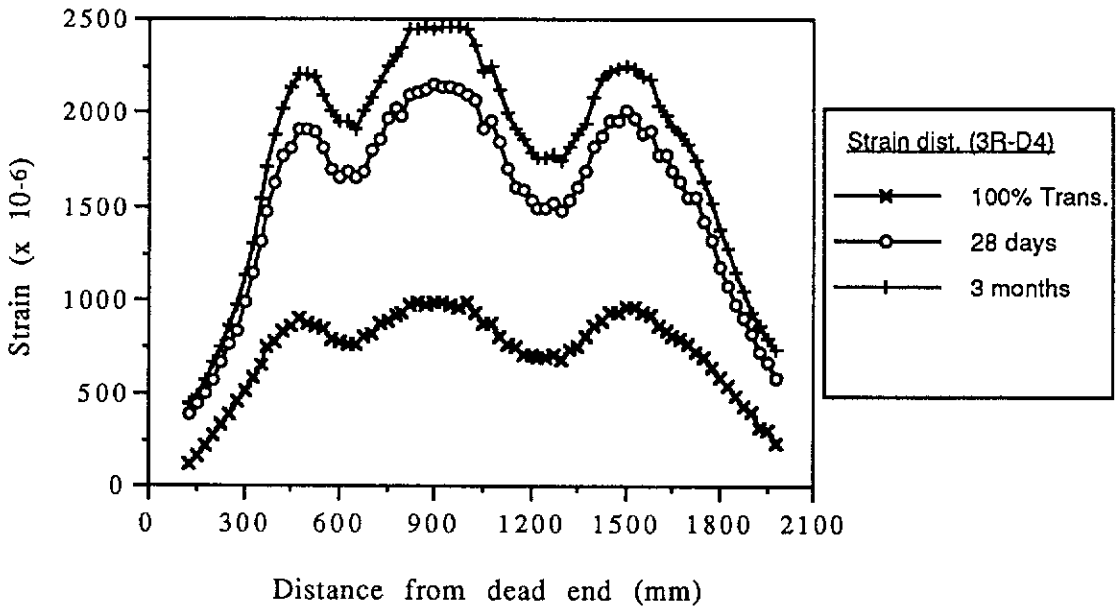

Figure A.21 Longitudinal Strain Distributions for Beam 3R-D4

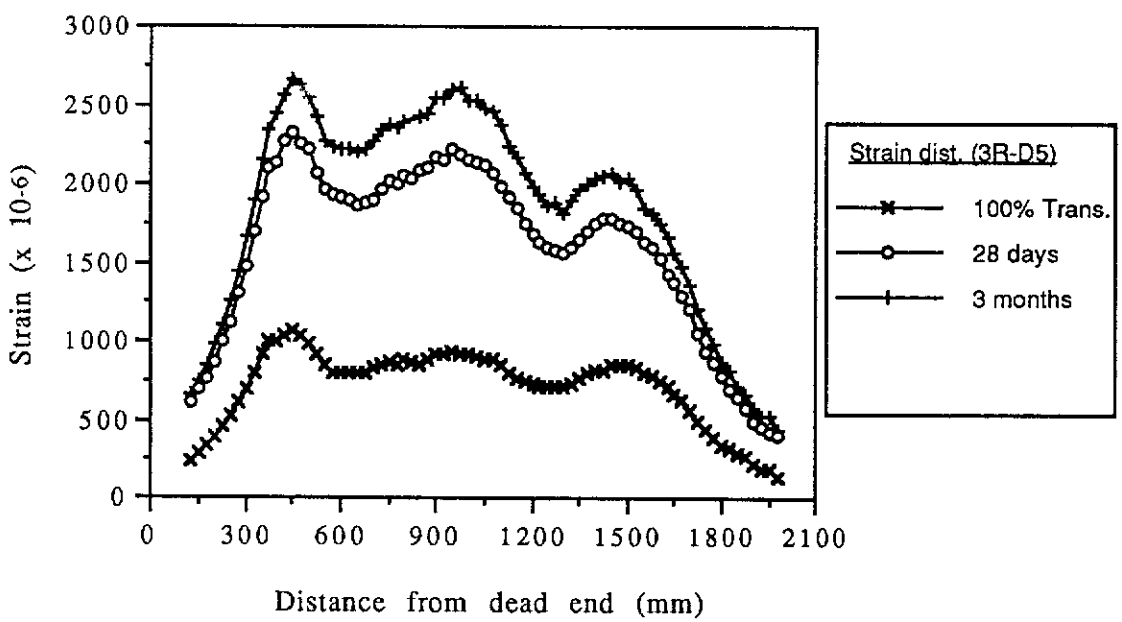

Figure A.22 Longitudinal Strain Distributions for Beam 3R-D5

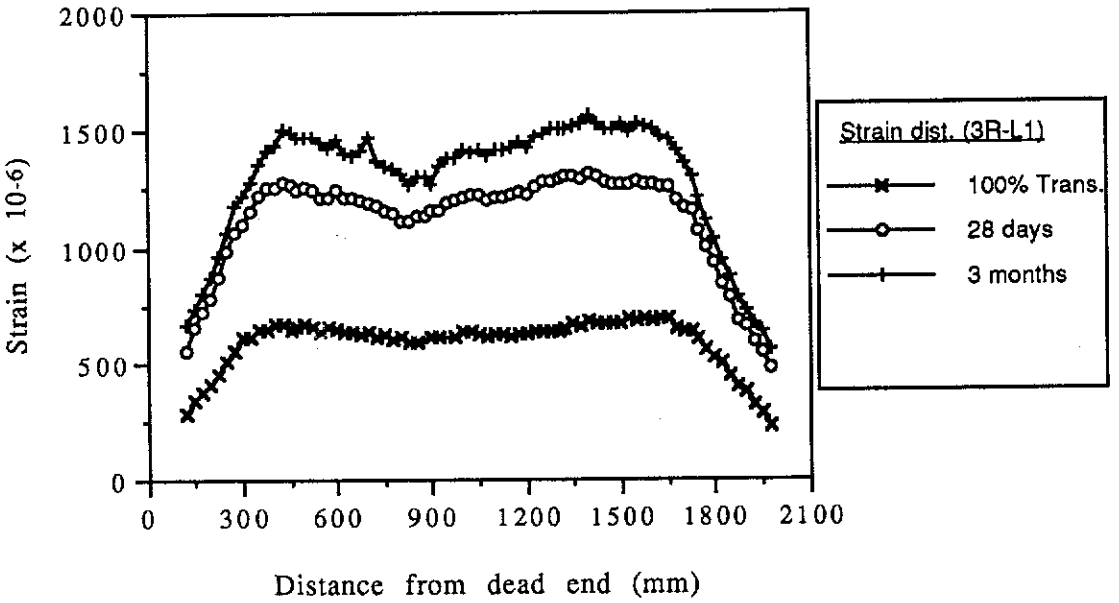

Figure A.23 Longitudinal Strain Distributions for Beam 3R-L1

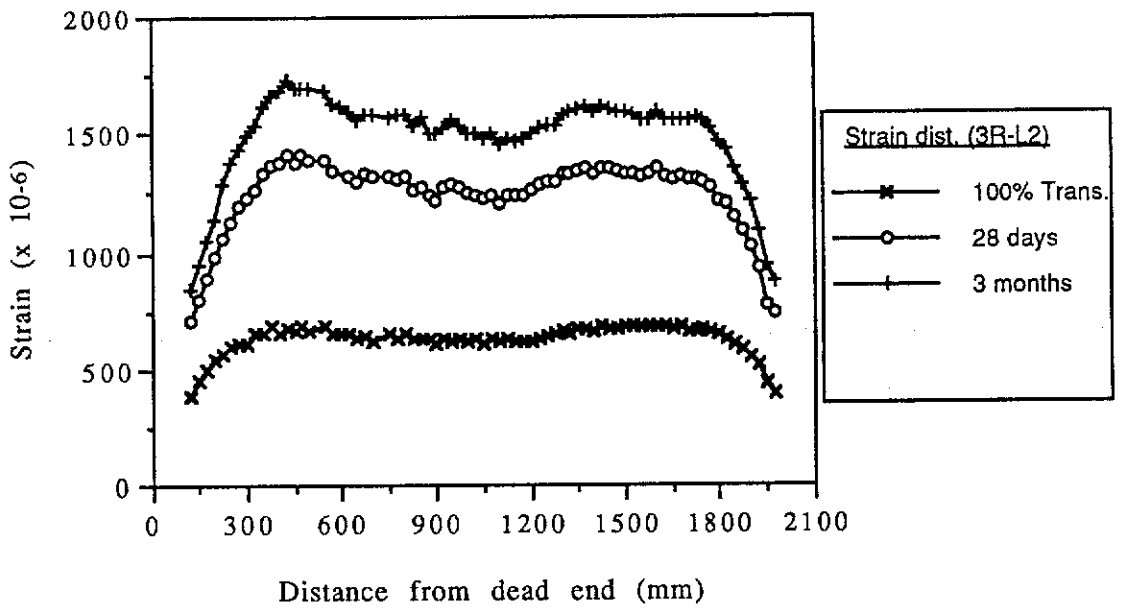

Figure A.24 Longitudinal Strain Distributions for Beam 3R-L2

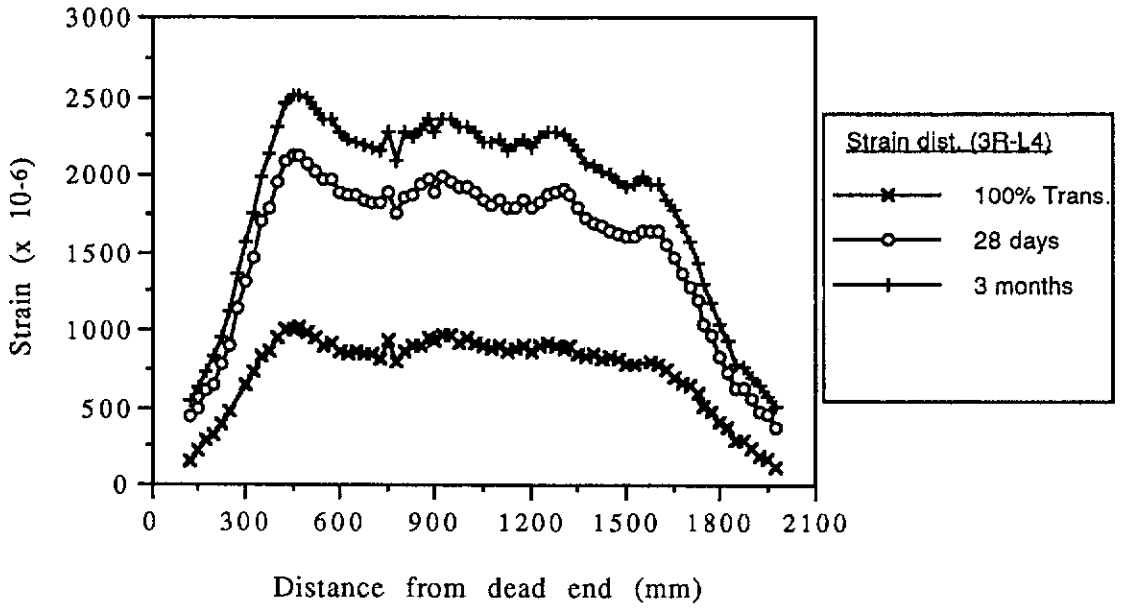

Figure A.25 Longitudinal Strain Distributions for Beam 3R-L4

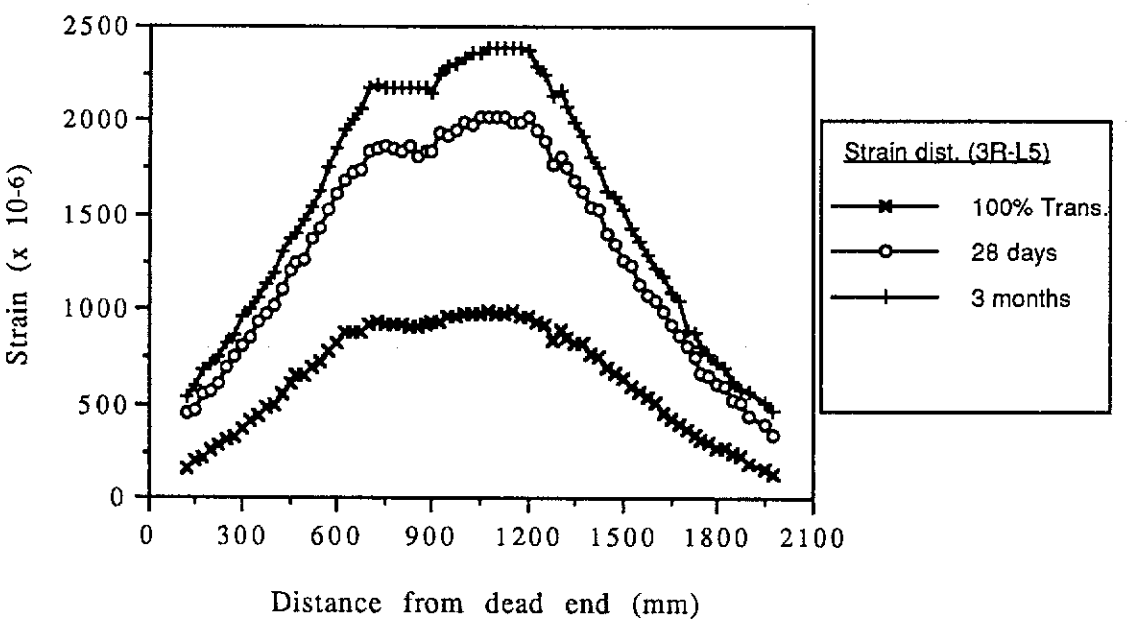

Figure A.26 Longitudinal Strain Distributions for Beam 3R-L5

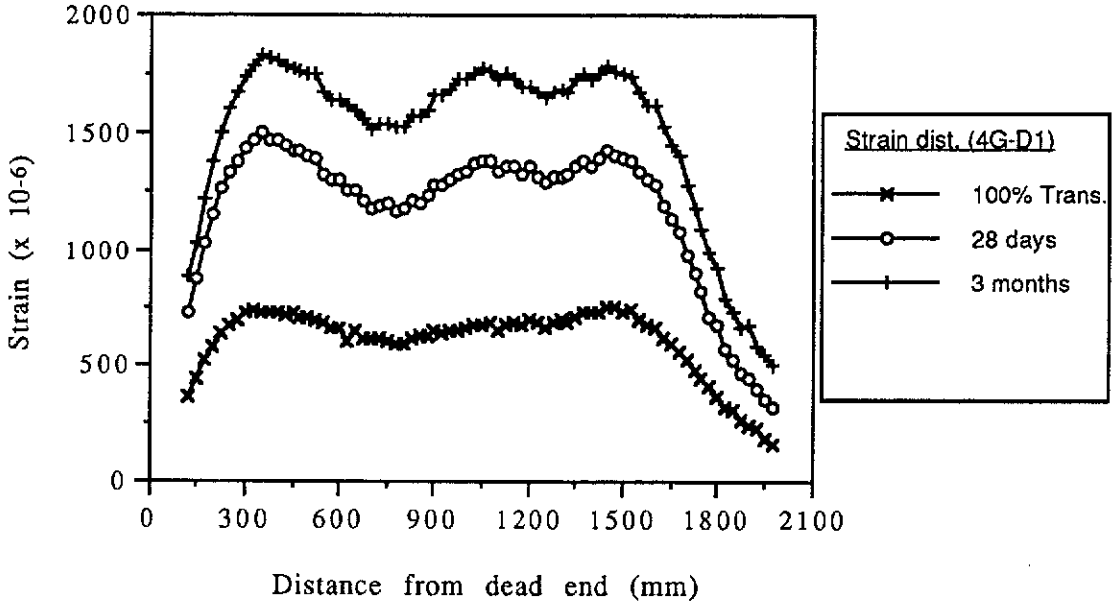

Figure A.27 Longitudinal Strain Distributions for Beam 4G-D1

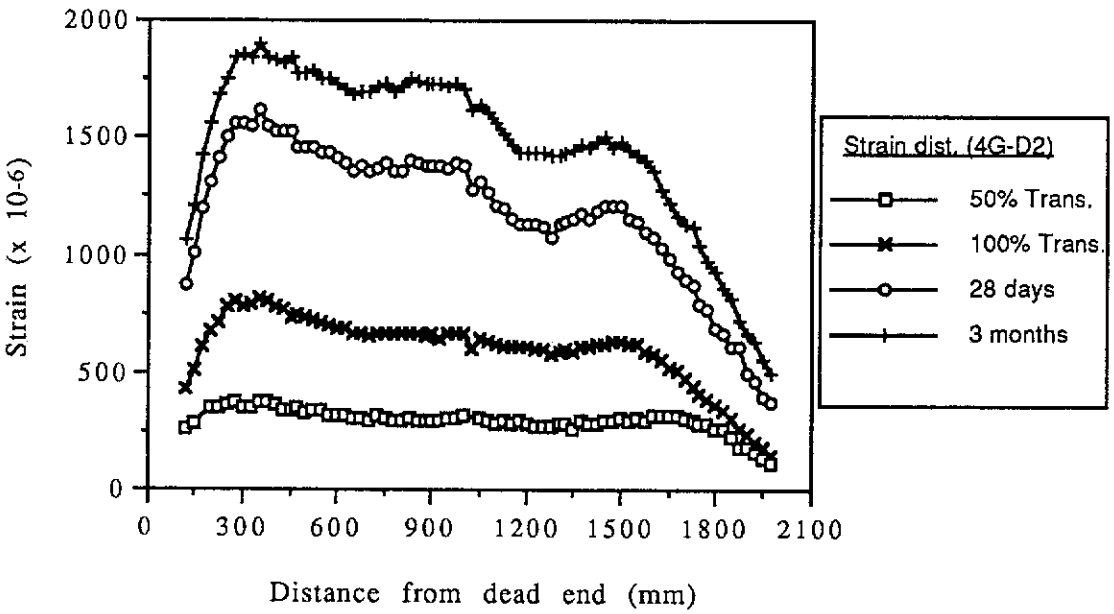

Figure A.28 Longitudinal Strain Distributions for Beam 4G-D2

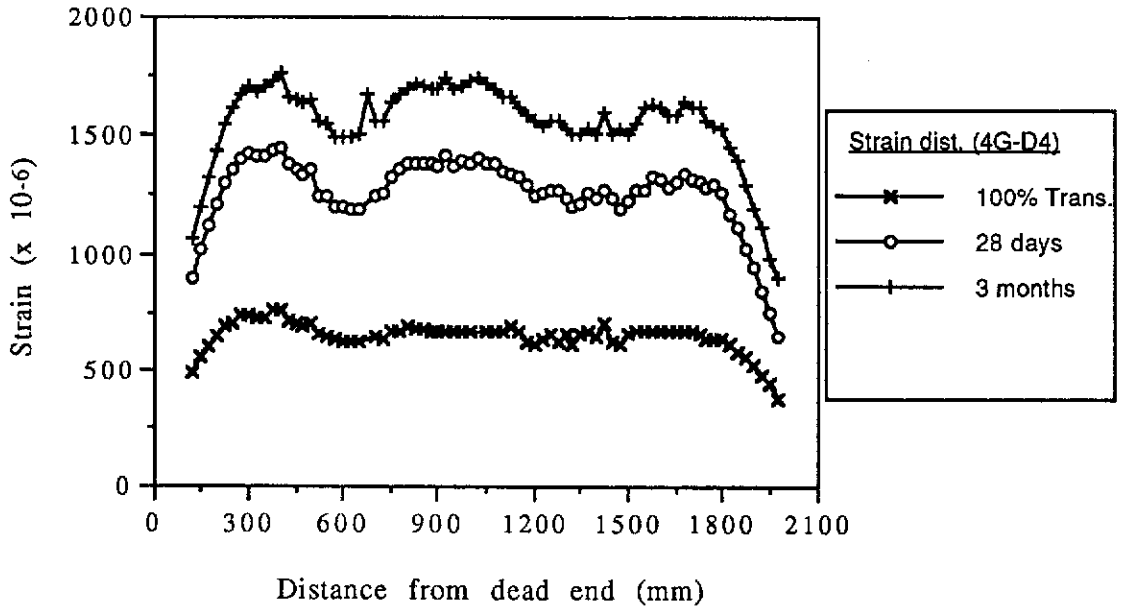

Figure A.29 Longitudinal Strain Distributions for Beam 4G-D4

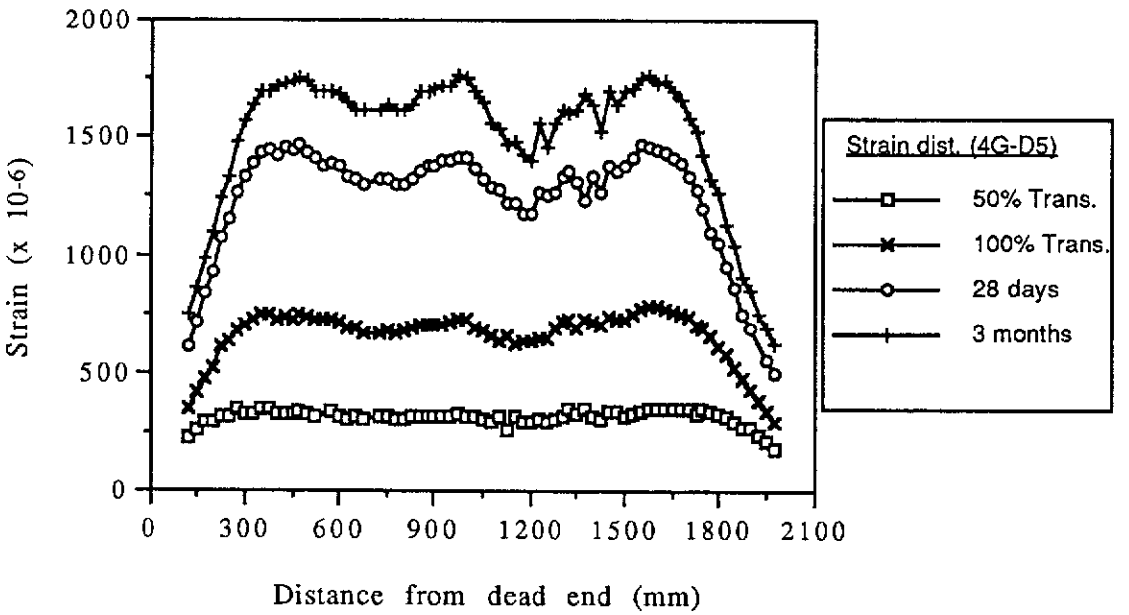

Figure A.30 Longitudinal Strain Distributions for Beam 4G-D5

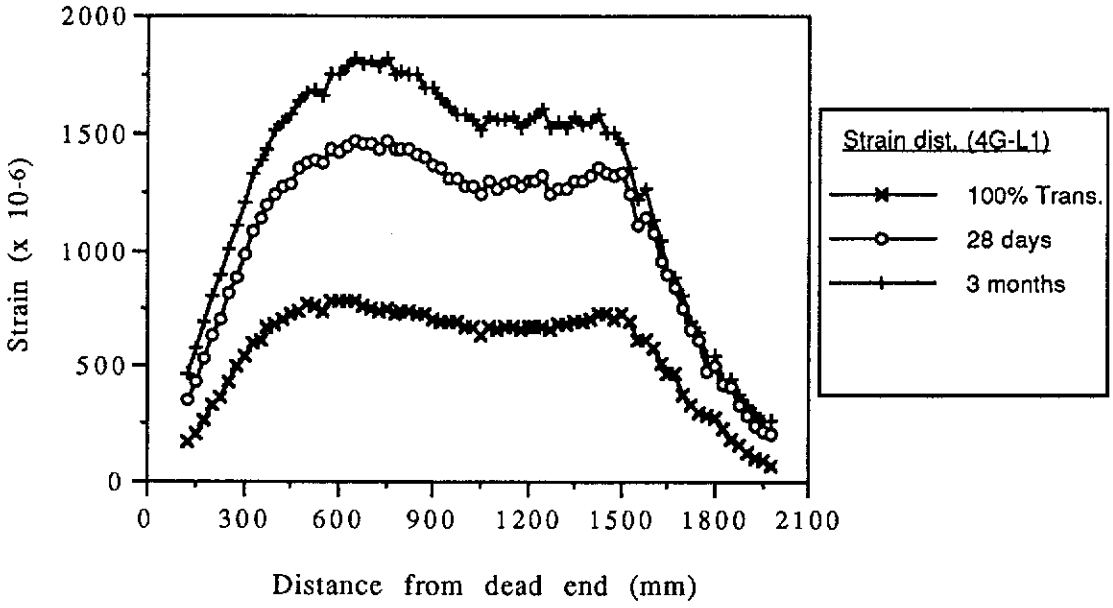

Figure A.31 Longitudinal Strain Distributions for Beam 4G-L1

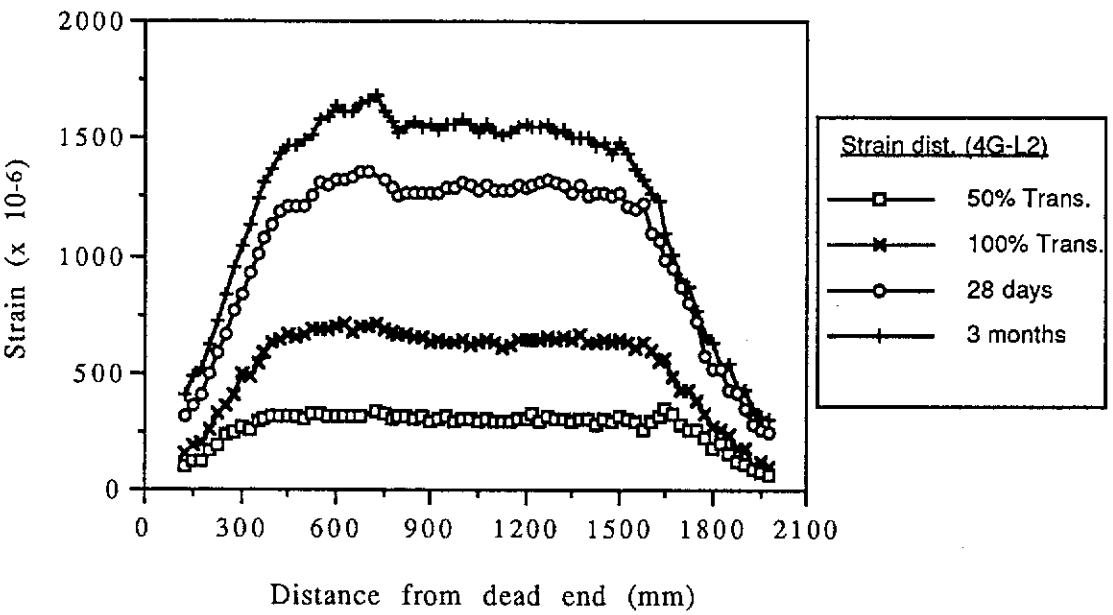

Figure A.32 Longitudinal Strain Distributions for Beam 4G-L2

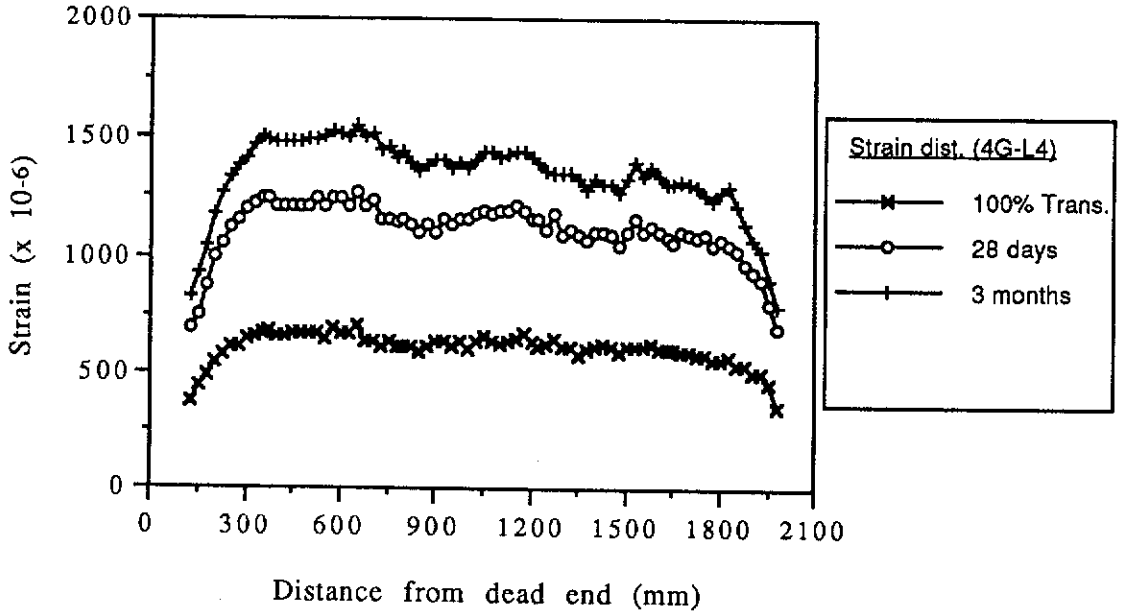

Figure A.33 Longitudinal Strain Distributions for Beam 4G-L4

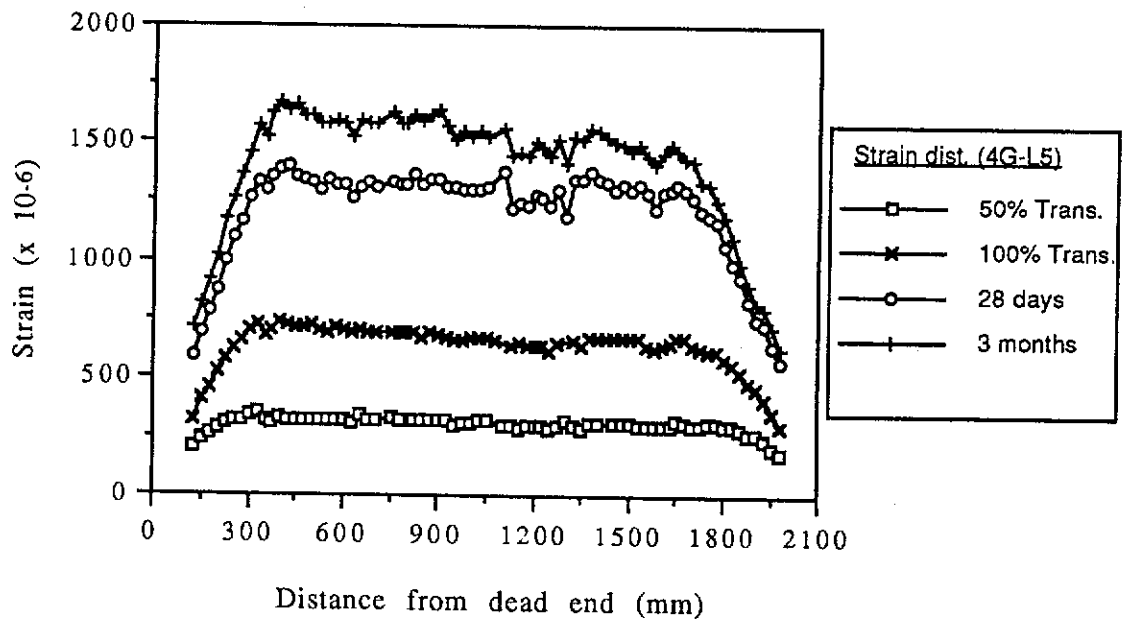

Figure A.34 Longitudinal Strain Distributions for Beam 4G-L5

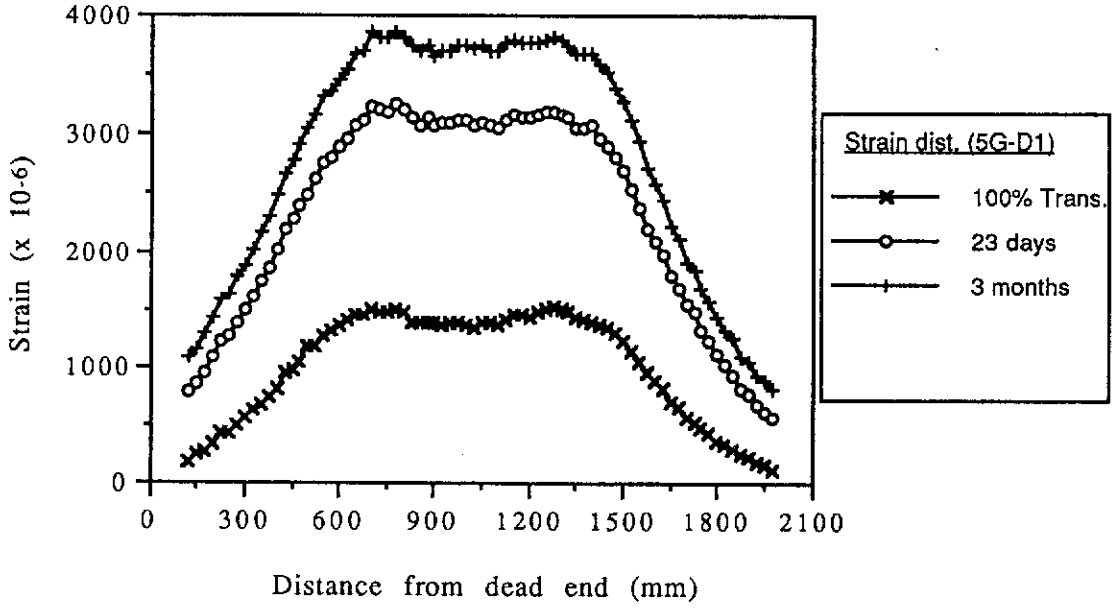

Figure A.35 Longitudinal Strain Distributions for Beam 5G-D1

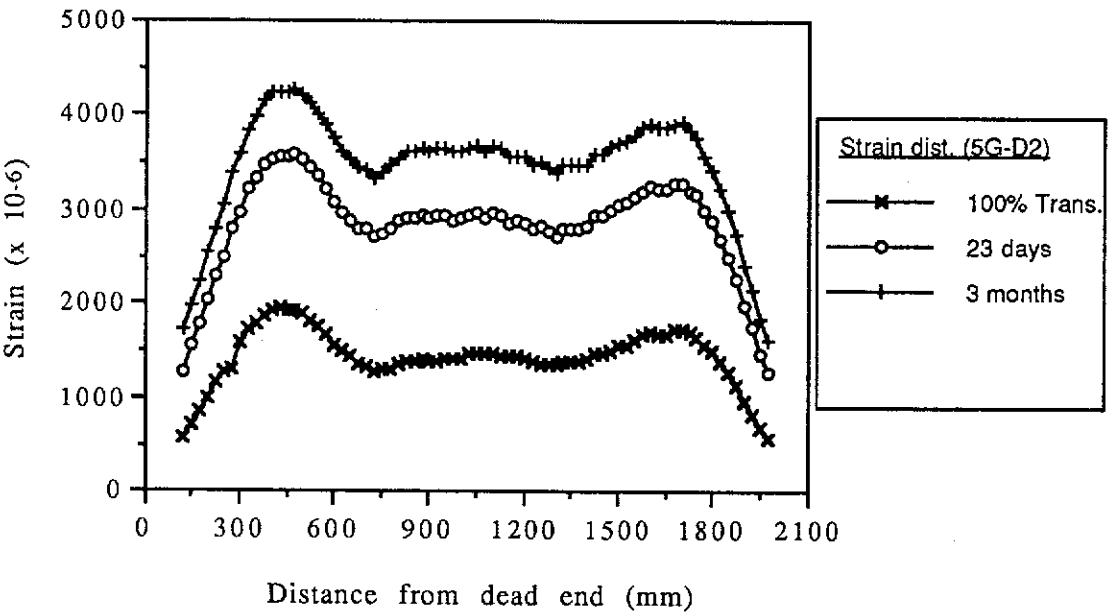

Figure A.36 Longitudinal Strain Distributions for Beam 5G-D2

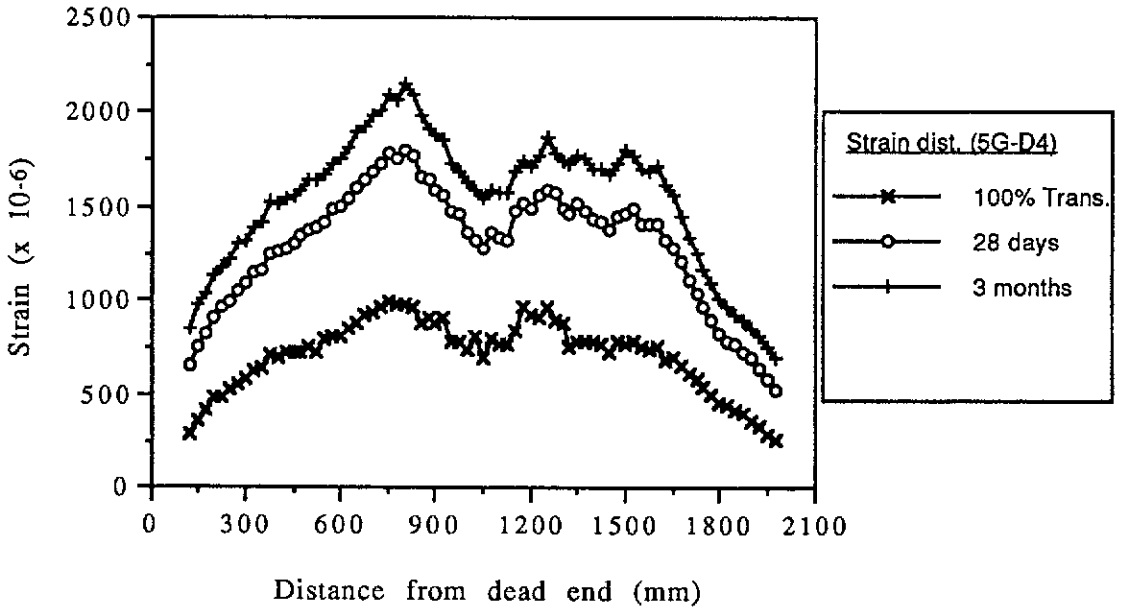

Figure A.37 Longitudinal Strain Distributions for Beam 5G-D4

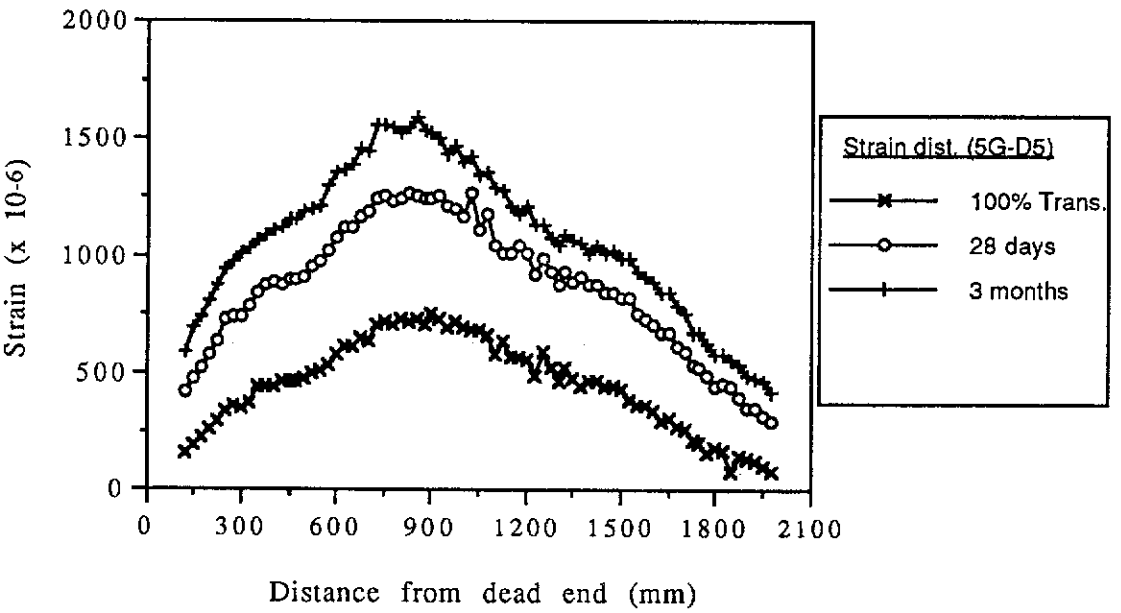

Figure A.38 Longitudinal Strain Distributions for Beam 5G-D5

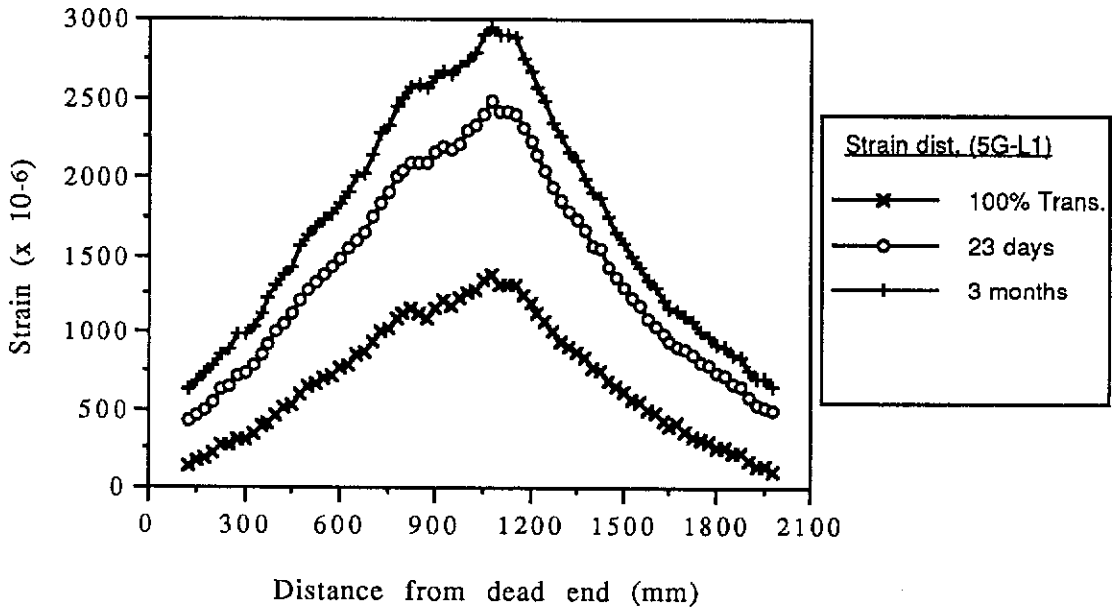

Figure A.39 Longitudinal Strain Distributions for Beam 5G-L1

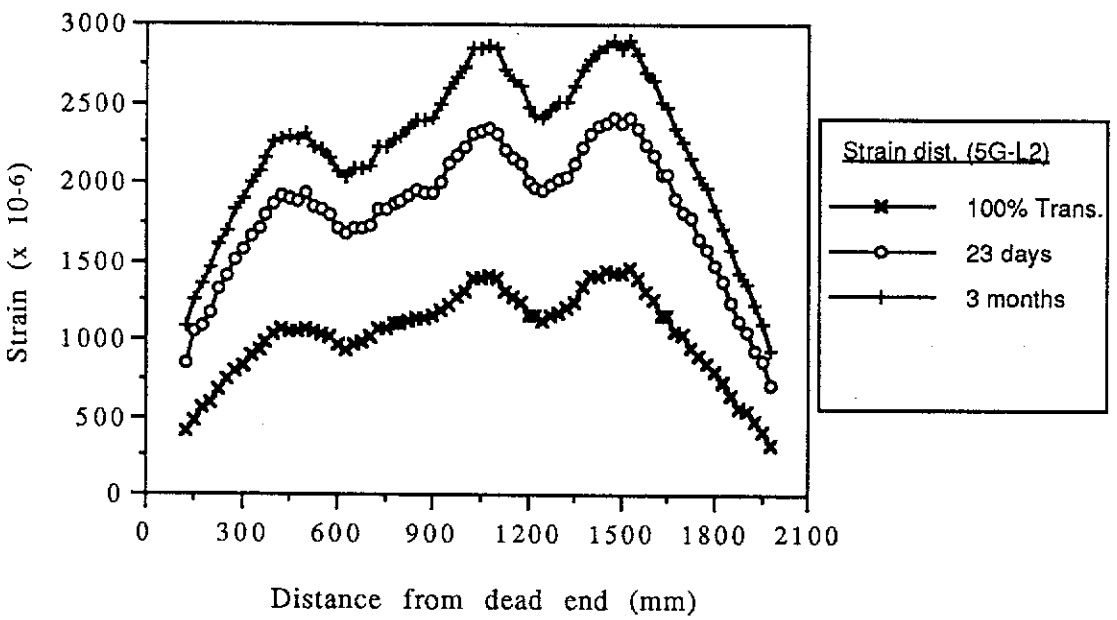

Figure A.40 Longitudinal Strain Distributions for Beam 5G-L2

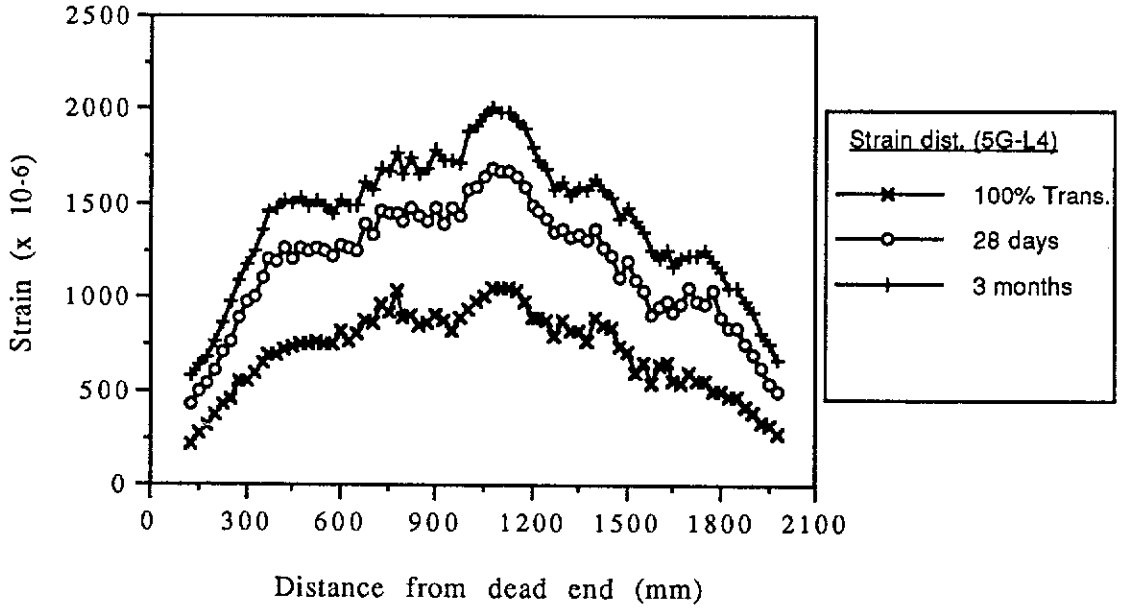

Figure A.41 Longitudinal Strain Distributions for Beam 5G-L4

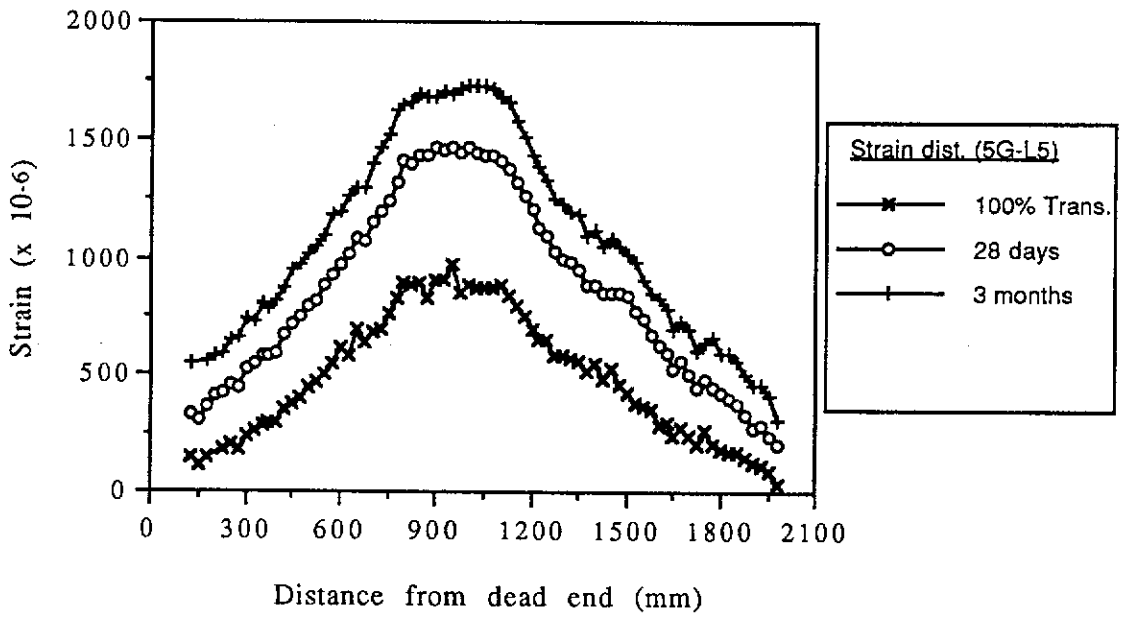

Figure A.42 Longitudinal Strain Distributions for Beam 5G-L5

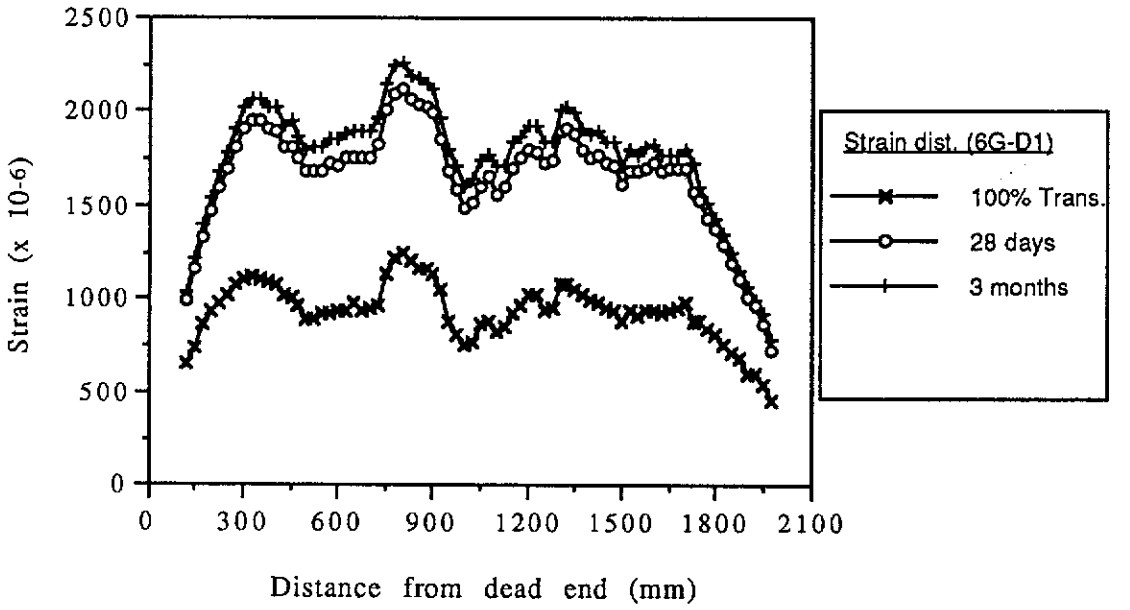

Figure A.43 Longitudinal Strain Distributions for Beam 6G-D1

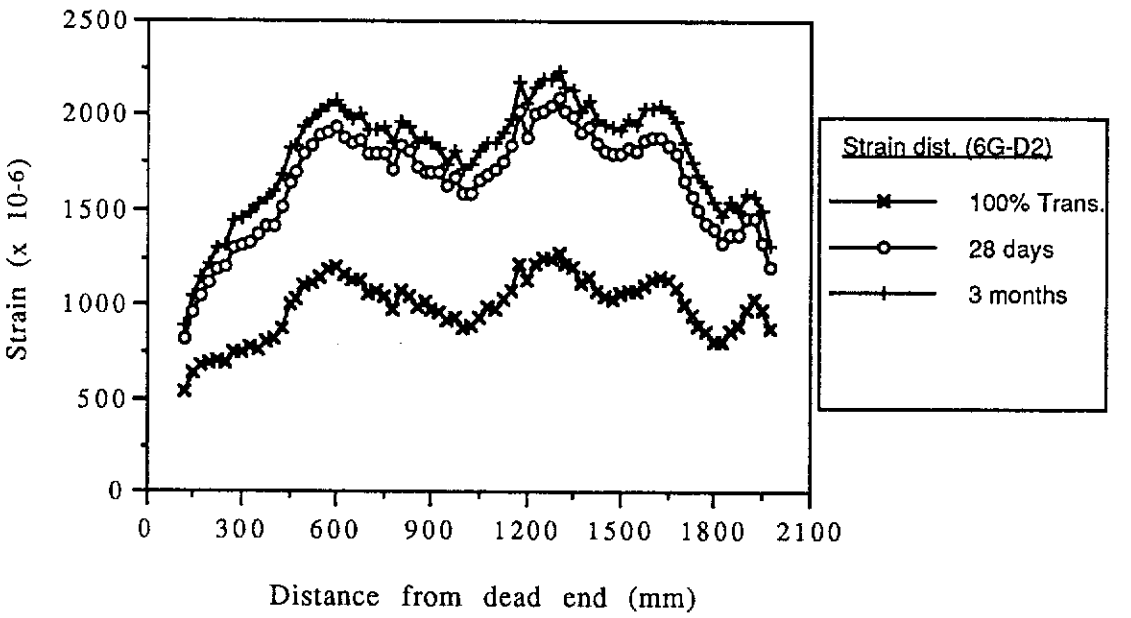

Figure A.44 Longitudinal Strain Distributions for Beam 6G-D2

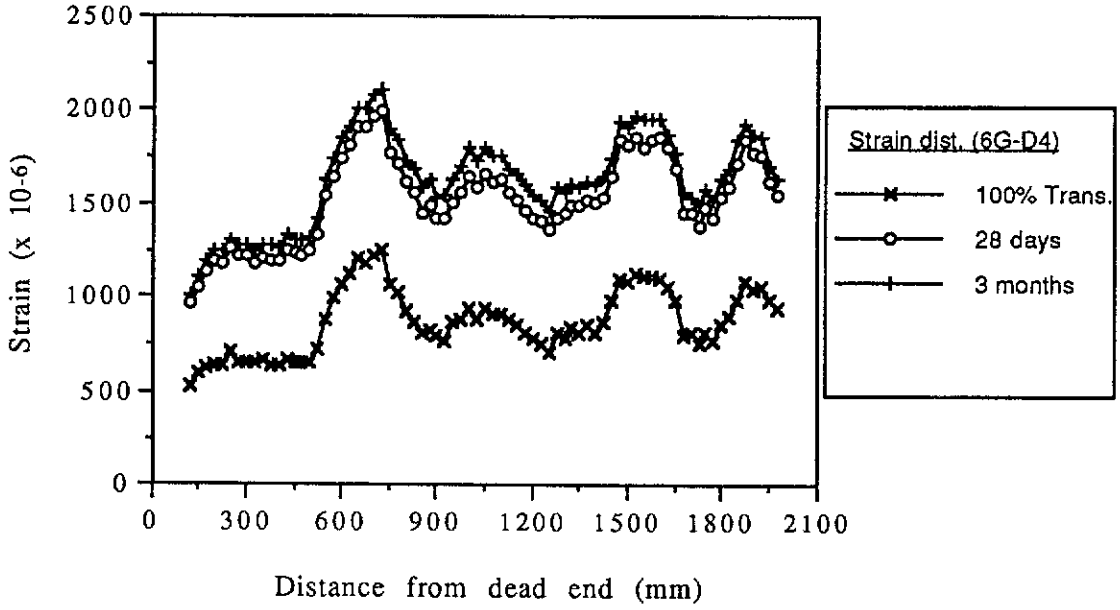

Figure A.45 Longitudinal Strain Distributions for Beam 6G-D4

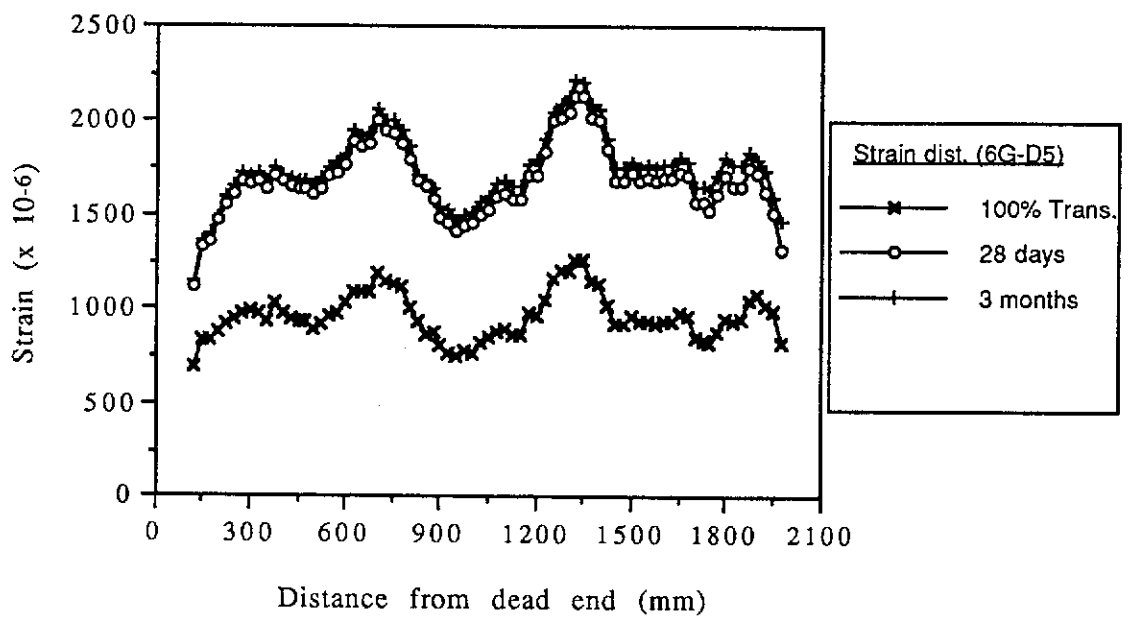

Figure A.46 Longitudinal Strain Distributions for Beam 6G-D5

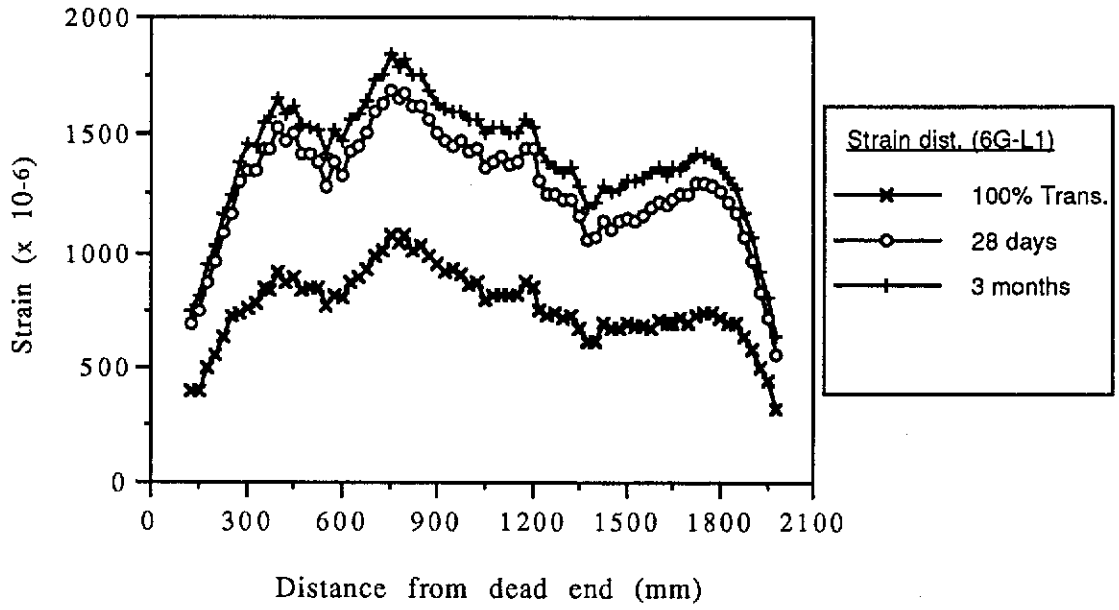

Figure A.47 Longitudinal Strain Distributions for Beam 6G-L1

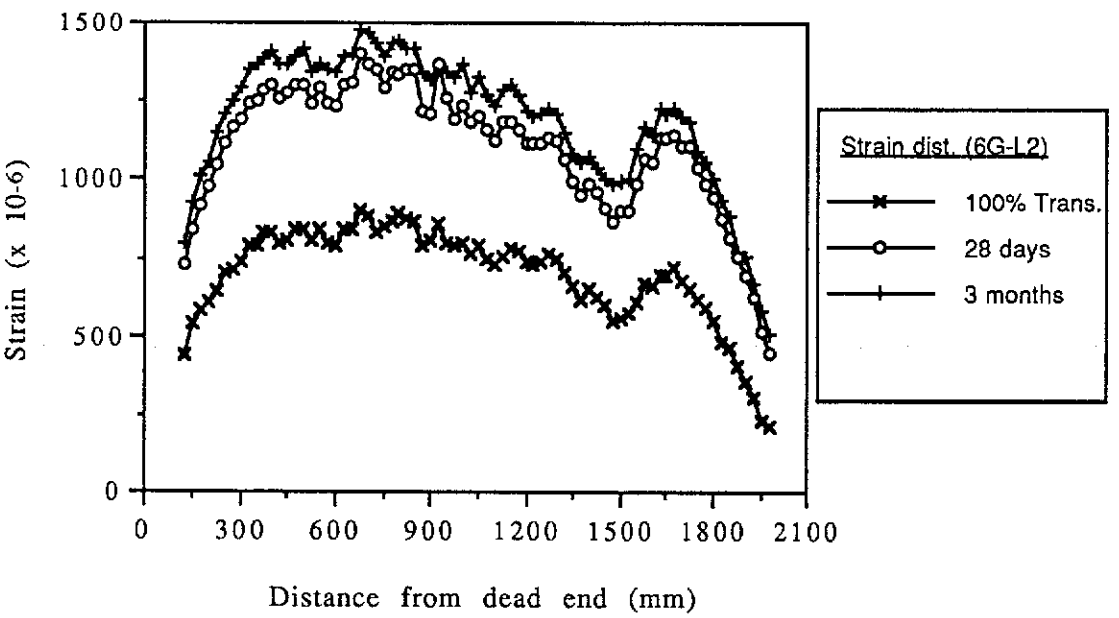

Figure A.48 Longitudinal Strain Distributions for Beam 6G-L2

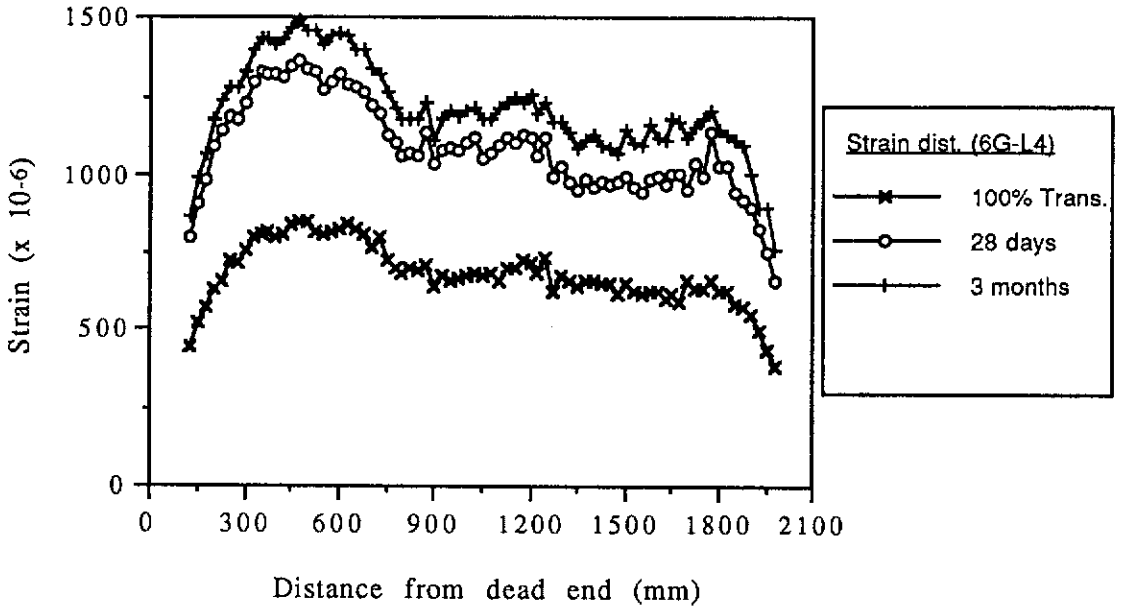

Figure A.49 Longitudinal Strain Distributions for Beam 6G-L4

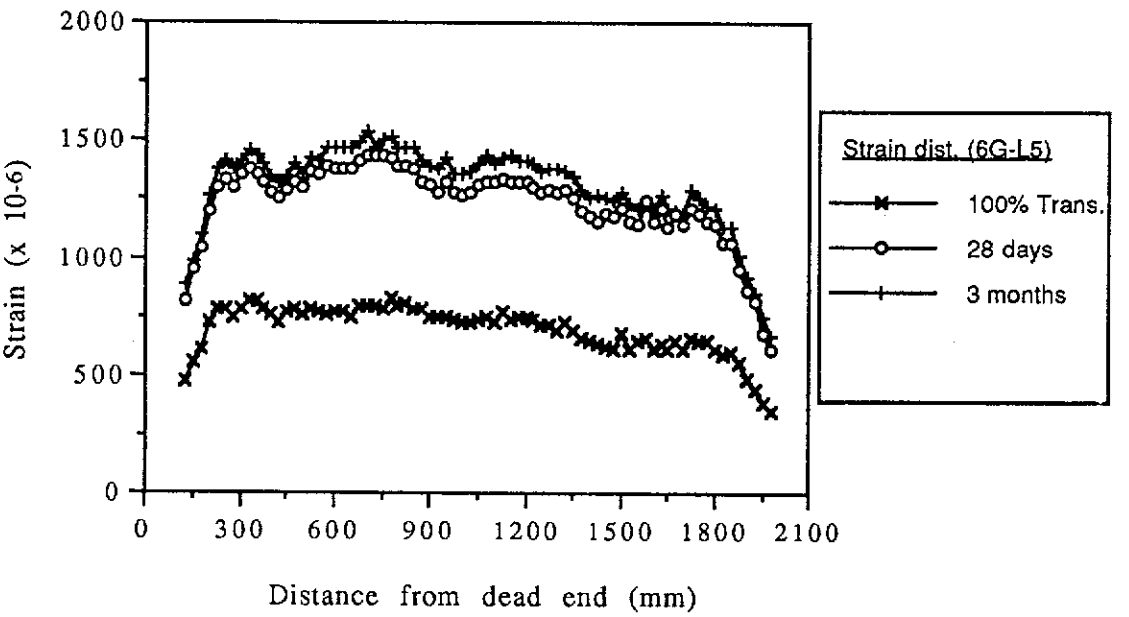

Figure A.50 Longitudinal Strain Distributions for Beam 6G-L5

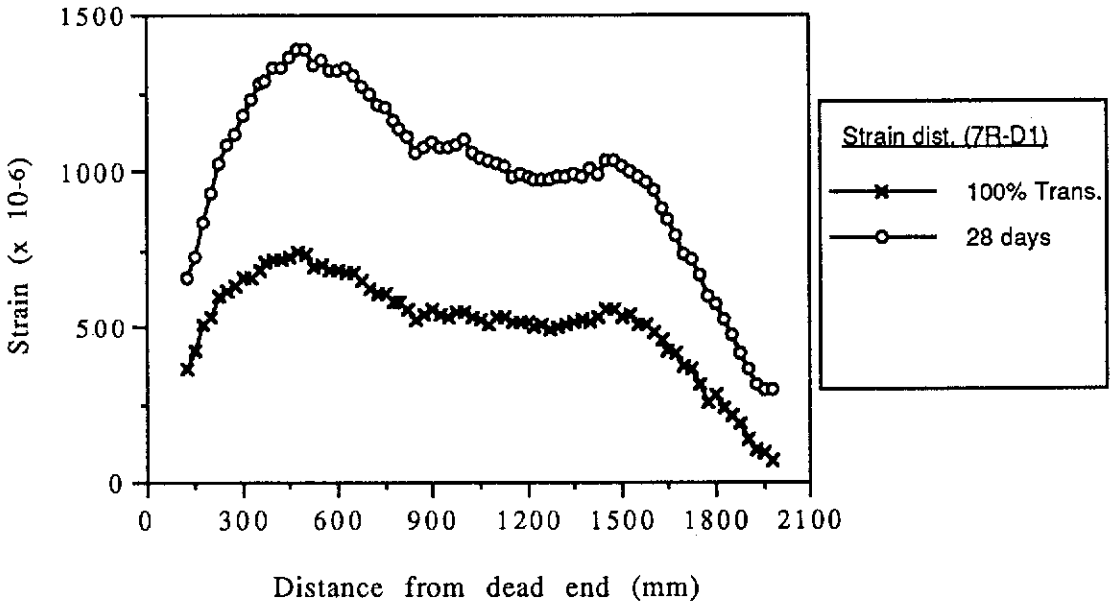

Figure A.51 Longitudinal Strain Distributions for Beam 7R-D1

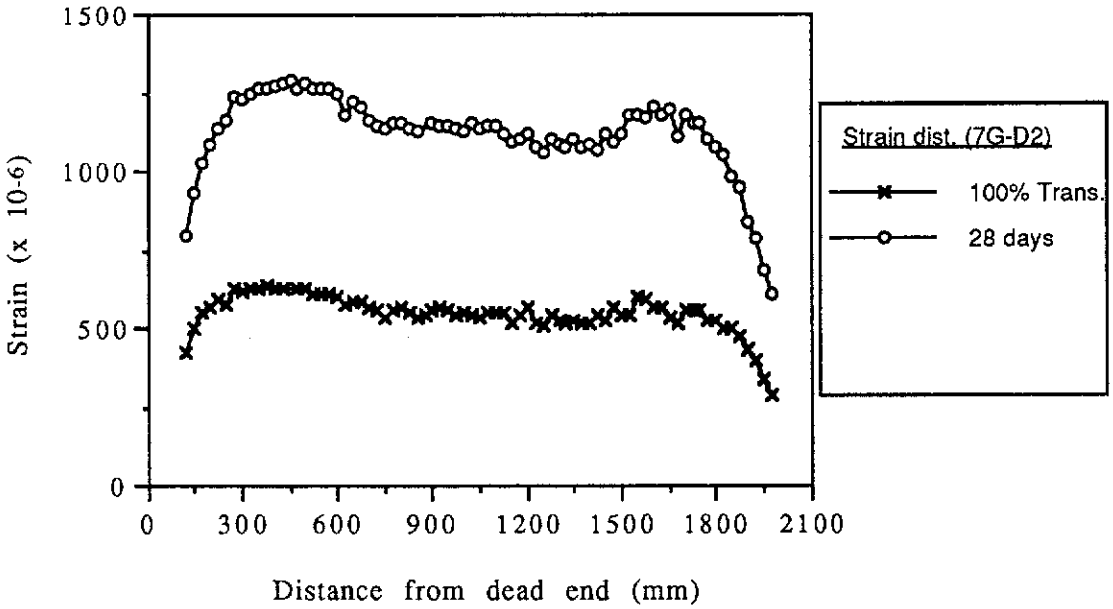

Figure A.52 Longitudinal Strain Distributions for Beam 7G-D2

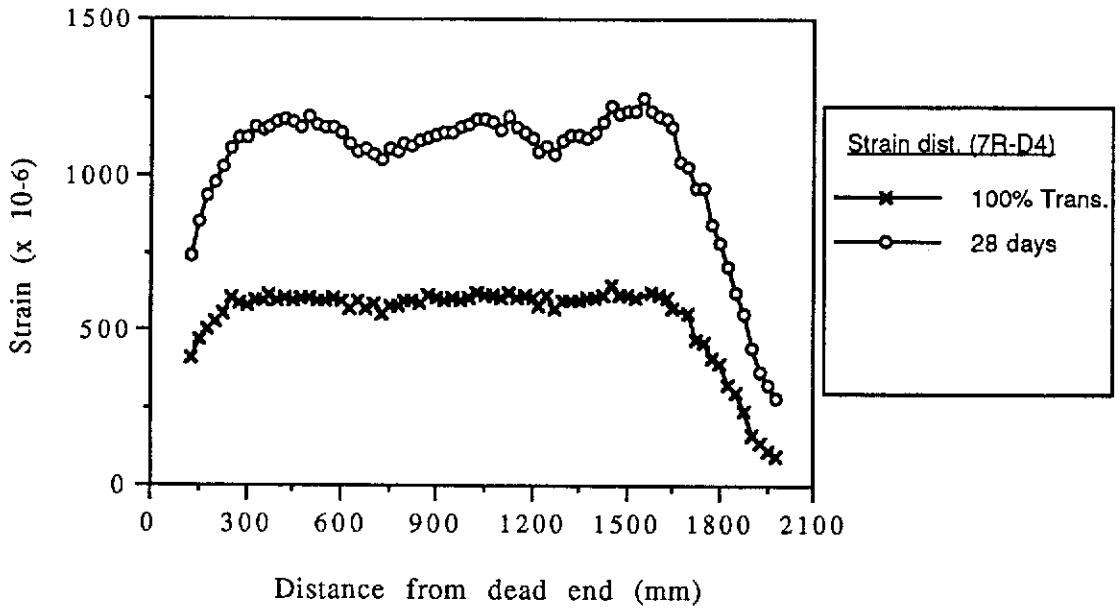

Figure A.53 Longitudinal Strain Distributions for Beam 7R-D4

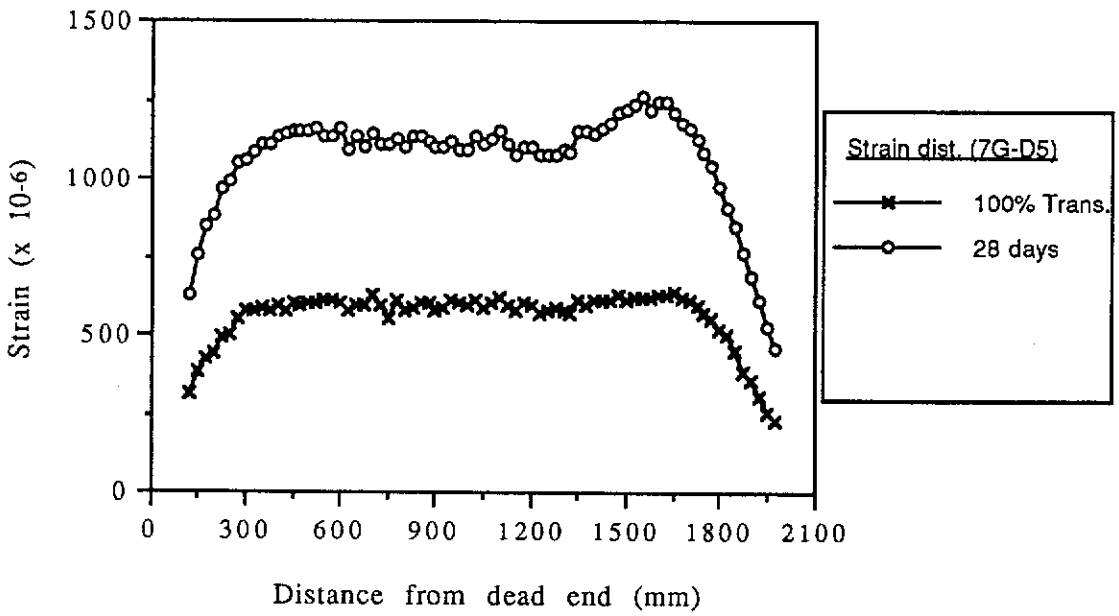

Figure A.54 Longitudinal Strain Distributions for Beam 7G-D5

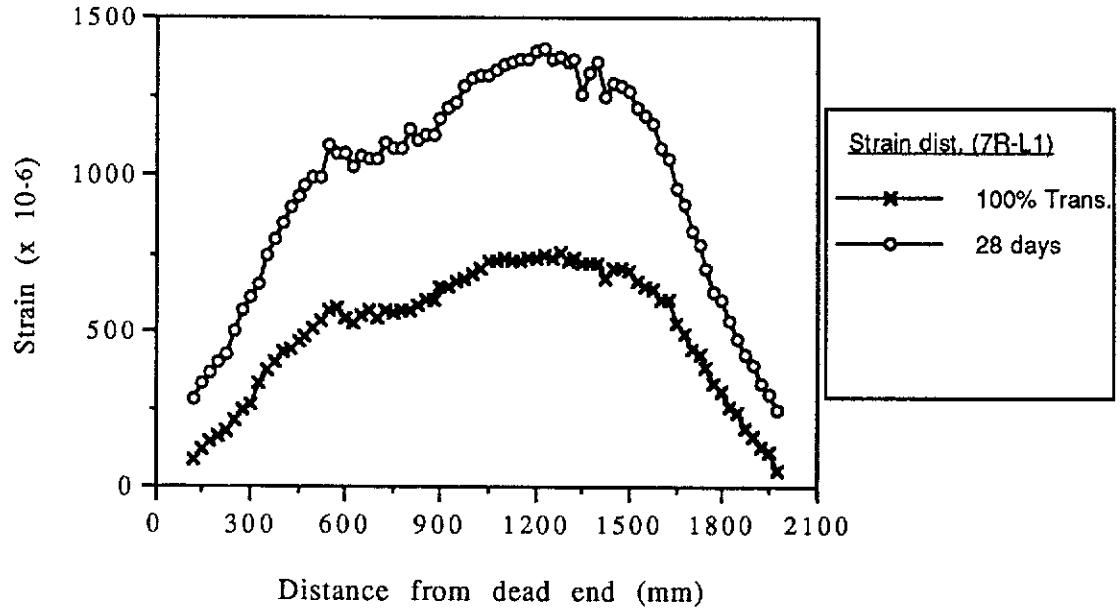

Figure A.55 Longitudinal Strain Distributions for Beam 7R-L1

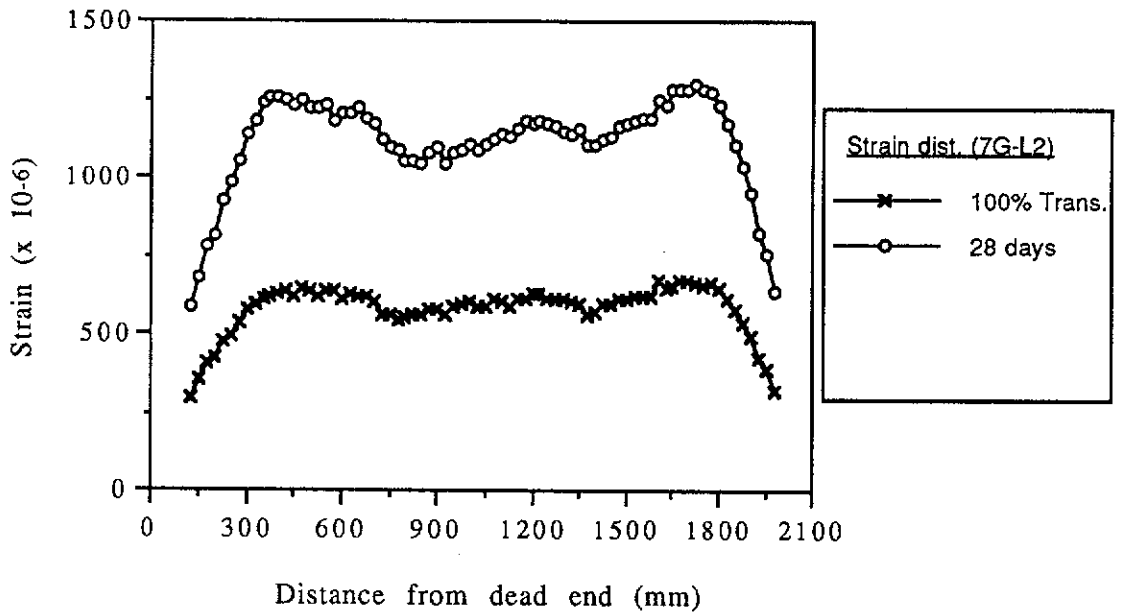

Figure A.56 Longitudinal Strain Distributions for Beam 7G-L2

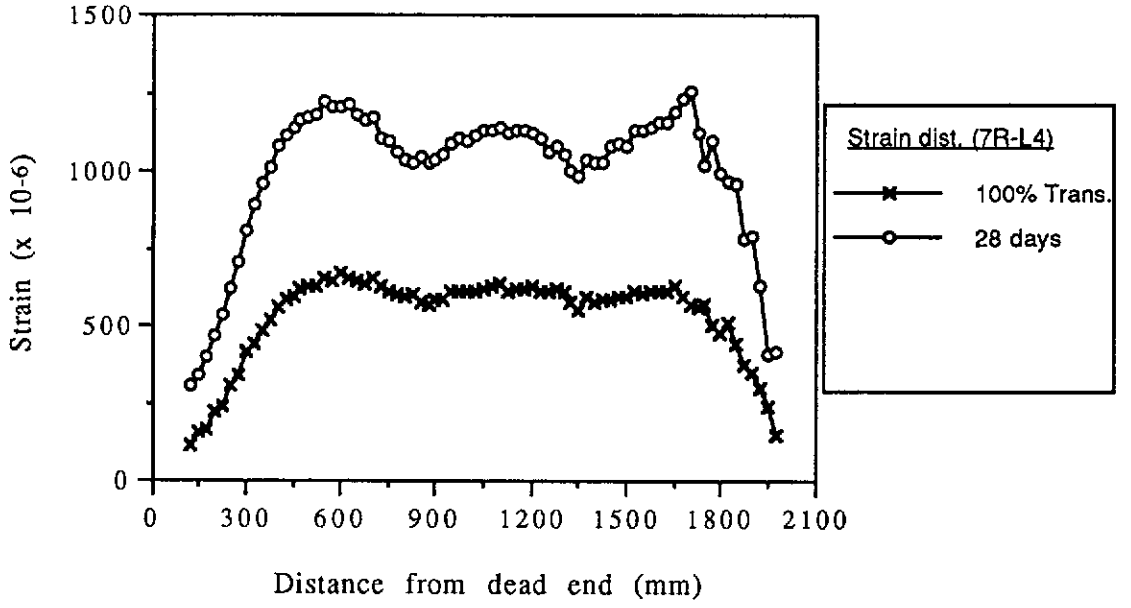

Figure A.57 Longitudinal Strain Distributions for Beam 7R-L4

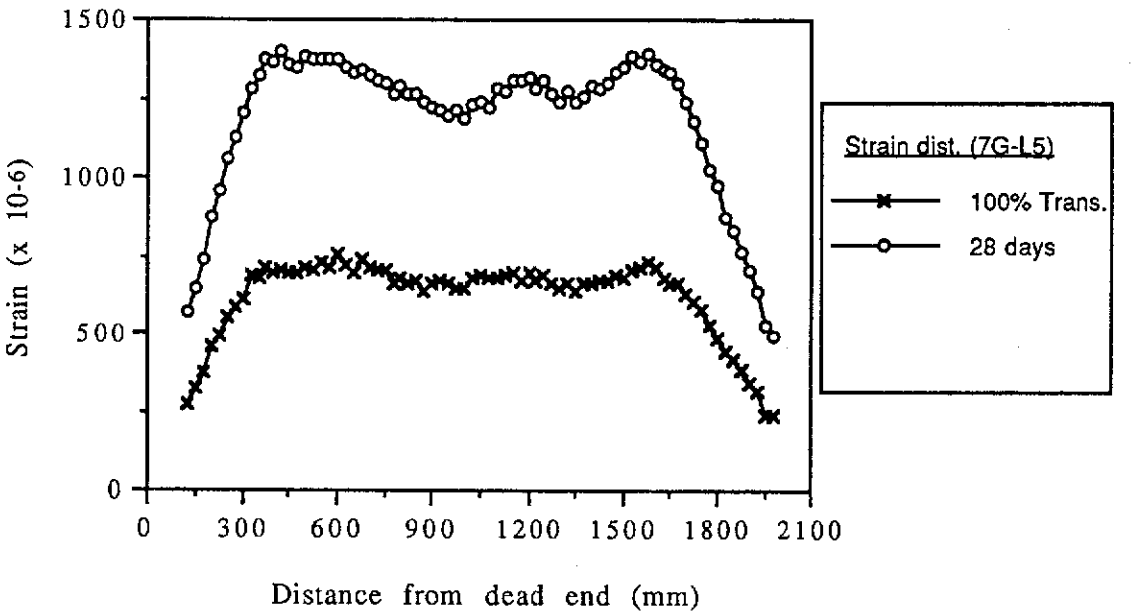

Figure A.58 Longitudinal Strain Distributions for Beam 7G-L5

Plots of Percentage Load Transfer Against Pull-in

Plots of percentage load transfer against pull-in are given for all the beams which had the prestress released gradually. The gradual releases were intended to have ten equal increments (increase in the percentage of load transferred but decrease in the jacking force). It was found that the 5 mm dia. wires released slightly more rapidly than the 7 mm dia. wires. For this reason, most beams with 7 mm dia. wires would have ten reasonably equal increments but the beams with 5 mm dia. wires were generally fully prestressed in nine increments. Plots for beams with four 5 mm dia. wires are given in two figures, one for the dead end and the other for the live end. This avoids congestion caused by having all the curves in a single graph.

Recordings were taken after each increment of load transfer. By plotting these curves, it was possible to understand the behaviour of the transfer better. These curves complement for the determination of transmission lengths from longitudinal strain distributions (refer to Chapter 4).

These curves are not available for Test 3 beam specimens and beams 7R-D1, 7R-D4, 7R-L1 and 7R-L4 since these beams were sudden and shock released. The beams 7G-D2, 7G-D5, 7G-L2 and 7G-L5 were gradually released in one increment by slowly releasing the jacks. Therefore, the pull-in plots are also not available for them.

Some of the plots indicate that the pull-ins at 100% transfer are small and fairly similar among all the wires at one or both ends of the beams. When the average pull-in at full transfer for a beam end was 0.5 mm or less, and the curves plotted were closely grouped together, the graphs were considered not significant and were omitted from this Appendix. Further details of the pull-ins can be referred to in Appendix C.

A summary of the beam ends where the average pull-ins at transfer were equal to or less than 0.5 mm is given in Table B.1:

Table B.1 Beam Ends with Average Pull-ins of 0.5 mm or Less.

Beam End	Average Δ_o (mm)
2G-D2 (dead end)	0.46
2G-D4 (dead end)	0.32
2G-L4 (dead end)	0.48
2G-L4 (live end)	0.48
4G-L4 (live end)	0.50
6G-D2 (dead end)	0.45
6G-D2 (live end)	0.40
6G-D4 (dead end)	0.31
6G-D4 (live end)	0.31
6G-D5 (dead and live ends)	0.49
6G-L2 (dead end)	0.34
6G-L2 (live end)	0.40
6G-L4 (dead end)	0.33
6G-L4 (live end)	0.33

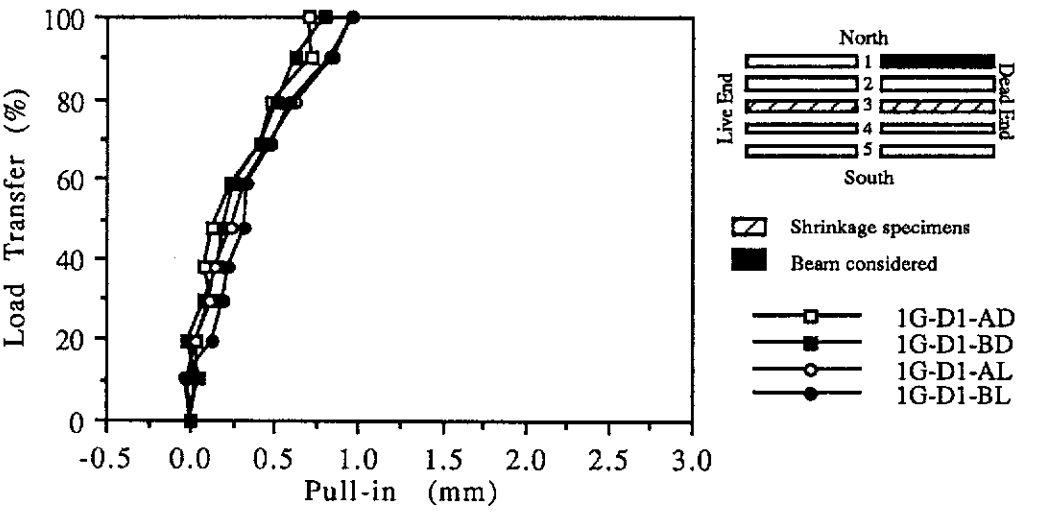

Figure B.1 Percentage Load Transfer vs. Pull-in for Beam 1G-D1 (At 7-day Transfer)

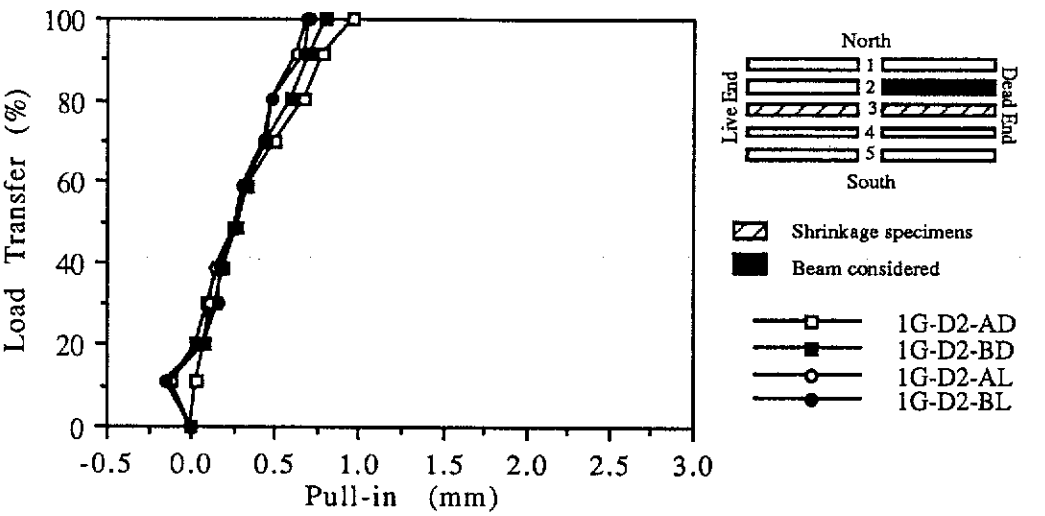

Figure B.2 Percentage Load Transfer vs. Pull-in for Beam 1G-D2 (At 7-day Transfer)

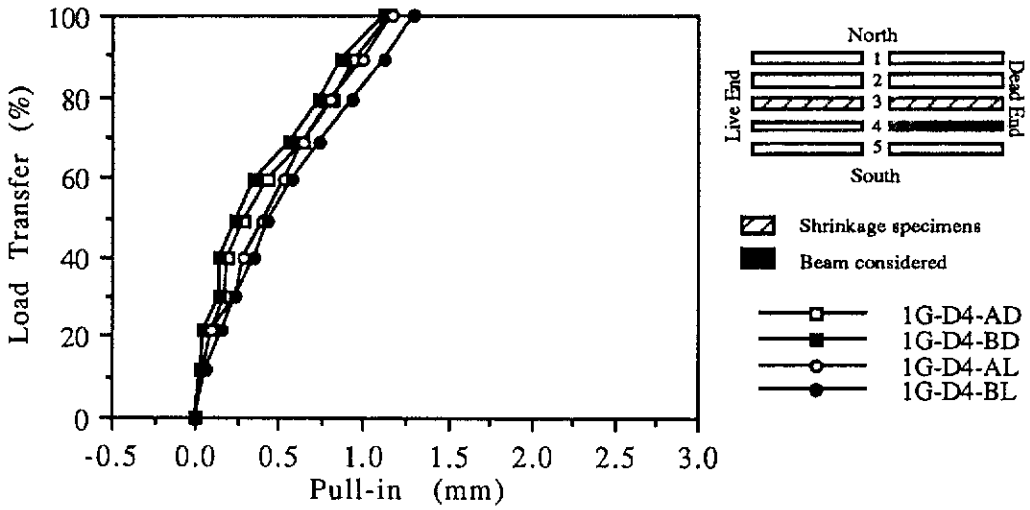

Figure B.3 Percentage Load Transfer vs. Pull-in for Beam 1G-D4 (At 7-day Transfer)

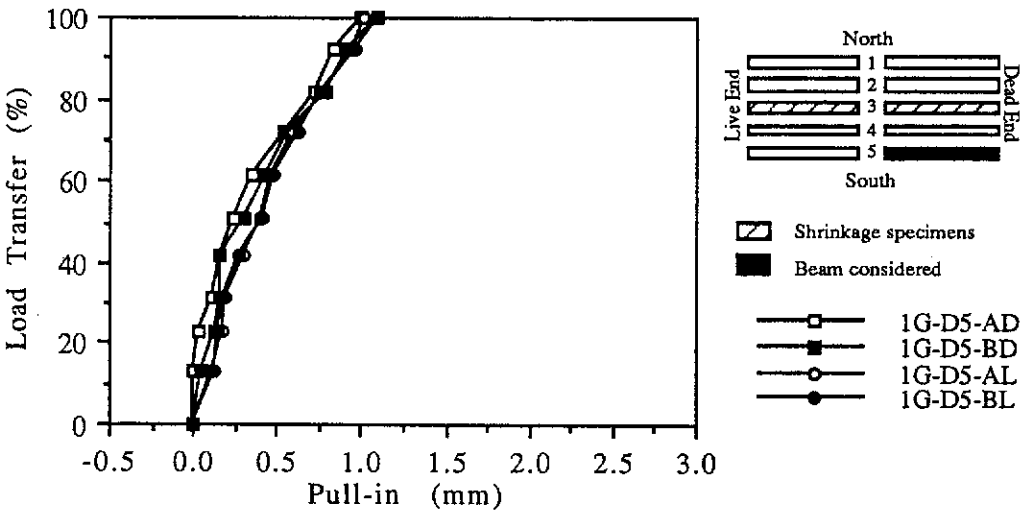

Figure B.4 Percentage Load Transfer vs. Pull-in for Beam 1G-D5 (At 7-day Transfer)

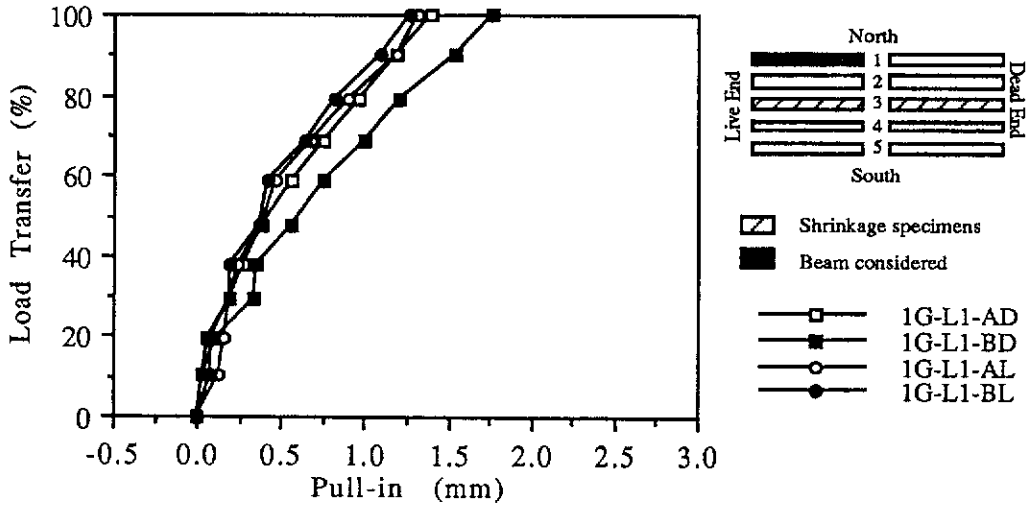

Figure B.5 Percentage Load Transfer vs. Pull-in for Beam 1G-L1 (At 7-day Transfer)

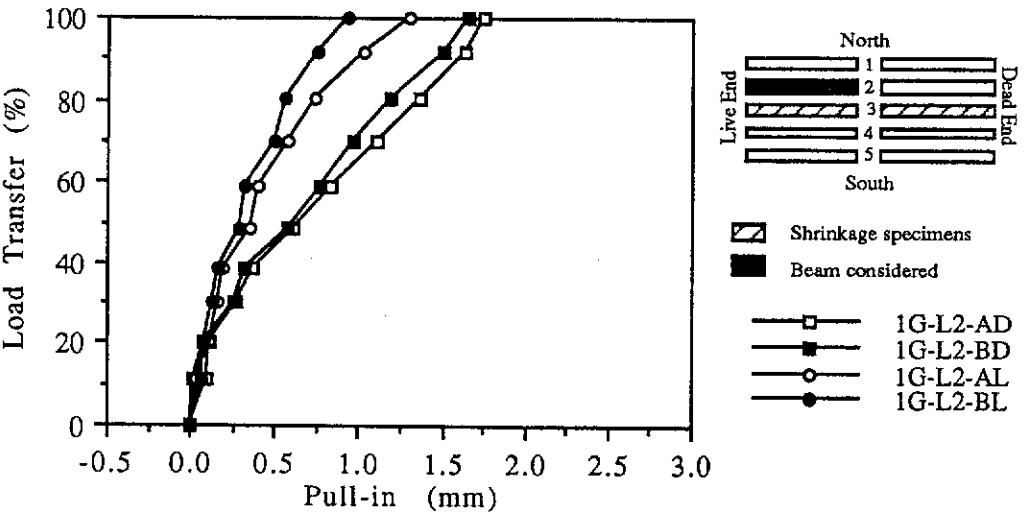

Figure B.6 Percentage Load Transfer vs. Pull-in for Beam 1G-L2 (At 7-day Transfer)

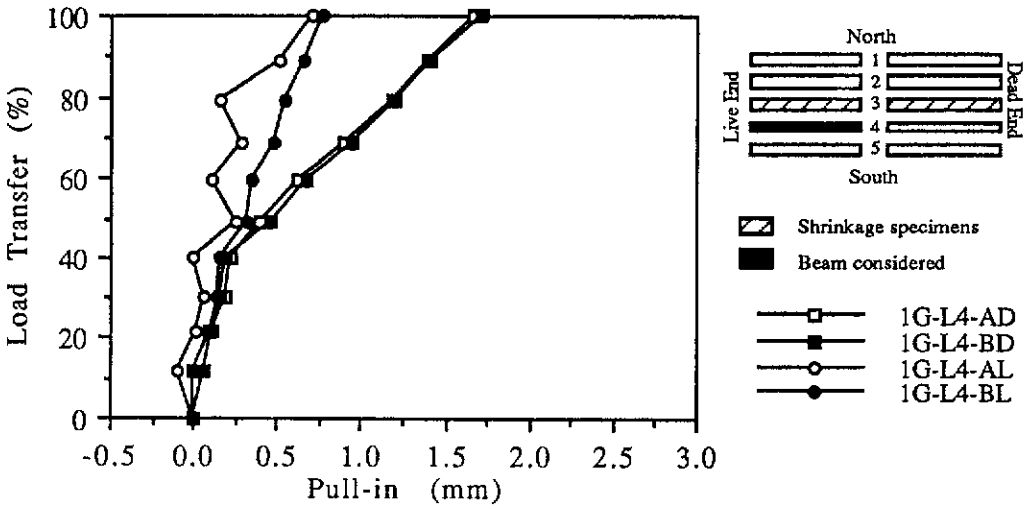

Figure B.7 Percentage Load Transfer vs. Pull-in for Beam 1G-L4 (At 7-day Transfer)

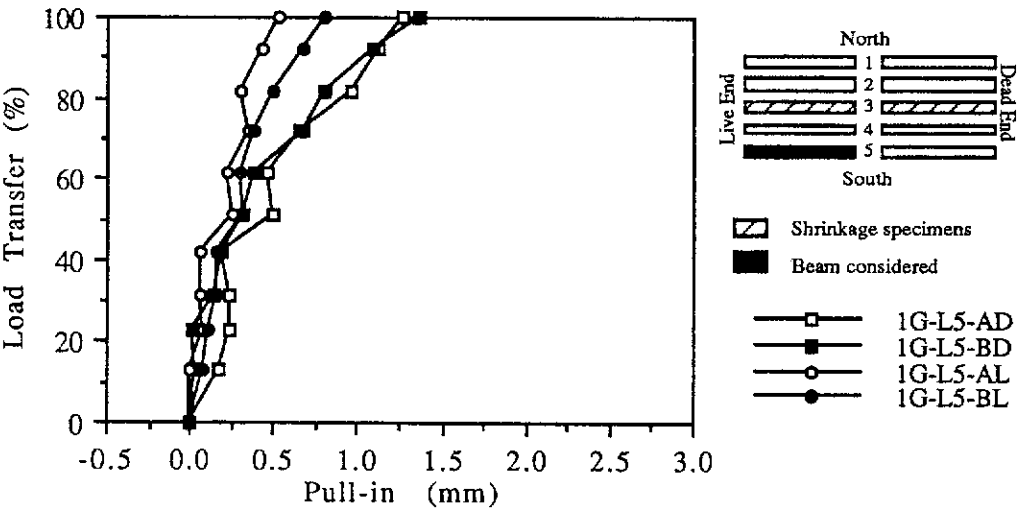

Figure B.8 Percentage Load Transfer vs. Pull-in for Beam 1G-L5 (At 7-day Transfer)

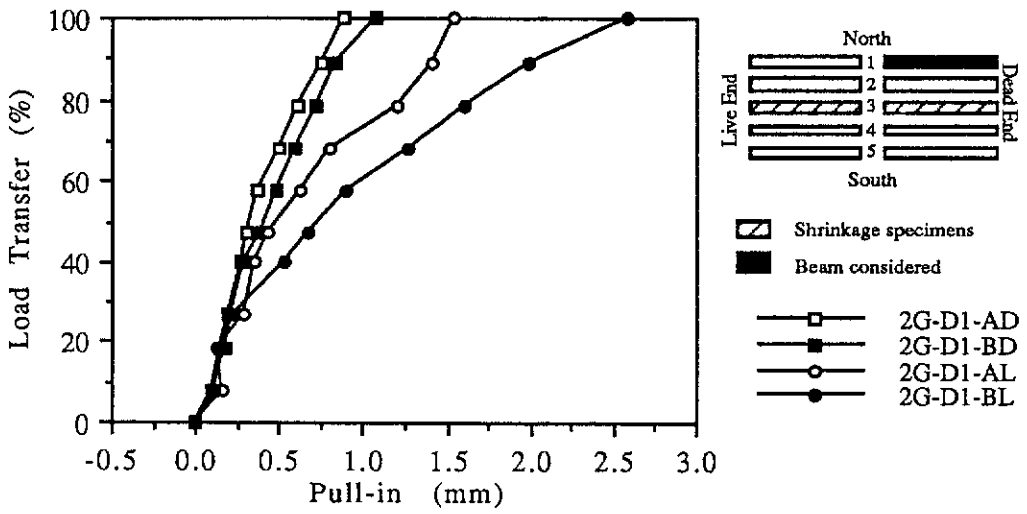

Figure B.9 Percentage Load Transfer vs. Pull-in for Beam 2G-D1 (At 7-day Transfer)

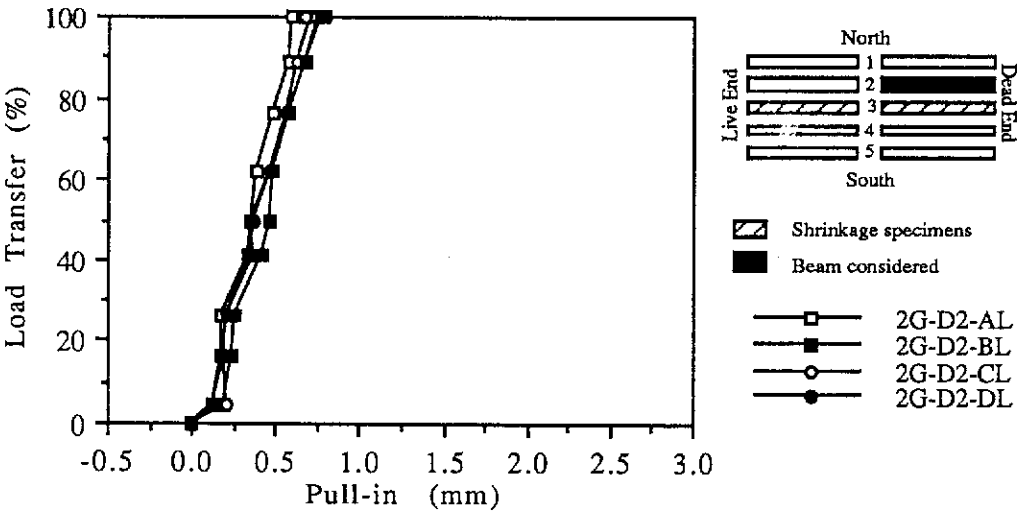

Figure B.10 Percentage Load Transfer vs. Pull-in for Beam 2G-D2 At the Live End (At 7-day Transfer)

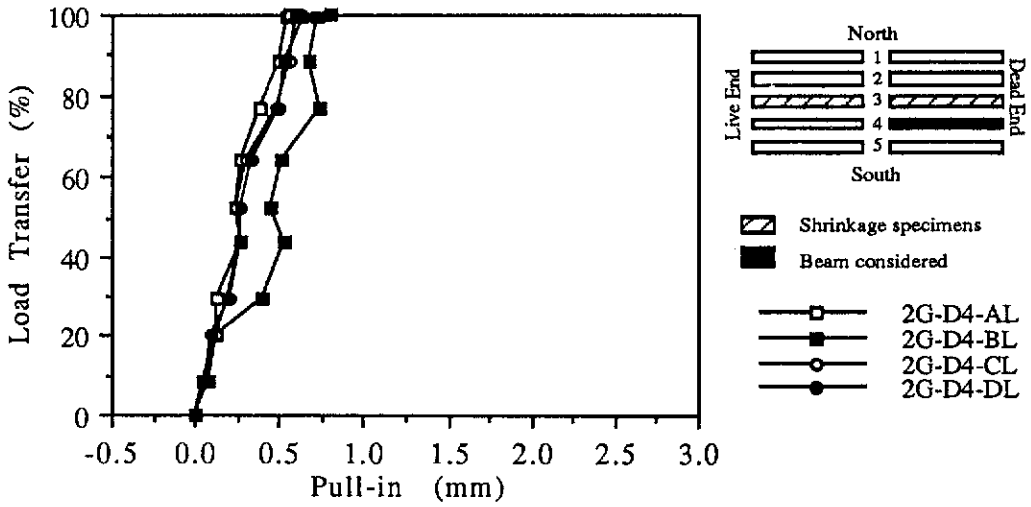

Figure B.11 Percentage Load Transfer vs. Pull-in for Beam 2G-D4 At the Live End (At 7-day Transfer)

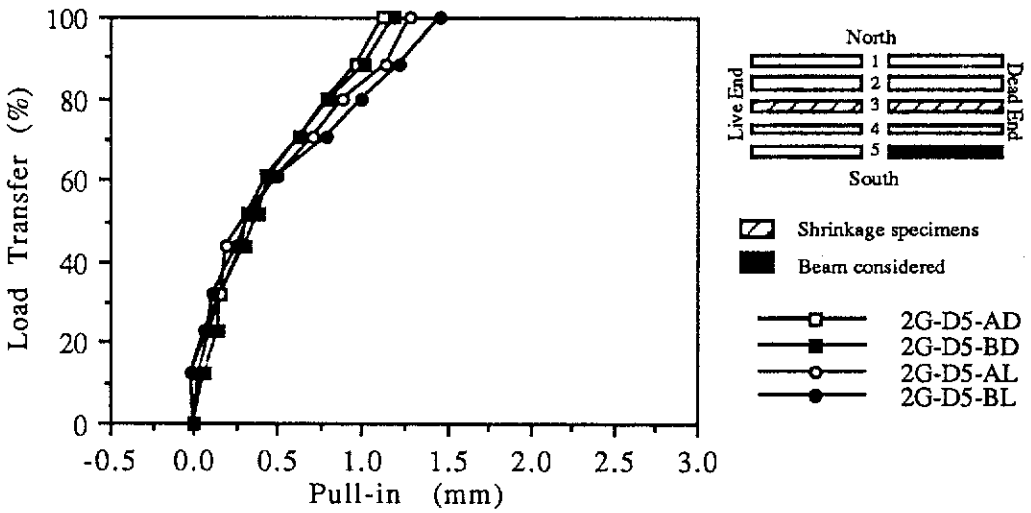

Figure B.12 Percentage Load Transfer vs. Pull-in for Beam 2G-D5 (At 7-day Transfer)

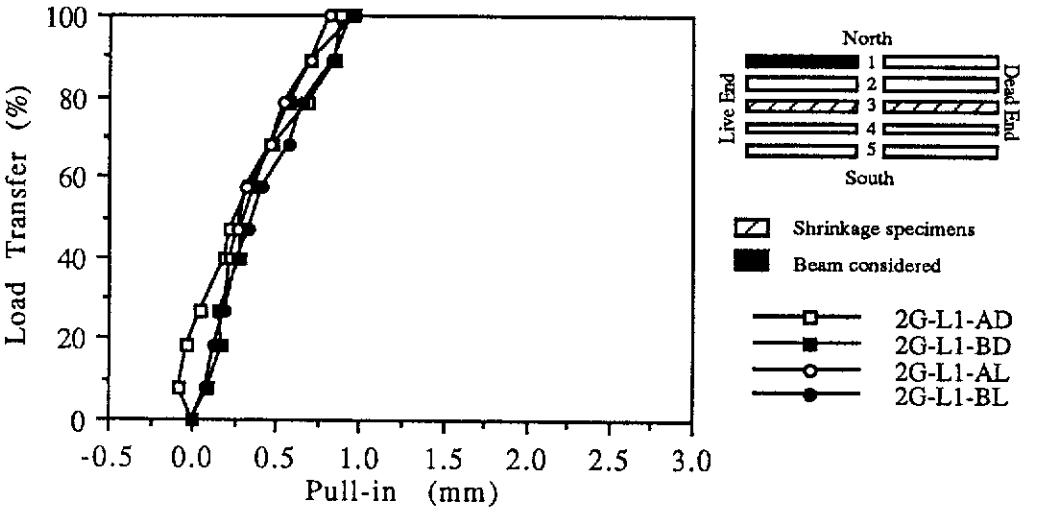

Figure B.13 Percentage Load Transfer vs. Pull-in for Beam 2G-L1 (At 7-day Transfer)

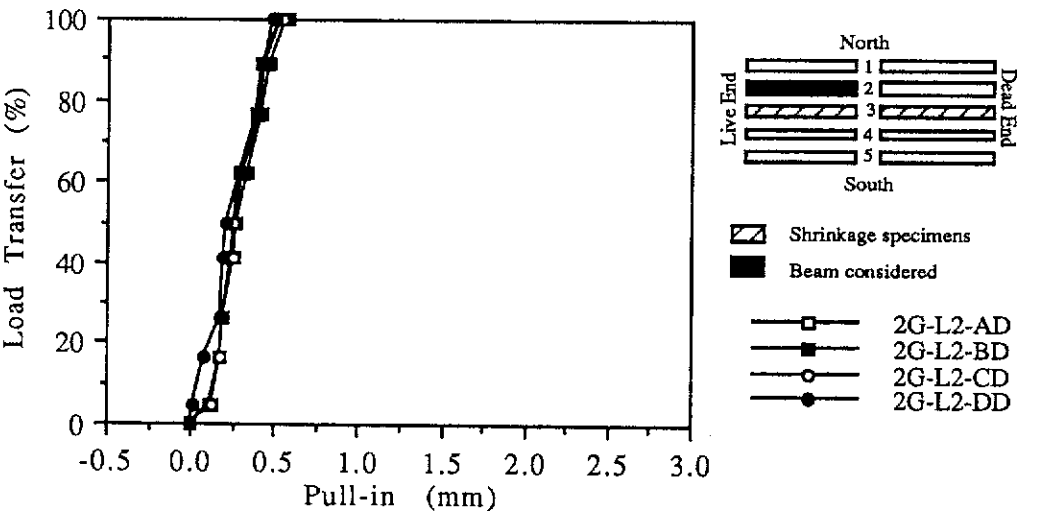

Figure B.14 Percentage Load Transfer vs. Pull-in for Beam 2G-L2 At the Dead End (At 7-day Transfer)

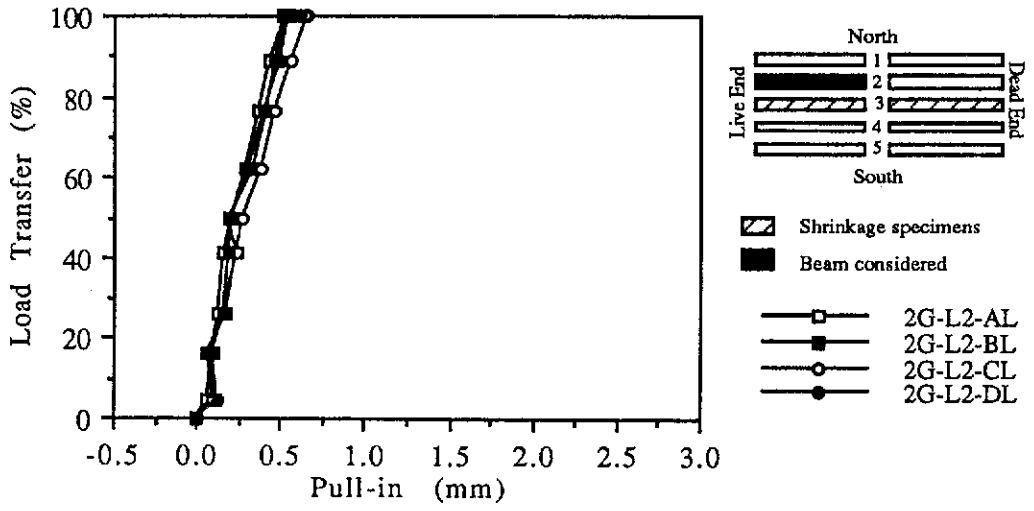

Figure B.15 Percentage Load Transfer vs. Pull-in for Beam 2G-L2 At the Live End (At 7-day Transfer)

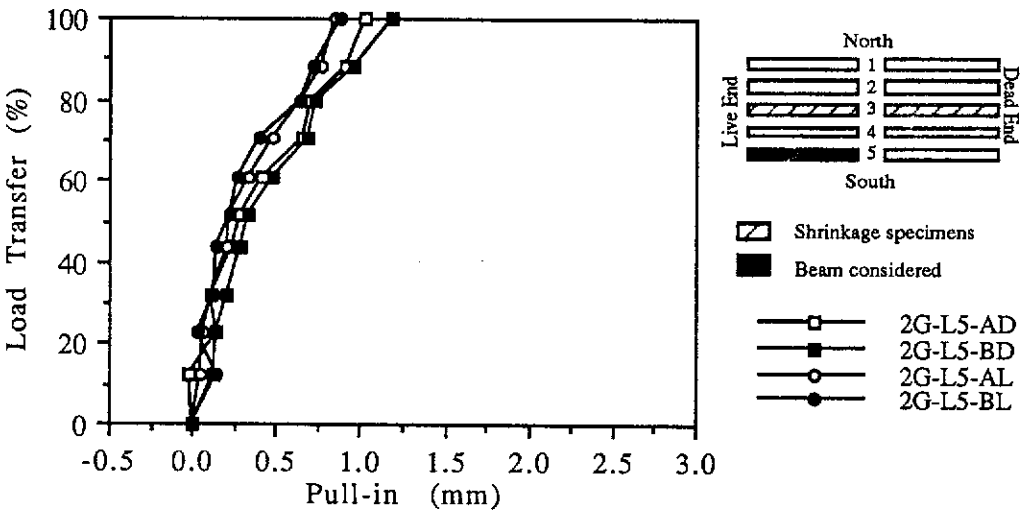

Figure B.16 Percentage Load Transfer vs. Pull-in for Beam 2G-L5 (At 7-day Transfer)

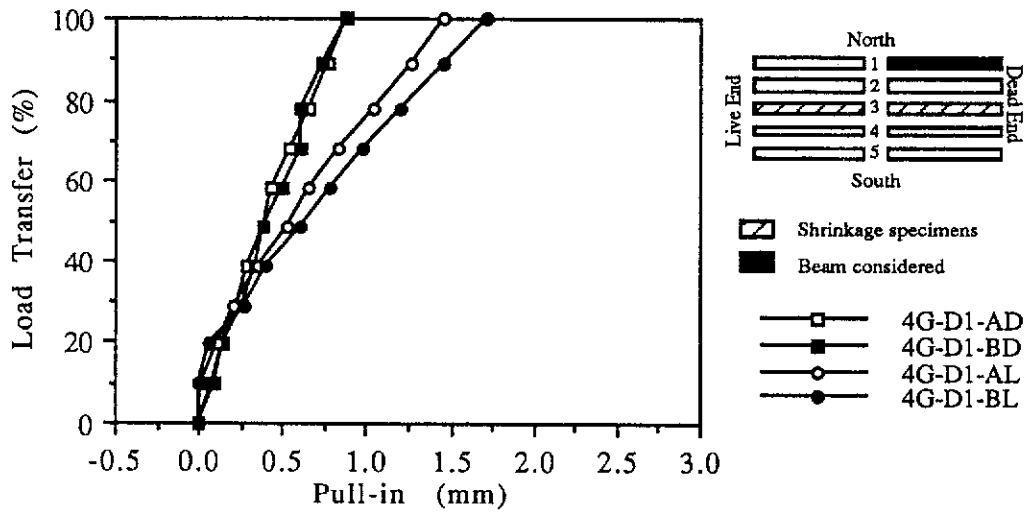

Figure B.17 Percentage Load Transfer vs. Pull-in for Beam 4G-D1 (At 7-day Transfer)

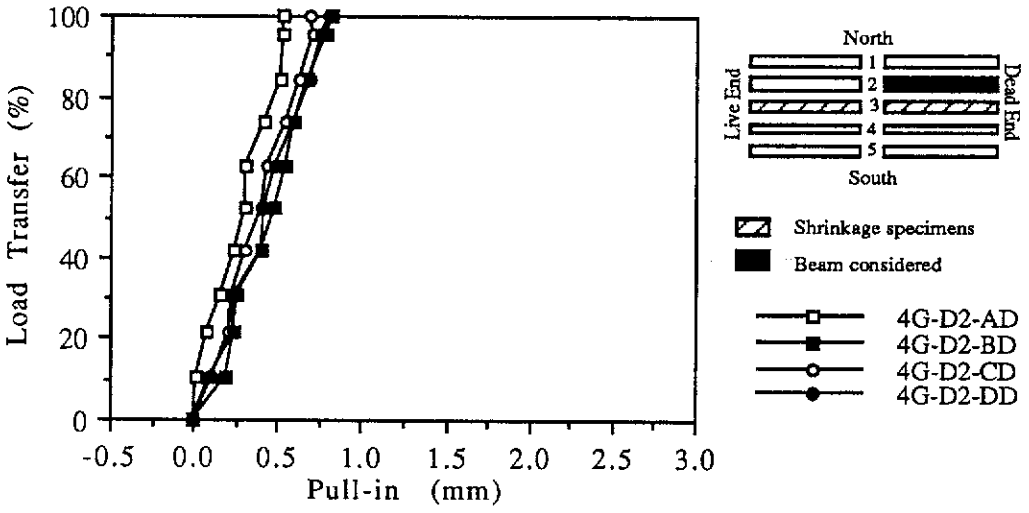

Figure B.18 Percentage Load Transfer vs. Pull-in for Beam 4G-D2 At the Dead End (At 7-day Transfer)

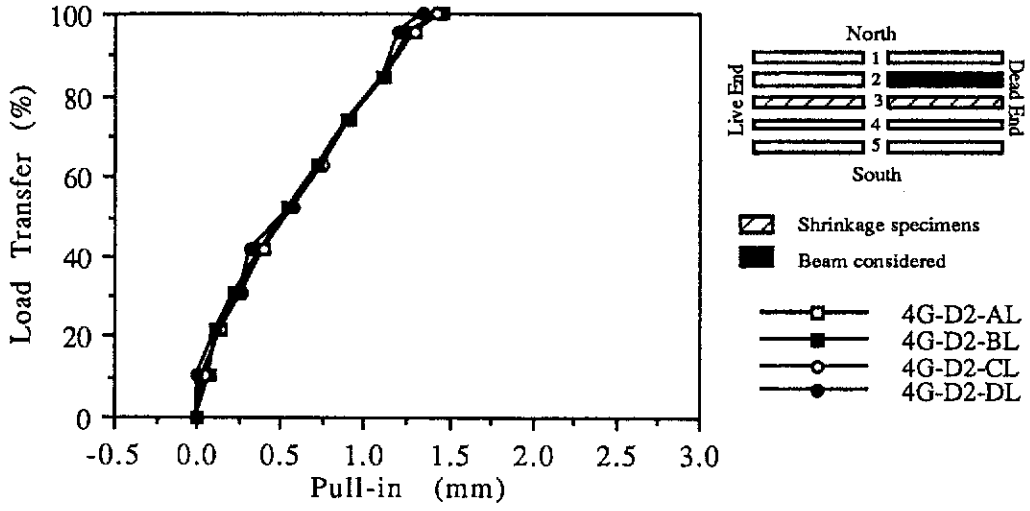

Figure B.19 Percentage Load Transfer vs. Pull-in for Beam 4G-D2 At the Live End (At 7-day Transfer)

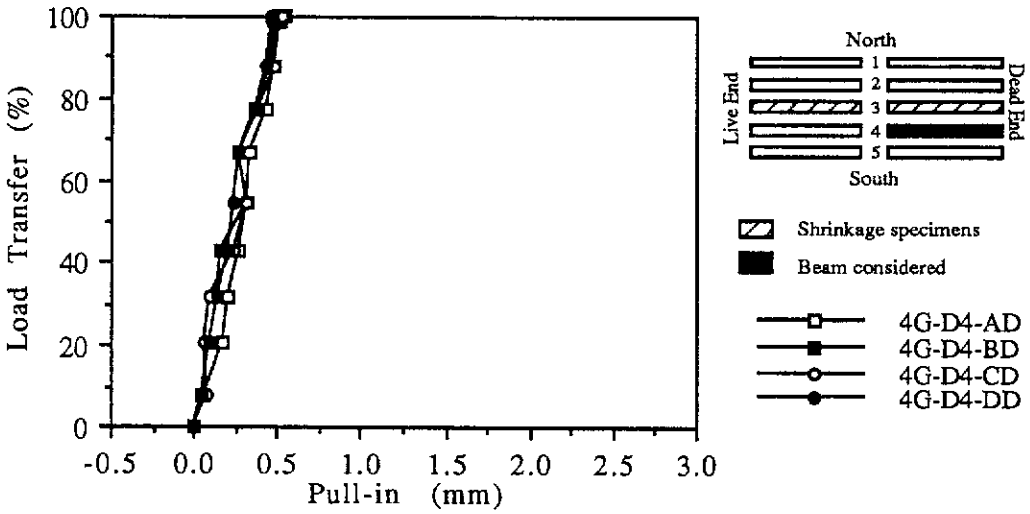

Figure B.20 Percentage Load Transfer vs. Pull-in for Beam 4G-D4 At the Dead End (At 7-day Transfer)

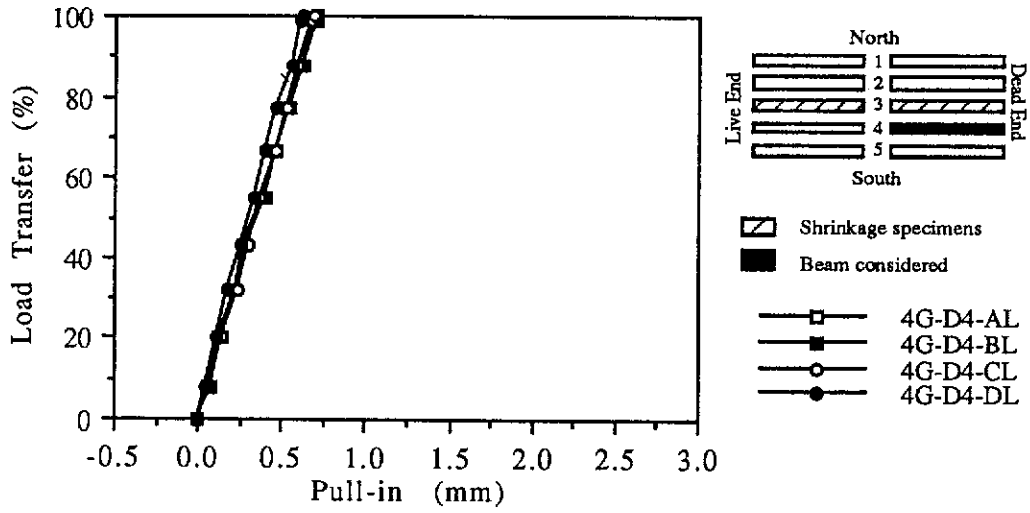

Figure B.21 Percentage Load Transfer vs. Pull-in for Beam 4G-D4 At the Live End (At 7-day Transfer)

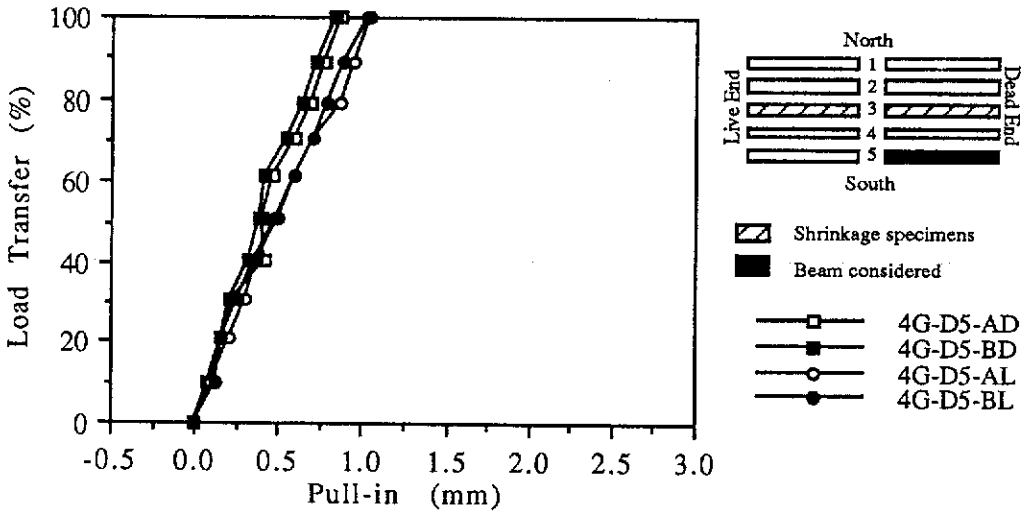

Figure B.22 Percentage Load Transfer vs. Pull-in for Beam 4G-D5 (At 7-day Transfer)

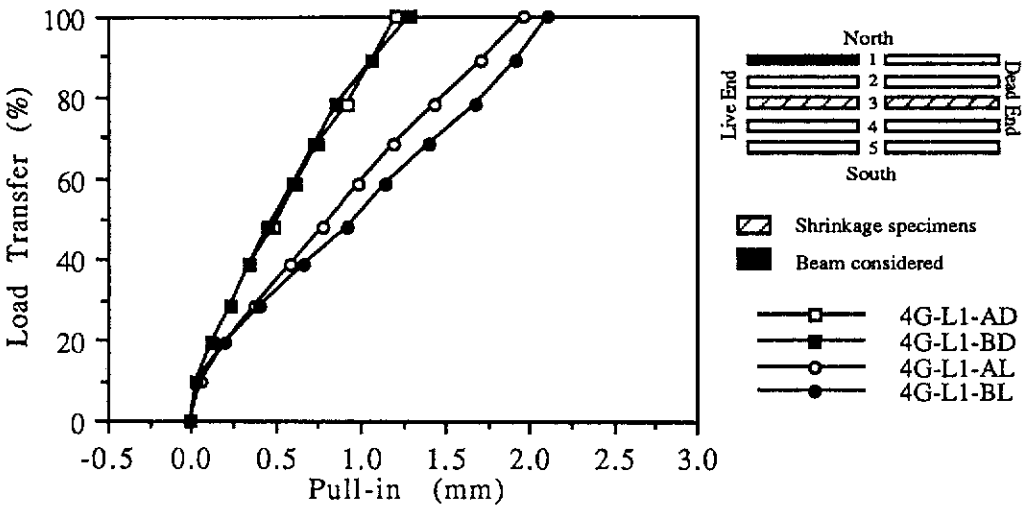

Figure B.23 Percentage Load Transfer vs. Pull-in for Beam 4G-L1 (At 7-day Transfer)

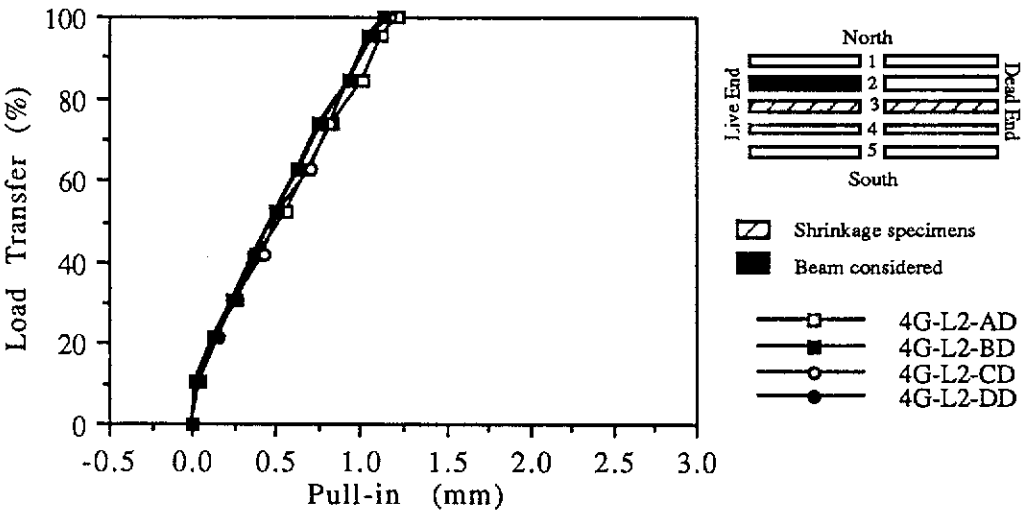

Figure B.24 Percentage Load Transfer vs. Pull-in for Beam 4G-L2 At the Dead End (At 7-day Transfer)

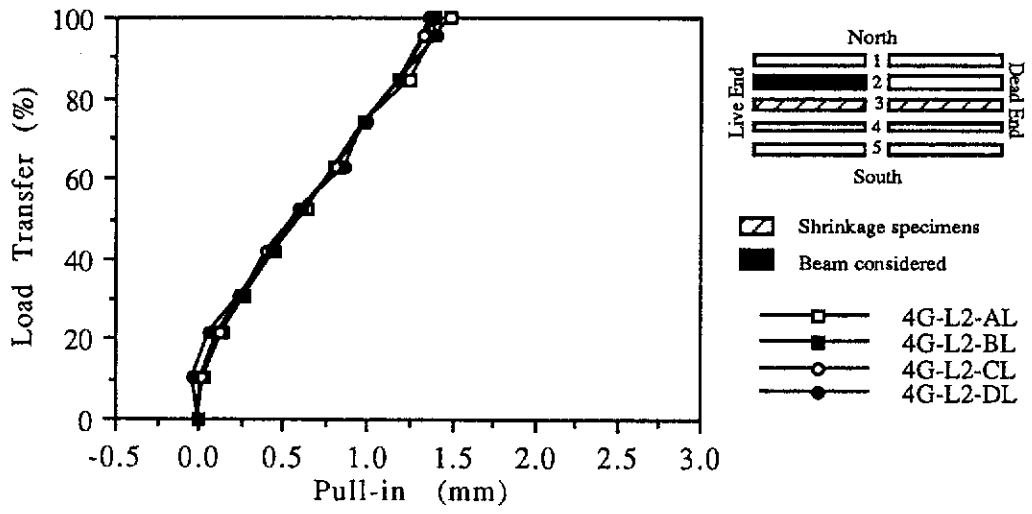

Figure B.25 Percentage Load Transfer vs. Pull-in for Beam 4G-L2 At the Live End (At 7-day Transfer)

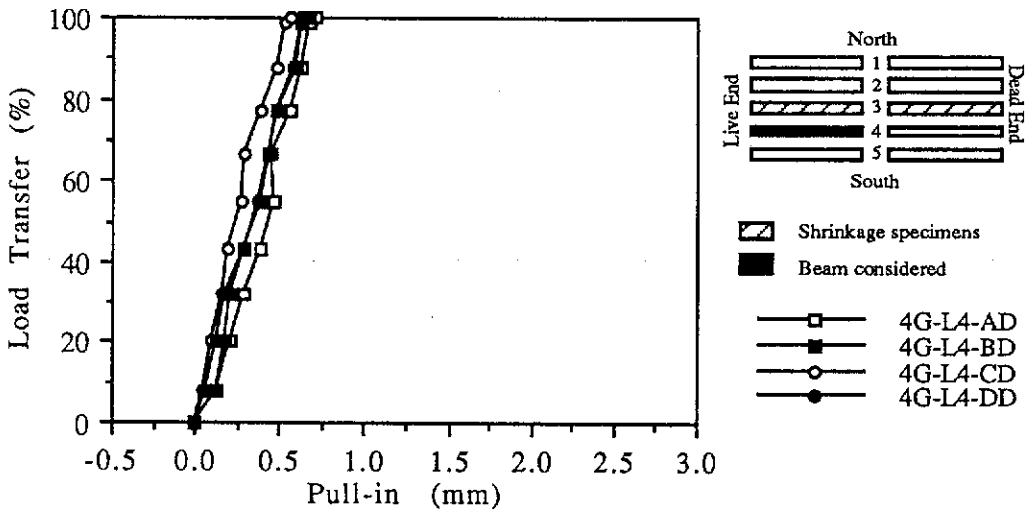

Figure B.26 Percentage Load Transfer vs. Pull-in for Beam 4G-L4 At the Dead End (At 7-day Transfer)

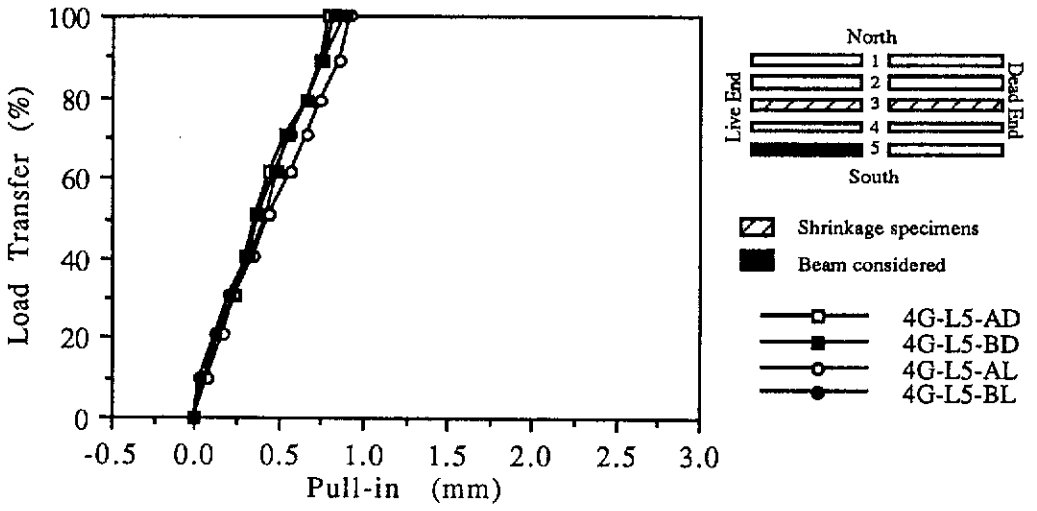

Figure B.27 Percentage Load Transfer vs. Pull-in for Beam 4G-L5 (At 7-day Transfer)

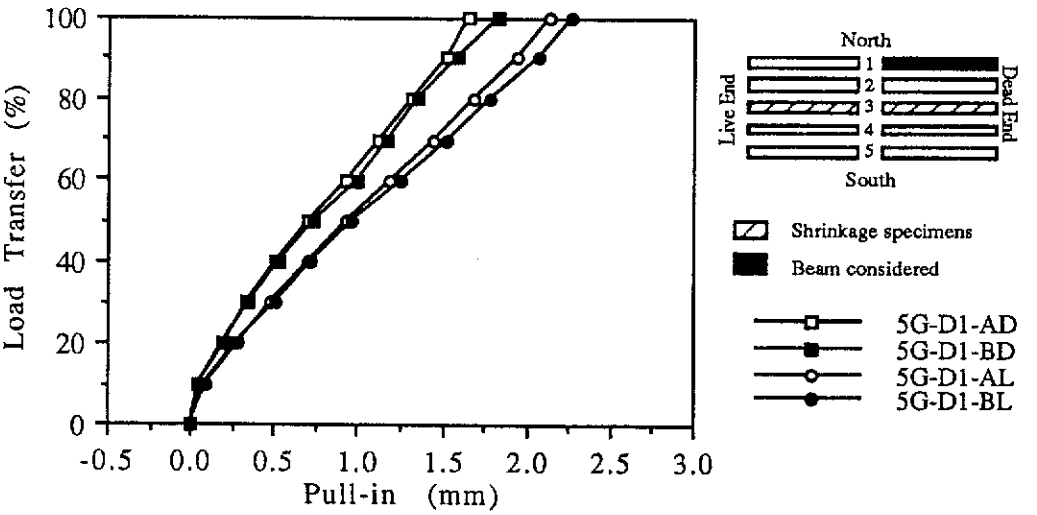

Figure B.28 Percentage Load Transfer vs. Pull-in for Beam 5G-D1 (At 2-day Transfer)

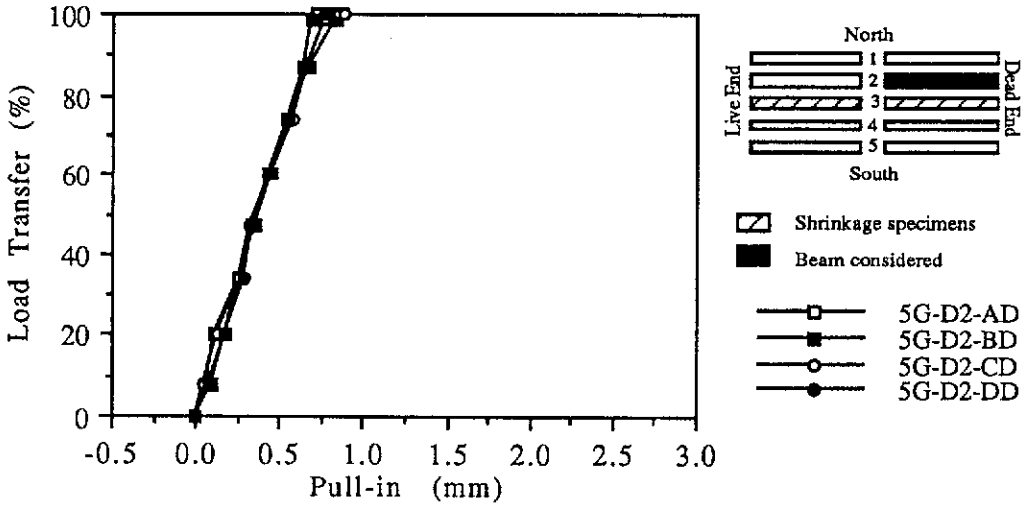

Figure B.29 Percentage Load Transfer vs. Pull-in for Beam 5G-D2 At the Dead End (At 2-day Transfer)

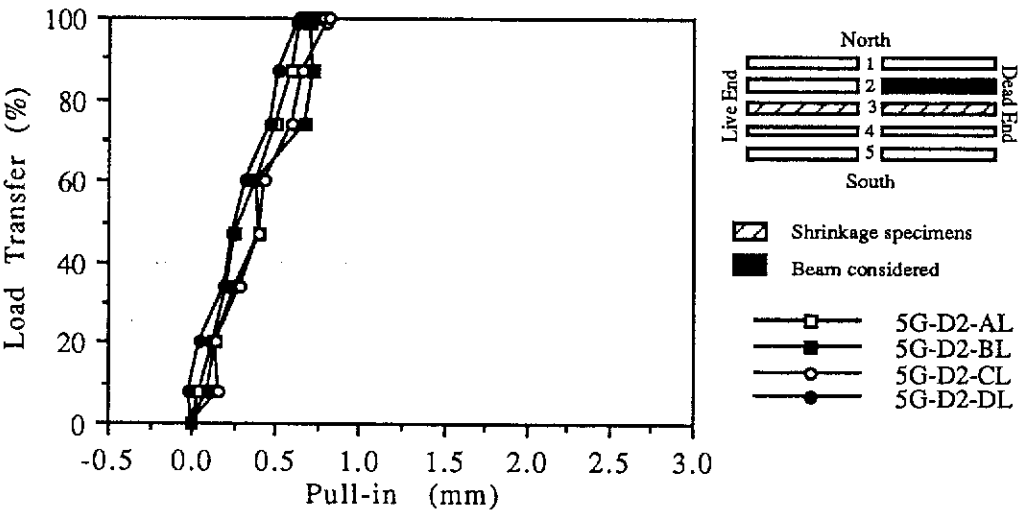

Figure B.30 Percentage Load Transfer vs. Pull-in for Beam 5G-D2 At the Live End (At 2-day Transfer)

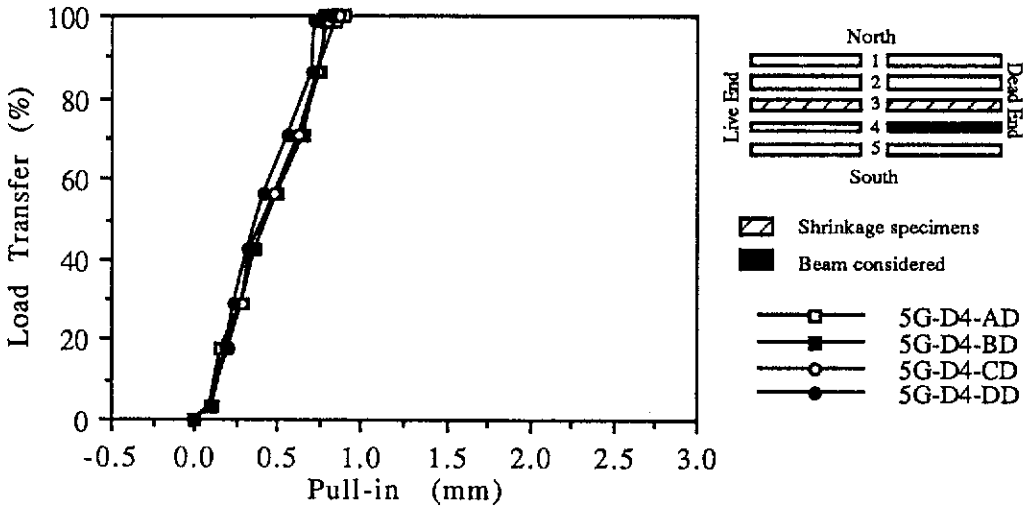

Figure B.31 Percentage Load Transfer vs. Pull-in for Beam 5G-D4 At the Dead End (At 7-day Transfer)

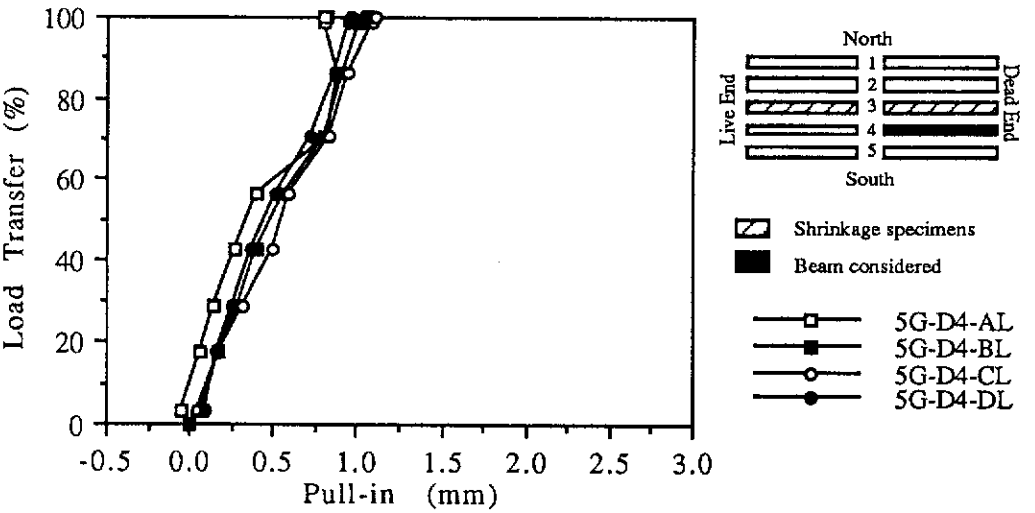

Figure B.32 Percentage Load Transfer vs. Pull-in for Beam 5G-D4 At the Live End (At 7-day Transfer)

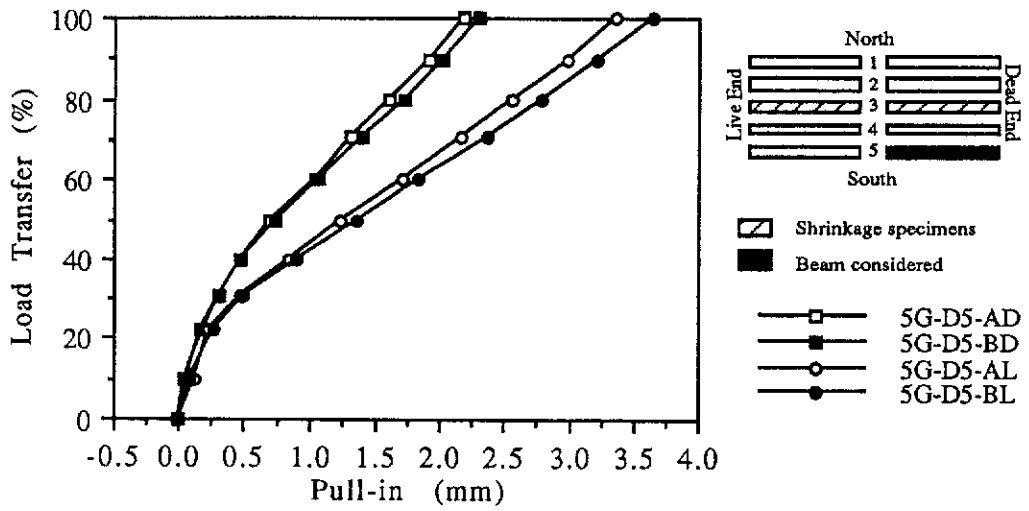

Figure B.33 Percentage Load Transfer vs. Pull-in for Beam 5G-D5 (At 7-day Transfer)

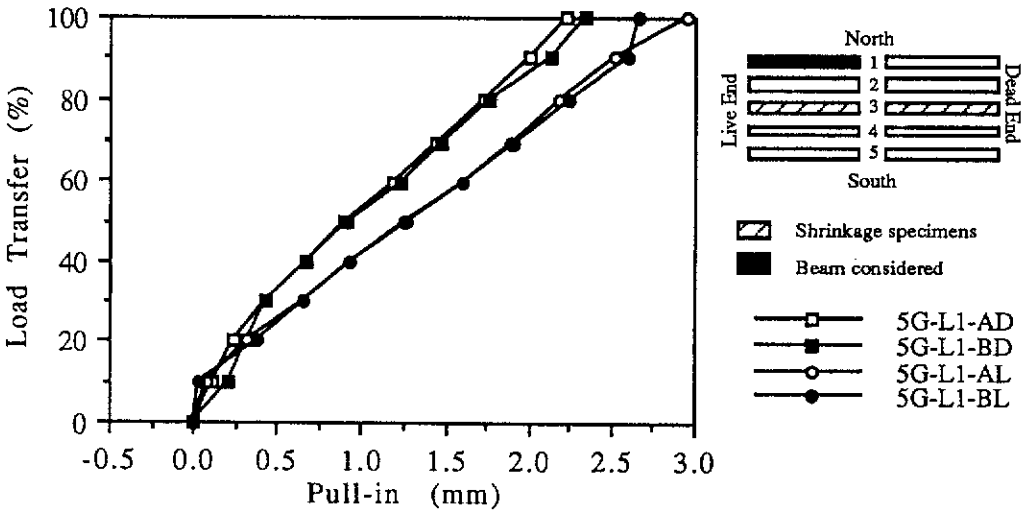

Figure B.34 Percentage Load Transfer vs. Pull-in for Beam 5G-L1 (At 2-day Transfer)

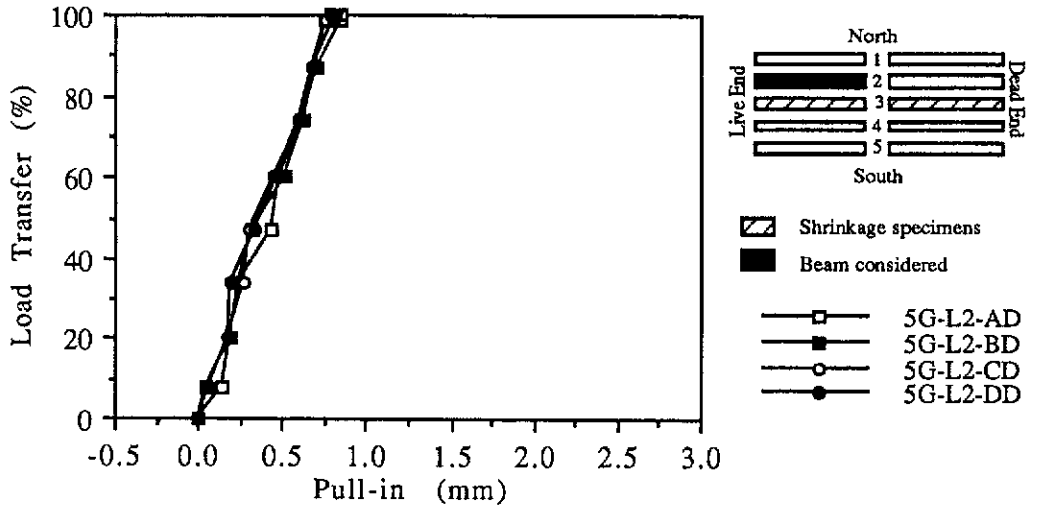

Figure B.35 Percentage Load Transfer vs. Pull-in for Beam 5G-L2 At the Dead End (At 2-day Transfer)

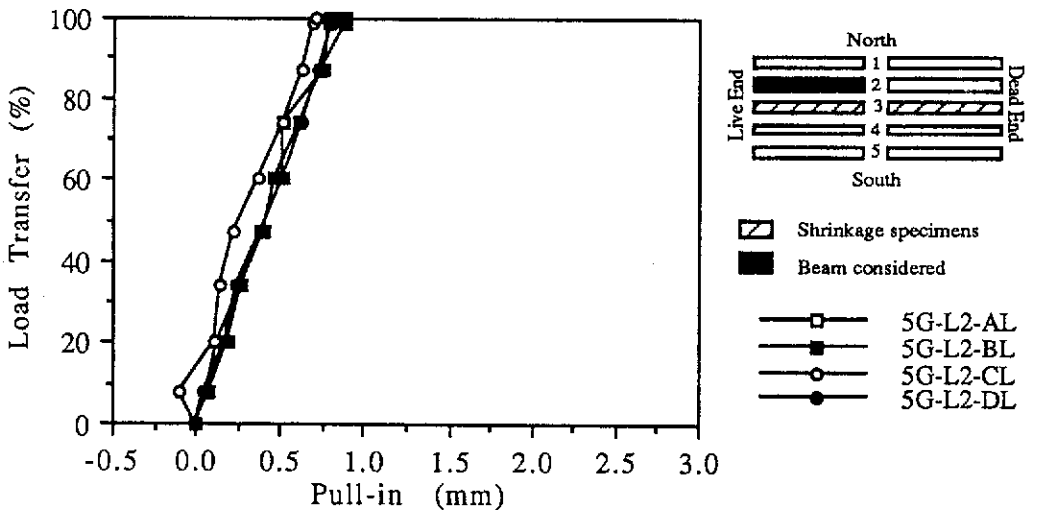

Figure B.36 Percentage Load Transfer vs. Pull-in for Beam 5G-L2 At the Live End (At 2-day Transfer)

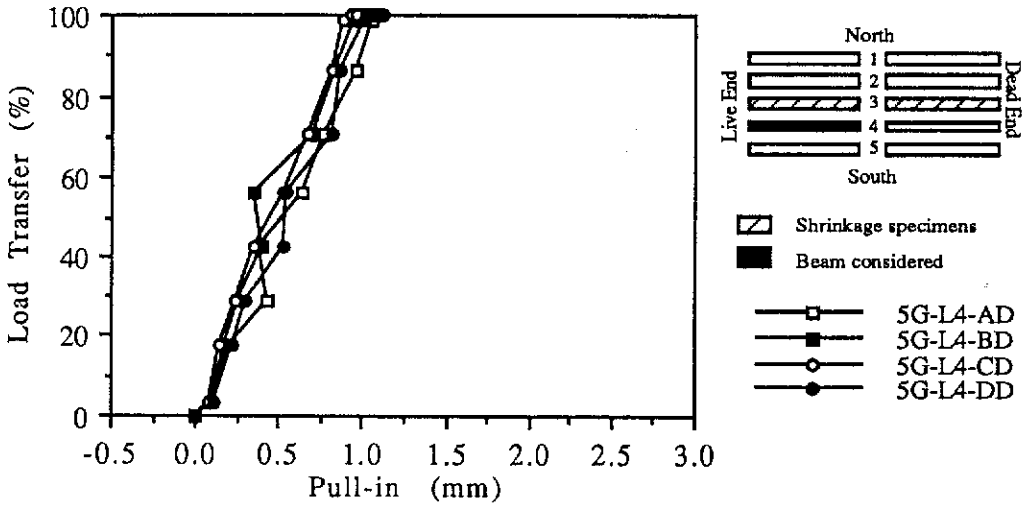

Figure B.37 Percentage Load Transfer vs. Pull-in for Beam 5G-L4 At the Dead End (At 7-day Transfer)

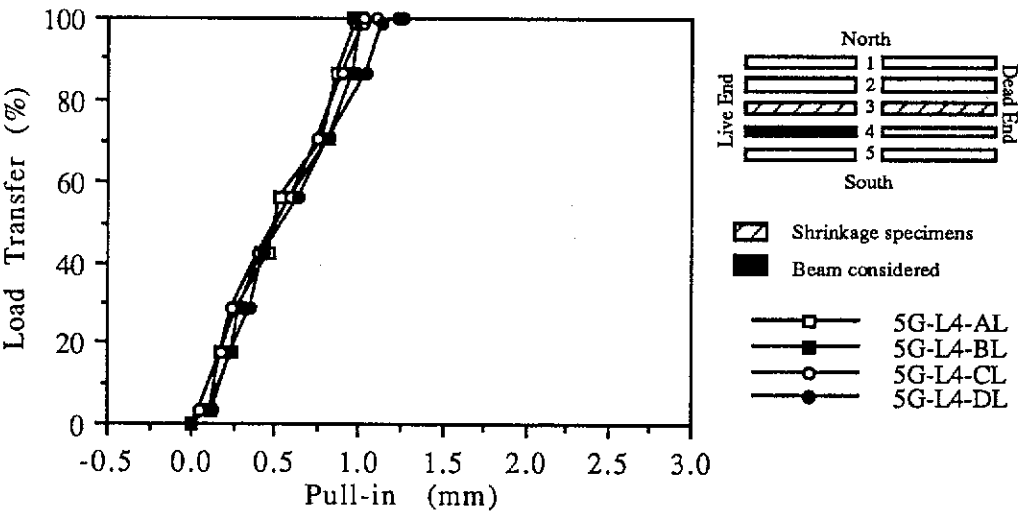

Figure B.38 Percentage Load Transfer vs. Pull-in for Beam 5G-L4 At the Live End (At 7-day Transfer)

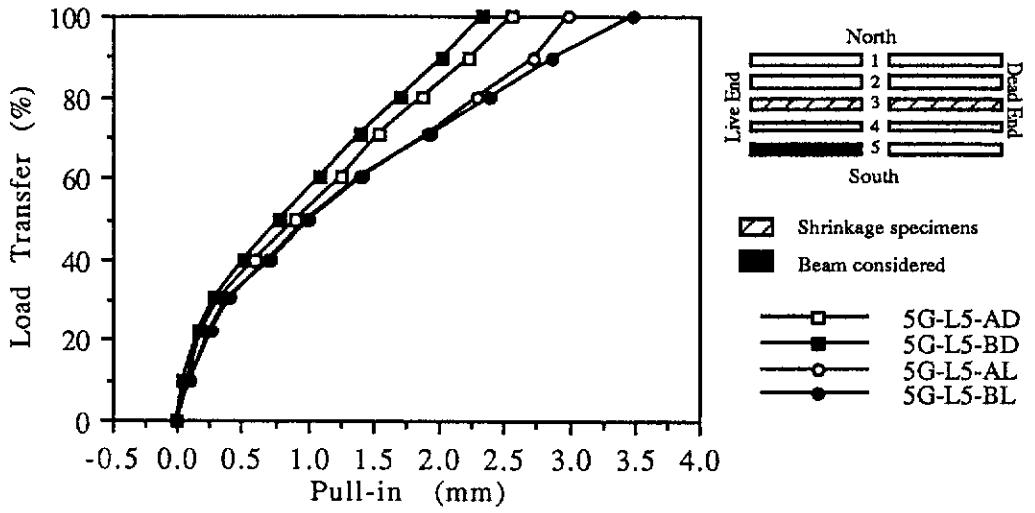

Figure B.39 Percentage Load Transfer vs. Pull-in for Beam 5G-L5 (At 7-day Transfer)

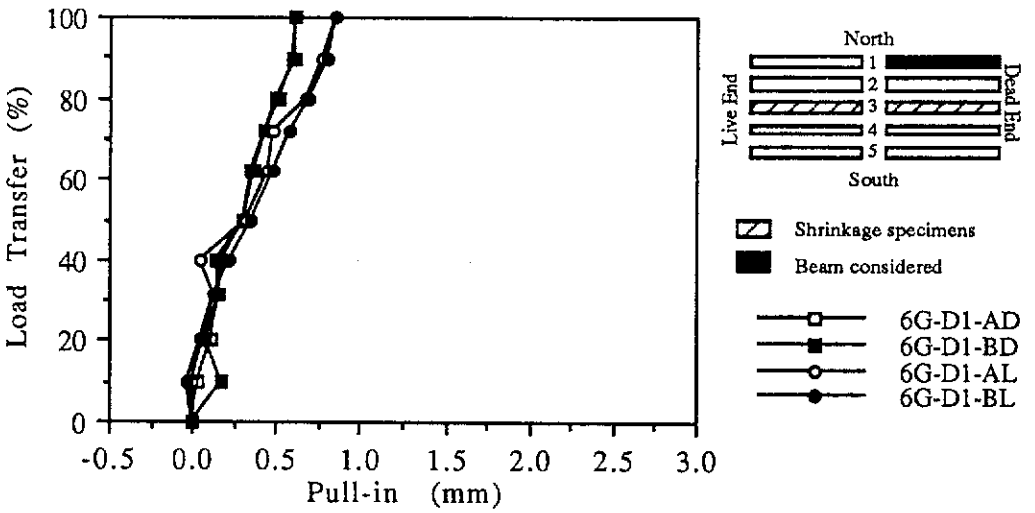

Figure B.40 Percentage Load Transfer vs. Pull-in for Beam 6G-D1 (At 7-day Transfer)

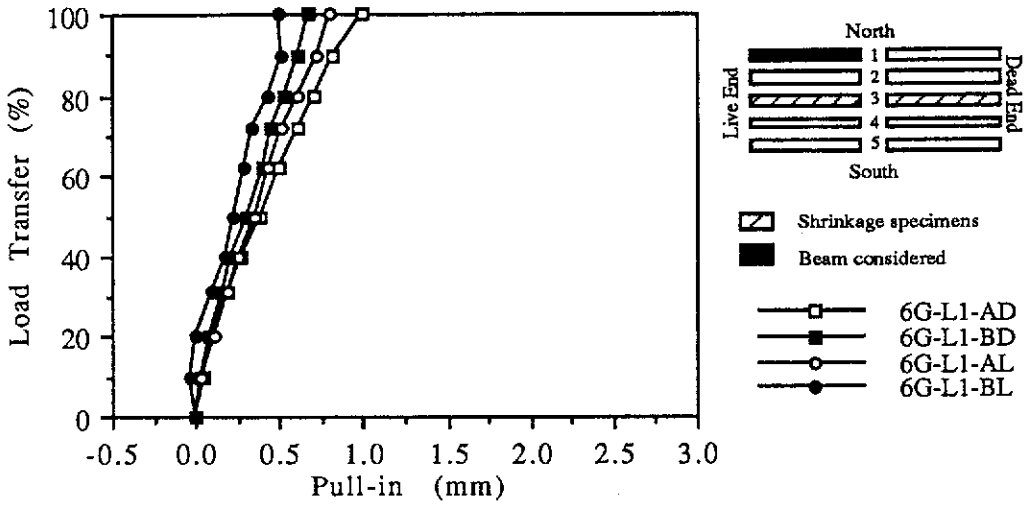

Figure B.41 Percentage Load Transfer vs. Pull-in for Beam 6G-L1 (At 7-day Transfer)

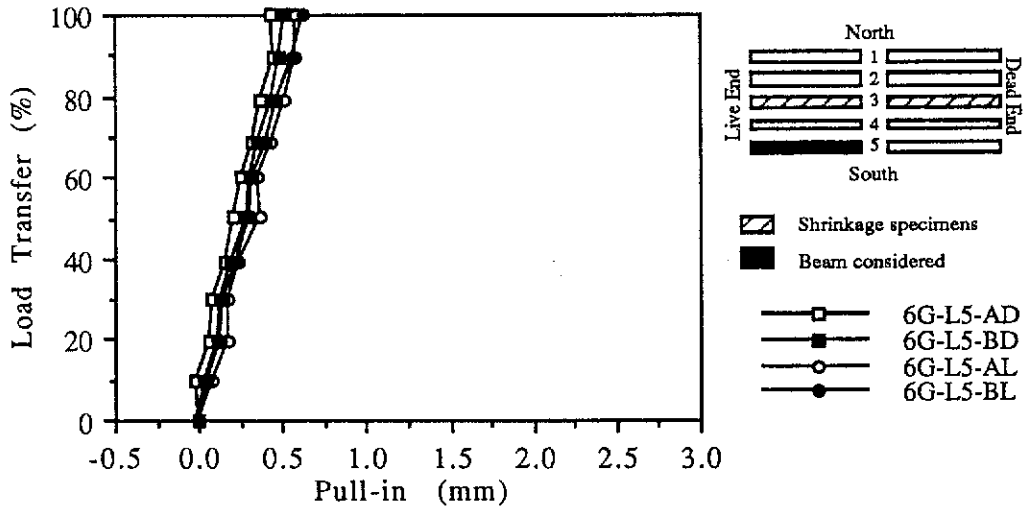

Figure B.42 Percentage Load Transfer vs. Pull-in for Beam 6G-L5 (At 7-day Transfer)

Laboratory Test Results

The full set of measurements for the transmission lengths and pull-ins are recorded here. The initial tendon stress and the concrete strength (standardised to 100 mm dia. x 200 mm cylinder strengths) during and after transfer are also given. Tests 1 and 2 were monitored for 6 months whereas Tests 3, 4, 5 and 6 were monitored for 3 months. Test 7 had recordings taken at transfer and at 28 days only.

The results in Tables C.1 to C.4 are tabulated according to the four types of wires used in Tests 1 to 7; namely the 5 mm dia. Plain, 5 mm dia. Chevron, 7 mm dia. Plain and 7 mm dia. Belgian wires. In most instances, one transmission length value was assigned to all the wires at the end of the beam under consideration although in some cases two transmission length values were obtained from a single demec line, eg. beam 2G-D1 at the live end where 450 and 850 mm were assigned to the wires at transfer (this was done after checking the pull-in diagram and pull-in values for full transfer). The only exceptions were beams 1G-D1 and 1G-L1 where two demec lines were used. For all the beams tested, there were two or four pull-ins for each beam end corresponding to the number of wire tendons used.

The results given in Table C.5 are average values of the transmission lengths and pull-ins from Tables C.1 to C.4. Averaged transmission length and pull-in values were determined for each beam end. All the analyses detailed in this thesis are based on these average values, except for comparisons of pull-ins in statistical inference tests.

Table C.1 Results for Transmission Length and Pull-in from Laboratory Tests (5 mmØ Plain Wire)

Transfer (%)	Wire End (Beam End)	Wire Type	Diameter (mm)	fsi (MPa)	Concrete Strength fcp (MPa)		Transmission Length Lp (mm)						Pull-in Δo (mm)					
					2-day	7-day	2-day	7-day	23-day	28-day	3-mth	6-mth	2-day	7-day	23-day	28-day	3-mth	6-mth
50	4G-D2 (D)	Plain	5	1156		48.7	350											
	4G-D2 (L)			1156		48.7	450											
	4G-L2 (D)			1156		48.7	400											
	4G-L2 (L)			1156		48.7	450											
100	4G-D2-AD	Plain	5	1156		48.7	350			350	350			0.53			0.45	0.71
	4G-D2-BD			1156		48.7	350			350	350			0.82			0.59	0.51
	4G-D2-CD			1156		48.7	350			350	350			0.69			0.53	0.47
	4G-D2-DD			1156		48.7	350			350	350			0.81			0.63	0.67
	4G-D2-AL			1156		48.7	600			625	625			1.46			1.62	1.60
	4G-D2-BL			1156		48.7	600			625	625			1.44			1.50	1.46
	4G-D2-CL			1156		48.7	600			625	625			1.42			1.42	1.38
	4G-D2-DL			1156		48.7	600			625	625			1.34			1.30	1.32
	4G-L2-AD			1156		48.7	525			550	550			1.22			1.18	1.28
	4G-L2-BD			1156		48.7	525			550	550			1.14			0.96	0.98
	4G-L2-CD			1156		48.7	525			550	550			1.16			0.99	1.08
	4G-L2-DD			1156		48.7	525			550	550			1.14			0.94	0.98
	4G-L2-AL			1156		48.7	600			600	600			1.50			1.42	1.64
	4G-L2-BL			1156		48.7	600			600	600			1.40			1.22	1.30
	4G-L2-CL			1156		48.7	600			600	600			1.36			1.24	1.26
	4G-L2-DL			1156		48.7	600			600	600			1.38			1.32	1.42
100	6G-D2-AD	Plain	5	1161		65.1	*200?*			*275?*	*275?*			0.43			0.37	0.35
	6G-D2-BD			1161		65.1	*200?*			*275?*	*275?*			0.47			0.55	0.57
	6G-D2-CD			1161		65.1	*200?*			*275?*	*275?*			0.47			0.51	0.53

Table C.1 Results for Transmission Length and Pull-in from Laboratory Tests (5 mmØ Plain Wire)

Transfer (%)	Wire End (Beam End)	Wire Type	Diameter (mm)	fsi (MPa)	Concrete Strength fcp (MPa)		Transmission Length Lp (mm)						Pull-in Δo (mm)					
					2-day	7-day	2-day	7-day	23-day	28-day	3-mth	6-mth	2-day	7-day	23-day	28-day	3-mth	6-mth
100	6G-D2-DD	Plain	5	1161		65.1		*200?*		*275?*	*275?*			0.43		0.55	0.59	
	6G-D2-AL			1161		65.1		*175?*		*175?*	*200?*			0.39		0.49	0.59	
	6G-D2-BL			1161		65.1		*175?*		*175?*	*200?*			0.35		0.47	0.45	
	6G-D2-CL			1161		65.1		*175?*		*175?*	*200?*			0.43		0.55	0.55	
	6G-D2-DL			1161		65.1		*175?*		*175?*	*200?*			0.43		0.55	0.57	
	6G-L2-AD			1161		65.1		375		400	400			0.41		0.51	0.49	
	6G-L2-BD			1161		65.1		375		400	400			0.35		0.35	0.31	
	6G-L2-CD			1161		65.1		375		400	400			0.33		0.39	0.47	
	6G-L2-DD			1161		65.1		375		400	400			0.25		0.35	0.35	
	6G-L2-AL			1161		65.1		425		425	425			0.51		0.61	0.67	
	6G-L2-BL			1161		65.1		425		425	425			0.39		0.49	0.53	
	6G-L2-CL			1161		65.1		425		425	425			0.37		0.39	0.47	
	6G-L2-DL			1161		65.1		425		425	425			0.33		0.45	0.47	

Note: *(?)* refers to transmission length determined with less degree of certainty due to indistinct end.

Table C.2 Results for Transmission Length and Pull-in from Laboratory Tests (5 mmØ Chevron Wire)

Transfer (%)	Wire End (Beam End)	Wire Type	Diameter (mm)	fsi (MPa)	Concrete Strength fcp (MPa)		Transmission Length Lp (mm)						Pull-in Δo (mm)					
					2-day	7-day	2-day	7-day	23-day	28-day	3-mth	6-mth	2-day	7-day	23-day	28-day	3-mth	6-mth
50	2G-D2 (D)	Chev	5	1120		48.7	200											
	2G-D2 (L)			1120		48.7	275											
	2G-L2 (D)			1120		48.7	175											
	2G-L2 (L)			1120		48.7	225											
100	2G-D2 AD	Chev	5	1120		48.7	250		275	325	275		0.38		0.54	0.58	0.58	
	2G-D2-BD			1120		48.7	250		275	325	275		0.44		0.42	0.52	0.54	
	2G-D2-CD			1120		48.7	250		275	325	275		0.48		0.54	0.56	0.54	
	2G-D2-DD			1120		48.7	250		275	325	275		0.54		0.64	0.68	0.66	
	2G-D2-AL			1120		48.7	325		325	325	325		0.68		0.74	0.82	0.80	
	2G-D2-BL			1120		48.7	325		325	325	325		0.78		0.90	0.93	0.92	
	2G-D2-CL			1120		48.7	325		325	325	325		0.68		0.88	0.90	0.92	
	2G-D2-DL			1120		48.7	325		325	325	325		0.78		0.99	0.99	1.15	
	2G-D4-AD			1120		35.8	250		250	275	275		0.33		0.42	0.48	0.50	
	2G-D4-BD			1120		35.8	250		250	275	275		0.42		0.52	0.52	0.56	
	2G-D4-CD			1120		35.8	250		250	275	275		0.14		0.20	0.18	0.24	
	2G-D4-DD			1120		35.8	250		250	275	275		0.38		0.48	0.46	0.54	
	2G-D4-AL			1120		35.8	350		350	300	300		0.56		0.58	0.52	0.60	
	2G-D4-BL			1120		35.8	350		350	300	300		0.80		0.78	0.58	0.62	
	2G-D4-CL			1120		35.8	350		350	300	300		0.60		0.68	0.64	0.70	
	2G-D4-DL			1120		35.8	350		350	300	300		0.62		0.70	0.70	0.76	
	2G-L2-AD			1120		48.7	275		325	325	325		0.54		0.60	0.50	0.54	
	2G-L2-BD			1120		48.7	275		325	325	325		0.58		0.64	0.60	0.62	
	2G-L2-CD			1120		48.7	275		325	325	325		0.54		0.62	0.52	0.58	
	2G-L2-DD			1120		48.7	275		325	325	325		0.50		0.52	0.56	0.62	

Table C.2 Results for Transmission Length and Pull-in from Laboratory Tests (5 mmØ Chevron Wire)

Transfer (%)	Wire End (Beam End)	Wire Type	Diameter (mm)	fsi (MPa)	Concrete Strength fcp (MPa)		Transmission Length Lp (mm)						Pull-in Δo (mm)					
					2-day	7-day	2-day	7-day	23-day	28-day	3-mth	6-mth	2-day	7-day	23-day	28-day	3-mth	6-mth
100	2G-L2-AL	Chev	5	1120		48.7	275			350	350	375	0.54			0.62	0.66	0.68
	2G-L2-BL			1120		48.7	275			350	350	375	0.52			0.66	0.70	0.72
	2G-L2-CL			1120		48.7	275			350	350	375	0.64			0.74	0.70	0.74
	2G-L2-DL			1120		48.7	275			350	350	375	0.60			0.64	0.62	0.68
	2G-L4-AD			1120		35.8	350			500	500	475	0.48			0.56	0.46	0.56
	2G-L4-BD			1120		35.8	350			500	500	475	0.46			0.52	0.44	0.54
	2G-L4-CD			1120		35.8	350			500	500	475	0.50			0.56	0.52	0.56
	2G-L4-DD			1120		35.8	350			500	500	475	0.46			0.54	0.48	0.66
	2G-L4-AL			1120		35.8	250			225	225	225	0.40			0.44	0.52	0.52
	2G-L4-BL			1120		35.8	250			225	225	225	0.47			0.49	0.45	0.51
	2G-L4-CL			1120		35.8	250			225	225	225	0.52			0.62	0.64	0.70
	2G-L4-DL			1120		35.8	250			225	225	225	0.52			0.56	0.54	0.60
100	3R-D2-AD	Chev	5	1141		53.1	325			325	350		0.38			0.49	0.45	
	3R-D2-BD			1141		53.1	325			325	350		0.32			0.43	0.43	
	3R-D2-CD			1141		53.1	325			325	350		0.33			0.47	0.47	
	3R-D2-DD			1141		53.1	325			325	350		0.32			0.61	0.61	
	3R-D2-AL			1141		53.1	525			575	600		0.43			0.57	0.51	
	3R-D2-BL			1141		53.1	525			575	600		0.45			0.61	0.55	
	3R-D2-CL			1141		53.1	525			575	600		0.55			0.73	0.65	
	3R-D2-DL			1141		53.1	525			575	600		0.49			0.59	0.59	
	3R-D4-AD			1100		33.8	475			475	475		1.39			1.59	1.55	
	3R-D4-BD			1100		33.8	475			475	475		1.31			1.57	1.49	
	3R-D4-CD			1100		33.8	475			475	475		1.33			1.55	1.49	
	3R-D4-DD			1100		33.8	475			475	475		1.31			1.53	1.45	

Table C.2 Results for Transmission Length and Pull-in from Laboratory Tests (5 mmØ Chevron Wire)

Transfer (%)	Wire End (Beam End)	Wire Type	Diameter (mm)	fsi (MPa)	Concrete Strength fcp (MPa)		Transmission Length Lp (mm)						Pull-in Δo (mm)					
					2-day	7-day	2-day	7-day	23-day	28-day	3-mth	6-mth	2-day	7-day	23-day	28-day	3-mth	6-mth
100	3R-D4-AL	Chev	5	1100		33.8		575		600	600			0.73		0.85	0.75	
	3R-D4-BL			1100		33.8		575		600	600			0.82		1.00	0.98	
	3R-D4-CL			1100		33.8		575		600	600			1.04		1.11	1.10	
	3R-D4-DL			1100		33.8		575		600	600			0.88		1.11	1.15	
	3R-L2-AD			1141		53.1		375		425	425			0.38		0.61	0.57	
	3R-L2-BD			1141		53.1		375		425	425			0.41		0.53	0.49	
	3R-L2-CD			1141		53.1		375		425	425			0.49		0.69	0.59	
	3R-L2-DD			1141		53.1		375		425	425			0.61		0.77	0.67	
	3R-L2-AL			1141		53.1		350		350	375			0.39		0.61	0.49	
	3R-L2-BL			1141		53.1		350		350	375			0.53		0.67	0.69	
	3R-L2-CL			1141		53.1		350		350	375			0.47		0.59	0.49	
	3R-L2-DL			1141		53.1		350		350	375			0.45		0.69	0.61	
	3R-L4-AD			1100		33.8		450		450	475			1.27		1.37	1.25	
	3R-L4-BD			1100		33.8		450		450	475			1.25		1.47	1.35	
	3R-L4-CD			1100		33.8		450		450	475			1.31		1.49	1.41	
	3R-L4-DD			1100		33.8		450		450	475			1.55		1.65	1.57	
	3R-L4-AL			1100		33.8		*500?*		*500?*	*525?*			1.07		1.17	1.21	
	3R-L4-BL			1100		33.8		*500?*		*500?*	*525?*			1.27		1.41	1.33	
	3R-L4-CL			1100		33.8		*775?*		*800?*	*825?*			1.59		1.77	N/A	
	3R-L4-DL			1100		33.8		*775?*		*800?*	*825?*			1.93		2.07	1.99	
100	4G-D4-AD	Chev	5	1075		48.7		375		400	400			0.51		0.45	0.49	
	4G-D4-BD			1075		48.7		375		400	400			0.55		0.45	0.47	
	4G-D4-CD			1075		48.7		375		400	400			0.53		0.43	0.37	
	4G-D4-DD			1075		48.7		375		400	400			0.47		0.37	0.43	

Table C.2 Results for Transmission Length and Pull-in from Laboratory Tests (5 mmØ Chevron Wire)

Transfer (%)	Wire End (Beam End)	Wire Type	Diameter (mm)	fsi (MPa)	Concrete Strength fcp (MPa)		Transmission Length Lp (mm)						Pull-in Δo (mm)					
					2-day	7-day	2-day	7-day	23-day	28-day	3-mth	6-mth	2-day	7-day	23-day	28-day	3-mth	6-mth
100	4G-D4-AL	Chev	5	1075		48.7		400		425	425			0.71		0.61	0.63	
	4G-D4-BL			1075		48.7		400		425	425			0.71		0.59	0.61	
	4G-D4-CL			1075		48.7		400		425	425			0.69		0.55	0.51	
	4G-D4-DL			1075		48.7		400		425	425			0.63		0.51	0.57	
	4G-L4-AD			1075		48.7		375		350	350			0.71		0.59	0.57	
	4G-L4-BD			1075		48.7		375		350	350			0.65		0.49	0.55	
	4G-L4-CD			1075		48.7		375		350	350			0.57		0.37	0.41	
	4G-L4-DD			1075		48.7		375		350	350			0.67		0.45	0.53	
	4G-L4-AL			1075		48.7		*450?*		*425?*	*425?*			0.49		0.25	0.47	
	4G-L4-BL			1075		48.7		*450?*		*425?*	*425?*			0.47		0.31	0.43	
	4G-L4-CL			1075		48.7		*450?*		*425?*	*425?*			0.51		0.41	0.49	
	4G-L4-DL			1075		48.7		*450?*		*425?*	*425?*			0.53		0.45	0.61	
100	5G-D2-AD	Chev	5	1090		20.1	425		425		425		0.78		0.70		0.76	
	5G-D2-BD			1090		20.1	425		425		425		0.86		0.94		0.98	
	5G-D2-CD			1090		20.1	425		425		425		0.88		0.80		0.86	
	5G-D2-DD			1090		20.1	425		425		425		0.78		0.72		0.74	
	5G-D2-AL			1090		20.1	400		400		400		0.70		0.62		0.66	
	5G-D2-BL			1090		20.1	400		400		400		0.74		0.72		0.86	
	5G-D2-CL			1090		20.1	400		400		400		0.82		0.76		0.86	
	5G-D2-DL			1090		20.1	400		400		400		0.66		0.58		0.62	
	5G-D4-AD			1080		26.8		750		750	750			0.90		0.88	0.92	
	5G-D4-BD			1080		26.8		750		750	750			0.84		0.84	0.88	
	5G-D4-CD			1080		26.8		750		750	750			0.86		0.82	0.78	
	5G-D4-DD			1080		26.8		750		750	750			0.82		0.96	0.96	

Table C.2 Results for Transmission Length and Pull-in from Laboratory Tests (5 mmØ Chevron Wire)

Transfer (%)	Wire End (Beam End)	Wire Type	Diameter (mm)	fsi (MPa)	Concrete Strength fcp (MPa)		Transmission Length Lp (mm)						Pull-in Δo (mm)					
					2-day	7-day	2-day	7-day	23-day	28-day	3-mth	6-mth	2-day	7-day	23-day	28-day	3-mth	6-mth
100	5G-D4-AL	Chev	5	1080		26.8		575		575	600			0.80		0.84	1.04	
	5G-D4-BL			1080		26.8		575		575	600			1.06		1.12	1.20	
	5G-D4-CL			1080		26.8		575		575	600			1.10		1.16	1.24	
	5G-D4-DL			1080		26.8		575		575	600			1.04		1.12	1.18	
	5G-L2-AD			1090		20.1	425		425		450		0.84		0.76		0.86	
	5G-L2-BD			1090		20.1	425		425		450		0.82		0.80		0.84	
	5G-L2-CD			1090		20.1	425		425		450		0.80		0.84		0.88	
	5G-L2-DD			1090		20.1	425		425		450		0.82		0.80		0.72	
	5G-L2-AL			1090		20.1	575		575		575		0.86		0.82		0.88	
	5G-L2-BL			1090		20.1	575		575		575		0.88		0.84		0.92	
	5G-L2-CL			1090		20.1	575		575		575		0.78		0.72		0.74	
	5G-L2-DL			1090		20.1	575		575		575		0.76		0.78		0.80	
	5G-L4-AD			1080		26.8		475		475	475			1.08		1.10	1.02	
	5G-L4-BD			1080		26.8		475		475	475			0.96		0.96	1.02	
	5G-L4-CD			1080		26.8		475		475	475			0.96		1.00	1.00	
	5G-L4-DD			1080		26.8		475		475	475			1.12		1.10	1.18	
	5G-L4-AL			1080		26.8		*700?*		*700?*	*700?*			0.98		0.96	0.98	
	5G-L4-BL			1080		26.8		*700?*		*700?*	*700?*			1.00		1.00	1.06	
	5G-L4-CL			1080		26.8		*700?*		*700?*	*700?*			1.10		1.08	1.14	
	5G-L4-DL			1080		26.8		*700?*		*700?*	*700?*			1.26		1.24	1.28	
100	6G-D4-AD	Chev	5	1176		65.1		200		250	250			0.33		0.31	0.37	
	6G-D4-BD			1176		65.1		200		250	250			0.37		0.33	0.35	
	6G-D4-CD			1176		65.1		200		250	250			0.29		0.31	0.29	
	6G-D4-DD			1176		65.1		200		250	250			0.23		0.25	0.29	

Table C.2 Results for Transmission Length and Pull-in from Laboratory Tests (5 mmØ Chevron Wire)

Transfer (%)	Wire End (Beam End)	Wire Type	Diameter (mm)	fsi (MPa)	Concrete Strength fcp (MPa)		Transmission Length Lp (mm)						Pull-in Δo (mm)					
					2-day	7-day	2-day	7-day	23-day	28-day	3-mth	6-mth	2-day	7-day	23-day	28-day	3-mth	6-mth
100	6G-D4-AL	Chev	5	1176		65.1		225		225	225			0.31		0.29	0.29	
	6G-D4-BL			1176		65.1		225		225	225			0.31		0.31	0.33	
	6G-D4-CL			1176		65.1		225		225	225			0.29		0.37	0.33	
	6G-D4-DL			1176		65.1		225		225	225			0.31		0.29	0.35	
	6G-L4-AD			1176		65.1		375		350	350			0.45		0.39	0.47	
	6G-L4-BD			1176		65.1		375		350	350			0.37		0.29	0.33	
	6G-L4-CD			1176		65.1		375		350	350			0.23		0.29	0.23	
	6G-L4-DD			1176		65.1		375		350	350			0.27		0.23	0.27	
	6G-L4-AL			1176		65.1		325		325	325			0.35		0.33	0.43	
	6G-L4-BL			1176		65.1		325		325	325			0.31		0.33	0.43	
	6G-L4-CL			1176		65.1		325		325	325			0.35		0.33	0.39	
	6G-L4-DL			1176		65.1		325		325	325			0.29		0.31	0.37	
100	7G-D2-AD	Chev	5	1176		53.9		275		275				0.41		0.57		
	7G-D2-BD			1176		53.9		275		275				0.45		0.52		
	7G-D2-CD			1176		53.9		275		275				0.45		0.47		
	7G-D2-DD			1176		53.9		275		275				0.37		0.41		
	7G-D2-AL			1176		53.9		350		350				0.56		0.60		
	7G-D2-BL			1176		53.9		350		350				0.64		0.68		
	7G-D2-CL			1176		53.9		350		350				0.56		0.72		
	7G-D2-DL			1176		53.9		350		350				0.58		0.66		
	7R-D4-AD			1151		53.9		325		325				0.28		0.31		
	7R-D4-BD			1151		53.9		325		325				0.43		0.43		
	7R-D4-CD			1151		53.9		325		325				0.51		0.49		
	7R-D4-DD			1151		53.9		325		325				0.37		0.47		

Table C.2 Results for Transmission Length and Pull-in from Laboratory Tests (5 mmØ Chevron Wire)

Transfer (%)	Wire End (Beam End)	Wire Type	Diameter (mm)	fsi (MPa)	Concrete Strength fcp (MPa)		Transmission Length Lp (mm)						Pull-in Δo (mm)					
					2-day	7-day	2-day	7-day	23-day	28-day	3-mth	6-mth	2-day	7-day	23-day	28-day	3-mth	6-mth
100	7R-D4-AL	Chev	5	1151		53.9		525		525				N/A		N/A		
	7R-D4-BL			1151		53.9		525		525				N/A		N/A		
	7R-D4-CL			1151		53.9		525		525				N/A		N/A		
	7R-D4-DL			1151		53.9		525		525				N/A		N/A		
	7G-L2-AD			1176		53.9		425		400				0.57		0.61		
	7G-L2-BD			1176		53.9		425		400				0.65		0.72		
	7G-L2-CD			1176		53.9		425		400				0.57		0.62		
	7G-L2-DD			1176		53.9		425		400				0.59		0.62		
	7G-L2-AL			1176		53.9		325		350				0.60		0.70		
	7G-L2-BL			1176		53.9		325		350				0.43		0.64		
	7G-L2-CL			1176		53.9		325		350				0.35		0.58		
	7G-L2-DL			1176		53.9		325		350				0.52		0.58		
	7R-L4-AD			1151		53.9		600		575				N/A		N/A		
	7R-L4-BD			1151		53.9		600		575				N/A		N/A		
	7R-L4-CD			1151		53.9		600		575				N/A		N/A		
	7R-L4-DD			1151		53.9		600		575				N/A		N/A		
	7R-L4-AL			1151		53.9		450		450				0.71		0.73		
	7R-L4-BL			1151		53.9		450		450				0.89		0.87		
	7R-L4-CL			1151		53.9		450		450				0.67		0.67		
	7R-L4-DL			1151		53.9		450		450				N/A		N/A		

Note: *(?)* refers to transmission length determined with less degree of certainty due to indistinct end.

Table C.3 Results for Transmission Length and Pull-in from Laboratory Tests (7 mmØ Plain Wire)

Transfer (%)	Wire End (Beam End)	Wire Type	Diameter (mm)	fsi (MPa)	Concrete Strength fcp (MPa)		Transmission Length Lp (mm)						Pull-in Δo (mm)					
					2-day	7-day	2-day	7-day	23-day	28-day	3-mth	6-mth	2-day	7-day	23-day	28-day	3-mth	6-mth
50	1G-D1-AD	Plain	7	1193		49.0	225											
	1G-D1-BD			1193		49.0	225											
	1G-D1-AL			1193		49.0	275											
	1G-D1-BL			1193		49.0	225											
	1G-D2 (D)			1159		49.0	225											
	1G-D2 (L)			1159		49.0	225											
	1G-L1-AD			1193		49.0	400											
	1G-L1-AL			1193		49.0	275											
	1G-L2 (D)			1159		49.0	475											
	1G-L2 (L)			1159		49.0	225											
100	1G-D1-AD	Plain	7	1193		49.0	375		375	425	425		0.70		0.84	1.13	1.25	
	1G-D1-BD			1193		49.0	325		325	425	425		0.80		0.84	1.31	1.39	
	1G-D1-AL			1193		49.0	425		425	475	475		0.97		1.01	1.38	1.60	
	1G-D1-BL			1193		49.0	475		475	475	475		0.96		1.00	1.47	1.69	
	1G-D2-AD			1159		49.0	425		425	475	525		0.96		0.94	1.06	1.30	
	1G-D2-BD			1159		49.0	425		425	475	525		0.81		0.81	1.04	1.26	
	1G-D2-AL			1159		49.0	425		425	425	425		0.69		0.88	1.18	1.28	
	1G-D2-BL			1159		49.0	425		425	425	425		0.71		0.79	1.08	1.32	
	1G-D4-AD			1193		49.0	600		625	650	650		1.15		1.37	1.39	1.61	
	1G-D4-BD			1193		49.0	600		625	650	650		1.11		1.13	1.09	1.47	
	1G-D4-AL			1193		49.0	475		475	525	600		1.17		1.13	1.55	1.85	
	1G-D4-BL			1193		49.0	475		475	525	600		1.29		1.33	1.81	2.12	
	1G-D5-AD			1193		49.0	625		625	625	625		1.00		1.37	1.49	1.73	
	1G-D5-BD			1193		49.0	625		625	625	625		1.08		1.08	1.14	1.38	

Table C.3 Results for Transmission Length and Pull-in from Laboratory Tests (7 mmØ Plain Wire)

Transfer (%)	Wire End (Beam End)	Wire Type	Diameter (mm)	fsi (MPa)	Concrete Strength fcp (MPa)		Transmission Length Lp (mm)						Pull-in Δo (mm)					
					2-day	7-day	2-day	7-day	23-day	28-day	3-mth	6-mth	2-day	7-day	23-day	28-day	3-mth	6-mth
100	1G-D5-AL	Plain	7	1193		49.0	425			425	475	475	1.02			1.13	1.41	1.67
	1G-D5-BL			1193		49.0	425			425	475	475	1.08			1.14	1.54	1.89
	1G-L1-AD			1193		49.0	525			525	525	525	1.39			1.43	1.33	1.77
	1G-L1-BD			1193		49.0	525			525	600	600	1.77			1.69	1.87	2.28
	1G-L1-AL			1193		49.0	525			525	525	525	1.31			N/A	N/A	N/A
	1G-L1-BL			1193		49.0	525			525	600	625	1.27			N/A	N/A	N/A
	1G-L2-AD			1159		49.0	625			625	625	625	1.75			1.91	2.09	2.43
	1G-L2-BD			1159		49.0	625			625	625	625	1.65			1.61	1.73	2.06
	1G-L2-AL			1159		49.0	*575?*			*575?*	*575?*	*575?*	1.30			N/A	N/A	N/A
	1G-L2-BL			1159		49.0	*325?*			*325?*	*325?*	*325?*	0.92			N/A	N/A	N/A
	1G-L4-AD			1193		49.0	650			650	650	650	1.67			1.57	1.59	1.98
	1G-L4-BD			1193		49.0	650			650	650	650	1.72			1.76	2.21	2.51
	1G-L4-AL			1193		49.0	475			475	475	475	0.71			N/A	N/A	N/A
	1G-L4-BL			1193		49.0	475			475	475	475	0.77			N/A	N/A	N/A
	1G-L5-AD			1193		49.0	*325?*			*325?*	*325?*	*325?*	1.27			1.19	1.90	2.18
	1G-L5-BD			1193		49.0	*725?*			*725?*	*725?*	*725?*	1.36			1.38	2.23	2.57
	1G-L5-AL			1193		49.0	325			375	375	375	0.53			N/A	N/A	N/A
	1G-L5-BL			1193		49.0	325			375	375	375	0.80			N/A	N/A	N/A
50	2G-D1 (D)	Plain	7	1190		48.7	300											
	2G-D1 (L)			1190		48.7	475											
	2G-L1 (D)			1190		48.7	300											
	2G-L1 (L)			1190		48.7	250											

Table C.3 Results for Transmission Length and Pull-in from Laboratory Tests (7 mmØ Plain Wire)

Transfer (%)	Wire End (Beam End)	Wire Type	Diameter (mm)	fsi (MPa)	Concrete Strength fcp (MPa)		Transmission Length Lp (mm)						Pull-in Δo (mm)					
					2-day	7-day	2-day	7-day	23-day	28-day	3-mth	6-mth	2-day	7-day	23-day	28-day	3-mth	6-mth
100	2G-D1-AD	Plain	7	1190		48.7	400			425	450	*450?*		0.88		0.98	1.37	1.51
	2G-D1-BD			1190		48.7	400			425	450	*450?*		1.07		1.11	1.63	1.87
	2G-D1-AL			1190		48.7	*450?*			*475?*	*475?*	*475?*		1.54		1.55	1.75	1.97
	2G-D1-BL			1190		48.7	*850?*			*800?*	*800?*	*800?*		2.58		2.88	3.15	3.43
	2G-D5-AD			1174		35.8	450			450	450	475		1.12		1.20	1.10	1.12
	2G-D5-BD			1174		35.8	450			450	450	475		1.18		1.20	1.10	1.06
	2G-D5-AL			1174		35.8	550			600	625	625		1.28		1.58	1.50	1.52
	2G-D5-BL			1174		35.8	550			600	625	625		1.46		1.60	1.52	1.52
	2G-L1-AD			1190		48.7	*300?*			*300?*	*300?*	*300?*		0.87		0.97	1.25	1.43
	2G-L1-BD			1190		48.7	*450?*			*400?*	*450?*	*475?*		0.96		1.04	1.37	1.59
	2G-L1-AL			1190		48.7	*275?*			*275?*	*275?*	*275?*		0.82		1.00	1.31	1.45
	2G-L1-BL			1190		48.7	*425?*			*375?*	*425?*	*425?*		0.94		0.90	1.22	1.33
	2G-L5-AD			1174		35.8	450			450	450	450		1.02		1.02	1.26	1.36
	2G-L5-BD			1174		35.8	450			450	450	450		1.18		1.34	1.40	1.48
	2G-L5-AL			1174		35.8	350			350	525	525		0.84		0.92	1.14	1.20
	2G-L5-BL			1174		35.8	350			350	525	525		0.88		0.94	1.23	1.27
100	3R-D1-AD	Plain	7	1174		53.1	300			350	350			0.37		0.64	0.68	
	3R-D1-BD			1174		53.1	300			350	350			0.51		0.78	0.92	
	3R-D1-AL			1174		53.1	600			600	600			1.20		1.38	1.42	
	3R-D1-BL			1174		53.1	600			600	600			1.59		1.99	1.85	
	3R-D5-AD			1187		33.8	450			450	450			1.27		1.45	1.51	
	3R-D5-BD			1187		33.8	450			450	450			1.00		1.26	1.29	
	3R-D5-AL			1187		33.8	600			650	650			1.51		1.85	1.93	
	3R-D5-BL			1187		33.8	600			650	650			2.48		2.82	2.68	

Table C.3 Results for Transmission Length and Pull-in from Laboratory Tests (7 mmØ Plain Wire)

Transfer (%)	Wire End (Beam End)	Wire Type	Diameter (mm)	fsi (MPa)	Concrete Strength fcp (MPa)		Transmission Length Lp (mm)						Pull-in Δo (mm)					
					2-day	7-day	2-day	7-day	23-day	28-day	3-mth	6-mth	2-day	7-day	23-day	28-day	3-mth	6-mth
100	3R-L1-AD	Plain	7	1174		53.1		425		425	425			0.78		0.90	1.06	
	3R-L1-BD			1174		53.1		425		425	425			0.96		1.14	1.22	
	3R-L1-AL			1174		53.1		450		450	525			0.96		1.06	1.20	
	3R-L1-BL			1174		53.1		450		450	525			1.06		1.16	1.30	
	3R-L5-AD			1187		33.8		725		750	725			1.73		1.79	1.67	
	3R-L5-BD			1187		33.8		725		750	725			2.05		2.30	2.40	
	3R-L5-AL			1187		33.8		*925?*		*900?*	*900?*			1.69		1.89	1.91	
	3R-L5-BL			1187		33.8		*925?*		*900?*	*900?*			2.58		2.97	2.89	
100	4G-D1-AD	Plain	7	1182		48.7		325		350	350			0.88		0.68	0.76	
	4G-D1-BD			1182		48.7		325		350	350			0.88		0.70	0.74	
	4G-D1-AL			1182		48.7		650		650	650			1.45		1.34	1.34	
	4G-D1-BL			1182		48.7		650		650	650			1.72		1.72	1.70	
	4G-L1-AD			1182		48.7		500		525	525			1.22		1.08	1.18	
	4G-L1-BD			1182		48.7		500		525	525			1.30		1.26	1.28	
	4G-L1-AL			1182		48.7		600		600	625			1.97		1.89	2.32	
	4G-L1-BL			1182		48.7		600		600	625			2.11		1.99	2.30	
100	5G-D1-AD	Plain	7	1162		20.1	700		700		700		1.65		1.73		1.71	
	5G-D1-BD			1162		20.1	700		700		700		1.83		1.79		1.73	
	5G-D1-AL			1162		20.1	825		800		800		2.13		2.03		2.01	
	5G-D1-BL			1162		20.1	825		800		800		2.27		2.29		2.27	
	5G-D5-AD			1172		26.8		*725?*		*725?*	*725?*			2.19		2.40	2.52	
	5G-D5-BD			1172		26.8		*725?*		*725?*	*725?*			2.31		2.37	2.42	
	5G-D5-AL			1172		26.8		*1050?*		*1075?*	*1175?*			3.35		3.73	3.77	

Table C.3 Results for Transmission Length and Pull-in from Laboratory Tests (7 mmØ Plain Wire)

Transfer (%)	Wire End (Beam End)	Wire Type	Diameter (mm)	fsi (MPa)	Concrete Strength fcp (MPa)		Transmission Length Lp (mm)						Pull-in Δo (mm)					
					2-day	7-day	2-day	7-day	23-day	28-day	3-mth	6-mth	2-day	7-day	23-day	28-day	3-mth	6-mth
100	5G-D5-BL	Plain	7	1172		26.8		*1050?*		*1075?*	*1175?*			3.65		3.99	4.01	
	5G-L1-AD			1162		20.1	*1075?**		*1075?**		*1075?**		2.23		2.25		2.27	
	5G-L1-BD			1162		20.1	*1075?**		*1075?**		*1075?**		2.35		2.33		2.33	
	5G-L1-AL			1162		20.1	*1025?**		*1025?**		*1025?**		2.96		3.00		3.02	
	5G-L1-BL			1162		20.1	*1025?**		*1025?**		*1025?**		2.66		2.56		2.56	
	5G-L5-AD			1172		26.8		800		800	800			2.56		3.02	3.06	
	5G-L5-BD			1172		26.8		800		800	800			2.33		2.84	2.90	
	5G-L5-AL			1172		26.8		1000		1025	1025			3.00		3.51	3.53	
	5G-L5-BL			1172		26.8		1000		1025	1025			3.49		4.10	4.10	
100	6G-D1-AD	Plain	7	1216		65.1		325		325	325			0.62		0.75	0.81	
	6G-D1-BD			1216		65.1		325		325	325			0.61		0.77	0.75	
	6G-D1-AL			1216		65.1		400		400	400			0.85		0.99	1.11	
	6G-D1-BL			1216		65.1		400		400	400			0.85		1.05	0.95	
	6G-L1-AD			1216		65.1		400		400	400			0.99		1.05	1.05	
	6G-L1-BD			1216		65.1		400		400	400			0.68		0.69	0.66	
	6G-L1-AL			1216		65.1		325		350	350			0.79		0.75	0.83	
	6G-L1-BL			1216		65.1		325		350	350			0.50		0.64	0.54	
100	7R-D1-AD	Plain	7	1182		53.9		475		475				N/A		N/A		
	7R-D1-BD			1182		53.9		475		475				N/A		N/A		
	7R-D1-AL			1182		53.9		625		625				N/A		N/A		
	7R-D1-BL			1182		53.9		625		625				N/A		N/A		
	7G-D5-AD			1177		53.9		300		350				0.80		0.82		
	7G-D5-BD			1177		53.9		300		350				0.55		0.55		

Table C.3 Results for Transmission Length and Pull-in from Laboratory Tests (7 mmØ Plain Wire)

Transfer (%)	Wire End (Beam End)	Wire Type	Diameter (mm)	fsi (MPa)	Concrete Strength fcp (MPa)		Transmission Length Lp (mm)						Pull-in Δo (mm)					
					2-day	7-day	2-day	7-day	23-day	28-day	3-mth	6-mth	2-day	7-day	23-day	28-day	3-mth	6-mth
100	7G-D5-AL	Plain	7	1177		53.9		450		475				1.04		1.08		
	7G-D5-BL			1177		53.9		450		475				1.12		1.14		
	7R-L1-AD			1182		53.9		575		575				N/A		N/A		
	7R-L1-BD			1182		53.9		575		575				N/A		N/A		
	7R-L1-AL			1182		53.9		*700?*		*700?*				N/A		N/A		
	7R-L1-BL			1182		53.9		*700?*		*700?*				N/A		N/A		
	7G-L5-AD			1177		53.9		375		375				0.88		0.94		
	7G-L5-BD			1177		53.9		375		375				0.82		0.78		
	7G-L5-AL			1177		53.9		525		525				1.08		1.16		
	7G-L5-BL			1177		53.9		525		525				1.28		1.30		

Note: *(?)* refers to transmission length determined with less degree of certainty due to indistinct end.
(?)* refers to estimated transmission length which may have been affected by overlapping of end zones.

Table C.4 Results for Transmission Length and Pull-in from Laboratory Tests (7 mmØ Belgian Wire)

Transfer (%)	Wire End (Beam End)	Wire Type	Diameter (mm)	fsi (MPa)	Concrete Strength fcp (MPa)		Transmission Length Lp (mm)						Pull-in Δo (mm)					
					2-day	7-day	2-day	7-day	23-day	28-day	3-mth	6-mth	2-day	7-day	23-day	28-day	3-mth	6-mth
50	4G-D5 (D)	Belg	7	1133		48.7	350											
	4G-D5 (L)			1133		48.7	350											
	4G-L5 (D)			1133		48.7	325											
	4G-L5 (L)			1133		48.7	325											
100	4G-D5-AD	Belg	7	1133		48.7	375			375	350			0.87			0.73	0.75
	4G-D5-BD			1133		48.7	375			375	350			0.83			0.73	0.79
	4G-D5-AL			1133		48.7	500			500	525			1.05			1.05	1.03
	4G-D5-BL			1133		48.7	500			500	525			1.03			0.99	1.05
	4G-L5-AD			1133		48.7	325			350	375			0.79			0.71	0.79
	4G-L5-BD			1133		48.7	325			350	375			0.83			0.73	0.87
	4G-L5-AL			1133		48.7	450			450	450			0.93			0.81	0.99
	4G-L5-BL			1133		48.7	450			450	450			0.89			0.81	0.93
100	6G-D5-AD	Belg	7	1151		65.1	300			325	325			0.45			0.51	0.57
	6G-D5-BD			1151		65.1	300			325	325			0.47			0.55	0.53
	6G-D5-AL			1151		65.1	200			225	225			0.45			0.55	0.55
	6G-D5-BL			1151		65.1	200			225	225			0.59			0.69	0.73
	6G-L5-AD			1151		65.1	250			250	250			0.43			0.57	0.61
	6G-L5-BD			1151		65.1	250			250	250			0.51			0.59	0.59
	6G-L5-AL			1151		65.1	325			375	375			0.57			0.59	0.61
	6G-L5-BL			1151		65.1	325			375	375			0.63			0.67	0.67

This page has been left blank intentionally.

Table C.5 in the following pages gives the average values of transmission lengths and pull-ins extracted from Tables C.1 to C.4.

Table C.5 Average Transmission Lengths and Pull-ins from Laboratory Tests

Test No.	Beam End	Wire Type	Diameter (mm)	fsi (MPa)	Concrete Strength fcp (MPa)		Transmission Length Lp (mm)						Pull-in Δo (mm)					
					2-day	7-day	2-day	7-day	23-day	28-day	3-mth	6-mth	2-day	7-day	23-day	28-day	3-mth	6-mth
1	1G-D1 (D)	Plain	7	1193		49.0		350		350	425	425		0.75		0.84	1.22	1.32
	1G-D1 (L)	Plain	7	1193		49.0		450		450	475	475		0.97		1.01	1.43	1.65
	1G-D2 (D)	Plain	7	1159		49.0		425		425	475	525		0.89		0.88	1.05	1.28
	1G-D2 (L)	Plain	7	1159		49.0		425		425	425	425		0.70		0.84	1.13	1.30
	1G-D4 (D)	Plain	7	1193		49.0		600		625	650	650		1.13		1.25	1.24	1.54
	1G-D4 (L)	Plain	7	1193		49.0		475		475	525	600		1.23		1.23	1.68	1.99
	1G-D5 (D)	Plain	7	1193		49.0		625		625	625	625		1.04		1.23	1.32	1.56
	1G-D5 (L)	Plain	7	1193		49.0		425		425	475	475		1.05		1.14	1.48	1.78
	1G-L1 (D)	Plain	7	1193		49.0		525		525	563	563		1.58		1.56	1.60	2.03
	1G-L1 (L)	Plain	7	1193		49.0		525		525	563	575		1.29		N/A	N/A	N/A
	1G-L2 (D)	Plain	7	1159		49.0		625		625	625	625		1.70		1.76	1.91	2.25
	1G-L2 (L)	Plain	7	1159		49.0		*450?*		*450?*	*450?*	*450?*		1.11		N/A	N/A	N/A
	1G-L4 (D)	Plain	7	1193		49.0		650		650	650	650		1.70		1.67	1.90	2.25
	1G-L4 (L)	Plain	7	1193		49.0		475		475	475	475		0.74		N/A	N/A	N/A
	1G-L5 (D)	Plain	7	1193		49.0		*525?*		*525?*	*525?*	*525?*		1.32		1.29	2.07	2.38
	1G-L5 (L)	Plain	7	1193		49.0		325		375	375	375		0.67		N/A	N/A	N/A
2	2G-D1 (D)	Plain	7	1190		48.7		400		425	450	*450?*		0.98		1.05	1.50	1.69
	2G-D1 (L)	Plain	7	1190		48.7		*650?*		*638?*	*638?*	*638?*		2.06		2.22	2.45	2.70
	2G-D2 (D)	Chev	5	1120		48.7		250		275	325	275		0.46		0.54	0.59	0.58
	2G-D2 (L)	Chev	5	1120		48.7		325		325	325	325		0.73		0.88	0.91	0.95
	2G-D4 (D)	Chev	5	1120		35.8		250		250	275	275		0.32		0.41	0.41	0.46
	2G-D4 (L)	Chev	5	1120		35.8		350		350	300	300		0.65		0.69	0.61	0.67
	2G-D5 (D)	Plain	7	1174		35.8		450		450	450	475		1.15		1.20	1.10	1.09
	2G-D5 (L)	Plain	7	1174		35.8		550		600	625	625		1.37		1.59	1.51	1.52

Table C.5 Average Transmission Lengths and Pull-ins from Laboratory Tests

Test No.	Beam End	Wire Type	Diameter (mm)	fsi (MPa)	Concrete Strength fcp (MPa)		Transmission Length Lp (mm)						Pull-in Δo (mm)					
					2-day	7-day	2-day	7-day	23-day	28-day	3-mth	6-mth	2-day	7-day	23-day	28-day	3-mth	6-mth
2	2G-L1 (D)	Plain	7	1190		48.7		*375?*		*350?*	*375?*	*388?*		0.92		1.01	1.31	1.51
	2G-L1 (L)	Plain	7	1190		48.7		*350?*		*325?*	*350?*	*350?*		0.88		0.95	1.27	1.39
	2G-L2 (D)	Chev	5	1120		48.7		275		325	325	325		0.54		0.60	0.55	0.59
	2G-L2 (L)	Chev	5	1120		48.7		275		350	350	375		0.58		0.67	0.67	0.71
	2G-L4 (D)	Chev	5	1120		35.8		350		500	500	475		0.48		0.55	0.48	0.58
	2G-L4 (L)	Chev	5	1120		35.8		250		225	225	225		0.48		0.53	0.54	0.58
	2G-L5 (D)	Plain	7	1174		35.8		450		450	450	450		1.10		1.18	1.33	1.42
	2G-L5 (L)	Plain	7	1174		35.8		350		350	525	525		0.86		0.93	1.19	1.24
3	3R-D1 (D)	Plain	7	1174		53.1		300		350	350			0.44		0.71	0.80	
	3R-D1 (L)	Plain	7	1174		53.1		600		600	600			1.40		1.69	1.64	
	3R-D2 (D)	Chev	5	1141		53.1		325		325	350			0.34		0.50	0.49	
	3R-D2 (L)	Chev	5	1141		53.1		525		575	600			0.48		0.63	0.58	
	3R-D4 (D)	Chev	5	1100		33.8		475		475	475			1.34		1.56	1.50	
	3R-D4 (L)	Chev	5	1100		33.8		575		600	600			0.87		1.02	1.00	
	3R-D5 (D)	Plain	7	1187		33.8		450		450	450			1.14		1.36	1.40	
	3R-D5 (L)	Plain	7	1187		33.8		600		650	650			2.00		2.34	2.31	
	3R-L1 (D)	Plain	7	1174		53.1		425		425	425			0.87		1.02	1.14	
	3R-L1 (L)	Plain	7	1174		53.1		450		450	525			1.01		1.11	1.25	
	3R-L2 (D)	Chev	5	1141		53.1		375		425	425			0.47		0.65	0.58	
	3R-L2 (L)	Chev	5	1141		53.1		350		350	375			0.46		0.64	0.57	
	3R-L4 (D)	Chev	5	1100		33.8		450		450	475			1.35		1.50	1.40	
	3R-L4 (L)	Chev	5	1100		33.8		*638?*		*650?*	*675?*			1.47		1.61	1.51	
	3R-L5 (D)	Plain	7	1187		33.8		725		750	725			1.89		2.05	2.04	
	3R-L5 (L)	Plain	7	1187		33.8		*925?*		*900?*	*900?*			2.14		2.43	2.40	

Table C.5 Average Transmission Lengths and Pull-ins from Laboratory Tests

Test No.	Beam End	Wire Type	Diameter (mm)	fsi (MPa)	Concrete Strength fcp (MPa)		Transmission Length Lp (mm)						Pull-in Δo (mm)					
					2-day	7-day	2-day	7-day	23-day	28-day	3-mth	6-mth	2-day	7-day	23-day	28-day	3-mth	6-mth
4	4G-D1 (D)	Plain	7	1182		48.7		325		350	350			0.88		0.69	0.75	
	4G-D1 (L)	Plain	7	1182		48.7		650		650	650			1.59		1.53	1.52	
	4G-D2 (D)	Plain	5	1156		48.7		350		350	350			0.71		0.55	0.59	
	4G-D2 (L)	Plain	5	1156		48.7		600		625	625			1.42		1.46	1.44	
	4G-D4 (D)	Chev	5	1075		48.7		375		400	400			0.52		0.43	0.44	
	4G-D4 (L)	Chev	5	1075		48.7		400		425	425			0.69		0.57	0.58	
	4G-D5 (D)	Belg	7	1133		48.7		375		375	350			0.85		0.73	0.77	
	4G-D5 (L)	Belg	7	1133		48.7		500		500	525			1.04		1.02	1.04	
	4G-L1 (D)	Plain	7	1182		48.7		500		525	525			1.26		1.17	1.23	
	4G-L1 (L)	Plain	7	1182		48.7		600		600	625			2.04		1.94	2.31	
	4G-L2 (D)	Plain	5	1156		48.7		525		550	550			1.17		1.02	1.08	
	4G-L2 (L)	Plain	5	1156		48.7		600		600	600			1.41		1.30	1.41	
	4G-L4 (D)	Chev	5	1075		48.7		375		350	350			0.65		0.48	0.52	
	4G-L4 (L)	Chev	5	1075		48.7		*450?*		*425?*	*425?*			0.50		0.36	0.50	
	4G-L5 (D)	Belg	7	1133		48.7		325		350	375			0.81		0.72	0.83	
	4G-L5 (L)	Belg	7	1133		48.7		450		450	450			0.91		0.81	0.96	
5	5G-D1 (D)	Plain	7	1162		20.1	700		700		700		1.74		1.76		1.72	
	5G-D1 (L)	Plain	7	1162		20.1	825		800		800		2.20		2.16		2.14	
	5G-D2 (D)	Chev	5	1090		20.1	425		425		425		0.83		0.79		0.84	
	5G-D2 (L)	Chev	5	1090		20.1	400		400		400		0.73		0.67		0.75	
	5G-D4 (D)	Chev	5	1080		26.8		750		750	750			0.86		0.88	0.89	
	5G-D4 (L)	Chev	5	1080		26.8		575		575	600			1.00		1.06	1.17	
	5G-D5 (D)	Plain	7	1172		26.8		*725?*		*725?*	*725?*			2.25		2.39	2.47	
	5G-D5 (L)	Plain	7	1172		26.8		*1050?*		*1075?*	*1175?*			3.50		3.86	3.89	

Table C.5 Average Transmission Lengths and Pull-ins from Laboratory Tests

Test No.	Beam End	Wire Type	Diameter (mm)	fsi (MPa)	Concrete Strength fcp (MPa)		Transmission Length Lp (mm)						Pull-in Δo (mm)					
					2-day	7-day	2-day	7-day	23-day	28-day	3-mth	6-mth	2-day	7-day	23-day	28-day	3-mth	6-mth
5	5G-L1 (D)	Plain	7	1162		20.1	*1075?**		*1075?**		*1075?**		2.29		2.29		2.30	
	5G-L1 (L)	Plain	7	1162		20.1	*1025?**		*1025?**		*1025?**		2.81		2.78		2.79	
	5G-L2 (D)	Chev	5	1090		20.1	425		425		450		0.82		0.80		0.83	
	5G-L2 (L)	Chev	5	1090		20.1	575		575		575		0.82		0.79		0.84	
	5G-L4 (D)	Chev	5	1080		26.8		475		475	475			1.03		1.04	0.80	
	5G-L4 (L)	Chev	5	1080		26.8		*700?*		*700?*	*700?*			1.09		1.07	1.12	
	5G-L5 (D)	Plain	7	1172		26.8		800		800	800			2.45		2.93	2.98	
	5G-L5 (L)	Plain	7	1172		26.8		1000		1025	1025			3.25		3.81	3.82	
6	6G-D1 (D)	Plain	7	1216		65.1		325		325	325			0.62		0.76	0.78	
	6G-D1 (L)	Plain	7	1216		65.1		400		400	400			0.85		1.02	1.03	
	6G-D2 (D)	Plain	5	1161		65.1		*200?*		*275?*	*275?*			0.45		0.50	0.51	
	6G-D2 (L)	Plain	5	1161		65.1		*175?*		*175?*	*200?*			0.40		0.52	0.54	
	6G-D4 (D)	Chev	5	1176		65.1		200		250	250			0.31		0.30	0.33	
	6G-D4 (L)	Chev	5	1176		65.1		225		225	225			0.31		0.32	0.33	
	6G-D5 (D)	Belg	7	1151		65.1		300		325	325			0.46		0.53	0.55	
	6G-D5 (L)	Belg	7	1151		65.1		200		225	225			0.52		0.62	0.64	
	6G-L1 (D)	Plain	7	1216		65.1		400		400	400			0.84		0.87	0.86	
	6G-L1 (L)	Plain	7	1216		65.1		325		350	350			0.65		0.70	0.69	
	6G-L2 (D)	Plain	5	1161		65.1		375		400	400			0.34		0.40	0.41	
	6G-L2 (L)	Plain	5	1161		65.1		425		425	425			0.40		0.49	0.54	
	6G-L4 (D)	Chev	5	1176		65.1		375		350	350			0.33		0.30	0.33	
	6G-L4 (L)	Chev	5	1176		65.1		325		325	325			0.33		0.33	0.41	
	6G-L5 (D)	Belg	7	1151		65.1		250		250	250			0.47		0.58	0.60	
	6G-L5 (L)	Belg	7	1151		65.1		325		375	375			0.60		0.63	0.64	

Table C.5 Average Transmission Lengths and Pull-ins from Laboratory Tests

Test No.	Beam End	Wire Type	Diameter (mm)	fsi (MPa)	Concrete Strength fcp (MPa)		Transmission Length Lp (mm)						Pull-in Δo (mm)					
					2-day	7-day	2-day	7-day	23-day	28-day	3-mth	6-mth	2-day	7-day	23-day	28-day	3-mth	6-mth
7	7R-D1 (D)	Plain	7	1182		53.9		475		475				N/A		N/A		
	7R-D1 (L)	Plain	7	1182		53.9		625		625				N/A		N/A		
	7G-D2 (D)	Chev	5	1176		53.9		275		275				0.42		0.49		
	7G-D2 (L)	Chev	5	1176		53.9		350		350				0.59		0.67		
	7R-D4 (D)	Chev	5	1151		53.9		325		325				0.40		0.43		
	7R-D4 (L)	Chev	5	1151		53.9		525		525				N/A		N/A		
	7G-D5 (D)	Plain	7	1177		53.9		300		350				0.68		0.69		
	7G-D5 (L)	Plain	7	1177		53.9		450		475				1.08		1.11		
	7R-L1 (D)	Plain	7	1182		53.9		575		575				N/A		N/A		
	7R-L1 (L)	Plain	7	1182		53.9		*700?*		*700?*				N/A		N/A		
	7G-L2 (D)	Chev	5	1176		53.9		425		400				0.60		0.64		
	7G-L2 (L)	Chev	5	1176		53.9		325		350				0.48		0.63		
	7R-L4 (D)	Chev	5	1151		53.9		600		575				N/A		N/A		
	7R- L4 (L)	Chev	5	1151		53.9		450		450				0.76		0.76		
	7G-L5 (D)	Plain	7	1177		53.9		375		375				0.85		0.86		
	7G-L5 (L)	Plain	7	1177		53.9		525		525				1.18		1.23		

Note: *(?)* refers to transmission length determined with less degree of certainty due to indistinct end.
(?)* refers to estimated transmission length which may have been affected by overlapping of end zones.

APPENDIX D

Results from Past Investigations

Results of transmission lengths and pull-ins from previous investigations are presented here. All the results given are with respect to pretensioned prestressed concrete using wire tendons.

The commonly used wires were the 5 mm dia. Plain and 5 mm dia. Belgian patterned wires. Some results were also obtained for the 7 mm dia. Plain wire. Some investigators did not specifically mention the type of 5 mm dia. indented wires used while others have utilised less commonly found types of wires and both these groups of results were combined under the category of "5 mmØ (Other Types)".

The concrete cube strengths were converted to the equivalent strength values for the 100 mm dia. x 200 mm cylinder. This cylinder size was adopted as the standard in this thesis.

Table D.1 Summary of Results from Past Investigations

Measurements	f_{si} (MPa) Initial Steel Stress	f_{cp} (MPa) (Cube) Transfer	f_{cp} (MPa) (Eq. Cylinder Strength)	Transmission Length, L_p (mm)				Δ_o Pull-in (mm)	Remarks
				5 mmØ Plain	5 mmØ Belgian	5 mmØ Other Types	7 mmØ Plain		
Marshall [1949]									2 sets of 10 columns.
5 mmØ wire (Good quality conc.)	1064	N/A	N/A	635-762				0.08?	100 mm square and 100 to 1830 mm long. One set prestressed with 12/5 mm dia. wires.
5 mmØ wire (Badly placed conc.)	1064	N/A	N/A	2000				N/A	Type of release unknown. Gauge pins and travelling microscope used to determine strain distribution. Equivalent concrete cylinder strength=66 MPa. Transfer at 4 days (transfer strength unknown). Krishnamurthy [1973] stated 0.08 mm for pull-in but this value could not be found in Marshall [1949].
Base [1958]									
(i) Building Research Station									Six castings of beams. 5 mm dia. Plain wires compared to 5 mm dia.
Cast 1 (5 mmØ plain) (Ave. of 6 results)	N/A	38.2	31.8	318				N/A	indented wires (indentation type unknown). Average L_p given for each set casting.
Cast 2 (5 mmØ large indentations) (Ave. of 6 results)	N/A	51.1	42.5			258		N/A	Individual pull-ins were not available. All wires cleaned from rust. Concrete cube strength given at transfer.
Cast 3 (5 mmØ large indentations) (Ave. of 8 results)	N/A	45.7	38.0			298		N/A	Assume standard concrete cube used. Concrete units stressed to 13.8 MPa.
Cast 4 (5 mmØ small indentations) (Ave. of 8 results)	N/A	42.1	35.0			257		N/A	

Table D.1 Summary of Results from Past Investigations

Measurements	f_{si} (MPa) Initial Steel Stress	f_{cp} (MPa) (Cube) Transfer	f_{cp} (MPa) (Eq. Cylinder Strength)	Transmission Length, L_p (mm)				Δ_o Pull-in (mm)	Remarks
				5 mmØ Plain	5 mmØ Belgian	5 mmØ Other Types	7 mmØ Plain		
(i) Building Research Station (cont'd.)									
Cast 4 (5 mmØ large indentations) (Ave. of 8 results)	N/A	42.1	35.0			232		N/A	
Cast 5 (5 mmØ plain) (Ave. of 8 results)	N/A	33.5	27.9	356				N/A	
Cast 6 (5 mmØ plain) (Ave. of 8 results)	N/A	34.2	28.5	340				N/A	
Cast 6 (7 mmØ plain) (Ave. of 8 results)	N/A	34.2	28.5				454	N/A	
(ii) Cement and Conc. Association									28 units; 14 units of 75 x 50 mm section and 8 units of 100 x 75 mm section were stressed
P1(1)	N/A	27.6	23.0	660				N/A	to 16.6 MPa, and 6 units of 150 x 100 mm
P2(1)	N/A	27.6	23.0	610				N/A	section were stressed to 13.8 MPa.
P3(1)	N/A	27.6	23.0	737				N/A	12 results each were given for the 5 mmØ Plain
P4(1)	N/A	27.6	23.0	813				N/A	and crimped wires.
P1(2)	N/A	27.6	23.0	432				N/A	Smallest section has equivalent f_{cp} = 57.4 MPa
P2(2)	N/A	27.6	23.0	635				N/A	Concrete cube strengths given at transfer.
P3(2)	N/A	27.6	23.0	635				N/A	Assume standard concrete cube used.
P4(2)	N/A	27.6	23.0	660				N/A	Time of transfer unknown.
P1(3)	N/A	69.0	57.4	229				N/A	
P2(3)	N/A	69.0	57.4	254				N/A	
P3(3)	N/A	69.0	57.4	356				N/A	
P4(3)	N/A	69.0	57.4	152				N/A	

Table D.1 Summary of Results from Past Investigations

Measurements	f_{si} (MPa) Initial Steel Stress	f_{cp} (MPa) (Cube) Transfer	f_{cp} (MPa) (Eq. Cylinder Strength)	Transmission Length, L_p (mm)				Δ_o Pull-in (mm)	Remarks
				5 mmØ Plain	5 mmØ Belgian	5 mmØ Other Types	7 mmØ Plain		
Arthur and Ganguli [1965]									23 I-beams of different sizes (4 beams for establishing experimental procedure).
A1(1)	1020	27.2	24.7		490			N/A	5 mm dia. Belgian indented wires in flanges.
A1(2)	1020	33.8	30.7		485			N/A	Gradual release, generally 16 equal steps.
A1(3)	1020	37.2	33.7		500			N/A	Wires free from rust.
A2(1)	1020	36.6	33.2		500			N/A	200 mm gauge length strain gauge.
A2(2)	1020	33.8	30.7		490			N/A	L_p was taken to the point of first flattening.
A2(3)	1020	32.1	29.1		465			N/A	Concrete strength (transfer) from 200 mm cubes.
A3(5)	1020	39.0	35.4		465			N/A	Transfer at 7 days.
A3(6)	1020	36.9	33.5		490			N/A	Of 19 beams, 13 cracked at one or both
A3(7)	1020	15.5	14.1		450			N/A	ends in the web.
B1(1)	1140	39.0	35.4		460			N/A	Nominal steel stresses given:
B1(2)	1140	34.5	31.3		475			N/A	Series A - 7 wires in bottom flange and 2
B1(3)	1140	27.6	25.0		475			N/A	wires in top flange,
B2(1)	1140	34.1	30.9		450			N/A	Series B - 4 wires each in top and bottom
B2(2)	1140	34.8	31.6		460			N/A	flanges.
B2(3)	1140	34.8	31.6		450			N/A	Total prestress force for each beam = 185 kN.
B3(1)	1140	42.8	38.8		475			N/A	
B3(2)	1140	41.0	37.2		475			N/A	
B3(3)	1140	40.7	36.9		460			N/A	
B3(4)	1140	26.9	24.4		475			N/A	

Table D.1 Summary of Results from Past Investigations

Measurements	f_{si} (MPa) Initial Steel Stress	f_{cp} (MPa) (Cube) Transfer	f_{cp} (MPa) (Eq. Cylinder Strength)	Transmission Length, L_p (mm)				Δ_o Pull-in (mm)	Remarks
				5 mmØ Plain	5 mmØ Belgian	5 mmØ Other Types	7 mmØ Plain		
Krishnamurthy [1970, 1971, 1972 & 1973] and Marshall and Krishnamurthy [1969] (i)									Over 80 units of I-section beams.
D11-A	N/A	15.0	12.0		572			0.74	5 mm dia. Belgian indented wires (B-type).
D12-A	N/A	29.0	23.2		489			1.35	Concrete strength (transfer) from 100 mm cubes.
D13-A	N/A	29.0	23.2		568			1.24	Transmission lengths were averaged for two ends of each beam.
D21-A	N/A	15.0	12.0		493			0.49	$L_p = 1.35\ L_{(80\%\ \text{strain build-up})}$
D22-A	N/A	25.1	20.1		511			0.95	Beams in mix A were all gradually released
D23-A	N/A	27.8	22.2		498			0.84	in 8 approximately equal steps.
D24-A	N/A	31.7	25.3		508			0.91	Total prestress force for each beam = 188 kN.
D31 to D34-A	N/A	N/A			566			N/A	Average result of four beams.
D41 to D44-A	N/A	N/A			570			N/A	Average result of four beams.
D11-B(1) (8 steps)	N/A	47.2	37.7		455			0.61	32 I-beams with mix B, 4 similar specimens
D11-B(2) (4 steps)	N/A	38.1	30.4		605			1.36	for eight different cross-sections.
D11-B(3) (2 steps)	N/A	47.3	37.8		554			1.62	Beams in mix B had gradual and sudden
D11-B(4) (Sudden)	N/A	57.2	45.7		574			1.15	releases in 8, 4, 2 and 1 steps in each set.
D12-B(1) (8 steps)	N/A	45.4	36.3		556			1.28	
D12-B(2) (4 steps)	N/A	46.6	37.2		617			1.65	
D12-B(3) (2 steps)	N/A	50.9	40.7		673			1.80	
D12-B(4) (Sudden)	N/A	48.1	38.4		599			1.31	

Table D.1 Summary of Results from Past Investigations

Measurements	f_{si} (MPa) Initial Steel Stress	f_{cp} (MPa) (Cube) Transfer	f_{cp} (MPa) (Eq. Cylinder Strength)	Transmission Length, L_p (mm)				Δ_o Pull-in (mm)	Remarks
				5 mmØ Plain	5 mmØ Belgian	5 mmØ Other Types	7 mmØ Plain		
(i) (cont'd.)									
D21-B(1) (8 steps)	N/A	47.2	37.7		437			0.49	
D21-B(2) (4 steps)	N/A	38.1	30.4		480			0.99	
D21-B(3) (2 steps)	N/A	47.3	37.8		561			2.00	
D21-B(4) (Sudden)	N/A	57.2	45.7		523			0.96	
D22-B(1) (8 steps)	N/A	27.0	21.6		455			0.69	
D22-B(2) (4 steps)	N/A	46.6	37.2		564			1.12	
D22-B(3) (2 steps)	N/A	50.9	40.7		610			1.44	
D22-B(4) (Sudden)	N/A	48.1	38.4		599			1.33	
D31-B(1) (8 steps)	N/A	54.2	43.3		617			1.12	
D31-B(2) (4 steps)	N/A	60.9	48.7		579			1.18	
D31-B(3) (2 steps)	N/A	43.1	34.4		643			1.52	
D31-B(4) (Sudden)	N/A	56.3	45.0		579			1.07	
D32-B(1) (8 steps)	N/A	51.5	41.1		518			0.99	
D32-B(2) (4 steps)	N/A	49.9	39.9		528			1.05	
D32-B(3) (2 steps)	N/A	47.7	38.1		561			1.16	
D32-B(4) (Sudden)	N/A	48.8	39.0		511			1.05	
D41-B(1) (8 steps)	N/A	54.2	43.3		544			1.09	
D41-B(2) (4 steps)	N/A	60.9	48.7		610			1.41	
D41-B(3) (2 steps)	N/A	43.1	34.4		574			1.16	
D41-B(4) (Sudden)	N/A	56.3	45.0		503			1.21	
D42-B(1) (8 steps)	N/A	51.5	41.1		541			1.08	
D42-B(2) (4 steps)	N/A	49.9	39.9		610			1.32	
D42-B(3) (2 steps)	N/A	47.7	38.1		574			1.57	
D42-B(4) (Sudden)	N/A	48.8	39.0		625			1.46	

Table D.1 Summary of Results from Past Investigations

Measurements	f_{si} (MPa) Initial Steel Stress	f_{cp} (MPa) (Cube) Transfer	f_{cp} (MPa) (Eq. Cylinder Strength)	Transmission Length, L_p (mm)				Δ_o Pull-in (mm)	Remarks
				5 mmØ Plain	5 mmØ Belgian	5 mmØ Other Types	7 mmØ Plain		
(ii) British Railways [1943], cited by Krishnamurthy [1973].									Concrete strength given at transfer. 5 mm dia. Plain wires used. Assume standard concrete cube used.
Sleeper units (7 results obtained)	973	41.2	34.3	380-610				0.61-1.60	
(iii) Leeds University Evans and Robinson [1955], cited by Krishnamurthy [1973].									Columns 38 x 32 x 1067 mm. Concrete strains determined by using X-ray & travelling microscope technique by Evans.
Col-K	N/A	59.3	49.3	609				0.81	Data from Figure 7(a) and Table 3 of reference.
Col-L	N/A	59.3	49.3				703	1.58	Data from Figure 8(a) of reference. Gradual release (transfer at 7 days). Concrete columns stressed to 20.7 MPa.
Evans and Williams [1957], cited by Krishnamurthy [1973].									
No designation	N/A	58.4	48.6				635	1.78	7 mm dia. Plain and corroded wire.
(iv) Rusch and Rehm [1963], cited by Krishnamurthy [1973].									Assume standard concrete cube strength given at transfer. 5 mm dia. indented wires used.
No. 11 (5 mmØ patterned wires)	785	15.2	12.6			500		0.74	Type of indentation unknown.

Table D.1 Summary of Results from Past Investigations

Measurements	f_{si} (MPa) Initial Steel Stress	f_{cp} (MPa) (Cube) Transfer	f_{cp} (MPa) (Eq. Cylinder Strength)	Transmission Length, L_p (mm)				Δ_o Pull-in (mm)	Remarks
				5 mmØ Plain	5 mmØ Belgian	5 mmØ Other Types	7 mmØ Plain		
(v) Ratz, Holmjanski and Kolner [1958], cited by Krishnamurthy [1973].									Concrete strength given at transfer. Assume standard concrete cube used. No. 6, 5T IT 5 mm dia. wires with indentations on two sides.
5 mmØ indented wire	417	29.4	24.5			237		0.22	Results were obtained from a line of best fit on the data points. The steel stress was varied but the concrete strength remained unchanged. Assume standard concrete cube used. From Figure 10(b) and Table 2 of reference (v).
	706	29.4	24.5			262		0.45	
	863	29.4	24.5			294		0.65	
Sengupta and Som [1976]									72 beams; T, unsymmetrical I, I, inverted T and rectangular shapes.
45 beams	N/A	N/A	N/A	600				N/A	5 mm dia. Plain wires. Gradual release. 200 mm gauge length strain gauge. L_p was taken to the point of first flattening. Cylinder strength (28 days) = 17.7 to 39.2 MPa. Age of transfer and transfer strength unknown. Average transmission lengths given.
17 beams	N/A	N/A	N/A	700				N/A	

Table D.1 Summary of Results from Past Investigations

Measurements	f_{si} (MPa) Initial Steel Stress	f_{cp} (MPa) (Cube) Transfer	f_{cp} (MPa) (Eq. Cylinder Strength)	Transmission Length, L_p (mm)				Δ_o Pull-in (mm)	Remarks
				5 mmØ Plain	5 mmØ Belgian	5 mmØ Other Types	7 mmØ Plain		
Srinivasa Rao, Kalyanasundaram and Fazlullah Sharief [1977]									8 prismatic beams 100 x 100 x 2500 mm. 5 mm dia. Plain wires and 10 mm dia. Tor90 ribbed bars (4 beams each). Gradual and shock (arc cutting) releases.
5P-1-1 (Shock)	1250	33.4	27.8	920				1.39	100 mm gauge length strain gauge.
5P-1-2 (Shock)	1250	33.4	27.8	783				1.30	$L_p = 1.35\ L_{(80\%\ max.\ strain)}$
5P-3-1 (Gradual)	1250	34.1	28.4	638				0.95	L_p average value of two ends of each beam.
5P-3-2 (Gradual)	1250	34.1	28.4	605				0.92	Assume standard concrete cubes used. Transfer at 7 days. Concrete strength given at transfer. Nominal steel stress given. Total prestress force = 10 ton., $\left(\frac{P}{A_c}\right)$ = 10 MPa.

APPENDIX E

Concrete Cylinder Strengths

The following tables present all the concrete cylinder compressive and Brazilian tensile test results. Concrete crushing tests and Brazilian tensile tests were carried out according to the Australian Standards, AS 1012.9 (1986) and AS 1012.10 (1985) respectively.

A simple code was designated to each individual cylinder in order to distinguish them (this code is not used within the thesis), for example:

C6 - 12 - X*

where, 6 refers to Test 6, 1 refers to the mix number (Tests 1, 4, 6 and 7 had only one mix whereas Tests 2, 3 and 5 had two different mixes each), 2 refers to the batch number (each mix may be made up of one, two or three batches) and X refers to the cylinder (a number for compressive test cylinder and an alphabet for Brazilian tensile test cylinder). A prefix C is only used when a commercial concrete mix was utilised. Finally, the symbol * refers to the usage of 150 mm dia. x 300 mm cylinders; otherwise, all the control cylinders were of the size of 100 mm dia. x 200 mm. All of the cylinders used for the compression tests were 100 mm dia. x 200 mm except for Test 1 which had 150 mm dia. x 300 mm cylinders. Cylinders of the size of 150 mm dia. x 300 mm were used in all the Brazilian tensile tests.

The tabulated compressive strengths are original values for the tests on 100 mm dia. x 200 mm and 150 mm dia. x 300 mm cylinders. The strength values for the 150 mm dia. x 300 mm cylinders taken from this Appendix (Test 1 only) have to be factored by 1.04 to convert to the equivalent 100 mm dia. x 200 mm cylinder strengths.

For tests 2, 3 and 5, the results for the second mix (Mix 2) are given in ***italics*** to differentiate from the results for Mix 1.

Both tests 4 and 6 had cylinders made from the first two of three batches of the same mix. Test 7 had cylinders from the first batch only.

Table E.1 Compressive and Brazilian Tensile Test Results

Test No.	Type of Test	Cylinder Mark	Failure Strength (MPa)		
			7 days	28 days	3 months
1	Compression Test	1-11-1*	44.4		
		1-12-1*	49.5		
		1-13-1*	47.5		
		1-11-2*		56.3	
		1-12-2*		60.3	
		1-13-2*		55.6	
		1-11-3*			65.2
		1-12-3*			66.7
		1-13-3*			68.4
1	Brazilian Tensile Test	1-11-A*	3.16		
		1-12-A*	3.67		
		1-13-A*	4.17		
		1-11-B*		3.69	
		1-12-B*		4.32	
		1-13-B*		4.13	
		1-11-C*			4.18
		1-12-C*			4.72
		1-13-C*			4.35
2	Compression Test	2-11-1	38.0		
		2-12-1	33.5		
		C2-21-1	*48.3*		
		C2-21-2	*49.0*		
		2-11-2		49.0	
		2-12-2		45.8	
		C2-21-3		*59.2*	
		C2-21-4		*52.9*	
		2-11-3			49.0
		2-12-3			48.1
		C2-21-5			*65.0*
		C2-21-6			*66.6*
2	Brazilian Tensile Test	2-11-A*	3.12		
		2-12-A*	3.21		
		C2-21-A*	*3.15*		
		C2-21-B*	*3.51*		
		2-11-B*		3.43	
		2-12-B*		3.34	
		C2-21-C*		*4.18*	
		C2-21-D*		*3.88*	
		2-11-C*			3.37
		2-12-C*			3.72
		C2-21-E*			*4.74*
		C2-21-F*			*4.86*

Table E.2 Compressive and Brazilian Tensile Test Results

Test No.	Type of Test	Cylinder Mark	Failure Strength (MPa)		
			7 days	28 days	3 months
3	Compression Test	3-11-1	36.7		
		3-12-1	30.9		
		3-21-1	***55.1***		
		3-22-1	***51.0***		
		3-11-2		41.9	
		3-12-2		40.9	
		3-21-2		***62.5***	
		3-22-2		***66.8***	
		3-11-3			51.0
		3-12-3			51.6
		3-21-3			***71.1***
		3-22-3			***72.2***
3	Brazilian Tensile Test	3-11-A*	3.20		
		3-12-A*	3.17		
		3-21-A*	***4.51***		
		3-22-A*	***3.89***		
		3-11-B*		3.87	
		3-12-B*		3.70	
		3-21-B*		***4.25***	
		3-22-B*		***4.23***	
		3-11-C*			3.64
		3-12-C*			3.54
		3-21-C*			***5.16***
		3-22-C*			***5.01***

Table E.3 Compressive and Brazilian Tensile Test Results

Test No.	Type of Test	Cylinder Mark	Failure Strength (MPa)		
			7 days	28 days	3 months
4	Compression Test	4-11-1	47.9		
		4-11-2	48.0		
		4-12-1	50.2		
		4-12-2	44.3#		
		4-11-3		61.9	
		4-11-4		63.7	
		4-12-3		59.0	
		4-12-4		66.4	
		4-11-5			73.6
		4-11-6			69.4
		4-12-5			71.0
		4-12-6			68.5
4	Brazilian Tensile Test	4-11-A*	3.63		
		4-11-B*	3.83		
		4-12-A*	3.44		
		4-12-B*	2.87#		
		4-11-C*		4.36	
		4-11-D*		4.32	
		4-12-C*		4.62	
		4-12-D*		4.88	
		4-11-E*			4.43
		4-11-F*			4.53
		4-12-E*			4.69
		4-12-F*			4.63

Note: # indicates that the cylinder was poorly compacted and showed significant amount of voids; result may have been adversely affected.

Table E.4 Compressive and Brazilian Tensile Test Results

Test No.	Type of Test	Cylinder Mark	Failure Strength (MPa)				
			2 days	7 days	23 days	28 days	3 mths
5	Compression Test	5-11-1		28.3			
		5-12-1		25.3			
		5-21-1	*20.2*				
		5-22-1	*20.0*				
		5-11-2				30.3	
		5-12-2				34.0	
		5-21-2			*38.4*		
		5-22-2			*39.9*		
		5-11-3					38.1
		5-12-3					36.5
		5-21-3					*43.7*
		5-22-3					*46.8*
5	Brazilian Tensile Test	5-11-A*		2.40			
		5-12-A*		2.26			
		5-21-A*	*2.42*				
		5-22-A*	*2.16*				
		5-11-B*				2.54	
		5-12-B*				2.83	
		5-21-B*			*3.21*		
		5-22-B*			*3.50*		
		5-11-C*					2.67
		5-12-C*					2.73
		5-21-C*					*3.68*
		5-22-C*					*3.26*

Table E.5 Compressive and Brazilian Tensile Test Results

Test No.	Type of Test	Cylinder Mark	Failure Strength (MPa)		
			7 days	28 days	3 months
6	Compression Test	C6-11-1	65.6		
		C6-11-2	63.4		
		C6-12-1	64.6		
		C6-12-2	66.9		
		C6-11-3		87.5	
		C6-11-4		90.1	
		C6-12-3		88.3	
		C6-11-5			87.6
		C6-11-6			90.2
		C6-12-5			99.9
		C6-12-6			94.9
6	Brazilian Tensile Test	C6-11-A*	3.92#		
		C6-11-B*	5.03		
		C6-12-A*	4.76		
		C6-12-B*	5.06		
		C6-11-C*			
		C6-11-D*		3.92°	
		C6-12-C*		5.03°	
		C6-12-D*		4.76°	
		C6-11-E*		5.06°	5.41
		C6-11-F*			5.41
		C6-12-E*			5.97
		C6-12-F*			5.27
7	Compression Test	7-11-1	54.0		
		7-11-2	52.7		
		7-11-3	55.1		
		7-11-4		61.1	
		7-11-5		59.8	
		7-11-6		56.1	
7	Brazilian Tensile Test	7-11-A*	3.82		
		7-11-B*	3.88		
		7-11-A*	4.13		
		7-11-B*		4.23	
		7-11-C*		4.32	
		7-11-D*		4.16	

Note: # indicates that the cylinder was poorly compacted and showed significant amount of voids; result may have been adversely affected.

° indicates that the cylinders were tested at 31 days instead of 28 days due to breakdown of the testing machine.
Result for C6-12-4 was omitted as the cylinder failed by creep when maximum ram travel was reached.

Statistical Inference Tests - Hypothesis Tests

Comparisons have been made between transmission lengths and pull-ins for different variables such as:

(a) surface condition - plain and indented wires.

(b) size of wire - 5 mm dia. and 7 mm dia. Plain wires.

(c) type of release - gradual, sudden and shock releases.

(d) different concrete transfer strength.

The t-statistic had been used for sample tests with either one or both sample sizes less than 30; otherwise, the z-statistic was used. Statistical inferences were made from the samples with regard to the behaviour of the populations by testing the null hypothesis, H_0 (which was generally one-tailed). Confidence levels considered were in the order of 99.99, 99.9, 99.5, 99.0, 95.0 and 90.0% when checking whether the test statistic had entered the critical region(s). When the test statistic showed that there was insufficient evidence to reject H_0, it was accepted but when it was critical, the alternative hypothesis H_a was adopted.

A brief summary page of each set of comparisons given in Chapter 4 precedes the actual calculations provided in this Appendix. All the values given for both the transmission lengths and pull-ins are in unit millimetres.

F.1 Comparisons of L_p and Δ_o for Plain Wires with L_p and Δ_o for Indented Wires (Gradual Release Only)

(A) Test 4 only (48.7 MPa concrete)

(i) 7 mm dia. Plain wire vs. 7 mm dia. Belgian wire

L_p (Plain) = L_p (Belgian) 90% C.L.

$\{n = 4, \bar{L}_p = 519, s = 143\}$, $\{n = 4, \bar{L}_p = 413, s = 78\}$

Δ_o (Plain) > Δ_o (Belgian) 99% C.L.

$\{n = 8, \bar{\Delta}_o = 1.44, s = 0.46\}$, $\{n = 8, \bar{\Delta}_o = 0.90, s = 0.09\}$

(ii) 5 mm dia. Plain wire vs. 5 mm dia. Chevron wire

L_p (Plain) > L_p (Chevron) 90% C.L.

$\{n = 4, \bar{L}_p = 519, s = 118\}$, $\{n = 4, \bar{L}_p = 400, s = 35\}$

Δ_o (Plain) > Δ_o (Chevron) 99.99% C.L.

$\{n = 16, \bar{\Delta}_o = 1.18, s = 0.30\}$, $\{n = 16, \bar{\Delta}_o = 0.59, s = 0.09\}$

(B) Test 6 only (65.1 MPa concrete)

(i) 7 mm dia. Plain wire vs. 7 mm dia. Belgian wire

L_p (Plain) > L_p (Belgian) 95% C.L.

$\{n = 4, \bar{L}_p = 363, s = 43\}$, $\{n = 4, \bar{L}_p = 269, s = 55\}$

Δ_o (Plain) > Δ_o (Belgian) 99.5% C.L.

$\{n = 8, \bar{\Delta}_o = 0.74, s = 0.16\}$, $\{n = 8, \bar{\Delta}_o = 0.51, s = 0.08\}$

(ii) 5 mm dia. Plain wire vs. 5 mm dia. Chevron wire

L_p (Plain) = L_p (Chevron) 90% C.L.

$\{n = 4, \bar{L}_p = 294, s = 125\}$, $\{n = 4, \bar{L}_p = 281, s = 83\}$

Δ_o (Plain) > Δ_o (Chevron) 99.9% C.L.

$\{n = 16, \bar{\Delta}_o = 0.40, s = 0.07\}$, $\{n = 16, \bar{\Delta}_o = 0.32, s = 0.06\}$

(C) Test 2 (48.7 MPa) and Test 4 (48.7 MPa)

(i) 7 mm dia. Plain wire vs. 7 mm dia. Belgian wire

L_p (Plain) = L_p (Belgian) 90% C.L.

$\{n = 8, \bar{L}_p = 481, s = 137\}$, $\{n = 4, \bar{L}_p = 413, s = 78\}$

Δ_o (Plain) > Δ_o (Belgian) 99% C.L.

$\{n = 16, \bar{\Delta}_o = 1.32, s = 0.53\}$, $\{n = 8, \bar{\Delta}_o = 0.90, s = 0.09\}$

(ii) 5 mm dia. Plain wire vs. 5 mm dia. Chevron wire

L_p (Plain) > L_p (Chevron) 95% C.L.

$\{n = 4, \bar{L}_p = 519, s = 118\}$, $\{n = 8, \bar{L}_p = 341, s = 71\}$

Δ_o (Plain) > Δ_o (Chevron) 99.99% C.L.

$\{n = 16, \bar{\Delta}_o = 1.18, s = 0.30\}$, $\{n = 32, \bar{\Delta}_o = 0.58, s = 0.10\}$

(D) Test 1 (49.0 MPa), Test 2 (48.7 MPa) and Test 4 (48.7 MPa)

(i) 7 mm dia. Plain wire vs. 7 mm dia. Belgian wire

L_p (Plain) > L_p (Belgian) 90% C.L.

$\{n = 24, \bar{L}_p = 489, s = 109\}$, $\{n = 4, \bar{L}_p = 413, s = 78\}$

Δ_o (Plain) > Δ_o (Belgian) 99.99% C.L.

$\{n = 48, \bar{\Delta}_o = 1.19, s = 0.42\}$, $\{n = 8, \bar{\Delta}_o = 0.90, s = 0.09\}$

Test 4 (f_{cp} = 48.7 MPa, Gradual Release)
(L_p for 7 mmØ Plain wire vs. L_p for 7 mmØ Belgian wire)

7 mmØ Plain wire[1]		7 mmØ Belgian wire[2]	
4G-D1-D	325	4G-D5-D	375
4G-D1-L	650	4G-D5-L	500
4G-L1-D	500	4G-L5-D	325
4G-L1-L	600	4G-L5-L	450

H_o: $\mu_1 = \mu_2$
H_a: $\mu_1 > \mu_2$

$\bar{L}_{p1} = 518.75$
$s_1 = 143.43$
$n_1 = 4$
$\frac{s_1^2}{n_1} = 5143.23$

$\bar{L}_{p2} = 412.5$
$s_2 = 77.73$
$n_2 = 4$
$\frac{s_2^2}{n_2} = 1510.42$

$$t_{test} = \frac{(\bar{L}_{p1} - \bar{L}_{p2})}{\sqrt{(s_1^2/n_1) + (s_2^2/n_2)}} = 1.303$$

$$\nu = \frac{\left(s_1^2/n_1 + s_2^2/n_2\right)^2}{\frac{(s_1^2/n_1)^2}{n_1 - 1} + \frac{(s_2^2/n_2)^2}{n_2 - 1}} = 4.62 \quad (\cong 5)$$

$t_{\nu=5,5\%} = 2.015$ $t_{\nu=5,10\%} = 1.476$

∴ Not significant, accept H_o @ 90.0% C.L., L_{p1} (7 mmØ Plain) = L_{p2} (7 mmØ Belgian).

Test 4 (f_{cp} = 48.7 MPa, Gradual Release)
(L_p for 5 mmØ Plain wire vs. L_p for 5 mmØ Chevron wire)

5 mmØ Plain wire[1]		5 mmØ Chevron wire[2]	
4G-D2-D	350	4G-D4-D	375
4G-D2-L	600	4G-D4-L	400
4G-L2-D	525	4G-L4-D	375
4G-L2-L	600	4G-L4-L	450

H_o: $\mu_1 = \mu_2$
H_a: $\mu_1 > \mu_2$

$\bar{L}_{p1} = 518.75$
$s_1 = 117.92$
$n_1 = 4$
$\frac{s_1^2}{n_1} = 3476.56$

$\bar{L}_{p2} = 400$
$s_2 = 35.36$
$n_2 = 4$
$\frac{s_2^2}{n_2} = 312.5$

$t_{test} = 1.929$

$\nu = 3.54 \quad (\cong 4)$

$t_{\nu=4,5\%} = 2.132$ $t_{\nu=4,10\%} = 1.533$

∴ Significant, reject H_o @ 90.0% C.L., L_{p1} (5 mmØ Plain) > L_{p2} (5 mmØ Chevron).

Test 6 (f_{cp} = 65.1 MPa, Gradual Release)
(L_p for 7 mmØ Plain wire vs. L_p for 7 mmØ Belgian wire)

7 mmØ Plain wire[1]		7 mmØ Belgian wire[2]	
6G-D1-D	325	6G-D5-D	300
6G-D1-L	400	6G-D5-L	200
6G-L1-D	400	6G-L5-D	250
6G-L1-L	325	6G-L5-L	325

H_o: $\mu_1 = \mu_2$
H_a: $\mu_1 > \mu_2$

$\bar{L}_{p1} = 362.5$
$s_1 = 43.30$
$n_1 = 4$
$\frac{s_1^2}{n_1} = 468.75$

$\bar{L}_{p2} = 268.75$
$s_2 = 55.43$
$n_2 = 4$
$\frac{s_2^2}{n_2} = 768.23$

$t_{test} = 2.666$

$\nu = 5.67 \ (\cong 6)$

$t_{\nu=6,5\%} = 1.943 \qquad t_{\nu=6,1\%} = 3.143$

$\therefore$ Significant, reject H_o @ 95.0% C.L., L_{p1} (7 mmØ Plain) > L_{p2} (7 mmØ Belgian).

Test 6 (f_{cp} = 65.1 MPa, Gradual Release)
(L_p for 5 mmØ Plain wire vs. L_p for 5 mmØ Chevron wire)

5 mmØ Plain wire[1]		5 mmØ Chevron wire[2]	
6G-D2-D	200	6G-D4-D	200
6G-D2-L	175	6G-D4-L	225
6G-L2-D	375	6G-L4-D	375
6G-L2-L	425	6G-L4-L	325

H_o: $\mu_1 = \mu_2$
H_a: $\mu_1 > \mu_2$

$\bar{L}_{p1} = 293.75$
$s_1 = 124.79$
$n_1 = 4$
$\frac{s_1^2}{n_1} = 3893.23$

$\bar{L}_{p2} = 281.25$
$s_2 = 82.60$
$n_2 = 4$
$\frac{s_2^2}{n_2} = 1705.73$

$t_{test} = 0.16$

$\therefore$ Very small, accept H_o @ 90.0% C.L., L_{p1} (5 mmØ Plain) = L_{p2} (5 mmØ Chevron).

Test 2 (f_{cp} = 48.7 MPa, Gradual Release) and Test 4 (f_{cp} = 48.7 MPa, Gradual Release)
(L_p for 7 mmØ Plain wire vs. L_p for 7 mmØ Belgian wire)

7 mmØ Plain wire[1]		7 mmØ Belgian wire[2]		
2G-D1-D	400	4G-D5-D	375	H_o: $\mu_1 = \mu_2$
2G-D1-L	650	4G-D5-L	500	H_a: $\mu_1 > \mu_2$
2G-L1-D	375	4G-L5-D	325	
2G-L1-L	350	4G-L5-L	450	
4G-D1-D	325			
4G-D1-L	650			
4G-L1-D	500			
4G-L1-L	600			

$\bar{L}_{p1} = 481.25$
$s_1 = 136.77$
$n_1 = 8$
$\frac{s_1^2}{n_1} = 2338.17$

$\bar{L}_{p2} = 412.5$
$s_2 = 77.73$
$n_2 = 4$
$\frac{s_2^2}{n_2} = 1510.42$

$t_{test} = 1.108$
$\nu = 9.61 \ (\cong 10)$
$t_{\nu=10,5\%} = 1.813$ $t_{\nu=10,10\%} = 1.372$

∴ Not significant, accept H_o @ 90.0% C.L., L_{p1} (7 mmØ Plain) = L_{p2} (7 mmØ Belgian).

Test 2 (f_{cp} = 48.7 MPa, Gradual Release) and Test 4 (f_{cp} = 48.7 MPa, Gradual Release)
(L_p for 5 mmØ Plain wire vs. L_p for 5 mmØ Chevron wire)

5 mmØ Plain wire[1]		5 mmØ Chevron wire[2]		
4G-D2-D	350	2G-D2-D	250	H_o: $\mu_1 = \mu_2$
4G-D2-L	600	2G-D2-L	325	H_a: $\mu_1 > \mu_2$
4G-L2-D	525	2G-L2-D	275	
4G-L2-L	600	2G-L2-L	275	
		4G-D4-D	375	
		4G-D4-L	400	
		4G-L4-D	375	
		4G-L4-L	450	

$\bar{L}_{p1} = 518.75$
$s_1 = 117.92$
$n_1 = 4$
$\frac{s_1^2}{n_1} = 3476.56$

$\bar{L}_{p2} = 340.63$
$s_2 = 70.63$
$n_2 = 8$
$\frac{s_2^2}{n_2} = 623.60$

$t_{test} = 2.782$
$\nu = 4.12 \ (\cong 4)$
$t_{\nu=4,5\%} = 2.132$ $t_{\nu=4,1\%} = 3.747$

∴ Significant, reject H_o @ 95.0% C.L., L_{p1} (5 mmØ Plain) > L_{p2} (5 mmØ Chevron).

Test 1 (f_{cp} = 49.0 MPa, Gradual Release), Test 2 (f_{cp} = 48.7 MPa, Gradual Release) and Test 4 (f_{cp} = 48.7 MPa, Gradual Release) (L_p for 7 mmØ Plain wire vs. L_p for 7 mmØ Belgian wire)

7 mmØ Plain wire[1]		7 mmØ Belgian wire[2]		
1G-D1-D	350	4G-D5-D	375	H_o: $\mu_1 = \mu_2$
1G-D1-L	450	4G-D5-L	500	H_a: $\mu_1 > \mu_2$
1G-D2-D	425	4G-L5-D	325	
1G-D2-L	425	4G-L5-L	450	
1G-D4-D	600			
1G-D4-L	475			
1G-D5-D	625			
1G-D5-L	425			
1G-L1-D	525			
1G-L1-L	525			
1G-L2-D	625			
1G-L2-L	450			
1G-L4-D	650			
1G-L4-L	475			
1G-L5-D	525			
1G-L5-L	325			
2G-D1-D	400			
2G-D1-L	650			
2G-L1-D	375			
2G-L1-L	350			
4G-D1-D	325			
4G-D1-L	650			
4G-L1-D	500			
4G-L1-L	600			

$\bar{L}_{p1} = 488.54$
$s_1 = 108.84$
$n_1 = 24$
$\frac{s_1^2}{n_1} = 493.61$

$\bar{L}_{p2} = 412.5$
$s_2 = 77.73$
$n_2 = 4$
$\frac{s_2^2}{n_2} = 1510.42$

$t_{test} = 1.699$

$\nu = 5.18 \ (\cong 5)$

$t_{\nu=5,5\%} = 2.015$ $\quad t_{\nu=5,10\%} = 1.476$

$\therefore$ Significant, reject H_o @ 90.0% C.L., L_{p1} (7 mmØ Plain) > L_{p2} (7 mmØ Belgian).

Test 4 (f_{cp} = 48.7 MPa, Gradual Release)
(Δ_o for 7 mmØ Plain wire vs. Δ_o for 7 mmØ Belgian wire)

7 mmØ Plain wire[1]		7 mmØ Belgian wire[2]	
4G-D1-AD	0.88	4G-D5-AD	0.87
4G-D1-BD	0.88	4G-D5-BD	0.83
4G-D1-AL	1.45	4G-D5-AL	1.05
4G-D1-BL	1.72	4G-D5-BL	1.03
4G-L1-AD	1.22	4G-L5-AD	0.79
4G-L1-BD	1.30	4G-L5-BD	0.83
4G-L1-AL	1.97	4G-L5-AL	0.93
4G-L1-BL	2.11	4G-L5-BL	0.89

H_o: $\mu_1 = \mu_2$
H_a: $\mu_1 > \mu_2$

$\bar{\Delta}_{o1} = 1.441$
$s_1 = 4.63 \times 10^{-1}$
$n_1 = 8$
$\frac{s_1^2}{n_1} = 2.685 \times 10^{-2}$

$\bar{\Delta}_{o2} = 9.025 \times 10^{-1}$
$s_2 = 9.498 \times 10^{-2}$
$n_2 = 8$
$\frac{s_2^2}{n_2} = 1.128 \times 10^{-3}$

$$t_{test} = \frac{(\bar{\Delta}_{o1} - \bar{\Delta}_{o2})}{\sqrt{(s_1^2/n_1) + (s_2^2/n_2)}} = 3.219 \qquad \nu = \frac{\left(s_1^2/n_1 + s_2^2/n_2\right)^2}{\frac{(s_1^2/n_1)^2}{n_1 - 1} + \frac{(s_2^2/n_2)^2}{n_2 - 1}} = 7.59 \ (\cong 8)$$

$t_{\nu=8,5\%} = 1.860$ $t_{\nu=8,1\%} = 2.896$ $t_{\nu=8,0.5\%} = 3.355$

∴ Significant, reject H_o @ 99.0% C.L., Δ_{o1} (7 mmØ Plain) > Δ_{o2} (7 mmØ Belgian).

Test 4 (f_{cp} = 48.7 MPa, Gradual Release)
(Δ_o for 5 mmØ Plain wire vs. Δ_o for 5 mmØ Chevron wire)

5 mmØ Plain wire[1]		5 mmØ Chevron wire[2]	
4G-D2-AD	0.53	4G-D4-AD	0.51
4G-D2-BD	0.82	4G-D4-BD	0.55
4G-D2-CD	0.69	4G-D4-CD	0.53
4G-D2-DD	0.81	4G-D4-DD	0.47
4G-D2-AL	1.46	4G-D4-AL	0.71
4G-D2-BL	1.44	4G-D4-BL	0.71
4G-D2-CL	1.42	4G-D4-CL	0.69
4G-D2-DL	1.34	4G-D4-DL	0.63
4G-L2-AD	1.22	4G-L4-AD	0.71
4G-L2-BD	1.14	4G-L4-BD	0.65
4G-L2-CD	1.16	4G-L4-CD	0.57
4G-L2-DD	1.14	4G-L4-DD	0.67
4G-L2-AL	1.50	4G-L4-AL	0.49
4G-L2-BL	1.40	4G-L4-BL	0.47
4G-L2-CL	1.36	4G-L4-CL	0.51
4G-L2-DL	1.38	4G-L4-DL	0.53

H_o: $\mu_1 = \mu_2$
H_a: $\mu_1 > \mu_2$

$\bar{\Delta}_{o1} = 1.176$
$s_1 = 3.04 \times 10^{-1}$
$n_1 = 16$
$\frac{s_1^2}{n_1} = 5.777 \times 10^{-3}$

$\bar{\Delta}_{o2} = 5.875 \times 10^{-1}$
$s_2 = 9.147 \times 10^{-2}$
$n_2 = 16$
$\frac{s_2^2}{n_2} = 5.229 \times 10^{-4}$

$t_{test} = 7.410$ $\nu = 17.7 \ (\cong 18)$
$t_{\nu=18,0.1\%} = 3.610$ $t_{\nu=18,0.01\%} = 4.648$

∴ Significant, reject H_o @ 99.99% C.L., Δ_{o1} (5 mmØ Plain) > Δ_{o2} (5 mmØ Chevron).

Test 6 (f_{cp} = 65.1 MPa, Gradual Release)
(Δ_o for 7 mmØ Plain wire vs. Δ_o for 7 mmØ Belgian wire)

7 mmØ Plain wire[1]		7 mmØ Belgian wire[2]	
6G-D1-AD	0.62	6G-D5-AD	0.45
6G-D1-BD	0.61	6G-D5-BD	0.47
6G-D1-AL	0.85	6G-D5-AL	0.45
6G-D1-BL	0.85	6G-D5-BL	0.59
6G-L1-AD	0.99	6G-L5-AD	0.43
6G-L1-BD	0.68	6G-L5-BD	0.51
6G-L1-AL	0.79	6G-L5-AL	0.57
6G-L1-BL	0.50	6G-L5-BL	0.63

H_o: $\mu_1 = \mu_2$
H_a: $\mu_1 > \mu_2$

$\bar{\Delta}_{o1} = 7.363 \times 10^{-1}$
$s_1 = 1.611 \times 10^{-1}$
$n_1 = 8$
$\frac{s_1^2}{n_1} = 3.243 \times 10^{-3}$

$\bar{\Delta}_{o2} = 5.125 \times 10^{-1}$
$s_2 = 7.517 \times 10^{-2}$
$n_2 = 8$
$\frac{s_2^2}{n_2} = 7.063 \times 10^{-4}$

$t_{test} = 3.561$ $\quad \nu = 9.91 \ (\cong 10)$

$t_{\nu=10,1\%} = 2.764$ $\quad t_{\nu=10,0.1\%} = 4.144$ $\quad t_{\nu=10,0.5\%} = 3.169$

∴ Significant, reject H_o @ 99.5% C.L., Δ_{o1} (7 mmØ Plain) > Δ_{o2} (7 mmØ Belgian).

Test 6 (f_{cp} = 65.1 MPa, Gradual Release)
(Δ_o for 5 mmØ Plain wire vs. Δ_o for 5 mmØ Chevron wire)

5 mmØ Plain wire[1]		5 mmØ Chevron wire[2]	
6G-D2-AD	0.43	6G-D4-AD	0.33
6G-D2-BD	0.47	6G-D4-BD	0.37
6G-D2-CD	0.47	6G-D4-CD	0.29
6G-D2-DD	0.43	6G-D4-DD	0.23
6G-D2-AL	0.39	6G-D4-AL	0.31
6G-D2-BL	0.35	6G-D4-BL	0.31
6G-D2-CL	0.43	6G-D4-CL	0.29
6G-D2-DL	0.43	6G-D4-DL	0.31
6G-L2-AD	0.41	6G-L4-AD	0.45
6G-L2-BD	0.35	6G-L4-BD	0.37
6G-L2-CD	0.33	6G-L4-CD	0.23
6G-L2-DD	0.25	6G-L4-DD	0.27
6G-L2-AL	0.51	6G-L4-AL	0.35
6G-L2-BL	0.39	6G-L4-BL	0.31
6G-L2-CL	0.37	6G-L4-CL	0.35
6G-L2-DL	0.33	6G-L4-DL	0.29

H_o: $\mu_1 = \mu_2$
H_a: $\mu_1 > \mu_2$

$\bar{\Delta}_{o1} = 3.963 \times 10^{-1}$
$s_1 = 6.52 \times 10^{-2}$
$n_1 = 16$
$\frac{s_1^2}{n_1} = 2.657 \times 10^{-4}$

$\bar{\Delta}_{o2} = 3.163 \times 10^{-1}$
$s_2 = 5.50 \times 10^{-2}$
$n_2 = 16$
$\frac{s_2^2}{n_2} = 1.891 \times 10^{-4}$

$t_{test} = 3.750$ $\quad \nu = 29.2 \ (\cong 29)$

$t_{\nu=29,1\%} = 2.462$ $\quad t_{\nu=29,0.1\%} = 3.396$

∴ Significant, reject H_o @ 99.9% C.L., Δ_{o1} (5 mmØ Plain) > Δ_{o2} (5 mmØ Chevron).

Test 2 (f_{cp} = 48.7 MPa, Gradual Release) and Test 4 (f_{cp} = 48.7 MPa, Gradual Release)
(Δ_o for 7 mmØ Plain wire vs. Δ_o for 7 mmØ Belgian wire)

7 mmØ Plain wire[1]		7 mmØ Belgian wire[2]	
2G-D1-AD	0.88	4G-D5-AD	0.87
2G-D1-BD	1.07	4G-D5-BD	0.83
2G-D1-AL	1.54	4G-D5-AL	1.05
2G-D1-BL	2.58	4G-D5-BL	1.03
2G-L1-AD	0.87	4G-L5-AD	0.79
2G-L1-BD	0.96	4G-L5-BD	0.83
2G-L1-AL	0.82	4G-L5-AL	0.93
2G-L1-BL	0.94	4G-L5-BL	0.89
4G-D1-AD	0.88		
4G-D1-BD	0.88		
4G-D1-AL	1.45		
4G-D1-BL	1.72		
4G-L1-AD	1.22		
4G-L1-BD	1.30		
4G-L1-AL	1.97		
4G-L1-BL	2.11		

H_o: $\mu_1 = \mu_2$
H_a: $\mu_1 > \mu_2$

$\bar{\Delta}_{o1} = 1.324$
$s_1 = 5.316 \times 10^{-1}$
$n_1 = 16$
$\frac{s_1^2}{n_1} = 1.766 \times 10^{-2}$

$\bar{\Delta}_{o2} = 9.025 \times 10^{-1}$
$s_2 = 9.498 \times 10^{-2}$
$n_2 = 8$
$\frac{s_2^2}{n_2} = 1.128 \times 10^{-3}$

$t_{test} = 3.078$

$\nu = 16.8 \ (\cong 17)$

$t_{\nu=17,10\%} = 1.333$ $t_{\nu=17,1\%} = 2.567$ $t_{\nu=17,0.1\%} = 3.646$

$\therefore$ Significant, reject H_o @ 99.0% C.L., Δ_{o1} (7 mmØ Plain) > Δ_{o2} (7 mmØ Belgian).

Test 2 (f_{cp} = 48.7 MPa, Gradual Release) and Test 4 (f_{cp} = 48.7 MPa, Gradual Release)
(Δ_o for 5 mmØ Plain wire vs. Δ_o for 5 mmØ Chevron wire)

5 mmØ Plain wire[1]		5 mmØ Chevron wire[2]	
4G-D2-AD	0.53	2G-D2-AD	0.38
4G-D2-BD	0.82	2G-D2-BD	0.44
4G-D2-CD	0.69	2G-D2-CD	0.48
4G-D2-DD	0.81	2G-D2-DD	0.54
4G-D2-AL	1.46	2G-D2-AL	0.68
4G-D2-BL	1.44	2G-D2-BL	0.78
4G-D2-CL	1.42	2G-D2-CL	0.68
4G-D2-DL	1.34	2G-D2-DL	0.78
4G-L2-AD	1.22	2G-L2-AD	0.54
4G-L2-BD	1.14	2G-L2-BD	0.58
4G-L2-CD	1.16	2G-L2-CD	0.54
4G-L2-DD	1.14	2G-L2-DD	0.50
4G-L2-AL	1.50	2G-L2-AL	0.54
4G-L2-BL	1.40	2G-L2-BL	0.52
4G-L2-CL	1.36	2G-L2-CL	0.64
4G-L2-DL	1.38	2G-L2-DL	0.60
		4G-D4-AD	0.51
		4G-D4-BD	0.55
		4G-D4-CD	0.53
		4G-D4-DD	0.47
		4G-D4-AL	0.71
		4G-D4-BL	0.71
		4G-D4-CL	0.69
		4G-D4-DL	0.63
		4G-L4-AD	0.71
		4G-L4-BD	0.65
		4G-L4-CD	0.57
		4G-L4-DD	0.67
		4G-L4-AL	0.49
		4G-L4-BL	0.47
		4G-L4-CL	0.51
		4G-L4-DL	0.53

H_o: $\mu_1 = \mu_2$
H_a: $\mu_1 > \mu_2$

$\bar{\Delta}_{o1} = 1.176$
$s_1 = 3.040 \times 10^{-1}$
$n_1 = 16$
$\frac{s_1^2}{n_1} = 5.777 \times 10^{-3}$

$\bar{\Delta}_{o2} = 5.819 \times 10^{-1}$
$s_2 = 1.010 \times 10^{-1}$
$n_2 = 32$
$\frac{s_2^2}{n_2} = 3.188 \times 10^{-4}$

$t_{test} = 7.604$

$\nu = 16.7 \ (\cong 17)$

$t_{\nu=17,0.01\%} = 4.714$

∴ Significant, reject H_o @ 99.99% C.L., Δ_{o1} (5 mmØ Plain) > Δ_{o2} (5 mmØ Chevron).

Test 1 (f_{cp} = 49.0 MPa, Gradual Release), Test 2 (f_{cp} = 48.7 MPa, Gradual Release) and Test 4 (f_{cp} = 48.7 MPa, Gradual Release) (Δ_o for 7 mmØ Plain wire vs. Δ_o for 7 mmØ Belgian wire)

7 mmØ Plain wire[1]		7 mmØ Belgian wire[2]	
1G-D1-AD	0.70	4G-D5-AD	0.87
1G-D1-BD	0.80	4G-D5-BD	0.83
1G-D1-AL	0.97	4G-D5-AL	1.05
1G-D1-BL	0.96	4G-D5-BL	1.03
1G-D2-AD	0.96	4G-L5-AD	0.79
1G-D2-BD	0.81	4G-L5-BD	0.83
1G-D2-AL	0.69	4G-L5-AL	0.93
1G-D2-BL	0.71	4G-L5-BL	0.89
1G-D4-AD	1.15		
1G-D4-BD	1.11		
1G-D4-AL	1.17		
1G-D4-BL	1.29		
1G-D5-AD	1.00		
1G-D5-BD	1.08		
1G-D5-AL	1.02		
1G-D5-BL	1.08		
1G-L1-AD	1.39		
1G-L1-BD	1.77		
1G-L1-AL	1.31		
1G-L1-BL	1.27		
1G-L2-AD	1.75		
1G-L2-BD	1.65		
1G-L2-AL	1.30		
1G-L2-BL	0.92		
1G-L4-AD	1.67		
1G-L4-BD	1.72		
1G-L4-AL	0.71		
1G-L4-BL	0.77		
1G-L5-AD	1.27		
1G-L5-BD	1.36		
1G-L5-AL	0.53		
1G-L5-BL	0.80		
2G-D1-AD	0.88		
2G-D1-BD	1.07		
2G-D1-AL	1.54		
2G-D1-BL	2.58		
2G-L1-AD	0.87		
2G-L1-BD	0.96		
2G-L1-AL	0.82		
2G-L1-BL	0.94		
4G-D1-AD	0.88		
4G-D1-BD	0.88		
4G-D1-AL	1.45		
4G-D1-BL	1.72		
4G-L1-AD	1.22		
4G-L1-BD	1.30		
4G-L1-AL	1.97		
4G-L1-BL	2.11		

$\bar{\Delta}_{o2} = 9.025 \times 10^{-1}$

$s_2 = 9.498 \times 10^{-2}$

$n_2 = 8$

$s_2^2/n_2 = 1.128 \times 10^{-3}$

H_o: $\mu_1 = \mu_2$

H_a: $\mu_1 > \mu_2$

$t_{test} = 4.065$

$\nu = 49.3 \ (\cong 49)$

$t_{\nu=49,0.1\%} = 3.265$ $\quad t_{\nu=49,0.01\%} = 4.021$

$\bar{\Delta}_{o1} = 1.185$ (7 mmØ Plain)

$s_1 = 4.216 \times 10^{-1}$

$n_1 = 48$

$s_1^2/n_1 = 3.703 \times 10^{-3}$

$\therefore$ Significant, reject H_o @ 99.99% C.L., Δ_{o1} (7 mmØ Plain) > Δ_{o2} (7 mmØ Belgian).

F.2 Comparisons of L_p and Δ_o for Different Wire Sizes (Gradual Release Only)

(A) Test 4 only (48.7 MPa concrete)

(i) 5 mmØ Plain wire vs. 7 mmØ Plain wire

L_p (5 mmØ) = L_p (7 mmØ) 90% C.L.

$\{n = 4, \bar{L}_p = 519, s = 118\}$, $\{n = 4, \bar{L}_p = 519, s = 143\}$

Δ_o (5 mmØ) < Δ_o (7 mmØ) 90% C.L.

$\{n = 16, \bar{\Delta}_o = 1.18, s = 0.30\}$, $\{n = 8, \bar{\Delta}_o = 1.44, s = 0.46\}$

(ii) 5 mmØ Chevron wire vs. 7 mmØ Belgian wire

L_p (5 mmØ) = L_p (7 mmØ) 90% C.L.

$\{n = 4, \bar{L}_p = 400, s = 35\}$, $\{n = 4, \bar{L}_p = 413, s = 78\}$

Δ_o (5 mmØ) < Δ_o (7 mmØ) 99.99% C.L.

$\{n = 16, \bar{\Delta}_o = 0.59, s = 0.09\}$, $\{n = 8, \bar{\Delta}_o = 0.90, s = 0.09\}$

(B) Test 6 only (65.1 MPa concrete)

(i) 5 mmØ Plain wire vs. 7 mmØ Plain wire

L_p (5 mmØ) = L_p (7 mmØ) 90% C.L.

$\{n = 4, \bar{L}_p = 294, s = 125\}$, $\{n = 4, \bar{L}_p = 363, s = 43\}$

Δ_o (5 mmØ) < Δ_o (7 mmØ) 99.9% C.L.

$\{n = 16, \bar{\Delta}_o = 0.40, s = 0.07\}$, $\{n = 8, \bar{\Delta}_o = 0.74, s = 0.16\}$

(ii) 5 mmØ Chevron wire vs. 7 mmØ Belgian wire

L_p (5 mmØ) = L_p (7 mmØ) 90% C.L.

$\{n = 4, \bar{L}_p = 281, s = 83\}$, $\{n = 4, \bar{L}_p = 269, s = 55\}$

Δ_o (5 mmØ) < Δ_o (7 mmØ) 99.99% C.L.

$\{n = 16, \bar{\Delta}_o = 0.32, s = 0.06\}$, $\{n = 8, \bar{\Delta}_o = 0.51, s = 0.08\}$

Note that only 5 and 7 mm diameter wires could be compared. There was no data available for other sizes of wire where similar comparisons could be made.

Test 4 (f_{cp} = 48.7 MPa, Gradual Release)
(L_p for 5 mmØ Plain wire vs. L_p for 7 mmØ Plain wire)

5 mmØ Plain wire[1]		7 mmØ Plain wire[2]	
4G-D2-D	350	4G-D1-D	325
4G-D2-L	600	4G-D1-L	650
4G-L2-D	525	4G-L1-D	500
4G-L2-L	600	4G-L1-L	600

H_o: $\mu_1 = \mu_2$
H_a: $\mu_1 < \mu_2$

$\bar{L}_{p1} = 518.75$
$s_1 = 117.92$
$n_1 = 4$
$\frac{s_1^2}{n_1} = 3476.56$

$\bar{L}_{p2} = 518.75$
$s_2 = 143.43$
$n_2 = 4$
$\frac{s_2^2}{n_2} = 5143.04$

$t_{test} = 0$

∴ Not significant, accept H_o @ 90.0% C.L., L_{p1} (5 mmØ Plain) = L_{p2} (7 mmØ Plain).

Test 4 (f_{cp} = 48.7 MPa, Gradual Release)
(L_p for 5 mmØ Chevron wire vs. L_p for 7 mmØ Belgian wire)

5 mmØ Chevron wire[1]		7 mmØ Belgian wire[2]	
4G-D4-D	375	4G-D5-D	375
4G-D4-L	400	4G-D5-L	500
4G-L4-D	375	4G-L5-D	325
4G-L4-L	450	4G-L5-L	450

H_o: $\mu_1 = \mu_2$
H_a: $\mu_1 < \mu_2$

$\bar{L}_{p1} = 400$
$s_1 = 35.36$
$n_1 = 4$
$\frac{s_1^2}{n_1} = 312.5$

$\bar{L}_{p2} = 412.5$
$s_2 = 77.73$
$n_2 = 4$
$\frac{s_2^2}{n_2} = 1510.42$

$t_{test} = -0.293$

∴ Not significant, accept H_o @ 90.0% C.L., L_{p1} (5 mmØ Chevron) = L_{p2} (7 mmØ Belgian).

Test 6 (f_{cp} = 65.1 MPa, Gradual Release)
(L_p for 5 mmØ Plain wire vs. L_p for 7 mmØ Plain wire)

5 mmØ Plain wire[1]		7 mmØ Plain wire[2]	
6G-D2-D	200	6G-D1-D	325
6G-D2-L	175	6G-D1-L	400
6G-L2-D	375	6G-L1-D	400
6G-L2-L	425	6G-L1-L	325

H_o: $\mu_1 = \mu_2$
H_a: $\mu_1 < \mu_2$

$\bar{L}_{p1} = 293.75$
$s_1 = 124.79$
$n_1 = 4$
$\frac{s_1^2}{n_1} = 3893.23$

$\bar{L}_{p2} = 362.5$
$s_2 = 43.30$
$n_2 = 4$
$\frac{s_2^2}{n_2} = 468.75$

$t_{test} = -1.04$

$\nu = 3.71 \ (\cong 4)$

$t_{\nu=4,10\%} = -1.533$

∴ Not significant, accept H_o @ 90.0% C.L., L_{p1} (5 mmØ Plain) = L_{p2} (7 mmØ Plain).

Test 6 (f_{cp} = 65.1 MPa, Gradual Release)
(L_p for 5 mmØ Chevron wire vs. L_p for 7 mmØ Belgian wire)

5 mmØ Chevron wire[1]		7 mmØ Belgian wire[2]	
6G-D4-D	200	6G-D5-D	300
6G-D4-L	225	6G-D5-L	200
6G-L4-D	375	6G-L5-D	250
6G-L4-L	325	6G-L5-L	325

H_o: $\mu_1 = \mu_2$
H_a: $\mu_1 < \mu_2$

$\bar{L}_{p1} = 281.25$
$s_1 = 82.60$
$n_1 = 4$
$\frac{s_1^2}{n_1} = 1705.73$

$\bar{L}_{p2} = 268.75$
$s_2 = 55.43$
$n_2 = 4$
$\frac{s_2^2}{n_2} = 768.23$

$t_{test} = 0.25$ (results reversed, but t_{test} is small)

∴ Not significant, accept H_o @ 90.0% C.L., L_{p1} (5 mmØ Chevron) = L_{p2} (7 mmØ Belgian).

Test 4 (f_{cp} = 48.7 MPa, Gradual Release)
(Δ_o for 5 mmØ Plain wire vs. Δ_o for 7 mmØ Plain wire)

5 mmØ Plain wire[1]		7 mmØ Plain wire[2]	
4G-D2-AD	0.53	4G-D1-AD	0.88
4G-D2-BD	0.82	4G-D1-BD	0.88
4G-D2-CD	0.69	4G-D1-AL	1.45
4G-D2-DD	0.81	4G-D1-BL	1.72
4G-D2-AL	1.46	4G-L1-AD	1.22
4G-D2-BL	1.44	4G-L1-BD	1.30
4G-D2-CL	1.42	4G-L1-AL	1.97
4G-D2-DL	1.34	4G-L1-BL	2.11
4G-L2-AD	1.22		
4G-L2-BD	1.14		
4G-L2-CD	1.16		
4G-L2-DD	1.14		
4G-L2-AL	1.50		
4G-L2-BL	1.40		
4G-L2-CL	1.36		
4G-L2-DL	1.38		

H_o: $\mu_1 = \mu_2$
H_a: $\mu_1 < \mu_2$

$\bar{\Delta}_{o1} = 1.176$
$s_1 = 3.040 \times 10^{-1}$
$n_1 = 16$
$\frac{s_1^2}{n_1} = 5.777 \times 10^{-3}$

$\bar{\Delta}_{o2} = 1.441$
$s_2 = 4.634 \times 10^{-1}$
$n_2 = 8$
$\frac{s_2^2}{n_2} = 2.685 \times 10^{-2}$

$t_{test} = -1.471$ $\nu = 10.1$ ($\cong 10$)
$t_{\nu=10,10\%} = -1.372$

∴ Significant, reject H_o @ 90.0% C.L., Δ_{o1} (5 mmØ Plain) < Δ_{o2} (7 mmØ Plain).

Test 4 (f_{cp} = 48.7 MPa, Gradual Release)
(Δ_o for 5 mmØ Chevron wire vs. Δ_o for 7 mmØ Belgian wire)

5 mmØ Chevron wire[1]		7 mmØ Belgian wire[2]	
4G-D4-AD	0.51	4G-D5-AD	0.87
4G-D4-BD	0.55	4G-D5-BD	0.83
4G-D4-CD	0.53	4G-D5-AL	1.05
4G-D4-DD	0.47	4G-D5-BL	1.03
4G-D4-AL	0.71	4G-L5-AD	0.79
4G-D4-BL	0.71	4G-L5-BD	0.83
4G-D4-CL	0.69	4G-L5-AL	0.93
4G-D4-DL	0.63	4G-L5-BL	0.89
4G-L4-AD	0.71		
4G-L4-BD	0.65		
4G-L4-CD	0.57		
4G-L4-DD	0.67		
4G-L4-AL	0.49		
4G-L4-BL	0.47		
4G-L4-CL	0.51		
4G-L4-DL	0.53		

H_o: $\mu_1 = \mu_2$
H_a: $\mu_1 < \mu_2$

$\bar{\Delta}_{o1} = 0.588$
$s_1 = 9.147 \times 10^{-2}$
$n_1 = 16$
$\frac{s_1^2}{n_1} = 5.229 \times 10^{-4}$

$\bar{\Delta}_{o2} = 0.903$
$s_2 = 9.498 \times 10^{-2}$
$n_2 = 8$
$\frac{s_2^2}{n_2} = 1.128 \times 10^{-3}$

$t_{test} = -7.753$ $\nu = 13.63$ ($\cong 13$)
$t_{\nu=13,0.01\%} = -5.111$

∴ Significant, reject H_o @ 99.99% C.L., Δ_{o1} (5 mmØ Chevron) < Δ_{o2} (7 mmØ Belgian).

Test 6 (f_{cp} = 65.1 MPa, Gradual Release)
(Δ_0 for 5 mmØ Plain wire vs. Δ_0 for 7 mmØ Plain wire)

5 mmØ Plain wire[1]		7 mmØ Plain wire[2]	
6G-D2-AD	0.43	6G-D1-AD	0.62
6G-D2-BD	0.47	6G-D1-BD	0.61
6G-D2-CD	0.47	6G-D1-AL	0.85
6G-D2-DD	0.43	6G-D1-BL	0.85
6G-D2-AL	0.39	6G-L1-AD	0.99
6G-D2-BL	0.35	6G-L1-BD	0.68
6G-D2-CL	0.43	6G-L1-AL	0.79
6G-D2-DL	0.43	6G-L1-BL	0.50
6G-L2-AD	0.41		
6G-L2-BD	0.35		
6G-L2-CD	0.33		
6G-L2-DD	0.25		
6G-L2-AL	0.51		
6G-L2-BL	0.39		
6G-L2-CL	0.37		
6G-L2-DL	0.33		

H_o: $\mu_1 = \mu_2$
H_a: $\mu_1 < \mu_2$

$\bar{\Delta}_{o1} = 3.963 \times 10^{-1}$
$s_1 = 6.52 \times 10^{-2}$
$n_1 = 16$
$\frac{s_1^2}{n_1} = 2.657 \times 10^{-4}$

$\bar{\Delta}_{o2} = 7.363 \times 10^{-1}$
$s_2 = 1.611 \times 10^{-1}$
$n_2 = 8$
$\frac{s_2^2}{n_2} = 3.243 \times 10^{-3}$

$t_{test} = -5.740$ $\quad \nu = 8.2 \ (\cong 8)$
$t_{\nu=8,0.1\%} = -4.501$ $\quad t_{\nu=8,0.01\%} = -6.442$

∴ Significant, reject H_o @ 99.9% C.L., Δ_{o1} (5 mmØ Plain) < Δ_{o2} (7 mmØ Plain).

Test 6 (f_{cp} = 65.1 MPa, Gradual Release)
(Δ_0 for 5 mmØ Chevron wire vs. Δ_0 for 7 mmØ Belgian wire)

5 mmØ Chevron wire[1]		7 mmØ Belgian wire[2]	
6G-D4-AD	0.33	6G-D5-AD	0.45
6G-D4-BD	0.37	6G-D5-BD	0.47
6G-D4-CD	0.29	6G-D5-AL	0.45
6G-D4-DD	0.23	6G-D5-BL	0.59
6G-D4-AL	0.31	6G-L5-AD	0.43
6G-D4-BL	0.31	6G-L5-BD	0.51
6G-D4-CL	0.29	6G-L5-AL	0.57
6G-D4-DL	0.31	6G-L5-BL	0.63
6G-L4-AD	0.45		
6G-L4-BD	0.37		
6G-L4-CD	0.23		
6G-L4-DD	0.27		
6G-L4-AL	0.35		
6G-L4-BL	0.31		
6G-L4-CL	0.35		
6G-L4-DL	0.29		

H_o: $\mu_1 = \mu_2$
H_a: $\mu_1 < \mu_2$

$\bar{\Delta}_{o1} = 3.163 \times 10^{-1}$
$s_1 = 5.50 \times 10^{-2}$
$n_1 = 16$
$\frac{s_1^2}{n_1} = 1.891 \times 10^{-4}$

$\bar{\Delta}_{o2} = 5.125 \times 10^{-1}$
$s_2 = 7.517 \times 10^{-2}$
$n_2 = 8$
$\frac{s_2^2}{n_2} = 7.063 \times 10^{-4}$

$t_{test} = -6.557$ $\quad \nu = 10.9 \ (\cong 11)$
$t_{\nu=11,0.01\%} = -5.453$

∴ Significant, reject H_o @ 99.99% C.L., Δ_{o1} (5 mmØ Chevron) < Δ_{o2} (7 mmØ Belgian).

F.3 Comparisons of L_p and Δ_o for Gradual, Sudden and Shock Releases

(A) Test 2 Gradual Release (48.7 and 35.8 MPa) vs. Test 3 Sudden Release (53.1 and 33.8 MPa)

(i) 7 mm dia. Plain wire (Test 2-48.7 MPa vs. Test 3-53.1 MPa)

L_p (Gradual) = L_p (Sudden) 90% C.L.

$\{n = 4, \bar{L}_p = 444, s = 139\}$, $\{n = 4, \bar{L}_p = 444, s = 123\}$

Δ_o (Gradual) > Δ_o (Sudden) 90% C.L. (results reversed)

$\{n = 8, \bar{\Delta}_o = 1.21, s = 0.60\}$, $\{n = 8, \bar{\Delta}_o = 0.93, s = 0.39\}$

(ii) 7 mm dia. Plain wire (Test 2-35.8 MPa vs. Test 3-33.8 MPa)

L_p (Gradual) < L_p (Sudden) 90% C.L.

$\{n = 4, \bar{L}_p = 450, s = 82\}$, $\{n = 4, \bar{L}_p = 675, s = 201\}$

Δ_o (Gradual) < Δ_o (Sudden) 99% C.L.

$\{n = 8, \bar{\Delta}_o = 1.12, s = 0.21\}$, $\{n = 8, \bar{\Delta}_o = 1.79, s = 0.55\}$

(iii) 5 mm dia. Chevron wire (Test 2-48.7 MPa vs. Test 3-53.1 MPa)

L_p (Gradual) < L_p (Sudden) 95% C.L.

$\{n = 4, \bar{L}_p = 281, s = 31\}$, $\{n = 4, \bar{L}_p = 394, s = 90\}$

Δ_o (Gradual) > Δ_o (Sudden) 90% C.L. (results reversed)

$\{n = 16, \bar{\Delta}_o = 0.58, s = 0.11\}$, $\{n = 16, \bar{\Delta}_o = 0.44, s = 0.08\}$

(iv) 5 mm dia. Chevron wire (Test 2-35.8 MPa vs. Test 3-33.8 MPa)

L_p (Gradual) < L_p (Sudden) 99.5% C.L.

$\{n = 4, \bar{L}_p = 300, s = 58\}$, $\{n = 4, \bar{L}_p = 534, s = 87\}$

Δ_o (Gradual) < Δ_o (Sudden) 99.99% C.L.

$\{n = 16, \bar{\Delta}_o = 0.48, s = 0.14\}$, $\{n = 16, \bar{\Delta}_o = 1.25, s = 0.30\}$

(B) Test 7 Gradual Release vs. Shock Release (53.9 MPa)

(i) 7 mm dia. Plain wire

L_p (Gradual) < L_p (Shock) 95% C.L.

$\{n = 4, \bar{L}_p = 413, s = 97\}$, $\{n = 4, \bar{L}_p = 594, s = 94\}$

Δ_o (Not available for comparison)

(ii) 5 mm dia. Chevron wire

L_p (Gradual) < L_p (Shock) 90% C.L.

$\{n = 4, \bar{L}_p = 344, s = 63\}$, $\{n = 4, \bar{L}_p = 475, s = 117\}$

Δ_o (Gradual) = Δ_o (Shock) 90% C.L.

$\{n = 16, \bar{\Delta}_o = 0.52, s = 0.10\}$, $\{n = 7, \bar{\Delta}_o = 0.55, s = 0.21\}$

(C) Test 3 Sudden Release (53.1 MPa) vs. Test 7 Shock Release (53.9 MPa)

(i) 7 mm dia. Plain wire

L_p (Sudden) < L_p (Shock) 90% C.L.

$\{n = 4, \bar{L}_p = 444, s = 123\}$, $\{n = 4, \bar{L}_p = 594, s = 94\}$

Δ_o (Not available for comparison)

Test 2 (f_{cp} = 48.7 MPa, Gradual Release) and Test 3 (f_{cp} = 53.1 MPa, Sudden Release)
(L_p for 7 mmØ Plain wire (Gradual) vs. L_p for 7 mmØ Plain wire (Sudden))

7 mmØ Plain (Grad)[1]		7 mmØ Plain (Sudden)[2]	
2G-D1-D	400	3R-D1-D	300
2G-D1-L	650	3R-D1-L	600
2G-L1-D	375	3R-L1-D	425
2G-L1-L	350	3R-L1-L	450

H_o: $\mu_1 = \mu_2$
H_a: $\mu_1 < \mu_2$

$\bar{L}_{p1} = 443.75$
$s_1 = 139.01$
$n_1 = 4$
$\frac{s_1^2}{n_1} = 4830.73$

$\bar{L}_{p2} = 443.75$
$s_2 = 123.11$
$n_2 = 4$
$\frac{s_2^2}{n_2} = 3789.02$

$t_{test} = 0$

∴ Not significant, accept H_o @ 90.0% C.L., L_{p1} (Gradual) = L_{p2} (Sudden).

Test 2 (f_{cp} = 35.8 MPa, Gradual Release) and Test 3 (f_{cp} = 33.8 MPa, Sudden Release)
(L_p for 7 mmØ Plain wire (Gradual) vs. L_p for 7 mmØ Plain wire (Sudden))

7 mmØ Plain (Grad)[1]		7 mmØ Plain (Sudden)[2]	
2G-D5-D	450	3R-D5-D	450
2G-D5-L	550	3R-D5-L	600
2G-L5-D	450	3R-L5-D	725
2G-L5-L	350	3R-L5-L	925

H_o: $\mu_1 = \mu_2$
H_a: $\mu_1 < \mu_2$

$\bar{L}_{p1} = 450$
$s_1 = 81.65$
$n_1 = 4$
$\frac{s_1^2}{n_1} = 1666.68$

$\bar{L}_{p2} = 675$
$s_2 = 201.04$
$n_2 = 4$
$\frac{s_2^2}{n_2} = 10104.27$

$t_{test} = -2.07$

$\nu = 3.96 \ (\cong 4)$

$t_{\nu=4,10\%} = -1.533 \quad t_{\nu=4,5\%} = -2.132$

∴ Significant, reject H_o @ 90.0% C.L., L_{p1} (Gradual) < L_{p2} (Sudden).

Test 2 (f_{cp} = 48.7 MPa, Gradual Release) and Test 3 (f_{cp} = 53.1 MPa, Sudden Release)
(L_p for 5 mmØ Chevron wire (Gradual) vs. L_p for 5 mmØ Chevron wire (Sudden))

5 mmØ Chevron (Grad)[1]		5 mmØ Chevron (Sudden)[2]		
2G-D2-D	250	3R-D2-D	325	H_o: $\mu_1 = \mu_2$
2G-D2-L	325	3R-D2-L	525	H_a: $\mu_1 < \mu_2$
2G-L2-D	275	3R-L2-D	375	
2G-L2-L	275	3R-L2-L	350	

$\bar{L}_{p1} = 281.25$
$s_1 = 31.46$
$n_1 = 4$
$\frac{s_1^2}{n_1} = 247.40$

$\bar{L}_{p2} = 393.75$
$s_2 = 89.85$
$n_2 = 4$
$\frac{s_2^2}{n_2} = 2018.23$

$t_{test} = -2.36$

$\nu = 3.72 \ (\cong 4)$

$t_{\nu=4,1\%} = -3.747 \quad t_{\nu=4,5\%} = -2.132$

$\therefore$ Significant, reject H_o @ 95.0% C.L., L_{p1} (Gradual) < L_{p2} (Sudden).

Test 2 (f_{cp} = 35.8 MPa, Gradual Release) and Test 3 (f_{cp} = 33.8 MPa, Sudden Release)
(L_p for 5 mmØ Chevron wire (Gradual) vs. L_p for 5 mmØ Chevron wire (Sudden))

5 mmØ Chevron (Grad)[1]		5 mmØ Chevron (Sudden)[2]		
2G-D4-D	250	3R-D4-D	475	H_o: $\mu_1 = \mu_2$
2G-D4-L	350	3R-D4-L	575	H_a: $\mu_1 < \mu_2$
2G-L4-D	350	3R-L4-D	450	
2G-L4-L	250	3R-L4-L	637.5	

$\bar{L}_{p1} = 300$
$s_1 = 57.74$
$n_1 = 4$
$\frac{s_1^2}{n_1} = 833.33$

$\bar{L}_{p2} = 534.38$
$s_2 = 87.43$
$n_2 = 4$
$\frac{s_2^2}{n_2} = 1910.81$

$t_{test} = -4.47$

$\nu = 5.20 \ (\cong 5)$

$t_{\nu=5,0.5\%} = -4.032 \quad t_{\nu=5,0.1\%} = -5.890$

$\therefore$ Significant, reject H_o @ 99.5% C.L., L_{p1} (Gradual) < L_{p2} (Sudden).

Test 7 (f_{cp} = 53.9 MPa, Gradual and Shock Releases)
(L_p for 7 mmØ Plain wire (Gradual) vs. L_p for 7 mmØ Plain wire (Shock))

7 mmØ Plain (Grad)[1]		7 mmØ Plain (Shock)[2]	
7G-D5-D	300	7R-D1-D	475
7G-D5-L	450	7R-D1-L	625
7G-L5-D	375	7R-L1-D	575
7G-L5-L	525	7R-L1-L	700

H_o: $\mu_1 = \mu_2$
H_a: $\mu_1 < \mu_2$

$\bar{L}_{p1} = 412.5$
$s_1 = 96.83$
$n_1 = 4$
$\frac{s_1^2}{n_1} = 2343.75$

$\bar{L}_{p2} = 593.75$
$s_2 = 94.37$
$n_2 = 4$
$\frac{s_2^2}{n_2} = 2226.56$

$t_{test} = -2.681$

$\nu = 6.00 \ (\cong 6)$

$t_{\nu=6,1\%} = -3.143 \quad t_{\nu=6,5\%} = -1.943$

$\therefore$ Significant, reject H_o @ 95.0% C.L., L_{p1} (Gradual) < L_{p2} (Shock).

Test 7 (f_{cp} = 53.9 MPa, Gradual and Shock Releases)
(L_p for 5 mmØ Chevron wire (Gradual) vs. L_p for 5 mmØ Chevron wire (Shock))

5 mmØ Chevron (Grad)[1]		5 mmØ Chevron (Shock)[2]	
7G-D2-D	275	7R-D4-D	325
7G-D2-L	350	7R-D4-L	525
7G-L2-D	425	7R-L4-D	600
7G-L2-L	325	7R-L4-L	450

H_o: $\mu_1 = \mu_2$
H_a: $\mu_1 < \mu_2$

$\bar{L}_{p1} = 343.75$
$s_1 = 62.5$
$n_1 = 4$
$\frac{s_1^2}{n_1} = 976.56$

$\bar{L}_{p2} = 475$
$s_2 = 117.26$
$n_2 = 4$
$\frac{s_2^2}{n_2} = 3437.5$

$t_{test} = -1.976$

$\nu = 4.58 \ (\cong 5)$

$t_{\nu=5,5\%} = -2.015 \quad t_{\nu=5,10\%} = -1.476$

$\therefore$ Significant, reject H_o @ 90.0% C.L., L_{p1} (Gradual) < L_{p2} (Shock).

Test 3 (f_{cp} = 53.1 MPa, Sudden Release) and Test 7 (f_{cp} = 53.9 MPa, Shock Release)
(L_p for 7 mmØ Plain wire (Sudden) vs. L_p for 7 mmØ Plain wire (Shock))

7 mmØ Plain (Sudden)[1]		7 mmØ Plain (Shock)[2]	
3R-D1-D	300	7R-D1-D	475
3R-D1-L	600	7R-D1-L	625
3R-L1-D	425	7R-L1-D	575
3R-L1-L	450	7R-L1-L	700

H_o: $\mu_1 = \mu_2$
H_a: $\mu_1 < \mu_2$

$\bar{L}_{p1} = 443.75$
$s_1 = 123.11$
$n_1 = 4$
$\frac{s_1^2}{n_1} = 3789.06$

$\bar{L}_{p2} = 593.75$
$s_2 = 94.37$
$n_2 = 4$
$\frac{s_2^2}{n_2} = 2226.56$

$t_{test} = -1.934$

$\nu = 5.62 \ (\cong 6)$

$t_{\nu=6,5\%} = -3.143 \quad t_{\nu=6,10\%} = -1.440$

∴ Significant, reject H_o @ 90.0% C.L., L_{p1} (Sudden) < L_{p2} (Shock).

Test 2 (f_{cp} = 48.7 MPa, Gradual Release) and Test 3 (f_{cp} = 53.1 MPa, Sudden Release)
(Δ_o for 7 mmØ Plain wire (Gradual) vs. Δ_o for 7 mmØ Plain wire (Sudden))

7 mmØ Plain (Grad)[1]		7 mmØ Plain (Sudden)[2]	
2G-D1-AD	0.88	3R-D1-AD	0.37
2G-D1-BD	1.07	3R-D1-BD	0.51
2G-D1-AL	1.54	3R-D1-AL	1.20
2G-D1-BL	2.58	3R-D1-BL	1.59
2G-L1-AD	0.87	3R-L1-AD	0.78
2G-L1-BD	0.96	3R-L1-BD	0.96
2G-L1-AL	0.82	3R-L1-AL	0.96
2G-L1-BL	0.94	3R-L1-BL	1.06

H_o: $\mu_1 = \mu_2$
H_a: $\mu_1 < \mu_2$

$\bar{\Delta}_{o1} = 1.208$
$s_1 = 6.00 \times 10^{-1}$
$n_1 = 8$
$\frac{s_1^2}{n_1} = 4.495 \times 10^{-2}$

$\bar{\Delta}_{o2} = 9.288 \times 10^{-1}$
$s_2 = 3.854 \times 10^{-1}$
$n_2 = 8$
$\frac{s_2^2}{n_2} = 1.857 \times 10^{-2}$

$t_{test} = 1.106$ (should be a negative value)

∴ Not significant, accept H_o @ 90.0% C.L., Δ_{o1} (Gradual) = Δ_{o2} (Sudden).
Possible that Δ_{o1} (Gradual) > Δ_{o2} (Sudden).

Test 2 (f_{cp} = 35.8 MPa, Gradual Release) and Test 3 (f_{cp} = 33.8 MPa, Sudden Release)
(Δ_o for 7 mmØ Plain wire (Gradual) vs. Δ_o for 7 mmØ Plain wire (Sudden))

7 mmØ Plain (Grad)[1]		7 mmØ Plain (Sudden)[2]	
2G-D5-AD	1.12	3R-D5-AD	1.27
2G-D5-BD	1.18	3R-D5-BD	1.00
2G-D5-AL	1.28	3R-D5-AL	1.51
2G-D5-BL	1.46	3R-D5-BL	2.48
2G-L5-AD	1.02	3R-L5-AD	1.73
2G-L5-BD	1.18	3R-L5-BD	2.05
2G-L5-AL	0.84	3R-L5-AL	1.69
2G-L5-BL	0.88	3R-L5-BL	2.58

H_o: $\mu_1 = \mu_2$
H_a: $\mu_1 < \mu_2$

$\bar{\Delta}_{o1} = 1.120$
$s_1 = 2.051 \times 10^{-1}$
$n_1 = 8$
$\frac{s_1^2}{n_1} = 5.257 \times 10^{-3}$

$\bar{\Delta}_{o2} = 1.789$
$s_2 = 5.547 \times 10^{-1}$
$n_2 = 8$
$\frac{s_2^2}{n_2} = 3.847 \times 10^{-2}$

$t_{test} = -3.198$ $\quad \nu = 8.9 \ (\cong 9)$
$t_{\nu=9,1\%} = -2.821$ $\quad t_{\nu=9,0.5\%} = -3.250$

∴ Significant, reject H_o @ 99.0% C.L., Δ_{o1} (Gradual) < Δ_{o2} (Sudden).

Test 2 (f_{cp} = 48.7 MPa, Gradual Release) and Test 3 (f_{cp} = 53.1 MPa, Sudden Release)
(Δ_o for 5 mmØ Chevron wire (Gradual) vs. Δ_o for 5 mmØ Chevron wire (Sudden))

5 mmØ Chevron (Grad)[1]		5 mmØ Chevron (Sudden)[2]	
2G-D2-AD	0.38	3R-D2-AD	0.38
2G-D2-BD	0.44	3R-D2-BD	0.32
2G-D2-CD	0.48	3R-D2-CD	0.33
2G-D2-DD	0.54	3R-D2-DD	0.32
2G-D2-AL	0.68	3R-D2-AL	0.43
2G-D2-BL	0.78	3R-D2-BL	0.45
2G-D2-CL	0.68	3R-D2-CL	0.55
2G-D2-DL	0.78	3R-D2-DL	0.49
2G-L2-AD	0.54	3R-L2-AD	0.38
2G-L2-BD	0.58	3R-L2-BD	0.41
2G-L2-CD	0.54	3R-L2-CD	0.49
2G-L2-DD	0.50	3R-L2-DD	0.61
2G-L2-AL	0.54	3R-L2-AL	0.39
2G-L2-BL	0.52	3R-L2-BL	0.53
2G-L2-CL	0.64	3R-L2-CL	0.47
2G-L2-DL	0.60	3R-L2-DL	0.45

H_o: $\mu_1 = \mu_2$
H_a: $\mu_1 < \mu_2$

$\bar{\Delta}_{o1} = 5.763 \times 10^{-1}$
$s_1 = 1.125 \times 10^{-1}$
$n_1 = 16$
$\frac{s_1^2}{n_1} = 7.907 \times 10^{-4}$

$\bar{\Delta}_{o2} = 4.375 \times 10^{-1}$
$s_2 = 8.434 \times 10^{-2}$
$n_2 = 16$
$\frac{s_2^2}{n_2} = 4.446 \times 10^{-4}$

t_{test} = 3.949 (should be a negative value)

∴ Not significant, accept H_o @ 90.0% C.L., Δ_{o1} (Gradual) = Δ_{o2} (Sudden).
Possible that Δ_{o1} (Gradual) > Δ_{o2} (Sudden).

Test 2 (f_{cp} = 35.8 MPa, Gradual Release) and Test 3 (f_{cp} = 33.8 MPa, Sudden Release)
(Δ_o for 5 mmØ Chevron wire (Gradual) vs. Δ_o for 5 mmØ Chevron wire (Sudden))

5 mmØ Chevron (Grad)[1]		5 mmØ Chevron (Sudden)[2]	
2G-D4-AD	0.33	3R-D4-AD	1.39
2G-D4-BD	0.42	3R-D4-BD	1.31
2G-D4-CD	0.14	3R-D4-CD	1.33
2G-D4-DD	0.38	3R-D4-DD	1.31
2G-D4-AL	0.56	3R-D4-AL	0.73
2G-D4-BL	0.80	3R-D4-BL	0.82
2G-D4-CL	0.60	3R-D4-CL	1.04
2G-D4-DL	0.62	3R-D4-DL	0.88
2G-L4-AD	0.48	3R-L4-AD	1.27
2G-L4-BD	0.46	3R-L4-BD	1.25
2G-L4-CD	0.50	3R-L4-CD	1.31
2G-L4-DD	0.46	3R-L4-DD	1.55
2G-L4-AL	0.40	3R-L4-AL	1.07
2G-L4-BL	0.47	3R-L4-BL	1.27
2G-L4-CL	0.52	3R-L4-CL	1.59
2G-L4-DL	0.52	3R-L4-DL	1.93

H_o: $\mu_1 = \mu_2$
H_a: $\mu_1 < \mu_2$

$\bar{\Delta}_{o1} = 4.788 \times 10^{-1}$
$s_1 = 1.427 \times 10^{-1}$
$n_1 = 16$
$\frac{s_1^2}{n_1} = 1.272 \times 10^{-3}$

$\bar{\Delta}_{o2} = 1.253$
$s_2 = 3.027 \times 10^{-1}$
$n_2 = 16$
$\frac{s_2^2}{n_2} = 5.726 \times 10^{-3}$

$t_{test} = -9.256$ $\nu = 21.4$ ($\cong 21$)
$t_{\nu=21,0.01\%} = -4.493$

∴ Significant, reject H_o @ 99.99% C.L., Δ_{o1} (Gradual) < Δ_{o2} (Sudden).

Test 7 (f_{cp} = 53.9 MPa, Gradual and Shock Releases)
(Δ_o for 5 mmØ Chevron wire (Gradual) vs. Δ_o for 5 mmØ Chevron wire (Shock))

5 mmØ Chevron (Grad)[1]		5 mmØ Chevron (Shock)[2]	
7G-D2-AD	0.41	7R-D4-AD	0.28
7G-D2-BD	0.45	7R-D4-BD	0.43
7G-D2-CD	0.45	7R-D4-CD	0.51
7G-D2-DD	0.37	7R-D4-DD	0.37
7G-D2-AL	0.56	7R-D4-AL	N/A
7G-D2-BL	0.64	7R-D4-BL	N/A
7G-D2-CL	0.56	7R-D4-CL	N/A
7G-D2-DL	0.58	7R-D4-DL	N/A
7G-L2-AD	0.57	7R-L4-AD	N/A
7G-L2-BD	0.65	7R-L4-BD	N/A
7G-L2-CD	0.57	7R-L4-CD	N/A
7G-L2-DD	0.59	7R-L4-DD	N/A
7G-L2-AL	0.60	7R-L4-AL	0.71
7G-L2-BL	0.43	7R-L4-BL	0.89
7G-L2-CL	0.35	7R-L4-CL	0.67
7G-L2-DL	0.52	7R-L4-DL	N/A

H_o: $\mu_1 = \mu_2$
H_a: $\mu_1 < \mu_2$

$\bar{\Delta}_{o1} = 5.188 \times 10^{-1}$
$s_1 = 9.514 \times 10^{-2}$
$n_1 = 16$
$\frac{s_1^2}{n_1} = 5.657 \times 10^{-4}$

$\bar{\Delta}_{o2} = 5.514 \times 10^{-1}$
$s_2 = 2.148 \times 10^{-1}$
$n_2 = 7$
$\frac{s_2^2}{n_2} = 6.593 \times 10^{-3}$

$t_{test} = 0.385$

∴ Very small, accept H_o @ 90.0% C.L., Δ_{o1} (Gradual) = Δ_{o2} (Shock).

F.4 Comparisons of L_p and Δ_o for Different Concrete Strengths

(A) Test 2 Gradual Release (35.8 vs. 48.7 MPa)

(i) 7 mm dia. Plain wire

L_p (35.8 MPa) = L_p (48.7 MPa) 90% C.L.

$\{n = 4, \bar{L}_p = 450, s = 82\}$, $\{n = 4, \bar{L}_p = 444, s = 139\}$

Δ_o (35.8 MPa) = Δ_o (48.7 MPa) 90% C.L.

$\{n = 8, \bar{\Delta}_o = 1.12, s = 0.21\}$, $\{n = 8, \bar{\Delta}_o = 1.21, s = 0.60\}$

(ii) 5 mm dia. Chevron wire

L_p (35.8 MPa) = L_p (48.7 MPa) 90% C.L.

$\{n = 4, \bar{L}_p = 300, s = 58\}$, $\{n = 4, \bar{L}_p = 281, s = 31\}$

Δ_o (35.8 MPa) < Δ_o (48.7 MPa) 90% C.L. (results reversed)

$\{n = 16, \bar{\Delta}_o = 0.48, s = 0.14\}$, $\{n = 16, \bar{\Delta}_o = 0.58, s = 0.11\}$

(B) Test 3 Sudden Release (33.8 vs. 53.1 MPa)

(i) 7 mm dia. Plain wire

L_p (33.8 MPa) > L_p (53.1 MPa) 90% C.L.

$\{n = 4, \bar{L}_p = 675, s = 201\}$, $\{n = 4, \bar{L}_p = 444, s = 123\}$

Δ_o (33.8 MPa) > Δ_o (53.1 MPa) 99% C.L.

$\{n = 8, \bar{\Delta}_o = 1.79, s = 0.55\}$, $\{n = 8, \bar{\Delta}_o = 0.93, s = 0.39\}$

(ii) 5 mm dia. Chevron wire

L_p (33.8 MPa) > L_p (53.1 MPa) 95% C.L.

$\{n = 4, \bar{L}_p = 534, s = 87\}$, $\{n = 4, \bar{L}_p = 394, s = 90\}$

Δ_o (33.8 MPa) > Δ_o (53.1 MPa) 99.99% C.L.

$\{n = 16, \bar{\Delta}_o = 1.25, s = 0.30\}$, $\{n = 16, \bar{\Delta}_o = 0.44, s = 0.08\}$

(C) Test 5 Gradual Release (20.1 MPa at 2 days vs. 26.8 MPa at 7 days) - Two-tailed tests used

(i) 7 mm dia. Plain wire

L_p (20.1 MPa) = L_p (26.8 MPa) 90% C.L.

$\{n = 4, \bar{L}_p = 906, s = 175\}$, $\{n = 4, \bar{L}_p = 894, s = 156\}$

Δ_o (20.1 MPa) $\neq$ Δ_o (26.8 MPa) 95% C.L.

$\{n = 8, \bar{\Delta}_o = 2.26, s = 0.42\}$, $\{n = 8, \bar{\Delta}_o = 2.86, s = 0.59\}$

(ii) 5 mm dia. Chevron wire

L_p (20.1 MPa) $\neq$ L_p (26.8 MPa) 90% C.L.

$\{n = 4, \bar{L}_p = 456, s = 80\}$, $\{n = 4, \bar{L}_p = 625, s = 124\}$

Δ_o (20.1 MPa) $\neq$ Δ_o (26.8 MPa) 99.99% C.L.

$\{n = 16, \bar{\Delta}_o = 0.80, s = 0.06\}$, $\{n = 16, \bar{\Delta}_o = 0.99, s = 0.13\}$

(D) Test 4 Gradual Release (48.7 MPa) vs. Test 6 Gradual Release (65.1 MPa)

(i) 7 mm dia. Plain wire

L_p (48.7 MPa) > L_p (65.1 MPa) 90% C.L.

$\{n = 4, \bar{L}_p = 519, s = 143\}$, $\{n = 4, \bar{L}_p = 363, s = 43\}$

Δ_o (48.7 MPa) > Δ_o (65.1 MPa) 99% C.L.

$\{n = 8, \bar{\Delta}_o = 1.44, s = 0.46\}$, $\{n = 8, \bar{\Delta}_o = 0.74, s = 0.16\}$

(ii) 7 mm dia. Belgian wire

L_p (48.7 MPa) > L_p (65.1 MPa) 95% C.L.

$\{n = 4, \bar{L}_p = 413, s = 78\}$, $\{n = 4, \bar{L}_p = 269, s = 55\}$

Δ_o (48.7 MPa) > Δ_o (65.1 MPa) 99.99% C.L.

$\{n = 8, \bar{\Delta}_o = 0.90, s = 0.09\}$, $\{n = 8, \bar{\Delta}_o = 0.51, s = 0.08\}$

(iii) 5 mm dia. Plain wire

L_p (48.7 MPa) > L_p (65.1 MPa) 95% C.L.

$\{n = 4, \bar{L}_p = 519, s = 118\}$, $\{n = 4, \bar{L}_p = 294, s = 125\}$

Δ_o (48.7 MPa) > Δ_o (65.1 MPa) 99.99% C.L.

$\{n = 16, \bar{\Delta}_o = 1.18, s = 0.30\}$, $\{n = 16, \bar{\Delta}_o = 0.40, s = 0.07\}$

(iv) 5 mm dia. Chevron wire

L_p (48.7 MPa) > L_p (65.1 MPa) 95% C.L.

$\{n = 4, \bar{L}_p = 400, s = 35\}$, $\{n = 4, \bar{L}_p = 281, s = 83\}$

Δ_o (48.7 MPa) > Δ_o (65.1 MPa) 99.99% C.L.

$\{n = 16, \bar{\Delta}_o = 0.59, s = 0.09\}$, $\{n = 16, \bar{\Delta}_o = 0.32, s = 0.06\}$

(E) Test 5 Gradual Release (20.1 and 26.8 MPa) vs. Tests 1, 2, 4, 6 and 7 (33.8 to 65.1 MPa)

(i) 7 mm dia. Plain wire

L_p (20.1 and 26.8 MPa) > L_p (33.8 to 65.1 MPa) 99.99% C.L.

$\{n = 8, \bar{L}_p = 900, s = 154\}$, $\{n = 36, \bar{L}_p = 465, s = 107\}$

Δ_o (20.1 and 26.8 MPa) > Δ_o (33.8 to 65.1 MPa) 99.99% C.L.

$\{n = 16, \bar{\Delta}_o = 2.56, s = 0.58\}$, $\{n = 72, \bar{\Delta}_o = 1.10, s = 0.39\}$

(ii) 5 mm dia. Chevron wire

L_p (20.1 and 26.8 MPa) > L_p (33.8 to 65.1 MPa) 99.9% C.L.

$\{n = 8, \bar{L}_p = 541, s = 132\}$, $\{n = 20, \bar{L}_p = 321, s = 69\}$

Δ_o (20.1 and 26.8 MPa) > Δ_o (33.8 to 65.1 MPa) 99.99% C.L.

$\{n = 32, \bar{\Delta}_o = 0.90, s = 0.14\}$, $\{n = 80, \bar{\Delta}_o = 0.50, s = 0.14\}$

Test 2 (f_{cp} = 35.8 and 48.7 MPa, Gradual Release)
(L_p for 7 mmØ Plain wire (35.8 MPa) vs. L_p for 7 mmØ Plain wire (48.7 MPa))

7 mmØ Plain (35.8 MPa)[1]		7 mmØ Plain (48.7 MPa)[2]	
2G-D5-D	450	2G-D1-D	400
2G-D5-L	550	2G-D1-L	650
2G-L5-D	450	2G-L1-D	375
2G-L5-L	350	2G-L1-L	350

H_o: $\mu_1 = \mu_2$
H_a: $\mu_1 > \mu_2$

$\bar{L}_{p1} = 450$
$s_1 = 81.65$
$n_1 = 4$
$\frac{s_1^2}{n_1} = 1666.67$

$\bar{L}_{p2} = 443.75$
$s_2 = 139.01$
$n_2 = 4$
$\frac{s_2^2}{n_2} = 4830.73$

$t_{test} = 0.078$

∴ Very small, accept H_o @ 90.0% C.L., L_{p1} (35.8 MPa) = L_{p2} (48.7 MPa).

Test 2 (f_{cp} = 35.8 and 48.7 MPa, Gradual Release)
(L_p for 5 mmØ Chevron wire (35.8 MPa) vs. L_p for 5 mmØ Chevron wire (48.7 MPa))

5 mmØ Chev. (35.8 MPa)[1]		5 mmØ Chev. (48.7 MPa)[2]	
2G-D4-D	250	2G-D2-D	250
2G-D4-L	350	2G-D2-L	325
2G-L4-D	350	2G-L2-D	275
2G-L4-L	250	2G-L2-L	275

H_o: $\mu_1 = \mu_2$
H_a: $\mu_1 > \mu_2$

$\bar{L}_{p1} = 300$
$s_1 = 57.74$
$n_1 = 4$
$\frac{s_1^2}{n_1} = 833.33$

$\bar{L}_{p2} = 281.25$
$s_2 = 31.46$
$n_2 = 4$
$\frac{s_2^2}{n_2} = 247.40$

$t_{test} = 0.57$

$\nu = 4.64$ ($\cong 5$)

$t_{\nu=5,10\%} = 1.476$

∴ Not significant, accept H_o @ 90.0% C.L., L_{p1} (35.8 MPa) = L_{p2} (48.7 MPa).

Test 3 (f_{cp} = 33.8 and 53.1 MPa, Sudden Release)
(L_p for 7 mmØ Plain wire (33.8 MPa) vs. L_p for 7 mmØ Plain wire (53.1 MPa))

7 mmØ Plain (33.8 MPa)[1]		7 mmØ Plain (53.1 MPa)[2]		
3R-D5-D	450	3R-D1-D	300	H_o: $\mu_1 = \mu_2$
3R-D5-L	600	3R-D1-L	600	H_a: $\mu_1 > \mu_2$
3R-L5-D	725	3R-L1-D	425	
3R-L5-L	925	3R-L1-L	450	

$\bar{L}_{p1} = 675$
$s_1 = 201.04$
$n_1 = 4$
$\frac{s_1^2}{n_1} = 10104.2$

$\bar{L}_{p2} = 443.75$
$s_2 = 123.11$
$n_2 = 4$
$\frac{s_2^2}{n_2} = 3789.06$

$t_{test} = 1.96$

$\nu = 4.97 \ (\cong 5)$

$t_{\nu=5,10\%} = 1.476$ $t_{\nu=5,5\%} = 2.015$

∴ Significant, reject H_o @ 90.0% C.L., L_{p1} (33.8 MPa) > L_{p2} (53.1 MPa).

Test 3 (f_{cp} = 33.8 and 53.1 MPa, Sudden Release)
(L_p for 5 mmØ Chevron wire (33.8 MPa) vs. L_p for 5 mmØ Chevron wire (53.1 MPa))

5 mmØ Chev. (33.8 MPa)[1]		5 mmØ Chev. (53.1 MPa)[2]		
3R-D4-D	475	3R-D2-D	325	H_o: $\mu_1 = \mu_2$
3R-D4-L	575	3R-D2-L	525	H_a: $\mu_1 > \mu_2$
3R-L4-D	450	3R-L2-D	375	
3R-L4-L	637.5	3R-L2-L	350	

$\bar{L}_{p1} = 534.38$
$s_1 = 87.43$
$n_1 = 4$
$\frac{s_1^2}{n_1} = 1910.81$

$\bar{L}_{p2} = 393.75$
$s_2 = 89.85$
$n_2 = 4$
$\frac{s_2^2}{n_2} = 2018.23$

$t_{test} = 2.244$

$\nu = 6.0 \ (\cong 6)$

$t_{\nu=6,5\%} = 1.943$ $t_{\nu=6,1\%} = 3.143$

∴ Significant, reject H_o @ 95.0% C.L., L_{p1} (33.8 MPa) > L_{p2} (53.1 MPa).

Test 5 (f_{cp} = 20.1 (2 days) and 26.8 MPa (7 days), Gradual Release) (L_p for 7 mmØ Plain wire (20.1 MPa) vs. L_p for 7 mmØ Plain wire (26.8 MPa))

7 mmØ Plain (20.1 MPa)[1]		7 mmØ Plain (26.8 MPa)[2]		
5G-D1-D	700	5G-D5-D	725	H_o: $\mu_1 = \mu_2$
5G-D1-L	825	5G-D5-L	1050	H_a: $\mu_1 \neq \mu_2$
5G-L1-D	1075	5G-L5-D	800	(2-tailed Test)
5G-L1-L	1025	5G-L5-L	1000	

$\bar{L}_{p1} = 906.25$
$s_1 = 174.85$
$n_1 = 4$
$\frac{s_1^2}{n_1} = 7643.23$

$\bar{L}_{p2} = 893.75$
$s_2 = 155.96$
$n_2 = 4$
$\frac{s_2^2}{n_2} = 6080.73$

$t_{test} = 0.107$

∴ Not significant, accept H_o @ 90.0% C.L. (2-Tailed Test), L_{p1} (20.1 MPa) = L_{p2} (26.8 MPa).

Test 5 (f_{cp} = 20.1 (2 days) and 26.8 MPa (7 days), Gradual Release) (L_p for 5 mmØ Chevron wire (20.1 MPa) vs. L_p for 5 mmØ Chevron wire (26.8 MPa))

5 mmØ Chev. (20.1 MPa)[1]		5 mmØ Chev. (26.8 MPa)[2]		
5G-D2-D	425	5G-D4-D	750	H_o: $\mu_1 = \mu_2$
5G-D2-L	400	5G-D4-L	575	H_a: $\mu_1 \neq \mu_2$
5G-L2-D	425	5G-L4-D	475	(2-Tailed Test)
5G-L2-L	575	5G-L4-L	700	

$\bar{L}_{p1} = 456.25$
$s_1 = 80.04$
$n_1 = 4$
$\frac{s_1^2}{n_1} = 1601.56$

$\bar{L}_{p2} = 625.0$
$s_2 = 124.16$
$n_2 = 4$
$\frac{s_2^2}{n_2} = 3854.17$

$t_{test} = -2.285$

$\nu = 5.13 \ (\cong 5)$

$t_{\nu=5,\frac{5\%}{2}} = \pm 2.571$ $\quad t_{\nu=5,\frac{10\%}{2}} = \pm 2.015$

∴ Significant, reject H_o @ 90.0% C.L. (2-Tailed Test), L_{p1} (20.1 MPa) ≠ L_{p2} (26.8 MPa).

Test 4 (f_{cp} = 48.7 MPa, Gradual Release) and Test 6 (f_{cp} = 65.1 MPa, Gradual Release)
(L_p for 7 mmØ Plain wire (48.7 MPa) vs. L_p for 7 mmØ Plain wire (65.1 MPa))

7 mmØ Plain (48.7 MPa)[1]		7 mmØ Plain (65.1 MPa)[2]	
4G-D1-D	325	6G-D1-D	325
4G-D1-L	650	6G-D1-L	400
4G-L1-D	500	6G-L1-D	400
4G-L1-L	600	6G-L1-L	325

H_o: $\mu_1 = \mu_2$
H_a: $\mu_1 > \mu_2$

$\bar{L}_{p1} = 518.75$
$s_1 = 143.43$
$n_1 = 4$
$\frac{s_1^2}{n_1} = 5143.23$

$\bar{L}_{p2} = 362.5$
$s_2 = 43.30$
$n_2 = 4$
$\frac{s_2^2}{n_2} = 468.75$

$t_{test} = 2.086$

$\nu = 3.54 \ (\cong 4)$

$t_{\nu=4,10\%} = 1.533 \qquad t_{\nu=4,5\%} = 2.132$

∴ Significant, reject H_o @ 90.0% C.L., L_{p1} (48.7 MPa) > L_{p2} (65.1 MPa).

Test 4 (f_{cp} = 48.7 MPa, Gradual Release) and Test 6 (f_{cp} = 65.1 MPa, Gradual Release)
(L_p for 7 mmØ Belgian wire (48.7 MPa) vs. L_p for 7 mmØ Belgian wire (65.1 MPa))

7 mmØ Belg. (48.7 MPa)[1]		7 mmØ Belg. (65.1 MPa)[2]	
4G-D5-D	375	6G-D5-D	300
4G-D5-L	500	6G-D5-L	200
4G-L5-D	325	6G-L5-D	250
4G-L5-L	450	6G-L5-L	325

H_o: $\mu_1 = \mu_2$
H_a: $\mu_1 > \mu_2$

$\bar{L}_{p1} = 412.5$
$s_1 = 77.73$
$n_1 = 4$
$\frac{s_1^2}{n_1} = 1510.42$

$\bar{L}_{p2} = 268.75$
$s_2 = 55.43$
$n_2 = 4$
$\frac{s_2^2}{n_2} = 768.23$

$t_{test} = 3.011$

$\nu = 5.42 \ (\cong 5)$

$t_{\nu=5,5\%} = 2.015 \qquad t_{\nu=5,1\%} = 3.365$

∴ Significant, reject H_o @ 95.0% C.L., L_{p1} (48.7 MPa) > L_{p2} (65.1 MPa).

Test 4 (f_{cp} = 48.7 MPa, Gradual Release) and Test 6 (f_{cp} = 65.1 MPa, Gradual Release)
(L_p for 5 mmØ Plain wire (48.7 MPa) vs. L_p for 5 mmØ Plain wire (65.1 MPa))

5 mmØ Plain (48.7 MPa)[1]		5 mmØ Plain (65.1 MPa)[2]	
4G-D2-D	350	6G-D2-D	200
4G-D2-L	600	6G-D2-L	175
4G-L2-D	525	6G-L2-D	375
4G-L2-L	600	6G-L2-L	425

H_o: $\mu_1 = \mu_2$
H_a: $\mu_1 > \mu_2$

$\bar{L}_{p1} = 518.75$
$s_1 = 117.92$
$n_1 = 4$
$\frac{s_1^2}{n_1} = 3476.56$

$\bar{L}_{p2} = 293.75$
$s_2 = 124.79$
$n_2 = 4$
$\frac{s_2^2}{n_2} = 3893.23$

$t_{test} = 2.621$

$\nu = 5.98 \ (\cong 6)$

$t_{\nu=6,5\%} = 1.943$ $t_{\nu=6,1\%} = 3.143$

∴ Significant, reject H_o @ 95.0% C.L., L_{p1} (48.7 MPa) > L_{p2} (65.1 MPa).

Test 4 (f_{cp} = 48.7 MPa, Gradual Release) and Test 6 (f_{cp} = 65.1 MPa, Gradual Release)
(L_p for 5 mmØ Chevron wire (48.7 MPa) vs. L_p for 5 mmØ Chevron wire (65.1 MPa))

5 mmØ Chev. (48.7 MPa)[1]		5 mmØ Chev. (65.1 MPa)[2]	
4G-D4-D	375	6G-D4-D	200
4G-D4-L	400	6G-D4-L	225
4G-L4-D	375	6G-L4-D	375
4G-L4-L	450	6G-L4-L	325

H_o: $\mu_1 = \mu_2$
H_a: $\mu_1 > \mu_2$

$\bar{L}_{p1} = 400$
$s_1 = 35.36$
$n_1 = 4$
$\frac{s_1^2}{n_1} = 312.5$

$\bar{L}_{p2} = 281.25$
$s_2 = 82.60$
$n_2 = 4$
$\frac{s_2^2}{n_2} = 1705.73$

$t_{test} = 2.643$

$\nu = 4.06 \ (\cong 4)$

$t_{\nu=4,5\%} = 2.132$ $t_{\nu=4,1\%} = 3.747$

∴ Significant, reject H_o @ 95.0% C.L., L_{p1} (48.7 MPa) > L_{p2} (65.1 MPa).

Test 5 (f_{cp} = 20.1 and 26.8 MPa, Gradual Release) and Tests 1, 2, 4, 6 and 7 (f_{cp} = 35.8 to 65.1 MPa, Gradual Releases)
(L_p for 7 mmØ Plain wire (20.1 and 26.8 MPa) vs. L_p for 7 mmØ Plain wire (35.8 to 65.1 MPa))

7 mmØ Plain (20.1, 26.8 MPa)[1]	
5G-D1-D	700
5G-D1-L	825
5G-D5-D	725
5G-D5-L	1050
5G-L1-D	1075
5G-L1-L	1025
5G-L5-D	800
5G-L5-L	1000

7 mmØ Plain (35.8 to 65.1 MPa)[2]	
1G-D1-D	350
1G-D1-L	450
1G-D2-D	425
1G-D2-L	425
1G-D4-D	600
1G-D4-L	475
1G-D5-D	625
1G-D5-L	425
1G-L1-D	525
1G-L1-L	525
1G-L2-D	625
1G-L2-L	450
1G-L4-D	650
1G-L4-L	475
1G-L5-D	600
1G-L5-L	325
2G-D1-D	400
2G-D1-L	650
2G-D5-D	450
2G-D5-L	550
2G-L1-D	400
2G-L1-L	350
2G-L5-D	450
2G-L5-L	350
4G-D1-D	325
4G-D1-L	650
4G-L1-D	500
4G-L1-L	600
6G-D1-D	325
6G-D1-L	400
6G-L1-D	400
6G-L1-L	325
7G-D5-D	300
7G-D5-L	450
7G-L5-D	375
7G-L5-L	525

H_o: $\mu_1 = \mu_2$
H_a: $\mu_1 > \mu_2$

$\bar{L}_{p1} = 900$
$s_1 = 153.53$
$n_1 = 8$
$\frac{s_1^2}{n_1} = 2946.43$

$\bar{L}_{p2} = 464.58$
$s_2 = 107.47$
$n_2 = 36$
$\frac{s_2^2}{n_2} = 320.81$

$t_{test} = 7.62$

$\nu = 8.59 \ (\cong 9)$

$t_{\nu=9,0.1\%} = 4.297 \quad t_{\nu=9,0.01\%} = 6.010$

∴ Significant, reject H_o @ 99.99% C.L., L_{p1} (20.1 and 26.8 MPa) > L_{p2} (35.8 to 65.1 MPa).

Test 5 (f_{cp} = 20.1 and 26.8 MPa, Gradual Release) and Tests 2, 4, 6 and 7 (f_{cp} = 35.8 to 65.1 MPa, Gradual Releases)
(L_p for 5 mmØ Chevron wire (20.1 and 26.8 MPa) vs. L_p for 5 mmØ Chevron wire (35.8 to 65.1 MPa))

5 mmØ Chev. (20.1, 26.8 MPa)[1]		5 mmØ Chev. (35.8 to 65.1 MPa)[2]	
5G-D2-D	425	2G-D2-D	250
5G-D2-L	400	2G-D2-L	325
5G-D4-D	750	2G-D4-D	250
5G-D4-L	575	2G-D4-L	350
5G-L2-D	425	2G-L2-D	275
5G-L2-L	575	2G-L2-L	275
5G-L4-D	475	2G-L4-D	350
5G-L4-L	700	2G-L4-L	250
		4G-D4-D	375
		4G-D4-L	400
		4G-L4-D	375
		4G-L4-L	450
		6G-D4-D	200
		6G-D4-L	225
		6G-L4-D	375
		6G-L4-L	325
		7G-D2-D	275
		7G-D2-L	350
		7G-L2-D	425
		7G-L2-L	325

H_o: $\mu_1 = \mu_2$
H_a: $\mu_1 > \mu_2$

$\bar{L}_{p1} = 540.63$
$s_1 = 132.25$
$n_1 = 8$
$\frac{s_1^2}{n_1} = 2186.10$

$\bar{L}_{p2} = 321.25$
$s_2 = 68.96$
$n_2 = 20$
$\frac{s_2^2}{n_2} = 237.75$

$t_{test} = 4.456$ $\quad \nu = 8.57 \ (\cong 9)$

$t_{\nu=9,0.1\%} = 4.297$ $\quad t_{\nu=9,0.01\%} = 6.010$

∴ Significant, reject H_o @ 99.9% C.L., L_{p1} (20.1 and 26.8 MPa) > L_{p2} (35.8 to 65.1 MPa).

Test 2 (f_{cp} = 35.8 and 48.7 MPa, Gradual Release)
(Δ_o for 7 mmØ Plain wire (35.8 MPa) vs. Δ_o for 7 mmØ Plain wire (48.7 MPa))

7 mmØ Plain (35.8 MPa)[1]		7 mmØ Plain (48.7 MPa)[2]	
2G-D5-AD	1.12	2G-D1-AD	0.88
2G-D5-BD	1.18	2G-D1-BD	1.07
2G-D5-AL	1.28	2G-D1-AL	1.54
2G-D5-BL	1.46	2G-D1-BL	2.58
2G-L5-AD	1.02	2G-L1-AD	0.87
2G-L5-BD	1.18	2G-L1-BD	0.96
2G-L5-AL	0.84	2G-L1-AL	0.82
2G-L5-BL	0.88	2G-L1-AL	0.94

H_o: $\mu_1 = \mu_2$
H_a: $\mu_1 > \mu_2$

$\bar{\Delta}_{o1} = 1.12$
$s_1 = 2.051 \times 10^{-1}$
$n_1 = 8$
$\frac{s_1^2}{n_1} = 5.257 \times 10^{-3}$
$t_{test} = 0.390$

$\bar{\Delta}_{o2} = 1.208$
$s_2 = 5.997 \times 10^{-1}$
$n_2 = 8$
$\frac{s_2^2}{n_2} = 4.495 \times 10^{-2}$

∴ Very small, accept H_o @ 90.0% C.L., Δ_{o1} (35.8 MPa) = Δ_{o2} (48.7 MPa).

Test 2 (f_{cp} = 35.8 and 48.7 MPa, Gradual Release)
(Δ_0 for 5 mmØ Chevron wire (35.8 MPa) vs. Δ_0 for 5 mmØ Chevron wire (48.7 MPa))

5 mmØ Chev. (35.8 MPa)[1]		5 mmØ Chev. (48.7 MPa)[2]	
2G-D4-AD	0.33	2G-D2-AD	0.38
2G-D4-BD	0.42	2G-D2-BD	0.44
2G-D4-CD	0.14	2G-D2-CD	0.48
2G-D4-DD	0.38	2G-D2-DD	0.54
2G-D4-AL	0.56	2G-D2-AL	0.68
2G-D4-BL	0.80	2G-D2-BL	0.78
2G-D4-CL	0.60	2G-D2-CL	0.68
2G-D4-DL	0.62	2G-D2-DL	0.78
2G-L4-AD	0.48	2G-L2-AD	0.54
2G-L4-BD	0.46	2G-L2-BD	0.58
2G-L4-CD	0.50	2G-L2-CD	0.54
2G-L4-DD	0.46	2G-L2-DD	0.50
2G-L4-AL	0.40	2G-L2-AL	0.54
2G-L4-BL	0.47	2G-L2-BL	0.52
2G-L4-CL	0.52	2G-L2-CL	0.64
2G-L4-DL	0.52	2G-L2-DL	0.60

H_o: $\mu_1 = \mu_2$
H_a: $\mu_1 > \mu_2$

$\bar{\Delta}_{o1} = 4.788 \times 10^{-1}$ $\bar{\Delta}_{o2} = 5.763 \times 10^{-1}$

$s_1 = 1.427 \times 10^{-1}$ $s_2 = 1.125 \times 10^{-1}$

$n_1 = 16$ $n_2 = 16$

$\frac{s_1^2}{n_1} = 1.272 \times 10^{-3}$ $\frac{s_2^2}{n_2} = 7.907 \times 10^{-4}$

t_{test} = -2.150 (should be positive value)

∴ Not significant, accept H_o @ 90.0% C.L., Δ_{o1} (35.8 MPa) = Δ_{o2} (48.7 MPa).
Possible that Δ_{o1} (35.8 MPa) < Δ_{o2} (48.7 MPa).

Test 3 (f_{cp} = 33.8 and 53.1 MPa, Sudden Release)
(Δ_0 for 7 mmØ Plain wire (33.8 MPa) vs. Δ_0 for 7 mmØ Plain wire (53.1 MPa))

7 mmØ Plain (33.8 MPa)[1]		7 mmØ Plain (53.1 MPa)[2]	
3R-D5-AD	1.27	3R-D1-AD	0.37
3R-D5-BD	1.00	3R-D1-BD	0.51
3R-D5-AL	1.51	3R-D1-AL	1.20
3R-D5-BL	2.48	3R-D1-BL	1.59
3R-L5-AD	1.73	3R-L1-AD	0.78
3R-L5-BD	2.05	3R-L1-BD	0.96
3R-L5-AL	1.69	3R-L1-AL	0.96
3R-L5-BL	2.58	3R-L1-AL	1.06

H_o: $\mu_1 = \mu_2$
H_a: $\mu_1 > \mu_2$

$\bar{\Delta}_{o1} = 1.789$ $\bar{\Delta}_{o2} = 9.288 \times 10^{-1}$

$s_1 = 5.548 \times 10^{-1}$ $s_2 = 3.854 \times 10^{-1}$

$n_1 = 8$ $n_2 = 8$

$\frac{s_1^2}{n_1} = 3.847 \times 10^{-2}$ $\frac{s_2^2}{n_2} = 1.857 \times 10^{-2}$

t_{test} = 3.60 ν = 12.48 ($\cong$ 12)

$t_{\nu=12,1\%}$ = 2.681 $t_{\nu=12,0.1\%}$ = 3.930

∴ Significant, reject H_o @ 99.0% C.L., Δ_{o1} (33.8 MPa) > Δ_{o2} (53.1 MPa).

Test 3 (f_{cp} = 33.8 and 53.1 MPa, Sudden Release)
(Δ_o for 5 mmØ Chevron wire (33.8 MPa) vs. Δ_o for 5 mmØ Chevron wire (53.1 MPa))

5 mmØ Chev. (33.8 MPa)[1]		5 mmØ Chev. (53.1 MPa)[2]	
3R-D4-AD	1.39	3R-D2-AD	0.38
3R-D4-BD	1.31	3R-D2-BD	0.32
3R-D4-CD	1.33	3R-D2-CD	0.33
3R-D4-DD	1.31	3R-D2-DD	0.32
3R-D4-AL	0.73	3R-D2-AL	0.43
3R-D4-BL	0.82	3R-D2-BL	0.45
3R-D4-CL	1.04	3R-D2-CL	0.55
3R-D4-DL	0.88	3R-D2-DL	0.49
3R-L4-AD	1.27	3R-L2-AD	0.38
3R-L4-BD	1.25	3R-L2-BD	0.41
3R-L4-CD	1.31	3R-L2-CD	0.49
3R-L4-DD	1.55	3R-L2-DD	0.61
3R-L4-AL	1.02	3R-L2-AL	0.39
3R-L4-BL	1.27	3R-L2-BL	0.53
3R-L4-CL	1.59	3R-L2-CL	0.47
3R-L4-DL	1.93	3R-L2-DL	0.45

H_o: $\mu_1 = \mu_2$
H_a: $\mu_1 > \mu_2$

$\bar{\Delta}_{o1} = 1.250$
$s_1 = 3.049 \times 10^{-1}$
$n_1 = 16$
$\frac{s_1^2}{n_1} = 5.812 \times 10^{-3}$

$\bar{\Delta}_{o2} = 4.375 \times 10^{-1}$
$s_2 = 8.434 \times 10^{-2}$
$n_2 = 16$
$\frac{s_2^2}{n_2} = 4.446 \times 10^{-4}$

$t_{test} = 10.3$ $\quad \nu = 17.3 \ (\cong 17)$

$t_{\nu=17,1\%} = 2.567$ $\quad t_{\nu=17,0.01\%} = 4.714$

∴ Significant, reject H_o @ 99.99% C.L., Δ_{o1} (33.8 MPa) > Δ_{o2} (53.1 MPa).

Test 5 (f_{cp} = 20.1 MPa (2 days) and 26.8 MPa (7 days), Gradual Release)
(Δ_o for 7 mmØ Plain wire (20.1 MPa) vs. Δ_o for 7 mmØ Plain wire (26.8 MPa))

7 mmØ Plain (20.1 MPa)[1]		7 mmØ Plain (26.8 MPa)[2]	
5G-D1-AD	1.65	5G-D5-AD	2.19
5G-D1-BD	1.83	5G-D5-BD	2.31
5G-D1-AL	2.13	5G-D5-AL	3.35
5G-D1-BL	2.27	5G-D5-BL	3.65
5G-L1-AD	2.23	5G-L5-AD	2.56
5G-L1-BD	2.35	5G-L5-BD	2.33
5G-L1-AL	2.96	5G-L5-AL	3.00
5G-L1-BL	2.66	5G-L5-AL	3.49

H_o: $\mu_1 = \mu_2$
H_a: $\mu_1 \neq \mu_2$
(2-Tailed Test)

$\bar{\Delta}_{o1} = 2.26$
$s_1 = 4.197 \times 10^{-1}$
$n_1 = 8$
$\frac{s_1^2}{n_1} = 2.202 \times 10^{-2}$

$\bar{\Delta}_{o2} = 2.86$
$s_2 = 5.859 \times 10^{-1}$
$n_2 = 8$
$\frac{s_2^2}{n_2} = 4.291 \times 10^{-2}$

$t_{test} = -2.355$ $\quad \nu = 12.69 \ (\cong 13)$

$t_{\nu=13,\frac{1\%}{2}} = \pm 3.012$ $\quad t_{\nu=13,\frac{5\%}{2}} = \pm 2.160$

∴ Significant, reject H_o @ 95.0% C.L. (2-Tailed Test), Δ_{o1} (20.1 MPa) ≠ Δ_{o2} (26.8 MPa).

Test 5 (f_{cp} = 20.1 MPa (2 days) and 26.8 MPa (7 days), Gradual Release)
(Δ_o for 5 mmØ Chevron wire (20.1 MPa) vs. Δ_o for 5 mmØ Chevron wire (26.8 MPa))

5 mmØ Chev. (20.1 MPa)[1]		5 mmØ Chev. (26.8 MPa)[2]	
5G-D2-AD	0.78	5G-D4-AD	0.90
5G-D2-BD	0.86	5G-D4-BD	0.84
5G-D2-CD	0.88	5G-D4-CD	0.86
5G-D2-DD	0.78	5G-D4-DD	0.82
5G-D2-AL	0.70	5G-D4-AL	0.80
5G-D2-BL	0.74	5G-D4-BL	1.06
5G-D2-CL	0.82	5G-D4-CL	1.10
5G-D2-DL	0.66	5G-D4-DL	1.04
5G-L2-AD	0.84	5G-L4-AD	1.08
5G-L2-BD	0.82	5G-L4-BD	0.96
5G-L2-CD	0.80	5G-L4-CD	0.96
5G-L2-DD	0.82	5G-L4-DD	1.12
5G-L2-AL	0.86	5G-L4-AL	0.98
5G-L2-BL	0.88	5G-L4-BL	1.00
5G-L2-CL	0.78	5G-L4-CL	1.10
5G-L2-DL	0.76	5G-L4-DL	1.26

H_o: $\mu_1 = \mu_2$
H_a: $\mu_1 \neq \mu_2$
(2-Tailed Test)

$\bar{\Delta}_{o1} = 7.988 \times 10^{-1}$
$s_1 = 6.260 \times 10^{-2}$
$n_1 = 16$
$\frac{s_1^2}{n_1} = 2.449 \times 10^{-4}$

$\bar{\Delta}_{o2} = 9.925 \times 10^{-1}$
$s_2 = 1.275 \times 10^{-1}$
$n_2 = 16$
$\frac{s_2^2}{n_2} = 1.016 \times 10^{-3}$

$t_{test} = -5.454$ $\quad \nu = 21.8 \ (\cong 22)$
$t_{\nu=22,\frac{1\%}{2}} = \pm 2.819$ $\quad t_{\nu=22,\frac{0.01\%}{2}} = \pm 4.736$

∴ Significant, reject H_o @ 99.99% C.L. (2-Tailed Test), Δ_{o1} (20.1 MPa) ≠ Δ_{o2} (26.8 MPa).

Test 4 (f_{cp} = 48.7 MPa, Gradual Release) and Test 6 (f_{cp} = 65.1 MPa, Gradual Release)
(Δ_o for 7 mmØ Plain wire (48.7 MPa) vs. Δ_o for 7 mmØ Plain wire (65.1 MPa))

7 mmØ Plain (48.7 MPa)[1]		7 mmØ Plain (65.1 MPa)[2]	
4G-D1-AD	0.88	6G-D1-AD	0.62
4G-D1-BD	0.88	6G-D1-BD	0.61
4G-D1-AL	1.45	6G-D1-AL	0.85
4G-D1-BL	1.72	6G-D1-BL	0.85
4G-L1-AD	1.22	6G-L1-AD	0.99
4G-L1-BD	1.30	6G-L1-BD	0.68
4G-L1-AL	1.97	6G-L1-AL	0.79
4G-L1-BL	2.11	6G-L1-BL	0.50

H_o: $\mu_1 = \mu_2$
H_a: $\mu_1 > \mu_2$

$\bar{\Delta}_{o1} = 1.441$
$s_1 = 4.634 \times 10^{-1}$
$n_1 = 8$
$\frac{s_1^2}{n_1} = 2.685 \times 10^{-1}$

$\bar{\Delta}_{o2} = 7.363 \times 10^{-1}$
$s_2 = 1.611 \times 10^{-1}$
$n_2 = 8$
$\frac{s_2^2}{n_2} = 3.243 \times 10^{-3}$

$t_{test} = 4.064$ $\quad \nu = 8.7 \ (\cong 9)$
$t_{\nu=9,1\%} = 2.821$ $\quad t_{\nu=9,0.1\%} = 4.297$

∴ Significant, reject H_o @ 99.0% C.L., Δ_{o1} (48.7 MPa) > Δ_{o2} (65.1 MPa).

Test 4 (f_{cp} = 48.7 MPa, Gradual Release) and Test 6 (f_{cp} = 65.1 MPa, Gradual Release)
(Δ_0 for 7 mmØ Belgian wire (48.7 MPa) vs. Δ_0 for 7 mmØ Belgian wire (65.1 MPa))

7 mmØ Belg. (48.7 MPa)[1]		7 mmØ Belg. (65.1 MPa)[2]	
4G-D5-AD	0.87	6G-D5-AD	0.45
4G-D5-BD	0.83	6G-D5-BD	0.47
4G-D5-AL	1.05	6G-D5-AL	0.45
4G-D5-BL	1.03	6G-D5-BL	0.59
4G-L5-AD	0.79	6G-L5-AD	0.43
4G-L5-BD	0.83	6G-L5-BD	0.51
4G-L5-AL	0.93	6G-L5-AL	0.57
4G-L5-BL	0.89	6G-L5-BL	0.63

H_o: $\mu_1 = \mu_2$
H_a: $\mu_1 > \mu_2$

$\bar{\Delta}_{01} = 9.025 \times 10^{-1}$
$s_1 = 9.498 \times 10^{-2}$
$n_1 = 8$
$\frac{s_1^2}{n_1} = 1.128 \times 10^{-3}$

$\bar{\Delta}_{02} = 5.125 \times 10^{-1}$
$s_2 = 7.517 \times 10^{-2}$
$n_2 = 8$
$\frac{s_2^2}{n_2} = 7.063 \times 10^{-4}$

$t_{test} = 9.107$ $\quad \nu = 13.3 \ (\cong 13)$
$t_{\nu=13,1\%} = 2.650$ $\quad t_{\nu=13,0.01\%} = 5.111$

$\therefore$ Significant, reject H_0 @ 99.99% C.L., Δ_{01} (48.7 MPa) > Δ_{02} (65.1 MPa).

Test 4 (f_{cp} = 48.7 MPa, Gradual Release) and Test 6 (f_{cp} = 65.1 MPa, Gradual Release)
(Δ_0 for 5 mmØ Plain wire (48.7 MPa) vs. Δ_0 for 5 mmØ Plain wire (65.1 MPa))

5 mmØ Plain (48.7 MPa)[1]		5 mmØ Plain (65.1 MPa)[2]	
4G-D2-AD	0.53	6G-D2-AD	0.43
4G-D2-BD	0.82	6G-D2-BD	0.47
4G-D2-CD	0.69	6G-D2-CD	0.47
4G-D2-DD	0.81	6G-D2-DD	0.43
4G-D2-AL	1.46	6G-D2-AL	0.39
4G-D2-BL	1.44	6G-D2-BL	0.35
4G-D2-CL	1.42	6G-D2-CL	0.43
4G-D2-DL	1.34	6G-D2-DL	0.43
4G-L2-AD	1.22	6G-L2-AD	0.41
4G-L2-BD	1.14	6G-L2-BD	0.35
4G-L2-CD	1.16	6G-L2-CD	0.33
4G-L2-DD	1.14	6G-L2-DD	0.25
4G-L2-AL	1.50	6G-L2-AL	0.51
4G-L2-BL	1.40	6G-L2-BL	0.39
4G-L2-CL	1.36	6G-L2-CL	0.37
4G-L2-DL	1.38	6G-L2-DL	0.33

H_o: $\mu_1 = \mu_2$
H_a: $\mu_1 > \mu_2$

$\bar{\Delta}_{01} = 1.176$
$s_1 = 3.040 \times 10^{-1}$
$n_1 = 16$
$\frac{s_1^2}{n_1} = 5.777 \times 10^{-3}$

$\bar{\Delta}_{02} = 3.963 \times 10^{-1}$
$s_2 = 6.520 \times 10^{-2}$
$n_2 = 16$
$\frac{s_2^2}{n_2} = 2.657 \times 10^{-4}$

$t_{test} = 10.03$ $\quad \nu = 16.4 \ (\cong 16)$

$t_{\nu=16,0.01\%} = 4.791$

$\therefore$ Significant, reject H_0 @ 99.99% C.L., Δ_{01} (48.7 MPa) > Δ_{02} (65.1 MPa).

Test 4 (f_{cp} = 48.7 MPa, Gradual Release) and Test 6 (f_{cp} = 65.1 MPa, Gradual Release)
(Δ_o for 5 mmØ Chevron wire (48.7 MPa) vs. Δ_o for 5 mmØ Chevron wire (65.1 MPa))

5 mmØ Chev. (48.7 MPa)[1]		5 mmØ Chev. (65.1 MPa)[2]	
4G-D4-AD	0.51	6G-D4-AD	0.33
4G-D4-BD	0.55	6G-D4-BD	0.37
4G-D4-CD	0.53	6G-D4-CD	0.29
4G-D4-DD	0.47	6G-D4-DD	0.23
4G-D4-AL	0.71	6G-D4-AL	0.31
4G-D4-BL	0.71	6G-D4-BL	0.31
4G-D4-CL	0.69	6G-D4-CL	0.29
4G-D4-DL	0.63	6G-D4-DL	0.31
4G-L4-AD	0.71	6G-L4-AD	0.45
4G-L4-BD	0.65	6G-L4-BD	0.37
4G-L4-CD	0.57	6G-L4-CD	0.23
4G-L4-DD	0.67	6G-L4-DD	0.27
4G-L4-AL	0.49	6G-L4-AL	0.35
4G-L4-BL	0.47	6G-L4-BL	0.31
4G-L4-CL	0.51	6G-L4-CL	0.35
4G-L4-DL	0.53	6G-L4-DL	0.29

H_o: $\mu_1 = \mu_2$
H_a: $\mu_1 > \mu_2$

$\bar{\Delta}_{o1} = 5.875 \times 10^{-1}$
$s_1 = 9.147 \times 10^{-2}$
$n_1 = 16$
$\frac{s_1^2}{n_1} = 5.229 \times 10^{-4}$

$\bar{\Delta}_{o2} = 3.163 \times 10^{-1}$
$s_2 = 5.50 \times 10^{-2}$
$n_2 = 16$
$\frac{s_2^2}{n_2} = 1.891 \times 10^{-4}$

$t_{test} = 10.16$

$\nu = 24.59 \ (\cong 25)$

$t_{\nu=25,0.01\%} = 4.352$

$\therefore$ Significant, reject H_o @ 99.99% C.L., Δ_{o1} (48.7 MPa) > Δ_{o2} (65.1 MPa).

Test 5 (f_{cp} = 20.1 and 26.8 MPa, Gradual Release) and Tests 1, 2, 4, 6 and 7 (f_{cp} = 35.8 to 65.1 MPa, Gradual Releases)
(Δ_o for 7 mmØ Plain wire (20.1 and 26.8 MPa) vs. Δ_o for 7 mmØ Plain wire (35.8 to 65.1 MPa))

7 mmØ Plain (20.1, 26.8 MPa)[1]	
5G-D1-AD	1.65
5G-D1-BD	1.83
5G-D1-AL	2.13
5G-D1-BL	2.27
5G-D5-AD	2.19
5G-D5-BD	2.31
5G-D5-AL	3.35
5G-D5-BL	3.65
5G-L1-AD	2.23
5G-L1-BD	2.35
5G-L1-AL	2.96
5G-L1-BL	2.66
5G-L5-AD	2.56
5G-L5-BD	2.33
5G-L5-AL	3.00
5G-L5-BL	3.49

7 mmØ Plain (35.8 to 65.1 MPa)[2]			
1G-D1-AD	0.70	2G-D5-AD	1.12
1G-D1-BD	0.80	2G-D5-BD	1.18
1G-D1-AL	0.97	2G-D5-AL	1.28
1G-D1-BL	0.96	2G-D5-BL	1.46
1G-D2-AD	0.96	2G-L1-AD	0.87
1G-D2-BD	0.81	2G-L1-BD	0.96
1G-D2-AL	0.69	2G-L1-AL	0.82
1G-D2-BL	0.71	2G-L1-BL	0.94
1G-D4-AD	1.15	2G-L5-AD	1.02
1G-D4-BD	1.11	2G-L5-BD	1.18
1G-D4-AL	1.17	2G-L5-AL	0.84
1G-D4-BL	1.29	2G-L5-BL	0.88
1G-D5-AD	1.00	4G-D1-AD	0.88
1G-D5-BD	1.08	4G-D1-BD	0.88
1G-D5-AL	1.02	4G-D1-AL	1.45
1G-D5-BL	1.08	4G-D1-BL	1.72
1G-L1-AD	1.39	4G-L1-AD	1.22
1G-L1-BD	1.77	4G-L1-BD	1.30
1G-L1-AL	1.31	4G-L1-AL	1.97
1G-L1-BL	1.27	4G-L1-BL	2.11
1G-L2-AD	1.75	6G-D1-AD	0.62
1G-L2-BD	1.65	6G-D1-BD	0.61
1G-L2-AL	1.30	6G-D1-AL	0.85
1G-L2-BL	0.92	6G-D1-BL	0.85
1G-L4-AD	1.67	6G-L1-AD	0.99
1G-L4-BD	1.72	6G-L1-BD	0.68
1G-L4-AL	0.71	6G-L1-AL	0.79
1G-L4-BL	0.77	6G-L1-BL	0.50
1G-L5-AD	1.27	7G-D5-AD	0.80
1G-L5-BD	1.36	7G-D5-BD	0.55
1G-L5-AL	0.53	7G-D5-AL	1.04
1G-L5-BL	0.80	7G-D5-BL	1.12
2G-D1-AD	0.88	7G-L5-AD	0.88
2G-D1-BD	1.07	7G-L5-BD	0.82
2G-D1-AL	1.54	7G-L5-AL	1.08
2G-D1-BL	2.58	7G-L5-BL	1.28

H_o: $\mu_1 = \mu_2$
H_a: $\mu_1 > \mu_2$

$\bar{\Delta}_{o1} = 2.56$
$s_1 = 5.817 \times 10^{-1}$
$n_1 = 16$
$\frac{s_1^2}{n_1} = 2.115 \times 10^{-2}$

$\bar{\Delta}_{o2} = 1.101$
$s_2 = 3.899 \times 10^{-1}$
$n_2 = 72$
$\frac{s_2^2}{n_2} = 2.112 \times 10^{-3}$

$t_{test} = 9.56$

$\nu = 18.1 \ (\cong 18)$

$t_{\nu=18,0.01\%} = 4.648$

∴ Significant, reject H_o @ 99.99% C.L., Δ_{o1} (20.1 and 26.8 MPa) > Δ_{o2} (35.8 to 65.1 MPa).

Test 5 (f_{cp} = 20.1 and 26.8 MPa, Gradual Release) and Tests 1, 2, 4, 6 and 7 (f_{cp} = 35.8 to 65.1 MPa, Gradual Releases)
(Δ_0 for 5 mmØ Chevron wire (20.1 and 26.8 MPa) vs. Δ_0 for 5 mmØ Chevron wire (35.8 to 65.1 MPa))

5 mmØ Chev. (20.1, 26.8 MPa)[1]	
5G-D2-AD	0.78
5G-D2-BD	0.86
5G-D2-CD	0.88
5G-D2-DD	0.78
5G-D2-AL	0.70
5G-D2-BL	0.74
5G-D2-CL	0.82
5G-D2-DL	0.66
5G-D4-AD	0.90
5G-D4-BD	0.84
5G-D4-CD	0.86
5G-D4-DD	0.82
5G-D4-AL	0.80
5G-D4-BL	1.06
5G-D4-CL	1.10
5G-D4-DL	1.04
5G-L2-AD	0.84
5G-L2-BD	0.82
5G-L2-CD	0.80
5G-L2-DD	0.82
5G-L2-AL	0.86
5G-L2-BL	0.88
5G-L2-CL	0.78
5G-L2-DL	0.76
5G-L4-AD	1.08
5G-L4-BD	0.96
5G-L4-CD	0.96
5G-L4-DD	1.12
5G-L4-AL	0.98
5G-L4-BL	1.00
5G-L4-CL	1.10
5G-L4-DL	1.26

H_o: $\mu_1 = \mu_2$
H_a: $\mu_1 > \mu_2$

5 mmØ Chev. (35.8 to 65.1 MPa)[2]			
2G-D2-AD	0.38	4G-L4-AD	0.71
2G-D2-BD	0.44	4G-L4-BD	0.65
2G-D2-CD	0.48	4G-L4-CD	0.57
2G-D2-DD	0.54	4G-L4-DD	0.67
2G-D2-AL	0.68	4G-L4-AL	0.49
2G-D2-BL	0.78	4G-L4-BL	0.47
2G-D2-CL	0.68	4G-L4-CL	0.51
2G-D2-DL	0.78	4G-L4-DL	0.53
2G-D4-AD	0.33	6G-D4-AD	0.33
2G-D4-BD	0.42	6G-D4-BD	0.37
2G-D4-CD	0.14	6G-D4-CD	0.29
2G-D4-DD	0.38	6G-D4-DD	0.23
2G-D4-AL	0.56	6G-D4-AL	0.31
2G-D4-BL	0.80	6G-D4-BL	0.31
2G-D4-CL	0.60	6G-D4-CL	0.29
2G-D4-DL	0.62	6G-D4-DL	0.31
2G-L2-AD	0.54	6G-L4-AD	0.45
2G-L2-BD	0.58	6G-L4-BD	0.37
2G-L2-CD	0.54	6G-L4-CD	0.23
2G-L2-DD	0.50	6G-L4-DD	0.27
2G-L2-AL	0.54	6G-L4-AL	0.35
2G-L2-BL	0.52	6G-L4-BL	0.31
2G-L2-CL	0.64	6G-L4-CL	0.35
2G-L2-DL	0.60	6G-L4-DL	0.29
2G-L4-AD	0.48	7G-D2-AD	0.41
2G-L4-BD	0.46	7G-D2-BD	0.45
2G-L4-CD	0.50	7G-D2-CD	0.45
2G-L4-DD	0.46	7G-D2-DD	0.37
2G-L4-AL	0.40	7G-D2-AL	0.56
2G-L4-BL	0.47	7G-D2-BL	0.64
2G-L4-CL	0.52	7G-D2-CL	0.56
2G-L4-DL	0.52	7G-D2-DL	0.58
4G-D4-AD	0.51	7G-L2-AD	0.57
4G-D4-BD	0.55	7G-L2-BD	0.65
4G-D4-CD	0.53	7G-L2-CD	0.57
4G-D4-DD	0.47	7G-L2-DD	0.59
4G-D4-AL	0.71	7G-L2-AL	0.60
4G-D4-BL	0.71	7G-L2-BL	0.43
4G-D4-CL	0.69	7G-L2-CL	0.35
4G-D4-DL	0.63	7G-L2-DL	0.52

$\bar{\Delta}_{o1} = 8.956 \times 10^{-1}$
$s_1 = 1.395 \times 10^{-1}$
$n_1 = 32$
$\frac{s_1^2}{n_1} = 6.079 \times 10^{-4}$

$\bar{\Delta}_{o2} = 4.955 \times 10^{-1}$
$s_2 = 1.409 \times 10^{-1}$
$n_2 = 80$
$\frac{s_2^2}{n_2} = 2.482 \times 10^{-4}$

Both n_1 and n_2 are > 30, use z-statistic instead of t-statistic.

$$z_{test} = \frac{(\bar{\Delta}_{o1} - \bar{\Delta}_{o2})}{\sqrt{(s_1^2/n_1) + (s_2^2/n_2)}} = 13.7$$

$z_{0.01\%} = 3.719$

∴ Significant, reject H_o @ 99.99% C.L., Δ_{o1} (20.1 and 26.8 MPa) > Δ_{o2} (35.8 to 65.1 MPa).

Normalised Strain Distributions

The following graphs in this Appendix give the normalised longitudinal strain distributions for beam specimens of Tests 1 and 2. The distributions were corrected for shrinkage strains and then normalised by dividing each distribution by the largest strain value for that particular distribution.

The normalised curves were plotted for Tests 1 and 2 only as the beams in these tests were monitored up to six months after casting. The changes in the distributions over time can be better understood by comparing the normalised curves at 7 days (transfer) and at 3 or 6 months.

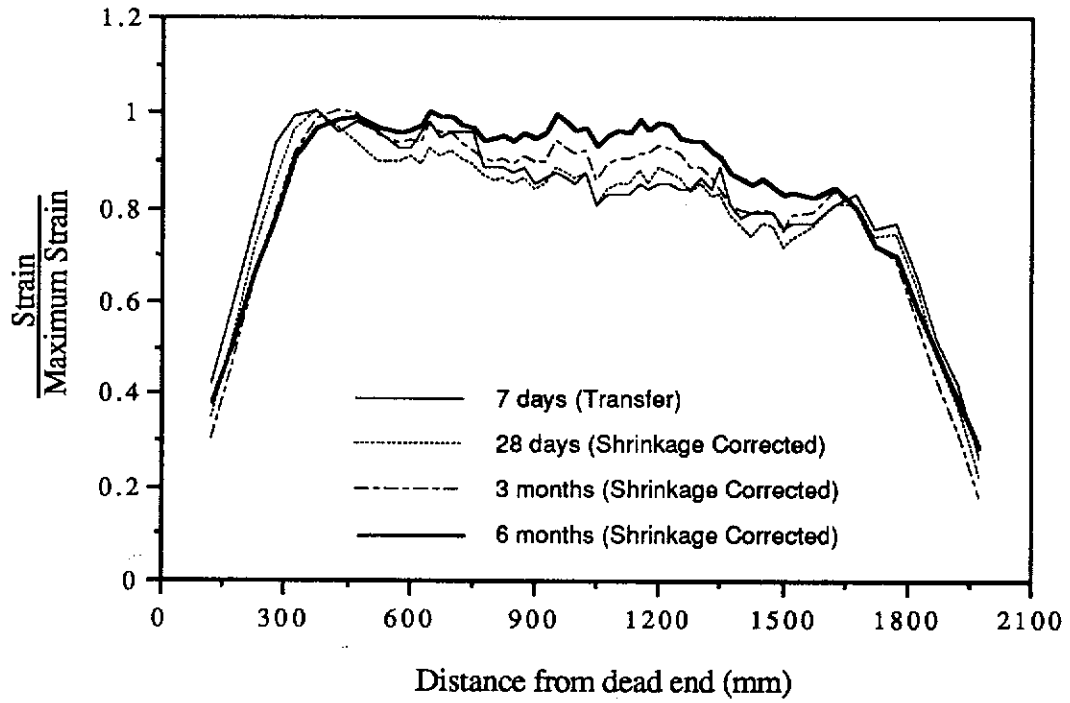

Figure G.1 Normalised Longitudinal Strains for Beam 1G-D1-A

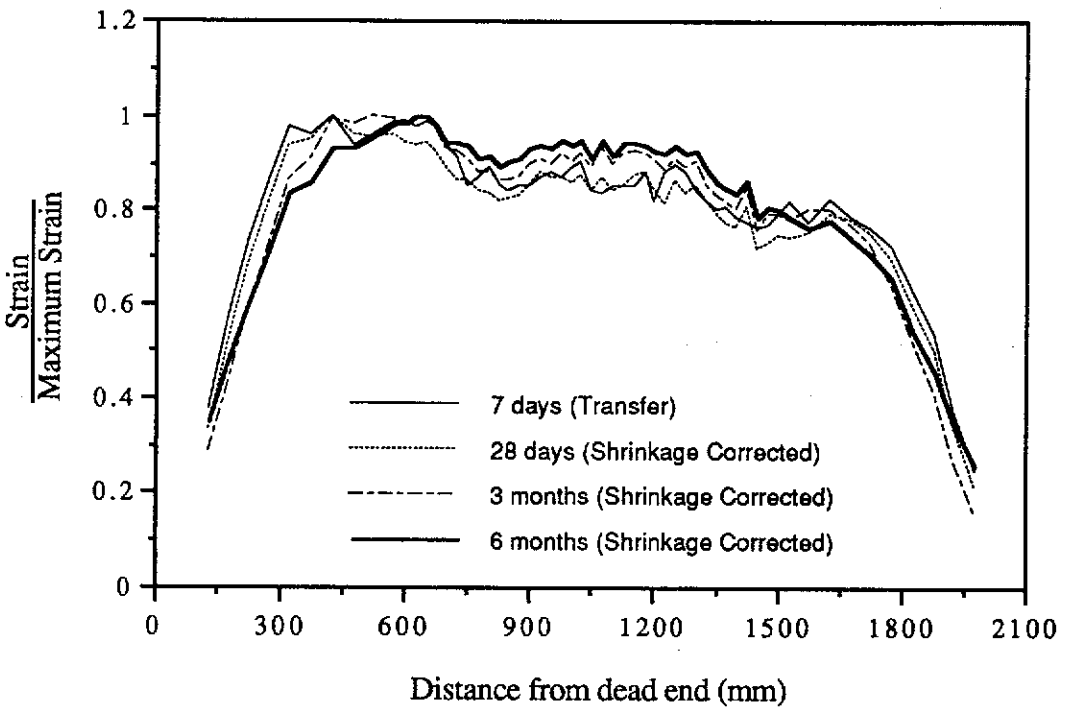

Figure G.2 Normalised Longitudinal Strains for Beam 1G-D1-B

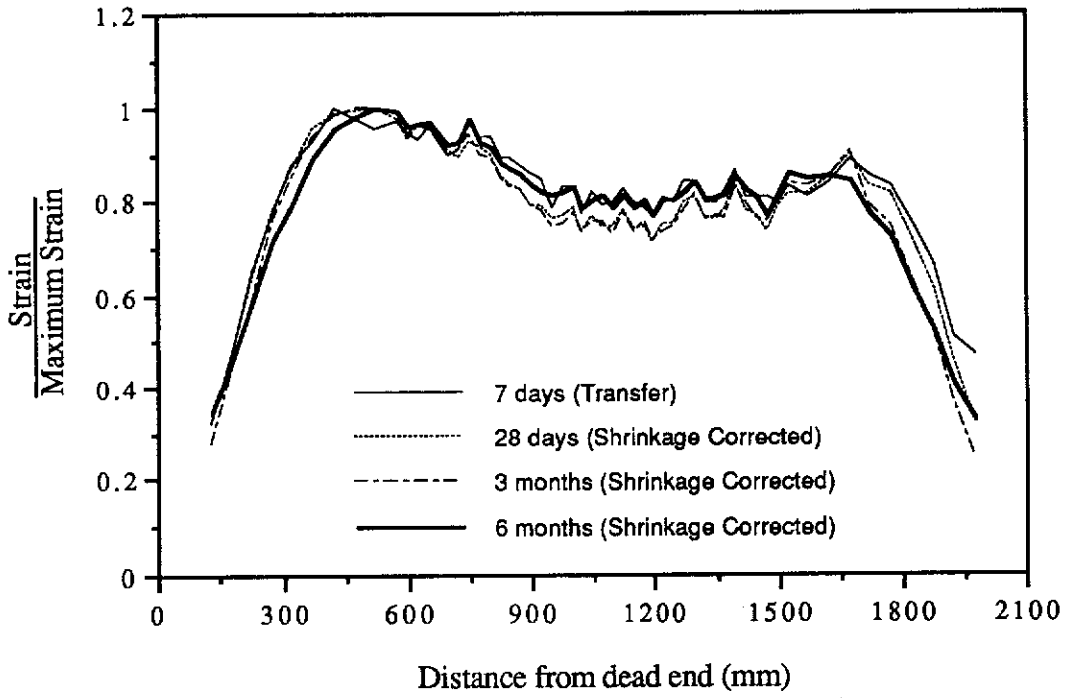

Figure G.3 Normalised Longitudinal Strains for Beam 1G-D2

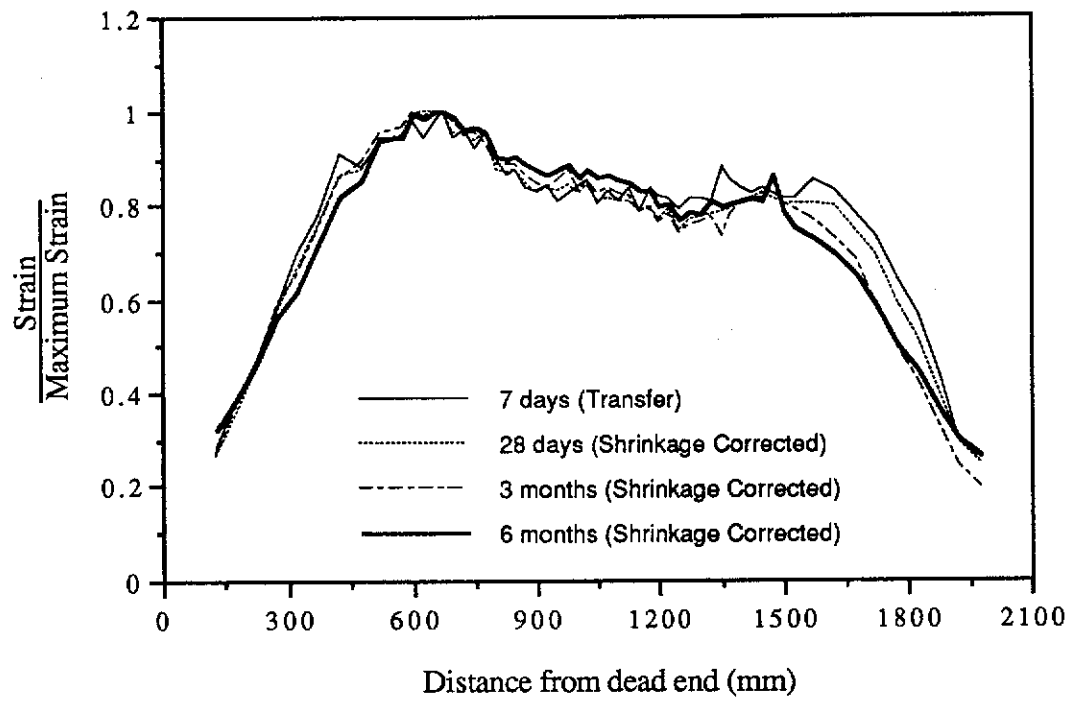

Figure G.4 Normalised Longitudinal Strains for Beam 1G-D4

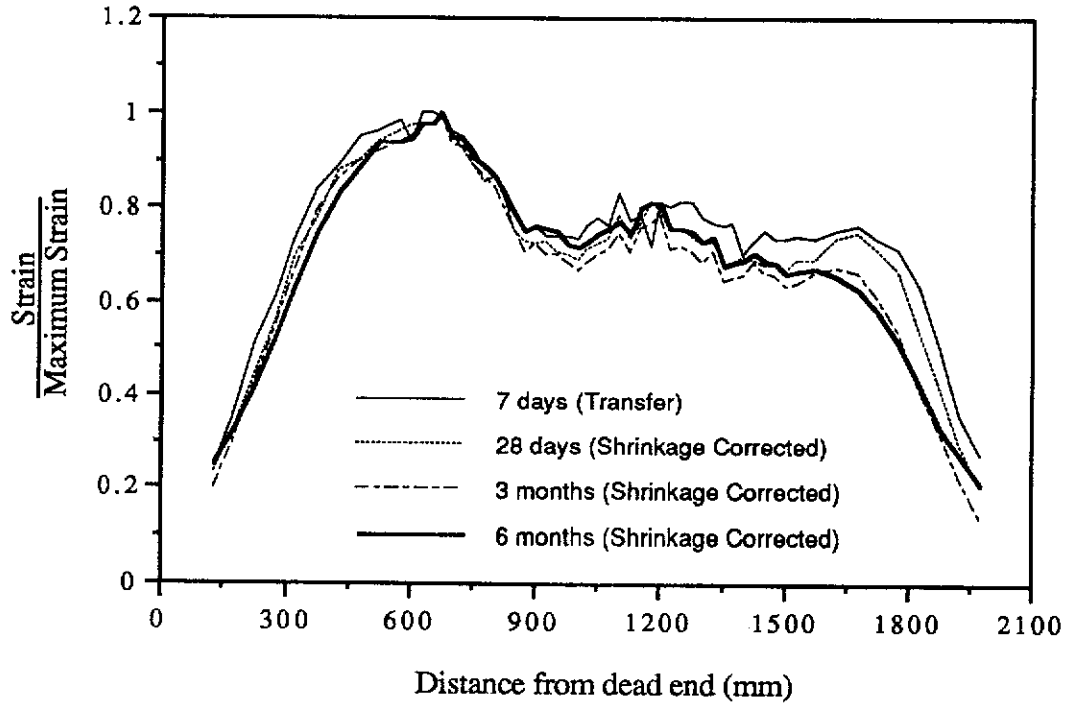

Figure G.5 Normalised Longitudinal Strains for Beam 1G-D5

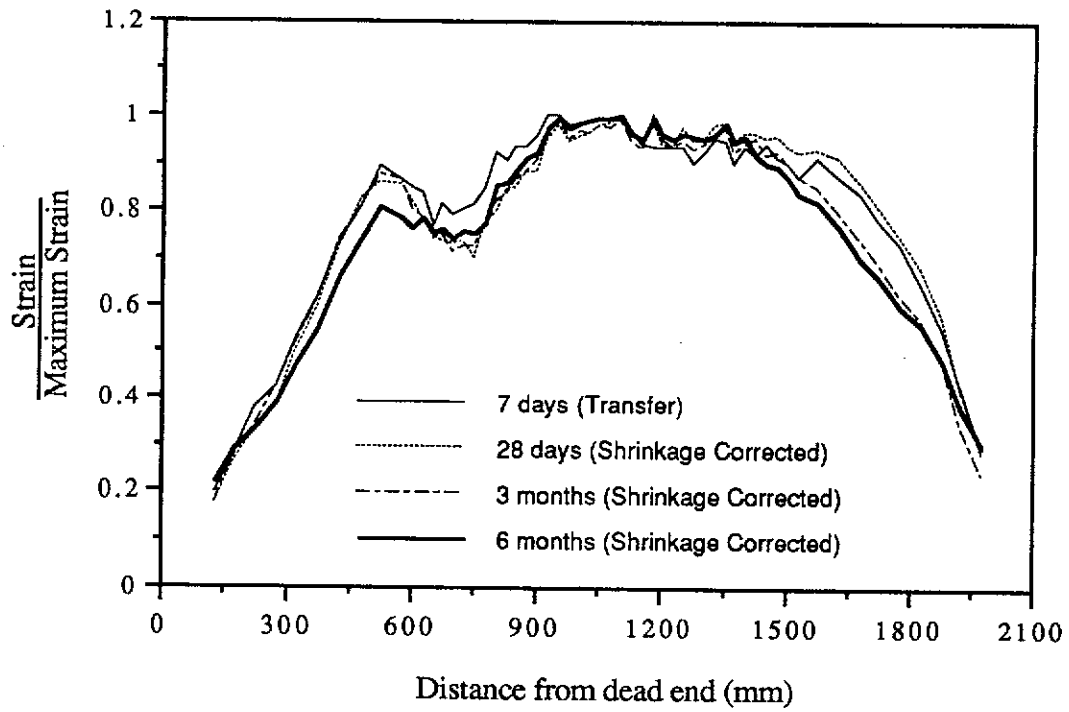

Figure G.6 Normalised Longitudinal Strains for Beam 1G-L1-A

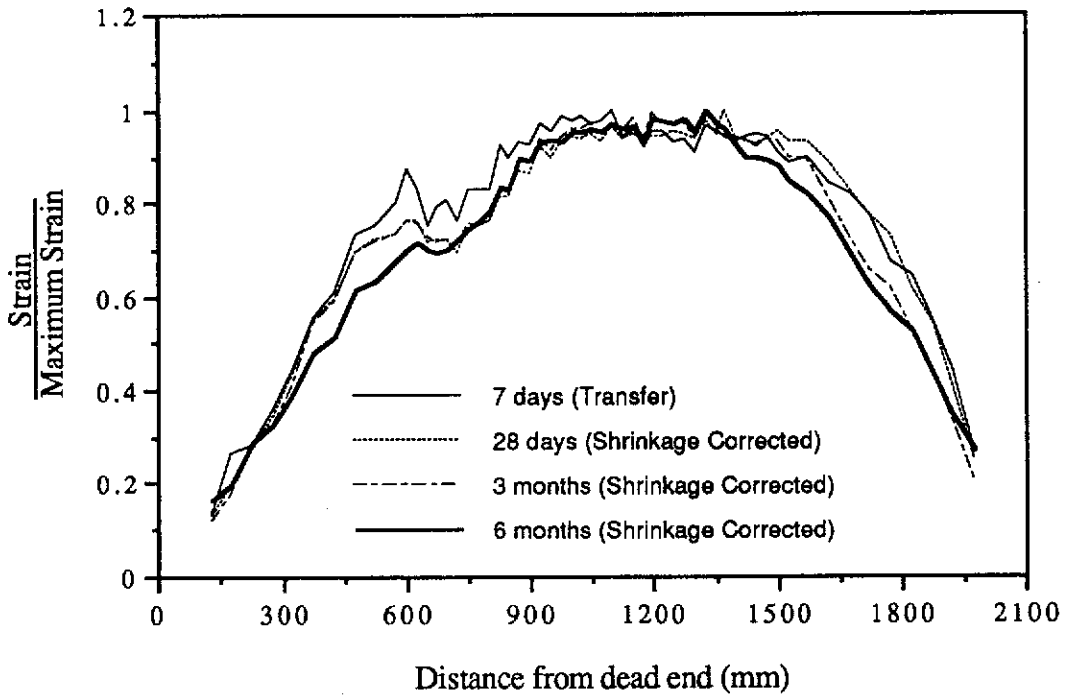

Figure G.7 Normalised Longitudinal Strains for Beam 1G-L1-B

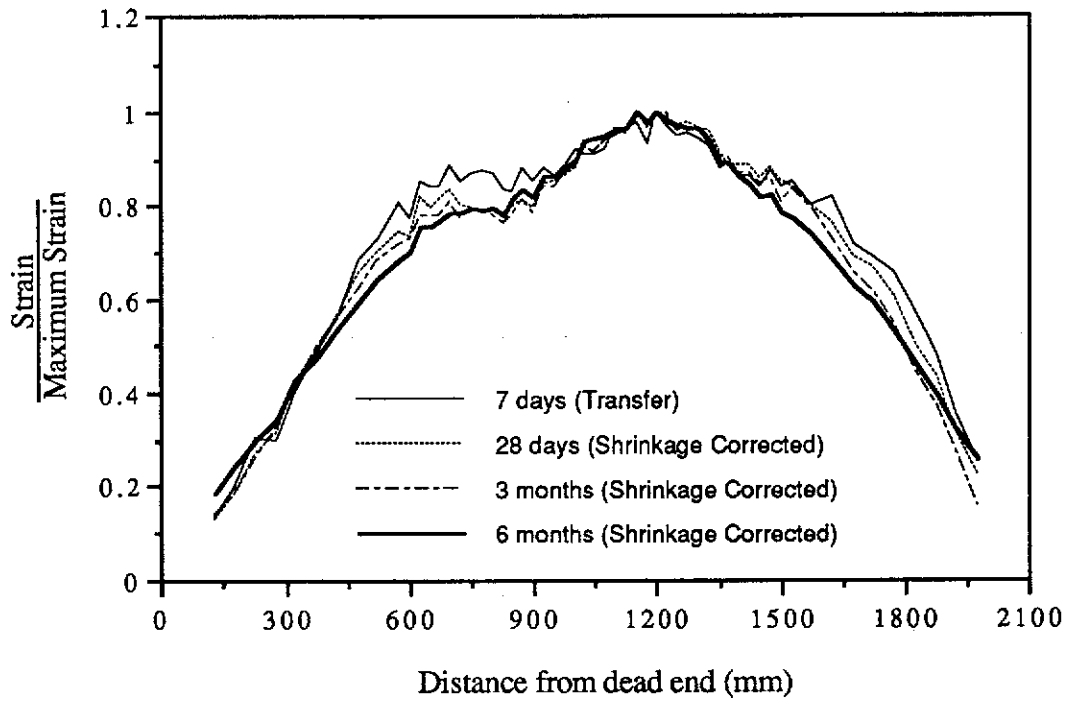

Figure G.8 Normalised Longitudinal Strains for Beam 1G-L2

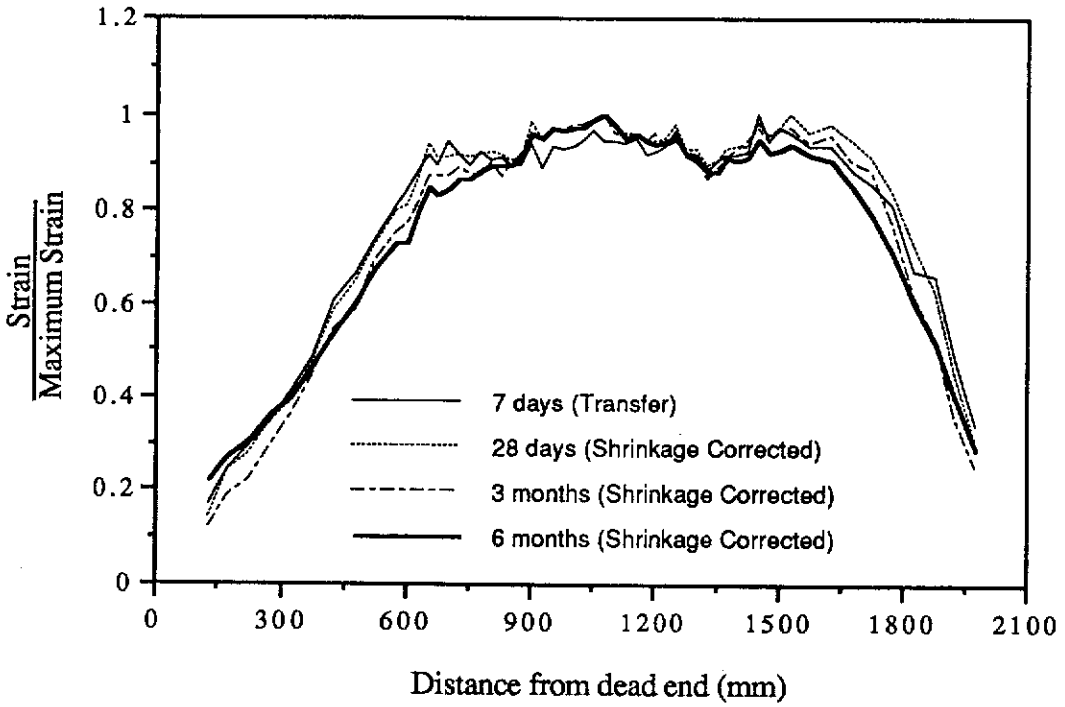

Figure G.9 Normalised Longitudinal Strains for Beam 1G-L4

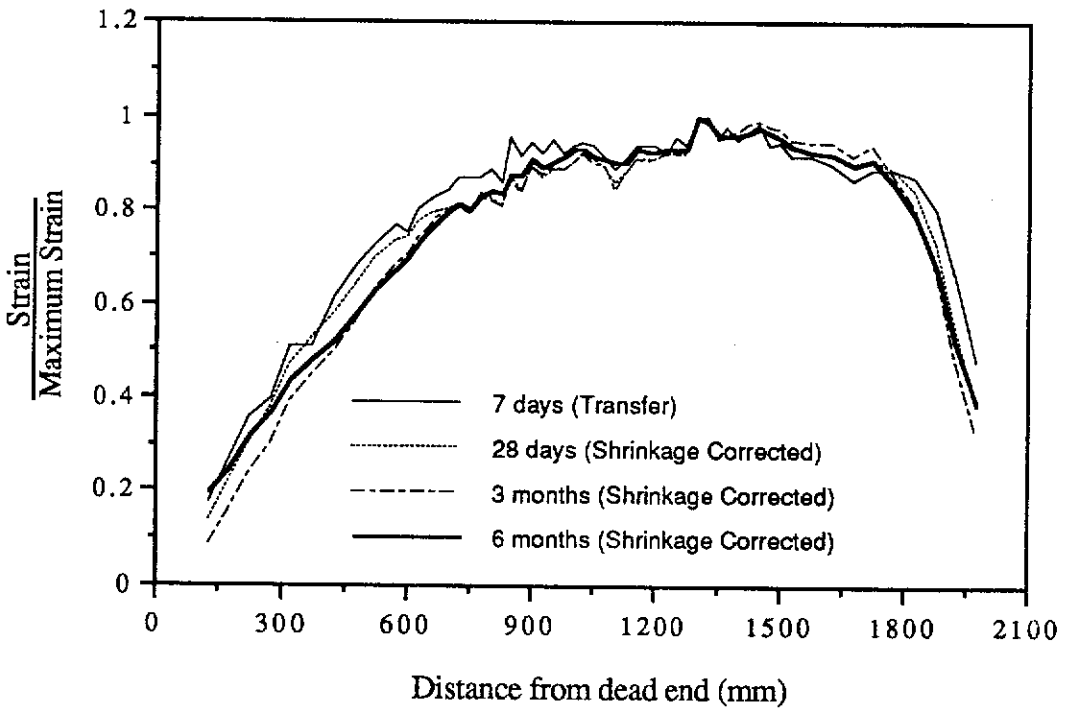

Figure G.10 Normalised Longitudinal Strains for Beam 1G-L5

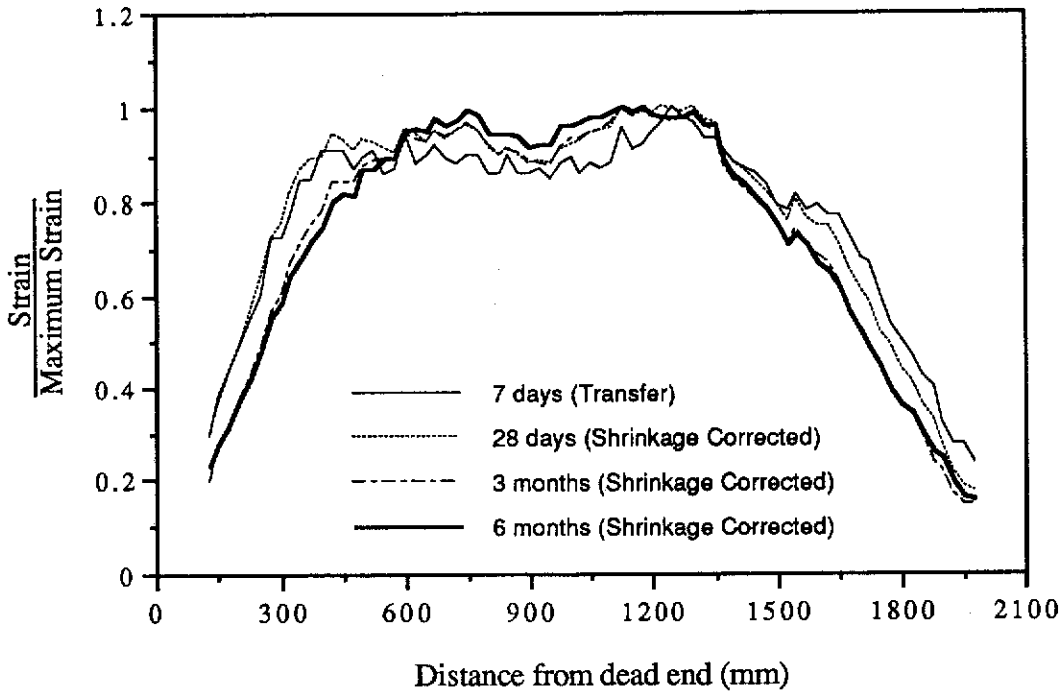

Figure G.11 Normalised Longitudinal Strains for Beam 2G-D1

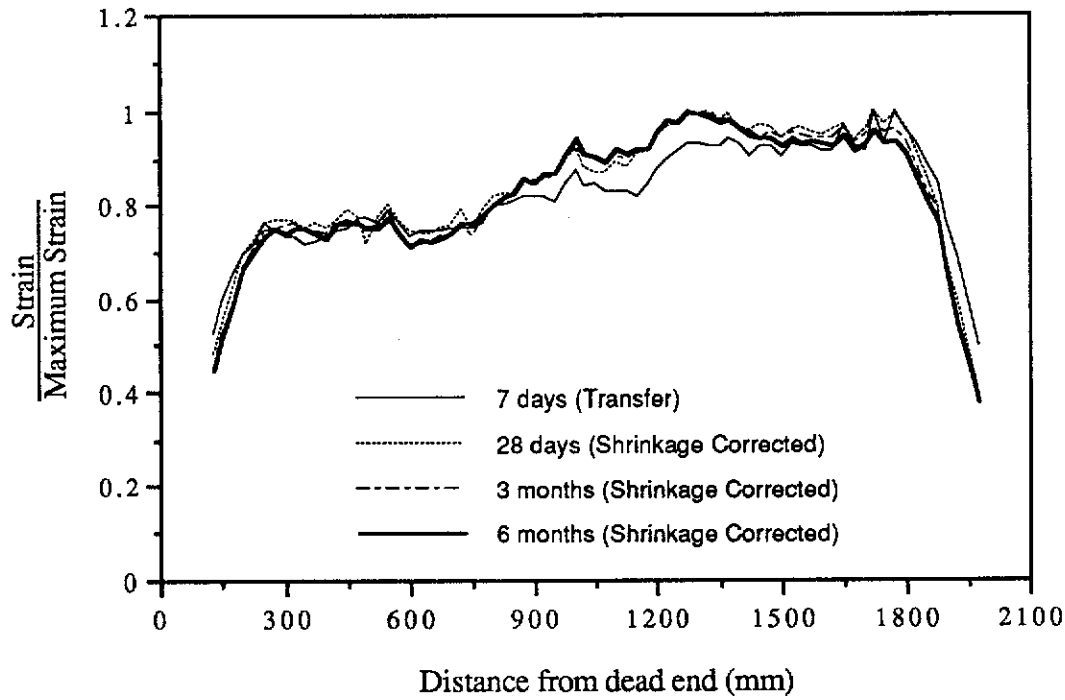

Figure G.12 Normalised Longitudinal Strains for Beam 2G-D2

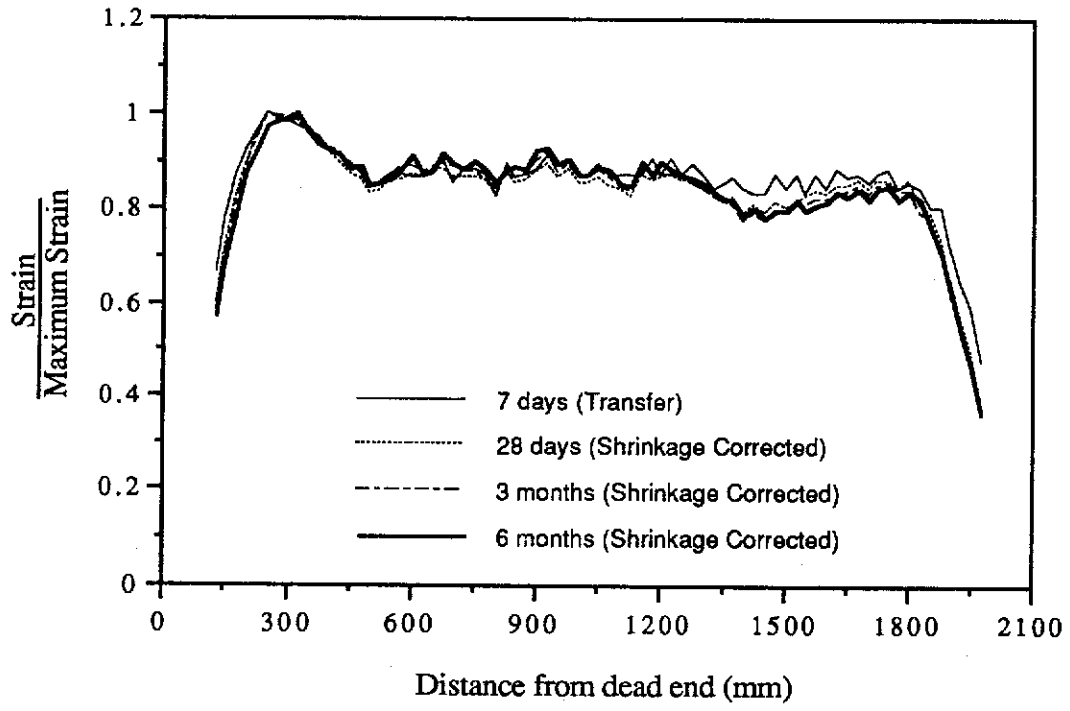

Figure G.13 Normalised Longitudinal Strains for Beam 2G-D4

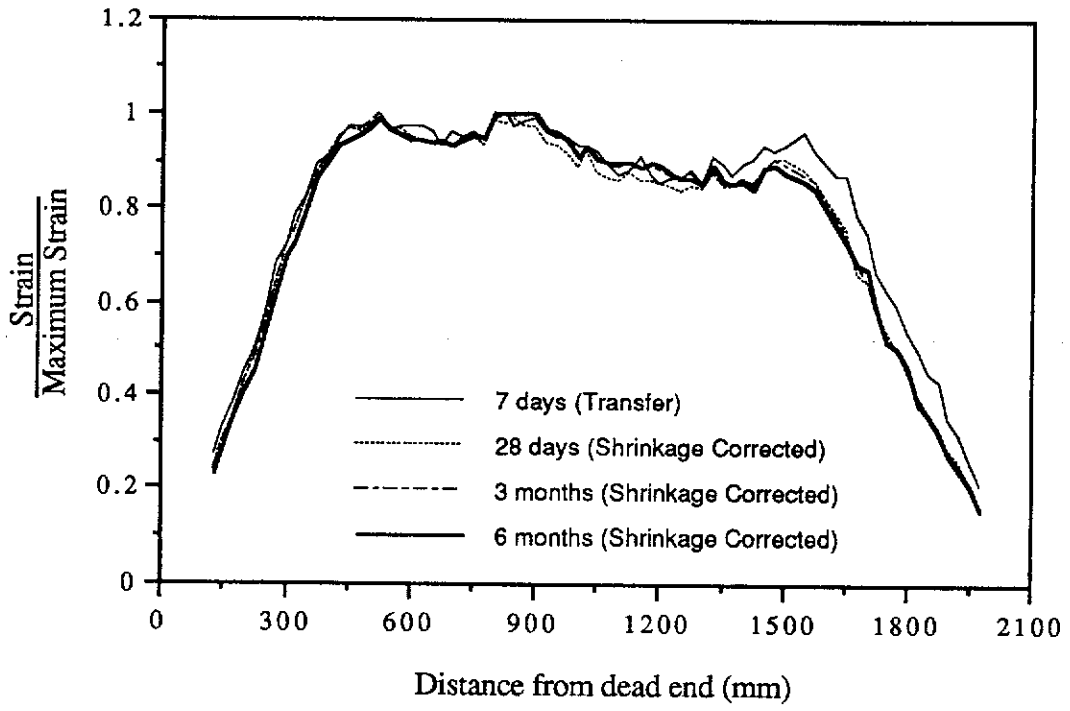

Figure G.14 Normalised Longitudinal Strains for Beam 2G-D5

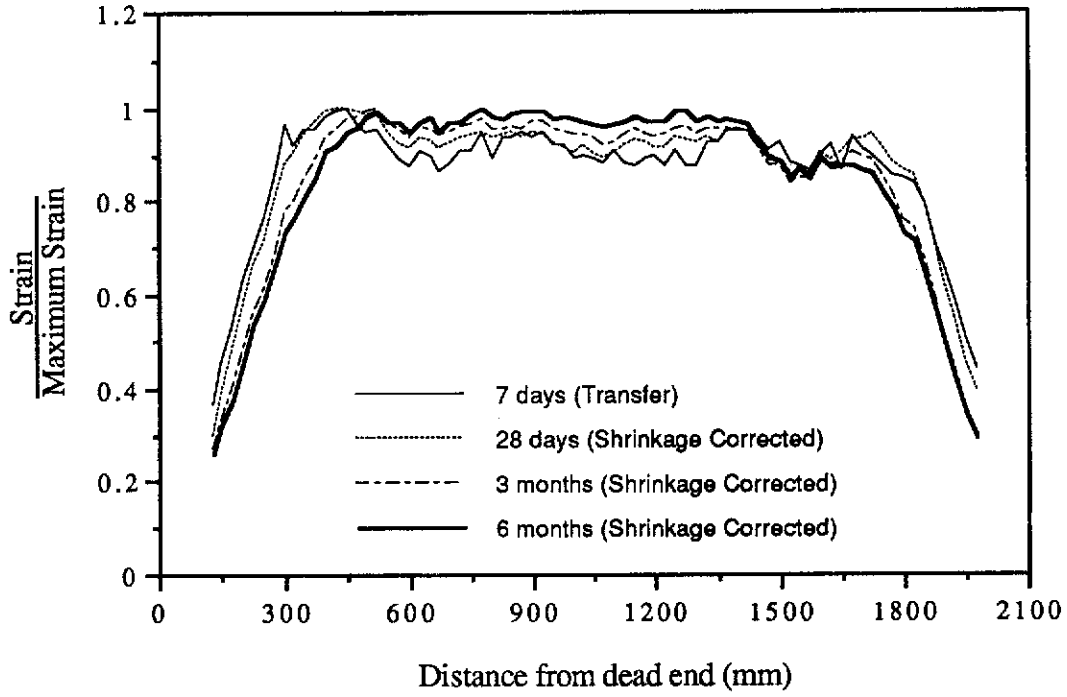

Figure G.15 Normalised Longitudinal Strains for Beam 2G-L1

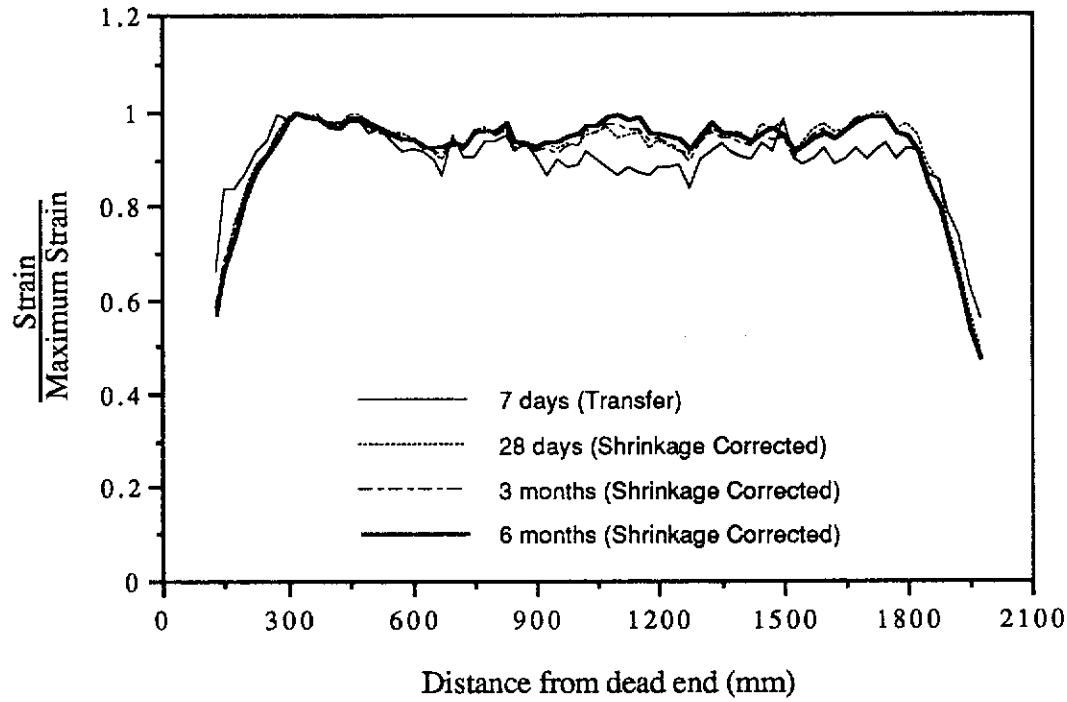

Figure G.16 Normalised Longitudinal Strains for Beam 2G-L2

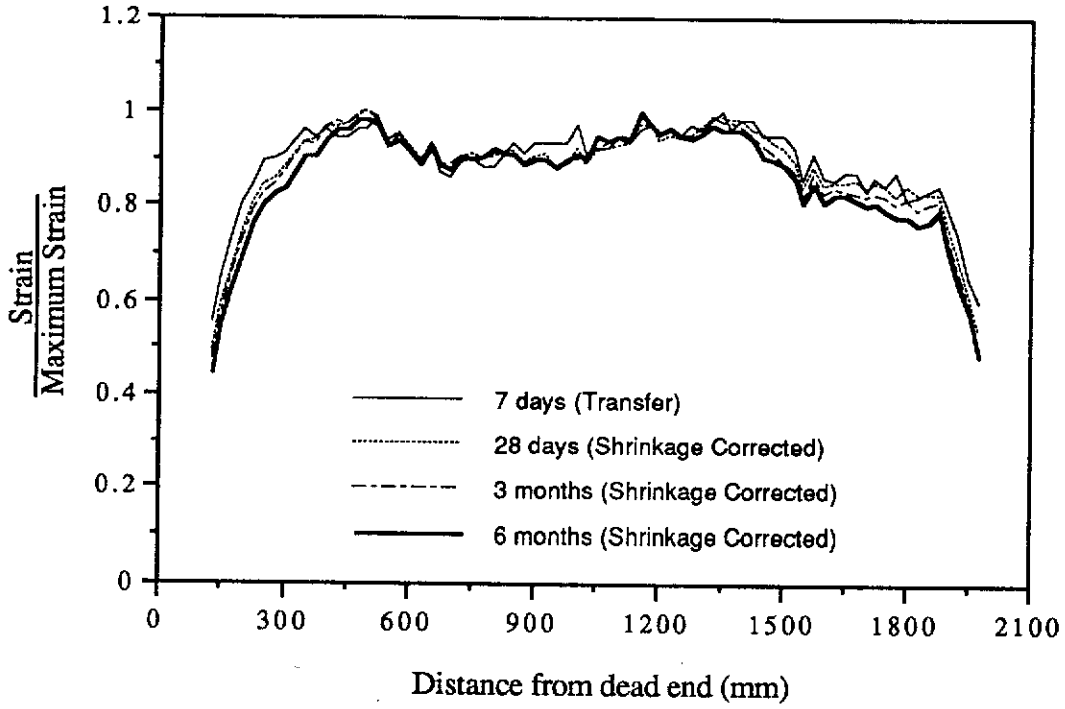

Figure G.17 Normalised Longitudinal Strains for Beam 2G-L4

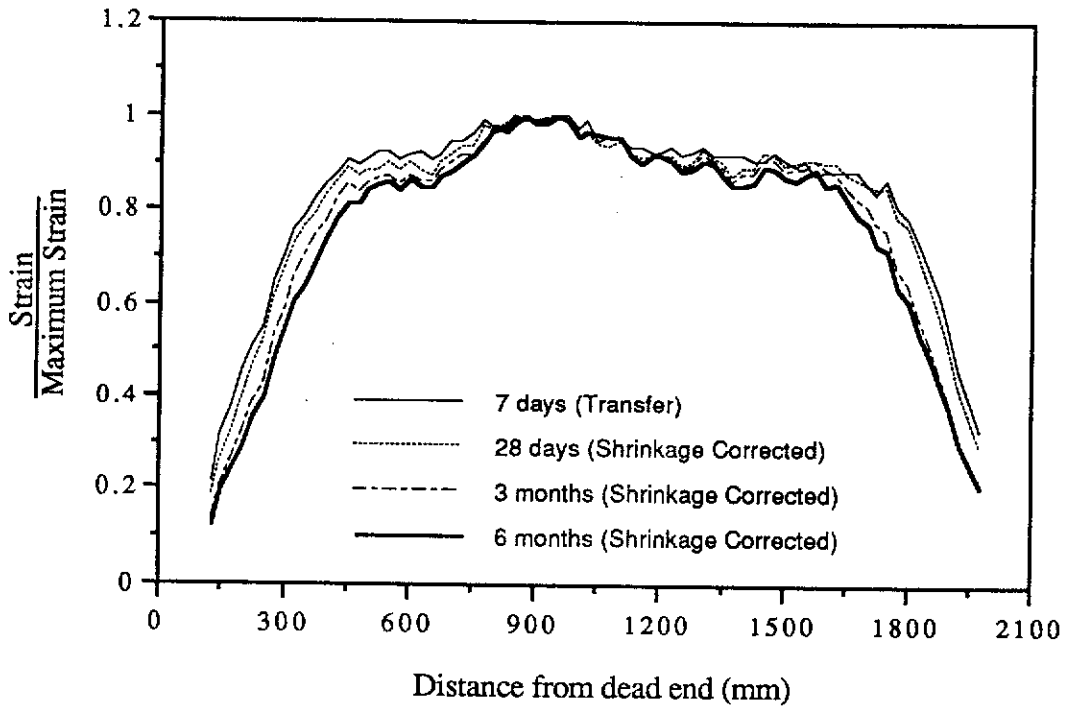

Figure G.18 Normalised Longitudinal Strains for Beam 2G-L5